frontiers | Research Topics

Updates on the complement system in kidney diseases

Edited by
Mihály Józsi and Roberta Bulla

Published in
Frontiers in Immunology

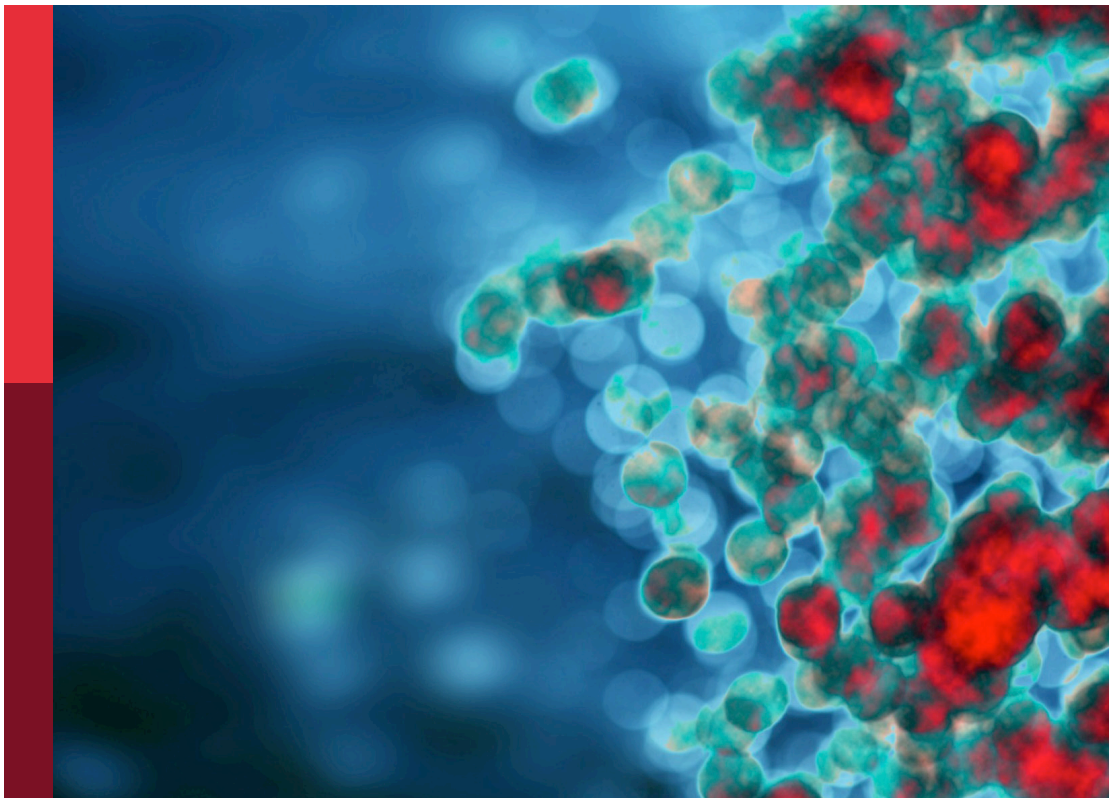

ISSN 1664-8714
ISBN 978-2-8325-2227-1
DOI 10.3389/978-2-8325-2227-1

About Frontiers

Frontiers is more than just an open access publisher of scholarly articles: it is a pioneering approach to the world of academia, radically improving the way scholarly research is managed. The grand vision of Frontiers is a world where all people have an equal opportunity to seek, share and generate knowledge. Frontiers provides immediate and permanent online open access to all its publications, but this alone is not enough to realize our grand goals.

Frontiers journal series

The Frontiers journal series is a multi-tier and interdisciplinary set of open-access, online journals, promising a paradigm shift from the current review, selection and dissemination processes in academic publishing. All Frontiers journals are driven by researchers for researchers; therefore, they constitute a service to the scholarly community. At the same time, the *Frontiers journal series* operates on a revolutionary invention, the tiered publishing system, initially addressing specific communities of scholars, and gradually climbing up to broader public understanding, thus serving the interests of the lay society, too.

Dedication to quality

Each Frontiers article is a landmark of the highest quality, thanks to genuinely collaborative interactions between authors and review editors, who include some of the world's best academicians. Research must be certified by peers before entering a stream of knowledge that may eventually reach the public - and shape society; therefore, Frontiers only applies the most rigorous and unbiased reviews. Frontiers revolutionizes research publishing by freely delivering the most outstanding research, evaluated with no bias from both the academic and social point of view. By applying the most advanced information technologies, Frontiers is catapulting scholarly publishing into a new generation.

What are Frontiers Research Topics?

Frontiers Research Topics are very popular trademarks of the *Frontiers journals series*: they are collections of at least ten articles, all centered on a particular subject. With their unique mix of varied contributions from Original Research to Review Articles, Frontiers Research Topics unify the most influential researchers, the latest key findings and historical advances in a hot research area.

Find out more on how to host your own Frontiers Research Topic or contribute to one as an author by contacting the Frontiers editorial office: frontiersin.org/about/contact

Updates on the complement system in kidney diseases

Topic editors

Mihály Józsi — Eötvös Loránd University, Hungary

Roberta Bulla — University of Trieste, Italy

Citation

Józsi, M., Bulla, R., eds. (2023). *Updates on the complement system in kidney diseases*. Lausanne: Frontiers Media SA. doi: 10.3389/978-2-8325-2227-1

Table of contents

frontiers | Frontiers in Immunology

TYPE Editorial
PUBLISHED 06 April 2023
DOI 10.3389/fimmu.2023.1196487

OPEN ACCESS

EDITED AND REVIEWED BY
Francesca Granucci,
University of Milano-Bicocca, Italy

*CORRESPONDENCE
Mihály Józsi
mihaly.jozsi@ttk.elte.hu

SPECIALTY SECTION
This article was submitted to Molecular Innate Immunity, a section of the journal Frontiers in Immunology

RECEIVED 29 March 2023
ACCEPTED 30 March 2023
PUBLISHED 06 April 2023

CITATION
Bulla R and Józsi M (2023) Editorial: Updates on the complement system in kidney diseases.
Front. Immunol. 14:1196487.
doi: 10.3389/fimmu.2023.1196487

Editorial: Updates on the complement system in kidney diseases

Roberta Bulla[1] and Mihály Józsi[2,3]*

[1]Department of Life Sciences, University of Trieste, Trieste, Italy, [2]Department of Immunology, ELTE Eötvös Loránd University, Budapest, Hungary, [3]MTA-ELTE Complement Research Group, Eötvös Loránd Research Network (ELKH), at the Department of Immunology, ELTE Eötvös Loránd University, Budapest, Hungary

KEYWORDS

COVID-19, atypical hemolytic uremic syndrome (aHUS), complement system, Factor H (FH), factor H-related protein (FHR), kidney injury, extracellular matrix (ECM), C3 glomerulopathy

Editorial on the Research Topic
Updates on the complement system in kidney diseases

The complement system is an ancient arm of the immune system. As such, it is involved in various physiological processes, including protection against pathogenic microbes and tumor cells, disposal of waste material such as dead cells and cell debris, and removal of immune complexes. In addition, several other "non-canonical" complement functions have been recognized, including roles in the activation of various cells, developmental processes, and synaptic pruning. Complement activation is potentially deleterious to the host if proceeds unchecked; thus, disturbance in the fine balance between its activation and inhibition can lead to various pathologies. The kidney is one of the organs involved in several complement-mediated diseases. This Research Topic features 13 papers covering various aspects of the role of the complement system in kidney diseases.

Role of the complement system in atypical hemolytic uremic syndrome

Atypical hemolytic uremic syndrome (aHUS) is a thrombotic microangiopathy (TMA) with complement abnormalities as predisposing factors. Pollack et al. reports a novel homozygous mutation in the central complement component C3, a deletion of four amino acids in the TED domain of the molecule. In the index patient, very low C3 levels were detected, indicating complement consumption due to overactivation. This is supported by molecular modeling, which showed that the deletion affects the interface between C3b and factor H (FH), a critical regulator of complement activation. In addition to C3 mutants, factor B (FB) variants can result in complement overactivation. Aradottir et al. studied three FB missense variants, two identified in aHUS patients and one in a patient with membranoproliferative glomerulonephritis. One of the FB mutants, D371G proved a gain-of-function variant, showed increased binding to C3b, causing enhanced formation of C3 convertase enzymes and thus excessive complement activation in assays using host cells.

Importantly, the authors demonstrated that by applying danicopan, an inhibitor of factor D, the enzyme that cleaves FB when bound to C3b and thus generates the C3bBb convertase, efficiently blocks FB cleavage and complement overactivation also in the case of the gain-of-function FB mutant.

Factor I is the key enzyme cleaving and thus inactivating C3b in the presence of cofactors. Saleem et al. report a patient with membranous nephropathy who underwent kidney transplantation and developed aHUS after the transplantation. Genetic analysis of the patient revealed the I357M mutation in factor I in heterozygosis. While factor I antigenic levels were normal in the patient, this variant showed reduced expression in 293T cells and, more importantly, reduced activity in the presence of the soluble regulator FH as cofactor, while its activity in the presence of complement receptor type 1 and membrane-cofactor protein (i.e., membrane-bound cofactors) was not affected. These data identify the I357M factor I variant as a risk factor for developing post-transplant aHUS.

FH is the main inhibitor of the alternative pathway (AP) of complement in body fluids and recognizes and binds to host cells *via* sialic acid and glycosaminoglycans and inhibits the AP on these surfaces as well. Five FH-related proteins arose through gene duplications from the FH-coding *CFH* gene, namely FHR-1 to FHR-5, encoded by five *CFHR* genes. In the FHRs the domains responsible for the complement regulatory activity of FH are not conserved and they may compete with FH for binding to certain ligands and surfaces. Due to their highly homologous sequences, the genomic region containing the *CFH* and the *CFHR* genes in proximity is prone to rearrangements, deletions and duplications of exons or whole genes. Such rearrangements and single-nucleotide polymorphisms affect the risk of several diseases, including that of aHUS and C3 glomerulopathy (C3G). Piras et al. describe a detailed analysis of this gene cluster in a large cohort of patients and identified various hybrid genes, including previously unreported ones, whole gene duplications or internal duplications in *CFH*. They found that such alterations are relatively frequent in primary aHUS while occur rarely in secondary aHUS forms. This work highlight the association of genomic rearrangements in the *CFH-CFHR* gene cluster with aHUS, and the complexity of these genetic factors that are often difficult to identify.

Role of the complement system in other renal diseases

Yoshida and Nishi in their mini review discussed the involvement of the complement system in TMA, a pathological condition caused by the formation of microvascular thrombi that leads to thrombocytopenia, microangiopathic hemolytic anemia, and organ damage. Kidney glomerular capillary thrombosis is mediated by complement dysregulation or complement overactivation. To understand how these vascular components interact will be fundamental for the creation of therapeutic strategies.

Complement activation contributes to the pathogenesis of acute kidney injury (AKI) in transplant patients. AKI is characterized by a rapid loss of renal function and is still associated to a high morbidity and mortality. The most common causes of AKI include renal ischemia-reperfusion injury, sepsis, and exogenous nephrotoxins such as drugs. AKI predisposes to the future development of chronic kidney disease (CKD) and subsequently to end-stage chronic renal disease. Currently, a specific treatment to arrest or attenuate progression in CKD is lacking. Franzin et al. reviewed recent findings on the role of complement in AKI-to-CKD transition. They also address how and when complement inhibitors might be used to prevent AKI and CKD progression improving graft function.

Renal damage and infections

The kidney is the second most common organ affected by COVID-19.

Pfister et al. analysed kidney biopsies with acute kidney failure for complement factors C1q, MASP-2, C3c, C3d, C4d and C5b-9. The classical pathway and C3 cleavage products were strongly detected. The membrane attack complex C5b-9 was also found deposited in peritubular capillaries, renal arterioles, and tubular basement membrane. They concluded that specific complement inhibition might be a promising therapeutic strategy in COVID-19 patients.

Bouwmeester et al. described the association between both Pfizer/BioNTech's (BNT162b2) mRNA-based and AstraZeneca's (ChAdOx1 nCoV-19) adenoviral-based COVID-19 vaccines and aHUS in the Dutch population. They identified COVID-19 vaccination as a potential trigger for aHUS onset or relapse in pediatric and adult patients who were not treated with C5 inhibition. Therefore, aHUS should be included in the differential diagnosis of patients with vaccine-induced thrombocytopenia, especially if co-occurring with mechanical hemolytic anemia and severe acute kidney injury, but in the absence of major neurological complications.

van Beek et al. demonstrated that renal failure was associated with the decrease of FH in the plasma as a consequence of the severity of meningococcal disease. In their study the serum levels of FH and all FHRs had been measured from a cohort of pediatric meningococcal disease patients during the acute stage of disease in relation to *Neisseria meningitidis* serogroup, diagnosis and severity parameters, and compared these with levels during convalescence in surviving patients. The authors concluded that plasma concentrations of all FH family proteins were greatly decreased during the acute phase of meningococcal disease. However, predominantly low FH plasma concentrations were associated with the severity of meningococcal disease and renal failure.

Role of extracellular matrix and heparan sulfate proteoglycans in the regulation of complement activation

Components of the extracellular matrix (ECM), when exposed to body fluids may promote local complement activation and inflammation. Binding of soluble complement inhibitors to the

ECM, such as factor H (FH), is important to prevent excessive complement activation locally. Pathologic complement activation at the glomerular basement membrane is implicated in renal diseases.

Papp et al. demonstrated that the FH-Related Proteins FHR-1 and FHR-5 can interact with the ECM and reduce FH regulatory activity and enhance complement activation. They showed that FHR-1 and FHR-5 bind to ECM elements like does FH, and that both FHRs competitively limit binding of FH, thus reducing complement regulation. By this activity, FHRs may influence the pathogenic and inflammatory conditions in kidney, eye, and joint diseases.

Another study by Loeven et al. demonstrated that the relative balance of FH and FHR-1/FHR-5 in the glomerular glycocalyx is affected by HS-mediated ligand selectivity, which alters complement AP regulation in this milieu. These findings offer novel insights into the pathogenesis of C3G and imply that genetic testing on C3G cohorts can identify patients who have mutations in HS proteoglycan production genes that result in a "permissive" milieu that promotes FHR over FH binding. In turn, this imbalance fosters complement dysregulation either directly or indirectly through additional triggering events. These results also point to a potential C3G therapy in which FHR-1 and FHR-5 are scavenged by short 2-O-desulfated heparin oligosaccharides, changing their affinity for the glomerular glycocalyx.

New experimental models for the diagnosis and treatment of kidney diseases

Overactivation of the AP of complement in the fluid phase and on the surface of the glomerular endothelial glycomatrix is the underlying cause of C3G. Pisarenka et al. developed an *in vitro* model of AP activation and regulation on a glycomatrix surface using an extracellular matrix substitute (MaxGel) for the reconstitution of AP C3 convertase. This ECM-based model of C3G offers a replicable method by which to evaluate the variable activity of the complement system in the context of disease.

Gaykema et al. demonstrated that CD55 over-expressing human induced pluripotent stem cells (iPSCs) and their derived kidney organoids are less susceptible to complement activation *in vitro*, providing evidence for the use of CD55 genetic manipulation to improve transplant outcomes of allogenic iPSC-derived tissues.

Conclusions

In summary, this Research Topic highlights novel aspects of the involvement of the complement system in kidney disease, including functional characterization of disease-associated mutations, mechanisms of activation and regulation, and association with infections. In addition, new experimental models are presented to aid improved diagnostics and research, and the potential of complement inhibition to prevent or mitigate kidney damage is discussed.

Author contributions

Both authors have made a substantial, direct, and intellectual contribution to the work and approved it for publication.

Funding

MJ is supported by the Kidneeds Foundation (Iowa, US), the European Union's Horizon 2020 research and innovation programme under grant agreement No. 899163 (SciFiMed), the National Research, Development and Innovation Fund of Hungary (grant no. 2020-1.1.6-JÖVŐ-2021-00010, and grant no. RRF-2.3.1-21-2022-00015 in frame of the National Pharmacological Research and Development Laboratory "PharmaLab"), and the Eötvös Loránd Research Network and the Hungarian Academy of Sciences (grant no. 0106307).

Conflict of interest

The authors declare that the research was conducted in the absence of any commercial or financial relationships that could be construed as a potential conflict of interest.

Publisher's note

frontiers in Immunology

REVIEW
published: 07 May 2020
doi: 10.3389/fimmu.2020.00734

Inflammaging and Complement System: A Link Between Acute Kidney Injury and Chronic Graft Damage

Rossana Franzin[1,2], Alessandra Stasi[1], Marco Fiorentino[1], Giovanni Stallone[3], Vincenzo Cantaluppi[2], Loreto Gesualdo[1] and Giuseppe Castellano[1,3]**

[1] Nephrology, Dialysis and Transplantation Unit, Department of Emergency and Organ Transplantation, University of Bari Aldo Moro, Bari, Italy, [2] Department Translational Medicine, University of Piemonte Orientale, Novara, Italy, [3] Nephrology, Dialysis and Transplantation Unit, Department of Medical and Surgical Sciences, University of Foggia, Foggia, Italy

The aberrant activation of complement system in several kidney diseases suggests that this pillar of innate immunity has a critical role in the pathophysiology of renal damage of different etiologies. A growing body of experimental evidence indicates that complement activation contributes to the pathogenesis of acute kidney injury (AKI) such as delayed graft function (DGF) in transplant patients. AKI is characterized by the rapid loss of the kidney's excretory function and is a complex syndrome currently lacking a specific medical treatment to arrest or attenuate progression in chronic kidney disease (CKD). Recent evidence suggests that independently from the initial trigger (i.e., sepsis or ischemia/reperfusions injury), an episode of AKI is strongly associated with an increased risk of subsequent CKD. The AKI-to-CKD transition may involve a wide range of mechanisms including scar-forming myofibroblasts generated from different sources, microvascular rarefaction, mitochondrial dysfunction, or cell cycle arrest by the involvement of epigenetic, gene, and protein alterations leading to common final signaling pathways [i.e., transforming growth factor beta (TGF-β), $p16^{ink4a}$, Wnt/β-catenin pathway] involved in renal aging. Research in recent years has revealed that several stressors or complications such as rejection after renal transplantation can lead to accelerated renal aging with detrimental effects with the establishment of chronic proinflammatory cellular phenotypes within the kidney. Despite a greater understanding of these mechanisms, the role of complement system in the context of the AKI-to-CKD transition and renal inflammaging is still poorly explored. The purpose of this review is to summarize recent findings describing the role of complement in AKI-to-CKD transition. We will also address how and when complement inhibitors might be used to prevent AKI and CKD progression, therefore improving graft function.

Keywords: renal aging, complement system, AKI-to-CKD transition, cellular senescence and SASP, complement inhibition therapy

OPEN ACCESS

Edited by:
Cees Van Kooten, Leiden University, Netherlands

Reviewed by:
Lourdes Isaac, University of São Paulo, Brazil
Behdad Afzali, National Institute of Diabetes and Digestive and Kidney Diseases, United States

****Correspondence:***
Rossana Franzin
rossanafranzin@hotmail.it
Giuseppe Castellano
giuseppe.castellano@unifg.it; castellanogiuseppe74@gmail.com

Specialty section:
This article was submitted to Molecular Innate Immunity, a section of the journal Frontiers in Immunology

Received: *02 November 2019*
Accepted: *31 March 2020*
Published: *07 May 2020*

Citation:
Franzin R, Stasi A, Fiorentino M, Stallone G, Cantaluppi V, Gesualdo L and Castellano G (2020) Inflammaging and Complement System: A Link Between Acute Kidney Injury and Chronic Graft Damage. Front. Immunol. 11:734. doi: 10.3389/fimmu.2020.00734

Abbreviations: ABMR, antibody-mediated rejection; AKI, acute kidney injury; AP, alternative pathway; C1-INH, C1 esterase inhibitor; CKD, chronic kidney injury; CP, classical pathway; DAMPs, damage-associated molecular patterns; DGF, delay graft function; EndMT, endothelial-to-mesenchymal transition; I/R, ischemia/reperfusion; IRI, ischemia/reperfusion injury; LP, lectin pathway; MAC, membrane attack complex; MASP, MBL-associated serine protease; MBL, mannose-binding lectin; PAI-1/*SERPINE1*, plasminogen activator inhibitor-1; PAMPs, pathogen-associated molecular patterns; PBMC, peripheral blood mononuclear cells; PMT, pericyte-to-myofibroblast transition; PRM, pattern recognition molecules; SASP, senescence-associated secretory phenotype.

OVERVIEW OF THE COMPLEMENT SYSTEM

Complement is an essential part of the innate immune system. Over a century ago, complement was first identified by Paul Ehrilch as a heat-labile component in serum that literally "complemented" the antibody- and cell-mediated immune responses against pathogens (1). Today, we do know that complement system consists of more than 40 blood-circulating, membrane-associated, and intracellular proteins. Complement can be activated in the serum, in local tissue, and at intracellular level (2) and exerts three major physiological functions. First, complement proteins are involved in host defense against infection (3). This activity is mediated by several events: (i) the pathogens opsonization (i.e., covalent C3b, C3d, C4b complement fragments deposition on microbial surfaces that boost phagocytosis), (ii) the leukocytes chemotaxis and activation that amplify the inflammatory process (i.e., the binding of complement anaphylatoxin to receptors on leukocytes), and (iii) the direct lysis of bacteria or infected cells. Second, complement can be considered as a connection between innate and adaptive immune response (4). Indeed, the C1q, the principal component of the classical pathway, can activate complement cascade after the binding to antibody–antigen complexes, which originated during the adaptive immune response. In addition, complement can also enhance the antibody response and consolidate the immunological memory since C3 receptors are expressed on B cells, antigen-presenting cells (APC), and follicular dendritic cells (5). Third, after the resolution of inflammatory injury, complement mediates the clearance of apoptotic/necrotic, ischemic, or damaged self-cells (i.e., by the binding of C1q or C3 fragments to host self-surfaces) (6).

In the serum and interstitial fluids, complement proteins circulate largely in an inactive form: however, in response to pathogen-associated molecular patterns (PAMPs) and/or damage-associated molecular patterns (DAMPs), they become activated through a sequential cascade of reactions (6) (7). The recognition of these highly conserved molecular patterns is achieved via different types of pattern recognition molecules (PRMs) (8) (**Figure 1**). The activation of complement system occurs via three different pathways: the classical pathway (CP), the alternative pathway (AP), and the lectin pathway (LP) (4). Independently from the signaling initiated, all the pathways lead to the formation of a central enzyme, the C3 convertase, that cleaves C3 into C3a and C3b. In the CP, immune complexes of immunoglobulin M (IgM) or hexameric IgG are recognized by C1q together with the associated proteases C1r and C1s (9). The LP contains six PRM: mannose-binding lectin (MBL), Ficolin-1, Ficolin-2, Ficolin-3, Collectin-10, and Collectin-11, which recognize carbohydrate and acetylated structures on pathogens and form a complex with MBL-associated serine proteases (MASPs) (10, 11). The AP is continuously activated at low level by the spontaneous hydrolysis of C3 called the "tick-over." This mechanism generates C3b that can then covalently bind to various proteins, lipids, and carbohydrate structures on microbial surfaces (4). As examples of DAMP-mediated complement activation, we could mention the CP induction by C-reactive protein (CRP) or Pentraxin-3 (12) (8); in IgA nephropathy, LP can be triggered by IgA (13), and after ischemia/reperfusion injury (IRI), L-fucose induced LP on stressed cells (7). With regard to AP, the cleavage of C3 can be induced by neutrophil enzyme elastase or myeloperoxidase (MPO) (14). Progressive C3 activation results in the formation of the C5 convertase, which cleaves C5 into C5b and C5a. C5 is the initiator of the terminal step, and C5b merged together with the components C6 till C9 assembling the membrane attack complex (MAC) pores (**Figure 1**). In the last steps of complement activation, the MAC leads to the direct lysis of the pathogen or target cells. Interestingly, MAC can also trigger a range of non-lethal effects on cells as NLRP3 inflammasome activation in the cytosol (15). Complement activation also leads to the generation of other effector molecules such as opsonins (C4b, C4d, C3b, iC3b, C3dg, and C3d) and anaphylatoxins (C3a, C5a), which can interact with their respective receptors and recruits granulocytes, monocytes, and other inflammatory cells on site of infection (16). Anaphylatoxins can bind specific receptors expressed not only on PBMCs but also on parenchymal cells such as tubular epithelial cells within the kidney, initiating inflammation and chemotaxis (C3aR, C5aR1 and C5aR2) (17) (**Figure 1**).

However, complement functions have been implicated in the pathogenesis of disorders not necessarily related to infections such as cancer (18), neurodegenerative and age-related disorders [i.e., age-related macular degeneration (AMD)], metabolic diseases (2), the progression of chronic kidney disease (CKD) (19, 20), and more importantly renal aging (21, 22). Therefore, increasing efforts are necessary to evaluate the efficacy of targeting complement to arrest the progression of renal aging during CKD (20, 23).

LOCAL PRODUCTION OF COMPLEMENT FACTORS AT RENAL LEVEL

Complement factors are produced predominantly by the liver; however, some factors as C1q (24), properdin, and C7 (25) are released by leukocytes (26); in addition, adipocytes can synthesize factors B and D (also known as adipsin) (27). In the kidney, tubular epithelial cells can produce virtually all complement proteins (28). The percentage of tubular complement biosynthesis can increase significantly during inflammation (29–31). Following IRI, complement C3 can be expressed by proximal tubular epithelial cells (32), endothelial cells (33), glomerular epithelial and mesangial cells (34). The C3 messenger RNA (mRNA) upregulation and the subsequent biosynthesis has been demonstrated to play a central role in kidney transplantation (35, 36). Pratt et al. demonstrated that wild-type (WT) mice with intact serum complement activity do not reject allogenic C3-deficient kidneys, underlying that kidney-derived complement is a key mediator of renal injury (37, 38). Thus, complement can switch the immune system balance toward a persistent and proinflammatory response that,

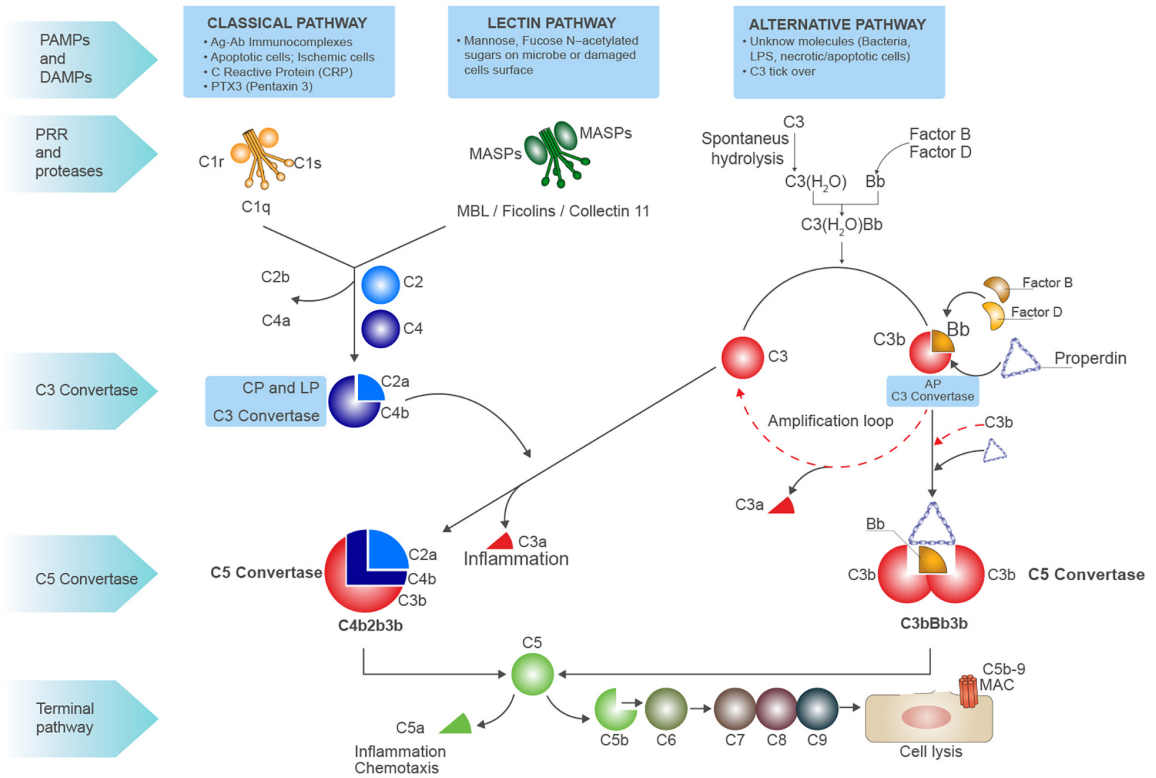

FIGURE 1 | Schematic overview of complement system. Complement system can be initiated by three different pathways: the classic pathway, the lectin pathway, and the alternative pathway, all converging to the formation of C3 convertases. The classic pathway is initiated by the binding of C1q globular domains to the Fc of immunoglobins bound to their antigen (immunocomplexes), apoptotic or ischemic cells, acute phase proteins [i.e., C-reactive protein (CRP) and Pentraxins]. When the binding of C1q to substrate occurs, a conformational change of C1q leads to activation of proteases C1r and C1s that are associated to C1q. It activates C1s, then cleaves C4 into C4b, subsequently C2 is cleaved which binds to C4b forming the CP (membrane-attached) C3 convertase, the C4b2a complex. This classical C3 convertase activates and cleaves C3 molecules to C3b and C3a. The pattern recognition receptor (PRR) of lectin pathway involves several molecules as MBL, Ficolins, and Collectin-11 that, after binding to mannose, fucose, or *N*-acetylated residues on microbial surfaces or damaged cells, can activate the serine proteases MASP1 and MASP2 leading to C3 convertase formation as for CP. At low level, the activation of alternative pathway (AP) can be induced by spontaneous hydrolysis of C3 into C3(H_2O), an event called C3 tick-over. The hydrolysis changes the structure of C3 by the translocation of the thiol ester domain that allows the new formed structure to form covalent bonds with -OH or -NH2 residues on the target surfaces. The C3(H_2O) can bind factor B (FB), resulting in the cleavage of FB by factor D (FD) and generating Ba and Bb and the formation of the AP C3 convertase C3(H_2O)Bb. The C3(H_2O)Bb complex is the initial C3 convertase of the AP (fluid phase C3 convertase) and can cleave C3 to C3a and C3b. The C3b fragment can bind to FB, and after the cleavage of FB by FD, the C3 convertase C3bBb (high level) is formed. This C3 convertase cleaves more C3 to C3b to generate even more C3 convertase in an amplification loop. The protein properdin stabilizes C3bBb. After formation of the classical C3 convertase C4b2a or the alternative C3 convertase C3bBb, the final pathway (common to all three pathways) may be initiated. An additional C3b molecule is incorporated in both the C3 convertases leading to the formation of the C5 convertase. Properdin stabilization occurs in AP C5 convertase formation (C3bBb3b). The C5 convertase cleavages C5 into C5a (the anaphylatoxin) and C5b, C5b then binds to C6, and this allow the binding of C7, C8, and C9 and results in the formation of the C5b-9 terminal membrane attack complex (MAC). The latter forms pores in the membrane of pathogens and damaged self-cells, thus promoting cell lysis. C3a and C5a are powerful anaphylatoxins able to induce chemotaxis and inflammation.

if directed against self-antigens, might promote the induction of autoimmunity or, if directed against donor antigens, might lead to rejection (23).

INTRACELLULAR COMPLEMENT ACTIVATION AND EVs CARRIED COMPLEMENT

Recent studies have revealed that complement activation is not confined in the serum or produced locally by resident and infiltrating cells into interstitial fluids. Complement cascade can also be initiated intracellularly. The intracellular complement activation, the Complosome, has been investigated mainly in human CD4 + T cells (2); however, it has also been described in adipocytes, monocytes, fibroblasts, B cell, and epithelial and endothelial cells. In resting T cells, the function of C3 and C5 intracellular activation has been associated to the homeostatic cell survival by keeping low level of mTOR signaling (2). Nevertheless, after T-cell receptor (TCR) activation, intracellularly cleaved C3 can induce the Th1 differentiation, the NLRP3 inflammasome activation, and the T cell metabolism reprogramming by regulation of glycolysis and mitochondrial oxidative phosphorylation (39). Interestingly, aging is also a process strongly integrated with chronic inflammation and metabolism; therefore, the recently discovered connection

between the Complosome and cellular metabolome might add a new layer of complexity in the impact of complement intracellular activation in several aging-related diseases (as obesity) and in the acceleration of renal aging during CKD.

Lastly, complement components can be also identified in circulating extracellular vesicles (EVs), particularly in microvesicles (MVs) with a size ranging from 0.1 to 1 μM. EVs can carry and modulate complement system in several age-related disease, such as AMD (40), providing a new, extracellular way to deliver complement in different body compartments.

COMPLEMENT IN KIDNEY DISEASE

The complement system is considered a crucial pathogenic mediator in the development of several renal diseases. The kidney is particularly susceptible to complement-mediated injury, mainly due to the ultrafiltration function, the low expression of complement regulators, and the local complement production (23). Complement aberrant activation, acquired or inherited dysregulation, and ineffective clearance have been observed in a wide spectrum of glomerulonephritis [lupus nephritis (41), C3 glomerulopathy, IgAN, antineutrophil cytoplasmic antibody (ANCA)-associated vasculitis], in thrombotic microangiopathy [atypical hemolytic uremic syndrome (aHUS)], in renal transplantation, and in the progression to CKD (20, 38). A predominant role for glomerular immunocomplex deposition has been observed in lupus nephritis with the involvement of CP, LP, and also AP. Moreover, the impairment of AP predominantly characterizes the aHUS and the C3 glomerulopathy. These findings have led to the clinical use of complement blocking therapeutics as Eculizumab in aHUS (42).

In the progression to CKD, the role of all the three pathways has been assessed, and promising results are coming from clinical trials. However, we are still far from the clinical use of complement inhibitors to delay the progression of renal fibrosis.

AKI-TO-CKD TRANSITION: THE ROLE OF COMPLEMENT

Acute kidney injury (AKI) characterized by a rapid loss of renal function and is still associated to a high morbidity and mortality (43). The most common causes of AKI include renal IRI, sepsis, or several exogenous nephrotoxins such as drugs. Currently, it is well known that AKI predisposes to the future development of CKD and subsequently to end-stage chronic renal disease (ESRD) (43). However, the cellular and molecular mechanisms underlying the progression from AKI to CKD remains incompletely understood.

Complement system was traditionally related to the early development of AKI (44); nonetheless, several evidence indicated that complement is a pivotal mediator of tubular senescence (21, 22) and interstitial fibrosis, the common hallmark of premature aging that characterizes the CKD (45). The major complement components involved in the AKI-to-CKD transition seems to be the anaphylatoxins C3a and C5a and the terminal C5b-9 that contribute to the damage during CKD progression through various mechanisms. After binding to C5aR and C3aR, these anaphylatoxins exert a proinflammatory and fibrogenic activity on tubular and endothelial cells (46, 47), pericytes (31, 48), and resident fibroblasts; moreover, they can mediate renal fibrosis by stimulating transforming growth factor beta 1 (TGF-β1) production in cultured murine tubular cells. As a consequence, activated endothelium, monocytes, and injured tubular epithelium (49) have all been shown to secrete profibrogenic factors such as TGF-β and platelet-derived growth factor (PDGF), able to activate resident fibroblasts promoting collagen deposition. In addition, we recently demonstrated that the complement anaphylatoxin C5a contribute to fibrosis inducing the pericytes to myofibroblast transdifferentiation (PMT) through pERK activation (48).

Other mechanisms of complement-mediated transition to CKD are the chemotactic effect on different infiltrating leukocytes (50) with the inhibition of the polarization of T-helper cells to Th1 cells (51) (52). The subsequent shift of T-helper cells to Th2 cells, together with their cytokines release, such as TGF-β, has been shown to act in a profibrotic manner (53). The predominant profibrotic effect of TGF-β signaling in AKI-to-CKD transition, in tubular cell cycle arrest, and myofibroblast transdifferentiation has been reviewed elsewhere (54).

Finally, the terminal C5b-9 complex is a powerful inducer of profibrotic and proinflammatory cytokines by a variety of renal cells. Incubation of human glomerular epithelial cells with sublytic doses of C5b-9 significantly increased the collagen synthesis (55) and the release of TGF-β1 and interleukin IL-6 (56). In addition, endothelial cells exposed to sublytic concentration of C5b-9 released profibrotic factors including fibroblast growth factor (FGF) and PDGF (57). Similar effects were observed in tubular epithelial cells; stimulating proximal tubular epithelial cells with C5b-9 led to increased expression of collagen type IV (58). Collectively, these *in vitro* evidence supported that C5b-9 can increase the profibrotic process associated with progressive renal injury. Uncontrolled complement activation may ultimately result in maladaptive tissue repair with irreversible development of fibrosis and renal aging.

THE ROLE OF COMPLEMENT IN IRI

Recent improvements in immunosuppressive therapy have made kidney transplantation the treatment of choice for ESRD patients (59). Complement system might have a detrimental role in different phases of renal transplantation from brain (DBD)/cardiac death (DCD) in deceased donors, to organ procurement, to IRI, allograft rejection, until the chronic graft deterioration (60). Increased systemic levels of sC5b-9 were observed in DBD and DCD but not in living donors, which correlate with increased acute rejection in the recipients (61). Furthermore, a strong association between chronic graft injury and overexpression of complement components has been found by proteomic analysis in kidney donor biopsies (62). These results indicated that shorter periods of ischemia are clearly

associated with less complement activation; in addition, the protein profiles of preservation solutions in which kidney from deceased donors had been stored revealed intense activity of complement effectors (as C3, factor B) during organ storage preceding transplantation (63).

Following organ procurement, the role of complement in renal IRI has been extensively investigated by several studies (64, 65). Importantly, renal IRI is the pivotal contributor in the development of delay graft function (DGF), traditionally defined as the requirement for dialysis during the first week after transplantation. IRI is initiated by the occlusion of blood flow that is necessary for organ collection and during hypothermic ischemia for the storage; in this conditions, renal cells are permanently damaged due to hypoxia, ATP depletion, and accumulation of metabolic waste, resulting in the production of reactive oxygen species (ROS) and DAMPs (i.e., histones, heat-shock proteins). Reperfusion leads to a more detrimental inflammatory response, resulting in further tissue damage characterized by early release of inflammatory cytokines such as IL-6, tumor necrosis factor alpha (TNFα), and IL-1α that represent a powerful inflammatory milieu capable to induce a cellular senescence-associated secretory phenotype (SASP).

A large body of evidence from both experimental (66–68) and clinical (20) studies has identified in complement activation a crucial mediator of chronic tubulointerstitial fibrosis following renal IRI (69). In the past years, using complement-deficient animals, the terminal C5b-9 was identified as principal inducer of tubular injury after IRI (70). In particular, Zhou et al. demonstrated that $C3^{-}$-, $C5^{-}$-, and $C6^{-}$-deficient mice were protected against ischemic damage, whereas $C4^{-}$-deficient mice were not (59). These initial findings underlined the importance of tubular (and not endothelial) injury in the I/R physiopathology. Next, we suggested a more significant role for the MAC and the AP pathway. The involvement of AP was also elegantly confirmed by Thruman et al. in transgenic mouse models (68, 71). More recent reports have focused on pattern recognition receptors of lectin pathway (LP-PRRs) (MBL, Collectin-11, Ficolin-3), CP-C1q, and C5aR1/C5aR2, indicating that all these complement components were able to trigger the IRI and fuel the progression to CKD (**Figure 2**). Hence, renal function in MBL-deficient mice was significantly preserved after IRI (67).

Furthermore, Collectin-11, a PRR that binds a ligand (L-fucose) (72) expressed on stressed tubular cells, was demonstrated capable to activate complement LP in C4-independent manner. This mechanism, called C2/C4 bypass, has been proposed by Yaseen et al. (73) and depends on the unique capacity of MASP2 to directly activate C3, leading to C3b and C3a fragment formation without the involvement of C4 or C2. These findings finally explained previous and contradictory results that showed protection from IRI in MASP2-deficient (74) but not in C4-deficient mice (70, 75, 76). More importantly, compared with wild-type, Collectin-11-deficient mice showed significantly reduced renal functional impairment and leukocyte infiltration, less chronic inflammation, and tubulointerstitial fibrosis after renal IRI (77). The analysis of other LP factors in patients showed that high pretransplant level of Ficolin-3 was strongly associated with poor allograft survival and age after kidney transplantation (78). In accordance, Ficolin-2 gene rs7851696 polymorphism influenced kidney allograft functions, with specific allele increasing the risk of DGF and rejection (79). These results revealed a central role of LP in the development of renal fibrosis after IRI, with strong clinical implication in the transition from AKI to CKD (77).

Even if the contribution of CP has been controversial (80), the CP and LP are effectively involved in development of early fibrosis. In a pig model of renal IRI injury, we demonstrated the deposition of C1q and MBL on peritubular capillaries colocalization with C4d after 15 min from reperfusion. The treatment with recombinant human C1-INH (C1 esterase inhibitor) (81), an inhibitor of CP and LP pathways, conferred protection not only reducing infiltrating cells but also modulating the generation of myofibroblasts by reducing endothelial-to-mesenchymal (EndMT) (82) and the pericytes-to-myofibroblast (PMT) transitions (48). Consistent with these results, Delpech et al. demonstrated that treatment by C1-INH appeared to be protective also after 3 months from IRI, reducing the development of chronic graft fibrosis (83). These data have been translated to humans, and the use of C1-INH in patients receiving deceased donor kidney transplants with high risk for DGF has been investigated in a recent clinical trial (84) and will be further discussed in the paragraphs below.

Next to C1 blockage, the C5aR1 and C5aR2 inhibition could offer promising results. C5aR receptors are expressed both on peripheral and infiltrating leukocytes (such as dendritic and T cells) and on renal parenchymal cells such as tubular epithelial cells, mediating the recruitment of leukocytes. Additionally, these receptors mediated allograft injury before (85) and after kidney transplantation (86) (**Figure 2**). Consistently, pathogenic roles for C5aR1 in renal tubulo-interstitial fibrosis have been reported in different models of renal IRI (66, 87–91), murine model of unilateral ureteral obstruction (UUO) (92), and chronic pyelonephritis (93). Remarkably, in clinical settings, donor urinary C5a concentrations before transplantation has been shown to be higher in the recipients with risk of DGF (92, 94).

Considering the C5aR1 profibrotic and complement-independent detrimental effect, the use of C5aR inhibitors should be taken into consideration. Recently, successful evidence are coming from trials using the Avacopan (CCX168), an orally administered, selective C5a receptor inhibitor in aHUS (NCT02464891), ANCA-associated vasculitis (NCT01363388, NCT02222155) (95), C3 glomerulonephitis (NCT03301467), and IgA nephropathy (13) (NCT02384317). The potential beneficial role of C5aR1 inhibition in the context of renal IRI should be encouraged.

FROM ANTIBODY-MEDIATED REJECTION TO CKD: THE ROLE OF COMPLEMENT

After kidney transplantation, antibody-mediated rejection (ABMR) is one of the leading cause of long-term graft failure and CKD in which complement system plays a

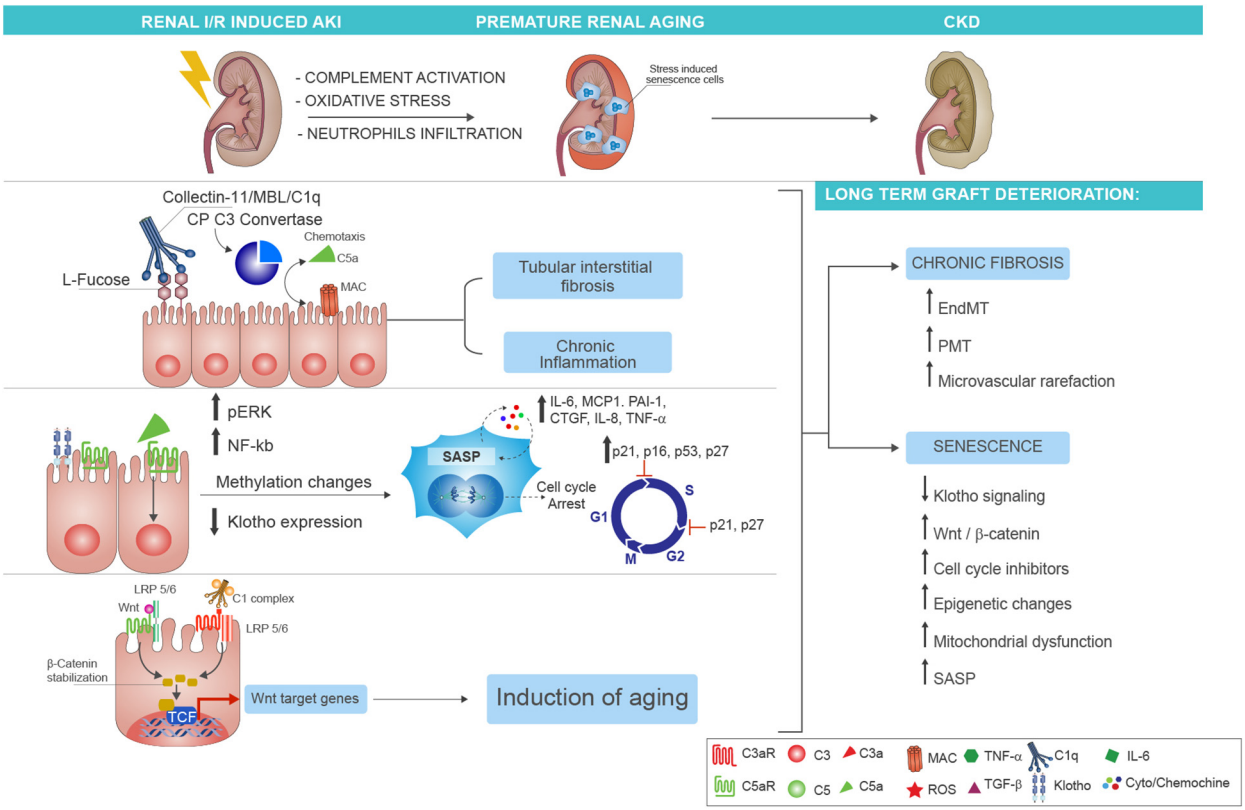

FIGURE 2 | Complement-driven accelerated renal senescence after IRI-AKI leading to CKD progression. During renal ischemia/reperfusion injury (IRI), activation of complement may lead to reactive oxygen species (ROS) generation and neutrophils infiltration, thereby establishing a prosenescence microenvironment that promotes accelerated renal aging. Several molecular mechanisms can be responsible for the establishment of tubular senescence after complement activation. First, renal tubular epithelial cells expressed fucosylated glucose patterns upon IRI, which can be recognized by the lectin pathway pattern recognition receptor (PRR) (as Collectin-11), therefore inducing complement activation and tubular interstitial fibrosis with persistent chronic inflammation (upper part). Second, the release of C5a anaphylatoxin, through methylation changes, can induce cellular senescence characterized by growth arrest, inhibition of apoptosis, and acquirement of a senescence-associated secretory phenotype (SASP). The molecular mediators of the growth arrest are mainly G1-S cell cycle inhibitors as p16INK4a, p21 WAF/CIP1, p53, and p27. The p21 and p27 proteins can mediate the cell cycle arrest also during the transition from phase S to phase G2 of cellular cycle. The SASP is maintained and amplified by the increased expression of proinflammatory [such as interleukin (IL)-6, monocyte chemoattractant protein-1 (MCP-1), IL-8, PAI-1, tumor necrosis factor alpha (TNFα)] and profibrotic cytokines [as connective tissue growth factor (CTGF)] (in the middle). Finally, another molecular mechanism of complement-induced renal inflammaging is mediated by Wnt/β-catenin signaling. The C1 complex (that is composed by the association of C1q with C1s and C1r serine proteases), after binding the serpentine Frizzled receptor (indicated in red), can cleave the N-terminal domain of LRP5/6 and stabilize the β-catenin protein (in the left). The function to bind Frizzled receptors and to cleave the LPR5/6 extracellular domain is normally exerted by the Wnt protein (indicated in green). The β-catenin stabilization allows the nuclear translocation, the interaction with transcription factors, and the augmented gene expression of proaging Wnt target genes. The final and common event of all these complement-mediated pathways is represented by the generation of stress-induced senescence cells, indicated in the figure as enlarged cells, indicated as blue cells to highlight the positivity to SA-βGal enzymatic assay. The persistence of these cells and the higher increase in SASP chemokines result in chronic fibrosis by the induction of endothelial-to-mesenchymal transition (EndMT) and pericyte-to-myofibroblast transition (PMT) that can amplify microvascular rarefaction together with generation of new myofibroblast and proliferation of resident fibroblast. Lastly, several mechanisms are involved in the maintenance of renal inflammaging such as the downregulation of Klotho, the increased Wnt signaling, mitochondrial dysfunction, the epigenetic changes, and the increased and stable expression of cell cycle inhibitors.

key role (96, 97). ABMR is characterized by glomerulitis, peritubular capillaritis, acute thrombotic microangiopathy tubular injury, C4d deposition in the peritubular capillaries, and microvascular inflammation (98, 99). As a consequence of these immunological attack to the graft, there is a significant increased incidence of late graft loss after ABMR (100–103). Even in presence of early acute rejection, several pathogenic mechanisms will progressively contribute to the later development of tubulo-interstitial fibrosis and progression to CKD (104, 105).

In the recipients, the presence of donor-specific antibodies (DSAs), i.e., natural IgM and IgG directed against donor endothelial human leukocyte antigen (HLA) or ABO antigens is referred as sensitization and represents the principal risk factor for ABMR. The immune complexes generated will activate CP by C1q-r-s complexes, therefore leading to covalent C4d deposition on peritubular capillaries. Consistently, for several years, the C4d deposition has been considered the gold standard for ABMR diagnosis; however, today, it is recognized that up to 55% of patients can develop ABMR without detectable capillary C4d

deposits. Indeed, a C4d-negative ABMR phenotype has been included in Banff 2013 classification (106–109).

Interestingly, all complement pathways are involved in ABMR (110, 111), leading to recruitment of leukocytes such as natural killer cell, monocyte/macrophage-mediated damage, endothelial injury, and increased intragraft coagulation (112, 113). Besides HLA matching and alloimmune response, other factors can influence the development of ABMR as donor and patient ages, cardiovascular complications, time on dialysis, glomerular disease recurrence, or more commonly hypertension, dyslipidemia, proteinuria, anemia, and diabetes. Interestingly, a significant complement activation has been observed also in these conditions. Bobka et al. demonstrated an increased complement activation in pretransplant biopsies from diabetic, hypertensive, or smoking donors (97). The authors showed a predictive value of complement activation in donor biopsies for later outcome; effective analyses of these deposits in the donor were characterized by C1q, factor D, C3c, and C5b-9 and tubular MASP2 and Collectin-11 in kidney that would have developed ABMR. Interestingly, at the diagnosis of ABMR, the expressions of these complement component were associated with higher serum creatinine and morphological changes.

Although is not clear whether the complement deposition occurred already in the donor or during the following IRI, a role of intragraft complement release has been hypothesized. We do know from the animal model of acute renal transplant rejection that early complement deposition can be associated by local synthesis of complement. By performing renal transplantation of a donor $C3^{-/-}$ kidney in a wild-type recipient mice (donor, $C3^{-/-}$; recipient: wild type), Pratt et al. demonstrated a significant increased long-term survival and less rejection incidence compared to wild-type mice recipients transplanted with allogenic wild-type kidney (Wtype/Wtype). Therefore, locally synthesized C3 is the most important trigger of rejection than circulating C3 and a powerful inducer of chronic damage (92). Other experimental evidence to support the role of complement in rejection were provided by Wang et al. (114). In a mouse model of ABMR induced after heart transplantation, Wang et al. showed that C5 blocking prevented ABMR and allowed long-term renal function. In conclusion, all these data support the use of complement inhibitors as therapeutic strategy to prevent the long-term complications of ABMR.

COMPLEMENT AND RENAL INFLAMMAGING: AN UNEXPLORED FIELD

Complement in Aging Diseases

Complement activation has been investigated in diseases of aging such as Alzheimer's and Parkinson's disease, amyotrophic lateral sclerosis, and multiple sclerosis or AMD (115). For instance, polymorphisms in factor H are known to increase several folds the risk of AMD, the most common cause of irreversible blindness. In addition, C3 gene expression is upregulated with aging in humans (116). Furthermore, C1q levels, which mediate synapse elimination in CNS, are dramatically increased in aged brains (117).

Interestingly, systemic protein C1q level increases with aging and can activate the Wnt/β-catenin signaling that is primarily involved in mammalian skeletal muscle aging (118, 119). The canonical Wnt signaling is activated by two kinds of receptors: the Frizzled family of serpentine proteins and the single-transmembrane protein low-density lipoprotein receptor-related protein 5/6 (LRP5/6) (120, 121) (**Figure 2**). Recently, Naito et al. demonstrated that C1q-r-s complex, after binding to Frizzled receptors, could induce the N-terminal cleavage of the ectodomain of LRP6, thereby activating Wnt pathway (119). In renal tubular epithelial cells, we found that C5a induced aberrant methylation changes in Wnt signaling related genes and in particular in Frizzled 6 (*FZD6*) receptor gene (22). This unexpected role of complement C1q in inducing an impaired regenerative capacity of skeletal muscle in aged animals has been further confirmed by several studies (122) showing that C1q secretion led to muscle fibrosis (122) and induced an increased proliferation of vascular smooth muscle cells via β-catenin signaling. From these observations (123), a role of C1q in the development of arteriosclerosis and arterial stiffening that occurs in advancing aging has been hypothesized. By the analysis of the circulating C1q and other cytokines associated with cardiovascular diseases (as TNF-α and IL-6), there emerged a significant correlation between C1q and aging-induced arterial stiffness. Regarding the role of LP in aging, evidence from Tomaiuolo et al. (124) showed that the specific MBL2 gene haplotypes (in particular, the high-activity-associated haplotypes as HYPA and LYQA) were significantly lower in centenarians than in the general population. The investigators identified also a role of MBL in the clearance of senescent cells. However, the mechanism underlying this peculiar connection between reduced MBL levels and longevity deserves more investigations.

In the healthy subjects, the correlation between complement and aging has its roots in earlier studies (125). In 1978, Yonemasu (126) demonstrated that, in a cohort of healthy volunteers (from birth up to 75 years), C1q and C3 levels independently oscillated with age. C1q increased gradually from birth to 60 years, whereas C3 reached higher level at 1 year, decreased until puberty, and augmented steadily after this age. Accordingly, in another cohort, Nagaki et al. detected an increased levels of CH50 activity, C1q, and C3 and decrease in factor B in older healthy subjects (127).

From these studies emerged a predominant role of C1q-CP in physiological aging. However, more recently, the findings from Gaya da Costa et al. provided strong evidence that also the AP was significantly activated in the elderly (76). In addition, authors also revealed increased terminal pathway components with age: these results are in line with the capability of complement to contribute to the clearance of senescent cells by MAC deposition (128).

The link between complement activation and physiological aging has been clarified in several experimental knockout models. Qiaoqiao Shi et al. (129) demonstrate that C3-deficient mice were protected from the synapse, neuron loss, and cognitive decline typically observed in older mice, suggesting an important role of C3 in the aging brain. Accordingly, in a model of AMD, $CD59a^{-/-}$ mice showed an age-dependent increased expression

of activators of the alternative complement pathway (C3, FB, FB) in the retinal pigment epithelium (RPE) choroid (130).

Furthermore, an age-related increase in complement C1q, C4, C3, and factor B expression was found in wild-type mouse brain (116).

All together, these studies demonstrate that aging is linked to a dysregulation of complement system, in particular of CP and AP, therefore to a progressive impairment of immune response.

Moreover, aging is associated to the establishment of a proinflammatory milieu generated by the hypersecretion of several cytokines [TNFα, IL-6, monocyte chemoattractant protein-1 (MCP-1), PAI-1] associated to higher risk for cardiovascular morbidity and mortality (131, 132).

More importantly, premature renal aging immediately after kidney transplantation could be modulated by soluble and circulating factors and, virtually, also by complement system. Liu et al. (133) showed that blood from young mouse was able to reduce IRI-induced AKI in older mouse (134). Using an experimental model of parabiosis, a surgical procedure that allowed a shared circulation between older and younger mice, Liu et al. demonstrated that a youthful systemic milieu was able to attenuate inflammation, oxidative stress, and apoptosis after renal IRI (133). These results are in line with previous findings demonstrating that bone marrow from young donor mice alleviated renal aging (135) and with recent data indicating that transplantation of young bone marrow can rejuvenate the hematopoietic system and preserved cognitive function in old recipient mice (136, 137).

Mechanisms of Renal Inflammaging

The term *renal senescence* reflects the complex interplay between genetics, immunological, and hormonal factors able to lead to structural and functional changes observed in aged kidneys (138).

During physiological aging that occurs in the elderly, a low-grade of systemic inflammation and the dysregulation of innate and acquired immune responses are normally observed. This systemic, chronic proinflammatory status has been defined for the first time by Claudio Franceschi as inflammaging, and the associated immunological impairment has been named immunosenescence. [all reviewed in more detail by Franceschi et al. (139)]. Inflammaging is a risk factor for multiple chronic diseases, such as CKD, cardiovascular diseases, cancer, depression, dementia, osteoporosis, sarcopenia, and anemia. Besides physiological aging, several mechanisms can induce inflammaging such as oxidative stress, mitochondrial dysfunction, complement activation, DNA damage, changes to microbiota composition, NLRP3 inflammasome activation, visceral obesity, and cellular senescence. In the kidney, inflammaging has been strongly connected to tubular senescence, characterized by cell cycle arrest and the acquirement of a SASP. The common features of renal aging have been observed in a wide range of kidney disorders as pretransplant cold storage preservation, IRI, ABMR, diabetic nephropathy, and IgA nephropathy (114). Histological features of kidney aging include glomerulosclerosis, interstitial fibrosis, glomerular basement membrane thickness, microvascular rarefaction, and tubular atrophy. Interestingly, similar changes are also observed in transplant injured kidney, suggesting that maladaptive repair after acute insults can be considered as the fuel for kidney inflammaging (140).

The SASP cell secretome involves the increased release of a large spectrum of proinflammatory [IL-6, IL-1α, IL-1β, IL-8, MCP-1, C–X–C motif chemokine ligand 1 (CXCL-1)], profibrotic [TGF-β, connective tissue growth factor (CTGF)] cytokines, growth factors (fibroblast growth factor 2 and hepatocyte growth factor), and matrix metalloproteinases (MMPs) (141). These factors acting on neighboring health cells and in the circulation exacerbate the progression of the inflammation, lately of the fibrosis and then progression to CKD (138, 142) (**Figure 2**). Healthy aging must rely on the ability to maintain a balanced immunological response between pro- and anti-inflammatory factors, allowing the inflammation resolution in a timely effective manner (143). In senescent cells, the persistent, chronic inflammaging is maintained by controlled downregulation or unchanged stable levels of anti-inflammatory cytokines as IL-10, IL-4, IL-2, IL-11, IL-12 or Fractalkine (CX3CL-1). For that reason, another well-described consequence of the SASP secretome is the tumor initiation and progression in cells residing in proximity of senescent cells (141). The list of molecular processes involved in premature kidney aging is complex; below, we will focus on the main processes that have been shown to link inflammaging with renal transplantation and complement system such as Klotho signaling, Wnt/β-catenin pathway, increased expression of cell cycle inhibitors, epigenetic changes, and mitochondrial dysfunction (144).

Klotho and the Aging Kidney

The Klotho protein, expressed predominantly in epithelial distal convolute (DCT) and proximal tubules, is an antisenescence factor. Although the transmembrane form of Klotho functions as a coreceptor for FGF23 signaling, the extracellular domain is cleaved and released into the blood, urine, and the cerebrospinal fluid acting as an endocrine factor on several distant organs, such as the heart (145).

Klotho gene is strongly involved in human aging and longevity. For instance, Klotho-deficient mice exhibit a shortened life span, skin and muscle atrophy, cognitive impairment, osteoporosis, and hearing loss, resembling an accelerated aging phenotype (146). In contrast, overexpression in Klotho gene in transgenic mice has been associated to increased life span (147, 148). In human, serum levels of Klotho decrease with age and are downregulated in several forms of AKI and chronic kidney injury (149–153). The principle function of Klotho, which acts in the FGF 23 signaling, is mainly implicated with calcium, phosphate, and Vitamin D metabolism, explaining the central involvement in aging-related-vascular calcification and osteoporosis (154).

A huge body of literature describes the reduced Klotho expression in the kidney, blood, and urine after IRI in mouse (155, 156), rat (155, 157, 158), and swine (21) models. Hu et al. (155) induced IRI in mice with different genetic background that led to various endogenous Klotho levels ranged from heterozygous Klotho haploinsufficient (with low/absent Klotho expression), to wild-type (WT, normal Klotho expression), to transgenic mice overexpressing Klotho. Compared with WT

mice, after I/R, Klotho levels were lower in haploinsufficient and higher in transgenic. In addition, the haploinsufficient mice had more deleterious functional and histological damage compared with WT mice, whereas these changes were milder in overexpressing transgenic mice. These results support the concept that reduced Klotho levels predispose the kidney to injury, accelerating renal fibrosis, and senescence, therefore promoting to transition from AKI to CKD (159).

In accordance, the restoring of Klotho level by exogeneous supplementation has been demonstrated to be renoprotective from fibrosis, senescence, and apoptosis (157). Although the Klotho expression was spontaneously restored with recovery in the WT [after 7 days from IRI (155)], preventing the early Klotho drop is crucial to avoid or to delay the AKI-to-CKD progression, together with cardiovascular complications (156). Different methods of Klotho supplementation have been evaluated, from exogenous administration of recombinant α-Klotho (155, 156) to forced expression by adenoviral vectors (157, 160), to minicircle vectors that allowed self-production of Klotho protein in the cells (161).

Other therapeutic strategies to reduce the Klotho loss with significant limitation of chronic damage could arise from complement inhibition. Our group recently demonstrated in a pig model of IRI significant downregulation of Klotho by 24 h from injury; importantly, Klotho was efficiently preserved after treatment with C1-INH, which efficiently modulated nuclear factor kappa B (NF-kB) signaling (21). Furthermore, the C5a anaphylatoxin led to a significant Klotho protein and gene expression decrease through a mechanism mediated by NF-kB (21). In addition, tubular cells exposed to C5a acquired a senescent phenotype as demonstrated by increased SA-βgal positivity, cell cycle arrest induced by increased p53, p21, and p16, and the acquirement of a SASP as detected by *IL-6, MCP-1*, *CTGF*, SERPINE 1 (*PAI-1*) gene expression. Interestingly, C5aR1 inhibition by monoclonal antibody protected the tubular cells from senescence (22).

Between all the cytokine involved in the SASP development, PAI-1 is also an essential mediator of cellular senescence (162) and could offer a target to counteract renal inflammaging. PAI-1 is expressed in senescent cells and tissue and is particularly highly increased in Klotho-deficient (kl/kl) mice. Furthermore, PAI-1 can be induced by C5a in human macrophages (163) and renal tubular cells (22). Using Klotho- and PAI-1 deficient mice (kl/kl$^{-/-}$pai-1$^{-/-}$) (164), it was demonstrated that PAI-1 deficiency in kl/kl$^{-/-}$ led to reduced senescence, preserved organ structure, and function with a fourfold increase in lifespan. Therefore, PAI-1 could be considered as a downstream effector of the IRI-induced Klotho loss; both the PAI-1 inhibition, by the development of selective PAI-1 antagonists (such as TM5441), together with the C5a blocking, could offer a new possibility to modulate the impairment in Klotho expression (165).

Wnt/β-Catenin Pathway in Renal Aging

Wnt/β-catenin signaling, a pathway involved in organ development, normally is kept silent in normal adult kidneys (166) but reactivated during aging (118), renal tubulointerstitial fibrosis (167), vascular calcification, and progression to CKD (121, 168, 169). Wnt signaling is antagonized by the protein Klotho that can bind to multiple Wnt ligands and inhibit the signal transduction mediated by Frizzled receptors (118, 170).

Recently, Luo et al. (171) identified a predominant role for component Wnt9 in promoting renal fibrosis by accelerating tubular senescence both in human and in experimental model of renal IRI and CKD (171). Interestingly, Wnt9a expression level correlated with the extent of tubular senescence and interstitial fibrosis and, functionally, with decline of estimated glomerular filtration rate (eGFR). The Wnt/β-catenin signaling constitutive activation has already been demonstrated to induce myofibroblast activation in the absence of other type of injury (172), with Wnt4 playing a pivotal role in chronic fibrosis (173). We have already discussed the capacity of C1q to activate Wnt signaling, leading to mammalian aging. Our *in vivo* studies confirmed that renal IRI activated Wnt4/β-catenin signaling, whereas the C1-INH treatment, blocking CP and LP, abrogated Wnt4/β-catenin activation preventing renal senescence and inflammaging (22). Lastly, in renal tubular cells, mitochondria are essential for energy production and are dysfunctional in AKI and CKD, leading to fibrosis and accelerated aging. Recent evidence indicated that Wnt/β-catenin signaling mediates age-related renal fibrosis and is associated with mitochondrial dysfunction (174) (**Figure 2**).

Cell Cycle Arrest and Renal Senescence

Tubular epithelial cells have a great regenerative potential after an ischemic or toxic injury (175) (176). Early after an episode of AKI, in damaged tubular cells, cell cycle is arrested by specific inhibitors in order to provide time for DNA repair, avoiding exaggerate progression to apoptosis. However, after IRI induced AKI, the prolonged injury can lead to a permanently arrested cell cycle maintained by a persistent increase in cell cycle inhibitors. Cell cycle arrest is a common marker of cellular senescence and is regulated by three major proteins belonging to cyclin-dependent kinase (CDK) inhibitors: p16^{ink4a}, p21$^{waf1/cip}$, and p53 (177) (**Figure 2**). p16^{ink4a}, encoded by the Ink4a/Arf locus, also known as CDKN2A, binds the kinases CDK4 and CDK6 that are necessary for cyclin D activation, therefore arresting cell cycle in G1 phase (178); the pivotal role of p16^{ink4a} in multiorgan aging has been revealed by Baker et al. (179). Interestingly, the elimination of naturally occurring p16^{ink4a}-positive cells during physiological aging attenuated glomerulosclerosis and tubular senescence, extending lifespan. In rodents models of renal I/R, several evidence have been provided for p16 ^{ink4a} involvement in long-term graft deterioration (180–182). In particular, Braun et al. (180) demonstrated that after IRI, p16ink4a-deficient mice showed less interstitial fibrosis and tubular atrophy. Furthermore, p16^{ink4a}(-/-) mice were associated with improved renal function, preservations of nephron mass, and transplant survival compared with wild-type controls. Consistently, mice that received kidney transplants from p16^{Ink4a} (-/-) donors had significantly better survival and developed a reduced amount of tubulointerstitial fibrosis (180). Similar results were obtained by other groups (182) even if some discrepancies exists in term of timing of p16 increased expression (181) or in correlation to the type of injury (183).

These results, describing the crucial role of p16 in mice model of aging, were confirmed in human kidney biopsies. In a seminal paper, Melk et al. (184) provided evidences that in normal human renal biopsies, nuclear p16INK4a staining was increased with aging. However, transplanted kidney with interstitial fibrosis and tubular atrophy or transplanted biopsies with chronic allograft dysfunction, exhibited a strongest nuclear and cytoplasmic staining, beyond the level expected from physiological aging. From this initial study, the hypothesis that the assessment of senescence by p16 measurement in time zero kidney biopsies could have a value for the prediction of chronic renal dysfunction in the recipient was investigated by other groups (185–187).

Another cell cycle inhibitor is $p21^{WAF1/Cip1}$, a protein that after binding to CDK2, can block the CDK2-cyclin E complex, therefore arresting cell cycle in G1/S checkpoint. Megyesi et al. (188) demonstrated the role of p21 in tubular interstitial fibrosis and CKD progression in proximal tubular cells. In large experimental models, using an *ex vivo* hemoperfusion of pig kidneys after I/R, cold preservation, and machine perfusion, Chktoua et al. (189) found an increased p16 and p21 expression at tubular level after 180 min of reperfusion. In contrast with these results, in our swine model of renal I/R, p16 increased expression was not detectable before 24 h from reperfusion, and interestingly, the p16 and p21 protein level appeared to be modulated by C1-INH treatment (22). In accordance with these findings, C5a stimulated renal proximal tubular cells and exhibited a higher increase in p21 protein after both short time (3 h) and longer time (24 h) of C5a exposure. However, p21 seemed to be downregulated after 24 h of C5a exposition, followed by 24 h of normal culture, indicating a potential recovery of tubular cells. These *in vitro* results are in line with findings that indicated that p21 could transiently increase after injury (190), describing that p21 is essential for the beneficial effects of renal ischemic preconditioning. Temporary cell cycle arrest induced by a p21-dependent pathway could be important for subsequent tubular cell proliferation after I/R (190, 191). To confirm the establishment of cellular senescence, we also assessed the p16INK4a protein level. Stimulation with C5a significantly induced a constant augment in protein expression of p16INK4a compared to untreated condition (22).

Complement and Epigenetic Changes in Aging

Epigenetic modifications are stable, heritable, and reversible genome changes that occur without the presence of alterations in the original DNA sequence (192). These modifications include DNA methylation, histone, phosphorylation, acetylation, methylation ubiquitylation, sumoylation, and miRNA pattern variations (193). There is an emerging evidence that epigenetics is crucial in healthy and accelerated renal aging (194). Not only physiological environmental factors (i.e., diet, exercise, education, and lifestyle factors) (195) but also acute inflammation, oxidative stress, or uremic toxins can contribute to susceptibility to CKD progression by epigenome changes (196, 197).

During transplantation, several stressors such as IRI, cold ischemia, and acute rejection can induce aberrant DNA methylation changes with serious implications for graft outcomes and acceleration of renal aging (198) (**Figure 2**). A great body of evidence recently provided the epigenomic, transcriptomic, and proteomic signature that characterize the biological older allografts (199–202) and the CKD methylation patterns (203, 204). Comparable results showing the importance of epigenetic modifications in AKI-to-CKD progression were obtained by rat and mice model of IRI, CKD, and premature renal aging.

Shasha Yin et al., in a mouse model of UUO, demonstrated that TGF-β can inhibit Klotho expression by epigenetic mechanisms leading to progression to renal fibrosis; TGF-β induces aberrant expression of DNMT1 and DNMT3a through inhibiting miR-152 and miR-30a, subsequently leading to Klotho promoter hypermethylation and Klotho protein suppression (205). In a rat model of IRI, Pratt et al. (206) found aberrant methylation in the C3 promoter gene in response to 24 h of cold ischemia and a subsequent 2 h of reperfusion, indicating an increased C3 release, therefore an amplification of local complement activation following the oxidative stress. However, these studies neither demonstrate a correlation between C3 aberrant methylation and increased gene expression (207) nor provided clinical translation data (208).

Recently, Denisenko et al. (209), in rat old kidneys, found an abnormal epigenetic pattern of extracellular matrix laminins that are involved in the development of glomerulosclerosis and tubulointerstitial fibrosis. *In vitro*, a predominant role for DNA methylation changes was identified by Bechtel et al. (210), who correlated the hypermethylation of *RASAL1*, a gene encoding an inhibitor of the RAS oncoprotein, with the fibrogenesis in the kidney. In our studies, we demonstrated that complement component C5a can induce a global tubular epithelial cell DNA hypomethylation (22), as observed in premature and accelerated renal aging (195, 211, 212). Furthermore, we found that C5a induced methylation modification-regulated genes involved in the prosenescence Wnt/β-catenin pathway and induced a SASP phenotype and cell cycle arrest (22) (**Figure 2**).

CELL-SPECIFIC EFFECTS OF COMPLEMENT IN AKI-TO-CKD TRANSITION

Renal Tubular Epithelial Cells and Complement

The impairment of tubular function is considered a critical step in many cases of AKI (213). During tubular injury, tubular cells dedifferentiate to replace the lost epithelial cells, but some of them fail in the recovery process and continue to produce factors that stimulate inflammation leading to fibrosis. This maladaptive response contributes to the development of CKD (214).

Activation of complement factors on tubular epithelium (215) is considered a key factor in tubulointerstitial inflammation and in the progression of renal dysfunction (216). Proteinuria is a common feature of kidney transplantation, and the

association between proteinuria, complement activation, and tubulointerstitial fibrosis is well established (217). Indeed, the proteinuric condition provides a source of complement proteins to renal tubuli with amplification of the cascade (20).

The increase in albumin, which is associated to a higher risk of adverse transplant outcomes (218), compromised the balance between complement activation and inhibition, reducing factor H binding at tubular level (219). Several data also showed that urinary pH or ammonia released from stressed epithelial cells directly activated C3 (20) (**Figure 3**).

Recent studies indicated a key role of properdin in complement activation and in progression of proteinuria-induced tubulointerstitial injury. Properdin binds the glycosaminoglycans of the apical surface of tubular epithelium and stabilizes the AP convertase, enhancing AP activation. Then, interfering with properdin binding to tubular cells may provide a therapeutic option for the treatment of renal disease and prevention of CKD progression (20) (**Figure 3**).

Complement-cleavage products, C5a and C3a, are important mediators of renal inflammation and injury (20). These mediators bind their receptors C3aR and C5aR expressed on renal tubular, endothelial, and innate immune cells. When tubular cells were exposed to C3a and/or C5a, they synthesized collagen I and acquired a mesenchymal profibrotic phenotype contributing to renal fibrosis (47). The effects of C5a and C3a on tubular cells were mediated by TGF-β synthesis that consequently promoted epithelial-mesenchymal transition (EMT) (220). In accordance, studies in rodent knockout showed that the absence of C3aR and C5aR on renal tubular epithelial cells or circulating leukocytes attenuated renal IRI. Treatment *in vivo* using antagonist for C3aR and C5aR and for factor B could improve graft survival, reducing the decrease in renal injury, tubular apoptosis, and inflammation (216, 220, 221).

In addition, there are evidence that complement might contribute to renal injury in diabetic nephropathy. Complement activation and subsequent deposition of MAC on tubular epithelial cells induced a significant production of proinflammatory cytokines, as IL-6 and TNF-α, ROS, and components of matrix that contributed to amplify renal injury and fibrosis process. In this setting, tubular cells increased the expression of histocompatibility antigens stimulating T-cell response and autoimmunity process (20).

Therefore, complement has to be considered one of the principal actor in the progression from AKI to CKD, and its modulation could prevent tubular dysfunction. In our previous studies, we demonstrated the pathogenic role of the complement cascade in a swine model of IRI (222). We showed the link between oxidative stress/NOX activity, complement activation, and EMT process at tubular level (223). We also demonstrated the ability of C1-INH to reduce tubular dysfunction with prevention of I/R-induced renal injury (82) (**Figure 3**).

Endothelial Cells and Complement System

Several studies highlighted the interactions between complement and the endothelium in pathogenesis of different renal diseases, including IRI, hemolytic uremic syndrome, and renal allograft injury (224). During inflammation, endothelium is continuously exposed to autologous complement (225) generated by the local or systemic activation of all complement pathways. Complement components such as C1q, C3a, C5a, and C5b-9 have direct effects on endothelial cells impairing their function. It is well known that C5b-9 not only induces cell lysis but also stimulates endothelial cells to acquire a prothrombotic cell surface. Furthermore, C5b-9 also contributes to platelet clumping as well as increased leukocyte adhesion and subsequent proinflammatory cytokine release (226) (**Figure 3**).

Accordingly, our group demonstrated that complement was primarily activated on peritubular and glomerular capillaries in a swine model of renal IRI, suggesting that endothelial cells are the primary target of injury (222). We also investigated an intriguing pathogenic process named EndMT in a swine model of renal IRI (82). EndMT has been shown to play a significant role in cardiac fibrosis, in arteriovenous fistula stenosis (227), and also in the recruitment of carcinoma-associated fibroblasts (228–230). In this model, a relevant portion of activated fibroblasts coexpress the endothelial marker CD31, indicating that these fibroblasts likely carry an endothelial imprint. This observation was also supported in renal diseases such as diabetic nephropathy (231–233) by colabeling the tissue with the endothelial marker CD31 and the fibroblast markers α-smooth muscle actin (α-SMA) and fibroblast-specific protein 1 (FSP1). In our study, we found that complement played a central role in this pathogenic process regulating fibrosis development within the graft (82). We also showed the effects of C1-INH in preventing C5b-9 deposition along peritubular capillaries, decreasing endothelial dysfunction and subsequent fibrosis (47, 222) (**Figure 3**).

A number of recent studies have shown that diseases of the vasculature and kidneys, including CKD, are associated with increased numbers of circulating endothelial microparticles and complement activation (224). EVs are actively shed from cells in response to injury. In particular, the microparticles found in the plasma of CKD patients presented increased levels of factor D that contributes to alternative pathway activation and systemic inflammation. Interfering with complement activation and microparticle release may be a potential therapeutic strategy to ameliorate kidney dysfunction in these patients (224).

In aHUS, complement-mediated injury is particularly active in renal glomerular capillaries and arterioles (234). Circulating complement fragments and local renal complement production lead to uncontrolled complement activation that induced platelet, leukocyte, and endothelial cell activation and systemic thrombotic microangiopathy with end organ damage or failure (235).

Pericytes Dysfunction Upon Complement Activation

The tubular interstitial fibrosis and glomerulosclerosis are considered the principal responsible for progression of renal disease. The principal source of interstitial fibrosis in

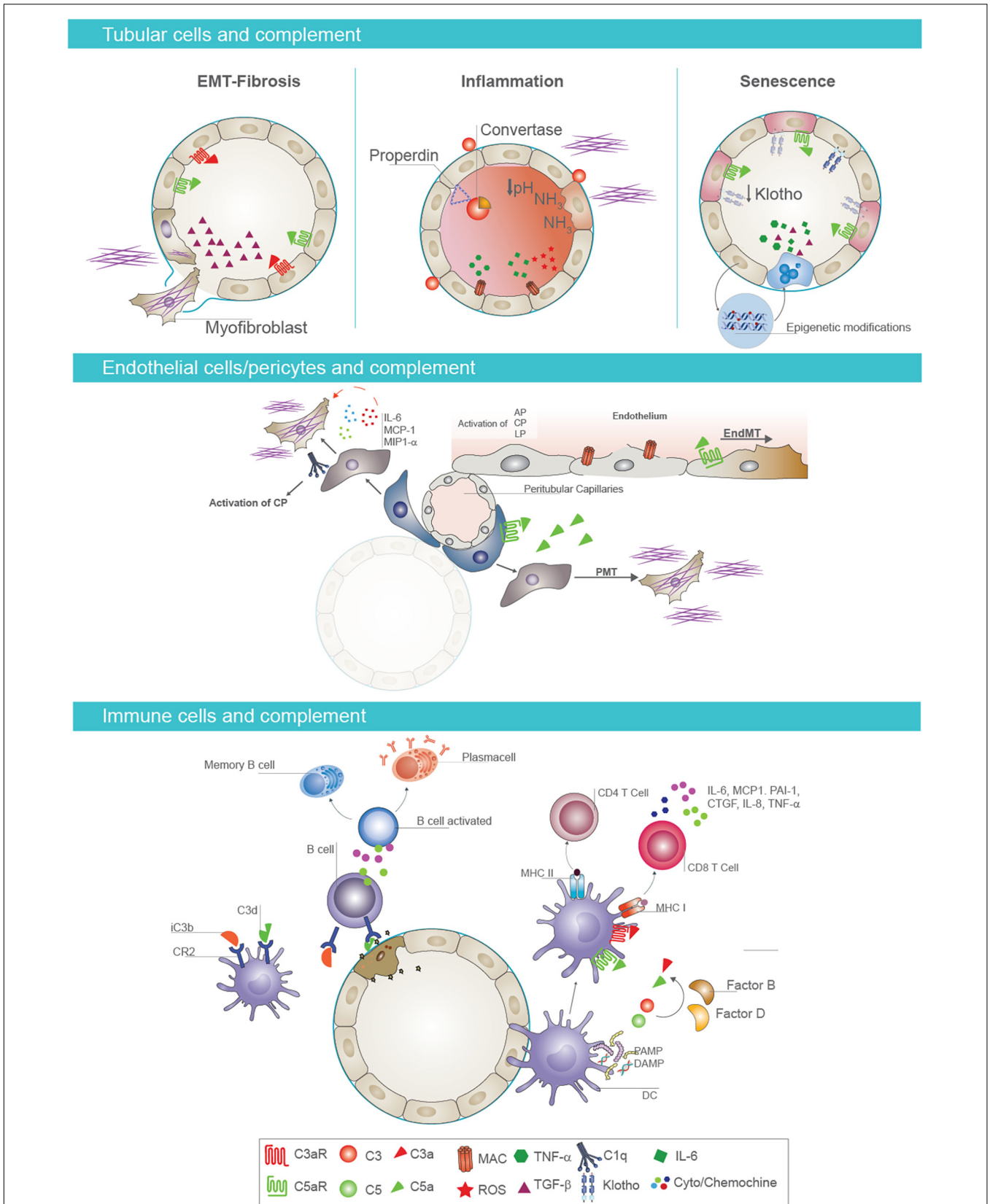

FIGURE 3 | Continued

FIGURE 3 | Cell-specific effects of complement in AKI-to-CKD transition. Tubular epithelial cells and complement activation (first panel). Activation of complement mediators on tubular epithelium is considered a key factor in renal fibrosis, inflammation, and senescence. Proximal tubular epithelial cells synthesize most components of the activation cascade as C4, C2, C3, factor B, and factor H. Reperfusion of the kidney following ischemia induces endothelial activation and release of nitrous oxide, leading to vasodilatation and leakage of complement components into the interstitial space In addition, complement proteins can be abnormally filtered across the altered glomerular barrier, leading to intratubular deposition of C3 and formation of membrane attack complex (MAC). When tubular cells are exposed to C3a and/or C5a, they synthesize transforming growth factor beta (TGF-β) that consequently promotes the EMT and fibrotic processes (on the left). Properdin, a key regulator of the complement system, enhances alternative pathway activation on the apical surface of tubular epithelium. Urinary pH and ammonia released from stressed tubular cells directly activate complement factor C3. This local complement activation and subsequent deposition of MAC on tubular cells induces a significant production of proinflammatory cytokines, contributing to renal inflammation (in the middle). Complement activation also induces a decrease in tubular expression of Klotho protein, an important antiaging factor. Complement promotes the acquirement of senescent tubular phenotype through epigenetic mechanisms, as DNA methylation (on the right). Endothelial cell/pericytes axis and complement activation (second panel). Complement also primes fibrotic process by inducing endothelial-to-mesenchymal transition (EndMT) and pericyte-to-mesenchymal transition (PMT) processes. In particular, C5a enhances EndMT process, causing phenotypic changes, with a decrease in endothelial markers and gain of fibroblast markers. In addition, pericytes, after C5a stimulation, acquire myofibroblast phenotype contributing to kidney fibrosis. Immune cells and complement (third panel). Complement components influence immune response in renal parenchyma. The binding of C3 fragments, iC3b and C3dg, to CR2 on B cells modulates B-cell response, increasing their activation and the development of memory B cells. Follicular DC also expressed CR2 and bind C3 fragments. After renal injury, PAMP and DAMP induce an increased expression of C3aR, C5aR1, and MHC class II on the surface of follicular DC and the synthesis and secretion of complement components C3 and C5 and factors B and D with local generation of C3a and C5a. These anaphylatoxins are strongly required for T-cell stimulation and activation in renal parenchyma.

kidney disease is represented by activated fibroblasts, named myofibroblasts (236). These cells derive from different precursors such as renal resident fibroblasts, endothelial cells, tubular cells, circulating bone-marrow-derived cells and pericytes (237). Recent studies highlighted the role of pericytes in the pathogenesis of renal fibrosis (238). Numerous secreted factors are involved in the generation and persistence of fibrotic process such as TGF-β, VEGF, CTGF, MMP, WNT ligands, and PDGF (31) (**Figure 3**).

Recent advances demonstrated that complement system not only contributed to local renal inflammation and adaptive immune response but also primed fibrotic process (239). Specifically, Xavier et al. demonstrated a local synthesis and secretion of C1q, C1r, and C1s by PDGFRβ-positive pericytes in two different animal model of CKD (31). Moreover, they showed that the C1q released by UUO-mice pericytes was associated to increased expression of extracellular matrix components, collagens, and augmented Wnt/β-catenin signaling, all common hallmark of myofibroblast activation. Finally, the C1q local synthesis amplified interstitial inflammation by the release of IL-6, MCP-1, and macrophage inflammatory protein 1-alpha (MIP1-α) that in turn contributed to fibrosis by macrophages recruitment (31, 240).

In addition to C1q, we recently demonstrated for the first time that also complement component C5a promoted the PMT, amplifying tubulo-interstitial fibrosis (48). *In vitro*, C5a-exposed pericytes downregulated the constitutive marker PDGFR-β and upregulated $aSMA^{+}$ stress fibers, the collagen I production, and the CTGF expression by TGF-β signaling. The C5aR blocking counteracted the PMT, reduced the C5a-induced collagen production, and more importantly inhibited the TGF-β pathway. In a swine model of I/R injury, we observed that C1-INH, acting upstream of C5 activation, indirectly reduced the release of C5a, preventing PMT process and ameliorating progressive kidney disease (48). Furthermore, also $C5aR1^{-/-}$ were spared from PMT in a mouse model of bilateral I/R.

These data indicate that pericytes are an important source of complement components at renal level and expressed receptors for complement anaphylatoxins. Therefore, pericytes are pivotal target for complement inhibition therapy to delay progression from AKI to CKD.

Immune Cells and Complement System

Next to direct effects on renal resident cells, complement components can influence the priming of alloantigen-specific immunity, modulating the interaction between dendritic cells (DCs) and T lymphocytes.

DCs are able to initiate an immune response by stimulating naive T cells, regulating the balance between Th1 and Th2 responses (241, 242). Moreover, complement components cooperate with DC to modulate T-cell response, and DCs themselves express complement factors, receptors, and regulators (243). Accordingly, we have demonstrated that C1q impaired DC activation leading to a limited T-cell response and preventing the overall immune response (244) (**Figure 3**).

Since the renal microenvironment has a strong influence on DC behavior, recent studies demonstrated the impact of local complement C3 on the differentiation and activation of DC. DC are considered the principal constituent of the tubulointerstitial compartment (245), and they produced C1q (41) and C3 in quantities similar to macrophages (246–248). Therefore, the contribution of C3 produced by these APC is strongly required for T-cell stimulation and activation in renal parenchyma. As a consequence, in C3-knockout organ, DCs have a reduced surface expression of major histocompatibility complex (MHC) class II and CD86, and they produce less IL-12 leading to a decrease in T-cell responsiveness (240, 249). Then, T-cell stimulation was reduced, and there was a shift for the generation of regulatory T cells (**Figure 3**).

This observation was confirmed *in vivo* in a skin allograft model. In this setting, infusion of mice with C3-knockout DC resulted in a less vigorous rejection of the skin allograft compared to mice infused with wild-type DC (248). Production of C3 has also been demonstrated for human monocyte-derived DC (240). The development of human monocyte-derived DC in either normal or C3-deficient

human serum resulted in a reduced expression of HLA-DR, CD1a, CD80, and CD86 in the absence of C3, leading to a reduced responsiveness upon lipopolysaccharide (LPS) activation (240).

Finally, other studies clearly demonstrated that generation of C3a and signaling through C3a receptors was a very important event at the interface between DC and T lymphocytes interaction and had a major role in immune activation (240, 249).

Moreover, it is well known that complement receptor type 2 (CR2, also known as CD21) is expressed on B cells and follicular DC, and it binds C3 fragments iC3b and C3d,g when associated to antigens (250). This binding modulates B-cell response, and the blockade of CR2 may be a potential strategy to reduce immune response in renal transplantation. Interestingly, the increase in C3 plasma levels also controls the development of memory B cells in kidney diseases (251).

Follicular DC can arise anywhere in the body, during chronic inflammatory reactions. Krautler et al. showed in a murine model of chronic inflammation that mature follicular DC localized in renal tissue and generated from tissue intrinsic precursors (252). Therefore, this finding proved that follicular DC may be ubiquitous and could regulate renal local immune response. These observations point toward an important role of complement activation at the immunological synapse and the contribution of complement regulators in this process.

Notably, C3aR and C5aR1 are extra- and intracellularly expressed in human CD4 + T cells and regulate the activation of mTOR pathway and NLRP3 inflammasome (109). In a mouse model of renal transplantation, the expression of these two receptors have been reported in regulatory T (Treg) cells, and they are shown to drive Th1 cells maturation and activation.

Moreover, PAMP or DAMP induced an increased expression of C3aR, C5aR1, and MHC class II on the surface of DC (109, 253), and the synthesis and secretion of complement components C3, C5, and factors B and D can locally generate C3a and C5a. Several data showed that both C3a and C5a stimulated CD4 + T cells to release interferon gamma (IFNγ) and IL-2 and induced TH1 and TH17 cell responses. Moreover, CD4 + T cells secreted IFNγ also upon C5aR1 activation (253). Therefore, therapeutic blockade of either C3aR or C5aR1 signaling could induce human tolerance to alloantigens and may prolong allogenic graft survival. Altogether, these data strongly suggest that the inhibition of complement acting on immune cells may represent a potential target for preventing rejection and progression of kidney diseases.

COMPLEMENT TARGETS STRATEGIES IN KIDNEY TRANSPLANTATION TO PREVENT AKI AND PROGRESSION TO CHRONIC DISFUNCTION

The involvement of complement in a broad range of disease processes renders this system an interesting and promising target for therapeutic interventions (254). Several clinical trials evaluating dozen of candidate drugs targeting specific complement's components are ongoing to date; most of them act as protein-protein interaction inhibitors, while others are physiological regulators or act on the genetic level, impairing the production of complement components (42). Eculizumab, the humanized monoclonal IgG2/4-antibody targeting C5, was the first complement drug available in the clinic, approved by the Food and Drug Administration (FDA) for the treatment of paroxysmal nocturnal hemoglobinuria (PNH) in 2007. PNH is a life-threatening disease characterized by an intravascular hemolytic anemia due to the destruction of red blood cells mediated by the complement system. In 2011, Eculizumab was also approved in the treatment of aHUS, where an uncontrolled activation of AP of the complement system (mutations in the complement regulatory proteins or acquired neutralizing autoantibodies against these regulatory factors) leads to a systemic thrombotic microangiopathy (255).

More than 10 years from its approval, the off-label usage of Eculizumab has been impressive, and several clinical trials are still assessing the potential indications, such as in kidney transplantation (42). As previously described, complement plays a major role in the IRI, such as DGF after kidney transplantation, and may be involved in the maladaptive repair leading to the progression to renal fibrosis and CKD (256). The role of Eculizumab in preventing and treating aHUS recurrence (255, 257) or *de novo* aHUS after kidney transplantation is well established to date (258). Recent evidence suggested its efficacy in the treatment of severe, progressive ABMR, or preventing ABMR in recipients with positive crossmatch against their living donors (rate of ABMR within 3 months after transplantation is 7.7% compared to 41.2% in patients receiving only plasma exchange) (259). However, the authors showed no differences between the treated and control groups in the incidence of chronic ABMR and death-censored graft survival, suggesting that the blockage of more proximal elements of the complement system may be pivotal in preventing the progression to chronic allograft disfunction (259).

Complement inhibition with Eculizumab to prevent IRI and DGF is still under investigation. In a single-center randomized controlled trial (RCT) of 57 children receiving a single dose of Eculizumab (700 mg/m^2) prior to transplantation, Eculizumab-treated patients had a significantly better early graft function, less arteriolar hyalinosis, and chronic glomerulopathy on protocol biopsies taken on day 30, 1 year, and 3 years after transplantation; however, an increased number of early graft losses due to flu-like infection has been documented (260).

Other complement-blocking agents have been used in kidney transplantation, and there are ongoing clinical trials evaluating the efficacy of recombinant C1-INH in preventing the development of IRI and DGF, as well as in the prevention and treatment of ABMR (258). C1-INH inhibits both the CP and LP of complement activation during IRI, reducing the release of renal microvesicles by inhibiting the

kallikrein-kinin system, and inhibits the coagulation pathway and, consequently, the formation of microthrombi in renal vessels (84, 254, 261). C1-INH is already licensed in many countries for the prevention and treatment of relapse of hereditary angioedema with important results and safety. However, its usage has been extended in other settings in order to prevent the acute development of organ disease and progression to chronic condition, particularly in the setting of kidney transplantation. Vo et al. conducted a phase I/II RCT evaluating the role of C1-INH in preventing ABMR in 20 highly HLA-sensitized recipients (262). After desensibilization, patients randomly received C1-INH 20 IU/kg or placebo intraoperatively and then another seven additional doses in the first month: DGF developed only in one patient in the treatment group, while four patients in the placebo group developed DGF (262). Moreover, no C1-INH-treated patients developed ABMR within 1 month; serum C4 levels recovered more quickly in the study group, and C3 and C4 levels were significantly higher, suggesting that C1-INH treatment may be effective in reducing antigen presentation and DSA production in this setting (262). The same investigators conducted a double-blind RCT where 70 high-risk and/or DCD donor kidney recipients were randomized to receive C1-INH 50 IU/kg intraoperatively and 24 h later versus placebo (263). The development of DGF (need of dialysis in the first post-transplantation week) was reduced in the study group but not statistically significant (42.9 versus 60% in the placebo group) (264); however, dialysis requirement and the mean number of dialysis sessions were reduced in C1-INH-treated group, particularly among recipients of grafts with KDPI. Furthermore, eGFR at 1 year was significantly higher in the treated group compared to the control group (p = 0.006), suggesting that C1-INH treatment safely reduces the need for dialysis and prevents progression to chronic graft disfunction (263).

The potential beneficial effect of C1-INH has been recently investigated in two recent studies. In a double-blind RCT performed in 18 DSA-positive recipients with an episode of biopsy-proven ABMR, randomized to placebo or C1-INH treatment in addition to alternate day plasmapheresis and IVIG, Montgomery et al. showed that there was no difference between groups with respect to the primary end points of 20-day graft survival or histological findings, but the C1-INH group showed a sustained improvement in renal function (264). Moreover, transplant glomerulopathy in 14 patients with available allograft biopsies at 6 months was significantly higher in the placebo group (3 of 7 patients) compared to none who received C1-INH (264). Viglietti et al. investigated the usage of C1-INH in six patients with acute ABMR and allograft disfunction that was refractory to standard therapy (steroids, plasmapheresis, high-dose IVIg, and rituximab). The authors showed a significant improvement in renal function (eGFR at 6 months) and, interestingly, a decrease in C1q binding anti-HLA DSA and the proportion of patients with C4d staining in peritubular capillaries in the treated patients: however, no differences in the typical histological findings of ABMR were described (265).

Overall, the main limitation in these studies using complement blockers is the small sample size; moreover, there is no direct competing trial with the use of eculizumab versus C1-INH; therefore, comparison of efficacy of different inhibitors of the complement system in clinical settings is not yet available. Several clinical trials evaluating C1-INH are currently ongoing and will guarantee a better understanding of the opportunities for the use of these agents in clinical transplantation.

In addition to eculizumab and C1-INH, other complement inhibitors have been studied in the transplantation setting, mostly in preclinical studies. These included engineered forms of complement receptor type 1 (CR1) (14), like TP-10 and Mirococept, and synthetic inhibitors of complement convertases (Compstatin) (266). TP-10 has been evaluated to reduce IRI in lung transplantation, showing reduced time of extubation, ventilatory days, and intensive care unit stay compared to patients in the placebo group (267). Furthermore, in a humanized mouse model of islet allograft, pretreatment with Mirococept reduced significantly intraislet inflammation, preserving insulin production by beta cells (268). The EMPIRIKAL trial is ongoing to evaluate the efficacy of an *ex vivo* administered complement inhibitor (Mirococept) in preventing DGF in cadaveric human renal transplantation (269). Pegcetacoplan (APL-2) is a pegylated Compstatin analog that acts as a cyclic peptide inhibitor of C3 and prevents both intravascular and extravascular hemolysis in patients with PHN. In a phase II clinical trial, APL-2 showed significant reduction in lactate dehydrogenas (LDH), total bilirubin, and absolute reticulocyte count with a sustained increase in hemoglobin (270). A phase III study (NCT03500549) comparing eculizumab and APL-2 in patients with PHN is ongoing. Finally, CCX168 (Avacopan), a selective C5a receptor inhibitor, has been investigated in preclinical and clinical studies in patients with ANCA-associated vasculitis. The important advantage of Avacopan is the preservation of the final common pathway of complement activation (MAC); thus, the innate immune response toward microbial agents remains fully active. Results from two phase II clinical trial CLEAR (NCT01363388) and CLASSIC (NCT0222155) showed that Avacopan is safe and effective in patients with ANCA-associated vasculitis allowing a safe reduction or suspension of corticosteroids (95, 271). Preliminary reports from the pivotal phase III ADVOCATE clinical trial (NCT02994927) showed the superiority of Avacopan in terms of sustained remission at 52 weeks and improvement in renal function in patients with ANCA-associated vasculitis in order to replace oral glucocorticoids (95). In this scenario, this therapeutic approach could represent an interesting alternative option also in other complement-based settings, such as IRI in transplantation.

The role of complement in heath and disease as an important component of the antimicrobial defense system raises questions about the safety and feasibility of complement inhibitors. The clinical experience with extended use of these drugs showed that they are considered safe and effective options with limited risk for complications (as infusion-related

effects, developing immunogenicity or severe infections): in this scenario, prophylactic measures (meningococcal vaccination before the use of eculizumab or vaccines for other bacteria such as pneumococci) and the prompt antibiotic treatment upon initial signs of infection may minimize the onset of severe adverse effects (272).

CONCLUSION AND FUTURE PROSPECTIVE

In summary, a growing body of experimental evidence indicates that complement activation contributes to the pathogenesis of renal inflammaging, particularly in the context of AKI-to-CKD transition. Complement components may regulate a wide range of molecular mechanisms both on infiltrating cells and renal parenchymal cells including scar-forming myofibroblasts, pericytes endothelial, and smooth muscle cells. We provided evidence supporting the pathogenic role of the complement system in promoting tubular epithelial cells senescence by genetic, epigenetic, and protein changes. Cellular senescence and the development of a SASP are involved in the progression from AKI to CKD, leading to common final signaling pathways involved in renal aging and fibrosis.

Currently, there are no validated therapeutic strategies to prevent renal inflammaging. However, promising results in clinical trials using new complement inhibitors suggest that interfering with this pivotal pathway of innate immune system may preserve the kidney from detrimental effect of AKI, reducing the progression of renal fibrosis and the accelerated renal aging.

AUTHOR CONTRIBUTIONS

RF and GC mainly contributed to the conception, the design and the writing of the manuscript. AS and MF contributed to writing of the parts relative to: cell-specific effects (for AS) and Complement therapeutics (for MF) and to literature bibliography search. GS and VC supported the final draft editing and revised the manuscript critically for final acceptance for publication. LG and GC supported and supervised the overall design of the article. RF and AS conceived of all figures. RF took the lead in writing the manuscript,reviewers revisions and figure changes. All authors gave final approval for the present version to be submitted.

FUNDING

This work was supported by University of Bari "Aldo Moro" and the Italian Ministry of Health (Giovani Ricercatori 2011-2012, GR-2011-02351027, AIM 1810057-activity 2 granted to AS, and Giovani Ricercatori GR-2009-1608662 granted to GC). LG was supported by a Regional Strategic Grant, Apulia Region (PSR 094). This work was supported in part by a grant from "Fondazione Cassa di Risparmio di Puglia" to RF.

ACKNOWLEDGMENTS

The authors thank Eustacchio Montemurno for excellent image conception and editing of all figures.

REFERENCES

1. Thurman JM, Le Quintrec M. Targeting the complement cascade: novel treatments coming down the pike. *Kidney Int*. (2016) 90:746–52. doi: 10.1016/j.kint.2016.04.018
2. Arbore G, Kemper C. A novel "complement–metabolism–inflammasome axis" as a key regulator of immune cell effector function. *Eur J Immunol*. (2016) 46:1563–73. doi: 10.1002/eji.201546131
3. Walport MJ. Complement. First of two parts. *N Engl J Med*. (2001) 344:1058–66. doi: 10.1056/NEJM200104053441406
4. Walport MJ. Complement. Second of two parts. *N Engl J Med*. (2001) 344:1140–4. doi: 10.1056/NEJM200104123441506
5. Wills-Karp M. Complement activation pathways: a bridge between innate and adaptive immune responses in asthma. *Proc Am Thorac Soc*. (2007) 4:247–51. doi: 10.1513/pats.200704-046AW
6. Koenderman L, Buurman W, Daha MR. The innate immune response. *Immunol Lett*. (2014) 162:95–102. doi: 10.1016/j.imlet.2014.10.010
7. Nauser CL, Farrar CA, Sacks SH. Complement recognition pathways in renal transplantation. *J Am Soc Nephrol*. (2017) 28:2571–8. doi: 10.1681/ASN.2017010079
8. Inforzato A, Bottazzi B, Garlanda C, Valentino S, Mantovani A. Pentraxins in humoral innate immunity. *Adv Exp Med Biol*. (2012) 946:1–20. doi: 10.1007/978-1-4614-0106-3_1
9. Ricklin D, Hajishengallis G, Yang K, Lambris JD. Complement: a key system for immune surveillance and homeostasis. *Nat Immunol*. (2010) 11:785–97. doi: 10.1038/ni.1923
10. Beltrame MH, Catarino SJ, Goeldner I, Boldt ABW, de Messias-Reason IJ. The lectin pathway of complement and rheumatic heart disease. *Front Pediatr*. (2014) 2:148. doi: 10.3389/fped.2014.00148
11. Garred P, Genster N, Pilely K, Bayarri-Olmos R, Rosbjerg A, Ma YJ, et al. A journey through the lectin pathway of complement-MBL and beyond. *Immunol Rev*. (2016) 274:74–97. doi: 10.1111/imr.12468
12. Mogensen TH. Pathogen recognition and inflammatory signaling in innate immune defenses. *Clin Microbiol Rev*. (2009) 22:240–73. doi: 10.1128/CMR.00046-08
13. Daha MR, van Kooten C. Role of complement in IgA nephropathy. *J Nephrol*. (2016) 29:1–4. doi: 10.1007/s40620-015-0245-6
14. O'Flynn J, Dixon KO, Faber Krol MC, Daha MR, van Kooten C. Myeloperoxidase directs properdin-mediated complement activation. *J Innate Immun*. (2014) 6:417–25. doi: 10.1159/000356980
15. Triantafilou K, Hughes TR, Triantafilou M, Morgan PP. The complement membrane attack complex triggers intracellular Ca2+ fluxes leading to NLRP3 inflammasome activation. *J Cell Sci*. (2013) 126(Pt 13):2903–13. doi: 10.1242/jcs.124388
16. Noris M, Remuzzi G. Overview of complement activation and regulation. *Semin Nephrol*. (2013) 33:479–92. doi: 10.1016/j.semnephrol.2013.08.001
17. Peng Q, Li K, Sacks SH, Zhou W. The role of anaphylatoxins C3a and C5a in regulating innate and adaptive immune responses. *Inflamm Allergy Drug Targets*. (2009) 8:236–46. doi: 10.2174/187152809788681038
18. Kourtzelis I, Rafail S. The dual role of complement in cancer and its implication in anti-tumor therapy. *Ann Transl Med*. (2016) 4:265. doi: 10.21037/atm.2016.06.26

19. Leslie JD, Mayor R. Complement in animal development: unexpected roles of a highly conserved pathway. *Semin Immunol*. (2013) 25:39–46. doi: 10.1016/j.smim.2013.04.005
20. Fearn A, Sheerin NS. Complement activation in progressive renal disease. *World J Nephrol*. (2015) 4:31–40. doi: 10.5527/wjn.v4.i1.31
21. Castellano G, Intini A, Stasi A, Divella C, Gigante M, Pontrelli P, et al. Complement modulation of anti−aging factor klotho in ischemia/reperfusion injury and delayed graft function. *Am J Transplant*. (2016) 16:325–33. doi: 10.1111/ajt.13415
22. Castellano G, Franzin R, Sallustio F, Stasi A, Banelli B, Romani M, et al. Complement component C5a induces aberrant epigenetic modifications in renal tubular epithelial cells accelerating senescence by Wnt4/βcatenin signaling after ischemia/reperfusion injury. *Aging (Albany NY)*. (2019) 11:4382–406. doi: 10.18632/aging.102059
23. Ricklin D, Reis ES, Lambris JD. Complement in disease: a defence system turning offensive. *Nat Rev Nephrol*. (2016) 12:383–401. doi: 10.1038/nrneph.2016.70
24. Clarke EV, Weist BM, Walsh CM, Tenner AJ. Complement protein C1q bound to apoptotic cells suppresses human macrophage and dendritic cell-mediated Th17 and Th1 T cell subset proliferation. *J Leukoc Biol*. (2015) 97:147–60. doi: 10.1189/jlb.3A0614-278R
25. Høgåsen AK, Würzner R, Abrahamsen TG, Dierich MP. Human polymorphonuclear leukocytes store large amounts of terminal complement components C7 and C6, which may be released on stimulation. *J Immunol*. (1995) 154:4734–40.
26. Blatt AZ, Pathan S, Ferreira VP. Properdin: a tightly regulated critical inflammatory modulator. *Immunol Rev*. (2016) 274:172–90. doi: 10.1111/imr.12466
27. Song N-J, Kim S, Jang B-H, Chang S-H, Yun UJ, Park K-M, et al. Small molecule-induced complement factor D (Adipsin) promotes lipid accumulation and adipocyte differentiation. *PLoS One*. (2016) 11:e0162228. doi: 10.1371/journal.pone.0162228
28. Tang S, Zhou W, Sheerin NS, Vaughan RW, Sacks SH. Contribution of renal secreted complement C3 to the circulating pool in humans. *J Immunol*. (1999) 162:4336–41.
29. Zhou W, Marsh JE, Sacks SH. Intrarenal synthesis of complement. *Kidney Int*. (2001) 59:1227–35. doi: 10.1046/j.1523-1755.2001.0590041227.x
30. Cui J, Wan J, You D, Zou Z, Chen Y, Li Z, et al. Interstitial complement C3 activation and macrophage infiltration in patients with hypertensive nephropathy. *Clin Nephrol*. (2017) 88:328–37. doi: 10.5414/CN109154
31. Xavier S, Sahu RK, Landes SG, Yu J, Taylor RP, Ayyadevara S, et al. Pericytes and immune cells contribute to complement activation in tubulointerstitial fibrosis. *Am J Physiol Physiol*. (2017) 312:F516–32. doi: 10.1152/ajprenal.00604.2016
32. Brooimans RA, Stegmann AP, van Dorp WT, van der Ark AA, van der Woude FJ, van Es LA, et al. Interleukin 2 mediates stimulation of complement C3 biosynthesis in human proximal tubular epithelial cells. *J Clin Invest*. (1991) 88:379–84. doi: 10.1172/JCI115314
33. Sheerin NS, Zhou W, Adler S, Sacks SH. TNF-alpha regulation of C3 gene expression and protein biosynthesis in rat glomerular endothelial cells. *Kidney Int*. (1997) 51:703–10. doi: 10.1038/ki.1997.101
34. Sacks S, Zhou W, Campbell RD, Martin J. C3 and C4 gene expression and interferon-gamma-mediated regulation in human glomerular mesangial cells. *Clin Exp Immunol*. (1993) 93:411–7. doi: 10.1111/j.1365-2249.1993.tb08193.x
35. Pratt JR, Abe K, Miyazaki M, Zhou W, Sacks SH. In situ localization of C3 synthesis in experimental acute renal allograft rejection. *Am J Pathol*. (2000) 157:825–31. doi: 10.1016/S0002-9440(10)64596-8
36. Farrar CA, Zhou W, Lin T, Sacks SH. Local extravascular pool of C3 is a determinant of postischemic acute renal failure. *FASEB J Off Publ Fed Am Soc Exp Biol*. (2006) 20:217–26. doi: 10.1096/fj.05-4747com
37. Pratt JR, Basheer SA, Sacks SH. Local synthesis of complement component C3 regulates acute renal transplant rejection. *Nat Med*. (2002) 8:582–7. doi: 10.1038/nm0602-582
38. Thurman JM. Complement in kidney disease: core curriculum 2015. *Am J Kidney Dis*. (2015) 65:156–68. doi: 10.1053/j.ajkd.2014.06.035
39. Liszewski MK, Kolev M, Le Friec G, Leung M, Bertram PG, Fara AF, et al. Intracellular complement activation sustains T cell homeostasis and mediates effector differentiation. *Immunity*. (2013) 39:1143–57. doi: 10.1016/j.immuni.2013.10.018
40. Karasu E, Eisenhardt SU, Harant J, Huber-Lang M. Extracellular vesicles: packages sent with complement. *Front Immunol*. (2018) 9:721. doi: 10.3389/fimmu.2018.00721
41. Castellano G, Trouw LA, Fiore N, Daha MR, Schena FP, van Kooten C. Infiltrating dendritic cells contribute to local synthesis of C1q in murine and human lupus nephritis. *Mol Immunol*. (2010) 47:2129–37. doi: 10.1016/j.molimm.2010.02.006
42. Ricklin D, Mastellos DC, Reis ES, Lambris JD. The renaissance of complement therapeutics. *Nat Rev Nephrol*. (2018) 14:26–47. doi: 10.1038/nrneph.2017.156
43. Hoste EAJ, Kellum JA, Selby NM, Zarbock A, Palevsky PM, Bagshaw SM, et al. Global epidemiology and outcomes of acute kidney injury. *Nat Rev Nephrol*. (2018) 14:607–25. doi: 10.1038/s41581-018-0052-0
44. Brar JE, Quigg RJ. Complement activation in the tubulointerstitium: AKI, CKD, and in between. *Kidney Int*. (2014) 86:663–6. doi: 10.1038/ki.2014.168
45. Humphreys BD. Mechanisms of renal fibrosis. *Annu Rev Physiol*. (2018) 80:309–26. doi: 10.1146/annurev-physiol-022516-034227
46. Yiu WH, Li RX, Wong DWL, Wu HJ, Chan KW, Chan LYY, et al. Complement C5a inhibition moderates lipid metabolism and reduces tubulointerstitial fibrosis in diabetic nephropathy. *Nephrol Dial Transplant*. (2018) 33:1323–32. doi: 10.1093/ndt/gfx336
47. Tang Z, Lu B, Hatch E, Sacks SH, Sheerin NS. C3a mediates epithelial-to-mesenchymal transition in proteinuric nephropathy. *J Am Soc Nephrol*. (2009) 20:593–603. doi: 10.1681/ASN.2008040434
48. Castellano G, Franzin R, Stasi A, Divella C, Sallustio F, Pontrelli P, et al. Complement activation during ischemia/reperfusion injury induces pericyte-to-myofibroblast transdifferentiation regulating peritubular capillary lumen reduction through pERK signaling. *Front Immunol*. (2018) 9:1002. doi: 10.3389/fimmu.2018.01002
49. Boor P, Konieczny A, Villa L, Schult A-L, Bucher E, Rong S, et al. Complement C5 mediates experimental tubulointerstitial fibrosis. *J Am Soc Nephrol*. (2007) 18:1508–15. doi: 10.1681/ASN.2006121343
50. Sean Eardley K, Cockwell P. Macrophages and progressive tubulointerstitial disease. *Kidney Int*. (2005) 68:437–55. doi: 10.1111/j.1523-1755.2005.00422.x
51. Heeger PS, Kemper C. Novel roles of complement in T effector cell regulation. *Immunobiology*. (2012) 217:216–24. doi: 10.1016/j.imbio.2011.06.004
52. Wenderfer SE, Ke B, Hollmann TJ, Wetsel RA, Lan HY, Braun MC. C5a receptor deficiency attenuates T cell function and renal disease in MRLlpr mice. *J Am Soc Nephrol*. (2005) 16:3572–82. doi: 10.1681/ASN.2005040373
53. Wynn TA. Fibrotic disease and the T(H)1/T(H)2 paradigm. *Nat Rev Immunol*. (2004) 4:583–94. doi: 10.1038/nri1412
54. Gewin LS. Transforming growth factor-beta in the acute kidney injury to chronic kidney disease transition. *Nephron*. (2019) 143:154–7. doi: 10.1159/000500093
55. Torbohm I, Schonermark M, Wingen AM, Berger B, Rother K, Hansch GM. C5b-8 and C5b-9 modulate the collagen release of human glomerular epithelial cells. *Kidney Int*. (1990) 37:1098–104. doi: 10.1038/ki.1990.91
56. Zhang J, Li Y, Shan K, Wang L, Qiu W, Lu Y, et al. Sublytic C5b-9 induces IL-6 and TGF-beta1 production by glomerular mesangial cells in rat Thy-1 nephritis through p300-mediated C/EBPbeta acetylation. *FASEB J Off Publ Fed Am Soc Exp Biol*. (2014) 28:1511–25. doi: 10.1096/fj.13-242693
57. Benzaquen LR, Nicholson-Weller A, Halperin JA. Terminal complement proteins C5b-9 release basic fibroblast growth factor and platelet-derived growth factor from endothelial cells. *J Exp Med*. (1994) 179:985–92. doi: 10.1084/jem.179.3.985
58. Abe K, Li K, Sacks SH, Sheerin NS. The membrane attack complex, C5b-9, up regulates collagen gene expression in renal tubular epithelial cells. *Clin Exp Immunol*. (2004) 136:60–6. doi: 10.1111/j.1365-2249.2004.02411.x
59. Suthanthiran M, Strom TB. Renal transplantation. *N Engl J Med*. (1994) 331:365–76. doi: 10.1056/NEJM199408113310606
60. Jager NM, Poppelaars F, Daha MR, Seelen MA. Complement in renal transplantation: the road to translation. *Mol Immunol*. (2017) 89:22–35. doi: 10.1016/j.molimm.2017.05.014
61. Damman J, Seelen MA, Moers C, Daha MR, Rahmel A, Leuvenink HG, et al. Systemic complement activation in deceased donors is associated with acute

rejection after renal transplantation in the recipient. *Transplantation*. (2011) 92:163–9. doi: 10.1097/TP.0b013e318222c9a0
62. Nakorchevsky A, Hewel JA, Kurian SM, Mondala TS, Campbell D, Head SR, et al. Molecular mechanisms of chronic kidney transplant rejection via large-scale proteogenomic analysis of tissue biopsies. *J Am Soc Nephrol*. (2010) 21:362–73. doi: 10.1681/ASN.2009060628
63. Coskun A, Baykal AT, Kazan D, Akgoz M, Senal MO, Berber I, et al. Proteomic analysis of kidney preservation solutions prior to renal transplantation. *PLoS One*. (2016) 11:e0168755. doi: 10.1371/journal.pone.0168755
64. de Vries B, Walter SJ, Peutz-Kootstra CJ, Wolfs TGAM, van Heurn LWE, Buurman WA. The mannose-binding lectin-pathway is involved in complement activation in the course of renal ischemia-reperfusion injury. *Am J Pathol*. (2004) 165:1677–88. doi: 10.1016/S0002-9440(10)63424-4
65. Damman J, Nijboer WN, Schuurs TA, Leuvenink HG, Morariu AM, Tullius SG, et al. Local renal complement C3 induction by donor brain death is associated with reduced renal allograft function after transplantation. *Nephrol Dial Transplant*. (2011) 26:2345–54. doi: 10.1093/ndt/gfq717
66. De Vries B, Matthijsen RA, Wolfs TGAM, Van Bijnen AAJHM, Heeringa P, Buurman WA. Inhibition of complement factor C5 protects against renal ischemia-reperfusion injury: inhibition of late apoptosis and inflammation. *Transplantation*. (2003) 75:375–82. doi: 10.1097/01.TP.0000044455.05584.2A
67. Møller-Kristensen M, Wang W, Ruseva M, Thiel S, Nielsen S, Takahashi K, et al. Mannan-binding lectin recognizes structures on ischaemic reperfused mouse kidneys and is implicated in tissue injury. *Scand J Immunol*. (2005) 61:426–34. doi: 10.1111/j.1365-3083.2005.01591.x
68. Thurman JM, Ljubanovic D, Edelstein CL, Gilkeson GS, Holers VM. Lack of a functional alternative complement pathway ameliorates ischemic acute renal failure in mice. *J Immunol*. (2003) 170:1517–23. doi: 10.4049/jimmunol.170.3.1517
69. Danobeitia JS, Djamali A, Fernandez LA. The role of complement in the pathogenesis of renal ischemia-reperfusion injury and fibrosis. *Fibrogenes Tissue Repair*. (2014) 7:16. doi: 10.1186/1755-1536-7-16
70. Zhou W, Farrar CA, Abe K, Pratt JR, Marsh JE, Wang Y, et al. Predominant role for C5b-9 in renal ischemia/reperfusion injury. *J Clin Invest*. (2000) 105:1363–71. doi: 10.1172/JCI8621
71. Thurman JM, Ljubanoviæ D, Royer PA, Kraus DM, Molina H, Barry NP, et al. Altered renal tubular expression of the complement inhibitor Crry permits complement activation after ischemia/reperfusion. *J Clin Invest*. (2006) 116:357–68. doi: 10.1172/JCI24521
72. Howard MC, Nauser CL, Farrar CA, Wallis R, Sacks SH. l-Fucose prevention of renal ischaemia/reperfusion injury in mice. *FASEB J*. (2020) 34:822–34. doi: 10.1096/fj.201901582R
73. Yaseen S, Demopulos G, Dudler T, Yabuki M, Wood CL, Cummings WJ, et al. Lectin pathway effector enzyme mannan-binding lectin-associated serine protease-2 can activate native complement C3 in absence of C4 and/or C2. *FASEB J*. (2017) 31:2210–9. doi: 10.1096/fj.201601306R
74. Asgari E, Farrar CA, Lynch N, Ali YM, Roscher S, Stover C, et al. Mannan-binding lectin-associated serine protease 2 is critical for the development of renal ischemia reperfusion injury and mediates tissue injury in the absence of complement C4. *FASEB J*. (2014) 28:3996–4003. doi: 10.1096/fj.13-246306
75. Farrar CA, Tran D, Li K, Wu W, Peng Q, Schwaeble W, et al. Collectin-11 detects stress-induced L-fucose pattern to trigger renal epithelial injury. *J Clin Invest*. (2016) 126:1911–25. doi: 10.1172/JCI83000
76. Gaya da Costa M, Poppelaars F, Berger SP, Daha MR, Seelen MA. The lectin pathway in renal disease: old concept and new insights. *Nephrol Dial Transplant*. (2018) 33:2073–9. doi: 10.1093/ndt/gfy073
77. Wu W, Liu C, Farrar CA, Ma L, Dong X, Sacks SH, et al. Collectin-11 promotes the development of renal tubulointerstitial fibrosis. *J Am Soc Nephrol*. (2018) 29:168–81. doi: 10.1681/ASN.2017050544
78. Smedbraten YV, Sagedal S, Mjoen G, Hartmann A, Fagerland MW, Rollag H, et al. High ficolin-3 level at the time of transplantation is an independent risk factor for graft loss in kidney transplant recipients. *Transplantation*. (2015) 99:791–6. doi: 10.1097/TP.0000000000000422
79. Dabrowska-Zamojcin E, Czerewaty M, Malinowski D, Tarnowski M, Sluczanowska-Glabowska S, Domanski L, et al. Ficolin-2 Gene rs7851696 polymorphism is associated with delayed graft function and acute rejection in kidney allograft recipients. *Arch Immunol Ther Exp (Warsz)*. (2018) 66:65–72. doi: 10.1007/s00005-017-0475-5
80. Park P, Haas M, Cunningham PN, Bao L, Alexander JJ, Quigg RJ. Injury in renal ischemia-reperfusion is independent from immunoglobulins and T lymphocytes. *Am J Physiol Renal Physiol*. (2002) 282:F352–7. doi: 10.1152/ajprenal.00160.2001
81. Berger M, Baldwin WM III, Jordan SC. Potential roles for C1 inhibitor in transplantation. *Transplantation*. (2016) 100:1415–24. doi: 10.1097/TP.0000000000000995
82. Curci C, Castellano G, Stasi A, Divella C, Loverre A, Gigante M, et al. Endothelial-to-mesenchymal transition and renal fibrosis in ischaemia/reperfusion injury are mediated by complement anaphylatoxins and Akt pathway. *Nephrol Dial Transplant*. (2014) 29:799–808. doi: 10.1093/ndt/gft516
83. Delpech P-O, Thuillier R, SaintYves T, Danion J, Le Pape S, van Amersfoort ES, et al. Inhibition of complement improves graft outcome in a pig model of kidney autotransplantation. *J Transl Med*. (2016) 14:277. doi: 10.1186/s12967-016-1013-7
84. Berger M, Lefaucheur C, Jordan SC. Update on C1 esterase inhibitor in human solid organ transplantation. *Transplantation*. (2019) 103:1763–75. doi: 10.1097/TP.0000000000002717
85. van Werkhoven MB, Damman J, van Dijk MCRF, Daha MR, de Jong IJ, Leliveld A, et al. Complement mediated renal inflammation induced by donor brain death: role of renal C5a-C5aR interaction. *Am J Transplant*. (2013) 13:875–82. doi: 10.1111/ajt.12130
86. van Werkhoven MB, Damman J, Daha MR, Krikke C, van Goor H, van Son WJ, et al. Novel insights in localization and expression levels of C5aR and C5L2 under native and post-transplant conditions in the kidney. *Mol Immunol*. (2013) 53:237–45. doi: 10.1016/j.molimm.2012.08.013
87. Zhang K, Li G-Q, He Q-H, Li Y, Tang M, Zheng Q-Y, et al. C5a/C5aR pathway accelerates renal ischemia-reperfusion injury by downregulating PGRN expression. *Int Immunopharmacol*. (2017) 53:17–23. doi: 10.1016/j.intimp.2017.10.006
88. Lewis AG, Kohl G, Ma Q, Devarajan P, Kohl J. Pharmacological targeting of C5a receptors during organ preservation improves kidney graft survival. *Clin Exp Immunol*. (2008) 153:117–26. doi: 10.1111/j.1365-2249.2008.03678.x
89. Poppelaars F, van Werkhoven MB, Kotimaa J, Veldhuis ZJ, Ausema A, Broeren SGM, et al. Critical role for complement receptor C5aR2 in the pathogenesis of renal ischemia-reperfusion injury. *FASEB J Off Publ Fed Am Soc Exp Biol*. (2017) 31:3193–204. doi: 10.1096/fj.201601218R
90. Thorenz A, Derlin K, Schroder C, Dressler L, Vijayan V, Pradhan P, et al. Enhanced activation of interleukin-10, heme oxygenase-1, and AKT in C5aR2-deficient mice is associated with protection from ischemia reperfusion injury-induced inflammation and fibrosis. *Kidney Int*. (2018) 94:741–55. doi: 10.1016/j.kint.2018.04.005
91. Gueler F, Rong S, Gwinner W, Mengel M, Brocker V, Schon S, et al. Complement 5a receptor inhibition improves renal allograft survival. *J Am Soc Nephrol*. (2008) 19:2302–12. doi: 10.1681/ASN.2007111267
92. Feucht HE, Felber E, Gokel MJ, Hillebrand G, Nattermann U, Brockmeyer C, et al. Is early complement activation in renal transplantation associated with later graft outcome? *Kidney Int*. (2018) 4:45–51. doi: 10.1159/000494014
93. Choudhry N, Li K, Zhang T, Wu K-Y, Song Y, Farrar CA, et al. The complement factor 5a receptor 1 has a pathogenic role in chronic inflammation and renal fibrosis in a murine model of chronic pyelonephritis. *Kidney Int*. (2016) 90:540–54. doi: 10.1016/j.kint.2016.04.023
94. Schroppel B, Heeger PS, Thiessen-Philbrook H, Hall IE, Doshi MD, Weng FL, et al. Donor urinary C5a levels independently correlate with posttransplant delayed graft function. *Transplantation*. (2019) 103:e29–35. doi: 10.1097/TP.0000000000002494
95. Jayne DRW, Bruchfeld AN, Harper L, Schaier M, Venning MC, Hamilton P, et al. Randomized trial of C5a receptor inhibitor avacopan in ANCA-associated vasculitis. *J Am Soc Nephrol*. (2017) 28:2756–67. doi: 10.1681/ASN.2016111179
96. Carminatti M, Tedesco-Silva H, Silva Fernandes NM, Sanders-Pinheiro H. Chronic kidney disease progression in kidney transplant recipients: a focus on traditional risk factors. *Nephrology (Carlton)*. (2019) 24:141–7. doi: 10.1111/nep.13483

97. Bobka S, Ebert N, Koertvely E, Jacobi J, Wiesener M, Buttner-Herold M, et al. Is early complement activation in renal transplantation associated with later graft outcome? *Kidney Blood Press Res*. (2018) 43:1488–504.
98. Feucht HE, Felber E, Gokel MJ, Hillebrand G, Nattermann U, Brockmeyer C, et al. Vascular deposition of complement-split products in kidney allografts with cell-mediated rejection. *Clin Exp Immunol*. (1991) 86:464–70. doi: 10.1111/j.1365-2249.1991.tb02954.x
99. Gosset C, Lefaucheur C, Glotz D. New insights in antibody-mediated rejection. *Curr Opin Nephrol Hypertens*. (2014) 23:597–604. doi: 10.1097/MNH.0000000000000069
100. Dunn TB, Noreen H, Gillingham K, Maurer D, Ozturk OG, Pruett TL, et al. Revisiting traditional risk factors for rejection and graft loss after kidney transplantation. *Am J Transplant*. (2011) 11:2132–43. doi: 10.1111/j.1600-6143.2011.03640.x
101. Orandi BJ, Chow EHK, Hsu A, Gupta N, Van Arendonk KJ, Garonzik-Wang JM, et al. Quantifying renal allograft loss following early antibody-mediated rejection. *Am J Transplant*. (2015) 15:489–98. doi: 10.1111/ajt.12982
102. Schinstock C, Stegall MD. Acute antibody-mediated rejection in renal transplantation: current clinical management. *Curr Transplant Rep*. (2014) 1:78–85. doi: 10.1007/s40472-014-0012-y
103. Djamali A, Kaufman DB, Ellis TM, Zhong W, Matas A, Samaniego M. Diagnosis and management of antibody-mediated rejection: current status and novel approaches. *Am J Transplant*. (2014) 14:255–71. doi: 10.1111/ajt.12589
104. Zhang R. Donor-specific antibodies in kidney transplant recipients. *Clin J Am Soc Nephrol*. (2018) 13:182–92. doi: 10.2215/CJN.00700117
105. Nankivell BJ, Alexander SI. Rejection of the kidney allograft. *N Engl J Med*. (2010) 363:1451–62. doi: 10.1056/NEJMra0902927
106. Orandi BJ, Alachkar N, Kraus ES, Naqvi F, Lonze BE, Lees L, et al. Presentation and outcomes of C4d-negative antibody-mediated rejection after kidney transplantation. *Am J Transplant*. (2016) 16:213–20. doi: 10.1111/ajt.13434
107. Loupy A, Hill GS, Suberbielle C, Charron D, Anglicheau D, Zuber J, et al. Significance of C4d Banff scores in early protocol biopsies of kidney transplant recipients with preformed donor-specific antibodies (DSA). *Am J Transplant*. (2011) 11:56–65. doi: 10.1111/j.1600-6143.2010.03364.x
108. Haas M, Sis B, Racusen LC, Solez K, Glotz D, Colvin RB, et al. Banff 2013 meeting report: inclusion of c4d-negative antibody-mediated rejection and antibody-associated arterial lesions. *Am J Transplant*. (2014) 14:272–83. doi: 10.1111/ajt.12590
109. Biglarnia AR, Huber-Lang M, Mohlin C, Ekdahl KN, Nilsson B. The multifaceted role of complement in kidney transplantation. *Nat Rev Nephrol*. (2018) 14:767–81. doi: 10.1038/s41581-018-0071-x
110. Cernoch M, Viklicky O. Complement in kidney transplantation. *Front Med*. (2017) 4:66. doi: 10.3389/fmed.2017.00066
111. Montero RM, Sacks SH, Smith RA. Complement-here, there and everywhere, but what about the transplanted organ? *Semin Immunol*. (2016) 28:250–9. doi: 10.1016/j.smim.2016.04.007
112. Stegall MD, Chedid MF, Cornell LD. The role of complement in antibody-mediated rejection in kidney transplantation. *Nat Rev Nephrol*. (2012) 8:670–8. doi: 10.1038/nrneph.2012.212
113. Farrar CA, Sacks SH. Mechanisms of rejection: role of complement. *Curr Opin Organ Transplant*. (2014) 19:8–13. doi: 10.1097/MOT.0000000000000037
114. Wang H, Arp J, Liu W, Faas SJ, Jiang J, Gies DR, et al. Inhibition of terminal complement components in presensitized transplant recipients prevents antibody-mediated rejection leading to long-term graft survival and accommodation. *J Immunol*. (2007) 179:4451–63. doi: 10.4049/jimmunol.179.7.4451
115. Maugeri A, Barchitta M, Mazzone MG, Giuliano F, Agodi A. Complement system and age-related macular degeneration: Implications of gene-environment interaction for preventive and personalized medicine. *Biomed Res Int*. (2018) 2018:7532507. doi: 10.1155/2018/7532507
116. Cribbs DH, Berchtold NC, Perreau V, Coleman PD, Rogers J, Tenner AJ, et al. Extensive innate immune gene activation accompanies brain aging, increasing vulnerability to cognitive decline and neurodegeneration: a microarray study. *J Neuroinflammation*. (2012) 9:179. doi: 10.1186/1742-2094-9-179
117. Stephan AH, Madison DV, Mateos JM, Fraser DA, Lovelett EA, Coutellier L, et al. A dramatic increase of C1q protein in the CNS during normal aging. *J Neurosci*. (2013) 33:13460–74. doi: 10.1523/JNEUROSCI.1333-13.2013
118. Liu H, Fergusson MM, Castilho RM, Liu J, Cao L, Chen J, et al. Augmented Wnt signaling in a mammalian model of accelerated aging. *Science*. (2007) 317:803–6. doi: 10.1126/science.1143578
119. Naito AT, Sumida T, Nomura S, Liu M-L, Higo T, Nakagawa A, et al. Complement C1q activates canonical Wnt signaling and promotes aging-related phenotypes. *Cell*. (2012) 149:1298–313. doi: 10.1016/j.cell.2012.03.047
120. Angers S, Moon RT. Proximal events in Wnt signal transduction. *Nat Rev Mol Cell Biol*. (2009) 10:468–77. doi: 10.1038/nrm2717
121. MacDonald BT, Tamai K, He X. Wnt/beta-catenin signaling: components, mechanisms, and diseases. *Dev Cell*. (2009) 17:9–26. doi: 10.1016/j.devcel.2009.06.016
122. Watanabe S, Sato K, Hasegawa N, Kurihara T, Matsutani K, Sanada K, et al. Serum C1q as a novel biomarker of sarcopenia in older adults. *FASEB J Off Publ Fed Am Soc Exp Biol*. (2015) 29:1003–10. doi: 10.1096/fj.14-262154
123. Hasegawa N, Fujie S, Horii N, Uchida M, Toyama Y, Inoue K, et al. Aging-induced elevation in circulating complement C1q level is associated with arterial stiffness. *Exp Gerontol*. (2019) 124:110650. doi: 10.1016/j.exger.2019.110650
124. Tomaiuolo R, Ruocco A, Salapete C, Carru C, Baggio G, Franceschi C, et al. Activity of mannose-binding lectin in centenarians. *Aging Cell*. (2012) 11:394–400. doi: 10.1111/j.1474-9726.2012.00793.x
125. Kohler PF, Müller-Eberhard HJ. Immunochemical quantitation of the third, fourth and fifth components of human complement: concentrations in the serum of healthy adults. *J Immunol*. (1967) 99:1211–6.
126. Yonemasu K, Kitajima H, Tanabe S, Ochi T, Shinkai H. Effect of age on C1q and C3 levels in human serum and their presence in colostrum. *Immunology*. (1978) 35:523–30.
127. Nagaki K, Hiramatsu S, Inai S, Sasaki A. The effect of aging on complement activity (CH50) and complement protein levels. *J Clin Lab Immunol*. (1980) 3:45–50.
128. Cole DS, Morgan BP. Beyond lysis: how complement influences cell fate. *Clin Sci*. (2003) 104:455–66. doi: 10.1042/CS20020362
129. Shi Q, Colodner KJ, Matousek SB, Merry K, Hong S, Kenison JE, et al. Complement C3-deficient mice fail to display age-related hippocampal decline. *J Neurosci*. (2015) 35:13029–42. doi: 10.1523/JNEUROSCI.1698-15.2015
130. Herrmann P, Cowing JA, Cristante E, Liyanage SE, Ribeiro J, Duran Y, et al. Cd59a deficiency in mice leads to preferential innate immune activation in the retinal pigment epithelium-choroid with age. *Neurobiol Aging*. (2015) 36:2637–48. doi: 10.1016/j.neurobiolaging.2015.05.019
131. Glasser SP, Dudenbostel T. The global burden of cardiovascular disease: the role of endothelial function and arterial elasticity in cardiovascular disease as novel and emerging biomarkers. *Curr Cardiovasc Risk Rep*. (2011) 5:187–95. doi: 10.1007/s12170-010-0151-3
132. Tuttolomondo A, Di Raimondo D, Pecoraro R, Arnao V, Pinto A, Licata G. Atherosclerosis as an inflammatory disease. *Curr Pharm Des*. (2012) 18:4266–88. doi: 10.2174/138161212802481237
133. Liu D, Lun L, Huang Q, Ning Y, Zhang Y, Wang L, et al. Youthful systemic milieu alleviates renal ischemia-reperfusion injury in elderly mice. *Kidney Int*. (2018) 94:268–79. doi: 10.1016/j.kint.2018.03.019
134. Plotkin M. Young blood for old kidneys? More questions than answers so far. *Kidney Int*. (2018) 94:235–6. doi: 10.1016/j.kint.2018.04.015
135. Yang H-C, Rossini M, Ma L-J, Zuo Y, Ma J, Fogo AB. Cells derived from young bone marrow alleviate renal aging. *J Am Soc Nephrol*. (2011) 22:2028–36. doi: 10.1681/ASN.2010090982
136. Das MM, Godoy M, Chen S, Moser VA, Avalos P, Roxas KM, et al. Young bone marrow transplantation preserves learning and memory in old mice. *Commun Biol*. (2019) 2:73. doi: 10.1038/s42003-019-0298-5
137. Gan KJ, Südhof TC. Specific factors in blood from young but not old mice directly promote synapse formation and NMDA-receptor recruitment. *Proc Natl Acad Sci USA*. (2019) 116:12524–33. doi: 10.1073/pnas.1902672116

138. Schmitt R, Melk A. Molecular mechanisms of renal aging. *Kidney Int*. (2017) 92:569–79. doi: 10.1016/j.kint.2017.02.036
139. Shanley DP, Aw D, Manley NR, Palmer DB. An evolutionary perspective on the mechanisms of immunosenescence. *Trends Immunol*. (2009) 30:374–81. doi: 10.1016/j.it.2009.05.001
140. Delanaye P, Jager KJ, Bokenkamp A, Christensson A, Dubourg L, Eriksen BO, et al. CKD: a call for an Age-adapted definition. *J Am Soc Nephrol*. (2019) 30:1785–805. doi: 10.1681/ASN.2019030238
141. Coppé J-P, Desprez P-Y, Krtolica A, Campisi J. The senescence-associated secretory phenotype: the dark side of tumor suppression. *Annu Rev Pathol Mech Dis*. (2010) 5:99–118. doi: 10.1146/annurev-pathol-121808-102144
142. Perlman AS, Chevalier JM, Wilkinson P, Liu H, Parker T, Levine DM, et al. Serum inflammatory and immune mediators are elevated in early stage diabetic nephropathy. *Ann Clin Lab Sci*. (2015) 45:256–63.
143. Rea IM, Gibson DS, McGilligan V, McNerlan SE, Denis Alexander H, Ross OA. Age and age-related diseases: role of inflammation triggers and cytokines. *Front Immunol*. (2018) 9:586. doi: 10.3389/fimmu.2018.00586
144. Sturmlechner I, Durik M, Sieben CJ, Baker DJ, van Deursen JM. Cellular senescence in renal ageing and disease. *Nat Rev Nephrol*. (2017) 13:77–89. doi: 10.1038/nrneph.2016.183
145. Neyra JA, Hu MC. Potential application of klotho in human chronic kidney disease. *Bone*. (2017) 100:41–9. doi: 10.1016/j.bone.2017.01.017
146. Kuro-o M, Matsumura Y, Aizawa H, Kawaguchi H, Suga T, Utsugi T, et al. Mutation of the mouse klotho gene leads to a syndrome resembling ageing. *Nature*. (1997) 390:45–51. doi: 10.1038/36285
147. Kuro-o M. Klotho and aging. *Biochim Biophys Acta*. (2009) 1790:1049–58. doi: 10.1016/j.bbagen.2009.02.005
148. Bian A, Neyra JA, Zhan M, Hu MC. Klotho, stem cells, and aging. *Clin Interv Aging*. (2015) 10:1233–43. doi: 10.2147/CIA.S84978
149. Keles N, Caliskan M, Dogan B, Keles NN, Kalcik M, Aksu F, et al. Low serum level of klotho is an early predictor of atherosclerosis. *Tohoku J Exp Med*. (2015) 237:17–23. doi: 10.1620/tjem.237.17
150. Xu Y, Sun Z. Molecular basis of Klotho: from gene to function in aging. *Endocr Rev*. (2015) 36:174–93. doi: 10.1210/er.2013-1079
151. Arking DE, Krebsova A, Macek MS, Macek MJ, Arking A, Mian IS, et al. Association of human aging with a functional variant of klotho. *Proc Natl Acad Sci USA*. (2002) 99:856–61. doi: 10.1073/pnas.022484299
152. Nitta K, Nagano N, Tsuchiya K. Fibroblast growth factor 23/klotho axis in chronic kidney disease. *Nephron Clin Pract*. (2014) 128:1–10. doi: 10.1159/000365787
153. Barker SL, Pastor J, Carranza D, Quinones H, Griffith C, Goetz R, et al. The demonstration of alphaKlotho deficiency in human chronic kidney disease with a novel synthetic antibody. *Nephrol Dial Transplant*. (2015) 30:223–33. doi: 10.1093/ndt/gfu291
154. Li X. The FGF metabolic axis. *Front Med*. (2019) 13:511–30. doi: 10.1007/s11684-019-0711-y
155. Hu M-C, Shi M, Zhang J, Quinones H, Kuro-o M, Moe OW. Klotho deficiency is an early biomarker of renal ischemia-reperfusion injury and its replacement is protective. *Kidney Int*. (2010) 78:1240–51. doi: 10.1038/ki.2010.328
156. Hu MC, Shi M, Gillings N, Flores B, Takahashi M, Kuro-O M, et al. Recombinant alpha-Klotho may be prophylactic and therapeutic for acute to chronic kidney disease progression and uremic cardiomyopathy. *Kidney Int*. (2017) 91:1104–14. doi: 10.1016/j.kint.2016.10.034
157. Sugiura H, Yoshida T, Tsuchiya K, Mitobe M, Nishimura S, Shirota S, et al. Klotho reduces apoptosis in experimental ischaemic acute renal failure. *Nephrol Dial Transplant*. (2005) 20:2636–45. doi: 10.1093/ndt/gfi165
158. Liu Q-F, Ye J-M, Deng Z-Y, Yu L-X, Sun Q, Li S-S. Ameliorating effect of Klotho on endoplasmic reticulum stress and renal fibrosis induced by unilateral ureteral obstruction. *Iran J Kidney Dis*. (2015) 9:291–7.
159. Zou D, Wu W, He Y, Ma S, Gao J. The role of klotho in chronic kidney disease. *BMC Nephrol*. (2018) 19:285. doi: 10.1186/s12882-018-1094-z
160. Haruna Y, Kashihara N, Satoh M, Tomita N, Namikoshi T, Sasaki T, et al. Amelioration of progressive renal injury by genetic manipulation of Klotho gene. *Proc Natl Acad Sci USA*. (2007) 104:2331–6. doi: 10.1073/pnas.0611079104
161. Shin YJ, Luo K, Quan Y, Ko EJ, Chung BH, Lim SW, et al. Therapeutic challenge of minicircle vector encoding klotho in animal model. *Am J Nephrol*. (2019) 49:413–24. doi: 10.1159/000499863
162. Baker DJ, Wijshake T, Tchkonia T, LeBrasseur NK, Childs BG, van de Sluis B, et al. Clearance of p16Ink4a-positive senescent cells delays ageing-associated disorders. *Nature*. (2011) 479:232–6. doi: 10.1038/nature10600
163. Kastl SP, Speidl WS, Kaun C, Rega G, Assadian A, Weiss TW, et al. The complement component C5a induces the expression of plasminogen activator inhibitor-1 in human macrophages via NF-kappaB activation. *J Thromb Haemost*. (2006) 4:1790–7. doi: 10.1111/j.1538-7836.2006.02046.x
164. Eren M, Boe AE, Murphy SB, Place AT, Nagpal V, Morales-Nebreda L, et al. PAI-1-regulated extracellular proteolysis governs senescence and survival in Klotho mice. *Proc Natl Acad Sci USA*. (2014) 111:7090–5. doi: 10.1073/pnas.1321942111
165. Tashiro Y, Nishida C, Sato-Kusubata K, Ohki-Koizumi M, Ishihara M, Sato A, et al. Inhibition of PAI-1 induces neutrophil-driven neoangiogenesis and promotes tissue regeneration via production of angiocrine factors in mice. *Blood*. (2012) 119:6382–93. doi: 10.1182/blood-2011-12-399659
166. Gewin LS. Renal tubule repair: is Wnt/beta-catenin a friend or foe? *Genes (Basel)*. (2018) 9:58. doi: 10.3390/genes9020058
167. Maarouf OH, Aravamudhan A, Rangarajan D, Kusaba T, Zhang V, Welborn J, et al. Paracrine Wnt1 drives interstitial fibrosis without inflammation by tubulointerstitial cross-talk. *J Am Soc Nephrol*. (2016) 27:781–90. doi: 10.1681/ASN.2014121188
168. Xiao L, Zhou D, Tan RJ, Fu H, Zhou L, Hou FF, et al. Sustained activation of Wnt/beta-catenin signaling drives AKI to CKD progression. *J Am Soc Nephrol*. (2016) 27:1727–40. doi: 10.1681/ASN.2015040449
169. Tan RJ, Zhou D, Zhou L, Liu Y. Wnt/beta-catenin signaling and kidney fibrosis. *Kidney Int Suppl*. (2014) 4:84–90. doi: 10.1038/kisup.2014.16
170. Tang X, Wang Y, Fan Z, Ji G, Wang M, Lin J, et al. Klotho: a tumor suppressor and modulator of the Wnt/beta-catenin pathway in human hepatocellular carcinoma. *Lab Invest*. (2016) 96:197–205. doi: 10.1038/labinvest.2015.86
171. Luo C, Zhou S, Zhou Z, Liu Y, Yang L, Liu J, et al. Wnt9a promotes renal fibrosis by accelerating cellular senescence in tubular epithelial cells. *J Am Soc Nephrol*. (2018) 29:1238–56. doi: 10.1681/ASN.2017050574
172. DiRocco DP, Kobayashi A, Taketo MM, McMahon AP, Humphreys BD. Wnt4/beta-catenin signaling in medullary kidney myofibroblasts. *J Am Soc Nephrol*. (2013) 24:1399–412. doi: 10.1681/ASN.2012050512
173. Surendran K, McCaul SP, Simon TC. A role for Wnt-4 in renal fibrosis. *Am J Physiol Renal Physiol*. (2002) 282:F431–41. doi: 10.1152/ajprenal.0009.2001
174. Miao J, Liu J, Niu J, Zhang Y, Shen W, Luo C, et al. Wnt/beta-catenin/RAS signaling mediates age-related renal fibrosis and is associated with mitochondrial dysfunction. *Aging Cell*. (2019) 18:e13004. doi: 10.1111/acel.13004
175. Bonventre JV, Yang L. Cellular pathophysiology of ischemic acute kidney injury. *J Clin Invest*. (2011) 121:4210–21. doi: 10.1172/JCI45161
176. Humphreys BD, Valerius MT, Kobayashi A, Mugford JW, Soeung S, Duffield JS, et al. Intrinsic epithelial cells repair the kidney after injury. *Cell Stem Cell*. (2008) 2:284–91. doi: 10.1016/j.stem.2008.01.014
177. Singh B, Wu P-YJ. Regulation of the program of DNA replication by CDK: new findings and perspectives. *Curr Genet*. (2019) 65:79–85. doi: 10.1007/s00294-018-0860-6
178. Campisi J, d'Adda di Fagagna F. Cellular senescence: when bad things happen to good cells. *Nat Rev Mol Cell Biol*. (2007) 8:729–40. doi: 10.1038/nrm2233
179. Baker DJ, Childs BG, Durik M, Wijers ME, Sieben CJ, Zhong J, et al. Naturally occurring p16(Ink4a)-positive cells shorten healthy lifespan. *Nature*. (2016) 530:184–9. doi: 10.1038/nature16932
180. Braun H, Schmidt BMW, Raiss M, Baisantry A, Mircea-Constantin D, Wang S, et al. Cellular senescence limits regenerative capacity and allograft survival. *J Am Soc Nephrol*. (2012) 23:1467–73. doi: 10.1681/ASN.2011100967
181. Rodrigues CE, Capcha JMC, de Braganca AC, Sanches TR, Gouveia PQ, de Oliveira PAF, et al. Human umbilical cord-derived mesenchymal stromal cells protect against premature renal senescence resulting from oxidative stress in rats with acute kidney injury. *Stem Cell Res Ther*. (2017) 8:19. doi: 10.1186/s13287-017-0475-8
182. Lee DH, Wolstein JM, Pudasaini B, Plotkin M. INK4a deletion results in improved kidney regeneration and decreased capillary rarefaction after

ischemia-reperfusion injury. *Am J Physiol Renal Physiol*. (2012) 302:F183–91. doi: 10.1152/ajprenal.00407.2011
183. Wolstein JM, Lee DH, Michaud J, Buot V, Stefanchik B, Plotkin MD. INK4a knockout mice exhibit increased fibrosis under normal conditions and in response to unilateral ureteral obstruction. *Am J Physiol Renal Physiol*. (2010) 299:F1486–95. doi: 10.1152/ajprenal.00378.2010
184. Melk A, Schmidt BMW, Vongwiwatana A, Rayner DC, Halloran PF. Increased expression of senescence-associated cell cycle inhibitor p16INK4a in deteriorating renal transplants and diseased native kidney. *Am J Transplant*. (2005) 5:1375–82. doi: 10.1111/j.1600-6143.2005.00846.x
185. Koppelstaetter C, Schratzberger G, Perco P, Hofer J, Mark W, Ollinger R, et al. Markers of cellular senescence in zero hour biopsies predict outcome in renal transplantation. *Aging Cell*. (2008) 7:491–7. doi: 10.1111/j.1474-9726.2008.00398.x
186. McGlynn LM, Stevenson K, Lamb K, Zino S, Brown M, Prina A, et al. Cellular senescence in pretransplant renal biopsies predicts postoperative organ function. *Aging Cell*. (2009) 8:45–51. doi: 10.1111/j.1474-9726.2008.00447.x
187. Sis B, Tasanarong A, Khoshjou F, Dadras F, Solez K, Halloran PF. Accelerated expression of senescence associated cell cycle inhibitor p16INK4A in kidneys with glomerular disease. *Kidney Int*. (2007) 71:218–26. doi: 10.1038/sj.ki.5002039
188. Megyesi J, Tarcsafalvi A, Li S, Hodeify R, Seng NSHL, Portilla D, et al. Increased expression of p21WAF1/CIP1 in kidney proximal tubules mediates fibrosis. *Am J Physiol Renal Physiol*. (2015) 308:F122–30. doi: 10.1152/ajprenal.00489.2014
189. Chkhotua AB, Abendroth D, Froeba G, Schelzig H. Up-regulation of cell cycle regulatory genes after renal ischemia/reperfusion: differential expression of p16(INK4a), p21(WAF1/CIP1) and p27(Kip1) cyclin-dependent kinase inhibitor genes depending on reperfusion time. *Transpl Int*. (2006) 19:72–7. doi: 10.1111/j.1432-2277.2005.00227.x
190. Nishioka S, Nakano D, Kitada K, Sofue T, Ohsaki H, Moriwaki K, et al. The cyclin-dependent kinase inhibitor p21 is essential for the beneficial effects of renal ischemic preconditioning on renal ischemia/reperfusion injury in mice. *Kidney Int*. (2014) 85:871–9. doi: 10.1038/ki.2013.496
191. Canaud G, Bonventre JV. Cell cycle arrest and the evolution of chronic kidney disease from acute kidney injury. *Nephrol Dial Transplant*. (2015) 30:575–83. doi: 10.1093/ndt/gfu230
192. Nangaku M, Hirakawa Y, Mimura I, Inagi R, Tanaka T. Epigenetic changes in the acute kidney injury-to-chronic kidney disease transition. *Nephron*. (2017) 137:256–9. doi: 10.1159/000476078
193. Shiels PG, McGuinness D, Eriksson M, Kooman JP, Stenvinkel P. The role of epigenetics in renal ageing. *Nat Rev Nephrol*. (2017) 13:471–82. doi: 10.1038/nrneph.2017.78
194. Jones MJ, Goodman SJ, Kobor MS. DNA methylation and healthy human aging. *Aging Cell*. (2015) 14:924–32. doi: 10.1111/acel.12349
195. Quach A, Levine ME, Tanaka T, Lu AT, Chen BH, Ferrucci L, et al. Epigenetic clock analysis of diet, exercise, education, and lifestyle factors. *Aging (Albany NY)*. (2017) 9:419–46. doi: 10.18632/aging.101168
196. Morgado-Pascual JL, Marchant V, Rodrigues-Diez R, Dolade N, Suarez-Alvarez B, Kerr B, et al. Epigenetic Modification Mechanisms Involved in Inflammation and Fibrosis in Renal Pathology. *Mediators Inflamm*. (2018) 2018:2931049. doi: 10.1155/2018/2931049
197. Chu AY, Tin A, Schlosser P, Ko Y-A, Qiu C, Yao C, et al. Epigenome-wide association studies identify DNA methylation associated with kidney function. *Nat Commun*. (2017) 8:1286. doi: 10.1038/s41467-017-01297-7
198. Parker MD, Chambers PA, Lodge JPA, Pratt JR. Ischemia- reperfusion injury and its influence on the epigenetic modification of the donor kidney genome. *Transplantation*. (2008) 86:1818–23. doi: 10.1097/TP.0b013e31818fe8f9
199. McGuinness D, Mohammed S, Monaghan L, Wilson PA, Kingsmore DB, Shapter O, et al. A molecular signature for delayed graft function. *Aging Cell*. (2018) 17:e12825. doi: 10.1111/acel.12825
200. Rowland J, Akbarov A, Eales J, Xu X, Dormer JP, Guo H, et al. Uncovering genetic mechanisms of kidney aging through transcriptomics, genomics, and epigenomics. *Kidney Int*. (2019) 95:624–35. doi: 10.1016/j.kint.2018.10.029
201. Melk A, Mansfield ES, Hsieh S-C, Hernandez-Boussard T, Grimm P, Rayner DC, et al. Transcriptional analysis of the molecular basis of human kidney aging using cDNA microarray profiling. *Kidney Int*. (2005) 68:2667–79. doi: 10.1111/j.1523-1755.2005.00738.x
202. Wang Z, Gerstein M, Snyder MRNA-. Seq: a revolutionary tool for transcriptomics. *Nat Rev Genet*. (2009) 10:57–63. doi: 10.1038/nrg2484
203. Smyth LJ, McKay GJ, Maxwell AP, McKnight AJ. DNA hypermethylation and DNA hypomethylation is present at different loci in chronic kidney disease. *Epigenetics*. (2014) 9:366–76. doi: 10.4161/epi.27161
204. Wing MR, Devaney JM, Joffe MM, Xie D, Feldman HI, Dominic EA, et al. DNA methylation profile associated with rapid decline in kidney function: findings from the CRIC study. *Nephrol Dial Transplant*. (2014) 29:864–72. doi: 10.1093/ndt/gft537
205. Yin S, Zhang Q, Yang J, Lin W, Li Y, Chen F, et al. TGFbeta-incurred epigenetic aberrations of miRNA and DNA methyltransferase suppress Klotho and potentiate renal fibrosis. *Biochim Biophys acta Mol cell Res*. (2017) 1864:1207–16. doi: 10.1016/j.bbamcr.2017.03.002
206. Pratt JR, Parker MD, Affleck LJ, Corps C, Hostert L, Michalak E, et al. Ischemic epigenetics and the transplanted kidney. *Transplant Proc*. (2006) 38:3344–6. doi: 10.1016/j.transproceed.2006.10.112
207. Heylen L, Thienpont B, Naesens M, Lambrechts D, Sprangers B. The emerging role of DNA methylation in kidney transplantation: a perspective. *Am J Transplant*. (2016) 16:1070–8. doi: 10.1111/ajt.13585
208. Cai G, Huang Z, Yu L, Li L. A preliminary study showing no association between methylation levels of C3 gene promoter and the risk of CAD. *Lipids Health Dis*. (2019) 18:5. doi: 10.1186/s12944-018-0949-4
209. Denisenko O, Mar D, Trawczynski M, Bomsztyk K. Chromatin changes trigger laminin genes dysregulation in aging kidneys. *Aging (Albany NY)*. (2018) 10:1133–45. doi: 10.18632/aging.101453
210. Bechtel W, McGoohan S, Zeisberg EM, Muller GA, Kalbacher H, Salant DJ, et al. Methylation determines fibroblast activation and fibrogenesis in the kidney. *Nat Med*. (2010) 16:544–50. doi: 10.1038/nm.2135
211. Day K, Waite LL, Thalacker-Mercer A, West A, Bamman MM, Brooks JD, et al. Differential DNA methylation with age displays both common and dynamic features across human tissues that are influenced by CpG landscape. *Genome Biol*. (2013) 14:R102. doi: 10.1186/gb-2013-14-9-r102
212. Johansson A, Enroth S, Gyllensten U. Continuous aging of the human DNA methylome throughout the human lifespan. *PLoS One*. (2013) 8:e67378. doi: 10.1371/journal.pone.0067378
213. Fattah H, Vallon V. Tubular recovery after acute kidney injury. *Nephron*. (2018) 140:140–3. doi: 10.1159/000490007
214. Forni LG, Darmon M, Ostermann M, Oudemans-van Straaten HM, Pettilä V, Prowle JR, et al. Renal recovery after acute kidney injury. *Intensive Care Med*. (2017) 43:855–66. doi: 10.1007/s00134-017-4809-x
215. Castellano G, Cappiello V, Fiore N, Pontrelli P, Gesualdo L, Schena FP, et al. CD40 ligand increases complement C3 secretion by proximal tubular epithelial cells. *J Am Soc Nephrol*. (2005) 16:2003–11. doi: 10.1681/ASN.2002120972
216. Wada T, Nangaku M. Novel roles of complement in renal diseases and their therapeutic consequences. *Kidney Int*. (2013) 84:441–50. doi: 10.1038/ki.2013.134
217. Fernández MLS, Cosio FG. Causes and consequences of proteinuria following kidney transplantation. *Nefrologia*. (2011) 31:404–14. doi: 10.3265/Nefrologia.pre2011.May.10972
218. Lam NN, Tonelli M, Lentine KL, Hemmelgarn B, Ye F, Wen K, et al. Albuminuria and posttransplant chronic kidney disease stage predict transplant outcomes. *Kidney Int*. (2017) 92:470–8. doi: 10.1016/j.kint.2017.01.028
219. Buelli S, Abbate M, Morigi M, Moioli D, Zanchi C, Noris M, et al. Protein load impairs factor H binding promoting complement-dependent dysfunction of proximal tubular cells. *Kidney Int*. (2009) 75:1050–9. doi: 10.1038/ki.2009.8
220. Vieyra MB, Heeger PS. Novel aspects of complement in kidney injury. *Kidney Int*. (2010) 77:495–9. doi: 10.1038/ki.2009.491
221. Angeletti A, Reyes-Bahamonde J, Cravedi P, Campbell KN. Complement in non-antibody-mediated kidney diseases. *Front Med*. (2017) 4:99. doi: 10.3389/fmed.2017.00099
222. Castellano G, Melchiorre R, Loverre A, Ditonno P, Montinaro V, Rossini M, et al. Therapeutic targeting of classical and lectin pathways of complement

protects from ischemia-reperfusion-induced renal damage. *Am J Pathol*. (2010) 176:1648–59. doi: 10.2353/ajpath.2010.090276
223. Simone S, Rascio F, Castellano G, Divella C, Chieti A, Ditonno P, et al. Complement-dependent NADPH oxidase enzyme activation in renal ischemia/reperfusion injury. *Free Radic Biol Med*. (2014) 74:263–73. doi: 10.1016/j.freeradbiomed.2014.07.003
224. Jalal D, Renner B, Laskowski J, Stites E, Cooper J, Valente K, et al. Endothelial microparticles and systemic complement activation in patients with chronic kidney disease. *J Am Heart Assoc*. (2018) 7:e007818. doi: 10.1161/JAHA.117.007818
225. Castellano G, Di Vittorio A, Dalfino G, Loverre A, Marrone D, Simone S, et al. Pentraxin 3 and complement cascade activation in the failure of arteriovenous fistula. *Atherosclerosis*. (2010) 209:241–7. doi: 10.1016/j.atherosclerosis.2009.08.044
226. Kerr H, Richards A. Complement-mediated injury and protection of endothelium: lessons from atypical haemolytic uraemic syndrome. *Immunobiology*. (2012) 217:195–203. doi: 10.1016/j.imbio.2011.07.028
227. Simone S, Loverre A, Cariello M, Divella C, Castellano G, Gesualdo L, et al. Arteriovenous fistula stenosis in hemodialysis patients is characterized by an increased adventitial fibrosis. *J Nephrol*. (2014) 27:555–62. doi: 10.1007/s40620-014-0050-7
228. Leask A. Getting to the heart of the matter: new insights into cardiac fibrosis. *Circ Res*. (2015) 116:1269–76. doi: 10.1161/CIRCRESAHA.116.305381
229. Pardali E, Sanchez-Duffhues G, Gomez-Puerto MC, Ten Dijke P. TGF-β-Induced endothelial-mesenchymal transition in fibrotic diseases. *Int J Mol Sci*. (2017) 18:2157. doi: 10.3390/ijms18102157
230. Potenta S, Zeisberg E, Kalluri R. The role of endothelial-to-mesenchymal transition in cancer progression. *Br J Cancer*. (2008) 99:1375–9. doi: 10.1038/sj.bjc.6604662
231. Liu F, Zhang S, Xu R, Gao S, Yin J. Melatonin attenuates endothelial-to-mesenchymal transition of glomerular endothelial cells via regulating miR-497/ROCK in diabetic nephropathy. *Kidney Blood Press Res*. (2018) 43:1425–36. doi: 10.1159/000493380
232. Shang J, Zhang Y, Jiang Y, Li Z, Duan Y, Wang L, et al. NOD2 promotes endothelial-to-mesenchymal transition of glomerular endothelial cells via MEK/ERK signaling pathway in diabetic nephropathy. *Biochem Biophys Res Commun*. (2017) 484:435–41. doi: 10.1016/j.bbrc.2017.01.155
233. Li L, Chen L, Zang J, Tang X, Liu Y, Zhang J, et al. C3a and C5a receptor antagonists ameliorate endothelial-myofibroblast transition via the Wnt/β-catenin signaling pathway in diabetic kidney disease. *Metabolism*. (2015) 64:597–610. doi: 10.1016/j.metabol.2015.01.014
234. Zhang K, Lu Y, Harley KT, Tran M-H. Atypical hemolytic uremic syndrome: a brief review. *Hematol Rep*. (2017) 9:7053. doi: 10.4081/hr.2017.7053
235. Fakhouri F, Zuber J, Frémeaux-bacchi V, Loirat C. Haemolytic uraemic syndrome. *Lancet*. (2017) 390:681–96. doi: 10.1016/S0140-6736(17)30062-4
236. Lin S-L, Kisseleva T, Brenner DA, Duffield JS. Pericytes and perivascular fibroblasts are the primary source of collagen-producing cells in obstructive fibrosis of the kidney. *Am J Pathol*. (2008) 173:1617–27. doi: 10.2353/ajpath.2008.080433
237. Sun YBY, Qu X, Caruana G, Li J. The origin of renal fibroblasts/myofibroblasts and the signals that trigger fibrosis. *Differentiation*. (2016) 92:102–7. doi: 10.1016/j.diff.2016.05.008
238. Gomez IG, Duffield JS. The FOXD1 lineage of kidney perivascular cells and myofibroblasts: functions and responses to injury. *Kidney Int Suppl*. (2014) 4:26–33. doi: 10.1038/kisup.2014.6
239. Sim RB, Schwaeble W, Fujita T. Complement research in the 18th-21st centuries: Progress comes with new technology. *Immunobiology*. (2016) 221:1037–45. doi: 10.1016/j.imbio.2016.06.011
240. van Kooten C, Fiore N, Trouw LA, Csomor E, Xu W, Castellano G, et al. Complement production and regulation by dendritic cells: Molecular switches between tolerance and immunity. *Mol Immunol*. (2008) 45:4064–72. doi: 10.1016/j.molimm.2008.07.015
241. Rogers NM, Ferenbach DA, Isenberg JS, Thomson AW, Hughes J. Dendritic cells and macrophages i. the kidney: a spectrum of good and evil. *Nat Rev Nephrol*. (2014) 10:625–43. doi: 10.1038/nrneph.2014.170
242. Gu H, Mickler EA, Cummings OW, Sandusky GE, Weber DJ, Gracon A, et al. Crosstalk between TGF-β1 and complement activation augments epithelial injury in pulmonary fibrosis. *FASEB J*. (2014) 28:4223–34. doi: 10.1096/fj.13-247650
243. Luque A, Serrano I, Aran JM. Complement components as promoters of immunological tolerance in dendritic cells. *Semin Cell Dev Biol*. (2019) 85:143–52. doi: 10.1016/j.semcdb.2017.11.022
244. Castellano G, Woltman AM, Schlagwein N, Xu W, Schena FP, Daha MR, et al. Immune modulation of human dendritic cells by complement. *Eur J Immunol*. (2007) 37:2803–11. doi: 10.1002/eji.200636845
245. Loverre A, Capobianco C, Stallone G, Infante B, Schena A, Ditonno P, et al. Ischemia-reperfusion injury-induced abnormal dendritic cell traffic in the transplanted kidney with delayed graft function. *Kidney Int*. (2007) 72:994–1003. doi: 10.1038/sj.ki.5002468
246. Woltman AM, De Fijter JW, Zuidwijk K, Vlug AG, Bajema IM, Van Der Kooij SW, et al. Quantification of dendritic cell subsets in human renal tissue under normal and pathological conditions. *Kidney Int*. (2007) 71:1001–8. doi: 10.1038/sj.ki.5002187
247. Soos TJ, Sims TN, Barisoni L, Lin K, Littman DR, Dustin ML, et al. CX3CR1+ interstitial dendritic cells form a contiguous network throughout the entire kidney. *Kidney Int*. (2006) 70:591–6. doi: 10.1038/sj.ki.5001567
248. Peng Q, Li K, Patel H, Sacks SH, Zhou W. Dendritic cell synthesis of C3 is required for full T cell activation and development of a Th1 phenotype. *J Immunol*. (2006) 176:3330–41. doi: 10.4049/jimmunol.176.6.3330
249. Zhou W, Peng Q, Li K, Sacks SH. Role of dendritic cell synthesis of complement in the allospecific T cell response. *Mol Immunol*. (2007) 44:57–63. doi: 10.1016/j.molimm.2006.06.012
250. Kranich J, Krautler NJ. How follicular dendritic cells shape the B-cell antigenome. *Front Immunol*. (2016) 7:225. doi: 10.3389/fimmu.2016.00225
251. Heyman B, Wiersma EJ, Kinoshita T. In vivo inhibition of the antibody response by a complement receptor-specific monoclonal antibody. *J Exp Med*. (1990) 172:665–8. doi: 10.1084/jem.172.2.665
252. Krautler NJ, Kana V, Kranich J, Tian Y, Perera D, Lemm D, et al. Follicular dendritic cells emerge from ubiquitous perivascular precursors. *Cell*. (2012) 150:194–206. doi: 10.1016/j.cell.2012.05.032
253. Sheen J-H, Strainic MG, Liu J, Zhang W, Yi Z, Medof ME, et al. TLR-induced murine dendritic cell (DC) activation requires DC-intrinsic complement. *J Immunol*. (2017) 199:278–91. doi: 10.4049/jimmunol.1700339
254. Ricklin D, Barratt-Due A, Mollnes TE. Complement in clinical medicine: clinical trials, case reports and therapy monitoring. *Mol Immunol*. (2017) 89:10–21. doi: 10.1016/j.molimm.2017.05.013
255. Giordano M, Castellano G, Messina G, Divella C, Bellantuono R, Puteo F, et al. Preservation of renal function in atypical hemolytic uremic syndrome by eculizumab: a case report. *Pediatrics*. (2012) 130:e1385–8. doi: 10.1542/peds.2011-1685
256. Fiorentino M, Grandaliano G, Gesualdo L, Castellano G. Acute kidney injury to chronic kidney disease transition. *Contrib Nephrol*. (2018) 193:45–54. doi: 10.1159/000484962
257. Giordano P, Netti GS, Santangelo L, Castellano G, Carbone V, Torres DD, et al. A pediatric neurologic assessment score may drive the eculizumab-based treatment of *Escherichia coli*-related hemolytic uremic syndrome with neurological involvement. *Pediatr Nephrol*. (2019) 34:517–27. doi: 10.1007/s00467-018-4112-2
258. Grenda R, Durlik M. Eculizumab in renal transplantation: a 2017 update. *Ann Transplant*. (2017) 22:550–4. doi: 10.12659/aot.905917
259. Stegall MD, Diwan T, Raghavaiah S, Cornell LD, Burns J, Dean PG, et al. Terminal complement inhibition decreases antibody-mediated rejection in sensitized renal transplant recipients. *Am J Transplant*. (2011) 11:2405–13. doi: 10.1111/j.1600-6143.2011.03757.x
260. Kaabak M, Babenko N, Shapiro R, Zokoyev A, Dymova O, Kim E. A prospective randomized, controlled trial of eculizumab to prevent ischemia-reperfusion injury in pediatric kidney transplantation. *Pediatr Transplant*. (2018) 22:e13129. doi: 10.1111/petr.13129
261. Tatapudi VS, Montgomery RA. Pharmacologic complement inhibition in clinical transplantation. *Curr Transplant Rep*. (2017) 4:91–100. doi: 10.1007/s40472-017-0148-7
262. Vo AA, Zeevi A, Choi J, Cisneros K, Toyoda M, Kahwaji J, et al. A phase I/II placebo-controlled trial of C1-inhibitor for prevention of antibody-mediated rejection in HLA sensitized patients. *Transplantation*. (2015) 99:299–308. doi: 10.1097/TP.0000000000000592

263. Jordan SC, Choi J, Aubert O, Haas M, Loupy A, Huang E, et al. A phase I/II, double-blind, placebo-controlled study assessing safety and efficacy of C1 esterase inhibitor for prevention of delayed graft function in deceased donor kidney transplant recipients. *Am J Transplant*. (2018) 18:2955–64. doi: 10.1111/ajt.14767
264. Montgomery RA, Orandi BJ, Racusen L, Jackson AM, Garonzik-Wang JM, Shah T, et al. Plasma-derived C1 esterase inhibitor for acute antibody-mediated rejection following kidney transplantation: results of a randomized double-blind placebo-controlled Pilot study. *Am J Transplant*. (2016) 16:3468–78. doi: 10.1111/ajt.13871
265. Viglietti D, Gosset C, Loupy A, Deville L, Verine J, Zeevi A, et al. C1 inhibitor in acute antibody-mediated rejection nonresponsive to conventional therapy in kidney transplant recipients: a Pilot study. *Am J Transplant*. (2016) 16:1596–603. doi: 10.1111/ajt.13663
266. Mastellos DC, Yancopoulou D, Kokkinos P, Huber-Lang M, Hajishengallis G, Biglarnia AR, et al. Compstatin: a C3-targeted complement inhibitor reaching its prime for bedside intervention. *Eur J Clin Invest*. (2015) 45:423–40. doi: 10.1111/eci.12419
267. Keshavjee S, Davis RD, Zamora MR, de Perrot M, Patterson GA. A randomized, placebo-controlled trial of complement inhibition in ischemia-reperfusion injury after lung transplantation in human beings. *J Thorac Cardiovasc Surg*. (2005) 129:423–8. doi: 10.1016/j.jtcvs.2004.06.048
268. Xiao F, Ma L, Zhao M, Smith RA, Huang G, Jones PM, et al. APT070 (mirococept), a membrane-localizing C3 convertase inhibitor, attenuates early human islet allograft damage in vitro and in vivo in a humanized mouse model. *Br J Pharmacol*. (2016) 173:575–87. doi: 10.1111/bph.13388
269. Kassimatis T, Qasem A, Douiri A, Ryan EG, Rebollo-Mesa I, Nichols LL, et al. A double-blind randomised controlled investigation into the efficacy of Mirococept (APT070) for preventing ischaemia reperfusion injury in the kidney allograft (EMPIRIKAL): study protocol for a randomised controlled trial. *Trials*. (2017) 18:255. doi: 10.1186/s13063-017-1972-x
270. Wong RS, Pullon HWH, Deschatelets P, Francois CG, Hamdani M, Issaragrisil S, et al. Inhibition of C3 with APL-2 results in normalisation of markers of intravascular and extravascular hemolysis in patients with paroxysmal nocturnal hemoglobinuria (PNH). *Blood*. (2018) 32(Suppl. 1):2314. doi: 10.1182/blood-2018-99-110827
271. Merkel PA, Niles J, Jimenez R, Spiera RF, Rovin BH, Bomback A, et al. A randomized clinical trial of CCX168, an orally administered C5AR inhibitor for treatment of patients with ANCA-associated vasculitis. *Arthritis Rheumatol*. (2016). 68 (suppl 10):1297. doi: 10.1002/art.39977
272. Ricklin D, Lambris JD. New milestones ahead in complement-targeted therapy. *Semin Immunol*. (2016) 28:208–22. doi: 10.1016/j.smim.2016.06.001

Conflict of Interest: The authors declare that the research was conducted in the absence of any commercial or financial relationships that could be construed as a potential conflict of interest.

frontiers in Immunology

CORRECTION
published: 08 January 2021
doi: 10.3389/fimmu.2020.630855

Corrigendum: Inflammaging and Complement System: A Link Between Acute Kidney Injury and Chronic Graft Damage

Rossana Franzin[1,2*], *Alessandra Stasi*[1], *Marco Fiorentino*[1], *Giovanni Stallone*[3], *Vincenzo Cantaluppi*[2], *Loreto Gesualdo*[1] and *Giuseppe Castellano*[1,3*]

[1] Nephrology, Dialysis and Transplantation Unit, Department of Emergency and Organ Transplantation, University of Bari Aldo Moro, Bari, Italy, [2] Department Translational Medicine, University of Piemonte Orientale, Novara, Italy, [3] Nephrology, Dialysis and Transplantation Unit, Department of Medical and Surgical Sciences, University of Foggia, Foggia, Italy

OPEN ACCESS

Approved by:
Frontiers Editorial Office,
Frontiers Media SA, Switzerland

***Correspondence:**
Rossana Franzin
rossanafranzin@hotmail.it
Giuseppe Castellano
giuseppe.castellano@unifg.it;
castellanogiuseppe74@gmail.com

Specialty section:
This article was submitted to Molecular Innate Immunity, a section of the journal Frontiers in Immunology

Received: 18 November 2020
Accepted: 08 December 2020
Published: 08 January 2021

Citation:
Franzin R, Stasi A, Fiorentino M, Stallone G, Cantaluppi V, Gesualdo L and Castellano G (2021) Corrigendum: Inflammaging and Complement System: A Link Between Acute Kidney Injury and Chronic Graft Damage. Front. Immunol. 11:630855. doi: 10.3389/fimmu.2020.630855

Keywords: renal aging, complement system, AKI-to-CKD transition, cellular senescence and SASP, complement, inhibition therapy

A Corrigendum on

Inflammaging and Complement System: A Link Between Acute Kidney Injury and Chronic Graft Damage

By Franzin R, Stasi A, Fiorentino M, Stallone G, Cantaluppi V, Gesualdo L and Castellano G (2020). Front. Immunol. 11:734. doi: 10.3389/fimmu.2020.00734

MISSING FUNDING

In the original article, we neglected to include the funder the Italian Ministry of Health (AIM 1810057-activity 2 granted to AS; Giovani Ricercatori GR-2009-1608662 granted to GC).

The authors apologize for this error and state that this does not change the scientific conclusions of the article in any way. The original article has been updated.

frontiers in Immunology

ORIGINAL RESEARCH
published: 29 January 2021
doi: 10.3389/fimmu.2020.594849

Complement Activation in Kidneys of Patients With COVID-19

Frederick Pfister[1†], Eva Vonbrunn[1†], Tajana Ries[1], Hans-Martin Jäck[2], Klaus Überla[3], Günter Lochnit[4], Ahmed Sheriff[5], Martin Herrmann[6], Maike Büttner-Herold[1], Kerstin Amann[1] and Christoph Daniel[1]*

[1] Department of Nephropathology, Institute of Pathology, Friedrich-Alexander-University (FAU) Erlangen-Nürnberg, Erlangen, Germany, [2] Nikolaus-Fiebinger-Center FAU, Department of Medicine 3, Division of Molecular Immunology, Friedrich-Alexander-University (FAU) Erlangen-Nürnberg, Erlangen, Germany, [3] Department of Virology, Friedrich-Alexander-University (FAU) Erlangen-Nürnberg, Erlangen, Germany, [4] Department of Biochemistry, Division Protein Analystics, Justus-Liebig-University Giessen, Giessen, Germany, [5] Pentracor GmbH, Henningsdorf, Germany, [6] Department of Medicine 3, Institute for Rheumatology and Immunology, Friedrich-Alexander-University (FAU) Erlangen-Nürnberg, Erlangen, Germany

OPEN ACCESS

Edited by:
Robert Braidwood Sim, University of Oxford, United Kingdom

Reviewed by:
Felix Poppelaars, University Medical Center Groningen, Netherlands
Cees Van Kooten, Leiden University, Netherlands
Steven Howard Sacks, King's College London, United Kingdom

***Correspondence:**
Christoph Daniel
Christoph.Daniel@uk-erlangen.de

[†]These authors have contributed equally to this work

Specialty section:
This article was submitted to Molecular Innate Immunity, a section of the journal Frontiers in Immunology

Received: *14 August 2020*
Accepted: *22 December 2020*
Published: *29 January 2021*

Citation:
Pfister F, Vonbrunn E, Ries T, Jäck H-M, Überla K, Lochnit G, Sheriff A, Herrmann M, Büttner-Herold M, Amann K and Daniel C (2021) Complement Activation in Kidneys of Patients With COVID-19. Front. Immunol. 11:594849. doi: 10.3389/fimmu.2020.594849

Most patients who became critically ill following infection with COVID-19 develop severe acute respiratory syndrome (SARS) attributed to a maladaptive or inadequate immune response. The complement system is an important component of the innate immune system that is involved in the opsonization of viruses but also in triggering further immune cell responses. Complement activation was seen in plasma adsorber material that clogged during the treatment of critically ill patients with COVID-19. Apart from the lung, the kidney is the second most common organ affected by COVID-19. Using immunohistochemistry for complement factors C1q, MASP-2, C3c, C3d, C4d, and C5b-9 we investigated the involvement of the complement system in six kidney biopsies with acute kidney failure in different clinical settings and three kidneys from autopsy material of patients with COVID-19. Renal tissue was analyzed for signs of renal injury by detection of thrombus formation using CD61, endothelial cell rarefaction using the marker E-26 transformation specific-related gene (ERG-) and proliferation using proliferating cell nuclear antigen (PCNA)-staining. SARS-CoV-2 was detected by *in situ* hybridization and immunohistochemistry. Biopsies from patients with hemolytic uremic syndrome (HUS, n = 5), severe acute tubular injury (ATI, n = 7), zero biopsies with disseminated intravascular coagulation (DIC, n = 7) and 1 year protocol biopsies from renal transplants (Ctrl, n = 7) served as controls. In the material clogging plasma adsorbers used for extracorporeal therapy of patients with COVID-19 C3 was the dominant protein but collectin 11 and MASP-2 were also identified. SARS-CoV-2 was sporadically present in varying numbers in some biopsies from patients with COVID-19. The highest frequency of CD61-positive platelets was found in peritubular capillaries and arteries of COVID-19 infected renal specimens as compared to all controls. Apart from COVID-19 specimens, MASP-2 was detected in glomeruli with DIC and ATI. In contrast, the classical pathway (i.e. C1q) was hardly seen in COVID-19 biopsies. Both C3 cleavage products C3c and C3d were strongly detected in renal arteries but also occurs in glomerular capillaries of COVID-19 biopsies, while tubular C3d was stronger than C3c in biopsies from COVID-19 patients. The membrane attack complex C5b-9, demonstrating terminal pathway

activation, was predominantly deposited in COVID-19 biopsies in peritubular capillaries, renal arterioles, and tubular basement membrane with similar or even higher frequency compared to controls. In conclusion, various complement pathways were activated in COVID-19 kidneys, the lectin pathway mainly in peritubular capillaries and in part the classical pathway in renal arteries whereas the alternative pathway seem to be crucial for tubular complement activation. Therefore, activation of the complement system might be involved in the worsening of renal injury. Complement inhibition might thus be a promising treatment option to prevent deregulated activation and subsequent collateral tissue injury.

Keywords: complement—immunological term, COVID-19, kidney, endothelial injury, lectin pathway activation

INTRODUCTION

Patients who became critically ill due to SARS-Cov2 virus infection developed severe acute respiratory distress syndrome (ARDS). ARDS is induced by damage of lung alveoli by endothelial injury followed by a maladaptive immune response (1). Tissue damage is not restricted to the respiratory tract since patients with severe COVID-19 often developed multiorgan failure including cardiac and acute kidney injury (2, 3). In a consecutive study of 701 patients with COVID-19 hospitalized in Wuhan, 44% and 27% had proteinuria and hematuria on admission, respectively (4). Furthermore, kidney disease in COVID-19 patients was associated with in-hospital mortality (3). While some reports suggested a direct viral infection of the kidney with infection of glomerular (5) and tubular cells (6–8) other studies support indirect pathomechanisms (9–11). Histopathological findings in postmortem renal biopsies (8, 10, 11) or native and allograft kidney biopsies (9) reported a wide spectrum of glomerular and tubular injury. However, by far the most common renal complication is acute kidney injury (AKI) (8–11). Additionally, scarce focal kidney fibrin thrombi occur (11). The pathophysiology of COVID-19–induced kidney damage is not well understood, but is primarily a result of the host immune response driving hypercytokinemia and aggressive inflammation (12, 13). The cytokine storm that causes lung injury associated with infections is reportedly driven by factors of the complement system (14), which as part of the innate immune system plays an important role in defense against infections. Complement opsonizes viruses or bacteria, activates and attracts leukocytes and lyses bacteria and cells (15). The complement system can be activated by three different pathways, (i) the classical pathway, activated by any structure that is recognized by C1q (16), (ii) the lectin pathway, activated when mannan-binding lectin-associated serine protease 2 (MASP-2) complexes with mannose-binding lectin (MBL), ficolins, or collectin-11 bound to saccharide patterns expressed on bacteria or cells (17, 18) and (iii) the alternative pathway, activated through spontaneous hydrolysis of C3 (19). All complement activation pathways form C3 convertases, which finally initiate the formation of the C5 convertase, which leads to the assembly of C5b-9, the terminal membrane attack complex. In addition, cleavage products C3a and C5a serve as anaphylatoxins that activate and attract leukocytes (15). Since complement activation could be detected in plasma (20), lung and skin (21) from COVID-19 patients and seems to be involved in promoting inflammatory processes that lead to tissue damage in COVID-19 patients we here investigated complement activation in six renal biopsies and three postmortem kidneys from patients with COVID-19. Complement involvement was compared to renal biopsies of acute tubular injury (ATI), known kidney diseases with distinct endothelial cell injury including hemolytic uremic syndrome (HUS) and disseminated intravascular coagulation (DIC) and a control group of 1 year protocol biopsies from stable renal transplants (Ctrl).

MATERIALS AND METHODS

Analysis of Plasma Adsorber–Bound Proteins

Plasma adsorbers (Pentracor CRP, Pentracor, Henningsdorf, Germany) that clogged during the treatment of critically ill COVID-19 patients were analyzed to study proteins involved in this plasma reaction. A sample of 0.5 ml agarose (plasma adsorber material) was washed with 25 ml of 0.9% NaCl solution to remove unbound proteins. After that, 0.5 ml of 2 mg/ml DNase I (Roche, in 10 mM Tris HCl, 2.5 mM $MgCl_2$ and 0.5 mM $CaCl_2$, pH 7.6) was added and the mixture was incubated for 30 min at 37°C on a tilt shaker. The DNase I and released proteins were eluted with 5 ml PBS, boiled for 15 min in reducing SDS-buffer (10% SDS in 250 mM Tris pH 6.8 supplemented with 2.83 M mercaptoethanol) and then separated by gradient SDS polyacrylamide gel electrophoresis (4–20% Acrylamid). Bands of interest were excised from gels and the proteins were digested with trypsin (10 ng/µl sequencing grade Promega, Mannheim). Tryptic peptides were eluted from the gel slices with 1% trifluoric acid.

Matrix-Assisted Laser-Desorption Ionization Time-of-Flight Mass Spectrometry (MALDI-TOF-MS) and Protein Identification

MALDI-TOF-MS was performed on an Ultraflex TOF/TOF mass spectrometer (Bruker Daltonics, Bremen) equipped with a nitrogen laser and a LIFT-MS/MS facility. The instrument was

operated in the positive-ion reflectron mode using 2.5-dihydroxybenzoic acid and methylendiphosphonic acid as matrix. Sum spectra consisting of 200–400 single spectra were acquired. For data processing and instrument control the Compass 1.4 software package consisting of FlexControl 4.4, FlexAnalysis 3.4 4, Sequence Editor and BioTools 3.2 and ProteinScape 3.1. were used. External calibration was performed with a peptide standard (Bruker Daltonics).

Proteins were identified by MASCOT peptide mass fingerprint search (http://www.matrixscience.com) using the Uniprot Human database (version 20200226, 210438 sequence entries; $p<0.05$). For the search, a mass tolerance of 75 ppm was allowed and oxidation of methionine as the variable modification was used.

Human Renal Tissue Specimens

To evaluate the relevance of complement in mediation of renal pathological changes during COVID-19 we used six formalin-fixed paraffin-embedded (FFPE) kidney biopsies of patients with COVID-19 and renal insufficiency in different clinical settings (four transplant kidneys, one ANCA-associated vasculitis, one multiple organ dysfunction syndrome) and three FFPE autopsy kidneys of patients who died with multiple organ dysfunction syndrome following SARS-CoV-2 infection. Kidney biopsies of patients with hemolytic uremic syndrome (HUS, n = 5), severe acute tubular injury due to septic shock (ATI n = 7), zero-biopsies with disseminated intravascular coagulation (DIC, n = 7) and 1 year protocol biopsies from stable renal transplants (Ctl; n = 7) served as controls. All tissue samples were collected from the archive of the Department of Nephropathology, Friedrich-Alexander-University Erlangen-Nuremberg and analysis was approved by the local Ethics committee (reference number 4415). Patient characteristics of the investigated cases with COVID-19 are described in **Table 1**.

In Situ Hybridization

In situ hybridization, for detection of SARS-CoV-2 RNA in FFPE tissue, was performed using a V nCoV2019-S probe (848561; ACD, Hayward, CA, USA), specific for the S gene encoding the spike protein from SARS-CoV-2, and the RNAscope 2.5 HD RED Kit (ACD). Tissue sections of 4 µm thickness were deparaffinized in xylene, dehydrated in ethanol and blocked with peroxidase. Slides were boiled in kit-provided antigen retrieval buffer at 95°C for 15 min and digested afterwards with protease at 40°C for 30 min. The target probe were hybridized with kidney sections in the HybEZ hybridization oven (ACD) at 40°C for 2 h. Pre-amplification and amplification steps were conducted using kit-provided reagents according to the manufacturer's recommendations. For signal detection sections were incubated with Fast Red substrate for 10 min at room temperature followed by counterstaining with hematoxylin, drying at 60°C for 15 min and mounting with Eco Mount (ACD). The same procedure was used for *in situ* hybridization with the Hs-COLEC11 probe (542431; ACD) for the detection of human collectin 11 mRNA.

Immunohistochemistry

For immunohistochemical stainings formalin-fixed paraffin-embedded (FFPE) kidney biopsies were cut into 2 µm sections, deparaffinized and rehydrated. Antigen retrieval was performed using pronase E (Sigma Aldrich, Taufkirchen, Germany) digestion for 30 min at 37°C (C1q, C3c, C5b-9) or cooking in target retrieval solution pH 6 (DAKO Deutschland GmbH, Hamburg, Germany) for 2.5 min (C3d, C4d, MASP-2, CD61, COVID-19 spike protein). Endogenous peroxidase was blocked with 3% H_2O_2 and unspecific antigens with Avidin-Biotin (Vector laboratories, Burlingame, CA, USA) and normal goat or horse serum in blotto (1:5). The following primary antibodies were diluted in 50 mM Tris pH 7,4 and incubated over-night at 4°C or for 1 h at room temperature: C1q, a rabbit polyclonal antibody against human C1q (A0136; DAKO Deutschland GmbH); C3c, a rabbit polyclonal antibody against human C3c (A0062; DAKO Deutschland GmbH); C3d, a rabbit monoclonal antibody against human C3d (ab136916; Abcam, Cambridge, UK); C5b-9, a mouse monoclonal antibody against human C5b-9 (M0777; DAKO Deutschland GmbH); MASP-2, a rabbit polyclonal antibody against human Mannan-binding lectin serine peptidase 2 (HPA029313; Sigma Aldrich); CD61 a mouse monoclonal antibody against human platelet glycoprotein IIIa (M0753; DAKO Deutschland GmbH), C4d, a rabbit polyclonal antibody against human C4d (BI-RC4D;

TABLE 1 | Clinical, laboratory, and histopathological findings in patients with COVID-19 infection.

Pt	Age	Sex	Biopsy indication	Comorbidities/ circumstances	SARS-CoV-2 infection	PU	Serumcreatinine [mg/dl]	Bx diagnosis
1	40	M	AKI, PU, HU, ANCA positivity	HTN	Current	1 g/g	3,1	ANCA-asso. Crescentic GN, ATN
2	76	M	MODS, AKI	DM	Current	++	7,5	ATN
3	69	M	AKI, ESKD, RTx 2007	DM, HTN, acute enteritis	Current	0,7 g/g	2,1	ATN
4	52	F	AKI, progress PU, ESKD, RTx 2011	DM, HTN	Current	1,5 g/g	1,5	ATN
5	70	M	AKI, ESKD, RTx	Bacterial pneumonia	Current	++	1,4	ATN, infect-asso.GN, cellular borderline changes
6	35	M	AKI, progress PU, ESKD, RTx 2019	–	Current	1,5 g/g	2,1	ATN, recurrent FSGS
7	41	F	ARDS, MODS, AKI, post-mortem	Pregnancy (32gw)	Current	Nd	Nd	ATN
8	64	M	ARDS, MODS, AKI, post-mortem	HTN	Current	Nd	Nd	ATN
9	71	M	ARDS, MODS, AKI, LE, post-mortem	HTN	Current	Nd	Nd	ATN

Pt, patient; M, male; F, female; PU, proteinuria measured as g proteinuria/g creatinine or dipstick; HU, hematuria; AKI, acute kidney insufficiency; ESKD, end-stage kidney disease; RTx, renal transplantation; ARDS, acute respiratory distress syndrome; MODS, multiple organ dysfunction syndrome; HTN, hypertension; DM, diabetes mellitus; ATN, acute tubular necrosis; FSGS, focal-segmental glomerulosclerosis; ANCA, anti-neutrophilic cytoplasmatic antibody; GN, glomerulonephritis; Nd, unknown.

Biomedica, Vienna, Austria) and SARS-CoV-2 spike protein, a mouse monoclonal antibody against SARS-CoV-2 spike protein (clone 224.2, kindly provided by M.-H. Jäck, Department of Molecular Immunology, FAU Erlangen-Nürnberg). After washing with 50 mM Tris pH 7.4, sections were incubated with biotinylated secondary goat anti-rabbit IgG (BA-1000; Vector laboratories) or horse anti-mouse IgG (BA-2001, Vector laboratories). Detection of bound antibodies was conducted using ABC-Kit and DAB-Impact as a substrate (both from Vector laboratories), while nuclei were counter stained with hematoxylin. For negative controls primary antibody was substituted by antibody dilution buffer (50 mM Tris pH 7,4) (**Supplemental Figure 3**). An overview with representative stainings of all cases is shown in **Supplemental Figure 2**.

Immunofluorescence Double Staining

For evaluation of endothelial cell injury and proliferative activity we performed immunofluorescence double staining on rehydrated FFPE kidney sections using a rabbit anti-human E26-transformation- specific related gene (ERG) antibody for detection of endothelial cells (diluted 1:100 in 50 mM Tris pH 7,4; EP111, Cell Marque, Rocklin, CA, USA) and a mouse anti-human proliferating cell nuclear antigen (PCNA, M0879, diluted 1:1000 in 50 mM Tris pH 7.4; DAKO Deutschland GmbH, Hamburg Germany). After dewaxing, sections were incubated with primary antibodies over-night at 4°C followed by washing with 50 mM Tris pH 7.4 supplemented with 0.05% Tween 20. A donkey anti-rabbit IgG Alexa Fluor 568 and a donkey anti-mouse IgG Alexa633 (both from Thermo Fisher Scientific, Waltham, MA, USA) were used as secondary antibodies diluted 1:200 in 50 mM Tris pH 7.4 and incubated at room temperature for 30 min. After subsequent washing, cell nuclei were stained with DAPI (diluted 0.2 µg/ml in distilled water) for 5 min, followed by rinsing in Tris buffer. Finally, sections were covered with Mowiol mounting medium (Calbiochem, La Jolla, USA) and analyzed using laser scanning confocal microscopy (LSM Zeiss 710) and quantification of fluorescence positive area by Zen software (Zeiss GmbH, Jena, Germany).

Semi-Quantitative Evaluation of Complement and CD61 in Renal Biopsies

Complement staining in renal biopsies was graded in different vascular compartments of the kidney (i.e. in the glomeruli, peritubular capillaries and arteries), using a semi-quantitative immunohistochemical staining score (score 0, 1 or 2), which describes the distribution and intensity of staining signal in the micro- and macrovascular structures. In detail for CD61, score 0 was defined as no positive thrombocytes within vascular lumina, score 1 was defined as single/scattered positive thrombocytes in vascular lumina and score 2 was defined as presence of intravascular thrombocyte aggregates of any size. For the components of the complement system (C1q, C3c, C3d, C4dC5b-9, MASP-2) score 0 was defined as no specific granular reactivity along endothelial cell surfaces in the different vascular compartments or tubular basement membrane, score 1 was defined as minimal reactivity in single glomeruli and peritubular capillaries and mild reactivity along endothelial cells or in the intima of arteries and focal reactivity along the tubular basement membrane and score 2 was defined as reactivity in > 10% to 20% of glomeruli and peritubular capillaries and moderate reactivity in the majority (>50%) of arteries and diffuse clear reactivity along tubular basement membranes.

Transient Expression of SARS-CoV-2 Spike Protein

Cells producing membrane-anchored CoV-2 spike protein cells were established by co-transfecting HEK 293T with the PEI method with a GFP reporter plasmid and a pCG1-based expression vector for the spike protein of SARS-CoV-2 (position 21580 – 25400 from accession no. NC_045512).

Generation of Anti-SARS-CoV-2 Spike Protein Ab

The monoclonal IgG2c antibody against the CoV-2 spike protein was isolated from a hybridoma line that was established by the conventional hybridoma technology from spleen cells of Trianni mice that were immunized with DNA-encoding CoV-2 spike protein and purified CoV-2 spike protein. The Trianni mouse line (Patent US 2013/0219535 A1) carried the complete repertoire of human variable region gene segments of immunoglobulin (Ig) heavy (HC) and L chains (LC).

Statistical Analyses

After testing for normal distribution of values using Kolmogorov-Smirnov test, data were analyzed using Kruskal-Wallis test with Dunn's Multiple Comparison test as *post hoc* test for comparison of multiple groups. In all tests $p<0.05$ was accepted as statistically significant. Statistical analyses were performed using GraphPad Prism 8 for Windows software (version 8.3, GraphPad software Inc., San Diego, CA, USA).

RESULTS

Complement C3 Was the Main Component in Clotted Plasma Adsorber From Patients With COVID-19

When seriously ill patients with COVID-19 in our clinic were connected to plasma absorption columns for therapeutic purposes, we observed that these columns quickly clogged. From more than 90 patients treated with CRP apheresis with various diseases (including severe myocardial infarction (STEMI), cardiogenic shock, after bypass surgery, severe COVID-19, acute pancreatitis, sepsis, SIRS after failed bypass surgery) the massive clogging of the columns only occurred in patients with severe COVID-19. In patients with heart attack much smaller clots were observed on the sieve filters but not on the adsorber material. To identify the proteins that are involved in this clot-forming reaction of the plasma, the proteins were detached from the adsorber material and sieve filters by treatment with DNase1 and separated by electrophoresis.

Individual bands were digested with trypsin and finally examined by MALDI-TOF (**Figure 1A**). First, we analyzed the most prominent bands of an electrophoretic separation in an unbiased manner for the major peptides and detected C3 and C3 fragments with a sequence coverage of 52% (**Figure 1B**). Next, we analyzed the candidate peptides of mannose-binding protein-associated serine protease 2 (MASP-2) and collectin 11 involved in complement activation *via* the lectin pathway and detected both molecules (MASP-2; sequence coverage 12%) and collectin 11 (sequence coverage 33%) (**Figure 1B**). MASP-2. In contrast, the investigation of the clots from treatment of heart attack patients showed haptoglobin as main component and only little C3a (data not shown). This finding might indicate an important role of complement in the pathogenesis of COVID-19 disease and encouraged us to investigate complement activation in the kidneys of COVID-19 patients in more detail.

Histopathology, Proliferative Activity, and Loss of Endothelial Cells in Kidneys From Patients With COVID-19

In this study, six kidney biopsies of patients with COVID-19 infection (four transplant kidneys, 1 ANCA-associated vasculitis, one multiple organ dysfunction syndrome) and three autopsy kidneys of patients who died with multiple organ dysfunction syndrome following COVID-19 infection were analyzed (**Table 1**). In all tissue samples a moderate to severe acute tubular injury (ATI) with tubular dilatation and vacuolization of swollen tubular epithelial cells was found (**Figure 2A**) and in one of the postmortem tissue samples isolated glomerular microthrombi were present (**Figure 2B**). In addition, an infect-associated glomerulonephritis (most likely related to a bacterial pneumonia the patient developed secondary to the COVID-19) was diagnosed in one proteinuric transplant patient (patient 5), accompanied by acute T-cell mediated borderline-rejection. Another proteinuric transplant patient suffered from recurrence of podocytopathy with focal-segmental glomerulosclerosis in the transplanted kidney and in the biopsy of patient 1 an ANCA-associated crescentic glomerulonephritis was diagnosed. SARS-CoV-2 was sporadically detected by *in situ* hybridization in renal tubules and endothelial cells in six of nine kidney specimens of patients with COVID-19 (**Figure 2C**). However, renal infection with COVID-19 could be confirmed in only one case by immunohistochemistry with an antibody directed against the SARS-CoV-2 spike protein (**Figure 2D**), indicating at least low renal virus load. In contrast, this antibody sensitively recognized paraffin embedded HEK293T cells transfected with SARS-CoV-2 spike protein (**Figure 2E**). To further assess renal damage in patients with COVID-19, we examined proliferating cell nuclear antigen (PCNA) as a marker of increased repair and the expression of the endothelial cell marker ERG in COVID-19 kidney biopsies and compared these to biopsies of kidney diseases characterized by tubular or endothelial damage. Compared to biopsies with hemolytic uremic syndrome (HUS) the kidneys of patients with COVID-19 (COV) showed significantly lower proliferative activity measured as PCNA positive area, which was comparably low to those of biopsies with acute tubular injury (ATI), disseminated intravascular coagulation (DIC) and in 1 year protocol biopsies that served as controls (Ctrl) (**Figures 3A, C–G**, green staining). Capillarization of COVID-19 biopsies, measured as ERG-positive area, was less 50% and 40% than in Ctrl and HUS (**Figures 3B, C, E, G**, red staining). Only DIC showed higher endothelial cell loss while endothelial cell loss in ATI was comparable to COV (**Figures 3B, D, F**).

Thrombus-Forming CD61-Positive Platelets Were Frequently Detected in Kidneys From Patients With COVID-19

First, we investigated CD61-positive platelets in COVID-19 renal biopsies, which are involved in thrombus formation and detected glomerular CD61-positive platelets in 8/9 of the COVID-19 cases (**Figures 4A, B**). Glomerular CD61-positive platelets were comparable in Ctrl and COVID-19, and decreased compared to DIC and HUS glomeruli but ATI had the lowest number of CD61-positive platelets (**Figure 3A**). In peritubular capillaries and renal arteries, CD61-positive platelets counts were higher in COVID-19 biopsies as compared to DIC, HUS and ATI and Ctrl (**Figures 4C–F**). The overall score for CD61, summarizing the scores of all three vascular beds, was highest in COVID-19 compared to all controls (**Table 2**).

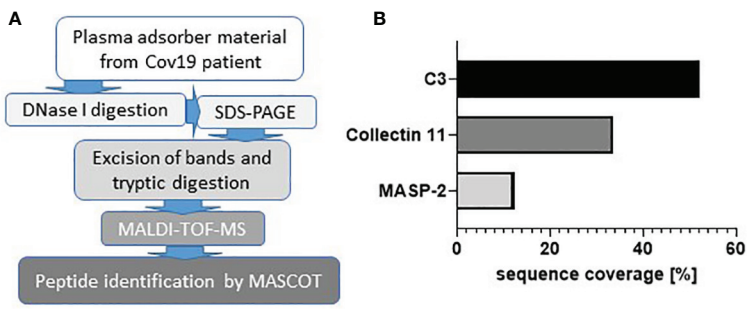

FIGURE 1 | Involvement of complement components in COVID-19. Workflow for the analysis of clotted material isolated from plasma adsorber material collected from treated COVID-19 patient **(A)**. Coverage rates of complement factors C3, collectin 11, and mannose-binding protein-associated serine protease 2 (MASP-2) analyzed by MALDI-TOF **(B)**.

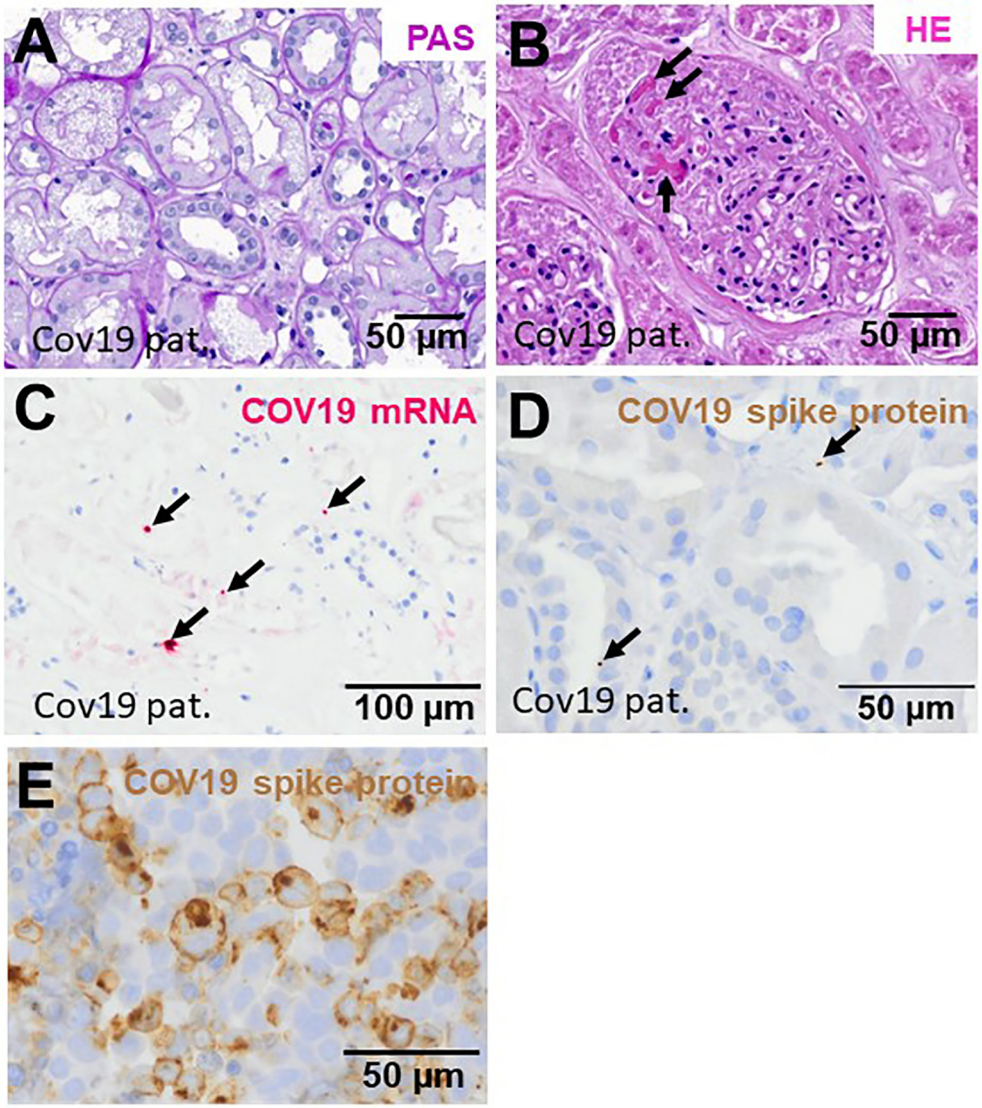

FIGURE 2 | Renal injury in kidney biopsies from patients infected with SARS-CoV-2. Representative pictures of a PAS-stained COVID-19 renal biopsy showing acute tubular injury with swollen and vacuolized cells **(A)** and glomerular microthrombi in HE-stained section (**B**, arrows). In situ hybridization for SARS-CoV-2 mRNA showed few positive signals in tubular and endothelial localization (**C**, pink signals marked by arrows). Immunohistochemistry for SARS-CoV-3 spike protein detected sporadic positive signals in renal biopsies from patients with COVID-19 (**D**, brown signals marked by arrows). As positive control, we employed HEK293T cells transfected with a plasmid expressing SARS-CoV-2 spike protein, fixed with formalin, embedded in paraffin followed by staining of sections by immunohistochemistry using anti-SARS-CoV-2 spike antibody (**E**, brown staining).

Marked Complement Activation Occurs in Kidney Vascular Beds of Patients With COVID-19

As first complement factor, we detected the glomerular deposition of MASP-2, a serine protease, that complexes with the lectin pathway initiators (MBL, ficolins, and collectins) and becomes activated upon binding to the lectin ligand and found it in 2/9 of the COVID-19 biopsies. Compared to COVID-19 glomerular MASP-2 expression was higher in DIC, comparable in Ctrl, slightly lower in ATI and did not occur at all in HUS (**Figures 5A, B**). Additionally, in peritubular capillaries and renal arteries, MASP-2 was detected in only 22% 2/9 of cases from patients with COVID-19 respectively, but could otherwise only be detected in renal arteries of HUS and in peritubular capillaries in HUS and ATI groups and not at all in the Ctrl biopsies (**Figures 5C–F**). Next, we studied the renal deposition of C1q, which is part of the classical pathway (**Figure 6**). We rarely detected C1q in glomerular and peritubular capillaries in a single COVID-19 biopsy (1/9), which was comparable to Ctrl. In HUS and DIC renal biopsies it was present in the glomeruli of all

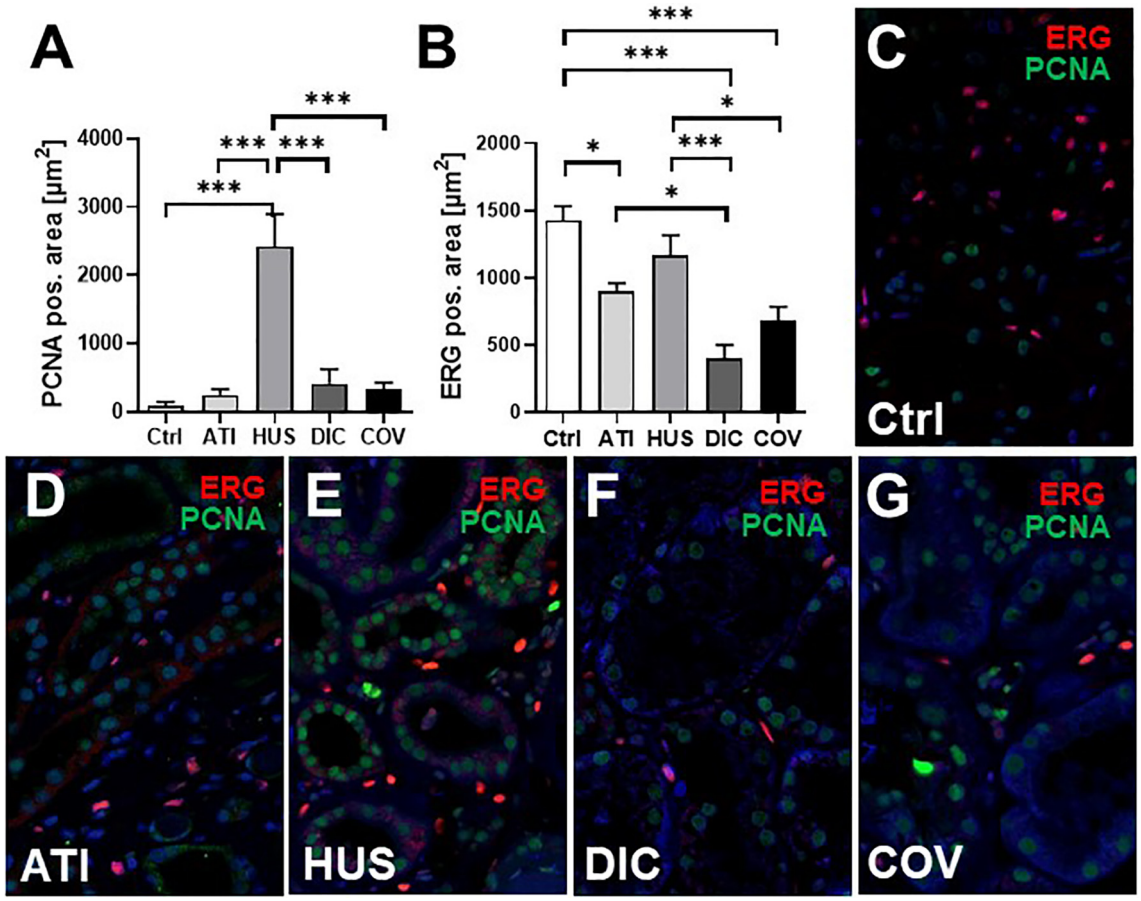

FIGURE 3 | Endothelial rarefaction and proliferative activity in kidney biopsies from patients infected with SARS-CoV-2. Renal proliferation, as assessed by PCNA-staining **(A)** and ERG-positive endothelial cells **(B)** were evaluated by immunofluorescence staining analyzed by confocal microscopy and quantification by ZEN-software in COVID-19 biopsies (COV, n = 7) compared to renal control biopsies taken 1 year after transplantation (Ctrl, n=7), biopsies with acute tubular injury (ATI, n = 7), hemolytic uremic syndrome (HUS, n = 5) and disseminated intravascular coagulation (DIC, n = 7). Representative pictures of immunofluorescence double staining showing PCNA (green staining) and ERG (red staining) double staining were shown in biopsies of Ctrl **(C)**, ATI **(D)**, HUS **(E)**, DIC **(F)**, and COV **(G)**. *$p < 0.05$; ***$p < 0.001$.

biopsies and peritubular capillaries in 40% to 60% of the biopsies (**Figures 6A–D**). In COVID-19, C1q deposition in the renal arteries was seen in 4/9 of biopsies (**Figures 6E, F**) and even more commonly in HUS and DIC (**Figure 6E**). In Ctrl C1q deposition was slightly lower compared to COVID-19 while renal biopsies of patients with ATI showed no C1q deposition at all (**Figures 6A, C, E**). Next, we analyzed fragments of C3 that are formed by all complement pathways: C3c, a stable activation fragment and C3d an activation fragment that is able to covalently bind to surfaces. The stable C3 fragment C3c was detectable in the glomeruli of 4/9 of the COVID-19 biopsies, while glomerular C3c signals were comparable in ATI and more frequent and stronger in HUS and DIC and lower in Ctrl (**Figures 7A, B**). In peritubular capillaries, C3c was visible in 2/9 of COVID-19 biopsies, one of them at high intensity, and was thus comparable in frequency to ATI and HUS (**Figures 7C, D**). Only in DIC peritubular C3c was present in 6/7 of biopsies but also occurred in 4/7 Ctrl biopsies (**Figure 7C**). In renal arteries, the deposition of C3c was common in all groups and showed less intensity in Ctrl while other groups frequently showed intense staining (**Figures 7E, F**). C3d,. was detectable in the glomeruli of 8/9 of COVID-19 biopsies, while glomerular C3d signals were lower in ATI and completely lacking in Ctrl (**Figures 8A, B**). In contrast, more frequent glomerular C3d deposition was detected in HUS and DIC (**Figures 8A, B**). In peritubular capillaries, C3d was negative in all investigated groups (**Figures 8C, D**). In renal arteries, the deposition of C3d was common in all groups but strongest staining was observed in COVID-19 (**Figures 8E, F**). Interestingly, the complement split product C4d, that was commonly used to assess whether antibodies are participating in antibody-mediated rejection of renal transplants, was not detected in any of the kidney samples tested; neither in biopsies of COVID-19 patients nor in the controls (**Supplemental Figure 3**, **Table 2**). Finally, we studied C5b-9 deposition in renal specimens, the membrane attack complex formed in the terminal complement pathway (**Figure 9**). While

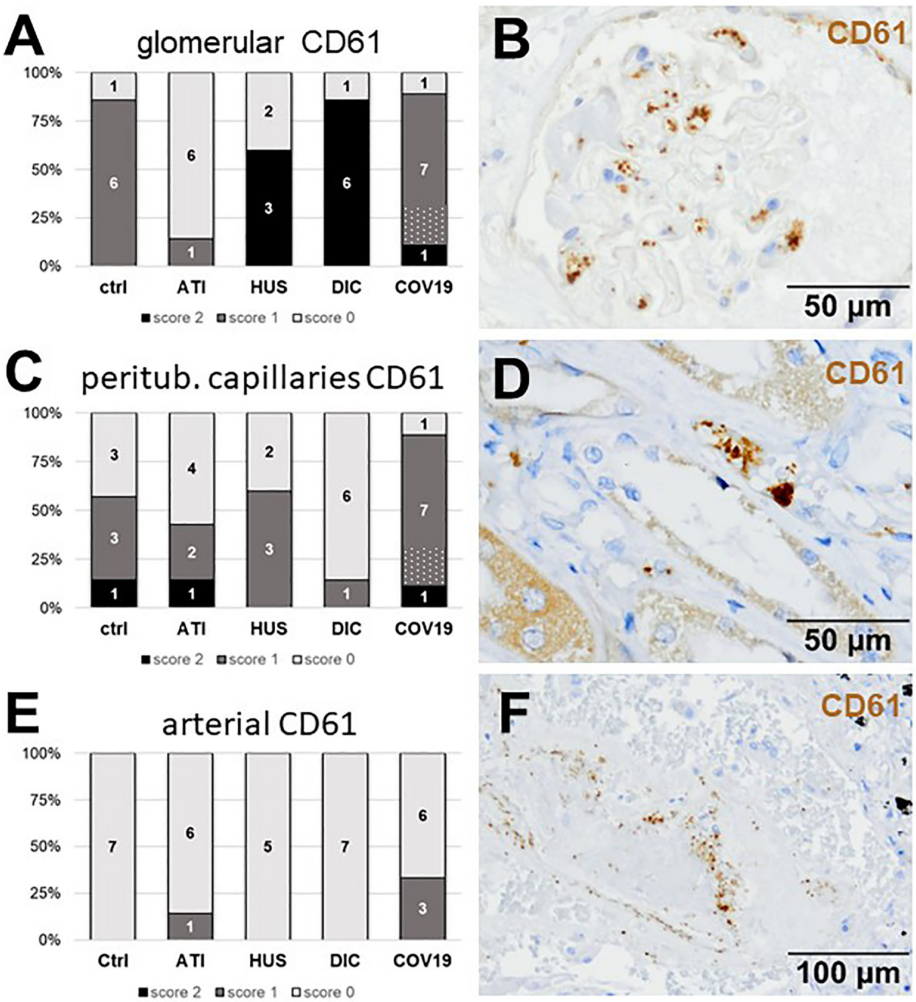

FIGURE 4 | Frequency and localization of CD61-positive platelets in renal biopsies with COVID-19 compared to Ctrl, ATI, HUS, and DIC. Frequency and amount of CD61-positive platelets was analyzed in glomerular capillaries **(A)**, peritubular capillaries **(C)** and renal arteries **(E)** in renal control biopsies taken 1 year after transplantation (Ctrl, n = 7), biopsies with acute tubular injury (ATI, n = 7), hemolytic uremic syndrome (HUS, n = 5), disseminated intravascular coagulation (DIC, n = 7), and COVID-19 (COVID-19, n = 9) using immunohistochemistry and semi-quantitative scoring. The proportion of CD61-positive stained cases that belongs to cases with comorbidities with known involvement of complement activation is marked by hatching in the bars representing the COVID-19 cohort. Representative pictures of COVID-19 biopsies positive for CD61 were shown for glomerular (**B**, brown staining), peritubular (**D**, brown staining), and arterial localization (**F**, brown staining).

TABLE 2 | Overview of renal complement deposition in patients with COVID-19 compared to Ctrl, ATI, HUS and DIC.

	Ctrl	ATI	HUS	DIC	COVID-19
CD61	0.52	0.29	0.6	0.61	0.78
MASP-2	0.07	0.07	0.1	0.2	0.22
C1q	0.14	0	0.8	0.79	0.19
C3c	0.54	0.89	1	1.25	0.75
C3d	0.39	0.48	0.55	0.61	0.89
C4d	0	0	0	0	0
C5b-9	0.5	0.43	0.65	0.93	1

The mean values of all semi-quantitative compartment-specific scores were summarized and displayed on a heat map.
Ctrl, 1 year renal transplant protocol biopsies; ATI, acute tubular injury; HUS, hemolytic uremic syndrome; DIC, disseminated intravascular coagulation.

C5b-9 was lacking in Ctrl and low in the glomeruli of ATI, it was deposited in four of nine COVID-19 cases, sometimes heavily (**Figures 9A, B**). The most intense deposition of C5b-9 was observed in DIC, while in HUS 3/5 of biopsies were also positive but showed only weak glomerular staining (**Figure 9A**). In contrast, peritubular C5b-9 was most common in COVID-19 (**Figures 9C, D**); in comparison Ctrl and DIC cases showed comparatively less C5b-9 and HUS showed less positive staining (**Figure 9C**). Comparable arterial C5b-9 deposits with light to intense staining were observed in COVID-19 and DIC, while in HUS arterial C5b-9 was similarly frequent but showed less intense staining (**Figure 9E**). Similar to most other complement components in this study, C5b-9 in renal arteries was lowest in ATI (**Figure 8E**) while Ctrl showed positive

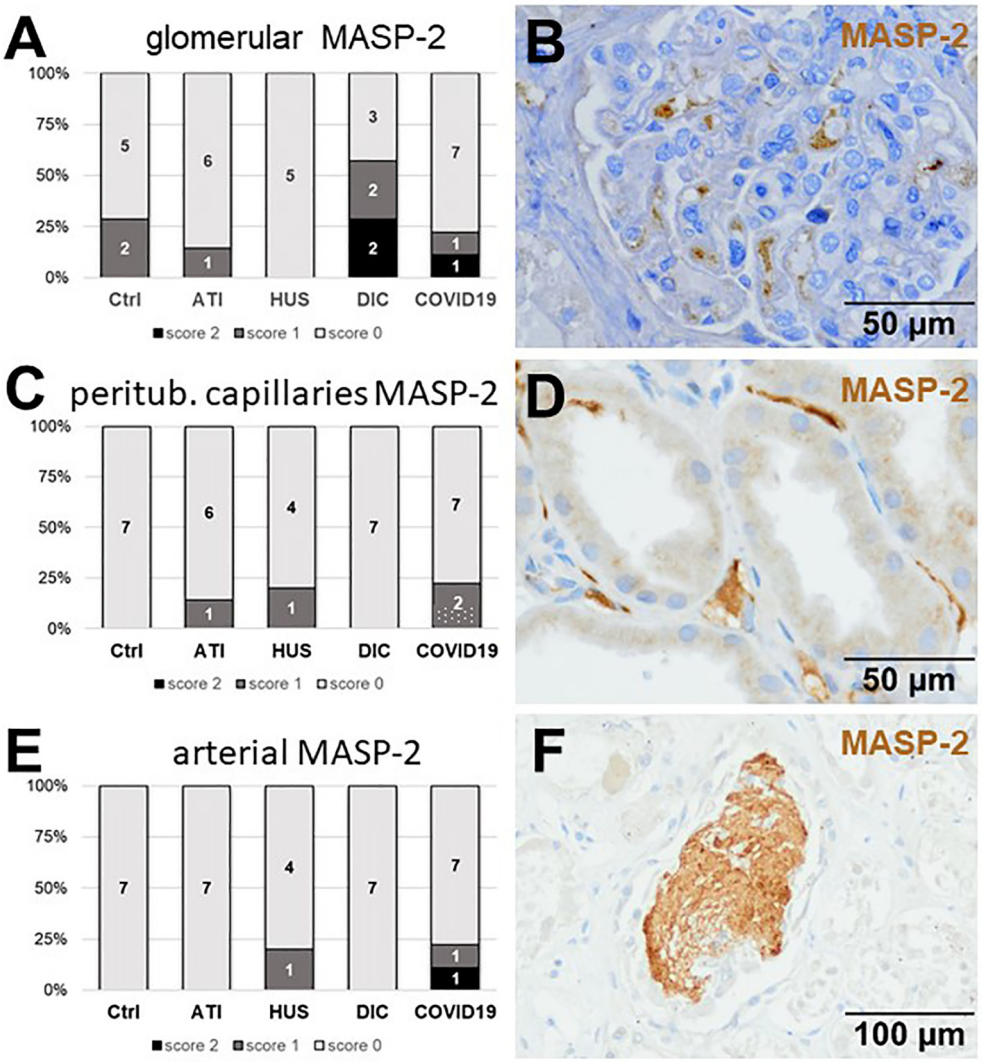

FIGURE 5 | Frequency and vascular localization of MASP-2 deposition in renal biopsies with COVID-19 compared to Ctrl, ATI, HUS, and DIC. Frequency and amount of mannose-binding protein-associated serine protease 2 (MASP-2) deposition was analyzed in glomerular capillaries **(A)**, peritubular capillaries **(C)** and renal arteries **(E)** in renal control biopsies taken 1 year after transplantation (Ctrl, n = 7), biopsies with acute tubular injury (ATI, n = 7), hemolytic uremic syndrome (HUS, n = 5), disseminated intravascular coagulation (DIC, n = 7), and COVID-19 (COVID-19, n = 9) using immunohistochemistry and semi-quantitative scoring. The proportion of MASP-2–positive stained cases that belongs to cases with comorbidities with known involvement of complement activation is marked by hatched bars representing the COVID-19 cohort. Representative pictures of COVID-19 biopsies positive for MASP-2 were shown for glomerular (**B**, brown staining), peritubular (**D**, brown staining) and arterial localization (**F**, brown staining).

staining in all cases but with less intensity (**Figure 9E**). In summary, COVID-19 leads to endothelial cell damage in the kidney with the accumulation of platelets and significant activation of the complement system (summarized in **Table 2**), which might at least in part occur *via* the lectin pathway.

Tubular Complement Activation Was Highest in Kidneys of Patients With COVID-19 and Restricted to C3c, C3d and C5b-9

Since we observed tubular injury in all biopsies from patients with COVID-19, we next investigated complement deposition in the tubular compartment and detected complement deposition along the tubular basement membranes (**Figures 10B, D, F**). No tubular deposition could be detected for MASP-2 and C1q in our cohort (data not shown). Tubular C3c, was detected in 5/9 biopsies from COVID-19 patients, while tubular C3c deposition in HUS was comparable and more frequent in ATI and DIC (**Figure 10A**). In contrast, tubular C3d was detectable in all COVID-19 biopsies and showed the most frequent and intense staining compared to all other groups (**Figure 10C**). Interestingly, the C3d staining was strongest in kidneys from patients who died due to severe COVID-19 infection, indicating that complement mediated tubular damage is might be dependent on the severity of the COVID-19 disease. Tubular

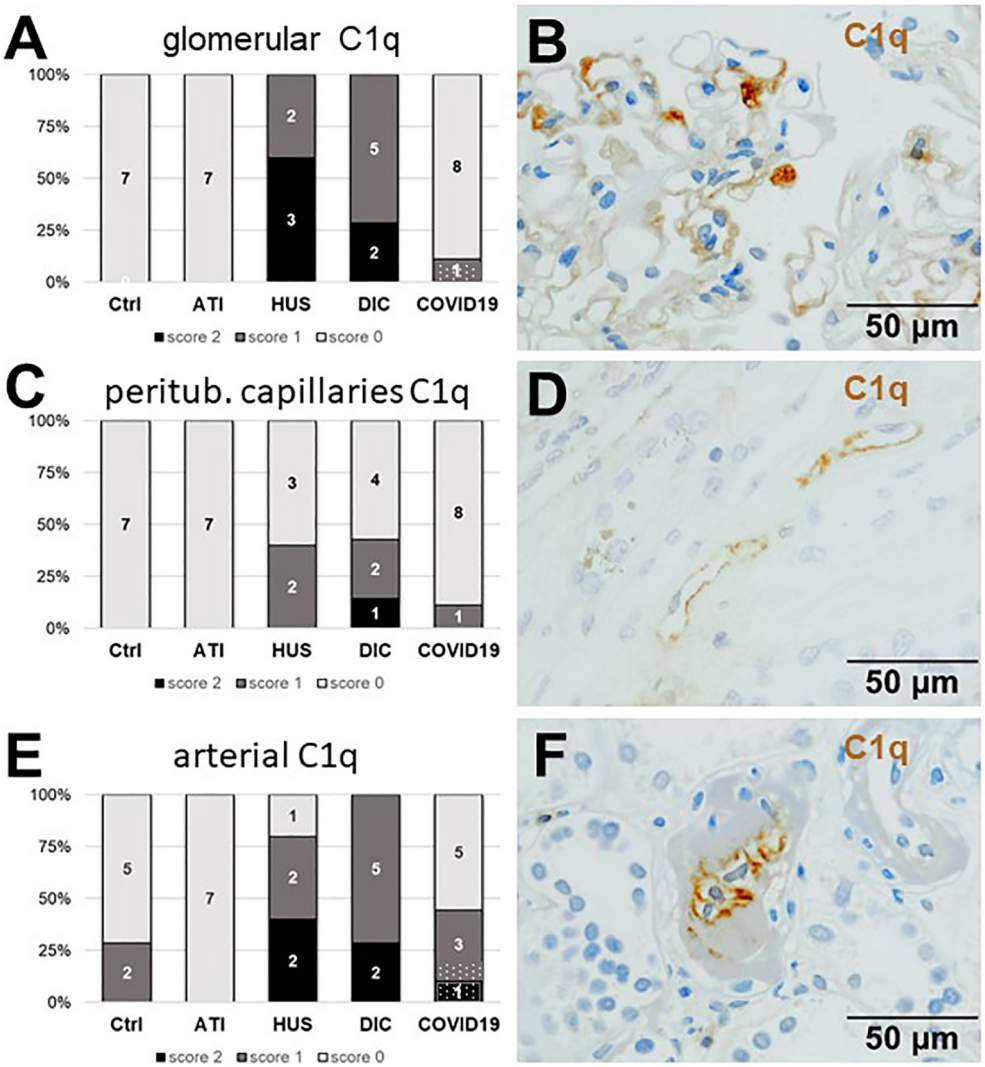

FIGURE 6 | Frequency and vascular localization of C1q deposition in renal biopsies with COVID-19 compared to Ctrl, ATI, HUS, and DIC. Frequency and amount of C1q deposition were analyzed in glomerular capillaries **(A)**, peritubular capillaries **(C)**, and renal arteries **(E)** in renal control biopsies taken 1 year after transplantation (Ctrl, n = 7), biopsies with acute tubular injury (ATI, n = 7), hemolytic uremic syndrome (HUS, n = 5), disseminated intravascular coagulation (DIC, n = 7) and COVID-19 (COVID-19, n = 9) using immunohistochemistry and semi-quantitative scoring. The proportion of C1q-positive stained cases that belongs to cases with comorbidities with known involvement of complement activation is marked by hatched bars representing the COVID-19 cohort. Representative pictures of COVID-19 biopsies positive for C1q were shown for glomerular (**B**, brown staining), peritubular (**D**, brown staining) and arterial localization (**F**, brown staining).

C5b-9 deposits could also be detected in 7/9 biopsies of patients with COVID-19 and again showed the highest intensity compared to the other groups (**Figure 10E**).

In summary, when the compartment-specific scores for all stainings were added up to a total score for the respective factor, biopsies of COVID-19 patients contained the highest number of CD61-positive platelets compared to the other groups (**Table 2**). This parallels with the deposition of C3d, C5b-9 and on a lower level with the deposition of MASP-2 (**Table 2**). C1q deposition in biopsies from patients with COVID-19 was comparable with Ctrl and even higher in HUS and DIC (**Table 2**), indicating that in COVID-19 renal complement was not activated *via* the classical but by the lectin or alternative pathway.

DISCUSSION

Complement factors were major components that clogged CRP adsorber columns during the treatment of critically ill patients with COVID-19 prompting further studies on a role of complement in COVID-19 infection. C5b-9 and the complement cleavage product and anaphylatoxin C5a were increased in the plasma of patients with moderate and severe disease compared to healthy controls (20). Furthermore, lung epithelial cells infected with SARS-CoV-2 highly expressed the complement factors C1r, C1s, C3 and factor B (22). Studies by immunohistology on complement-mediated microvascular damage showed deposits of MASP-2, C4d, and C5b-9 in the

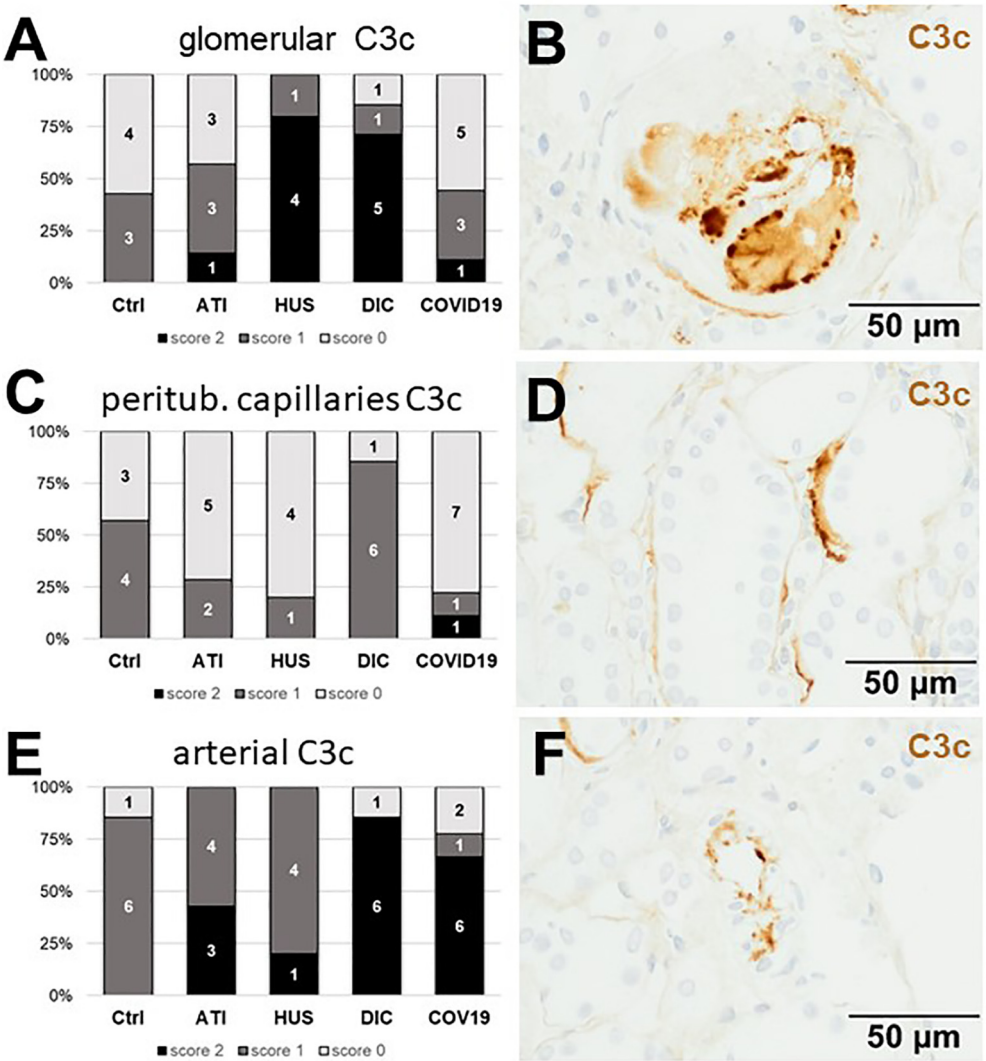

FIGURE 7 | Frequency and vascular localization of C3c deposition in renal biopsies with COVID-19 compared to Ctrl, ATI, HUS and DIC. Frequency and amount of C3c deposition were analyzed in glomerular capillaries **(A)**, peritubular capillaries **(C)**, and renal arteries **(E)** in renal control biopsies taken 1 year after transplantation (Ctrl, n = 7), biopsies with acute tubular injury (ATI, n = 7), hemolytic uremic syndrome (HUS, n = 5), disseminated intravascular coagulation (DIC, n = 7) and COVID-19 (COVID-19, n = 9) using immunohistochemistry and semi-quantitative scoring. The proportion of C3d-positive stained cases that belongs to cases with comorbidities with known involvement of complement activation is marked by hatched bars representing the COVID-19 cohort. Representative pictures of COVID-19 biopsies positive for C3c were shown for glomerular (**B**, brown staining), peritubular (**D**, brown staining) and arterial localization (**F**, brown staining).

lungs and skins of severely ill patients (21). In a preprint study Gao et al. demonstrated, that the SARS-CoV-2 nucleocapsid protein bound to MASP-2 and activated complement; blockade of this interaction improved the survival of mice with COVID-19 nucleocapsid potentiated LPS-induced pneumonia (23). In our study in kidney biopsies from patients with COVID-19, we for the first time detected enhanced renal complement deposition in vascular beds and tubuli supporting the idea that the complement system is a potential mediator of COVID-19–induced kidney injury. The observed kidney damage in COVID-19 biopsies was primarily acute kidney injury (AKI) with mild to severe tubular injury and in rare cases glomerular thrombi. This is consistent with the observations of other histopathological studies examining kidneys of the patients with COVID-19 and identifying AKI in 37% to 98% of all examined cases (9–11). Interestingly, especially the tubular deposition of C3d was highest in biopsies from patients with COVID-19 and seem to be dependent on the severity of the disease, supporting the role of complement as a mediator of tubular damage. In addition, we investigated endothelial cell loss in COVID-19 biopsies. The endothelium plays an important role in the pathogenesis of COVID-19–mediated tissue damage, both as an effector contributing to inflammation and thrombosis, and as a target organ, whose dysfunction may contribute to poor outcome (24). In an autopsy study from patients who died of COVID-19, pulmonary vessels showed widespread thrombosis,

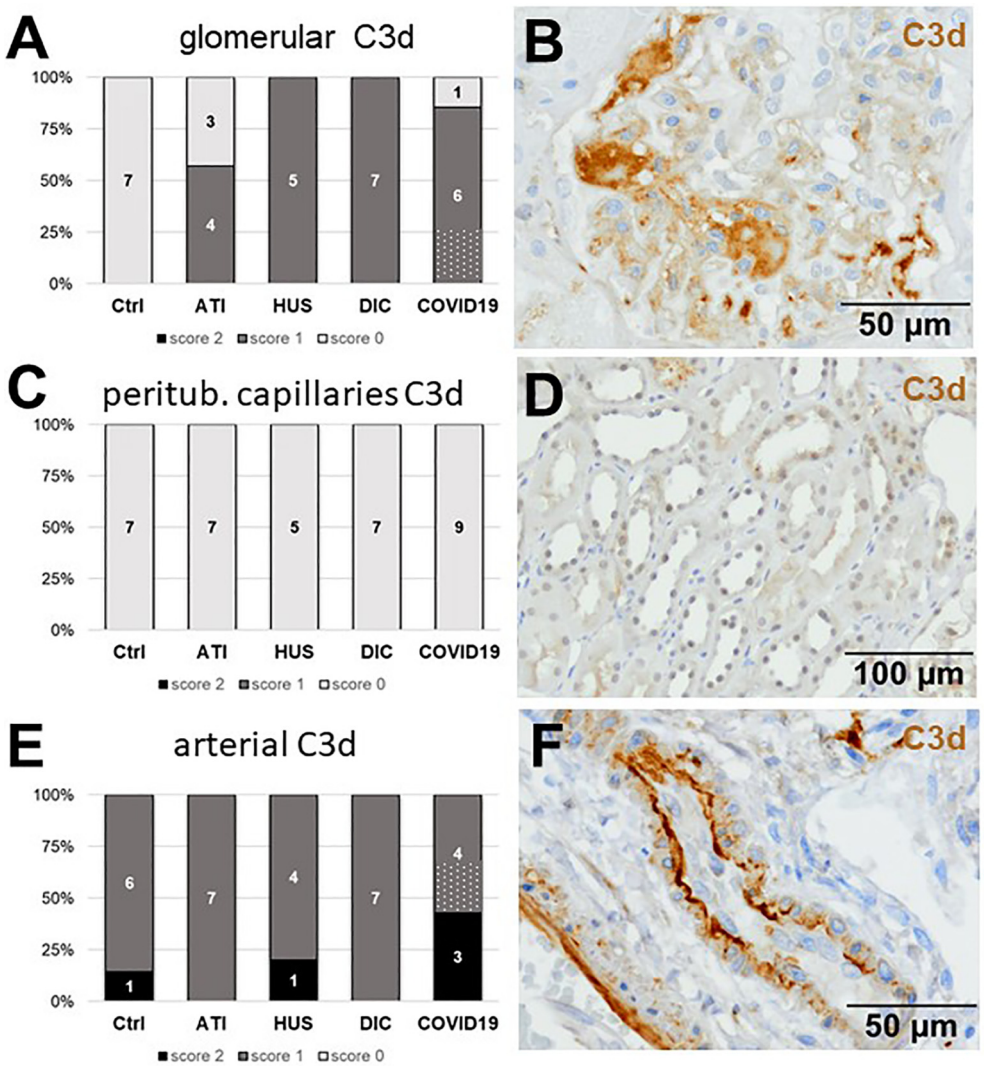

FIGURE 8 | Frequency and vascular localization of C3d deposition in renal biopsies with COVID-19 compared to Ctrl, ATI, HUS, and DIC. Frequency and amount of C3d deposition were analyzed in glomerular capillaries **(A)**, peritubular capillaries **(C)** and renal arteries **(E)** in renal control biopsies taken 1 year after transplantation (Ctrl, n = 7), biopsies with acute tubular injury (ATI, n = 7), hemolytic uremic syndrome (HUS, n = 5), disseminated intravascular coagulation (DIC, n = 7) and COVID-19 (COVID-19, n = 9) using immunohistochemistry and semi-quantitative scoring. The proportion of C3d-positive stained cases that belongs to cases with comorbidities with known involvement of complement activation is marked by hatched bars representing the COVID-19 cohort. Representative pictures of COVID-19 biopsies positive for C3d were shown for glomerular (**B**, brown staining), peritubular (**D**, brown staining) and arterial localization (**F**, brown staining).

capillary microthrombi and increased neovascularization (25). In renal biopsies we observed a reduction of the endothelial cell marker ERG, similar to the endothelial damage in ATI, but less pronounced than in DIC. Renal capillarization was highest in HUS, indicating that the endothelial cell damage already started to be repaired by high proliferative activity. In contrast to reports in the lung (25), microthrombi and endothelial proliferation were rare in COVID-19 renal biopsies. However, CD61-positive platelets in peritubular capillaries were highest in COVID-19 biopsies compared to all other groups. In comparison with other renal diseases with distinct endothelial cell injury, like HUS or DIC, we demonstrate similar complement activation in COVID-19 renal biopsies with some differences in the involved pathways.

The lectin pathway can be activated by sugar residues bound to pattern recognition molecules followed by activation of MASP-2 complexes with collectin 11. In ischemic kidneys, collectin 11 recognized an abnormal L-fucose pattern on tubular cells and consequently activated the lectin pathway (26). Interestingly, in tubuli from COVID-19 biopsies we observed a higher collectin 11 mRNA expression compared to 1 year biopsies, HUS and ATI controls (**Supplemental Figure 1**) and MASP-2 deposition in some of the COVID-19 cases, indicating that activation of the lectin pathway in COVID-19 was not restricted to lung or skin (21). Activation of the classical pathway can be mediated for example by natural IgM antibodies that recognize viral antigens or neo-antigens exposed on damaged host tissues (27). C1q, the

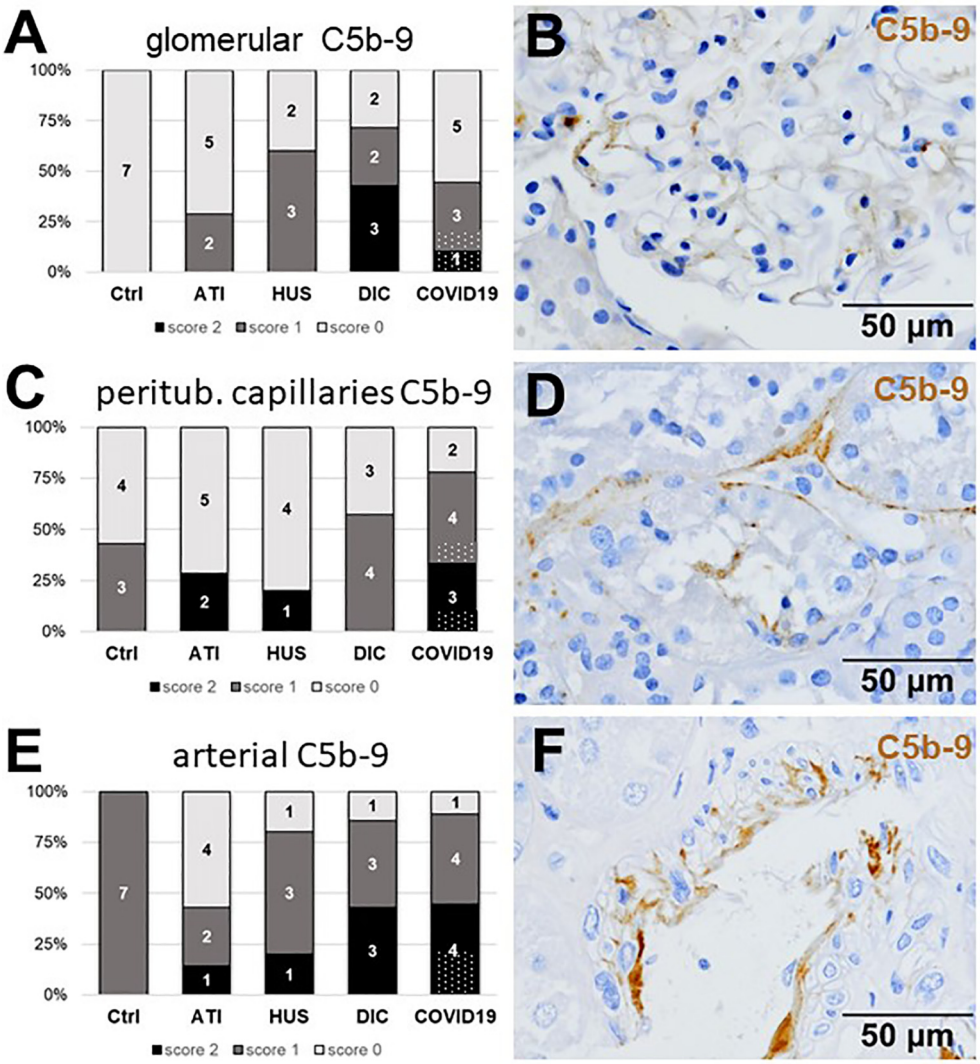

FIGURE 9 | Frequency and vascular localization of C5b-9 deposition in renal biopsies with COVID-19 compared to Ctrl, ATI, HUS, and DIC. Frequency and amount of C5b-9 deposition were analyzed in glomerular capillaries **(A)**, peritubular capillaries **(C)** and renal arteries **(E)** in renal control biopsies taken 1 year after transplantation (Ctrl, n = 7), biopsies with acute tubular injury (ATI, n = 7), hemolytic uremic syndrome (HUS, n = 5), disseminated intravascular coagulation (DIC, n = 7) and COVID-19 (COVID-19, n = 9) using immunohistochemistry and semi-quantitative scoring. The proportion of C5b-9–positive stained cases that belongs to cases with comorbidities with known involvement of complement activation is marked by hatched bars representing the COVID-19 cohort. Representative pictures of COVID-19 biopsies positive for C5b-9 were shown for glomerular (**B**, brown staining), peritubular (**D**, brown staining) and arterial localization (**F**, brown staining).

starter of the classical pathway, was more frequently detected in COVID-19 as compared to ATI but, nevertheless, rarely detected in glomeruli and peritubular capillaries compared to HUS and DIC cases. However, the highest C1q deposition in COVID-19 biopsies was seen in renal arteries. C3 cleavage products occur in all three complement activation pathways and were detected as the stable cleavage product C3c and C3d, which can bind covalently to cell surfaces. Interestingly, deposition of these C3 cleavage products were not similarly deposited in the renal biopsies. C3d was highest in biopsies from patients with COVID-19, C3c was also increased compared to controls but even higher in HUS and DIC. Differences in staining patterns are may be due to the specificity of the used antibodies. While the anti-C3c antibody also recognize C3 the anti-C3d do not detect intact C3. C5b-9, as a marker of the terminal complement cascade, was strongly and similarly detectable in glomerular capillaries and even more strongly deposited in the peritubular capillaries than in HUS and DIC biopsies. Significant C5b-9 deposition was also described in lung and skin biopsies from patients with COVID-19 (21).

In summary, in our study complement activation in COVID-19 was not restricted to a specific activation pathway. Complement was reportedly activated by all three known pathways during COVID-19 infection (28). It is conceivable that complement activation can occur both through direct interaction with the SARS-CoV-2 virus or indirectly by

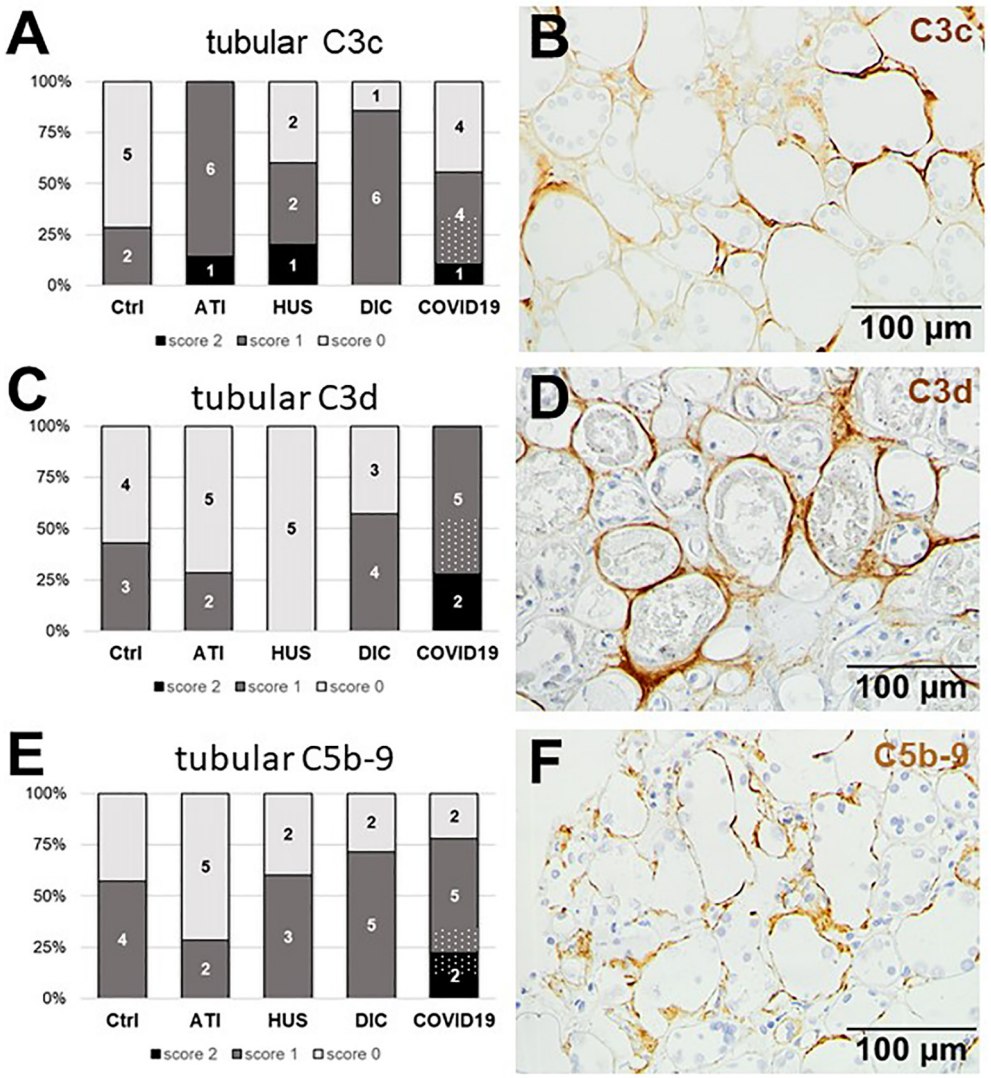

FIGURE 10 | Frequency and tubular localization of C3c, C3d, and C5b-9 deposition in renal biopsies with COVID-19 compared to Ctrl, ATI, HUS and DIC. Frequency and amount of tubular C3c **(A)**, C3d **(C)**, and C5b-9 **(E)** deposition were analyzed in renal control biopsies taken 1 year after transplantation (Ctrl, n = 7), biopsies with acute tubular injury (ATI, n = 7), hemolytic uremic syndrome (HUS, n = 5), disseminated intravascular coagulation (DIC, n = 7), and COVID-19 (COVID-19, n = 9) using immunohistochemistry and semi-quantitative scoring. The proportion of complement-positive stained cases that belongs to cases with comorbidities with known involvement of complement activation is marked by hatched bars representing the COVID-19 cohort. Representative pictures of COVID-19 biopsies positive for tubular C3c (**B**, brown staining), C3d (**D**, brown staining), and C5b-9 (**F**, brown staining) were shown.

tissue damage and dying cells. Presumably, the complement activation in kidneys of COVID-19 patients observed in our study was rather indirect, since we could hardly detect viruses by in-situ hybridization and even fewer pathogens by immunohistochemistry so that we cannot exclude that these are unspecific background signals. This goes inline with findings of other groups, which have also not found robust signals of SARS-CoV-2 in the kidneys (9–11). In contrast, in other studies SARS-CoV-2 was detected in the kidney (5, 7, 8), so that we cannot exclude the possibility that SARS-CoV-2 was present in the kidney at an earlier time interval before biopsy was taken and that complement was activated directly by the virus. Our own and data of other groups showed that complement activation might be an important pathomechanism of tissue damage in COVID-19 opening the possibility of treatment with complement inhibitors. Anecdotal reports of the successful treatment of seriously ill patients with COVID-19 employing the C5 inhibitor Eculizumab (29) or the C3 inhibitor AMY-101 (30) have already been published. Clinical studies with complement inhibitors in patients with COVID-19 will show the efficiency of this treatment. Several clinical trials are currently ongoing to investigate the protective effects of purified/recombinant complement regulators (e.g. C1-esterase inhibitor) or complement inhibitors directed against MASP-2, C3, C5, or

the C5a receptor on COVID-19 outcomes ranging from changes in oxygenation to mortality (31)(https://www.trialsitenews.com/category/masp-2/).

LIMITATION OF THE STUDY

Our study is limited by the small number of COVID-19 renal biopsies and the different co-morbidities of the investigated patients with kidney disease. At least 3 of the comorbidities are also known for the occurrence of complement activation, namely ANCA-associated GN, FSGS and infectious GN. To distinguish between COVID-19–related complement activation and complement activation that might be related to the diagnosed renal disease, the proportion of positively stained cases that belongs to the 3 above mentioned cases is marked in the figures by hatching. Indeed, we frequently but not necessarily always detected complement deposition outline biopsies with these diseases. However, the percentage of complement-positive cases in COVID-19 with known potential complement involvement represented on average 30.2% of all positive COVID-19 cases. Although we cannot rule out that the observed complement deposition in the cases with the above mentioned kidney diseases was due to this comorbidity and not to the COVID-19 infection, the renal complement deposition was by far not limited to these cases. Renal thrombi were only found in one investigated post-mortem biopsy, therefore it remains unclear if thrombi only occur in severely diseased kidneys or during peri-mortal processes. Since the antibody used for detection of MASP-2 also recognize the MASP-2 splice variant MAp19, lacking the catalytic domain, we cannot distinguish between complement activating MASP-2 and Map19. Although our initial observation that complement factors are an essential component of plasma clots in CRP adsorbers in critically ill patients with COVID-19 led to the studies in the kidney, the role of complement in the clotting process remains open and needs further investigation.

In conclusion, we observed marked complement deposition in kidneys of patients with COVID-19 similar to other known renal diseases with a distinct endothelial injury. Complement deposition could be also detected on tubular basement membranes in biopsies from patients with COVID-19. Therefore, we speculate that complement is, most likely involved in vascular and tubular kidney damage in COVID-19. Specific complement inhibition might thus be a promising treatment option to prevent deregulated complement activation and subsequent collateral tissue injury. Further studies with larger biopsy numbers are necessary to elucidate the involvement of the complement system in COVID-19–induced renal damage.

DATA AVAILABILITY STATEMENT

The original contributions presented in the study are included in the article/**Supplementary Material**. Further inquiries can be directed to the corresponding author.

ETHICS STATEMENT

The studies involving human participants were reviewed and approved by Ethics Committee of Friedrich-Alexander-University Erlangen-Nürnberg (Reference No. 4415). Written informed consent for participation was not required for this study in accordance with the national legislation and the institutional requirements.

AUTHOR CONTRIBUTIONS

EV and FP conducted experiments, analyzed data, and wrote the manuscript. TR carried out immunohistological staining. H-MJ and KÜ generated the anti-SARS-CoV-2 spike antibody, supplied transfected cells, and proofread the paper. GL performed MALDI-TOF. AS isolated proteins from plasma adsorber material. MH conceived and designed the plasma adsorber analysis and revised the manuscript. KA, MB-H, and CD conceived and designed the study, analyzed data, and wrote the manuscript. All authors contributed to the article and approved the submitted version.

FUNDING

This study was funded by the Deutsche Forschungsgemeinschaft (DFG, German Research Foundation), project number 387509280, SFB 1350 and supported by the DEFEAT Pandemics autopsy platform of the Federal Ministry of Education and Research (BMBF).

ACKNOWLEDGMENTS

The technical assistance of E. Roth, S. Söllner, Lisa Stelzer, Britta Hähnel, and M. Reutelshöfer is gratefully acknowledged.

SUPPLEMENTARY MATERIAL

The Supplementary Material for this article can be found online at: https://www.frontiersin.org/articles/10.3389/fimmu.2020.594849/full#supplementary-material

REFERENCES

1. Guan WJ, Ni ZY, Hu Y, Liang WH, Ou CQ, He JX, et al. Clinical Characteristics of Coronavirus Disease 2019 in China. *N Engl J Med* (2020) 382(18):1708–20. doi: 10.1056/NEJMoa2002032
2. Gupta A, Madhavan MV, Sehgal K, Nair N, Mahajan S, Sehrawat TS, et al. Extrapulmonary manifestations of COVID-19. *Nat Med* (2020) 26(7):1017–32. doi: 10.1038/s41591-020-0968-3
3. Chen YT, Shao SC, Hsu CK, Wu IW, Hung MJ, Chen YC. Incidence of acute kidney injury in COVID-19 infection: a systematic review and

meta-analysis. *Crit Care* (2020) 24(1):346. doi: 10.1186/s13054-020-03009-y
4. Cheng Y, Luo R, Wang K, Zhang M, Wang Z, Dong L, et al. Kidney disease is associated with in-hospital death of patients with COVID-19. *Kidney Int* (2020) 97(5):829–38. doi: 10.1016/j.kint.2020.03.005
5. Puelles VG, Lütgehetmann M, Lindenmeyer MT, Sperhake JP, Wong MN, Allweiss L, et al. Multiorgan and Renal Tropism of SARS-CoV-2. *N Engl J Med* (2020) 383(6) :590–2. doi: 10.1056/NEJMc2011400
6. Soleimani M. Acute Kidney Injury in SARS-CoV-2 Infection: Direct Effect of Virus on Kidney Proximal Tubule Cells. *Int J Mol Sci* (2020) 21(9):1–6. doi: 10.3390/ijms21093275
7. Farkash EA, Wilson AM, Jentzen JM. Ultrastructural Evidence for Direct Renal Infection with SARS-CoV-2. *J Am Soc Nephrol* (2020) 31(8):1683–7. doi: 10.1681/asn.2020040432
8. Su H, Yang M, Wan C, Yi LX, Tang F, Zhu HY, et al. Renal histopathological analysis of 26 postmortem findings of patients with COVID-19 in China. *Kidney Int* (2020) 98(1):219–27. doi: 10.1016/j.kint.2020.04.003
9. Kudose S, Batal I, Santoriello D, Xu K, Barasch J, Peleg Y, et al. Kidney Biopsy Findings in Patients with COVID-19. *J Am Soc Nephrol* (2020) 31(9):1959–68. doi: 10.1681/asn.2020060802
10. Golmai P, Larsen CP, DeVita MV, Wahl SJ, Weins A, Rennke HG, et al. Histopathologic and Ultrastructural Findings in Postmortem Kidney Biopsy Material in 12 Patients with AKI and COVID-19. *J Am Soc Nephrol* (2020) 31 (9):1944–7. doi: 10.1681/asn.2020050683
11. Santoriello D, Khairallah P, Bomback AS, Xu K, Kudose S, Batal I, et al. Postmortem Kidney Pathology Findings in Patients with COVID-19. *J Am Soc Nephrol* (2020) 31(9):2158–67. doi: 10.1681/asn.2020050744
12. Chen G, Wu D, Guo W, Cao Y, Huang D, Wang H, et al. Clinical and immunological features of severe and moderate coronavirus disease 2019. *J Clin Invest* (2020) 130(5):2620–9. doi: 10.1172/jci137244
13. Leppkes M, Knopf J, Naschberger E, Lindemann A, Singh J, Herrmann I, et al. Vascular occlusion by neutrophil extracellular traps in COVID-19. *EBioMedicine* (2020) 58:102925. doi: 10.1016/j.ebiom.2020.102925
14. Wang R, Xiao H, Guo R, Li Y, Shen B. The role of C5a in acute lung injury induced by highly pathogenic viral infections. *Emerg Microbes Infect* (2015) 4 (5):e28. doi: 10.1038/emi.2015.28
15. Noris M, Remuzzi G. Overview of complement activation and regulation. *Semin Nephrol* (2013) 33(6):479–92. doi: 10.1016/j.semnephrol.2013.08.001
16. Kojouharova M, Reid K, Gadjeva M. New insights into the molecular mechanisms of classical complement activation. *Mol Immunol* (2010) 47 (13):2154–60. doi: 10.1016/j.molimm.2010.05.011
17. Farrar CA, Zhou W, Sacks SH. Role of the lectin complement pathway in kidney transplantation. *Immunobiology* (2016) 221(10):1068–72. doi: 10.1016/j.imbio.2016.05.004
18. Dobo J, Pal G, Cervenak L, Gal P. The emerging roles of mannose-binding lectin-associated serine proteases (MASPs) in the lectin pathway of complement and beyond. *Immunol Rev* (2016) 274(1):98–111. doi: 10.1111/imr.12460
19. Pangburn MK, Schreiber RD, Muller-Eberhard HJ. Formation of the initial C3 convertase of the alternative complement pathway. Acquisition of C3b-like activities by spontaneous hydrolysis of the putative thioester in native C3. *J Exp Med* (1981) 154(3):856–67. doi: 10.1084/jem.154.3.856
20. Cugno M, Meroni PL, Gualtierotti R, Griffini S, Grovetti E, Torri A, et al. Complement activation in patients with COVID-19: A novel therapeutic target. *J Allergy Clin Immunol* (2020) 146(1):215–7. doi: 10.1016/j.jaci.2020.05.006
21. Magro C, Mulvey JJ, Berlin D, Nuovo G, Salvatore S, Harp J, et al. Complement associated microvascular injury and thrombosis in the pathogenesis of severe COVID-19 infection: a report of five cases. *Transl Res* (2020) 220:1–13. doi: 10.1016/j.trsl.2020.04.007
22. Yan B, Freiwald T, Chauss D, Wang L, West E, Bibby J, et al. SARS-CoV2 drives JAK1/2-dependent local and systemic complement hyper-activation. *Res Sq* (2020). doi: 10.21203/rs.3.rs-33390/v1
23. Gao T, Hu M, Zhang X, Li H, Zhu L, Liu H, et al. Highly pathogenic coronavirus N protein aggravates lung injury by MASP-2-mediated complement over-activation. *medRxiv* (2020). doi: 10.1101/2020.03.29.2004196
24. Evans PC, Ed Rainger G, Mason JC, Guzik TJ, Osto E, Stamataki Z, et al. Endothelial dysfunction in COVID-19: a position paper of the ESC Working Group for Atherosclerosis and Vascular Biology, and the ESC Council of Basic Cardiovascular Science. *Cardiovasc Res* (2020) 116(14) :2177–84. doi: 10.1093/cvr/cvaa230
25. Ackermann M, Verleden SE, Kuehnel M, Haverich A, Welte T, Laenger F, et al. Pulmonary Vascular Endothelialitis, Thrombosis, and Angiogenesis in Covid-19. *N Engl J Med* (2020) 383(2):120–8. doi: 10.1056/NEJMoa2015432
26. Farrar CA, Tran D, Li K, Wu W, Peng Q, Schwaeble W, et al. Collectin-11 detects stress-induced L-fucose pattern to trigger renal epithelial injury. *J Clin Invest* (2016) 126(5):1911–25. doi: 10.1172/jci83000
27. Zhang M, Carroll MC. Natural IgM-mediated innate autoimmunity: a new target for early intervention of ischemia-reperfusion injury. *Expert Opin Biol Ther* (2007) 7(10):1575–82. doi: 10.1517/14712598.7.10.1575
28. Song WC, FitzGerald GA. COVID-19, microangiopathy, hemostatic activation, and complement. *J Clin Invest* (2020) 130(8):3950–3. doi: 10.1172/jci140183
29. Diurno F, Numis FG, Porta G, Cirillo F, Maddaluno S, Ragozzino A, et al. Eculizumab treatment in patients with COVID-19: preliminary results from real life ASL Napoli 2 Nord experience. *Eur Rev Med Pharmacol Sci* (2020) 24 (7):4040–7. doi: 10.26355/eurrev_202004_20875
30. Mastaglio S, Ruggeri A, Risitano AM, Angelillo P, Yancopoulou D, Mastellos DC, et al. The first case of COVID-19 treated with the complement C3 inhibitor AMY-101. *Clin Immunol* (2020) 215:108450. doi: 10.1016/j.clim.2020.108450
31. Conigliaro P, Triggianese P, Perricone C, Chimenti MS, Perricone R. COVID-19: disCOVering the role of complement system. *Clin Exp Rheumatol* (2020) 38(4):587–91. doi: 10.1016/j.autrev.2020.102590

Conflict of Interest: Author AS was employed by the company Pentracor GmbH.

The remaining authors declare that the research was conducted in the absence of any commercial or financial relationships that could be construed as a potential conflict of interest.

frontiers in Immunology

ORIGINAL RESEARCH
published: 10 June 2021
doi: 10.3389/fimmu.2021.690821

Factor D Inhibition Blocks Complement Activation Induced by Mutant Factor B Associated With Atypical Hemolytic Uremic Syndrome and Membranoproliferative Glomerulonephritis

*Sigridur Sunna Aradottir[1], Ann-Charlotte Kristoffersson[1], Lubka T. Roumenina[2], Anna Bjerre[3,4], Pavlos Kashioulis[5], Runolfur Palsson[6,7] and Diana Karpman[1]**

[1] Department of Pediatrics, Clinical Sciences Lund, Lund University, Lund, Sweden, [2] Centre de Recherche des Cordeliers, INSERM, Sorbonne Université, Université de Paris, Paris, France, [3] Division of Pediatric and Adolescent Medicine, Oslo University Hospital, Oslo, Norway, [4] Institute of Clinical Medicine, University of Oslo, Oslo, Norway, [5] Department of Molecular and Clinical Medicine/Nephrology, Institute of Medicine, Sahlgrenska Academy, University of Gothenburg, Gothenburg, Sweden, [6] Landspitali - The National University Hospital of Iceland, Reykjavik, Iceland, [7] Faculty of Medicine, School of Health Sciences, University of Iceland, Reykjavík, Iceland

Complement factor B (FB) mutant variants are associated with excessive complement activation in kidney diseases such as atypical hemolytic uremic syndrome (aHUS), C3 glomerulopathy and membranoproliferative glomerulonephritis (MPGN). Patients with aHUS are currently treated with eculizumab while there is no specific treatment for other complement-mediated renal diseases. In this study the phenotype of three FB missense variants, detected in patients with aHUS (D371G and E601K) and MPGN (I242L), was investigated. Patient sera with the D371G and I242L mutations induced hemolysis of sheep erythrocytes. Mutagenesis was performed to study the effect of factor D (FD) inhibition on C3 convertase-induced FB cleavage, complement-mediated hemolysis, and the release of soluble C5b-9 from glomerular endothelial cells. The FD inhibitor danicopan abrogated C3 convertase-associated FB cleavage to the Bb fragment in patient serum, and of the FB constructs, D371G, E601K, I242L, the gain-of-function mutation D279G, and the wild-type construct, in FB-depleted serum. Furthermore, the FD-inhibitor blocked hemolysis induced by the D371G and D279G gain-of-function mutants. In FB-depleted serum the D371G and D279G mutants induced release of C5b-9 from glomerular endothelial cells that was reduced by the FD-inhibitor. These results suggest that FD inhibition can effectively block complement overactivation induced by FB gain-of-function mutations.

Keywords: complement, factor B, factor D, danicopan, atypical hemolytic uremic syndrome, C3 glomerulopathy

OPEN ACCESS

Edited by:
Roberta Bulla, University of Trieste, Italy

Reviewed by:
Richard Michael Burwick, Cedars Sinai Medical Center, United States
Eleni Gavriilaki, G. Papanikolaou General Hospital, Greece

***Correspondence:**
Diana Karpman
diana.karpman@med.lu.se

Specialty section:
This article was submitted to Molecular Innate Immunity, a section of the journal Frontiers in Immunology

Received: *04 April 2021*
Accepted: *10 May 2021*
Published: *10 June 2021*

Citation:
Aradottir SS, Kristoffersson A-C, Roumenina L, Bjerre A, Kashioulis P, Palsson R and Karpman D (2021) Factor D Inhibition Blocks Complement Activation Induced by Mutant Factor B Associated With Atypical Hemolytic Uremic Syndrome and Membranoproliferative Glomerulonephritis. Front. Immunol. 12:690821. doi: 10.3389/fimmu.2021.690821

INTRODUCTION

The innate immune system is a first line of defense against pathogens and contributes to removal of apoptotic host cells. One of the mainstays of protection is the complement system responding to non-self molecules and eliminating them or neutralizing their effects by opsonization or lysis as well as induction of leukocyte chemoattraction, inflammation and phagocytosis (1). The main enzymatic activity of the alternative complement pathway is mediated by the C3 convertase. For C3 convertase formation to occur C3b binds to factor B (FB) which is cleaved by factor D (FD) to the Ba and Bb fragments, the latter possessing catalytic activity. Bb remains bound to C3b and forms the C3bBb convertase that exponentially cleaves more C3 into C3a and C3b. Binding of additional C3b molecules generates the C5 convertase. The complement system is kept in balance by multiple cellular and soluble regulators (1).

FB is essential for defense against encapsulated bacteria, and thus individuals with FB deficiency are prone to infection with *Neisseria meningitidis* and *Streptococcus pneumoniae* (2). Conversely, an overactive FB can lead to excessive complement activation *via* the alternative pathway resulting in kidney diseases such as atypical hemolytic uremic syndrome (aHUS) or C3 glomerulopathy. In both of these rare conditions, patients may exhibit complement activation but there are distinct differences in clinical presentation and renal pathology. While aHUS is characterized by hemolytic anemia, thrombocytopenia and renal failure with lesions indicative of thrombotic microangiopathy (3), C3 glomerulopathy is a form of chronic glomerulonephritis presenting with hematuria and proteinuria leading to renal failure (4). These conditions can arise due to mutant variants in complement factors, including C*FB* mutations, or auto-antibodies against factor H (5). Autoantibodies against FB have been described in C3 glomerulopathy (6).

In aHUS the complement system is overactive due to loss-of-function mutations in complement regulators or gain-of-function mutations in *C3* or *CFB* (7). Gain-of-function variants in *CFB* are rare and have in certain cases been associated with low C3 levels in patient sera (8–11) indicating complement activation *in vivo*. Mutations have been shown to increase FB binding affinity to C3b thereby stabilizing the C3bBb convertase (12) and enhancing resistance to factor H mediated decay acceleration (9, 13). This was particularly demonstrated for mutations located in close proximity to the C3b binding region, i.e. the Mg^{2+}-binding site in the von Willebrand factor type A domain of FB (14). Of note, not all *CFB* mutations have been shown to induce complement activation and not all individuals carrying *CFB* mutations associated with aHUS develop disease (11, 12, 14), even if circulating C3 levels are low. In addition to aHUS, *CFB* mutations and rare variants have also been demonstrated in C3 glomerulopathy and immune complex-associated membranoproliferative glomerulonephritis (MPGN) (15–17).

Binding of C3b to FB elicits a conformational change exposing the scissile bond at position Arg^{234}-Lys^{235} enabling cleavage by FD (18). Small molecule FD inhibitors have been developed as potential treatments for complement-mediated diseases (19) and efficiently inhibited activation of the alternative pathway *in vitro* as well as in animal models (19, 20). FD inhibitors present the advantage of blocking complement activation at the level of the C3 convertase, while leaving the classical and lectin pathways intact. A phase 2 trial has been completed and a phase 3 trial with an oral FD inhibitor as an add-on therapy to C5 inhibition is ongoing in patients with paroxysmal nocturnal hemoglobinuria (PNH) (21, 22).

The aim of this study was to investigate if FD inhibition impacted complement overactivation induced by *CFB* mutations. To this end we investigated four *CFB* mutations associated with aHUS or MPGN, two of which mediate a gain-of-function phenotype. We studied the effect of FD inhibition in the presence of the FB mutations on C3 convertase-induced FB cleavage, complement-mediated hemolysis, and release of soluble C5b-9 from glomerular endothelial cells.

MATERIALS AND METHODS

Subjects

Patients from Iceland, Sweden and Norway with complement-mediated renal diseases are referred to the laboratory at the Dept of Pediatrics in Lund for genetic diagnostics. Three patients were found to have *CFB* mutations. The patients and their laboratory data are presented in **Table 1**. Samples were obtained from apparently healthy adult controls (n=12, 6 female) who were not using any medications. The study of patients and healthy controls was performed with the approval of the Ethics Review Board at Lund University. Approval included genetic analysis of Nordic patients and phenotypic studies of complement mutations. The study was also approved by the National Bioethics Committee of Iceland and the Data Protection Officer at Oslo University Hospital, Oslo Norway. Informed written consent was obtained from the patients or the parents of Patient 3 and the healthy controls.

Blood Samples

Whole blood in EDTA tubes was used for DNA purification. Serum samples were taken during chronic disease in Patients 1-3 and from healthy controls, centrifuged after one hour at room temperature and stored at -80°C until assayed.

Genetic Analysis and Mutation Screening

Next generation sequencing was performed focusing on a panel of genes encoding the following 17 proteins: complement C3, CFB, factor H (CFH), factor H-related proteins-1, -2, -3, -4, -5, C5, factor I, properdin, CD46 (membrane co-factor protein), a disintegrin and metalloproteinase with a thrombospondin type 1 motif 13 (ADAMTS13), diacylglycerol kinase epsilon (DGKE), plasminogen, thrombomodulin and clusterin.

Whole-exome sequencing was performed at the Center for Molecular Diagnostics, Skåne University Hospital and Clinical Genomics Lund, SciLifeLab. In brief, genomic DNA was subject to tagmentation-based library preparation and hybrid capture

TABLE 1 | Clinical characteristics of patients included in this study.

Pat	Sex	Age at presentation (yrs)	Diagnosis	Clinical presentation	Biopsy findings	Disease course	Complement levels		Genetic assay[a]			
							C3 g/L	Factor B %	Factor B	Factor H	DGKE	ADAMTS13
1	M	1	aHUS	Uremia Hypertension	TMA C3 deposition	CKD stage 5 Eculizumab Recurrences: 4 Kidney transplant x3[b]	0.4	100	D371G	–	–	–
2	F	54	aHUS	Uremia	NA	CKD stage 3 Eculizumab Recurrence 0	0.9	66	E601K	–	Q560R	–
3[c]	F	6	MPGN	Nephrotic syndrome	MPGN C3, C1q, C5b-9 and IgM deposition	CKD stage 5 Eculizumab	0.75	79	I242L	V62I N1050Y	–	P457L

[a]All genetic variants shown are heterozygous. [b]Two kidney transplants were performed before the eculizumab era, the first functioned for 15 years and the second for 7 years. Three years after the second transplant, treatment with eculizumab was initiated due to HUS recurrence and was continued until the patient returned to dialysis. Eculizumab therapy was restarted at the time of the third kidney transplant without evidence of recurrence. [c]This patient underwent two biopsies within 2 months, C3 deposits in capillary walls and mesangium increased in the second biopsy. The patient did not have circulating C3 nephritic factor. DGKE, diacylglycerol kinase epsilon; aHUS, atypical hemolytic uremic syndrome; TMA, thrombotic microangiopathy; CKD, chronic kidney disease; MPGN, membranoproliferative glomerulonephritis; NA, not available/not performed. Normal reference values for C3: 0.5-0.95 g/L (Patient 1) 0.77-1.38 g/L (Patients 2 and 3), reference values vary between different clinical laboratories; Factor B: 75-125% (Patient 1), 59-154% (Patients 2 and 3). Patients 1 and 2 did not have antibodies against factor H.

using the Illumina TruSeq Rapid Exome library kit according to the manufacturer's instructions. Captured exome libraries were sequenced 2 x 150 bp on a Next Seq 500 (Illumina, San Diego, CA). Alignment and variant calling were performed according to GATK "Best Practices for Germline SNP & Indel Discovery in Whole Genome and Exome Sequence". Sequence data was mapped to the hg19 genome build using BWA 0.7.15 (23) and variants were called using HaplotypeCaller from GATK 3.7 and processed according to the best practice recommendations (24, 25). Variants were annotated using Ensembl Variant Effect Predictor release 87. Reported variants with frequencies <2% according to Genome Aggregation Database (gnomAD) were included in the genetic evaluation.

Measurement of Anti-Factor B Antibodies

Factor B antibodies were measured in serum as previously described (6). A Nunc Maxisorp 96 well plate (Thermo Scientific, Roskilde, Denmark) was coated with FB (Complement Technologies, Tylor, Texas). Bound IgG was detected with anti-human IgG:horse radish peroxidase (DAKO, Glostrup, Denmark).

Mutagenesis

A plasmid containing wild-type *CFB*, or variants D279G, or I242L cDNA in the expression vector, pcDNA 3.1/V5-His TOPO (Invitrogen, Thermo Fisher, Carlsbad, CA) was previously described (12, 26). For the FB variants D371G and E601K mutagenesis was performed using the QuikChange II XL Site-Directed Mutagenesis Kit (Agilent Technologies, Santa Clara, CA). Primers are available upon request. Mutant sequences were verified by enzymatic digestion with restriction enzymes. XL-10 Gold ultracompetent cells (Agilent) were used for transformation. Constructs were Sanger sequenced to confirm that no additional mutations had been introduced.

Transient Transfection

Transfection was performed as previously described (27). Briefly, human embryonic kidney 293 cells (HEK) cells (ATCC, Teddington, Middlesex, UK) were seeded and grown in DMEM/high glucose Hyclone medium (GE Healthcare Life Sciences, South Logan, UT), supplemented with 100 U/mL penicillin, 100 µg/mL streptomycin and 10% fetal bovine serum to approximately 95% confluence before transfection. Plasmid DNA (2 µg) was added to each well and transfection performed with Lipofectamine (Invitrogen, Life Technologies, Waltham, MA) according to the manufacturer's instructions. Twenty-four h after transfection, the medium was changed to Optimem (Thermo Fisher Scientific) and cells were cultured for an additional 72 h. The media were collected and supplemented with protease inhibitors cOmplete Mini without EDTA (Roche Diagnostic, Mannheim, Germany) and centrifuged to remove cell debris.

Determination of Factor B Size by Immunoblotting

FB size in sera and cell media was determined by immunoblotting. Sera was diluted 1:2000, samples were reduced with mercapto-ethanol and incubated at 100°C for 5 minutes. Proteins were separated by SDS electrophoresis and transferred to a PVDF membrane. Plasma purified FB (1 mg/mL, Complement Technology, Tyler, Texas) was used as the control. Membranes were blocked overnight. Polyclonal goat anti-human FB antibody (1:1000, Complement Technology) was used as the primary antibody followed by rabbit anti-goat horse-radish-peroxidase (1:1000, DAKO, Glostrup, Denmark). Detection was performed by chemiluminescence (Pierce lECL2, Western Blotting Substrate, Rockford, IL) and detected using ChemiDoc™ Touch, Bio-Rad (Hercules, CA).

Measurement of Factor B Protein Levels

FB concentration of constructs was quantified by ELISA using mouse anti-human factor Ba (Quidel, San Diego, CA) for capture and goat anti-human FB polyclonal antibody (Complement Technology) for detection, followed by rabbit anti-goat horseradish-peroxidase (HRP, 1:1000, DAKO, Glostrup, Denmark), alternatively an ELISA kit for detection of human FB (Abcam, Cambridge UK) showing comparable FB levels. Plasma purified FB was used as the standard. Absorbance was measured at 450 nm using Glomax Discover (Promega, Madison, WI).

Complement Activation on Primary Glomerular Endothelial Cells

Primary glomerular endothelial cells (Cell Systems, Kirkland, WA) were plated on cell culture slides (Thermo Fisher Scientific) in endothelial growth medium (EGM-2, Lonza, Walkersville, MD), approximately 75000 cells per well and cultured to monolayer confluence. Cells were activated with adenosine diphosphate (ADP, 1 mM, Sigma-Aldrich) in serum-free EGM-2 for 10 min and washed with PBS with Mg/Ca (GE Life Sciences). Serum samples were diluted 1:4 in serum-free EGM-2 and magnesium-ethylene glycol-bis(2-aminoethylether)-N N N′N`-tetraacetic acid (Mg-EGTA, Complement Technology) 0.1M 1:10, incubated with the cells for 2 h at 37°C. Cells were washed, fixed in paraformaldehyde 4% for 30 min, washed thrice and blocked in 1% BSA for 30 min. C3c deposition on the cells was detected using rabbit anti-human C3c antibody:FITC (DAKO, Glostrup, Denmark) diluted 1:50 in 1% BSA for 1 h. Cells were stained with 4′,6-diamidino-2-phenylindole (DAPI, Thermo Fisher, Eugene, OR). Fluorescence was detected using a Ti-E inverted fluorescence microscope equipped with a Nikon structured illumination microscopy module (Nikon Instruments, Tokyo, Japan). Image stacks at 10 x magnification were converted to maximal intensity images. Stained cells were outlined with a threshold above the background to select the area occupied by cells (DAPI-positive). Quantification was performed using ImageJ Fiji Software (Version 1.53h, NIH, Bethesda, MD).

In certain experiments the cells were incubated with FB constructs (50 μg/mL) in FB-depleted serum diluted 1:4 in serum-free EGM-2. The FB constructs were preincubated with and without the FD inhibitor danicopan ACH- 4471 (MedChemtronica AB, Monmouth Junction, NJ) 10 μM for 15 min before a 2-hour incubation with the cells. Cell supernatants were collected and kept at -20°C until assayed using the sC5b-9 ELISA described below.

Hemolytic Assays Using Human Sera and Factor B Constructs

Complement activation in serum was assayed by incubation of the serum with sheep erythrocytes ($5x10^8$/mL, Håtunalab, Bro, Sweden). Serum (20%) was added to gelatin veronal buffer (GVB) with Mg-EGTA 0.1M 1:10 to which normal human serum (20%) was added, as a source of normal C3, for 10 min at 30°C (28). Ethylenediaminetetraacetic acid (EDTA) 10 mM was added, and samples were centrifuged. Rat serum in EDTA (1:5, Complement Technology) was added, as a source of the terminal complement pathway, for 1 h at 37°C and samples were centrifuged. Absorbance was measured at 405 nm using Glomax Discover (Promega, Madison, WI).

Rabbit erythrocytes ($5x10^8$/mL, Håtunalab) were used in GVB-Mg-EGTA buffer, as above, and incubated with FB constructs 5 μg/mL in FB-depleted serum (Complement Technology). Samples were incubated for 1 h on a shaker at 37°C, after which complement activation was terminated by addition of EDTA (Complement Technology). In certain experiments the FD inhibitor was incubated with erythrocytes in buffer to which FB-depleted serum was added before addition of the constructs. Absorbance was measured at 405 nm using Glomax Discover.

Binding of Factor B Constructs to C3 Measured by Surface Plasmon Resonance

Purified C3b (33 μg/mL in 10 mM sodium acetate (GE Healthcare Bio-Sciences), pH 5.0, Complement Technology) was amine-coupled to a CM5 sensor chip (GE Healthcare) corresponding to 5517.3 response units. The surface of the sensor chip was activated with a mixture of N-hydroxysuccinimide and 1-ethyl-3-(3-dimethylaminoipropyl) -carbomide. After covalent binding of C3b to the dextran matrix the surface was blocked with ethanolamine. Running buffer (10 mM Hepes (pH 7.4), 50 mM NaCl, 10 mM $MgCl_2$) was injected over the flow cells at a flow rate of 10 μL/min and 25°C. The C3 convertase was generated as previously described (29) by serial injections of FB 0.28 μg (60 nM) together with FD 0.02 μg in 50 μl running buffer followed by C3(H2O) 2 μg. After the last step (FB+FD) the surface was extensively washed with 3 M NaCl in acetate buffer (pH 5.2) and 50 mM NaOH to rinse away residual noncovalently bound proteins.

Additional experiments were performed to study the interaction between C3b and FB. C3b was diluted in 10 mM sodium acetate (pH 5.5) at a concentration of 20 μg/mL, and then immobilized as above. The D371G, D279G and wild-type constructs were injected at a flow rate of 30 μL/min and at 25°C over the flow cells using a running buffer containing 10 mM Hepes, 150 mm NaCl, 0.005% surfactant P20, 3.4 mM EDTA (pH 7.5) and 10 mM $MgCl_2$. The equilibrium constant (KD) was calculated. The regeneration buffers used were 10 mM glycine-HCl pH 1.5 and 0.5 M sodium chloride.

Assays were performed using a Biacore X100 instrument (GE Healthcare). Biacore X100 Evaluation Software version 2.0.1 and 1.0.1 was used for sensogram generation. Baseline values were adjusted to pre-sample injection levels at t=0 in each cycle in order to compare binding.

Factor B Cleavage by Factor D in Solid Phase

Microtiter wells were coated with C3b at 3 μg/mL diluted in phosphate-buffered-saline (PBS) overnight and blocked with bovine serum albumin (BSA, Sigma) for 1 h. Serum, 20% in Mg- PBS, or FB constructs 5 μg/mL in assembly buffer (Mg, FD 100 ng/mL in PBS with BSA 1%), were incubated for 30 min at 37°C and an additional 30 min with slow shaking. Samples were washed four times with PBS-Tween 20 0.1%. Twenty μl 10 mM EDTA with sodium dodecyl sulfate (SDS) 1% were added to the empty wells for 1 h on a microplate shaker 1000 rpm at rt.

Protein complexes were detached by scraping as described (30) and samples were stored at -20°C. In certain samples the FD inhibitor at 10 µM (final concentration) was preincubated with the samples for 15 min before addition to the plate.

Samples were reduced and loaded onto a Tris-TGX gel 10% (Bio Rad) and after protein separation transferred to PVDF membranes (Bio Rad) and electroblotted (Transblot Turbo, Bio Rad). Immunoblot was carried out with goat anti-FB and rabbit anti-goat:HRP and detected as described above.

Soluble C5b-9 Measurement

Soluble C5b-9 in the supernatant from activated glomerular endothelial cells was quantified using the MicroVue SC5-b9 Plus kit (Quidel, San Diego, CA) according to the manufacturer's protocol. Absorbance was measured at 450 nm using Glomax Discover.

Statistics

Kruskal-Wallis multiple-comparison test followed by Dunn's procedure was used for evaluating differences between more than two groups. A P value ≤ 0.05 was considered significant. Statistical analysis was performed using GraphPad prism 8 software (version 8.4.3, GraphPad Software, La Jolla, CA).

RESULTS

Factor B Variants

Three FB mutations were identified in Patients 1-3 (**Table 1**). The location of the gene products within FB domains is depicted in **Figure 1**. FB variants D371G (rs1258425617) (31) and I242L (rs1299040443) (7, 12, 32) have been reported before in patients with aHUS. Variant D371G (rs756325732) is located in the von Willebrand factor (VWF) type A domain of the Bb fragment, but far from the C3b binding site (**Figure 1**). The E601K variant has not been previously reported and is located in the serine protease domain, not near the catalytic site, at the VWF type A domain binding interface in the context of the pro-convertase C3bB (but not in the convertase C3bBb). The Bb fragment undergoes a conformational change upon release of Ba, leading to assembly of the metal ion dependent adhesion site (MIDAS). The mutated residue is far from the MIDAS, which participates in C3b binding, but may affect its assembly by allosteric effects (**Figure 1**). I242L is located in the linker between Ba and Bb fragments near the R234-K235 scissile bond (33). The D279G variant was used as a positive control as it was previously shown to induce a gain-of-function phenotype (34) and is located in proximity to the MIDAS in the von Willebrand factor A domain. The patients had normal serum FB levels (**Table 1**) and normal FB size (**Supplementary Figure 1**) and did not have autoantibodies to FB (data not shown).

Phenotypic Assays of the FB Mutations

Assays were performed to investigate the factor B phenotype using patient sera and mutant constructs, as outlined in **Table 2**.

C3 Deposition on Glomerular Endothelial Cells

Serum from Patients 1-3 and normal sera (n=10) were incubated with primary glomerular endothelial cells. Patient sera induced C3 deposition on the cells which was also detected for 3 normal

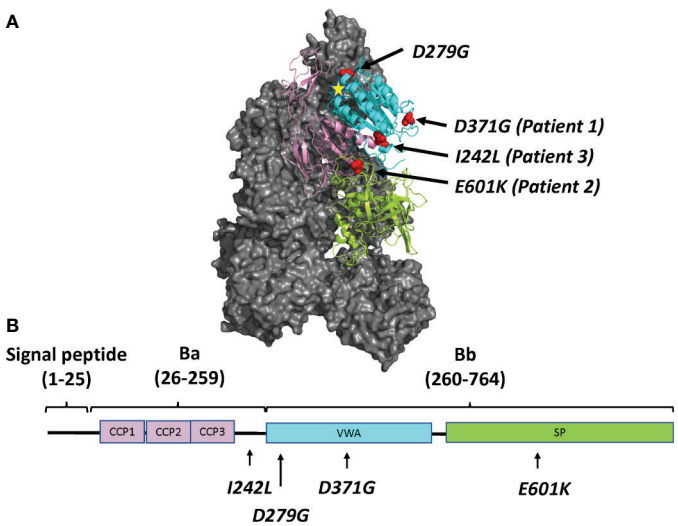

FIGURE 1 | The molecular structure of factor B and the location of mutations described in this study. **(A)** Location of the four mutated residues (D371G, E601K, I242L and D279G), visualized on the structure of the C3 pro-convertase C3bB depicted in grey (PDB ID 2XWJ) (18) using PyMol. The Metal Ion Dependent Adhesion Site (MIDAS) on C3b is depicted by a star. The colors of the domains correspond to the domains depicted in **(B)**. **(B)** The linear structure of factor B divided into the signal peptide/leader, Ba and Bb fragments with a linker sequence in between. The amino acid numbers are given in parentheses. The protein is composed of a complement control protein (CCP) domain with three CCPs, followed by the linker, the von Willebrand factor type A domain (VWA) and the serine protease (SP) domain. The location of mutations studied herein is depicted.

TABLE 2 | Complement functional assays performed in this study using patient sera and mutant constructs.

Complement assays	Patient 1 D371G		Patient 2 E601K		Patient 3 I242L		Positive control D279G	Normal controls	
	Serum[a]	Mutant construct	Serum[a]	Mutant construct	Serum[a]	Mutant construct	Mutant construct	Serum	Wild-type construct
C3 deposition on glomerular endothelial cells	+	ND	+	ND	+	ND	ND	3/10[b]	ND
Hemolysis sheep RBCs	+	ND	–	ND	+	ND	ND	0/2	ND
Factor B binding to C3b (surface plasmon resonance)	ND	+	ND	–	ND	–	+	ND	–
Factor B degradation by factor D	Degr	Degr	Degr	Degr	Degr	Degr	Degr	Degr	Degr
Hemolysis of rabbit RBCs	ND	+	ND	–	ND	–	+	ND	–
Soluble C5b-9 release from glomerular endothelial cells	ND	+	ND	–	ND	–	+	ND	–

[a]*Serum from Patients 1 and 2 was taken during eculizumab treatment. Serum from Patient 3 was taken before the start of eculizumab treatment.* [b]*3/10 indicates positive result in 3 of 10 controls. +, complement activation detected; -, complement activation was not detected; ND, Not done; RBCs, red blood cells; Degr, degradation detected.*

sera incubated with the cells (**Figure 2**). C5b-9 deposition on the cells could not be assayed because the patients were treated with the anti-C5 antibody eculizumab (**Table 1**).

Patient Sera Induced Hemolysis of Sheep Red Blood Cells

Sera from Patients 1-3 and normal serum from two healthy controls were incubated with sheep erythrocytes. Sera from Patients 1 (FB: D371G) and 3 (FB: I242L, CFH: V62I, N1050Y and ADAMTS13: P457L) induced hemolysis whereas samples from Patient 2 (FB: E601K, DGKE: Q560R) and the normal controls (n=2) did not (**Figure 3**).

Binding of Factor B Constructs to C3b and Formation of the C3 Convertase Determined by Surface Plasmon Resonance

In binding assays, we first examined FB binding to C3b. C3b was immobilized on a Biacore sensor surface. The purified FB constructs, D279G (positive control, gain-of-function mutation in aHUS) (13), D371G, I242L or E601K were injected together with FD. Sensograms were aligned at $t = 0$ for comparison and showed that the FB construct D371G bound most, followed by D279G. The I242L, E601K and wild-type constructs demonstrated similar binding capacity (see arrow in **Figure 4**).

The C3 convertase was assembled on the sensor chip by serial injections of purified FB and FD followed by C3 (**Figure 4**) and showed that the factor B variant D279G yielded the highest binding, indicating C3 convertase formation, followed by D371G, the wild-type, E601K and I242L (see arrowhead in **Figure 4**).

Binding experiments showed that the FB mutant constructs D279G and D371G exhibited stronger binding to C3 than the wild-type construct (**Figure 4B**). Using a concentration range of the D371G and wild-type constructs (**Figure 4C**) the Ka, Kd and KD constant were calculated showing that the D371G construct had a higher affinity for C3 than the wild-type construct.

Effects of Factor D Inhibition

Factor B Cleavage by the C3 Convertase

A functional C3bBb(Mg^{2+}) complex was formed in a microtiter plate by incubating C3b-coated wells with serum. In the presence

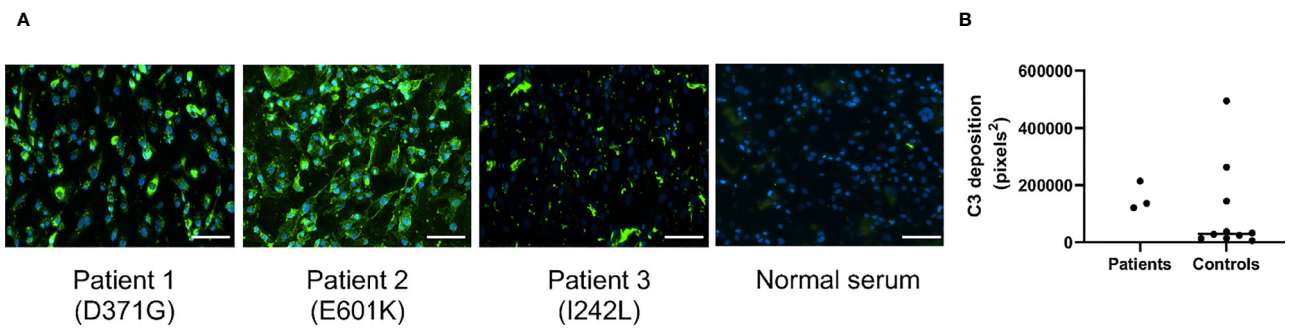

FIGURE 2 | C3 deposition on glomerular endothelial cells in the presence of serum from patients and controls. Sera from Patients 1-3 and controls (n = 10) were incubated with glomerular endothelial cells for 2 h and C3 detected by immunofluorescence. **(A)** Serum from Patients 1-3 induced excessive C3 deposition on the cells. The scale bar represents 100 µm. **(B)** Quantification of C3 deposition fluorescence showing that even 3/10 sera from apparently healthy adult controls exhibited C3 deposition. The bar represents the median.

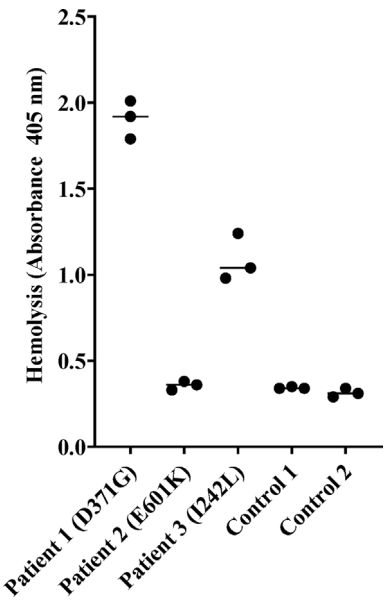

FIGURE 3 | Hemolysis of sheep erythrocytes in the presence of patient and normal serum. Serum from Patients 1 (factor B mutation D371G) and 3 (I242L) induced hemolysis of sheep erythrocytes whereas serum from Patient 2 and from the two normal controls did not. The results of three separate experiments are shown. The bar depicts the median.

of normal serum, as well as serum from Patients 1-3, the C3 convertase was formed and cleavage of FB to the Bb fragment was detected (**Figure 5A**). In the presence of the FD inhibitor, danicopan ACH- 4471, FB cleavage was inhibited in normal serum, as well as in the serum of Patients 2 and 3, and partially inhibited in the serum of Patient 1 in which a weak Bb band was still visible.

Similarly, the C3b-coated plates were incubated with purified FB constructs together with FD showing that all constructs, wild-type, D279G, D371G, E601K and I242L, exhibited FB cleavage to the Bb fragment, albeit weaker for the I242L variant, and that cleavage was entirely inhibited in the presence of the FD inhibitor (**Figure 5B**).

Complement-Mediated Hemolysis of Rabbit Red Blood Cells

Rabbit red blood cells were incubated with FB constructs in FB-depleted serum and underwent hemolysis in the presence of FB variants D279G and D371G whereas the wild-type, as well as E601K and I242L constructs did not induce hemolysis. The FD inhibitor inhibited D279G- and D371G-induced hemolysis (**Figure 6**).

Release of Soluble C5b-9 From Primary Glomerular Endothelial Cells

Soluble C5b-9 was detected in supernatants from primary glomerular endothelial cells that were incubated with FB constructs D279G and D371G in FB-depleted serum. The FB construct D371G induced increased C5b-9 release compared to the wild-type construct (**Figure 7**). In the presence of the FD inhibitor the soluble C5b-9 levels were comparable with those released in the presence of the wild-type construct (**Figure 7**). Factor B mutant constructs E601K and I242L did not induce C5b-9 release compared to the wild-type.

DISCUSSION

Complement activation is a hallmark of aHUS, C3 glomerulopathy and MPGN. Here we explored three patients with *CFB* variants. One of these variants, D371G, was shown to be a gain-of-function mutation, as indicated by enhanced binding to C3b, formation of the C3 convertase, increased hemolysis of rabbit erythrocytes and release of soluble C5b-9 from glomerular endothelial cells. Additionally, the D279G variant, also found in aHUS (13), was used a positive control and exhibited similar properties. Both *CFB* variants, D371G and D279G, could be effectively controlled by the FD small molecule-inhibitor danicopan (ACH-4471). The remaining two variants did not show gain-of-function but also did not perturb the inhibitory activity of danicopan. This suggests that FD inhibition should effectively inhibit complement activation in these patients.

CFB variants have been described in patients with aHUS (7–14, 31, 35, 36), in C3 glomerulopathy (15, 17) and in a few patients with immune-complex associated MPGN (16) but not all of them exhibit gain-of-function (12). Here we show that the mutant variant D371G, found in Patient 1, and reported previously (31), induces a clear-cut gain-of-function. These functional consequences can explain why the serum from Patient 1, without other complement mutations, induced C3 deposition on glomerular endothelial cells and hemolysis of sheep erythrocytes. Increased hemolysis in serum from this patient, treated with eculizumab at the time of sampling, is explained by the addition of rat serum, as a source of C5b-9, at which point the effect of eculizumab is eliminated by a washing step.

A novel *CFB* mutation E601K, in the serine protease domain of the protein, was found in Patient 2. This variant did not exhibit gain-of-function in the tests performed. Therefore, the increased complement deposition on endothelial cells cannot be explained by this genetic variant. The patient also had a mutation in the diacylglycerol kinase epsilon (DGKE) gene. DGKE mutations associated with aHUS do not directly cause complement activation and usually present during the first year of life (37), however this patient first presented with aHUS at mid-life. Thus, we assume that the DGKE variant was not associated with the patient's disease.

The FB mutant variant I242L was detected in Patient 3, a child with what initially appeared to be immune complex-mediated MPGN. However, a second biopsy within 2 months showed more C3 deposition and suggested that the child might develop C3 glomerulopathy over time. This mutation was previously described in patients with aHUS and did not induce a clear gain-of-function (12). Serum from the patient induced C3 deposition on glomerular endothelial cells and enhanced hemolysis of sheep erythrocytes. The child also has previously reported genetic variants in *CFH*, V62I and N1050Y (38), suggesting that complement activation on cells may be a

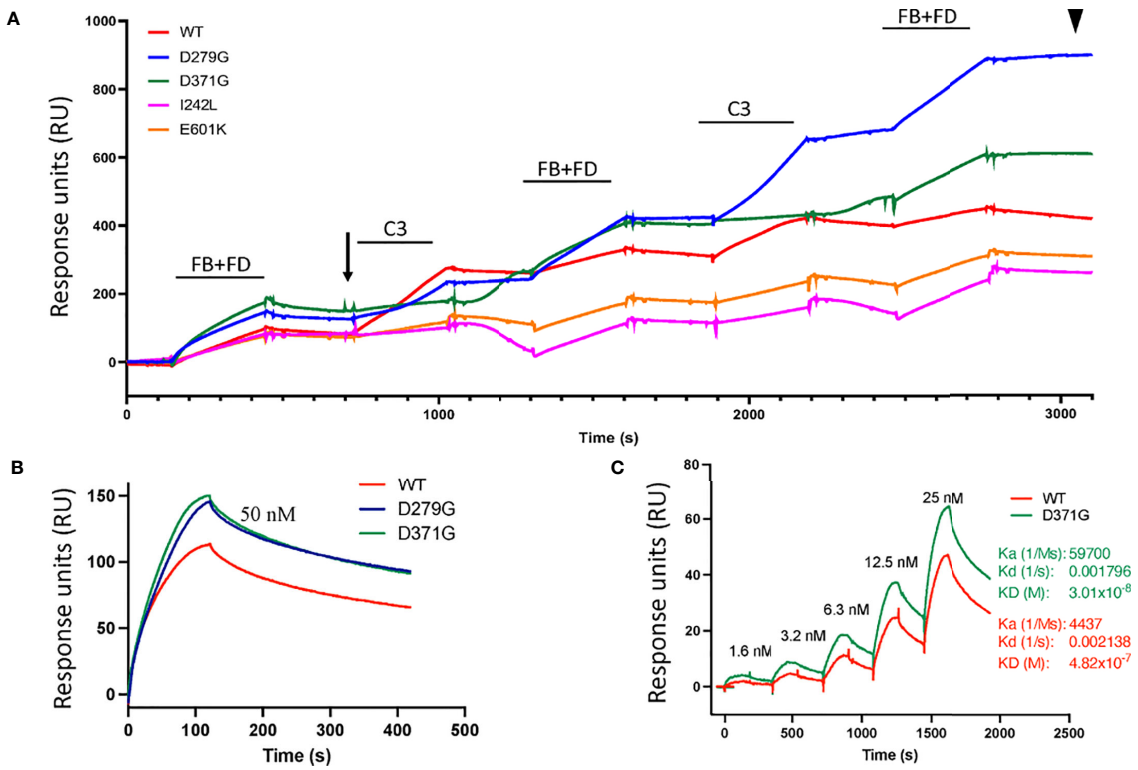

FIGURE 4 | Binding of factor B variants to C3b and formation of the C3 convertase. **(A)** Purified C3b was coupled to a CM5 sensor chip. Factor B (FB) variants and factor D (FD) were injected over the surface and binding curves visualized. The FB D371G mutant exhibited the strongest binding to the C3b-coated surface (see arrow) followed by D279G, I242L, the wild-type (WT) and E601K. This was followed by serial injections of C3 alternating with FB+FD to form the C3 convertase on the chip. The strongest C3 convertase generation was demonstrated for the D279G mutant (see arrowhead), followed by D371G, the wild-type, I242L and E601K. Baseline values were adjusted at $t = 0$ in each cycle for comparison. **(B)** Binding between C3b and FB alone was assessed using the wild-type construct, D371G and D279G showing that both mutant constructs, at 50 nM, exhibited stronger binding than the wild-type construct. **(C)** The coefficient of dissociation was evaluated using a range of FB concentrations comparing construct D371G to the wild-type.

combined effect of *CFB* and *CFH* variants, although functional data regarding the *CFH* variant N1050Y are lacking.

One limitation of this study was that only three patients were investigated and only one of the three (Patient 1) was found to have a gain-of-function mutation in factor B (D371G). In Patients 2 and 3 we could not determine a link between the patients' clinical disease and the factor B mutations. The absence of functional consequences of the two *CFB* mutant variants, E601K and I242L, is in apparent contradiction with the complement activation observed on endothelial cells, incubated with patient sera. Ex vivo complement activation on endothelial cells has been previously reported as positive in aHUS patients without identified genetic abnormalities (39). Moreover, it is positive in patients with sickle cell disease (40), preeclampsia and HELLP syndrome (41) and as shown herein, even in some apparently healthy controls. In sickle cell disease, the complement overactivation was mediated, at least in part, by heme (40, 42). Heme or other pro-inflammatory factors may be present in the patient sera, activating the endothelial cells, rendering them susceptible to complement activation. Furthermore, although serum from Patient 2 induced C3 deposition on endothelial cells the serum did not induce hemolysis (**Table 2**) which is in line with the presence of a pro-inflammatory factor inducing changes on the surface of endothelial cells which did not fully activate the terminal complement complex.

FD inhibition has been previously assessed in samples from patients with the complement-mediated diseases PNH and aHUS. Low concentrations of FD inhibitors were shown to reduce C3 fragment deposition on PNH erythrocytes as well as complement-mediated hemolysis (19, 20). Likewise, serum from aHUS patients induced complement-mediated cell death in *PIGA*-null PNH-like cells which was abrogated by the FD-inhibitor (20). The results of the current study focused on FB mutations utilizing both patient sera and recombinant mutants, showing that the FD inhibitor prevented FB cleavage to Bb, hemolysis and the formation of C5b-9 in the presence of gain-of-function mutations, thereby blocking excessive complement activation.

Danicopan was found to be effective in preventing complement-mediated hemolysis in a phase 2 trial in patients with PNH (43). A phase 3 trial is ongoing in which Danicopan is being investigated as add-on therapy to C5 inhibitor for patients with PNH with extravascular hemolysis (22). For patients with aHUS current consensus recommends treatment with intravenous eculizumab,

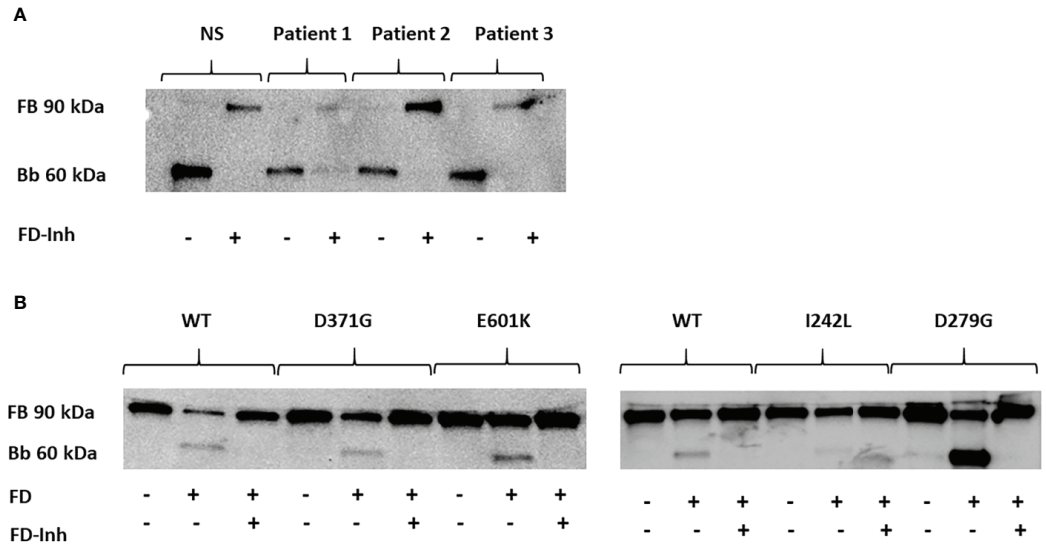

FIGURE 5 | The effect of factor D inhibition on C3 convertase formation using human serum or factor B mutants. An immunoblot assay was used to detect the Bb fragment of the alternative pathway C3bBb. **(A)** C3bBb(Mg^{2+}) complexes were formed by incubating C3b-coated wells with normal serum (NS) or patient serum (Patients 1-3). The C3 convertase formed in the presence of all sera effectively cleaved factor B to the Bb component and this reaction was inhibited by the factor D inhibitor. The factor D inhibitor only partially blocked the C3 convertase in the presence of serum from Patient 1(D371G mutation) as a weak Bb band was still visible. **(B)** The same assay was performed with the wild-type (WT) and mutant factor B constructs (D371G, E601K, I242L and D279G) showing cleavage to the Bb fragments and effective inhibition by the factor D inhibitor. FB, factor B; Bb, the Bb fragment of factor B; FD, factor D; FD-inh, factor D inhibitor.

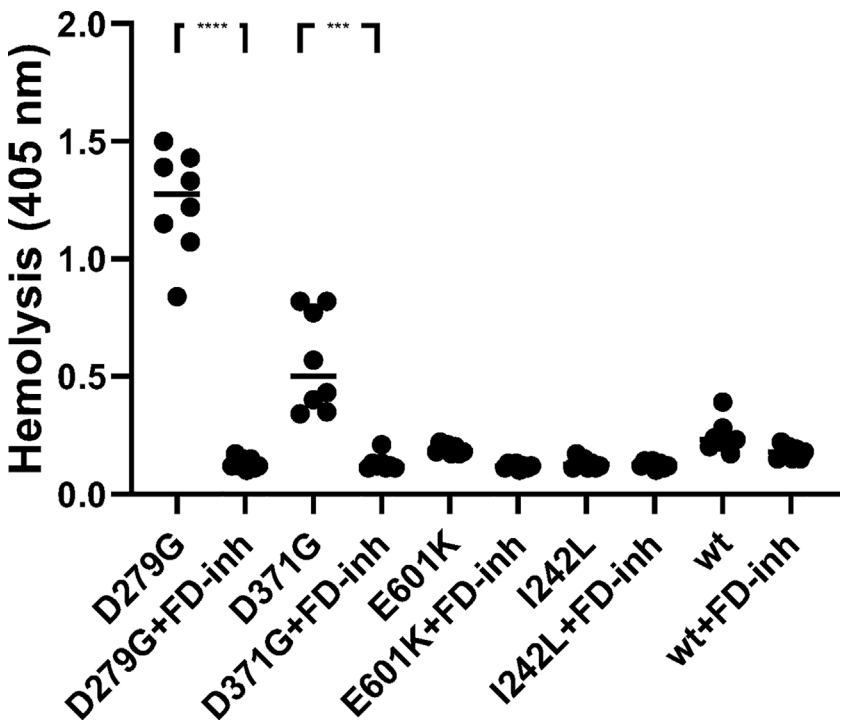

FIGURE 6 | The effect of factor D inhibition on hemolysis of rabbit erythrocytes. Factor B constructs were incubated in factor B-depleted serum with rabbit erythrocytes. The mutant variants D279G (positive control) and D371G (corresponding to Patient 1) induced hemolysis. The other mutant constructs (E601K, I242L) and wild-type (wt) did not induce hemolysis. The factor D inhibitor (FD-inh) inhibited hemolysis induced by factor B mutants D279G and D371G. Eight separate experiments are shown. ***$P < 0.001$, ****$P < 0.0001$.

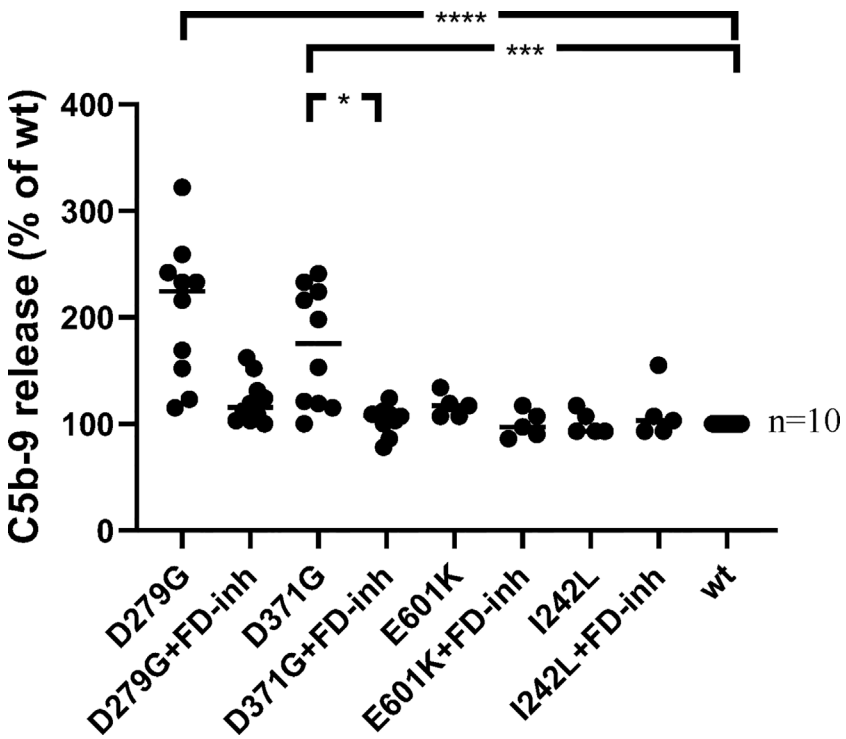

FIGURE 7 | The effect of factor D inhibition on C5b-9 release from glomerular endothelial cells. Factor B mutants D279G (positive control), D371G, E601K, I242L and the wild-type (wt) construct were combined with factor B-depleted serum and incubated with glomerular endothelial cells. The release of C5b-9 was detected in cell supernatants in the presence or absence of the factor D inhibitor. The mutant construct D371G induced the release of C5b-9 which was decreased by the factor D inhibitor. A tendency to decrease was noted when the mutant construct D279G was incubated with the factor D inhibitor but this did not achieve statistical significance (multivariate analysis). FD-inh, factor D inhibitor; *P < 0.05, ***P < 0.001, ****P < 0.0001.

or ravulizumab (5, 44) thereby blocking C5. FD inhibitors should also be evaluated in clinical trials either as add-on therapy for C3 glomerulopathy patients, or for aHUS patients in whom C5 inhibition is insufficient, or as an alternative therapy. FD inhibitors present certain advantages over eculizumab for the treatment of aHUS. In addition to the extremely high price of eculizumab (45) and the oral mode of administration of danicopan, FD blockade will selectively inhibit the alternative pathway and allow activity of the classic and lectin pathways. Patients treated with eculizumab are at risk of meningococcal infection due to blockade of C5b-9 mediated bacterial killing, a risk that is considerably less with FD inhibitors (46). However, C3 degradation fragments physiologically promote opsonization and phagocytosis (47) which are also important for defense against meningococcal infections. Inhibition of these proximal effects would not occur in the presence of eculizumab, while they would be impeded in the presence of an FD inhibitor. In line with this upstream inhibition, the spike protein of SARS-CoV-2 was shown to activate the alternative pathway of complement, and a small molecule FD inhibitor prevented the cellular deposition of C3 fragments and the generation of C5b-9 (48). Similarly, we could show that danicopan inhibited formation of the C3 convertase and FB cleavage as well as release of soluble C5b-9 from cells exposed to the gain-of-function *CFB* D371G mutation.

In summary, we describe at the molecular level, the response of FB mutations to FD inhibition and that FB mutations do not impact the effective response to FD inhibition. The data suggest that FD inhibition should be further studied in clinical trials as a possible treatment for complement-mediated kidney diseases aHUS, MPGN and C3 glomerulopathy.

DATA AVAILABILITY STATEMENT

The raw data supporting the conclusions of this article will be made available by the authors, without undue reservation, to any qualified researcher.

ETHICS STATEMENT

The study of patients and healthy controls was performed with the approval of the Ethics Review Board at Lund University. The study was also approved by the National Bioethics Committee of Iceland and the Data Protection Officer at Oslo University Hospital, Oslo Norway. Informed written consent was obtained from the patients or the parents of Patient 3 and the healthy controls.

AUTHOR CONTRIBUTIONS

SA conceived and designed the analysis, analyzed the data; performed experiments and wrote the paper. A-CK performed experiments and wrote the paper. LR contributed conceptually, contributed plasmids and wrote the paper. AB contributed patient data and write-up. PK contributed patient data and write-up. RP contributed patient data, design and write-up. DK conceived and designed the analysis and wrote the paper. All authors contributed to the article and approved the submitted version.

FUNDING

The Swedish Research Council (2017-01920), The Knut and Alice Wallenberg Foundation (Wallenberg Clinical Scholar 2015.0320), Skåne Centre of Excellence in Health, The IngaBritt and Arne Lundberg's Research Foundation, Olle Engkvist Byggmästare Foundation (all to DK).

ACKNOWLEDGMENTS

The authors wish to thank Dr Marina Noris and Dr Roberta Donadelli, Istituto di Ricerche Farmacologiche Mario Negri, Bergamo Italy for excellent technical advice for the assay of factor B cleavage by the C3 convertase. Dr Ravi Bhongir and Dr Sandra Jovic, Infection Medicine, Clinical Sciences Lund are acknowledged for their help with the surface plasmon resonance assays. The authors thank Drs Markus Heidenblad, Sofia Saal and Björn Hallström of the Center for Molecular Diagnostics, Region Skåne and Clinical Genomics Lund, SciLifeLab, Lund University for next-generation sequencing. Dr Henning Gong carried out part of the mutagenesis study as part of his master's thesis. The kidney biopsies of Patient 3 were assessed by Dr. Melinda Raki, Department of Pathology, Oslo University Hospital, Oslo Norway, Dr. Sabine Leh, Department of Pathology, Haukeland Univeristy Hospital Bergen, Norway, Professor Sanjeev Sethi and Professor Fernando Fervenza of the Department of Laboratory Medicine and Pathology, Mayo Clinic, Rochester, Minnesota. This work was presented in preliminary poster form at the17th Congress of the International Pediatric Nephrology Association, Iguacu Brazil, September 20-24, 2016, at the 6th International Conference "HUS & related diseases", Innsbruck, Austria, June 11-13, 2017, the 16th European Meeting of Complement in Human Disease, Copenhagen, Denmark, September 8-12, 2017, the 18th Congress of the International Pediatric Nephrology Association, Venice, Italy October 17-21, 2019.

SUPPLEMENTARY MATERIAL

The Supplementary Material for this article can be found online at: https://www.frontiersin.org/articles/10.3389/fimmu.2021.690821/full#supplementary-material

REFERENCES

1. Walport MJ. Complement. First of Two Parts. *N Engl J Med* (2001) 344:1058–66. doi: 10.1056/NEJM200104053441406
2. Slade C, Bosco J, Unglik G, Bleasel K, Nagel M, Winship I. Deficiency in Complement Factor B. *N Engl J Med* (2013) 369:1667–9. doi: 10.1056/NEJMc1306326
3. Karpman D, Loos S, Tati R, Arvidsson I. Haemolytic Uraemic Syndrome. *J Intern Med* (2017) 281:123–48. doi: 10.1111/joim.12546
4. Smith RJH, Appel GB, Blom AM, Cook HT, D'Agati VD, Fakhouri F, et al. C3 Glomerulopathy - Understanding a Rare Complement-Driven Renal Disease. *Nat Rev Nephrol* (2019) 15:129–43. doi: 10.1038/s41581-018-0107-2
5. Goodship TH, Cook HT, Fakhouri F, Fervenza FC, Fremeaux-Bacchi V, Kavanagh D, et al. Atypical Hemolytic Uremic Syndrome and C3 Glomerulopathy: Conclusions From a "Kidney Disease: Improving Global Outcomes" (Kdigo) Controversies Conference. *Kidney Int* (2017) 91:539–51. doi: 10.1016/j.kint.2016.10.005
6. Marinozzi MC, Roumenina LT, Chauvet S, Hertig A, Bertrand D, Olagne J, et al. Anti-Factor B and Anti-C3b Autoantibodies in C3 Glomerulopathy and Ig-Associated Membranoproliferative Gn. *J Am Soc Nephrol* (2017) 28:1603–13. doi: 10.1681/ASN.2016030343
7. Maga TK, Nishimura CJ, Weaver AE, Frees KL, Smith RJ. Mutations in Alternative Pathway Complement Proteins in American Patients With Atypical Hemolytic Uremic Syndrome. *Hum Mutat* (2010) 31:E1445–60. doi: 10.1002/humu.21256
8. Funato M, Uemura O, Ushijima K, Ohnishi H, Orii K, Kato Z, et al. A Complement Factor B Mutation in a Large Kindred With Atypical Hemolytic Uremic Syndrome. *J Clin Immunol* (2014) 34:691–5. doi: 10.1007/s10875-014-0058-8
9. Zhang Y, Kremsdorf R, Sperati CJ, Henriksen KJ, Mori M, Goodfellow RX, et al. Mutation of Complement Factor B Causing Massive Fluid-Phase Dysregulation of the Alternative Complement Pathway can Result in Atypical Hemolytic Uremic Syndrome. *Kidney Int* (2020) 98:1265–74. doi: 10.1016/j.kint.2020.05.028
10. Tawadrous H, Maga T, Sharma J, Kupferman J, Smith RJ, Schoeneman M. A Novel Mutation in the Complement Factor B Gene (CFB) and Atypical Hemolytic Uremic Syndrome. *Pediatr Nephrol* (2010) 25:947–51. doi: 10.1007/s00467-009-1415-3
11. Bekassy ZD, Kristoffersson AC, Cronqvist M, Roumenina LT, Rybkine T, Vergoz L, et al. Eculizumab in an Anephric Patient With Atypical Haemolytic Uraemic Syndrome and Advanced Vascular Lesions. *Nephrol Dial Transplant* (2013) 28:2899–907. doi: 10.1093/ndt/gft340
12. Marinozzi MC, Vergoz L, Rybkine T, Ngo S, Bettoni S, Pashov A, et al. Complement Factor B Mutations in Atypical Hemolytic Uremic Syndrome-Disease-Relevant or Benign? *J Am Soc Nephrol* (2014) 25:2053–65. doi: 10.1681/ASN.2013070796
13. Roumenina LT, Jablonski M, Hue C, Blouin J, Dimitrov JD, Dragon-Durey MA, et al. Hyperfunctional C3 Convertase Leads to Complement Deposition on Endothelial Cells and Contributes to Atypical Hemolytic Uremic Syndrome. *Blood* (2009) 114:2837–45. doi: 10.1182/blood-2009-01-197640
14. Goicoechea de Jorge E, Harris CL, Esparza-Gordillo J, Carreras L, Arranz EA, Garrido CA, et al. Gain-of-Function Mutations in Complement Factor B are Associated With Atypical Hemolytic Uremic Syndrome. *Proc Natl Acad Sci U S A* (2007) 104:240–5. doi: 10.1073/pnas.0603420103
15. Imamura H, Konomoto T, Tanaka E, Hisano S, Yoshida Y, Fujimura Y, et al. Familial C3 Glomerulonephritis Associated With Mutations in the Gene for Complement Factor B. *Nephrol Dial Transplant* (2015) 30:862–4. doi: 10.1093/ndt/gfv054
16. Iatropoulos P, Noris M, Mele C, Piras R, Valoti E, Bresin E, et al. Complement Gene Variants Determine the Risk of Immunoglobulin-Associated MPGN and C3 Glomerulopathy and Predict Long-Term Renal Outcome. *Mol Immunol* (2016) 71:131–42. doi: 10.1016/j.molimm.2016.01.010
17. Osborne AJ, Breno M, Borsa NG, Bu F, Fremeaux-Bacchi V, Gale DP, et al. Statistical Validation of Rare Complement Variants Provides Insights Into the

Molecular Basis of Atypical Hemolytic Uremic Syndrome and C3 Glomerulopathy. *J Immunol* (2018) 200:2464–78. doi: 10.4049/jimmunol.1701695
18. Forneris F, Ricklin D, Wu J, Tzekou A, Wallace RS, Lambris JD, et al. Structures of C3b in Complex With Factors B and D Give Insight Into Complement Convertase Formation. *Science* (2010) 330:1816–20. doi: 10.1126/science.1195821
19. Maibaum J, Liao SM, Vulpetti A, Ostermann N, Randl S, Rudisser S, et al. Small-Molecule Factor D Inhibitors Targeting the Alternative Complement Pathway. *Nat Chem Biol* (2016) 12:1105–10. doi: 10.1038/nchembio.2208
20. Yuan X, Gavriilaki E, Thanassi JA, Yang G, Baines AC, Podos SD, et al. Small-Molecule Factor D Inhibitors Selectively Block the Alternative Pathway of Complement in Paroxysmal Nocturnal Hemoglobinuria and Atypical Hemolytic Uremic Syndrome. *Haematologica* (2017) 102:466–75. doi: 10.3324/haematol.2016.153312
21. Wiles JA, Galvan MD, Podos SD, Geffner M, Huang M. Discovery and Development of the Oral Complement Factor D Inhibitor Danicopan (Ach-4471). *Curr Med Chem* (2020) 27:4165–80. doi: 10.2174/0929867326676191001130342
22. Kulasekararaj A, Risitano A, Lee JW, Huang M, Nishimura J-I, Ramirez-Santiago A, et al. Phase 3 Study of Danicopan, An Oral Complement Factor D Inhibitor, As Add-on Therapy to a C5 Inhibitor in Patients With Paroxysmal Nocturnal Hemoglobinuria With Clinically Evident Extravascular Hemolysis. *Blood* (2020) 136:6–7. doi: 10.1182/blood-2020-134388
23. Li H. Aligning Sequence Reads, Clone Sequences and Assembly Contigs With BWA-MEM. *arXiv* [Preprint] (2013) arXiv:13033997.
24. DePristo MA, Banks E, Poplin R, Garimella KV, Maguire JR, Hartl C, et al. A Framework for Variation Discovery and Genotyping Using Next-Generation DNA Sequencing Data. *Nat Genet* (2011) 43:491–8. doi: 10.1038/ng.806
25. Van der Auwera GA, Carneiro MO, Hartl C, Poplin R, Del Angel G, Levy-Moonshine A, et al. From FastQ Data to High Confidence Variant Calls: The Genome Analysis Toolkit Best Practices Pipeline. *Curr Protoc Bioinf* (2013) 43:11 0 1– 0 33. doi: 10.1002/0471250953.bi1110s43
26. Hourcade DE, Mitchell LM, Oglesby TJ. Mutations of the Type A Domain of Complement Factor B That Promote High-Affinity C3b-Binding. *J Immunol* (1999) 162:2906–11.
27. Sartz L, Olin AI, Kristoffersson AC, Stahl AL, Johansson ME, Westman K, et al. A Novel C3 Mutation Causing Increased Formation of the C3 Convertase in Familial Atypical Hemolytic Uremic Syndrome. *J Immunol* (2012) 188:2030–7. doi: 10.4049/jimmunol.1100319
28. Rother U. A New Screening Test for C3 Nephritis Factor Based on a Stable Cell Bound Convertase on Sheep Erythrocytes. *J Immunol Methods* (1982) 51:101–7. doi: 10.1016/0022-1759(82)90386-6
29. Jokiranta TS, Westin J, Nilsson UR, Nilsson B, Hellwage J, Lofas S, et al. Complement C3b Interactions Studied With Surface Plasmon Resonance Technique. *Int Immunopharmacol* (2001) 1:495–506. doi: 10.1016/s1567-5769(00)00042-4
30. Bettoni S, Galbusera M, Gastoldi S, Donadelli R, Tentori C, Sparta G, et al. Interaction Between Multimeric Von Willebrand Factor and Complement: A Fresh Look to the Pathophysiology of Microvascular Thrombosis. *J Immunol* (2017) 199:1021–40. doi: 10.4049/jimmunol.1601121
31. Phillips EH, Westwood JP, Brocklebank V, Wong EK, Tellez JO, Marchbank KJ, et al. The Role of ADAMTS-13 Activity and Complement Mutational Analysis in Differentiating Acute Thrombotic Microangiopathies. *J Thromb Haemost* (2016) 14:175–85. doi: 10.1111/jth.13189
32. Vaught AJ, Braunstein EM, Jasem J, Yuan X, Makhlin I, Eloundou S, et al. Germline Mutations in the Alternative Pathway of Complement Predispose to HELLP Syndrome. *JCI Insight* (2018) 3(6):e99128. doi: 10.1172/jci.insight.99128
33. Milder FJ, Gomes L, Schouten A, Janssen BJ, Huizinga EG, Romijn RA, et al. Factor B Structure Provides Insights Into Activation of the Central Protease of the Complement System. *Nat Struct Mol Biol* (2007) 14:224–8. doi: 10.1038/nsmb1210
34. Hourcade DE, Mitchell LM. Access to the Complement Factor B Scissile Bond is Facilitated by Association of Factor B With C3b Protein. *J Biol Chem* (2011) 286:35725–32. doi: 10.1074/jbc.M111.263418
35. Alfakeeh K, Azar M, Alfadhel M, Abdullah AM, Aloudah N, Alsaad KO. Rare Genetic Variant in the CFB Gene Presenting as Atypical Hemolytic Uremic Syndrome and Immune Complex Diffuse Membranoproliferative Glomerulonephritis, With Crescents, Successfully Treated With Eculizumab. *Pediatr Nephrol* (2017) 32:885–91. doi: 10.1007/s00467-016-3577-0
36. Noris M, Remuzzi G. Atypical Hemolytic Uremic Syndrome Associated With a Factor B Genetic Variant and Fluid-Phase Complement Activation: An Exception to the Rule? *Kidney Int* (2020) 98:1084–7. doi: 10.1016/j.kint.2020.06.026
37. Lemaire M, Frémeaux-Bacchi V, Schaefer F, Choi M, Tang WH, Le Quintrec M, et al. Recessive Mutations in DGKE Cause Atypical Hemolytic-Uremic Syndrome. *Nat Genet* (2013) 45:531–6. doi: 10.1038/ng.2590
38. Ståhl AL, Vaziri-Sani F, Heinen S, Kristoffersson AC, Gydell KH, Raafat R, et al. Factor H Dysfunction in Patients With Atypical Hemolytic Uremic Syndrome Contributes to Complement Deposition on Platelets and Their Activation. *Blood* (2008) 111:5307–15. doi: 10.1182/blood-2007-08-106153
39. Galbusera M, Noris M, Gastoldi S, Bresin E, Mele C, Breno M, et al. An *Ex Vivo* Test of Complement Activation on Endothelium for Individualized Eculizumab Therapy in Hemolytic Uremic Syndrome. *Am J Kidney Dis* (2019) 74:56–72. doi: 10.1053/j.ajkd.2018.11.012
40. Roumenina LT, Chadebech P, Bodivit G, Vieira-Martins P, Grunenwald A, Boudhabhay I, et al. Complement Activation in Sickle Cell Disease: Dependence on Cell Density, Hemolysis and Modulation by Hydroxyurea Therapy. *Am J Hematol* (2020) 95:456–64. doi: 10.1002/ajh.25742
41. Palomo M, Blasco M, Molina P, Lozano M, Praga M, Torramade-Moix S, et al. Complement Activation and Thrombotic Microangiopathies. *Clin J Am Soc Nephrol* (2019) 14:1719–32. doi: 10.2215/cjn.05830519
42. Merle NS, Grunenwald A, Rajaratnam H, Gnemmi V, Frimat M, Figueres ML, et al. Intravascular Hemolysis Activates Complement *Via* Cell-Free Heme and Heme-Loaded Microvesicles. *JCI Insight* (2018) 3(12):e96910. doi: 10.1172/jci.insight.96910
43. Risitano AM, Kulasekararaj AG, Lee JW, Maciejewski JP, Notaro R, Brodsky R, et al. Danicopan: An Oral Complement Factor D Inhibitor for Paroxysmal Nocturnal Hemoglobinuria. *Haematologica* (2020). doi: 10.3324/haematol.2020.261826
44. Tanaka K, Adams B, Aris AM, Fujita N, Ogawa M, Ortiz S, et al. The Long-Acting C5 Inhibitor, Ravulizumab, is Efficacious and Safe in Pediatric Patients With Atypical Hemolytic Uremic Syndrome Previously Treated With Eculizumab. *Pediatr Nephrol* (2021) 36:889–98. doi: 10.1007/s00467-020-04774-2
45. Karpman D, Höglund P. Orphan Drug Policies and Use in Pediatric Nephrology. *Pediatr Nephrol* (2017) 32:1–6. doi: 10.1007/s00467-016-3520-4
46. Konar M, Granoff DM. Eculizumab Treatment and Impaired Opsonophagocytic Killing of Meningococci by Whole Blood From Immunized Adults. *Blood* (2017) 130:891–9. doi: 10.1182/blood-2017-05-781450
47. Ricklin D, Hajishengallis G, Yang K, Lambris JD. Complement: A Key System for Immune Surveillance and Homeostasis. *Nat Immunol* (2010) 11:785–97. doi: 10.1038/ni.1923
48. Yu J, Yuan X, Chen H, Chaturvedi S, Braunstein EM, Brodsky RA. Direct Activation of the Alternative Complement Pathway by SARS-CoV-2 Spike Proteins is Blocked by Factor D Inhibition. *Blood* (2020) 136:2080–9. doi: 10.1182/blood.2020008248

Conflict of Interest: The authors declare that the research was conducted in the absence of any commercial or financial relationships that could be construed as a potential conflict of interest.

frontiers in Immunology

CASE REPORT
published: 24 June 2021
doi: 10.3389/fimmu.2021.608604

A Novel Homozygous In-Frame Deletion in Complement Factor 3 Underlies Early-Onset Autosomal Recessive Atypical Hemolytic Uremic Syndrome - Case Report

Shirley Pollack[1,2], Israel Eisenstein[1], Adi Mory[3], Tamar Paperna[3], Ayala Ofir[3], Hagit Baris-Feldman[3], Karin Weiss[3], Nóra Veszeli[4], Dorottya Csuka[4], Revital Shemer[5], Fabian Glaser[6], Zoltán Prohászka[4] and Daniella Magen[1,5]*

[1] Pediatric Nephrology Institute, Ruth Children's Hospital, Haifa, Israel, [2] Rappaport Faculty of Medicine, Technion - Israel Institute of Technology, Haifa, Israel, [3] Genetic Institute, Haifa, Israel, [4] Research Laboratory, Department of Internal Medicine and Haematology, and MTA-SE Research Group of Immunology and Hematology, Hungarian Academy of Sciences and Semmelweis University, Budapest, Hungary, [5] Laboratory of Molecular Medicine, Rappaport Faculty of Medicine, Technion - Israel Institute of Technology, Haifa, Israel, [6] Bioinformatics Knowledge Unit, The Lorry I. Lokey Interdisciplinary Center for Life Sciences and Engineering, Technion-Israel Institute of Technology, Haifa, Israel

Background and Objectives: Atypical hemolytic uremic syndrome (aHUS) is mostly attributed to dysregulation of the alternative complement pathway (ACP) secondary to disease-causing variants in complement components or regulatory proteins. Hereditary aHUS due to C3 disruption is rare, usually caused by heterozygous activating mutations in the *C3* gene, and transmitted as autosomal dominant traits. We studied the molecular basis of early-onset aHUS, associated with an unusual finding of a novel homozygous activating deletion in C3.

Design, Setting, Participants, & Measurements: A male neonate with eculizumab-responsive fulminant aHUS and C3 hypocomplementemia, and six of his healthy close relatives were investigated. Genetic analysis on genomic DNA was performed by exome sequencing of the patient, followed by targeted Sanger sequencing for variant detection in his close relatives. Complement components analysis using specific immunoassays was performed on frozen plasma samples from the patient and mother.

Results: Exome sequencing revealed a novel homozygous variant in exon 26 of *C3* (c.3322_3333del, p.Ile1108_Lys1111del), within the highly conserved thioester-containing domain (TED), fully segregating with the familial disease phenotype, as compatible with autosomal recessive inheritance. Complement profiling of the patient showed decreased C3 and FB levels, with elevated levels of the terminal membrane attack complex, while his healthy heterozygous mother showed intermediate levels of C3 consumption.

OPEN ACCESS

Edited by:
Cordula M. Stover, University of Leicester, United Kingdom

Reviewed by:
Kevin James Marchbank, Newcastle University, United Kingdom
Michal Malina, Newcastle Hospitals, United Kingdom
Elisabetta Valoti, Istituto di Ricerche Farmacologiche Mario Negri (IRCCS), Italy

***Correspondence:**
Shirley Pollack
s_pollack@rmc.gov.il

Specialty section:
This article was submitted to Molecular Innate Immunity, a section of the journal Frontiers in Immunology

Received: *21 September 2020*
Accepted: *24 May 2021*
Published: *24 June 2021*

Citation:
Pollack S, Eisenstein I, Mory A, Paperna T, Ofir A, Baris-Feldman H, Weiss K, Veszeli N, Csuka D, Shemer R, Glaser F, Prohászka Z and Magen D (2021) A Novel Homozygous In-Frame Deletion in Complement Factor 3 Underlies Early-Onset Autosomal Recessive Atypical Hemolytic Uremic Syndrome - Case Report. Front. Immunol. 12:608604. doi: 10.3389/fimmu.2021.608604

Conclusions: Our findings represent the first description of aHUS secondary to a novel homozygous deletion in C3 with ensuing unbalanced C3 over-activation, highlighting a critical role for the disrupted C3-TED domain in the disease mechanism.

Keywords: atypical hemolytic uremic syndrome (aHUS), complement factor C3, eculizumab, alternative complement pathway, homozygous deletion

INTRODUCTION

Atypical hemolytic uremic syndrome (aHUS) is a heterogeneous group of acquired and hereditary thrombotic microangiopathy (TMA), manifested by microangiopathic hemolytic anemia, thrombocytopenia and acute kidney injury, which are usually not preceded by the diarrheal prodromal phase of Shiga Toxin-related HUS. Most forms of aHUS are associated with dysregulation of the alternative complement pathway (ACP), resulting in complement-mediated endothelial cell injury, with ensuing end-organ tissue damage (1, 2).

To date, about two thirds of patients with aHUS carry identifiable mutations or likely-pathogenic risk variants in genes encoding complement pathway proteins (2–5). While loss-of-function mutations are commonly implicated in genes encoding regulatory complement components, including complement Factor H (*CFH*), complement Factor I (*CFI*) and membrane cofactor protein (MCP, *CD46*), gain-of-function mutations are usually associated with complement Factor B (*CFB*) and *C3* (6–8). In conjunction with genetic predisposition, acquired autoantibodies against Factor H (FH) have been implicated in the pathogenesis of aHUS in approximately 10% of cases, and are mostly attributed to genomic rearrangements or deletions in *CFH/CFHR1/CFHR3/CFHR4* genes within the regulators of complement activation gene cluster (9, 10). In addition to proteins directly related to the complement cascade, increasing evidence highlights the role of coagulation factors in the pathogenesis of aHUS, including thrombomodulin (*THBD*), which regulates Factor I-mediated C3b inactivation, and plasminogen (*PLG*), which enhances plasmin-mediated fibrinolysis and thrombi degradation (11, 12). Finally, mutations in *DGKE*, encoding diacylglycerol kinase-ϵ (DGKE) have been linked with infantile-onset aHUS, accompanied by nephrotic syndrome and chronic kidney disease (CKD), through an as yet unresolved mechanism (8, 13).

Given the central role of ACP over-activation in the pathogenesis of aHUS, a favorable response to targeted blockade of the complement cascade is highly conceivable. Eculizumab is a monoclonal antibody directed against the human C5 complement component, causing inhibition of C5a release, thereby preventing downstream generation of the membrane attack complex (MAC), C5b-9. As such, it is indicated in acute episodes of aHUS, and as prophylaxis in susceptible patients (3, 14).

In this report we describe a male neonate with a life-threatening presentation of aHUS, associated with a novel homozygous in-frame deletion in the *C3* gene. Complement profile analysis suggests unbalanced activation of the ACP, which is further supported by a favorable response to eculizumab therapy. To the best of our knowledge, this is the first report of a homozygous deletion in *C3* associated with severe neonatal presentation of aHUS, secondary to C3 over-activation.

CLINICAL PRESENTATION AND WORKUP

The patient is the 5th child of healthy, 1st-degree cousins of Arab-Muslim origin, born at term after normal pregnancy and delivery. Detailed family history was negative for renal, hematological, autoimmune or recurrent infectious disorders. He was admitted to a local hospital at the age of 3 days for evaluation of extensive jaundice, anemia, thrombocytopenia, and impaired kidney function. Following fulminant renal failure and acute respiratory insufficiency, he was urgently transferred to our care for further evaluation and management. On admission, the infant displayed clinical signs of encephalopathy, accompanied by fluid overload and pulmonary congestion secondary to anuric renal failure, which necessitated mechanical ventilation and renal replacement therapy.

Initial laboratory investigation was compatible with TMA, as evidenced by normocytic anemia, severe thrombocytopenia, significant schistocytosis on peripheral blood smear, a negative Coombs test, and extremely elevated lactate dehydrogenase (LDH) levels. A thorough microbiological workup was negative for an identifiable infectious trigger. Plasma ADAMTS-13 activity was normal, and anti-ADAMTS-13 antibodies were undetected, thereby excluding thrombotic thrombocytopenic purpura (TTP). Coagulation tests excluded diffuse intravascular coagulation (DIC). Metabolic screen showed normal blood levels of homocysteine, methionine and cobalamin C, with no evidence of organic aciduria, thereby excluding cobalamin C deficiency. Serum C3 levels were repeatedly extremely low, with normal C4 levels. A connective tissue disorder panel (collagenogram) was negative. Imaging studies, including renal echo-Doppler, brain ultrasonography and echocardiography were unremarkable.

With a working diagnosis of aHUS, the patient was managed with eculizumab therapy, in conjunction with mechanical ventilation, daily hemodialysis, red blood cell transfusions and prophylactic penicillin therapy. Within several days of eculizumb initiation, the infant showed dramatic clinical and laboratory improvement, followed by rapid neurological, hematological, respiratory and renal recovery. Currently, at the age of 2 years, the child is in sustained remission from aHUS under prophylactic eculizumab therapy, with a history of two reversible aHUS relapses following non-adherence to prescribed eculizumab prophylaxis. Each relapse appeared after 10-14 days delay in scheduled eculizumab therapy, manifesting with thrombotic microangiopathy and acute renal failure.

Sequelae of his fulminant presenting episode of aHUS include arterial hypertension, non-nephrotic range proteinuria with normal glomerular filtration rate (GFR), and gross motor developmental delay. His serum C3 levels are constantly low. He does not exhibit increased susceptibility to pyogenic bacterial infections, as reported in patients with homozygous loss-of-function variants in *C3* which cause C3 deficiency (15, 16), although infections may have been prevented by prophylactic antibiotic treatment.

MATERIALS AND METHODS

Genetic Analysis

Genomic DNA was extracted from the patient's peripheral lymphocytes for clinical exome sequencing, using the TruSight One Sequencing panel (Illumina, Inc., San Diego, CA, USA), according to manufacturer's instructions. Direct Sanger sequencing was performed on the coding regions and intron-exon boundaries of *CFH* (exons 1-9 & 11-23), *CFI* (exons 1-13), *MCP* (CD46, exons 1-14), *C3* (exons 1-41), and *CFB* (exons 1-18); *THBD* (exon 1).

Multiplex Ligation-Dependent Probe Amplification (MLPA) analysis was performed using a commercially available assay (P236-A3 ARMD probemix, MRC-Holland).

All available family members were Sanger sequenced for the *C3* variant and for additional variations and risk polymorphisms identified in the patient.

Pathogenicity of identified sequence variants was classified according to joint consensus recommendations by the American College of Medical Genetics and Genomics and the Association for Molecular Pathology (17).

Complement Profile Analysis

Levels of complement components, regulators and FH autoantibodies were determined on frozen plasma samples of the patient and his mother, according to previously published methods (18). Fresh plasma samples for complement analysis on additional family members were unavaliable.

C3b-FH Complex Modelling

Structural analysis of C3b-FH complex was based on the PDB 3OXU complex structure (19). Interfacial amino acids of C3b were defined as those within a distance < 5 Å of any atom of Factor H. The energy of the C3b-FH complex was computed with pyDock bindEy module for protein structure prediction (20), both for the wild-type and the inferred mutant C3 protein structure. Molecular graphics and analyses were performed with the UCSF ChimeraX program, developed by the Resource for Biocomputing, Visualization, and Informatics at the University of California, SF, with support from National Institutes of Health R01-GM129325 and the Office of Cyber Infrastructure and Computational Biology, National Institute of Allergy and Infectious Diseases (21).

RESULTS

Genetic Analysis

Sequence analysis of the patient revealed a homozygous in-frame deletion of 12bp in exon 26 of the *C3* gene (c.3322_3333del, p.Ile1108_Lys1111del) resulting in deletion of highly conserved four amino acids (ILEK) from the inferred protein sequence. The four deleted residues are predicted to be located in the α-chain of the encoded C3 protein, within its highly conserved thioester-containing domain (TED) (NCBI conserved domains). The p.Ile1108_Lys1111del-C3 variant was absent from public variation data bases [dbSNP; 1000 Genomes Projects; gnomAD; The Greater Middle East Variom Project (GME)], and was predicted harmful by mutation prediction software (Mutation Taster).

Several additional common polymorphisms and variants of unknown significance were identified in complement encoding genes of the patient (**Figure 1**). In detail, he was found to be heterozygous for a substitution in the *CFH* gene (c.3050C>T, p.Thr1017Ile). This variant has been previously classified as likely benign, based on comparable allele frequencies between healthy individuals and aHUS patients, combined with ambiguous prediction of pathogenicity, according to *in-silico* prediction software analysis (22). Further identified heterozygous polymorphisms in the patient included the *CFH* Y402H risk factor for dense deposit disease, as well as the *CD46* rs2796267, rs2796268 and rs1962149 polymorphisms, referred as part of the *MCP*ggaac risk haplotype for aHUS (**Figure 1**).

MLPA analysis excluded deletions or duplications within the Regulators of Complement Activation (RCA) gene cluster (*CFH, CFHR1, CFHR2, CFHR3* and *CFHR5*) on chromosome 1q31.3, as underlying the disease.

Targeted sequencing of all healthy close relatives excluded homozygosity for the p.Ile1108_Lys1111del-C3 variant. Heterozygosity for the *MCP*ggaac risk haplotype was identified in the healthy father and sister. The rare allele of the *CFH* Y402H risk polymorphism was identified in the healthy father, sister and brothers, but not in the healthy mother (**Figure 1**).

Complement Profile Analysis

As shown in **Table 1**, complement analysis of the patient indicated critically low C3 level, deficient activity of all three complement pathways, decreased complement factor B (FB) level, and increased level of the terminal pathway activation marker. C1q, C4, FI and FH levels were within or slightly below the reference range. Anti-FH antibody titer was negative, below the cut-off.

Taken together, complement profile analysis of the patient suggests spontaneous activation of the p.lle1108_Lys111de-C3 protein by FB, resulting in ongoing consumption of C3 and FB, and increased generation of the MAC.

C3b-FH Complex Modeling

Structural analysis of C3b-FH complex demonstrates strategic location of the four deleted amino acids (ILEK) within the TED domain, at the C3b-FH interface (**Figure 2C**). The energy difference between wild-type and mutant C3b-FH complex structure (ΔG-wild-type – ΔG mutant) is estimated to

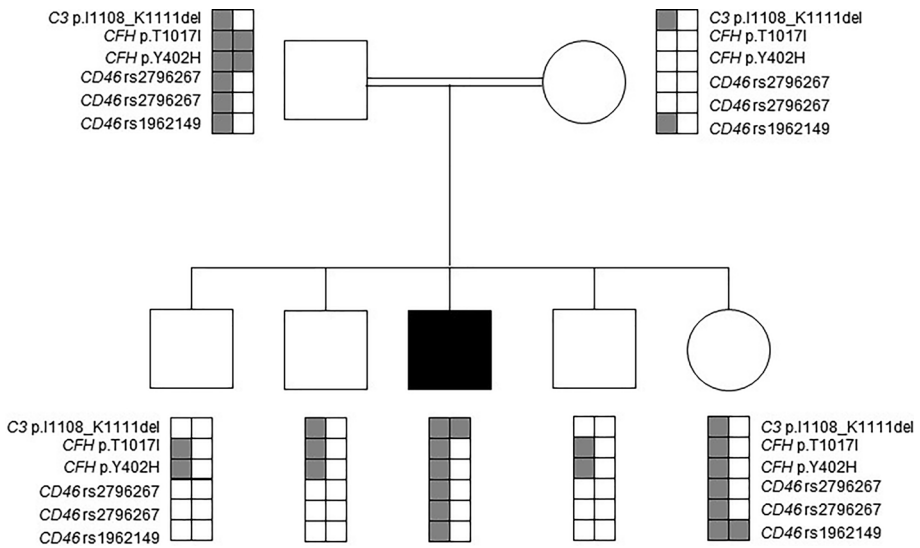

FIGURE 1 | Mutation analysis in the patient's nuclear family. Affected individual is marked by a black filled square. Rare alleles of the rs2796267, rs2796268 and rs1962149 polymorphisms and their haplotype referred as *MCP*ggaac were reported to be a risk factor for developing aHUS.

TABLE 1 | Complement profile of the patient and his mother.

	Patient	Healthy mother	Reference range
ADAMTS13 activity	99%	94%	67-150%
Total complement activity, classical pathway (hemolytic test)	0 CH50/ml	37 CH50/ml	48-103 CH50/ml
Total complement activity, alternative pathway (WIELISA-Alt)	0%	59%	70-125%
Total complement activity, lectin pathway (WIELISA-LP):	0%	4%	70-125%
C3	0.15 g/L	0.57 g/L	0.9-1.8 g/L
C4	0.21 g/L	0.28 g/L	0.15-0.55 g/L
Factor H antigen	222 mg/L	309 mg/L	250-880 mg/L
Factor I antigen	73%	87%	70-130%
Factor B antigen	39%	93%	70-130%
Anti- factor H IgG autoantibody	107 AU/mL	35 AU/mL	<110 AU/mL
C1q antigen	54 mg/mL	107 mg/mL	60-180 mg/mL
Anti-C1q IgG autoantibody	9 U/mL	3 U/mL	<52 U/mL
sC5b-9 (terminal complement complex)	456 ng/mL	239 ng/mL	110-252 ng/mL

be $\Delta\Delta G \sim -5$Kcal, suggesting a catastrophic effect exerted by the deletion on interface stability. Hence, the ILEK deletion in mutant C3 is highly likely to disrupt C3b-FH interaction, thereby disabling the inhibitory effect of FH on downstream activation of C3b.

DISCUSSION

We herein described the clinical and molecular investigation in a male infant from a consanguineous family, with neonatal presentation of fulminant aHUS and multi-organ failure, accompanied by extremely low serum levels of C3, a favorable systemic response to eculizumab therapy, and intolerance to eculizumab cessation. Mutation analysis revealed a small homozygous in-frame deletion of 12 bp in exon 26 of the *C3* gene, resulting in four amino acids deletion (ILEK) from the inferred TED of C3, in association with apparent C3 deficiency. However, complement profile analysis indicated unbalanced activation of the ACP, as evidenced by a reduced level of FB denoting its consumption, combined with excessive generation of the terminal MAC. Moreover, structural modelling of C3b-FH complex suggests a disruptive effect of ILEK-deletion on mutant C3b binding to FH, thereby supporting the hypothesis of unbalanced degradation of mutant C3 as underlying the mechanism of aHUS.

C3 is the most abundant complement component protein, playing a crucial role in activation of all three complement pathways. In its mature, unprocessed form, the C3 protein is composed of one α and one β chain linked by a disulfide bond,

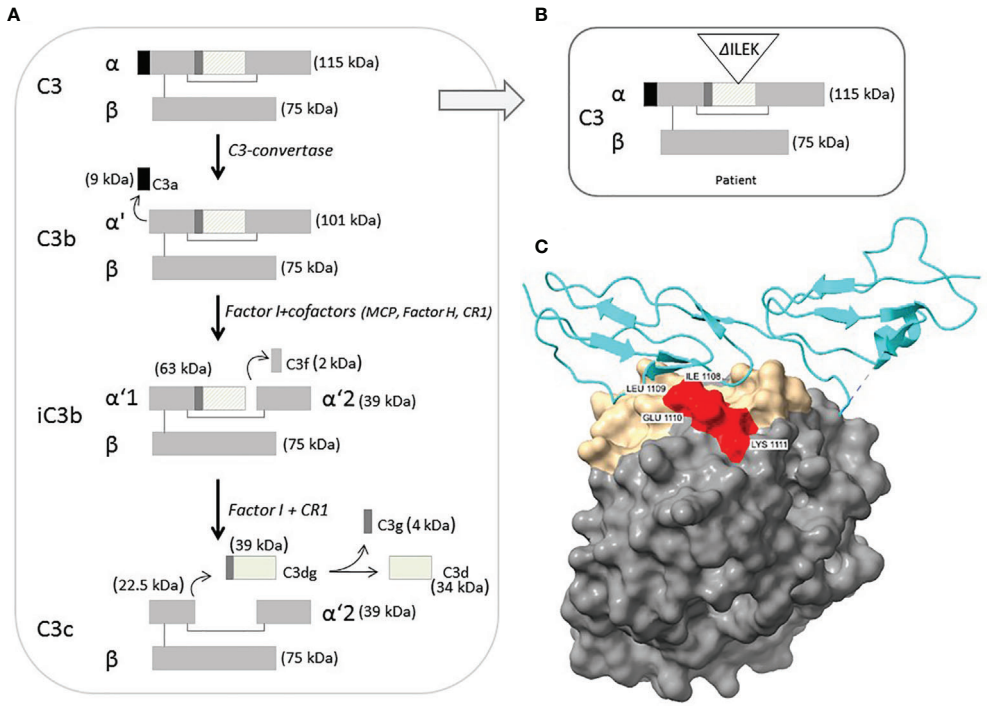

FIGURE 2 | **(A)** Schematic representation of intact C3 structure, processing and regulation. The diagonal-line filled rectangle represents the TED of C3. **(B)** Schematic representation of the position of four-residue deleted sequence (ΔILEK) within the TED domain of the patient's C3 alpha chain. **(C)** Modelling of the C3b (TED domain)-Factor H complex (from PDB 3OXU) (19), using the UCSF ChimeraX tool. C3b is shown in solvent-excluded molecular surface representation, and Factor H (P08603) in cyan ribbons. All C3b interfacial amino acids are colored gold, while the p.1008-1111 (ILEK) mutant region is colored red. As clearly demonstrated, amino acids ILEK are an integral part of the C3b-Factor H interface.

and consists of 13 domains, harboring intrinsic functional and binding capacity to various effector ligands. Intact C3 is an inert molecule, exhibiting its biological activity only after proteolytic cleavage to functional degradation product (**Figure 2A**). Under physiological condition, C3b is constantly produced at a very low rate, by spontaneous hydrolysis to C3(H2O). The C3b factor is able to attach to pathogens and host cell surfaces, where it binds FB, which in turn is cleaved by complement factor D (FD). The resulting C3bBb or C3 convertase further cleaves and activates C3, thereby leading to an amplification loop of the alternative complement cascade, culminating in MAC-related tissue damage (23, 24).

aHUS secondary to C3 disruption is relatively rare, especially during the pediatric age group, with an overall reported prevalence ranging between 4.5%-11.4 of aHUS cases (3, 4, 25). C3-associated aHUS is mostly attributed to heterozygous gain-of-function variants in the *C3* gene, leading to unbalanced activation of the complement cascade (8, 26–28). Furthermore, the presentation of aHUS in carriers of C3 gain-of-function mutations may be influenced by the presence of the *MCP*ggaac risk haplotype, as previously described (29). In contrast, homozygous loss-of-function variants in C3 are usually implicated in C3 deficiency, manifested by increased susceptibility to recurrent bacterial infections and autoimmunity, unrelated to aHUS (15, 16). To the best of our knowledge, the constellation of aHUS secondary to a small homozygous deletion in *C3* associated with unbalanced activation of the ACP has not been previously reported (OMIM databases).

According to the crystallographic structure of C3, the TED, located within residues 963-1268, contains a hidden thioester bond, which is exposed upon C3 cleavage, thereby facilitating covalent binding of C3b to target surface ligands (30, 31). Moreover, conformational displacement of the TED domain has been previously shown to disrupt the interaction of C3b with the ACP regulators, i.e., FH and MCP (32, 33). Hence, the inferred deletion of four highly conserved residues from the TED of the p.Ile1108_Lys1111del-C3 protein (**Figures 2B, C**), may impose a conformational change of functional significance on the TED, rendering mutant C3b resistant to inactivation, through impaired binding to FH. This hypothesis is further supported by previous reports on the functional significance of various aHUS-related *C3* missense variants within the TED, (i.e., p.L1109V, p.P1114L, p.D1115N, p.G1116R, I1157T), residing in close proximity to the location of p.Ile1108_Lys1111del-C3, with accumulating evidence for their disrupted cell surface interaction with FH, or resistance to inactivation by MCP, due to C3b altered conformation (4, 5, 26, 34, 35).

Of note, hereditary aHUS, in general, is well-known for its partial penetrance, resulting in phenotypic variability among carriers of a shared disease-causing variant. Incomplete penetrance is commonly attributed to the harmful effect of

background risk variants within ACP regulatory genes, including *CFH* and *MCP* risk haplotypes (5, 36, 37). The fact that all heterozygous carriers of the p.lle1108_Lys1111del-C3 variant within the studied family are disease-free, suggests that heterozygosity for this likely-pathogenic activating variant, either in the absence or presence of additional risk variants, is insufficient for the development of full-blown disease, albeit intermediated C3 consumption and ACP activation, as evidenced by the complement profile of the patient's mother.

In conclusion, we have identified a likely-pathogenic homozygous deletion in C3, associated with life-threatening aHUS secondary to over-activation of the ACP. Complement profile analysis suggests a damaging conformational effect of this deletion on the TED of the C3 protein, rendering it susceptible to unbalanced activation due to impaired interaction with regulatory FH. Our findings enable prenatal diagnosis and early treatment initiation in newly identified subjects at risk, while reinforcing the significance of an intact C3-TED for normal function and regulation of the ACP. Yet, the exact mechanism whereby the identified 4-residue deletion in C3 may affect molecular interactions of the C3 protein with additional regulators of the ACP, with ensuing downstream over-activation of terminal complement cascade, warrants further investigation.

DATA AVAILABILITY STATEMENT

The datasets presented in this study can be found in online repositories. The names of the repository/repositories and accession number(s) can be found below: https://www.ncbi.nlm.nih.gov/genbank/, 2384952.

ETHICS STATEMENT

The studies involving human participants were reviewed and approved by the Rambam Health Care Campus Institutional ethics committee. The patients/participants provided their written informed consent to participate in this study. Written informed consent to participate in this study was provided by the participants' legal guardian/next of kin.

AUTHOR CONTRIBUTIONS

SP: Writing – original draft – Preparation, creation and/or presentation of the published work, specifically writing the initial draft (including substantive translation). DM and ZP: Writing – review & editing – Preparation, creation and/or presentation of the published work by those from the original research group, specifically critical review, commentary or revision – including pre- or post-publication stages. IE, AM, TP, AO, HB-F, KW, NV, RS, FG, and DC: research activity - performed the clinical and laboratory analysis, reviewed and edited the paper. All authors contributed to the article and approved the submitted version.

FUNDING

The study was supported by the Premium Postdoctoral Fellowship Program of the Hungarian Academy of Sciences (PPD2018-016/2018), and by the Kaylie Kidney Research Center of Excellence at Rambam Medical Center.

REFERENCES

1. Noris M, Remuzzi G, Noris M. Atypical Hemolytic-Uremic Syndrome. *N Engl J Med* (2009) 361(17):1676–87. doi: 10.1056/NEJMra0902814
2. Schaefer F, Ardissino G, Ariceta G, Fakhouri F, Scully M, Isbel N, et al. Clinical and Genetic Predictors of Atypical Hemolytic Uremic Syndrome Phenotype and Outcome. *Kidney Int* (2018) 94(2):408–18. doi: 10.1016/j.kint.2018.02.029
3. Loirat C, Fakhouri F, Ariceta G, Besbas N, Bitzan M, Bjerre A, et al. An International Consensus Approach to the Management of Atypical Hemolytic Uremic Syndrome in Children. *Pediatr Nephrol* (2016) 31(1):15–39. doi: 10.1007/s00467-015-3076-8
4. Schramm EC, Roumenina LT, Rybkine T, Chauvet S, Vieira-Martins P, Hue C, et al. Mapping Interactions Between Complement C3 and Regulators Using Mutations in Atypical Hemolytic Uremic Syndrome. *Blood* (2015) 125(15):2359–69. doi: 10.1182/blood-2014-10-609073
5. Bresin E, Rurali E, Caprioli J, Sanchez-Corral P, Fremeaux-Bacchi V, Rodriguez de Cordoba S, et al. Combined Complement Gene Mutations in Atypical Hemolytic Uremic Syndrome Influence Clinical Phenotype. *J Am Soc Nephrol* (2013) 24(3):475–86. doi: 10.1681/ASN.2012090884
6. Rodriguez E, Rallapalli PM, Osborne AJ, Perkins SJ, Rodriguez E. New Functional and Structural Insights From Updated Mutational Databases for Complement Factor H, Factor I, Membrane Cofactor Protein and C3. *Biosci Rep* (2014) 34(5):e00146. doi: 10.1042/BSR20140117
7. Feitz WJC, van de Kar NCAJ, Orth-Höller D, van den Heuvel LPJW, Licht C. The Genetics of Atypical Hemolytic Uremic Syndrome. *Med Genet* (2018) 30(4):400–9. doi: 10.1007/s11825-018-0216-0
8. Yoshida Y, Kato H, Ikeda Y, Nangaku M, Yoshida Y. Pathogenesis of Atypical Hemolytic Uremic Syndrome. *J Atheroscler Thromb* (2019) 26(2):99–110. doi: 10.5551/jat.RV17026
9. Moore I, Strain L, Pappworth I, Kavanagh D, Barlow PN, Herbert AP, et al. Association of Factor H Autoantibodies With Deletions of CFHR1, Cfhr3, CFHR4, and With Mutations in CFH, Cfi, CD46, and C3 in Patients With Atypical Hemolytic Uremic Syndrome. *Blood* (2010) 115(2):379–87. doi: 10.1182/blood-2009-05-221549
10. Valoti E, Alberti M, Iatropoulos P, Piras R, Mele C, Breno M, et al. Rare Functional Variants in Complement Genes and Anti-FH Autoantibodies-Associated Ahus. *Front Immunol* (2019) 10:853. doi: 10.3389/fimmu.2019.00853
11. Dzik S. Complement and Coagulation: Cross Talk Through Time. *Transfus Med Rev* (2019) 33(4):199–206. doi: 10.1016/j.tmrv.2019.08.004
12. Bu F, Maga T, Meyer NC, Wang K, Thomas CP, Nester CM, et al. Comprehensive Genetic Analysis of Complement and Coagulation Genes in Atypical Hemolytic Uremic Syndrome. *J Am Soc Nephrol* (2014) 25(1):55–64. doi: 10.1681/ASN.2013050453
13. Lemaire M, Frémeaux-Bacchi V, Schaefer F, Choi M, Tang WH, Le Quintrec M, et al. Recessive Mutations in DGKE Cause Atypical Hemolytic-Uremic Syndrome. *Nat Genet* (2013) 45(5):531–6. doi: 10.1038/ng.2590
14. Fakhouri F, Loirat C. Anticomplement Treatment in Atypical and Typical Hemolytic Uremic Syndrome. *Semin Hematol* (2018) 55(3):150–8. doi: 10.1053/j.seminhematol.2018.04.009
15. Reis E S, Falcão DA, Isaac L. Clinical Aspects and Molecular Basis of Primary Deficiencies of Complement Component C3 and Its Regulatory Proteins Factor I and Factor H. *Scand J Immunol* (2006) 63(3):155–68. doi: 10.1111/j.1365-3083.2006.01729.x
16. Okura Y, Kobayashi I, Yamada M, Sasaki S, Yamada Y, Kamioka I, et al. Clinical Characteristics and Genotype-Phenotype Correlations in C3 Deficiency. *J Allergy Clin Immunol* (2016) 137(2):640–44.e1. doi: 10.1016/j.jaci.2015.08.017
17. Richards S, Aziz N, Bale S, Bick D, Das S, Gastier-Foster J, et al. Standards and Guidelines for the Interpretation of Sequence Variants: A Joint Consensus Recommendation of the American College of Medical Genetics and Genomics

and the Association for Molecular Pathology. *Genet Med* 17(5):405–24. doi: 10.1038/gim.2015.30

18. Richards S, Aziz N, Bale S, Bick D, Das S, Gastier-Foster J, et al. Standards and Guidelines for the Interpretation of Sequence Variants: A Joint Consensus Recommendation of the American College of Medical Genetics and Genomics and the Association for Molecular Pathology. *Genet Med* (2015) 17(5):405–24. doi: 10.1038/gim.2015.30
19. Morgan HP, Schmidt CQ, Guariento M, Blaum BS, Gillespie D, Herbert AP, et al. Structural Basis for Engagement by Complement Factor H of C3b on a Self Surface. *Nat Struct Mol Biol* (2011) 18(4):463–70. doi: 10.1038/nsmb.2018
20. Rosell M, Rodríguez-Lumbreras LA, Fernández-Recio M. Modeling of Protein Complexes and Molecular Assemblies With Pydock. *Methods Mol Biol* (2020) 2165:175–98. doi: 10.1007/978-1-0716-0708-4_10
21. Pettersen EF, Goddard TD, Huang CC, Meng EC, Couch GS, Croll TI, et al. Ucsf ChimeraX: Structure Visualization for Researchers, Educators, and Developers. *Protein Sci* (2021) 30(1):70–82. doi: 10.1002/pro.3943
22. Osborne AJ, Breno M, Borsa NG, Bu F, Frémeaux-Bacchi V, Gale DP, et al. Statistical Validation of Rare Complement Variants Provides Insights Into the Molecular Basis of Atypical Hemolytic Uremic Syndrome and C3 Glomerulopathy. *J Immunol* (2018) 200(7):2464–78. doi: 10.4049/jimmunol.1701695
23. de Bruijn MH, Fey GH. Human Complement Component C3: cDNA Coding Sequence and Derived Primary Structure. *Proc Natl Acad Sci USA* (1985) 82 (3):708–12. doi: 10.1073/pnas.82.3.708
24. Janssen BJ, Gros P, Janssen BJC. Structural Insights Into the Central Complement Component C3. *Mol Immunol* (2007) 44(1-3):3–10. doi: 10.1016/j.molimm.2006.06.017
25. Fremeaux-Bacchi V, Fakhouri F, Garnier A, Bienaimé F, Dragon-Durey MA, Ngo S, et al. Genetics and Outcome of Atypical Hemolytic Uremic Syndrome: A Nationwide French Series Comparing Children and Adults. *Clin J Am Soc Nephrol* (2013) 8(4):554–62. doi: 10.2215/CJN.04760512
26. Frémeaux-Bacchi V, Miller EC, Liszewski MK, Strain L, Blouin J, Brown AL, et al. Mutations in Complement C3 Predispose to Development of Atypical Hemolytic Uremic Syndrome. *Blood* (2008) 112(13):4948–52. doi: 10.1182/blood-2008-01-133702
27. Lhotta K, Janecke AR, Scheiring J, Petzlberger B, Giner T, Fally V, et al. A Large Family With a Gain-of-Function Mutation of Complement C3 Predisposing to Atypical Hemolytic Uremic Syndrome, Microhematuria, Hypertension and Chronic Renal Failure. *Clin J Am Soc Nephrol* (2009) 4 (8):1356–62. doi: 10.2215/CJN.06281208
28. Sartz L, Olin AI, Kristoffersson AC, Ståhl AL, Johansson ME, Westman K, et al. A Novel C3 Mutation Causing Increased Formation of the C3 Convertase in Familial Atypical Hemolytic Uremic Syndrome. *J Immunol* (2012) 188(4):2030–7. doi: 10.4049/jimmunol.1100319
29. Lumbreras J, Subias M, Espinosa N, Ferrer JM, Arjona E, Rodríguez de Córdoba S, et al. The Relevance of the MCP Risk Polymorphism to the Outcome of Ahus Associated With C3 Mutations. A Case Report. *Front Immunol* (2020) 11:1348. doi: 10.3389/fimmu.2020.01348
30. Janssen BJ, Huizinga EG, Raaijmakers HC, Roos A, Daha MR, Nilsson-Ekdahl K, et al. Structures of Complement Component C3 Provide Insights Into the Function and Evolution of Immunity. *Nature* (2005) 437(7058):505–11. doi: 10.1038/nature04005
31. Janssen BJ, Christodoulidou A, McCarthy A, Lambris JD, Gros P. Structure of C3b Reveals Conformational Changes That Underlie Complement Activity. *Nature* (2006) 444(7116):213–6. doi: 10.1038/nature05172
32. Wu J, Wu Y-Q, Ricklin D, Janssen BJC, Lambris JD, Grosl P. Structure of Complement Fragment C3b-Factor H and Implications for Host Protection by Complement Regulators. *Nat Immunol* (2009) 10(7):728–33 doi: 10.1038/ni.1755
33. Wu J, Wu YQ, Ricklin D, Janssen BJ, Lambris JD, Gros P.Wu J, et al. Structure of Complement Fragment C3b–Factor H and Implications for Host Protection by Complement Regulators. *Nat Immunol* (2009) 10(7):728–33. doi: 10.1038/ni.1755
34. Persson BD, Schmitz NB, Santiago C, Zocher G, Larvie M, Scheu U, et al. Structure of the Extracellular Portion of CD46 Provides Insights Into Its Interactions With Complement Proteins and Pathogens. *PloS Pathog* (2010) 6 (9):e1001122. doi: 10.1371/journal.ppat.1001122
35. Martínez-Barricarte R, Heurich M, López-Perrote A, Tortajada A, Pinto S, López-Trascasa M, et al. The Molecular and Structural Bases for the Association of Complement C3 Mutations With Atypical Hemolytic Uremic Syndrome. *Mol Immunol* (2015) 66(2):263–73. doi: 10.1016/j.molimm.2015.03.248
36. Sansbury FH, Cordell HJ, Bingham C, Bromilow G, Nicholls A, Powell R, et al. Factors Determining Penetrance in Familial Atypical Haemolytic Uraemic Syndrome. *J Med Genet* (2014) 51(11):756–64. doi: 10.1136/jmedgenet-2014-102498
37. Roumenina LT, Frimat M, Miller EC, Provot F, Dragon-Durey MA, Bordereau P, et al. A Prevalent C3 Mutation in aHUS Patients Causes a Direct C3 Convertase Gain of Function. *Blood* (2012) 119(18):4182–91. doi: 10.1182/blood-2011-10-383281

Conflict of Interest: The authors declare that the research was conducted in the absence of any commercial or financial relationships that could be construed as a potential conflict of interest.

frontiers in Immunology

ORIGINAL RESEARCH
published: 18 August 2021
doi: 10.3389/fimmu.2021.676662

Selective Binding of Heparin/Heparan Sulfate Oligosaccharides to Factor H and Factor H-Related Proteins: Therapeutic Potential for C3 Glomerulopathies

Markus A. Loeven[1†], Marissa L. Maciej-Hulme[1†], Cansu Yanginlar[1†], Melanie C. Hubers[1], Edwin Kellenbach[2], Mark de Graaf[1], Toin H. van Kuppevelt[3], Jack Wetzels[1], Ton J. Rabelink[4], Richard J. H. Smith[5] and Johan van der Vlag[1]*

[1] Department of Nephrology, Radboud Institute for Molecular Life Sciences, Radboud University Medical Center, Nijmegen, Netherlands, [2] Biochemical Technical Support Aspen Oss, Oss, Netherlands, [3] Department of Biochemistry, Radboud Institute for Molecular Life Sciences, Radboud University Medical Center, Nijmegen, Netherlands, [4] Department of Nephrology and Einthoven Laboratory for Vascular Medicine, Leiden University Medical Center, Leiden, Netherlands, [5] Departments of Internal Medicine and Otolaryngology, Carver College of Medicine, Iowa City, IA, United States

Complement dysregulation is characteristic of the renal diseases atypical hemolytic uremic syndrome (aHUS) and complement component 3 glomerulopathy (C3G). Complement regulatory protein Factor H (FH) inhibits complement activity, whereas FH-related proteins (FHRs) lack a complement regulatory domain. FH and FHRs compete for binding to host cell glycans, in particular heparan sulfates (HS). HS is a glycosaminoglycan with an immense structural variability, where distinct sulfation patterns mediate specific binding of proteins. Mutations in FH, FHRs, or an altered glomerular HS structure may disturb the FH : FHRs balance on glomerular endothelial cells, thereby leading to complement activation and the subsequent development of aHUS/C3G. In this study, we aimed to identify specific HS structures that could specifically compete off FHRs from HS glycocalyx (HS_{Glx}), without interfering with FH binding. FH/FHR binding to human conditionally immortalized glomerular endothelial cells (ciGEnCs) and HS_{Glx} purified from ciGEnC glycocalyx was assessed. HS modifications important for FH/FHR binding to HS_{Glx} were analyzed using selectively desulfated heparins in competition with purified HS_{Glx}. We further assessed effects of heparinoids on FHR1- and FHR5-mediated C3b deposition on ciGEnCs. In the presence of C3b, binding of FH, FHR1 and FHR5 to ciGEnCs was significantly increased, whereas binding of FHR2 was minimal. FHR1 and 5 competitively inhibited FH binding to HS_{Glx}, leading to alternative pathway dysregulation. FHR1 and FHR5 binding was primarily mediated by N-sulfation while FH binding depended on N-, 2-O- and 6-O-sulfation. Addition of 2-O-desulfated heparin significantly reduced FHR1- and FHR5-mediated C3b deposition on ciGEnCs. We identify 2-O-desulfated heparin derivatives as potential therapeutics for C3G and other diseases with dysregulated complement.

Keywords: complement, factor H (FH), factor H-related protein, heparan sulfate (HS), heparin, complement 3 glomerulopathy

OPEN ACCESS

Edited by:
Mihály Józsi, Eötvös Loránd University, Hungary

Reviewed by:
Bo Nilsson, Uppsala University, Sweden
Joshua Thurman, University of Colorado Anschutz Medical Campus, United States
Christoph Licht, Hospital for Sick Children, Canada

***Correspondence:**
Johan van der Vlag
Johan.vanderVlag@radboudumc.nl

[†]These authors have contributed equally to this work and share first authorship

Specialty section:
This article was submitted to Molecular Innate Immunity, a section of the journal Frontiers in Immunology

Received: *05 March 2021*
Accepted: *02 August 2021*
Published: *18 August 2021*

Citation:
Loeven MA, Maciej-Hulme ML, Yanginlar C, Hubers MC, Kellenbach E, de Graaf M, van Kuppevelt TH, Wetzels J, Rabelink TJ, Smith RJH and van der Vlag J (2021) Selective Binding of Heparin/Heparan Sulfate Oligosaccharides to Factor H and Factor H-Related Proteins: Therapeutic Potential for C3 Glomerulopathies. Front. Immunol. 12:676662. doi: 10.3389/fimmu.2021.676662

INTRODUCTION

The complement system serves an important role in immunity by removing pathogens and apoptotic debris. Three distinct pathways can induce complement activation, with the alternative pathway (AP) targeting both pathogens and host tissues. Complement activation results in the cleavage of complement component C3 to C3b, which attaches covalently to cell surfaces and extracellular matrix. C3b recruits complement factor B to form a catalytic complex called C3 convertase that results in feed-forward amplification of complement activation, culminating in the formation of the lytic pore C5b-9 complex (1).

Failure to control AP activation on host tissues can lead to disease, including the glomerular diseases complement component 3 glomerulopathy (C3G) (2) and atypical hemolytic uremic syndrome (aHUS) (3). C3G and aHUS have been associated with genetic variations in various complement genes, including complement factor H (*CFH*), which encodes Factor H (FH) the main inhibitor of the AP (4). FH, which consists of 20 homologous complement control protein (CCP) domains, binds to C3b (5) to displace factor B (decay accelerating activity, DAA) (6) and it also acts as cofactor for complement factor I-mediated cleavage of C3b into iC3b (cofactor activity) (7). FH differentiates between host tissues and pathogens by binding to heparan sulfate (HS) on host tissues using CCP7 (8, 9) and CCP20 (10), and to sialic acid using CCP20 (11). FH-mediated complement control is further modulated by six FH-related proteins (FHR1-3, 4A, 4B and 5) which contain CCPs with high homology to many but not all CCPs of FH. Notably the N-terminal complement regulatory domain present in FH is absent in FHRs. CCPs in FHR proteins that are homologous to CCP7 and CCP19-20 in FH facilitate FHR binding to FH ligands, including HS and C3b (12–14). FHRs have therefore been proposed to compete with FH for ligands on host tissues such as glomerular endothelial cells and the glomerular basement membrane, potentially leading to local dysregulation of AP activation and tissue damage (15).

FHRs can be divided into type 1 FHRs (FHR1, FHR2, and FHR5), which occur as homo- and heterodimers, and type 2 FHRs (FHR3, FHR4A, and FHR4B), which are monomeric in plasma (16, 17). Type 1 FHRs, particularly FHR1 and FHR5, are prominently found in renal biopsies of C3G patients (18). In addition, in both aHUS and C3G patients, pathologic type 1 FHR gene rearrangements have been described that generate novel FHRs proteins with increased abilities to compete with FH for cell surface and extracellular matrix binding (15, 19, 20).

We hypothesized that pathogenic changes, for example genetically inherited, or induced by infections or high blood pressure, in glomerular tissues, *e.g.* deviations in the HS structures, may also affect the balance between FH and FHR binding, thereby further contributing to disease development.

HS is a linear polysaccharide from the glycosaminoglycan family that is particularly prominent in the endothelial glycocalyx, a thick glycan layer lining the lumen of blood vessels (21). HS is synthesized by a complex biomachinery that involves more than 30 enzymes (22). Initially, a carbohydrate backbone is generated by the action of exostosin 1/exostosin 2 (EXT1/2) copolymerase that adds up to 100-200 repeating units of the glucuronic acid-N-acetylglucosamine (GlcA-GlcNAc) disaccharide motif. Subsequently, N-deacetylase/N-sulfotransferases (NDSTs) substitute acetyl groups in GlcNAc residues for sulfates, the first of several different sulfate modifications. GlcA can be converted to iduronic acid (IdoA) by glucuronic acid epimerase (GLCE), introducing additional structural variability (23). Finally, sulfate modifications are added by sulfotransferases (HS2STs, HS3STs, and HS6STs) at the 2-O-position of GlcA/IdoA and the 3-O- and/or 6-O-positions, respectively, of GlcNAc/GlcNS. The number of structural possibilities within an HS chain is immense; considering 48 possible disaccharides, regarding possible combinations of modifications, an average HS chain of 100 disaccharides has 48^{100} which equals 10^{168} possible structures. The structural diversity of HS, mainly dictated by distinct sulfation patterns, explains why HS mediates the specific binding and function of a myriad of proteins, including complement proteins (24, 25). Notably, heparin and highly sulfated domains within HS are similar, whereas heparin overall is more sulfated than HS.

While the cell surface recognition domains of FH and FHRs are highly homologous, they are not identical. It is known that small changes in the HS binding domains of FH significantly affect the specificity of protein interaction with certain sulfate modifications (26), and therefore it is reasonable to hypothesize that similar differences in specificity may exist between FH and FHRs. Theoretically, the relative binding affinities of FH and FHR to host tissues, *i.e.* endothelial glycocalyx, may be different, which could be selectively inhibited by HS or heparinoid oligosaccharides. Therefore, in this study, we sought to investigate whether HS structures can be identified, which differentially alter FH and/or FHR binding to the glycocalyx of glomerular endothelial cells. Indeed, we found that binding of FH, FHR1 and FHR5 proteins to glomerular endothelial HS is differentially mediated by N-, 2-O- and 6-O-sulfation. These findings offer novel insights into the underlying pathophysiology of C3G and may lead to novel treatments for C3G and other diseases with dysregulated complement activity.

MATERIALS AND METHODS

Participants

Patients with C3G referred to the Molecular Otolaryngology and Renal Research Laboratories (MORL) at the University of Iowa (UI) for a genetic evaluation of complement genes were enrolled in this study. C3G was diagnosed by the presence of C3 deposits by immunofluorescence in the absence, or comparatively reduced presence of other immunoreactants (C3 immunofluorescence at least two orders of magnitude greater intensity than for any other immunoreactant). Copy number variation in the *CFH-CFHR* genomic region was determined using multiplex ligation-dependent probe amplification. The study was approved by the Institutional Review Board of Carver College of Medicine at the University of Iowa.

Cell Culture

Conditionally immortalized human glomerular endothelial cells (ciGEnCs) were cultured as previously described (27) on 1.0 μg/cm^2

bovine fibronectin (Bio-Connect BV, Huissen, The Netherlands) coating. For proliferation, cells were cultured at 33°C in endothelial cell basal medium (EGM-2 MV; Lonza, Verviers, Belgium). For experiments, ciGEnCs were seeded at 25% confluence at 37°C and grown to confluent monolayers. Human umbilical vein endothelial cells (HUVECs) were cultured as previously described (28). Media were refreshed every two days.

Evaluation of FH/FHR ciGEnC Binding Using ELISA

ciGEnCs were differentiated in 96 well plates for five days. After differentiation, cells were washed twice using Hank's balanced salt solution including Mg^{2+}/Ca^{2+} (HBSS) and incubated for 30 minutes at RT with two-fold dilution series of serum-purified FH (Complement Technologies Inc., Tyler, TX, USA) or recombinant 6xHis-tagged FHR1, FHR2 and FHR5 (Novoprotein, Summit, NJ, USA) in HBSS with 2% (w/v) bovine serum albumin (BSA; Sigma-Aldrich Chemie, Zwijndrecht, The Netherlands). Binding was detected using monoclonal anti-FH antibody (Clone: Ox24; Bio-Rad) followed by goat anti-mouse IgG_1:horseradish peroxidase (HRP) conjugate (Sanbio BV, Uden, The Netherlands), or mouse anti-6xHis antibody (Sigma-Aldrich) followed by goat anti-mouse IgG : HRP conjugate (Jackson ImmunoResearch, West Grove, PA). Assays were developed using 3, 3', 5, 5' tetramethyl benzidine substrate A+B (Biolegend, London, UK). Based on the titrations, FH, FHR1, FHR2 and FHR5 were used at a concentration of 100, 70, 50 and 10 µg/ml for all subsequent assays, unless stated otherwise.

For evaluation of FH and FHR binding to C3b-labeled ciGEnCs, cells were cultured in 96 well plates for five days at 37°C, washed twice with HBSS and sensitized with anti-Jurkat/Ramos/THP-1 antiserum (1:30 in HBSS) (29). Classical pathway activation was then induced by incubation with 3.60 µg/ml C1, 1.00 µg/ml C2, 6.00 µg/ml C4 and 130 µg/ml C3 (Complement technologies Inc.) in HBSS for 20 minutes at 37°C. C3b labeling was confirmed using polyclonal sheep anti-C3 antibody (ICL Inc., Portland, OR, USA) followed by rabbit anti-sheep IgG: HRP conjugate (Sanbio BV). For competition assays between FH and FHRs on C3b-labeled ciGEnCs, ciGEnCs were preincubated with FHRs for 10 minutes before addition of FH for 20 minutes at RT. Binding of FH and FHRs to C3b-labeled ciGEnCs was determined as described above.

Alternative/Terminal Pathway Activation Assays

ciGEnCs and HUVECs were cultured in 24 or 48 well plates as described above. After differentiation, cells were washed twice with 0.2% (w/v) BSA in phosphate-buffered saline (PBS) and incubated for 30 minutes at 37°C with 20% (v/v) normal human serum (NHS; Complement Technologies Inc., Tyler, TX, USA) in veronal-buffered saline [15 mM barbitone, 145 mM NaCl, 5 mM $MgCl_2$, 5 mM EGTA, 0.025% NaN_3 (pH 7.3)] or 20% NHS supplemented with 35 µg/ml FHR1, 25 µg/ml FHR2 or 5 µg/ml FHR5 in veronal-buffered saline. 20% NHS supplemented with 10 mM EDTA was used to correct for cell surface binding of C3 in absence of complement activation. Monoclonal antibodies specific for decay-accelerating factor (Bio-Rad Laboratories BV, clone: BRIC-216) or membrane cofactor protein (Santa Cruz Biotechnology, Santa Cruz, CA, USA, clone: M177) were included to sensitize ciGEnCs to AP activation. To determine AP dysregulation on ciGEnCs in patient serum, cells were incubated with C3G patient sera including: patients with 3 to 4 copies of the *CFHR1* gene, the *CFHR1* and *CFHR3* gene deletion (Δ*CFHR3-CFHR1*), 402H/H or 402Y/Y haplotype. Since C3G patient sera samples were depleted of C3, the sera were supplemented with either 20% NHS or C3 (130 µg/ml), factor B (21 µg/ml) and factor D (0.2 µg/ml) (Complement Technologies Inc.) before addition to the cells. Patient sera samples that did not exceed the C3 signal of NHS supplemented with EDTA (MFI: 54819 ± 6202) by at least 2.5-fold after AP supplementation were rejected from analysis. To determine potential therapeutic effects, FHR-supplemented sera were spiked with 2-O-desulfated heparin (oligosaccharides) before addition to the cells. Cells were detached by incubation with 1% (w/v) BSA in non-enzymatic cell dissociation solution (Sigma-Aldrich Chemie) and gentle scraping, centrifuged at 500g and resuspended in 0.5% (w/v) BSA in ice-cold PBS. C3 and C9 deposition was detected using polyclonal sheep anti-C3 antibodies and goat anti-C9 antiserum (Quidel, San Diego, CA, USA). Antibody binding was quantified with Alexa 488-labeled donkey anti-sheep IgG and donkey anti-goat IgG (Life Technologies, Breda, The Netherlands) using a Beckman Coulter CytoFLEX flow cytometer with Kaluza 2.1 software. To determine if the classical pathway contributes to the observed C3b deposition, cells were sensitized with anti-Jurkat/Ramos/THP-1 antiserum and incubated with 20% NHS in either veronal-buffered saline or HBSS (**Supplementary Figure 1**). To validate the flow cytometry assay used to analyze C3b deposition, C3b deposition was also analyzed using SDS PAA gel electrophoresis and Western blotting.

Heparan Sulfate Purification Using Low Melting Agarose Barium Acetate Agarose Gel Electrophoresis

Glycosaminoglycan extractions were performed as described previously (30). GAGs were loaded on 1% (w/v) low-melting agarose gel (Boehringer Mannheim, Mannheim, Germany), and resolved by gel electrophoresis in 50 mM barium acetate buffer, pH 5.0 (Sigma-Aldrich). Gels were stained using Azure A (Sigma-Aldrich) and ciGEnC glycocalyx-derived HS (HS_{Glx}) bands were collected and melted at 65°C for 10 minutes. After extraction using an equal volume basic phenol (Boom BV, Meppel, The Netherlands), HS_{Glx} in the aqueous phase was collected and HS_{Glx} was precipitated by addition of 0.24 µl 27% (w/v) sodium acetate (Sigma-Aldrich) and 3.72 µl ethanol (Merck, Darmstadt, Germany) per µl aqueous phase, followed by overnight incubation at -20°C. Precipitates were collected by centrifugation at 15,700g for 10 minutes and resuspended in H_2O. Three consecutive precipitations were performed per HS_{Glx} extract.

2-O-Desulfated Heparin Oligosaccharide Library Generation

2-O-desulfated heparin was generated from 100 mg heparin (Aspen Oss BV, Oss, The Netherlands) as described previously (31). A 5% (w/v) solution of heparin in H_2O was alkalized by adding sodium hydroxide (Merck) to 0.5 M concentration,

snap-freezing and lyophilization. 1% (w/v) sodium borohydride (Sigma Aldrich) was included to minimize degradation by β-elimination. The resulting product was dissolved and neutralized by adding 5% (v/v) acetic acid and dialyzed extensively against H_2O. Selective 2-O-desulfation was confirmed by disaccharide analysis of 4 mg heparin or 2-O-desulfated heparin as described previously (32). 2-O-desulfated heparin oligosaccharide libraries were generated following the protocol described by Powell et al. (33). 40 mg 2-O-desulfated heparin were digested overnight at 37°C using 1.0 mU/mg heparinase II (Iduron, Macclesfield, UK) in 2.0 ml 100 mM acetate (pH 7.0), 1.5 mM calcium chloride. 5.00 to 8.75 mg/ separation of 2-O-desulfated heparin digest were resolved by size exclusion chromatography in 0.25 M ammonium bicarbonate at 0.22 mL/min flow speed over a BioGel P10 column (75 x 1.6 cm; Bio-Rad Laboratories BV) while monitoring the absorbance at 232 nm and collecting 1.0 mL fractions. Fractions corresponding to defined peaks were pooled, dialyzed against H_2O using 100-500 Da molecular weight cut-off Float-A-Lyzers (Repligen, Breda, Netherlands) and then concentrated by centrifugal evaporation. 2-O-desulfated heparin oligosaccharides were quantified using a Smart-Spec Plus spectrophotometer (Bio-Rad Laboratories BV) to measure the absorbance 232 nm and an extinction coefficient of 5500 $M^{-1}cm^{-1}$ (34). Successful digestion and size separation were confirmed using polyacrylamide gel electrophoresis compared to Arixtra, (GlaxoSmithKline, Brentford, UK) and size-defined heparin oligosaccharide standards (gifted from Prof. Jerry Turnbull's lab) (33) and silver-staining following Morrissey (35).

Competition Assays Using Selectively Desulfated Heparin (Oligosaccharides)

HS_{Glx} was immobilized on microtiter plates (NUNC, Roskilde, Denmark) at a concentration which resulted in ~70% of the EW4G2 (anti-HS antibody) signal obtained from 1.0 μg/well of heparan sulfate from bovine kidney (Sigma-Aldrich). Plates were washed using PBS/0.05% Tween-20 and blocked using 2% BSA in HBSS for 2 hours at RT. Binding of FH, FHR1, FHR2 and FHR5 after 1 hour incubation at RT was determined as described for cell surface binding assays. For competition between FH and FHRs, plates were preincubated with FHR1 or FHR5 in 2% BSA in HBSS for 1 hour at RT before incubation with FH. The role of HS modifications was evaluated by preincubating FH, FHR1 and FHR5 with 100 μg/ml heparin, N-, 2-O- and 6-O-desulfated heparin (Iduron, UK) for 1 hour at RT before addition to immobilized HS_{Glx}. To determine the minimum oligosaccharide size required for inhibition of FHR1 and FHR5 binding to HS_{Glx}, proteins were preincubated with 10 μM of the different size exclusion chromatography fractions.

Statistics

Groups were compared with Student's unpaired t-test or One-way ANOVA (>2 groups) followed by Tukey's *post-hoc* test using GraphPad Prism 9.1.2 (GraphPad Software Inc., San Diego, CA). Values are given as mean ± standard error of the mean unless stated otherwise. Statistical significance was accepted for $p \leq 0.05$.

RESULTS

FH and Type 1 FHRs Bind to (C3b-Labeled) Glomerular Endothelial Cells *In Vitro*

To investigate the role of specific HS/heparinoid sulfate modifications in the interaction between FH, type 1 FHRs and HS in the glomerular endothelial glycocalyx *in vitro*, we first evaluated the binding characteristics of FH and FHRs to ciGEnCs. All proteins, except FHR2, bound to the cell surface within their reported physiological concentrations (13, 36, 37) (**Figures 1A–D**). Notably, since FHR2 hardly binds to ciGEnCs, we mainly focused on FHR1 and FHR5 in our subsequent experiments. Next, we wondered whether the presence of C3b would influence FH and FHRs binding. To this end, we deposited C3b on antibody-sensitized ciGEnCs using classical pathway proteins (**Supplementary Figure 1** and **Figure 1E**), which significantly increased binding of FH and FHRs, though FHR2 binding remained relatively weak compared to FHR1 and FHR5 (**Figure 1F** and **Supplementary Figure 2A**).

FHR1 and FHR5 Cause Complement Activation on Glomerular Endothelium *In Vitro*

Next, we evaluated the effect of FHRs on complement regulation on ciGEnCs. Supplementing human serum with FHR1, FHR2 or FHR5 before incubation with ciGEnCs revealed significant dysregulation of AP activity, as measured by increased C3b deposition, in the case of FHR1 and FHR5 (**Figure 2A** and **Supplementary Figure 2B**), and the terminal pathway activity, as measured by C9 deposition, in the case of FHR1 (**Figure 2B** and **Supplementary Figure 2C**). Furthermore, when ciGEnCs were incubated with serum from C3G patients, significant dysregulation of AP activity was observed ($p=0.0011$) compared to healthy control serum (**Figure 2C**). Notably, to validate our flow cytometry assay to measure C3b deposition, we also analyzed C3b deposition in resolved cellular extracts followed by Western blotting, which essentially yielded quantitatively similar results (**Supplementary Figure 3**). To determine if the observed dysregulation of the AP by the added FHRs results from decreased FH binding to ciGEnCs, FH was added to cells after incubation with FHRs. While no significant inhibition of FH binding was observed on untreated ciGEnCs, FHR5 significantly reduced cell surface binding of FH after ciGEnCs were labeled with C3b using the classical pathway proteins (**Figure 2D** and **Supplementary Figure 2D**). Thus, HS-binding of type 1 FHRs deregulates complement activity on ciGEnCs, which may depend in part on C3b deposition.

FHR1 and FHR5 Compete With FH for Binding to HS Purified From Glomerular Endothelial Glycocalyx (HS_{Glx})

Since cells express other potential ligands for FH/FHR than only HS, we zoomed in on the interaction of FH and FHRs proteins with purified HS isolated from glycocalyx (HS_{Glx}) of cultured glomerular endothelial cells. FH and FHRs binding to purified and immobilized HS_{Glx} revealed similar results as for binding to

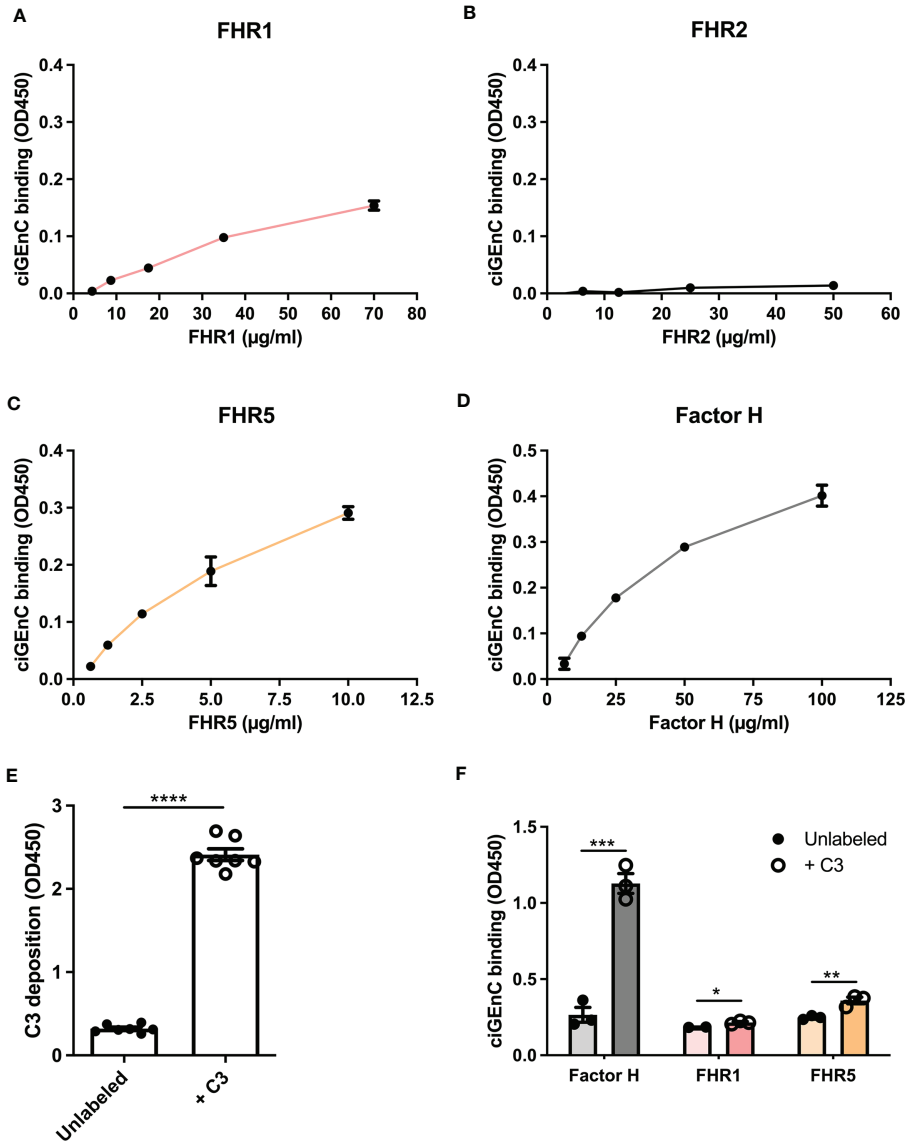

FIGURE 1 | Factor H and recombinant FHR1 and FHR5 bind to glomerular endothelial cells *in vitro*. Factor H-related proteins (FHRs) 1 **(A)**, 2 **(B)** and 5 **(C)** and factor H **(D)** were titrated on conditionally immortalized glomerular endothelial cells (ciGEnCs) and binding was determined using ELISA. Labeling antibody-sensitized ciGEnCs with C3b using classical pathway proteins (n=7) **(E)** significantly increased binding of factor H and FHR1 and FHR5 (n=3) **(F)**. (*p < 0.05, **p < 0.01, ***p < 0.001, ****p < 0.0001 *vs* Unlabeled).

ciGEnCs, i.e. FH, FHR1 and FHR5 bound to HS_{Glx}, whereas FHR2 did not (**Figure 3A** and **Supplementary Figure 2E**). Moreover, FHR1 and FHR5 efficiently competed with FH for binding to HS_{Glx}, since FH binding was reduced by the addition of FHR1 or FHR5 (**Figure 3B**).

2-O-Desulfated Heparin Oligosaccharides Selectively Inhibit FHR1 and FHR5 Binding, and Reduce C3b Deposition on Endothelial Cells

To identify the nature of the HS structures in purified HS_{Glx} that are important for FH and/or FHR binding, we performed competition assays with heparin and N-, 2-O- or 6-O-desulfated heparins. Unmodified heparin blocked HS binding sites on FH, FHR1 and FHR5, thereby reducing (for FH) or preventing (for FHR1 and FHR5) binding to HS_{Glx}, (**Figures 3C–E**). Removing any of the sulfates from heparin largely abolished the competition for FH binding to HS_{Glx} (**Figure 3C**). In contrast, 2-O- and 6-O-desulfated, and to a lesser degree, N-desulfated heparin, were still able to compete for FHR1 (**Figure 3D**) and FHR5 (**Figure 3E**). These results reveal that there is selectivity in binding of FH *versus* FHR1/FHR5 to structures within HS_{Glx}. Importantly, C3b deposition by patient sera on ciGEnC was significantly decreased in the presence of 2-O-desulfated

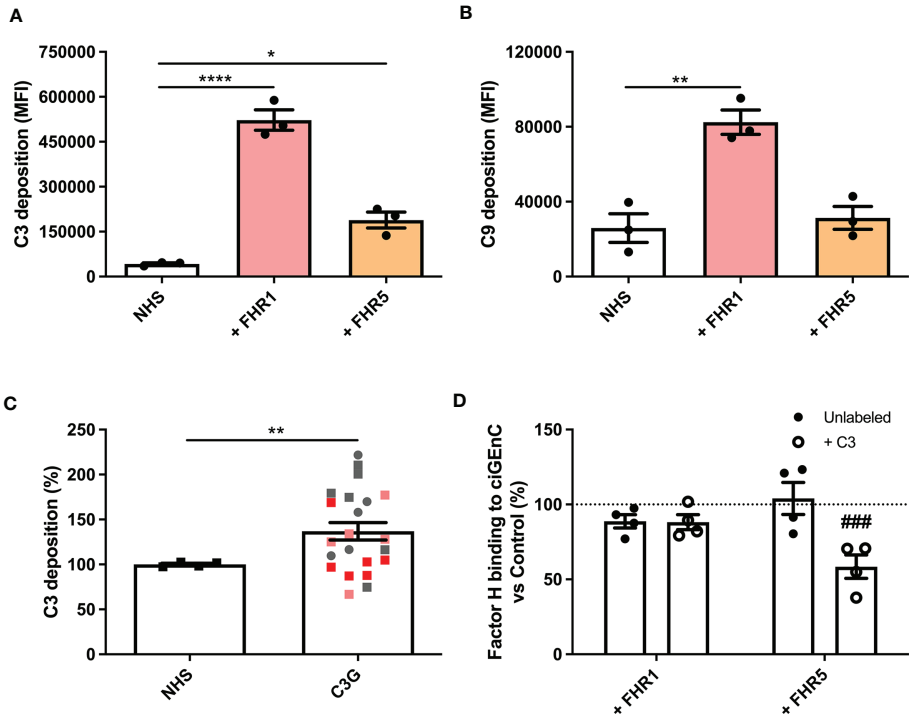

FIGURE 2 | Factor H-related proteins 1 and 5 deregulate alternative pathway activation on glomerular endothelial cells *in vitro*. ciGEnCs were incubated in 20% normal human serum (NHS) in veronal-buffered saline including 5 mM magnesium-EGTA, which prevents classical/lectin pathway activation. Serum was supplemented with factor H-related proteins (FHRs) 1 or 5 and effects on alternative pathway (n=3) **(A)** and terminal pathway (n=3) **(B)** activity were evaluated using flow cytometry. ciGEnCs were incubated with NHS or C3G patient sera (n=4, healthy controls; n=22, C3G patients) **(C)**, including patients: with 3 to 4 copies of the FHR1 gene (pink), FHR1 and FHR3 deletion (ΔCFHR3-1) (red), 402H/H haplotype (grey square) and 402Y/Y haplotype (grey circle). Sera were supplemented with C3, factor B and factor D to ensure the presence of sufficient amounts of AP components. To determine the effect of FHR competition on FH binding, unlabeled or C3b-labeled ciGEnCs were pre-incubated with buffer (Control) or FHRs 1 or 5, after which FH binding was detected using ELISA (n=4) **(D)**. (*$p < 0.05$, **$p < 0.01$, ****$p < 0.0001$ *vs* NHS; $^{###}p < 0.001$ *vs* Control).

heparin, thereby suggesting that 2-O-desulfated heparin has therapeutic value for complement-mediated glomerular disease (**Figure 3F**). Addition of 2-O-desulfated heparin to FHR-supplemented serum reverse the C3b deposition caused by FHR1 competition with FH on ciGEnCs (**Supplementary Figure 4**) as well as on HUVECs (**Supplementary Figure 5**) in a concentration-dependent manner. Considering the highly heterogenous structure of HS and heparin, associated with many functions, a possible therapeutic should be preferably of short length whilst retaining the functional activity. Therefore, to determine the minimal size of 2-O-desulfated heparin required for restoring complement regulation, a size-defined library of oligosaccharides was generated from 2-O-desulfated heparin (**Supplementalry Figure 6** and **Supplementary Table 1**). Addition of size-defined 2-O-desulfated fractions revealed that a minimum of a tetrasaccharide (dp 4) was required for significant binding to FHR1 and FHR5 in competition with HS_{Glx} (**Figure 4A**), thereby reducing FHR binding to glomerular endothelial cells (**Figure 4B**). Importantly, FH binding to HS_{Glx} was not altered by any of the fractions tested (**Figure 4A**). Thus, 2-O-desulfated heparin oligosaccharides were identified as highly selective competitors reducing/preventing FHR1 and FHR5 binding to HS_{Glx}, but not affecting FH binding to HS_{Glx}, thereby supporting their potential application in novel C3G therapies.

DISCUSSION

The pathogenesis of C3G is driven by dysregulation of AP complement activity in the fluid phase and/or glomerular microenvironment. The relative balance between FH and type 1 FHR proteins is especially relevant in the glomerulus, as the latter compete with the former for host tissue-associated ligands, thereby affecting the relative degree of complement control in this microenvironment. One of the most important host ligands for FH and FHRs on glomerular endothelial cells is HS (36, 37).

In this study, we found that while FH, FHR1 and FHR5 bound to ciGEnCs, the initial deposition of C3b significantly increased this binding. The biggest relative changes were observed for FHR5, the binding of which significantly reduced binding of FH, creating a microenvironment in which AP activity was dysregulated, although terminal pathway activity was not observed. FHR1, in contrast, did not inhibit FH binding to ciGEnCs but nevertheless did lead to dysregulated AP activity and activation of the terminal pathway.

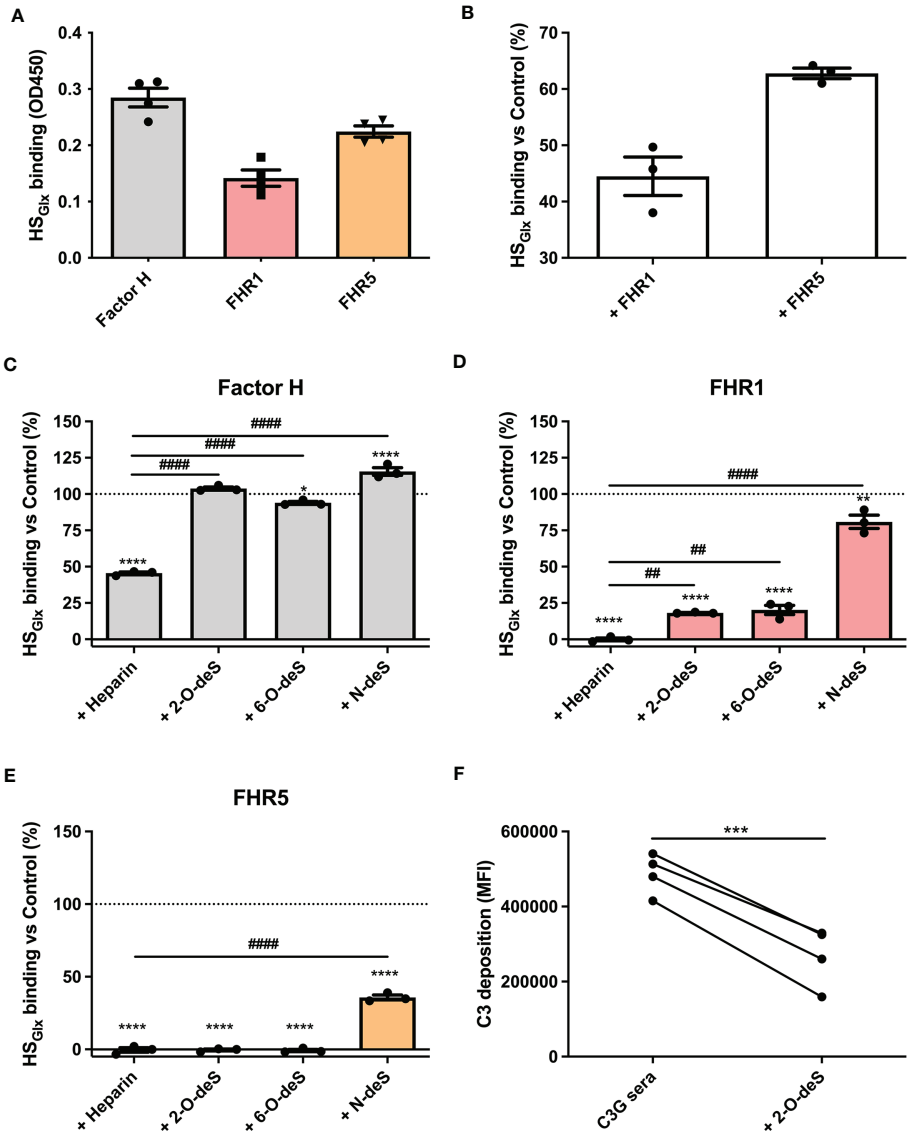

FIGURE 3 | O-desulfated heparins reduce FHR1 and FHR5 binding to purified glomerular endothelial glycocalyx-derived heparan sulfate (HS), without affecting FH binding. HS was purified from isolated glycocalyx from conditionally immortalized glomerular endothelial cells (HS_{Glx}) and immobilized on microtiter plates. Binding of factor H (FH) and factor H-related proteins (FHRs) was measured using ELISA (n=4) **(A)**. For competition assays, HS_{Glx} was incubated with FHR1 or FHR5 before binding of FH was determined (n=3) **(B)**. The contribution of specific sulfate modifications to HS_{Glx} binding of FH (n=3) **(C)**, FHR1 (n=3) **(D)** and FHR5 (n=3) **(E)** was evaluated by preincubating proteins with buffer (Control), heparin or 2-O-, 6-O- and N-desulfated (deS) heparin before addition to microtiter plates. To investigate potential therapeutic effects of 2-O-desulfated heparin in context of C3G patient sera (402H/H haplotype group with >1.5x increased C3 deposition compared to NHS), sera were supplemented with 50 µg/ml 2-O-desulfated heparin before addition to the cells (n=4) **(F)**. (*p < 0.05, **p < 0.01, ****p < 0.0001 *vs* Control; $^{\#\#}$p < 0.01, $^{\#\#\#\#}$p < 0.0001 *vs* Heparin; ***p<0.001 vs C3G sera.)

FHR1-mediated dysregulation therefore may differ on cell surfaces that have been C3b-labeled as compared to cell surfaces on which C3 convertase has already formed. This difference suggests that FHR1 may support the formation of C3 convertase, as has been described for properdin (38, 39). Of note, we found that FHR2, which is also a type 1 FHR, hardly bound to ciGEnCs.

Consistent with the results we observed with FHR1 and FHR5, we also measured a significant increase in AP activity in the sera of C3G patients, including patients with 3 or 4 copies of the *CFHR1* gene. This increase in AP activity was not seen in C3G patients with Δ*CFHR3-CFHR1* deficiency. These findings suggest that in addition to fluid-phase dysregulation of the AP, which is characteristic of C3G, dysregulation of complement can also occur in the glomerular microenvironment and is impacted by the relative levels of FH and FHR1/FHR5 in the circulation.

To further clarify the importance of HS modifications, we studied the interaction between FH, FHRs and HS using purified HS_{Glx}, *i.e.* in the absence of other cell surface ligands. In these

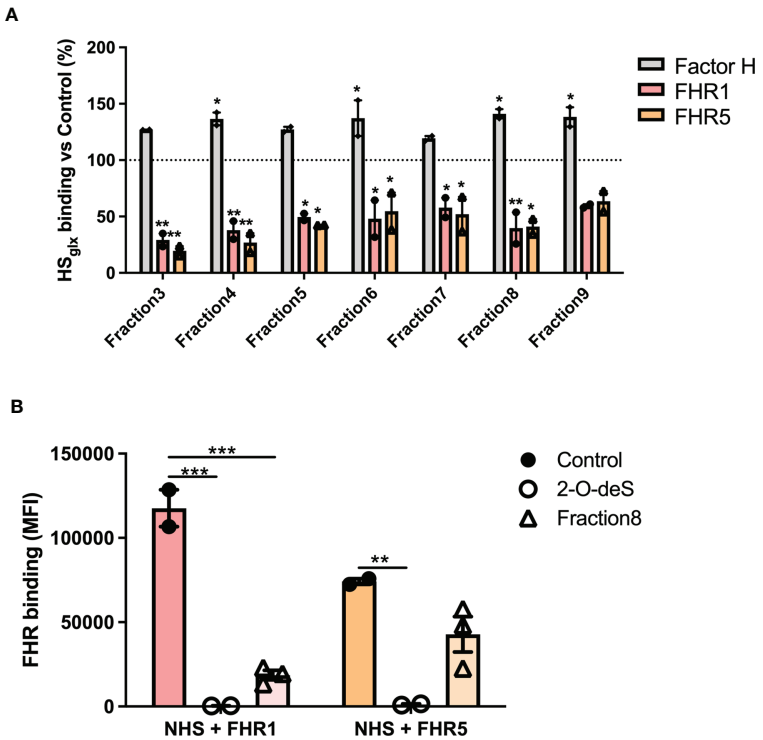

FIGURE 4 | 2-O-desulfated heparin fragments with a size equal to or larger than tetrasaccharides reduce FHR1 and 5 binding to purified glomerular endothelial HS_{Glx} and ciGEnCs, without affecting FH binding to HS_{Glx}. To determine the minimal oligosaccharide size required for FHR1 and FHR5 competition, proteins were preincubated with equimolar amounts of 2-O-desulfated heparin digest size exclusion chromatography fractions (n=2) **(A)**. Addition of 2-O-deS heparin or short 2-O-deS oligosaccharides (Fraction8) to FHR-supplemented serum significantly reduced FHR binding to ciGEnCs (n≥2) **(B)**. (*p < 0.05, **p < 0.01, ***p < 0.001 *vs* Control).

experiments, we compared heparin and HS_{Glx} and found that the former competed more efficiently for FHR1 and FHR5 than for FH. Selectively desulfated heparin did not influence binding of FH to HS_{Glx}, which shows that binding of FH to HS_{Glx} depends on N-, 2-O- and 6-O-sulfation. These results match previous reports involving FH-competition experiments with selectively desulfated heparins (9, 40). Selectively desulfated heparins were successful in preventing or reducing binding of FHR1 and FHR5 to HS_{Glx}, except for N-desulfated heparin that still allowed FHR1 binding, which shows that FHR1 binding is primarily mediated by N-sulfation.

Notably, although FHR5 bound more strongly to HS_{Glx} as compared with FHR1, FHR1 was the more potent competitor for FH binding to HS_{Glx}. This difference between FHR1 and FHR5 reflects the close homology between the HS binding domains of FHR1 (CCP5) and FH (CCP20), which share 97% identity. The two variant amino acids–L290 *vs* S1191 and A296 *vs* V1197–in FH and FHR1 are buried and therefore unlikely to interact directly with HS. They do however affect the structure of the surface-exposed loop that harbors the HS-binding amino acids K285/K1186 and K287/K1188 in FHR1 and FH, respectively (41), possibly altering surface charge distribution and consequently the HS binding characteristics of the domain. This remarkable degree of ligand specificity is also seen with age-related macular degeneration and the associated p.Tyr402His polymorphism (rs1061170) in CCP7 of FH, which affects FH binding to specific HS modifications in Buch's membrane and is a risk factor for disease (26). Type 1 FHRs (FHR1, 2 and 5) can also exist as heterodimers or homodimers, which we have not addressed in this study. However, we do not consider this as a major limitation, since homodimers of FHR1, 2 and 5 may have formed in our assays. Most likely, our primary finding that 2-O-desulfated heparin can prevent binding of FHR1 and FHR5 is also valid for heterodimers, since the monomers present in a heterodimer both will bind to 2-O-desulfated heparin, whereas FHR2 hardly binds to HS_{Glx}.

The ability of 2-O-desulfated heparin oligosaccharides to compete for FHR but not FH and thereby alter binding to HS_{Glx} suggests that providing a "sink" to scavenge FHR proteins represents a novel treatment approach for C3G. 2-O-desulfation by alkaline lyophilization is not only remarkably selective and simple, but it also removes the rare glucosamine 3-O-sulfate modification, which significantly reduces the anticoagulant activity of 2-O-desulfated heparin (42) and thus potential adverse effects. We observed that selective competition is retained with short 2-O-desulfated oligosaccharides (≥tetrasaccharides), potentially enabling the synthesis of therapeutically active oligosaccharides by chemoenzymatic methods (43).

In conclusion, we have demonstrated HS-mediated ligand specificity for FH and FHR1/FHR5 that impacts the relative balance of these proteins in the glomerular glycocalyx, thereby altering AP regulation in this microenvironment. These results

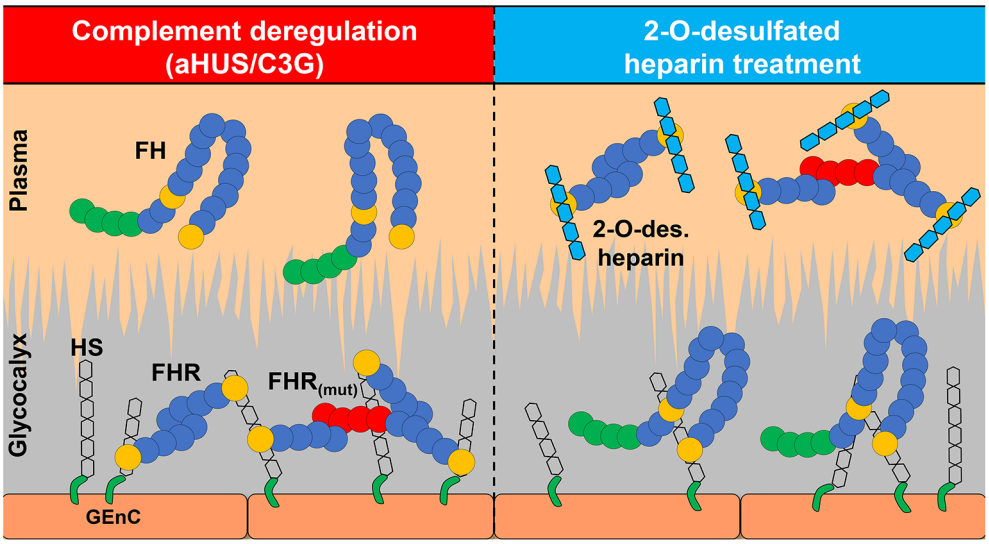

FIGURE 5 | 2-O-desulfated heparin oligosaccharides are potential therapeutics for C3G and other diseases with dysregulated complement. Pathogenic changes in complement components or glomerular glycocalyx affect the balance between FH and FHRs contributing to disease development. 2-O-desulfated heparin derivatives selectively inhibit FHR1 and FHR5 binding to glomerular endothelium without affecting FH binding, which makes them potential therapeutics for C3G and other diseases with dysregulated complement.

provide novel insights into the pathophysiology of C3G and suggest that genetic studies of C3G cohorts can identify patients with variants in genes involved in HS proteoglycan synthesis that create a "permissive" microenvironment, which favors FHR binding over FH binding. This imbalance, in turn, supports complement dysregulation either primarily or after secondary triggering events. Our data also suggest a novel treatment for C3G in which short 2-O-desulfated heparin oligosaccharides are used to scavenge FHR1 and FHR5, thereby altering the binding of these proteins to the glomerular glycocalyx (**Figure 5**).

DATA AVAILABILITY STATEMENT

The raw data supporting the conclusions of this article will be made available by the authors, without undue reservation.

ETHICS STATEMENT

The study was approved by the Institutional Review Board of Carver College of Medicine at the University of Iowa. Written informed consent to participate in this study was provided by the participants' legal guardian/next of kin.

AUTHOR CONTRIBUTIONS

JvdV initiated and supervised the study. ML and JvdV designed the study. MMH, ML, CY, MCH, MdG and EK carried out experiments. MMH, ML, CY and MCH analyzed the data and made the figures. MMH, ML, CY, MCH, EK, TvK, JW, TJR, RS and JvdV drafted and revised the manuscript. All authors contributed to the article and approved the submitted version.

FUNDING

This study was supported by the Radboud university medical center PhD fellow program, consortium grant LSHM16058-SGF (GLYCOTREAT, a collaboration project financed by the PPP Allowance made available by Top Sector Life Sciences & Health to the Dutch Kidney Foundation to stimulate public-private partnerships), Kidneeds, GCR foundation USA JV and the National Institutes of Health R01 DK110023 RS.

ACKNOWLEDGMENTS

The authors would like to thank Dr. Anna Blom for anti-Jurkat/Ramos/THP-1 antiserum, Dr. Simon Satchel for the conditionally immortalised glomerular endothelial cells (ciGEnCs), Prof. Jerry Turnbull for size-defined heparin oligosaccharide standards and Dr. Christian Viskov for performing disaccharide analyses.

SUPPLEMENTARY MATERIAL

The Supplementary Material for this article can be found online at: https://www.frontiersin.org/articles/10.3389/fimmu.2021.676662/full#supplementary-material

REFERENCES

1. Merle NS, Church SE, Fremeaux-Bacchi V, Roumenina LT. Complement System Part I - Molecular Mechanisms of Activation and Regulation. *Front Immunol* (2015) 6:262. doi: 10.3389/fimmu.2015.00262
2. Cook HT. C3 Glomerulopathy. *F1000Research* (2017) 6:248. doi: 10.12688/f1000research.10364.1
3. Nester CM, Barbour T, de Cordoba SR, Dragon-Durey MA, Fremeaux-Bacchi V, Goodship THJ, et al. Atypical aHUS: State of the Art. *Mol Immunol* (2015) 67:31–42. doi: 10.1016/j.molimm.2015.03.246
4. de Córdoba SR, de Jorge EG. Translational Mini-Review Series on Complement Factor H: Genetics and Disease Associations of Human Complement Factor H. *Clin Exp Immunol* (2008) 151:1–13. doi: 10.1111/j.1365-2249.2007.03552.x
5. Schmidt CQ, Herbert AP, Kavanagh D, Gandy C, Fenton CJ, Blaum BS, et al. A New Map of Glycosaminoglycan and C3b Binding Sites on Factor H. *J Immunol (Baltimore Md 1950)* (2008) 181:2610–9. doi: 10.4049/jimmunol.181.4.2610
6. Weiler JM, Daha MR, Austen KF, Fearon DT. Control of the Amplification Convertase of Complement by the Plasma Protein Beta1h. *Proc Natl Acad Sci USA* (1976) 73:3268–72. doi: 10.1073/pnas.73.9.3268
7. Pangburn MK, Schreiber RD, Müller-Eberhard HJ. Human Complement C3b Inactivator: Isolation, Characterization, and Demonstration of an Absolute Requirement for the Serum Protein Beta1H for Cleavage of C3b and C4b in Solution. *J Exp Med* (1977) 146:257–70. doi: 10.1084/jem.146.1.257
8. Blackmore TK, Sadlon TA, Ward HM, Lublin DM, Gordon DL. Identification of a Heparin Binding Domain in the Seventh Short Consensus Repeat of Complement Factor H. *J Immunol (Baltimore Md 1950)* (1996) 157:5422–7.
9. Clark SJ, Ridge LA, Herbert AP, Hakobyan S, Mulloy B, Lennon R, et al. Tissue-Specific Host Recognition by Complement Factor H Is Mediated by Differential Activities of Its Glycosaminoglycan-Binding Regions. *J Immunol (Baltimore Md 1950)* (2013) 190:2049–57. doi: 10.4049/jimmunol.1201751
10. Hellwage J, Jokiranta TS, Friese MA, Wolk TU, Kampen E, Zipfel PF, et al. Complement C3b/C3d and Cell Surface Polyanions Are Recognized by Overlapping Binding Sites on the Most Carboxyl-Terminal Domain of Complement Factor H. *J Immunol (Baltimore Md 1950)* (2002) 169:6935–44. doi: 10.4049/jimmunol.169.12.6935
11. Blaum BS, Hannan JP, Herbert AP, Kavanagh D, Uhrín D, Stehle T. Structural Basis for Sialic Acid-Mediated Self-Recognition by Complement Factor H. *Nat Chem Biol* (2015) 11:77–82. doi: 10.1038/nchembio.1696
12. Medjeral-Thomas N, Pickering MC. The Complement Factor H-Related Proteins. *Immunol Rev* (2016) 274:191–201. doi: 10.1111/imr.12477
13. Skerka C, Chen Q, Fremeaux-Bacchi V, Roumenina LT. Complement Factor H Related Proteins (CFHRs). *Mol Immunol* (2013) 56:170–80. doi: 10.1016/j.molimm.2013.06.001
14. Zipfel PF, Jokiranta TS, Hellwage J, Koistinen V, Meri S. The Factor H Protein Family. *Immunopharmacology* (1999) 42:53–60. doi: 10.1016/S0162-3109(99)00015-6
15. Józsi M, Tortajada A, Uzonyi B, Goicoechea de Jorge E, Rodríguez de Córdoba S. Factor H-Related Proteins Determine Complement-Activating Surfaces. *Trends Immunol* (2015) 36:374–84. doi: 10.1016/j.it.2015.04.008
16. Goicoechea de Jorge E, Caesar JJE, Malik TH, Patel M, Colledge M, Johnson S, et al. Dimerization of Complement Factor H-Related Proteins Modulates Complement Activation *In Vivo*. *Proc Natl Acad Sci* (2013) 110:4685–90. doi: 10.1073/pnas.1219260110
17. van Beek AE, Pouw RB, Brouwer MC, van Mierlo G, Geissler J, Ooijevaar-de Heer P, et al. Factor H-Related (FHR)-1 and FHR-2 Form Homo- and Heterodimers, While FHR-5 Circulates Only As Homodimer in Human Plasma. *Front Immunol* (2017) 8:1328. doi: 10.3389/fimmu.2017.01328
18. Sethi S, Fervenza FC, Zhang Y, Zand L, Vrana JA, Nasr SH, et al. C3 Glomerulonephritis: Clinicopathological Findings, Complement Abnormalities, Glomerular Proteomic Profile, Treatment, and Follow-Up. *Kidney Int* (2012) 82:465–73. doi: 10.1038/ki.2012.212
19. Barbour TD, Ruseva MM, Pickering MC. Update on C3 Glomerulopathy. *Nephrol Dialysis Transplant* (2016) 31:717–25. doi: 10.1093/ndt/gfu317
20. Holers VM. Human C3 Glomerulopathy Provides Unique Insights Into Complement Factor H–Related Protein Function. *J Clin Invest* (2013) 123:2357–60. doi: 10.1172/JCI69684
21. Reitsma S, Slaaf DW, Vink H, van Zandvoort MAMJ, Oude Egbrink MGA. The Endothelial Glycocalyx: Composition, Functions, and Visualization. *Pflugers Arch* (2007) 454:345–59. doi: 10.1007/s00424-007-0212-8
22. Esko JD, Selleck SB. Order Out of Chaos: Assembly of Ligand Binding Sites in Heparan Sulfate. *Annu Rev Biochem* (2002) 71:435–71. doi: 10.1146/annurev.biochem.71.110601.135458
23. Rudd TR, Yates EA. A Highly Efficient Tree Structure for the Biosynthesis of Heparan Sulfate Accounts for the Commonly Observed Disaccharides and Suggests a Mechanism for Domain Synthesis. *Mol Biosyst* (2012) 8:1499. doi: 10.1039/c2mb25019e
24. Langford-Smith A, Day AJ, Bishop PN, Clark SJ. Complementing the Sugar Code: Role of GAGs and Sialic Acid in Complement Regulation. *Front Immunol* (2015) 6:25. doi: 10.3389/fimmu.2015.00025
25. Ori A, Wilkinson MC, Fernig DG. The Heparanome and Regulation of Cell Function: Structures, Functions and Challenges. *Front Biosci* (2008) 13:4309–38. doi: 10.2741/3007
26. Clark SJ, Higman VA, Mulloy B, Perkins SJ, Lea SM, Sim RB, et al. His-384 Allotypic Variant of Factor H Associated With Age-Related Macular Degeneration has Different Heparin Binding Properties From the Non-Disease-Associated Form. *J Biol Chem* (2006) 281:24713–20. doi: 10.1074/jbc.M605083200
27. Satchell SC, Tasman CH, Singh A, Ni L, Geelen J, von Ruhland CJ, et al. Conditionally Immortalized Human Glomerular Endothelial Cells Expressing Fenestrations in Response to VEGF. *Kidney Int* (2006) 69:1633–40. doi: 10.1038/sj.ki.5000277
28. Rother N, Pieterse E, Lubbers J, Hilbrands L, van der Vlag J. Acetylated Histones in Apoptotic Microparticles Drive the Formation of Neutrophil Extracellular Traps in Active Lupus Nephritis. *Front Immunol* (2017) 8:1136. doi: 10.3389/fimmu.2017.01136
29. Escudero-Esparza A, Kalchishkova N, Kurbasic E, Jiang WG, Blom AM. The Novel Complement Inhibitor Human CUB and Sushi Multiple Domains 1 (CSMD1) Protein Promotes Factor I-Mediated Degradation of C4b and C3b and Inhibits the Membrane Attack Complex Assembly. *FASEB J* (2013) 27:5083–93. doi: 10.1096/fj.13-230706
30. Van Gemst JJ, Loeven MA, De Graaf MJJ, Berden JHM, Rabelink TJ, Smit CH, et al. RNA Contaminates Glycosaminoglycans Extracted From Cells and Tissues. *PloS One* (2016) 11(11):e0167336. doi: 10.1371/journal.pone.0167336
31. Jaseja M, Rej RN, Sauriol F, Perlin AS. Novel Regio- and Stereoselective Modifications of Heparin in Alkaline Solution. Nuclear Magnetic Resonance Spectroscopic Evidence. *Can J Chem* (1989) 67:1449–56. doi: 10.1139/v89-221
32. Mourier P, Anger P, Martinez C, Herman F, Viskov C. Quantitative Compositional Analysis of Heparin Using Exhaustive Heparinase Digestion and Strong Anion Exchange Chromatography. *Anal Chem Res* (2015) 3:46–53. doi: 10.1016/j.ancr.2014.12.001
33. Powell AK, Ahmed YA, Yates EA, Turnbull JE. Generating Heparan Sulfate Saccharide Libraries for Glycomics Applications. *Nat Protoc* (2010) 5:821–33. doi: 10.1038/nprot.2010.17
34. Skidmore MA, Guimond SE, Dumax-Vorzet AF, Atrih A, Yates EA, Turnbull JE. High Sensitivity Separation and Detection of Heparan Sulfate Disaccharides. *J Chromatogr A* (2006) 1135:52–6. doi: 10.1016/j.chroma.2006.09.064
35. Morrissey JH. Silver Stain for Proteins in Polyacrylamide Gels: A Modified Procedure With Enhanced Uniform Sensitivity. *Anal Biochem* (1981) 117:307–10. doi: 10.1016/0003-2697(81)90783-1
36. Heinen S, Hartmann A, Lauer N, Wiehl U, Dahse H-M, Schirmer S, et al. Factor H-Related Protein 1 (CFHR-1) Inhibits Complement C5 Convertase Activity and Terminal Complex Formation. *Blood* (2009) 114:2439–47. doi: 10.1182/blood-2009-02-205641
37. McRae JL, Duthy TG, Griggs KM, Ormsby RJ, Cowan PJ, Cromer BA, et al. Human Factor H-Related Protein 5 Has Cofactor Activity, Inhibits C3 Convertase Activity, Binds Heparin and C-Reactive Protein, and Associates With Lipoprotein. *J Immunol (Baltimore Md 1950)* (2005) 174:6250–6. doi: 10.4049/jimmunol.174.10.6250
38. Gaarkeuken H, Siezenga MA, Zuidwijk K, van Kooten C, Rabelink TJ, Daha MR, et al. Complement Activation by Tubular Cells Is Mediated by Properdin Binding. *Am J Physiol Renal Physiol* (2008) 295:F1397–403. doi: 10.1152/ajprenal.90313.2008
39. Zaferani A, Vivès RR, van der Pol P, Hakvoort JJ, Navis GJ, van Goor H, et al. Identification of Tubular Heparan Sulfate as a Docking Platform for the

Alternative Complement Component Properdin in Proteinuric Renal Disease. *J Biol Chem* (2011) 286:5359–67. doi: 10.1074/jbc.M110.167825

40. Zaferani A, Vivès RR, van der Pol P, Navis GJ, Daha MR, van Kooten C, et al. Factor H and Properdin Recognize Different Epitopes on Renal Tubular Epithelial Heparan Sulfate. *J Biol Chem* (2012) 287:31471–81. doi: 10.1074/jbc.M112.380386
41. Bhattacharjee A, Reuter S, Trojnár E, Kolodziejczyk R, Seeberger H, Hyvärinen S, et al. The Major Autoantibody Epitope on Factor H in Atypical Hemolytic Uremic Syndrome Is Structurally Different From Its Homologous Site in Factor H-Related Protein 1, Supporting a Novel Model for Induction of Autoimmunity in This Disease. *J Biol Chem* (2015) 290:9500–10. doi: 10.1074/jbc.M114.630871
42. Fryer A, Huang YC, Rao G, Jacoby D, Mancilla E, Whorton R, et al. Selective O-Desulfation Produces Nonanticoagulant Heparin That Retains Pharmacological Activity in the Lung. *J Pharmacol Exp Ther* (1997) 282:208–19.
43. Lu W, Zong C, Chopra P, Pepi LE, Xu Y, Amster IJ, et al. Controlled Chemoenzymatic Synthesis of Heparan Sulfate Oligosaccharides. *Angew Chem Int Ed* (2018) 57:5340–4. doi: 10.1002/anie.201800387

Conflict of Interest: Author EK was employed by company Aspen API.

The remaining authors declare that the research was conducted in the absence of any commercial or financial relationships that could be construed as a potential conflict of interest.

Publisher's Note: All claims expressed in this article are solely those of the authors and do not necessarily represent those of their affiliated organizations, or those of the publisher, the editors and the reviewers. Any product that may be evaluated in this article, or claim that may be made by its manufacturer, is not guaranteed or endorsed by the publisher.

frontiers in Immunology

ORIGINAL RESEARCH
published: 22 March 2022
doi: 10.3389/fimmu.2022.845953

Complement Factor H-Related Proteins FHR1 and FHR5 Interact With Extracellular Matrix Ligands, Reduce Factor H Regulatory Activity and Enhance Complement Activation

*Alexandra Papp[1], Krisztián Papp[2], Barbara Uzonyi[1,2], Marcell Cserhalmi[1], Ádám I. Csincsi[1], Zsóka Szabó[1], Zsófia Bánlaki[1], David Ermert[3], Zoltán Prohászka[4,5], Anna Erdei[2,6], Viviana P. Ferreira[7], Anna M. Blom[3] and Mihály Józsi[1,6]**

[1] MTA-ELTE Complement Research Group, Eötvös Loránd Research Network (ELKH), Department of Immunology, ELTE Eötvös Loránd University, Budapest, Hungary, [2] MTA-ELTE Immunology Research Group, Eötvös Loránd Research Network (ELKH), Department of Immunology, ELTE Eötvös Loránd University, Budapest, Hungary, [3] Department of Translational Medicine, Lund University, Malmo, Sweden, [4] Department of Internal Medicine and Haematology, Semmelweis University, Budapest, Hungary, [5] Research Group for Immunology and Haematology, Semmelweis University-Eötvös Loránd Research Network (Office for Supported Research Groups), Budapest, Hungary, [6] Department of Immunology, ELTE Eötvös Loránd University, Budapest, Hungary, [7] Department of Medical Microbiology and Immunology, University of Toledo College of Medicine, Toledo, OH, United States

OPEN ACCESS

Edited by:
Arvind Sahu,
National Centre for Cell Science, India

Reviewed by:
Simon John Clark,
University of Tübingen, Germany
József Dobó,
Hungarian Academy of Sciences (MTA), Hungary

***Correspondence:**
Mihály Józsi
mihaly.jozsi@ttk.elte.hu

Specialty section:
This article was submitted to Molecular Innate Immunity, a section of the journal Frontiers in Immunology

Received: *30 December 2021*
Accepted: *17 February 2022*
Published: *22 March 2022*

Citation:
Papp A, Papp K, Uzonyi B, Cserhalmi M, Csincsi ÁI, Szabó Z, Bánlaki Z, Ermert D, Prohászka Z, Erdei A, Ferreira VP, Blom AM and Józsi M (2022) Complement Factor H-Related Proteins FHR1 and FHR5 Interact With Extracellular Matrix Ligands, Reduce Factor H Regulatory Activity and Enhance Complement Activation. Front. Immunol. 13:845953. doi: 10.3389/fimmu.2022.845953

Components of the extracellular matrix (ECM), when exposed to body fluids may promote local complement activation and inflammation. Pathologic complement activation at the glomerular basement membrane and at the Bruch's membrane is implicated in renal and eye diseases, respectively. Binding of soluble complement inhibitors to the ECM, including factor H (FH), is important to prevent excessive complement activation. Since the FH-related (FHR) proteins FHR1 and FHR5 are also implicated in these diseases, our aim was to study whether these FHRs can also bind to ECM components and affect local FH activity and complement activation. Both FH and the FHRs showed variable binding to ECM components. We identified laminin, fibromodulin, osteoadherin and PRELP as ligands of FHR1 and FHR5, and found that FHR1 bound to these ECM components through its C-terminal complement control protein (CCP) domains 4-5, whereas FHR5 bound *via* its middle region, CCPs 3-7. Aggrecan, biglycan and decorin did not bind FH, FHR1 and FHR5. FHR5 also bound to immobilized C3b, a model of surface-deposited C3b, *via* CCPs 3-7. By contrast, soluble C3, C3(H_2O), and the C3 fragments C3b, iC3b and C3d bound to CCPs 8-9 of FHR5. Properdin, which was previously described to bind *via* CCPs 1-2 to FHR5, did not bind in its physiologically occurring serum forms in our assays. FHR1 and FHR5 inhibited the binding of FH to the identified ECM proteins in a dose-dependent manner, which resulted in reduced FH cofactor activity. Moreover, both FHR1 and FHR5 enhanced alternative complement pathway activation on immobilized ECM proteins when exposed to human serum, resulting in the increased deposition of C3-fragments, factor B and C5b-9. Thus, our results identify novel ECM ligands of FH family

proteins and indicate that FHR1 and FHR5 are competitive inhibitors of FH on ECM and, when bound to these ligands, they may enhance local complement activation and promote inflammation under pathological conditions.

Keywords: factor H-related protein (FHR), extracellular matrix (ECM), complement regulation, factor H (FH), laminin, glomerular basement membrane (GBM), Bruch's membrane (BM), kidney disease

INTRODUCTION

The complement system, being a powerful effector arm of innate immunity, requires proper regulation to focus its activation on target cells, such as invading microbes and dying host cells, yet at the same time avoid unwanted damage to healthy host cells and tissues (1, 2). Dysregulation of the alternative pathway is associated with complement-mediated damage and is implicated in the pathomechanism of several diseases, including age-related macular degeneration (AMD), rheumatoid arthritis (RA) and the kidney diseases atypical hemolytic uremic syndrome (aHUS) and C3 glomerulopathy (C3G) (3, 4). Factor H (FH), a 155-kDa serum glycoprotein, is the major inhibitor of the complement alternative pathway and as such it inhibits complement activation at the level of the central complement component C3. FH binds to the C3b fragment of C3, and acts as a cofactor for factor I in the enzymatic inactivation of C3b; it also prevents assembly of the C3 convertase enzyme (C3bBb) of the alternative pathway and accelerates decay of this convertase once already formed, as well as regulates the C5 convertases (5, 6).

The human factor H protein family also includes the FH splice variant factor H-like protein 1 (FHL1) and five factor H-related (FHR) proteins. All FH family members exclusively consist of complement control protein (CCP) domains (also known as short consensus repeats). The FHRs show high but varying degree of amino acid sequence identity with the corresponding domains of FH, especially in their C-terminal part (3, 7–9). The FHR proteins lack domains related to the N-terminal CCPs 1-4 of FH, which are responsible for the FH complement inhibitory activity (8, 9). Due to the sequence similarity, FHRs share ligand binding properties with FH and they can all bind to C3b, suggesting a role for them in the modulation of complement activation; other ligands shared by some of the FHRs and FH include heparin, DNA and the pentraxins C-reactive protein (its monomeric or pentameric form) and pentraxin 3 (3, 7–11). However, their role in complement regulation has been controversial (8). For FHR5, a weak cofactor activity was reported at relatively high concentration compared to the physiological serum level of FHR5 (12). In surface convertase assays using purified proteins, FHR5 was shown to inhibit C5 conversion (13). FHR1 in turn was reported to inhibit complement at the C5 level and/or the terminal pathway (14), but this report was not confirmed in independent studies (10, 15–17). Recent studies showed that both FHR1 and FHR5 can compete with FH for binding to C3b, and to support assembly of the alternative pathway C3 convertase (C3bBb), thereby enhancing alternative pathway activation (7, 10). FHR5 also inhibits FH binding to DNA, pentraxins, malondialdehyde epitopes and to extracellular matrix (ECM) proteins (7, 11, 18). Thus, current evidence supports a role for FHR1 and FHR5 as competitive inhibitors of FH for binding to different ligands and instead of inhibiting complement as FH, FHR1 and FHR5 rather enhance complement activation (3, 7, 10, 11, 15, 19–21).

According to genetic studies, mutations in the *CFHR1* and *CFHR5* genes are associated with kidney and eye diseases where inappropriate or excessive complement activation is implicated at the glomerular basement membrane (GBM) or at the Bruch's membrane (BM) (3, 8, 20–28). Quantitative and qualitative changes in FHR proteins apparently contribute to the pathological processes in diseases such as AMD, aHUS, C3G and IgA nephropathy (20, 21, 27, 28).

The GBM and BM are considered as specialized ECMs (29, 30). The ECM is mainly composed of collagen and/or elastin fibers, proteoglycans and glycoproteins. The GBM as a part of the glomerular filtration barrier mainly consists of collagen type IV, laminin and heparan sulphate among others (30). The multifunctional BM which is localized between the retinal pigment epithelium (RPE) and choroid, is mostly composed of elastin fibres, collagen fibres (mainly collagen type IV), laminin, fibronectin, heparan sulphate among other molecules (29).

Components of the ECM are not accessible to serum proteins under normal conditions. However, upon inflammation and tissue damage, ECM in the kidney and in the eye become exposed to interaction with complement components (31–34). Moreover, both anatomic sites are characterized by a fenestrated endothelium, and changes in the vasculature such as the loss of choriocapillaris that influences the Bruch's membrane composition likely contribute to the pathogenic process (35). The ECM has no integral/inherent complement regulators such as membrane-bound complement inhibitors (e.g. CD55, CD59), therefore surface-bound FH provides the main protection from complement-mediated attack and damage (36, 37). It was demonstrated that FH binds to fibroblast- and endothelial cell-derived ECM (3, 38). Moreover FH binds to short leucine-rich repeat glycoproteins like fibromodulin, osteoadherin, and proline/arginine-rich end leucine-rich repeat protein (PRELP) (31, 32, 34, 39, 40), which are components of the ECM in the

Abbreviations: aHUS, atypical hemolytic uremic syndrome; AMD, age-related macular degeneration; BM, Bruch's membrane; BSA, bovine serum albumin; C3G, C3 glomerulopathy; CCP, complement control protein domain; DPBS, Dulbecco's phosphate-buffered saline; ECM, extracellular matrix; FB, factor B; FD, factor D; FH, factor H; FHR, factor H-related; FHR1, factor H-related protein 1; FHR4, factor H-related protein 4; FHR5, factor H-related protein 5; FI, factor I; FP, factor P; GBM, glomerular basement membrane; HSA, human serum albumin; NHS, normal human serum; PRELP, proline/arginine-rich end leucine-rich repeat protein.

joints, kidney and eye (32, 33, 40). Next to FH, which keeps its regulatory activity when bound, both FHR1 and FHR5 bind to MaxGel, a fibroblast-derived ECM that is used as an *in vitro* model of ECM, and modulate complement activation (7, 10). Moreover, binding of FHR5 to human laminin has been described (18).

Based on the ligand binding similarities of FH and FHR proteins, we hypothesized that FHR1 and FHR5 can interact with various extracellular matrix components. The aim of the present study was to analyze FHR1 and FHR5 binding to selected extracellular matrix components and to determine how their binding affects the regulatory activity of FH and overall complement activation.

MATERIALS AND METHODS

Proteins, Abs, and Sera

Recombinant human FHR1, FHR2, FHR3, FHR4 and FHR5 produced by Novoprotein (Shanghai, China) were purchased from Gentaur (Kampenhout, Belgium). Polyclonal goat anti-human FHR5 was purchased from R&D Systems (Wiesbaden, Germany). Purified human factor H (FH), C3, C3b, iC3b, C3c, C3d, factor I (FI), properdin (FP), goat anti-human FH and goat anti-human FB Ab were obtained from Merck (Budapest, Hungary). The anti-human FH mAb A254 and the anti-properdin mAb A235, and normal human serum (NHS) were from Quidel (obtained *via* Biomedica, Budapest, Hungary). Rabbit anti-human C3d, and HRP-conjugated goat anti-mouse Ig, rabbit anti-goat Ig and swine anti-rabbit Ig were obtained from Dako (Hamburg, Germany) and the HRP-labeled goat anti-human C3 Ab was from MP Biomedicals (Solon, OH). Human laminin, aggrecan, biglycan, decorin, collagen IV, fibronectin and vitronectin were purchased from Sigma-Aldrich (Budapest, Hungary).

The ECM proteins fibromodulin, osteoadherin, and PRELP were expressed recombinantly in HEK293 cells and purified using affinity chromatography due to the presence of His-tag (41).

Human properdin was purified as described in (42). Properdin oligomeric forms (dimers, P2; trimers, P3; and tetramers, P4) were isolated from pure properdin by size exclusion chromatography, as previously described (42). Briefly, pure properdin (5 mg) was loaded onto a Phenomenex BioSep-Sec-S4000 column (600 x 7.8 mm) with a guard column (75 x 7.8 mm) and eluted at a 0.5 ml/min flow rate in PBS. Purified, physiological forms of properdin were stored at 4°C and used within 2 week of separation (42, 43).

Protein Expression and Purification

Recombinant human FHR5 fragments comprising CCPs 1-4, CCPs 3-7, and CCPs 8-9 were amplified by polymerase chain reaction using codon-optimized human FHR5 DNA template and specific primers (**Table 1**), and cloned into the pBSV-8His Baculo-virus expression vector (44). The proteins were expressed in *Spodoptera frugiperda* (Sf9) cells and purified by nickel-affinity chromatography. Purified proteins were analyzed by Western blot using 10% SDS-PAGE under non-reducing conditions and by silver staining.

Protein Microarray

ECM proteins (0.5 mg/ml), gelatin (0.5 mg/ml) and MaxGel (0.8 mg/ml) were printed onto nitrocellulose-covered slides in triplicates. Air-dried slides were washed three times with PBS containing 0.05% Tween 20 and blocked with 4% BSA. In binding assays, the immobilized ECM proteins were incubated with FHR1 (5 μg/ml; 25 μg/ml; 50 μg/ml) or FHR5 (0.5 μg/ml; 5 μg/ml; 20 μg/ml), then detected with goat anti-human FH or goat anti-human FHR5 followed by Alexa-647 labeled anti-goat IgG.

To measure competition, printed proteins were incubated with 25 μg/ml FH with or without FHR1 (5 μg/ml; 25 μg/ml; 50 μg/ml) or FHR5 (0.5 μg/ml; 5 μg/ml; 20 μg/ml). Bound FH was detected using monoclonal mouse anti-FH Ab (A254) that does not cross-react with FHR1 and FHR5, and Alexa-546-conjugated goat anti-mouse IgG. After scanning, fluorescence intensities were calculated as median of the triplicates and background was subtracted.

Complement activation on protein microarray was analyzed by incubating immobilized ECM components with 20% NHS in the presence or absence of recombinant FHR1 (50 μg/ml) or FHR5 (20 μg/ml) diluted in DPBS containing Mg^{2+} and Ca^{2+} (Lonza). C3 deposition was detected with Alexa-555 labelled anti-C3 $F(ab')_2$, and the sC5b-9 was detected with biotinylated monoclonal anti-sC5b-9 Ab and streptavidin-Alexa-488.

Microtiter Plate Binding Assays

To analyze the binding of C3b, iC3b, C3c and C3d to FHR5 fragments, 5 μg/ml FHR5, FHR5 CCPs 1-4, CCPs 3-7, CCPs 8-9, and human serum albumin (HSA) as a negative control were immobilized on microtiter plate. After blocking with 4% BSA, 20 μg/ml C3b, iC3b, C3c and 10 μg/ml C3d were added to the corresponding wells. Bound proteins were detected with HRP-conjugated anti-human C3 or polyclonal rabbit anti-human C3d followed by HRP-conjugated swine anti-rabbit Ig. TMB High Sensitivity substrate solution (BioLegend) was used to visualize binding, and the absorbance was measured at 450 nm.

TABLE 1 | The primers used to generate the FHR5 fragments used in this study.

Primer name	Length (nt)	Optimal temperature (°C)	Sequence (5'- 3')
optFHR-5 CCP1-4 fw	32	76.6	ATGTAACTGCAGGGCACTCTCTGTGATTTCCC
optFHR-5 CCP1-4 rev	25	77.2	ATATAACCCGGGGACGCATGTGGGC
optFHR-5 CCP3-7 fw	35	85.3	ATAATAGCGGCCGCAAAGGGCGAGTGTCACGTCCC
optFHR-5 CCP3-7 rev	37	86.5	ATAATACCCGGGTGCCACGCAACGTGGCAATGACTGC
optFHR-5 CCP8-9 fw	32	76.6	AGATATCTGCAGGAGTCGACCGCTTACTGTGG
optFHR-5 CCP8-9 rev	31	77.5	AGTAATCCCGGGCTCACAGATTGGGTACTCG

To measure binding in a reverse setting, 20 μg/ml C3b was immobilized and incubated with 20 μg/ml FHR5, the FHR5 fragments CCPs 1-4, CCPs 3-7 and CCPs 8-9 diluted in DPBS containing Mg^{2+} and Ca^{2+} (Lonza). HSA was used as a negative control protein. Bound proteins were detected with polyclonal goat anti-FHR5 Ab and HRP-conjugated rabbit anti-goat Ig antibody.

To further analyze the binding of C3 and C3(H_2O) to FHR5, 10 μg/ml FHR5, CCPs 1-4, CCPs 3-7, CCPs 8-9 and as a negative control alpha-1-antitrypsin were immobilized in microplate wells, and incubated with 5 μg/ml C3, C3(H_2O), and C3b, which was used as a positive control. C3(H_2O) form was generated from C3 with ten freeze/thaw cycles. After washing steps, bound proteins were detected with HRP-conjugated anti-human C3 antibody.

To measure properdin binding, FHR proteins and C3b were immobilized at 5 μg/ml in DPBS containing Mg^{2+} and Ca^{2+} at 4°C overnight. After washing with DPBS containing 0.05% Tween-20, free binding sites were blocked by incubation with 4% BSA dissolved in DPBS containing 0.05% Tween-20 at 20°C for 1 hr, then 20 μg/ml of the various properdin forms diluted in DPBS containing Mg^{2+} and Ca^{2+} was added at 20°C for 1 hr. After washing, properdin binding was detected using the anti-properdin mAb A235 (1:1000) and the corresponding secondary Ab (1:1000).

To analyze FHR1 binding to ECM proteins, 5 μg/ml laminin, fibromodulin, osteoadherin, PRELP and HSA were coated and incubated with FHR1 (5 μg/ml or 10 μg/ml). Bound FHR1 was detected with goat anti-human FH and the corresponding secondary Ab. Inhibition of FHR1 binding to ECM proteins was measured by incubating the immobilized ECM proteins with 5 μg/ml FHR1 and simultaneously added mAb C18 (10 μg/ml), which recognizes CCP5 of FHR1, or mAb A255 (10 μg/ml), which does not recognize FHR1 and was used as a control. Binding of FHR1 was detected as described above.

For FHR5, ECM proteins were immobilized (10 μg/ml) and incubated with FHR5 and its fragments (CCPs 1-4, CCPs 3-7, CCPs 8-9) in equimolar concentrations (100 nM or 200 nM). After washing, bound proteins were detected as described above.

To measure the competition between FHR5 and FH for the binding to ECM proteins in microplate format, immobilized ECM proteins (10 μg/ml) were incubated with 50 μg/ml FH in the presence or absence of 20 μg/ml FHR5. HSA was used as a negative control. Bound FH was detected with monoclonal anti-human FH (A254) and HRP-conjugated goat anti-mouse Ig antibody.

Complement Activation Assays

To measure complement activation and C3 convertase formation on ECM-bound FHR1/FHR5, microplate wells were coated with the ECM proteins (5 μg/ml or 10 μg/ml) and, after blocking with 4% BSA, incubated with 10% NHS diluted in 5 mM Mg^{2+}-EGTA in the absence or presence of FHR5 (10 μg/ml) or FHR1(10 μg/ml; 20 μg/ml) for 30 min at 37°C. Deposition of C3 fragments and factor B (FB) was detected using HRP-conjugated anti-human C3, and goat anti-human FB followed by HRP-conjugated rabbit anti-goat Ig, respectively.

Cofactor Assays

To assess the functional consequence of competition between FHR5 and FH, laminin was immobilized at 10 μg/ml and, after blocking with 4% BSA, 100 μg/ml FH was added in the absence or presence of 20 μg/ml FHR5. After washing, the wells were incubated with 140 nM C3b and 300 nM FI diluted in DPBS containing Mg^{2+} and Ca^{2+} for 1 hour at 37°C. Supernatants were collected and subjected to 7.5% SDS-PAGE and Western blotting under reducing conditions. C3 fragments were detected with a HRP-conjugated anti-human C3 Ab and an ECL detection kit (Merck).

Statistical Analysis

Statistical analysis was performed using GraphPad Prism version 5.00 for Windows (GraphPad Software, San Diego, California). A p value <0.05 was considered statistically significant.

RESULTS

FHR1 and FHR5 Bind to Several ECM Proteins

FH was previously shown to bind to several components of the extracellular matrix (ECM); moreover, FH represents the main alternative complement pathway inhibitor on ECM (31, 32), although its splice variant, factor H-like protein 1 (FHL-1) was reported as the major regulator in Bruch's membrane (45). We hypothesized that, due to their sequence similarities with FH (**Figure 1**), FHR1 and FHR5 could interact with certain ECM components, which is also supported by recent data (7, 10, 18).

To test this hypothesis, first we used protein microarray technique. Various ECM proteins were printed onto nitrocellulose-covered slides in triplicates. The slides were incubated with increasing concentrations of FHR1 (**Figure 2A**) and FHR5 (**Figure 2B**), and their binding was detected using polyclonal antibodies to FH and FHR5, respectively. Both FHRs bound to several ECM proteins, including laminin, osteoadherin, PRELP and vitronectin, in a dose-dependent manner. Binding of FHR1 and FHR5 to laminin, osteoadherin and PRELP was confirmed by ELISA; in addition, prominent binding to fibromodulin was also detected in ELISA (**Figure 3**). This difference between the two types of assays might be due to the different surfaces and measurement methods.

To determine the binding sites for the analyzed ECM proteins within FHR5, recombinant FHR5 fragments comprising CCPs 1-4, CCPs 3-7, and CCPs 8-9 were generated, expressed in insect cells and purified (**Figure 1**, **Table 1** and **Supplementary Figure 1**). Binding of these FHR5 fragments to the immobilized ECM proteins was determined by ELISA using polyclonal anti-FHR5. We found that CCPs 3-7 of FHR5 bound to laminin, fibromodulin, osteoadherin and PRELP, indicating that FHR5 binds to these ECM proteins through its middle part, whereas the other tested FHR5 fragments did not bind (**Figures 3A, B**). FHR1 also bound to immobilized laminin, fibromodulin, osteoadherin and PRELP in ELISA (**Figure 3C**). Presumably, FHR1 binds through its most C-terminal domain to

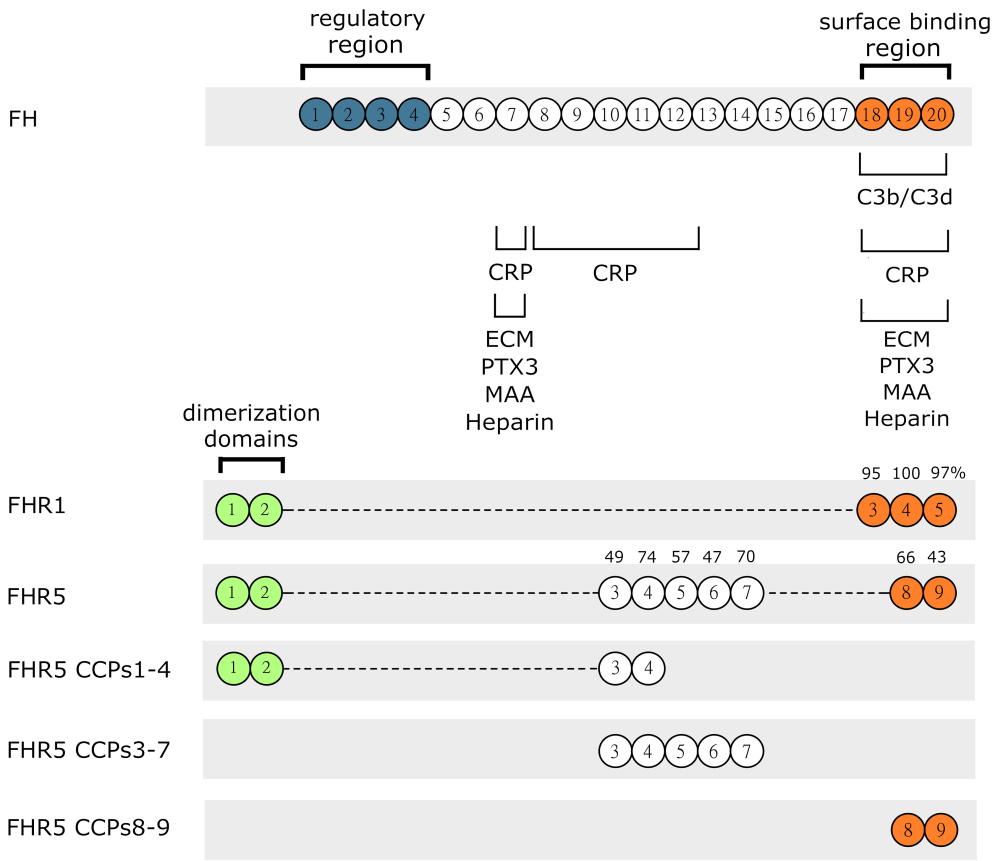

FIGURE 1 | Schematic drawing of FH, FHR1, FHR5 and the recombinant FHR5 fragments used in this study. FH, FHR1 and FHR5 are composed of individually folding globular domains called complement control protein domains (CCPs) or also known as short consensus repeats (SCRs). CCPs 1-4 of FH mediate complement regulatory activity while the CCPs 7 and 18-20 are responsible for binding different ligands and surface recognition. The CCPs of FHR1 and FHR5 share high amino acid sequence identity with the corresponding domains of FH, indicated by numbers above. The C-terminal part is well conserved indicating similar or identical ligand and surface binding between FHR1, FHR5 and FH. FHR proteins lack the N-terminal regulatory domains CCPs 1-4 of FH. CCPs 1-2 of FHR1 and FHR5 are very similar to each other and responsible for formation of homo and heterodimers.

these ECM proteins, in contrast to FHR5, since when FHR1 was preincubated with the monoclonal antibody C18, which recognizes the CCP5 domain of FHR1, FHR1 binding to laminin, fibromodulin, osteoadherin and PRELP was inhibited. In contrast, the mAb A255, which binds to FH but not to FHR1, did not affect FHR1 binding in this assay (**Figure 3D**). Since laminin binding has not been described for FH before, we tested laminin binding to the FH fragments comprising the N-terminal regulatory domains CCPs 1-4, the middle part CCPs 8-14 (which contains domains related to FHR5) and the C-terminal CCPs 15-20 that contains domains homologous to the FHR1 C-terminus. Laminin bound only to CCPs 15-20, supporting a C-terminal binding site in both FH and FHR1 (**Supplementary Figure 2**).

FHR1 and FHR5 Compete With FH for Binding to ECM Proteins

To further analyze the interaction of FHR1 and FHR5 with ECM proteins and their effect on the functional activity of FH, we tested whether FHR1 and FHR5 compete with FH for binding to ECM proteins. In the protein microarray setup, the immobilized ECM proteins were incubated with FH together with increasing amounts of FHR1 and FHR5. Binding of FH was detected with an anti-FH mAb that does not recognize FHR1 and FHR5. Both FHR1 and FHR5 inhibited the binding of FH to osteoadherin, PRELP, fibromodulin, laminin, vitronectin and collagen IV in a dose-dependent manner, as well as to MaxGel that was used as a control (**Figures 4A, B**). Competition between FHR5 and FH was confirmed by ELISA where laminin, osteoadherin, fibromodulin and PRELP were immobilized in microplate wells and incubated with 50 μg/ml FH in the absence or presence of 20 μg/ml FHR5. FHR5 strongly inhibited FH binding to these ECM proteins (**Figure 4C**).

To study whether the competitive inhibition of FH binding by FHR5 impairs the complement regulatory activity by removing FH, a surface cofactor assay was performed. Laminin was immobilized in microplate wells and incubated with FH together with or without FHR5. After removing the unbound proteins by extensive washing, FI and C3b were added to the wells to allow for cleavage of C3b. After incubation, the supernatants were collected, the proteins were separated by SDS-PAGE and the C3b cleavage products were visualized by

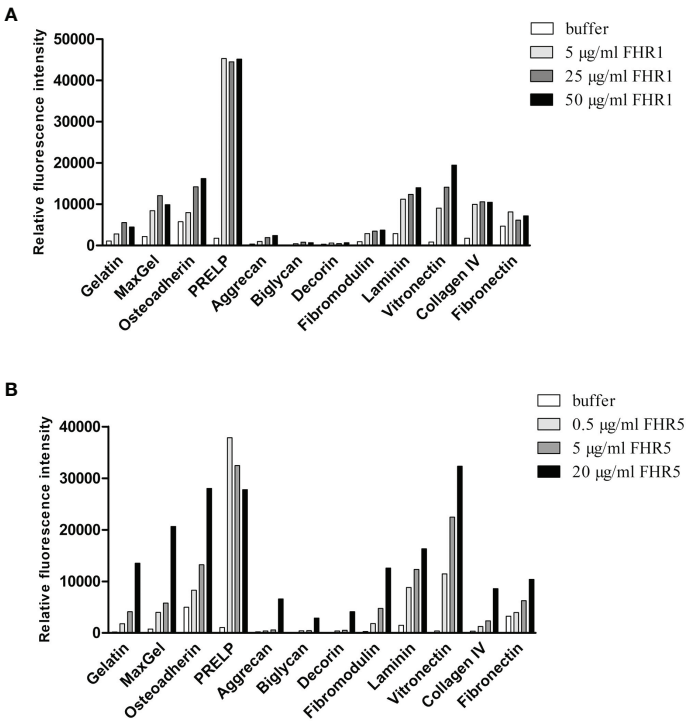

FIGURE 2 | Binding of FHR1 and FHR5 to ECM components. FHR1 **(A)** and FHR5 **(B)** binding to ECM ligands was analyzed by protein microarray. ECM proteins, gelatin and MaxGel were printed onto nitrocellulose-covered slides in triplicates. Air-dried slides were washed and blocked with 4% BSA, then incubated with FHR1 or FHR5 in increasing concentrations. Bound proteins were detected with polyclonal goat anti-human FH or polyclonal goat anti-human FHR5 Ab and Alexa-647 labeled goat-IgG. A signal higher than the one obtained for the negative control protein gelatin was defined as the threshold for binding. Data are representative of two experiments.

Western blot. FHR5 competitively inhibited the cofactor activity of FH on laminin coated surfaces as less C3b α'-chain was cleaved in the presence of FHR5 (**Figure 4D**).

FHR5 Binds iC3b and C3d *via* Its C-Terminal Domains but It Does Not Bind C3c, and Also Interacts With C3 and C3(H_2O)

All FHR proteins bind C3b, the main ligand of FH (3). FH has multiple recognition sites for C3b and other C3 fragments, but the C-terminal domains harbor the major binding site for surface-bound C3b. Because of the conserved FH C-terminal domains, FHRs are supposed to share this C-terminal C3b recognition site. We set out to determine the binding sites of various C3 fragments in the FHR5 protein, using recombinant FHR5 fragments comprising CCPs 1-4, CCPs 3-7 and CCPs 8-9 that cover the whole protein. FHR5 and its fragments were immobilized in microtiter plate wells and incubated with C3b, iC3b, C3c and C3d. FHR5 bound soluble C3b mainly *via* the C-terminal CCPs 8-9 (**Figures 5A, D**), in agreement with recent data (18). Similarly, both iC3b and C3d bound to the CCPs 8-9 fragment of FHR5, whereas C3c did not bind to any of the FHR5 fragments nor to the whole protein (**Figure 5A, B**). In reverse setting, where C3b was immobilized in microtiter plate wells and incubated with FHR5 fragments, CCPs 3-7 showed significant binding to surface-bound C3b (**Figure 5C**). Thus, FHR5 appears to have two C3b binding sites, one for surface-bound C3b and another for fluid-phase C3b, suggesting that FHR5 when bound to a surface either *via* deposited C3b or to other ligands exposed on the surface, such as bound pentraxins (11) or ECM proteins, it can potentially recruit C3b from fluid-phase and allow for alternative pathway activation by recruiting an active C3bBb convertase (7).

Since C3 fragments are generated upon complement activation, we also tested whether intact C3 and C3(H_2O), which is physiologically constantly generated in serum at a low rate, can bind to FHR5. Purified C3 was subjected to freeze-thaw cycles to generate C3(H_2O) (**Supplementary Figure 3**). Both C3 and C3(H_2O) bound to the C-terminal fragment CCPs 8-9 of FHR5 (**Figure 5E**); however, it cannot be excluded that during the experiment C3 was ticking over and actually C3(H_2O) what was bound.

FHR1 and FHR5 Do Not Bind Properdin Directly

Previously, we showed that FHR5 can activate the alternative pathway by binding C3b and recruiting an active C3 convertase enzyme, as showed by the deposition of C3b, Bb and properdin on immobilized FHR5. However, FHR5 did not bind FB or properdin directly (7). Rudnick et al. on the other hand described direct binding of properdin to FHR5 and suggested that properdin when bound to FHR5 recruits C3b and thus initiates complement activation (18). To resolve this

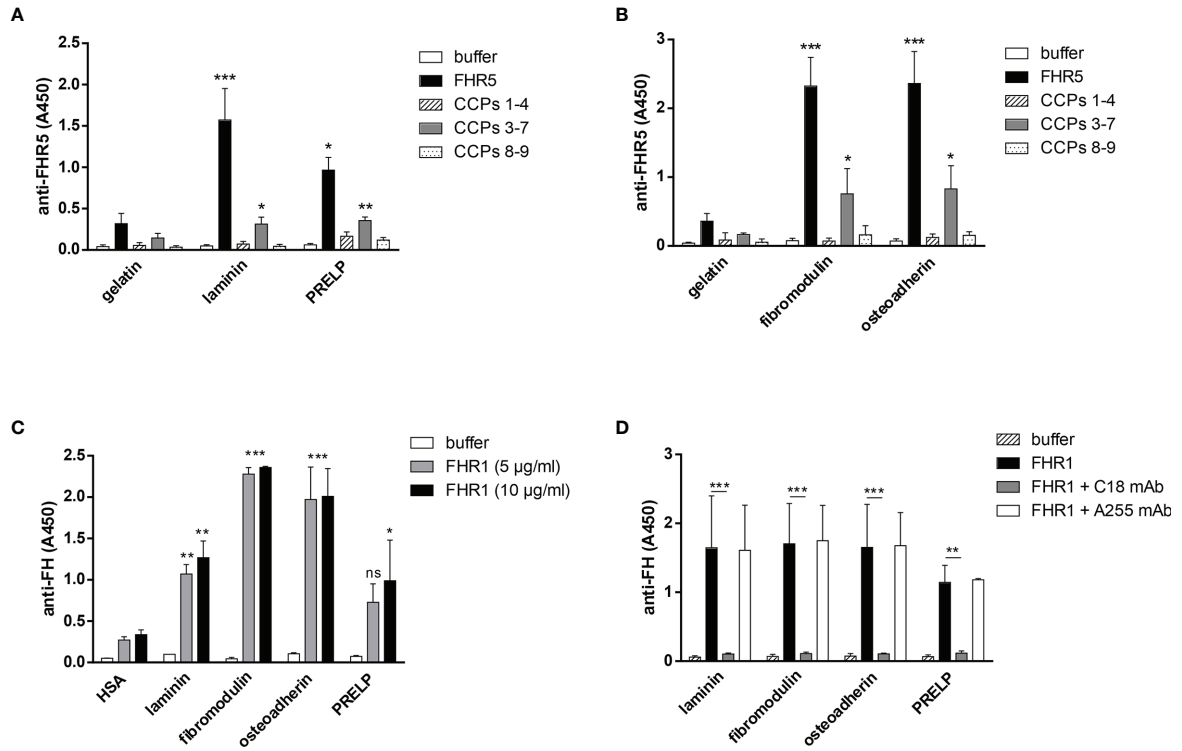

FIGURE 3 | FHR5 binds through its middle part, CCPs 3-7, and FHR1 binds *via* its C-terminal domain to ECM proteins. In ELISA 10 µg/ml of gelatin, laminin, PRELP **(A)**, osteoadherin and fibromodulin **(B)** were immobilized in microplate wells and after blocking, incubated with 200 nM **(A)** or 100 nM **(B)** FHR5, CCPs 1-4, CCPs 3-7 and CCPs 8-9. Binding of FHR5 and its fragments was measured with goat anti-human FHR5 Ab. Data are means ± SD derived from three experiments. *p < 0.05, **p < 0.01, ***p < 0.001 one-way ANOVA, compared to the negative control, gelatin. **(C)** Laminin, fibromodulin, osteoadherin and PRELP were immobilized (10 µg/ml) in microplate wells. After blocking, FHR1 was added in increasing concentrations. Binding of FHR1 was detected with polyclonal goat anti-human FH and the corresponding secondary antibody. Data are means ± SD derived from three independent experiments. *p <0.05, **p <0.01, ***p <0.001 two-way ANOVA, compared to the negative control, HSA; ns, not significant. **(D)** Immobilized ECM proteins were incubated with FHR1 (5 µg/ml) in the presence or absence of the monoclonal Ab C18, which recognizes the CCP 5 domain of FHR1. We used monoclonal Ab A255 as a negative control. Bound FHR1 was detected as described earlier. Data are means ± SD derived from three independent experiments. *p < 0.05, **p < 0.01, ***p < 0.001 two-way ANOVA.

contradiction, and since properdin notoriously tends to aggregate and generate higher order oligomers when stored for longer time or freeze-thawed (43), we analyzed the binding of purified commercial properdin (P), as well as purified properdin dimers, trimers, and tetramers (P2, P3, and P4, respectively). There was no significant binding of the physiologically occurring properdin forms to FHR5, nor to the other FHRs tested in parallel; however, there was prominent binding to C3b, used as a positive control (**Figure 6A**). In addition, since FHR5 CCPs 1-2 were proposed to harbor a properdin binding site (19), we analyzed our recombinant FHR5 fragments and no properdin binding to any of these was found in ELISA (**Figure 6B**). Altogether, these results suggest that physiological serum properdin forms are unlikely to bind directly to FHR5 and other FHRs.

FHR1 and FHR5 Enhance Complement Activation on ECM Proteins Through the Alternative Pathway

Competition between FH and FHR1 or FHR5 for binding to ECM is only one way how the regulation of complement activation can be compromised at such a surface. Previously, we demonstrated that both FHR1 and FHR5 allow formation of the alternative pathway C3 convertase when immobilized on microplate wells and rather support than inhibit complement activation. We tested whether FHR1 and FHR5 show this activity when bound to ECM proteins. To this end, ECM proteins were immobilized and incubated with NHS in the presence or absence of recombinant FHR1 or FHR5 in a buffer supplemented with 5 mM Mg^{2+}-EGTA to allow only the activation of alternative pathway. Generation of the alternative pathway C3 convertase on the surface bound FHR proteins was confirmed by measuring deposition of C3b and factor B (FB). Both FHR1 and FHR5 significantly enhanced the amount of bound C3-fragments on the ECM proteins (**Figures 7A**, **8A**). FHR5 also induced significant FB deposition, whereas FHR1 increased the amount of ECM-bound FB to a lesser extent and at higher serum concentration (**Figures 7B**, **8B**, and data not shown). These results indicate that both FHR1 and FHR5 support alternative pathway activation on ECM proteins.

In the case of FHR5, we further studied this using MaxGel and ECM produced *in vitro* by ARPE-19 cells. These two ECMs of different origin have different composition, laminin dominating in MaxGel and collagen IV in ARPE-derived ECM (**Supplementary Figure 4C**). When these ECMs were exposed to serum in the presence of FHR5, strongly increased deposition of all components

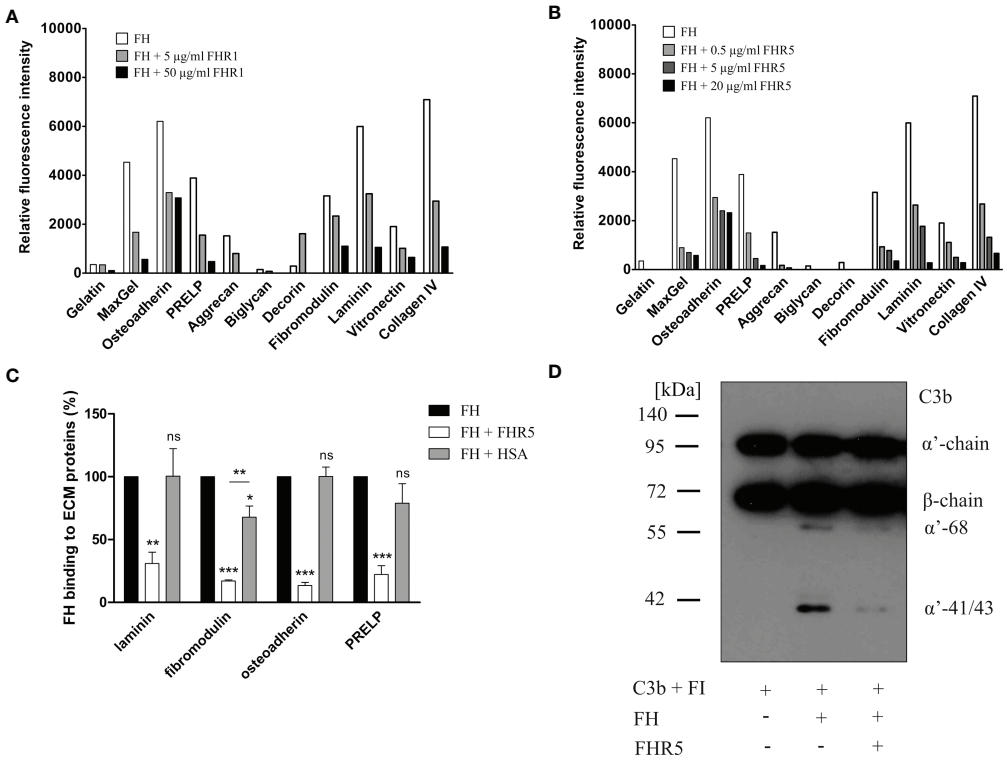

FIGURE 4 | FHR1 and FHR5 compete with FH for binding to several ECM components, and FHR5 competitively inhibits the cofactor activity of FH. ECM proteins were printed on slides and incubated with 25 µg/ml FH together with increasing concentrations of FHR1 **(A)** or FHR5 **(B)**. Binding of FH was measured by monoclonal mouse anti-FH (A254) that does not recognize FHR1 or FHR5 and Alexa546-conjugated goat anti-mouse IgG. Data are representative of two experiments. **(C)** Competition between FHR5 and FH was also measured in ELISA. Laminin, fibromodulin, osteoadherin and PRELP (10 µg/ml of each) were immobilized and incubated with 50 µg/ml FH with or without 20 µg/ml FHR5. FH binding to ECM proteins was detected as described earlier. The values were normalized for FH binding (100%) and show means ± SD derived from three independent experiments. *p <0.05, **p <0.01, ***p <0.001, one-way ANOVA; ns, not significant. **(D)** Laminin (10 µg/ml) was immobilized and after blocking, the wells were incubated with 100 µg/ml FH with or without 20 µg/ml FHR5. Then, 140 nM C3b and 220 nM FI were added to the wells for one hour at 37°C. After incubation, supernatants were analyzed on 7.5% SDS-PAGE and Western blot. The blot was developed by using HRP-conjugated anti-human C3 Ab that recognizes C3b and its fragments except for C3d. The molecular mass marker is indicated on the left, and the C3b chains and the C3b α'-chain cleavage fragments are indicated on the right. Results are representative of three experiments.

of a C3bBbP properdin-stabilized alternative pathway C3 convertase was detected (**Supplementary Figures 4A, B**).

FHR5 Increases the Deposition of C5b-9 on ECM Proteins

We used the ECM protein microarray to analyze the effect of FHR1 and FHR5 on terminal complement pathway activation by measuring the deposition of the C5b-9 complex. Immobilized ECM proteins were incubated with NHS with or without the addition of recombinant FHR1 or FHR5. In this assay, FHR5 increased the deposition of C5b-9, along with the deposition of C3 fragments, on osteoadherin, PRELP, fibromodulin and vitronectin (**Figure 9**), while FHR1 had no such effect.

DISCUSSION

The FH protein family is implicated in the regulation and modulation of complement activation, and members of this protein family were linked to various inflammatory and infectious diseases (46). Whereas the exact functions of the FHR proteins are still to be determined and currently in part controversial, a number of FHR ligands have already been identified. Recent studies show that both FHR1 and FHR5 rather support complement activation in contrast to FH (7, 10). Furthermore, FHR1 and FHR5 were shown to compete with FH for binding to different ligands such as C3b, monomeric/modified C-reactive protein, pentraxin 3, MaxGel (7, 10), and DNA (11), thereby FHRs indirectly enhance complement activation as well.

FHR1 and FHR5 were found in immune deposits in several kidney and eye diseases where excessive complement activation is implicated, indicating that FHRs play an important role in these pathological processes (3, 25, 26, 28, 47). Under these conditions, components of the ECM are exposed and available to interact with complement proteins (31–34). Previously, it was reported that FHR5 binds to MaxGel, an ECM extract (7) and to human laminin (18), an important component of the GBM, and

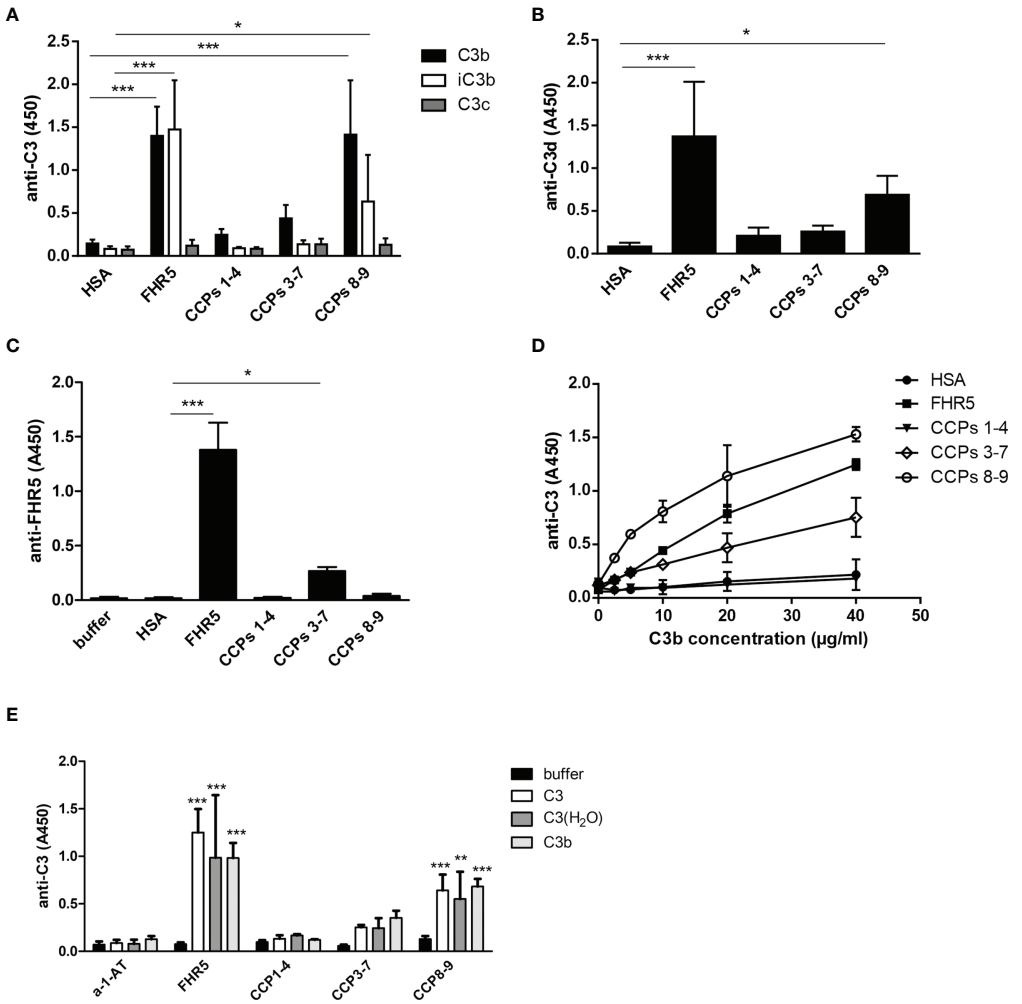

FIGURE 5 | Binding of FHR5 and its fragments to C3b, iC3b, C3c and C3d. **(A)** FHR5, CCPs 1-4, CCPs 3-7, CCPs 8-9 and HSA were immobilized at 5 µg/ml in microplate wells. After blocking, 20 µg/ml C3b, iC3b and C3c were added. Bound proteins were detected using HRP-conjugated anti-human C3 Ab. **(B)** C3d binding to FHR5 also was measured by ELISA. FHR5 and its fragments were coated and incubated with 10 µg/ml C3d. Binding of C3d was measured with an anti-human C3d Ab and the corresponding secondary Ab. **(C)** In reverse setting, C3b was coated (20 µg/ml) and, after blocking, microplate wells were incubated with 20 µg/ml FHR5, CCPs 1-4, CCPs 3-7 and CCPs 8-9. HSA was used as a control protein. Binding of FHR5 and its fragments was detected by a polyclonal goat anti-FHR5 and HRP-conjugated secondary Ab. **(D)** Dose-dependent binding of C3b to FHR5 and its fragments was measured as shown in **(A)**; C3b was added in increasing concentrations. Data are means ± SD derived from five **(A–C)** or two **(D)** independent experiments. *$p < 0.05$, ***$p < 0.001$, one-way ANOVA. **(E)** Binding of C3, C3(H_2O) and C3b to immobilized FHR5 and its fragments was measured by ELISA using HRP-conjugated polyclonal anti-C3 antibody. Data are means + SD derived from four experiments. **$p < 0.01$, ***$p < 0.001$, one-way ANOVA, compared to the negative control protein alpha-1-antitrypsin (a-1-AT).

FHR5 was also detected in the ECM of the eye (47); moreover, FHR5 promoted complement activation when bound to MaxGel (7).

In the present study, we show that next to FH, both FHR1 and FHR5 bind to different ECM components relevant in the kidney, eye and joints. Moreover, we show that FHR1 binds to these proteins through its C-terminal domains, while FHR5 binds *via* its middle domains (CCPs 3-7) (**Figures 2**, **3**). The higher signal detected in ELISA for the full-length FHR5 compared with CCPs 3-7 (**Figures 3A, B**) may be due to conformational differences and/or the higher avidity of the dimerized full-length protein and more available epitopes for the detection antibody. These results confirm previous data that FHR5 binds to human laminin by CCPs 5-7 (18). We demonstrate that the middle domains of FHR5 (CCPs 3-7) represent the binding site for immobilized C3b fragment as well, whereas the fluid phase C3b [as it was shown (18)], C3(H_2O), iC3b and the C3d fragment bind to CCPs 8-9 of FHR5 (**Figure 5**); however, conformational effects and steric hindrances may also influence the observed interactions. FHR1 and FHR5 inhibit the binding of FH to the same ECM components causing reduced cofactor activity of FH (**Figure 4**). These data are in accordance with other studies showing that FHRs compete with FH for different ligands and thereby reduce FH binding and, consequently, its complement activation inhibiting function locally (7, 15). Since

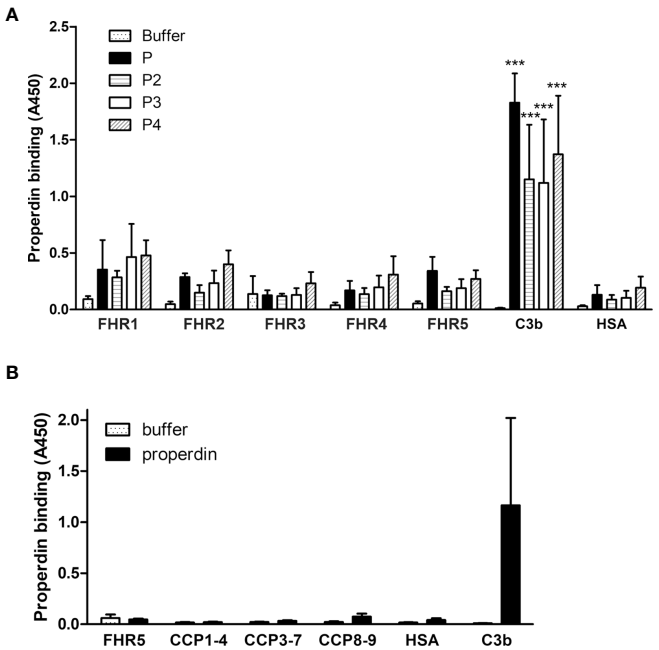

FIGURE 6 | Analysis of properdin binding to FHRs. **(A)** The five FHR proteins, C3b as positive control protein and HSA as negative control protein were immobilized and binding of purified properdin (P) and the isolated properdin dimers, trimers and tetramers (P2, P3 and P4, respectively) was measured by ELISA using anti-properdin antibody. **(B)** Properdin binding to the FHR5 deletion mutants CCPs 1-4, 3-7 and 8-9 was measured as in **(A)**. Data are means + SD from three experiments. ***p <0.001, one-way ANOVA, compared to the negative control protein HSA.

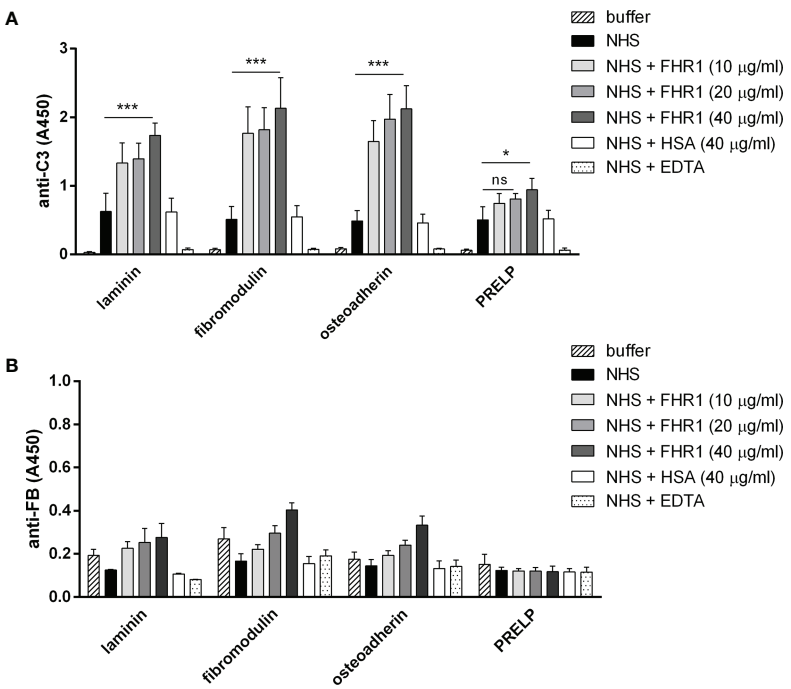

FIGURE 7 | FHR1 increases C3 fragment deposition on ECM proteins. Immobilized ECM proteins were incubated with 10% NHS with or without FHR1 added in increasing concentrations (10 μg/ml, 20 μg/ml, 40 μg/ml) diluted in 5 mM Mg^{2+}-EGTA. C3 fragment deposition **(A)** was measured with HRP-conjugated polyclonal anti-human C3 Ab and FB binding **(B)** was measured by goat anti-human FB and the corresponding secondary Ab. Data are means ± SD derived from four independent experiments. *p <0.05, ***p < 0.001, two-way ANOVA; ns, not significant.

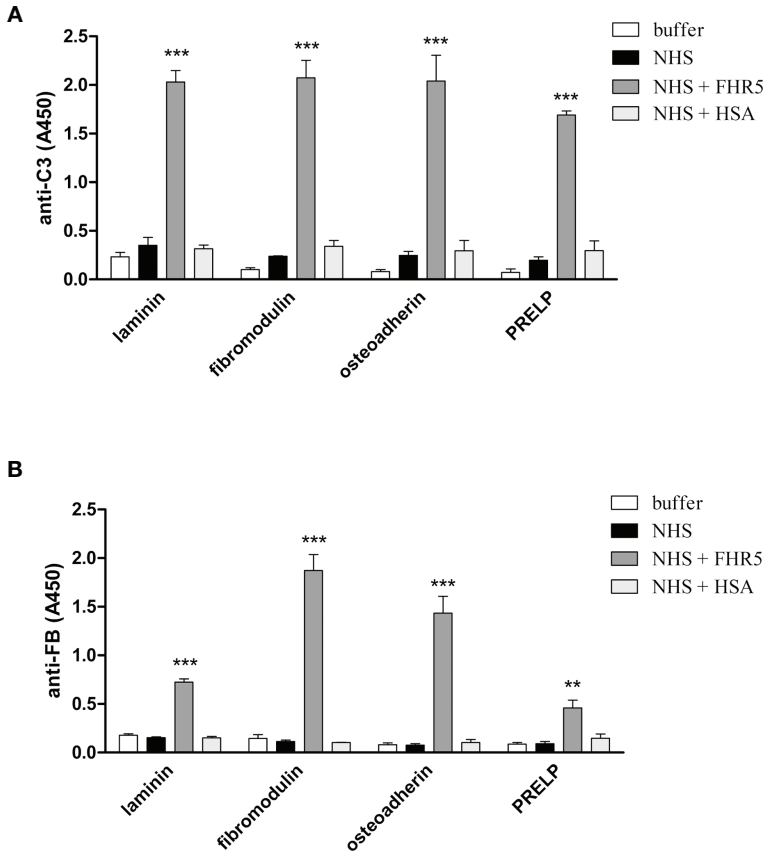

FIGURE 8 | FHR5 causes enhanced C3 fragment deposition and supports alternative pathway activation when bound to ECM proteins. Immobilized ECM proteins were incubated with 10% NHS in the presence or absence of 10 µg/ml FHR5, supplemented with 5 mM Mg^{2+}-EGTA which allows only alternative pathway activation. Binding of C3 fragments and factor B was detected with HRP-conjugated anti-human C3 Ab **(A)** and goat anti-human FB Ab **(B)**. Data are means ± SD derived from three experiments. **p < 0.01, ***p < 0.001, one-way ANOVA.

the FH splice variant FHL-1 was identified as the predominant complement regulator in Bruch's membrane (45), its binding to ECM components and the possible modulation of this interaction by FHR1 and FHR5 would be worth studying in the future.

FHR1, FHR4 and FHR5 were shown to directly promote complement activation by binding C3b and allowing formation of the alternative pathway C3 convertase, when bound on surfaces (7, 10, 11, 48, 49). A recent study found direct binding of C3 to FHR1 and proposed that this interaction would allow FHR1 to support complement activation in its vicinity (50). In light of our results with C3(H_2O) (**Figure 5E**) and the tendency of C3 to tick over at a low rate, we believe it more likely that it is not the abundant C3, but C3(H_2O) generated by tick-over and/or C3b generated nearby that binds to surface-bound FHRs and serves as a focal point to assemble a C3 convertase, further propagating alternative pathway activation. In our study we demonstrate that both FHR1 and FHR5 increase C3 and FB deposition on the surface of ECM components such as laminin, fibromodulin, osteoadherin and PRELP. Similar to previous results, FHR1 was less effective in triggering complement activation compared to FHR5, and in our assays only the latter enhanced also C5b-9 deposition under the same experimental conditions (**Figures 7–9**) (10, 11). To detect FHR1-induced complement activation, higher serum concentrations are required, since the avidity of surface binding depends on initial C3b deposition as well and may also be explained by the bigger dimers of FHR5 compared to the more compact FHR1. In addition, while FHR1 contains only one C3b binding site in its C terminus, in the case of FHR5 surface-bound ligands, including deposited C3b, are recognized by the central domains, while the C terminus remains available for recruiting C3(H_2O) or C3b (**Figures 3**, **5**).

It was also proposed that FHR5 would promote alternative pathway activation by recruiting properdin *via* the CCPs 1-2 (18, 19). We have re-analyzed this issue using separated physiological properdin forms and found that neither properdin dimers, trimers or tetramers showed significant binding to FHR5 and the other FHRs. In addition, unfractionated properdin that typically contains aggregated properdin multimers did not bind to FHR5 and its fragments, including CCPs 1-2 (**Figure 6**). Thus, while it cannot be excluded that cell-derived properdin may bind to FHR5, serum properdin binding could

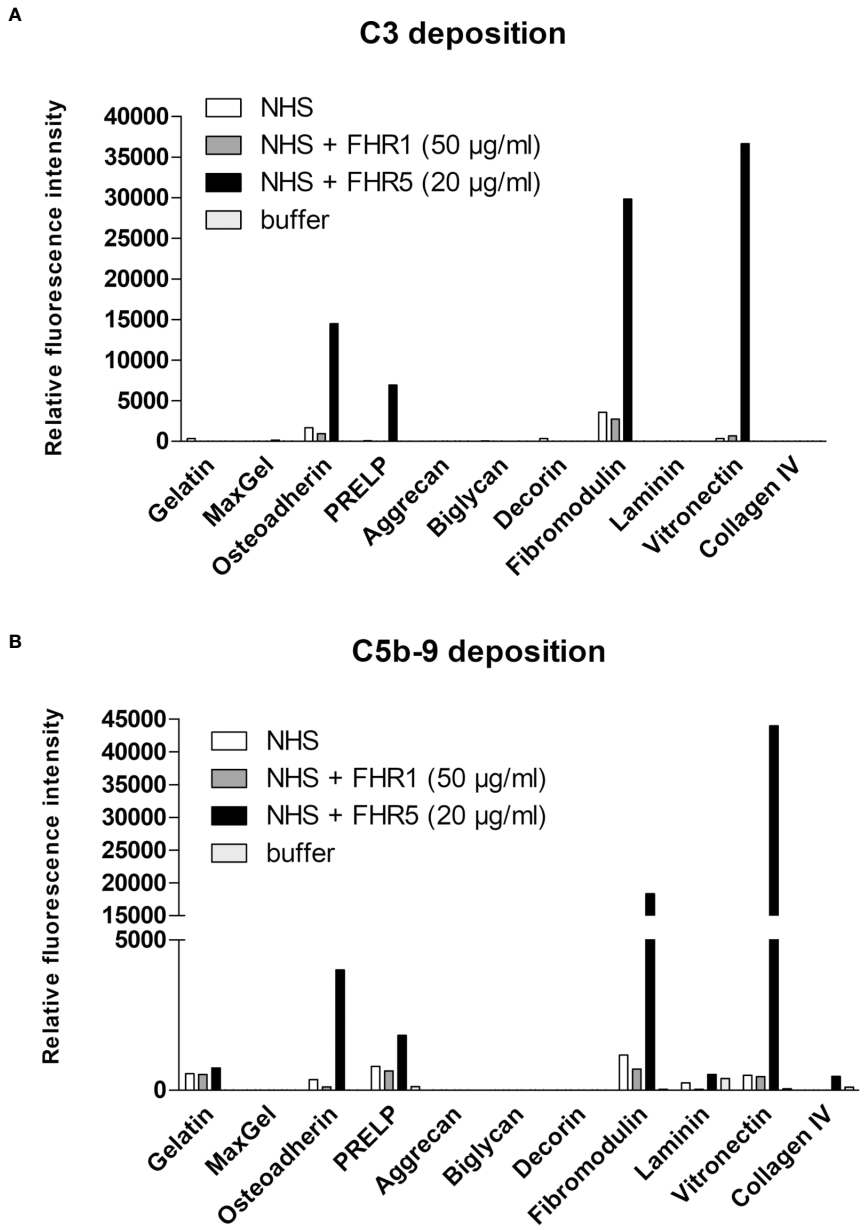

FIGURE 9 | FHR5 increases C5b-9 deposition on ECM ligands. ECM proteins were printed onto nitrocellulose-covered slides and after blocking, proteins were incubated with normal human serum (NHS) in the presence or absence of recombinant FHR1 (50 µg/ml) or FHR5 (20 µg/ml) for 1 hour at 37°C. Bound proteins were detected with polyclonal anti-C3 **(A)** or monoclonal anti-sC5b-9 **(B)** and with the corresponding secondary Ab. Data are representative of two independent experiments.

not be confirmed, in accordance with our previous results (7, 10). However, properdin binding can be detected once a C3 convertase is formed on surface bound FHRs (7, 10, 11).

It is increasingly recognized that the balance between the inhibitor FH and the deregulator FHR proteins determine the extent of complement activation (8, 46), which is influenced by the local and serum levels of FH and the FHRs. Increased FHR to FH ratios were detected in diseases such as IgA nephropathy, AMD, aHUS and rheumatoid arthritis (28, 51–54). Determination of the levels, ligands and functions of the FH family proteins will bring us closer to understand the pathomechanism of these diseases and will likely improve diagnostic, prognostic and therapeutic possibilities.

In summary, we show that FHR1 and FHR5 bind to ECM components as does FH; moreover, both FHRs competitively inhibit the binding of FH resulting in reduced complement regulatory activity (**Figure 10**). Furthermore, FHR1 and FHR5 enhance complement activation on ECM proteins indicating that FHRs may contribute to pathological and inflammatory conditions in kidney, eye and joint diseases by modulating the

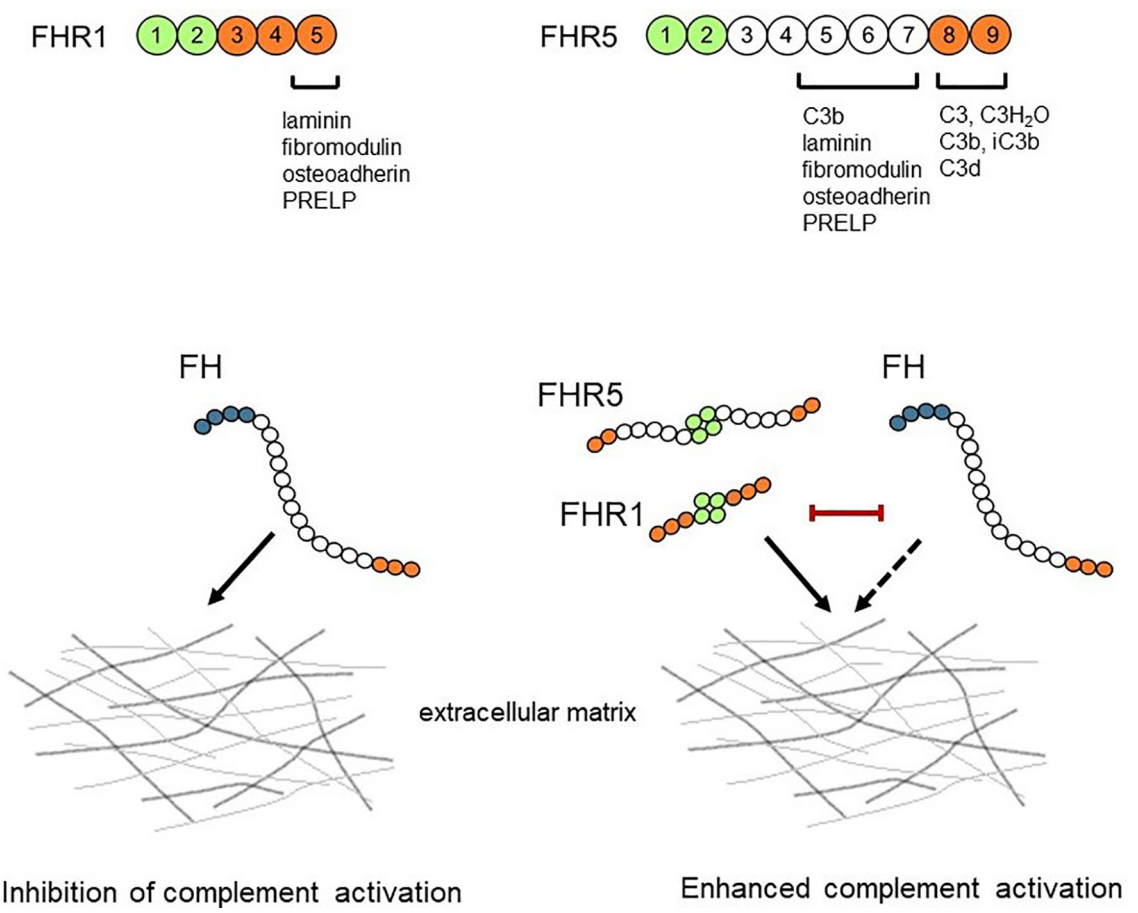

FIGURE 10 | Schematic overview of the interaction between FH/FHRs and the ECM. FHR1 and FHR5 can bind to ECM components and competitively inhibit the binding of FH, thus reducing the complement regulatory activity of FH. The ECM-bound FHR1 and FHR5 may also directly enhance alternative pathway activation by binding C3(H_2O) and C3b and allowing formation of C3 convertase.

regulatory activity of FH and directly complement activation on ECM.

DATA AVAILABILITY STATEMENT

The original contributions presented in the study are included in the article/**Supplementary Material**. Further inquiries can be directed to the corresponding author.

AUTHOR CONTRIBUTIONS

AP, KP, BU, MC, ÁIC, ZS, and ZB performed experiments. DE, ZP, VPF, and AMB contributed materials. All authors discussed the data. MJ supervised the study. AP and MJ wrote the manuscript with the help of the other authors. All authors listed have made a substantial, direct, and intellectual contribution to the work and approved it for publication.

FUNDING

This work was supported in part by the Kidneeds Foundation (Iowa, US), the MedInProt, the National Research, Development and Innovation Fund of Hungary (grants K 109055 and K 125219), the Institutional Excellence Program to ELTE (NKFIH-1157/8/2019, D11206), the Hungarian Academy of Sciences (0106307), the European Union's Horizon 2020 research and innovation programme under grant agreement No. 899163 (SciFiMed), all to MJ; the National Institutes of Health (grant R01HL112937 to VPF), and the Swedish Research Council (2018-02392, to AMB).

SUPPLEMENTARY MATERIAL

The Supplementary Material for this article can be found online at: https://www.frontiersin.org/articles/10.3389/fimmu.2022.845953/full#supplementary-material

REFERENCES

1. Merle NS, Church SE, Fremeaux-Bacchi V, Roumenina LT. Complement System Part I - Molecular Mechanisms of Activation and Regulation. *Front Immunol* (2015) 6:262. doi: 10.3389/fimmu.2015.00262
2. Merle NS, Noe R, Halbwachs-Mecarelli L, Fremeaux-Bacchi V, Roumenina LT. Complement System Part II: Role in Immunity. *Front Immunol* (2015) 6:257. doi: 10.3389/fimmu.2015.00257
3. Sanchez-Corral P, Pouw RB, López-Trascasa M, Józsi M. Self-Damage Caused by Dysregulation of the Complement Alternative Pathway: Relevance of the Factor H Protein Family. *Front Immunol* (2018) 9:1607. doi: 10.3389/fimmu.2018.01607
4. Thurman JM, Holers VM. The Central Role of the Alternative Complement Pathway in Human Disease. *J Immunol* (2006) 176(3):1305–10. doi: 10.4049/jimmunol.176.3.1305
5. Kopp A, Hebecker M, Svobodová E, Józsi M. Factor H: A Complement Regulator in Health and Disease, and a Mediator of Cellular Interactions. *Biomolecules* (2012) 2(1):46–75. doi: 10.3390/biom2010046
6. Rodriguez de Cordoba S, Esparza-Gordillo J, Goicoechea de Jorge E, Lopez-Trascasa M, Sánchez-Corral P. The Human Complement Factor H: Functional Roles, Genetic Variations and Disease Associations. *Mol Immunol* (2004) 41(4):355–67. doi: 10.1016/j.molimm.2004.02.005
7. Csincsi AI, Kopp A, Zöldi M, Bánlaki Z, Uzonyi B, Hebecker M, et al. Factor H-Related Protein 5 Interacts With Pentraxin 3 and the Extracellular Matrix and Modulates Complement Activation. *J Immunol* (2015) 194(10):4963–73. doi: 10.4049/jimmunol.1403121
8. Józsi M, Tortajada A, Uzonyi B, Goicoechea de Jorge E, Rodríguez de Córdoba S. Factor H-Related Proteins Determine Complement-Activating Surfaces. *Trends Immunol* (2015) 36(6):374–84. doi: 10.1016/j.it.2015.04.008
9. Skerka C, Chen Q, Fremeaux-Bacchi V, Roumenina LT. Complement Factor H Related Proteins (CFHRs). *Mol Immunol* (2013) 56(3):170–80. doi: 10.1016/j.molimm.2013.06.001
10. Csincsi AI, Szabó Z, Bánlaki Z, Uzonyi B, Cserhalmi M, Kárpáti É, et al. FHR-1 Binds to C-Reactive Protein and Enhances Rather Than Inhibits Complement Activation. *J Immunol* (2017) 199(1):292–303. doi: 10.4049/jimmunol.1600483
11. Karpati E, Papp A, Schneider AE, Hajnal D, Cserhalmi M, Csincsi ÁI, et al. Interaction of the Factor H Family Proteins FHR-1 and FHR-5 With DNA and Dead Cells: Implications for the Regulation of Complement Activation and Opsonization. *Front Immunol* (2020) 11:1297. doi: 10.3389/fimmu.2020.01297
12. McRae JL, Duthy TG, Griggs KM, Ormsby RJ, Cowan PJ, Cromer BA, et al. Human Factor H-Related Protein 5 has Cofactor Activity, Inhibits C3 Convertase Activity, Binds Heparin and C-Reactive Protein, and Associates With Lipoprotein. *J Immunol* (2005) 174(10):6250–6. doi: 10.4049/jimmunol.174.10.6250
13. Zwarthoff SA, Berends ETM, Mol S, Ruyken M, Aerts PC, Józsi M, et al. Functional Characterization of Alternative and Classical Pathway C3/C5 Convertase Activity and Inhibition Using Purified Models. *Front Immunol* (2018) 9:1691. doi: 10.3389/fimmu.2018.01691
14. Heinen S, Hartmann A, Lauer N, Wiehl U, Dahse HM, Schirmer S, et al. Factor H-Related Protein 1 (CFHR-1) Inhibits Complement C5 Convertase Activity and Terminal Complex Formation. *Blood* (2009) 114(12):2439–47. doi: 10.1182/blood-2009-02-205641
15. Goicoechea de Jorge E, Caesar JJ, Malik TH, Patel M, Colledge M, Johnson S, et al. Dimerization of Complement Factor H-Related Proteins Modulates Complement Activation *In Vivo*. *Proc Natl Acad Sci USA* (2013) 110 (12):4685–90. doi: 10.1073/pnas.1219260110
16. Strobel S, Abarrategui-Garrido C, Fariza-Requejo E, Seeberger H, Sánchez-Corral P, Józsi M. Factor H-Related Protein 1 Neutralizes Anti-Factor H Autoantibodies in Autoimmune Hemolytic Uremic Syndrome. *Kidney Int* (2011) 80(4):397–404. doi: 10.1038/ki.2011.152
17. Meszaros T, Csincsi ÁI, Uzonyi B, Hebecker M, Fülöp TG, Erdei A, et al. Factor H Inhibits Complement Activation Induced by Liposomal and Micellar Drugs and the Therapeutic Antibody Rituximab *In Vitro*. *Nanomedicine* (2016) 12(4):1023–31. doi: 10.1016/j.nano.2015.11.019
18. Rudnick RB, Chen Q, Stea ED, Hartmann A, Papac-Milicevic N, Person F, et al. FHR5 Binds to Laminins, Uses Separate C3b and Surface-Binding Sites, and Activates Complement on Malondialdehyde-Acetaldehyde Surfaces. *J Immunol* (2018) 200(7):2280–90. doi: 10.4049/jimmunol.1701641
19. Chen Q, Manzke M, Hartmann A, Büttner M, Amann K, Pauly D, et al. Complement Factor H-Related 5-Hybrid Proteins Anchor Properdin and Activate Complement at Self-Surfaces. *J Am Soc Nephrol* (2016) 27(5):1413–25. doi: 10.1681/ASN.2015020212
20. Chen Q, Wiesener M, Eberhardt HU, Hartmann A, Uzonyi B, Kirschfink M, et al. Complement Factor H-Related Hybrid Protein Deregulates Complement in Dense Deposit Disease. *J Clin Invest* (2014) 124(1):145–55. doi: 10.1172/JCI71866
21. Goicoechea de Jorge E, Tortajada A, García SP, Gastoldi S, Merinero HM, García-Fernández J, et al. Factor H Competitor Generated by Gene Conversion Events Associates With Atypical Hemolytic Uremic Syndrome. *J Am Soc Nephrol* (2018) 29(1):240–9. doi: 10.1681/ASN.2017050518
22. Zhai YL, Meng SJ, Zhu L, Shi SF, Wang SX, Liu LJ, et al. Rare Variants in the Complement Factor H-Related Protein 5 Gene Contribute to Genetic Susceptibility to IgA Nephropathy. *J Am Soc Nephrol* (2016) 27(9):2894–905. doi: 10.1681/ASN.2015010012
23. Osborne AJ, Breno M, Borsa NG, Bu F, Frémeaux-Bacchi V, Gale DP, et al. Statistical Validation of Rare Complement Variants Provides Insights Into the Molecular Basis of Atypical Hemolytic Uremic Syndrome and C3 Glomerulopathy. *J Immunol* (2018) 200(7):2464–78. doi: 10.4049/jimmunol.1701695
24. Gale DP, Pickering MC. Regulating Complement in the Kidney: Insights From CFHR5 Nephropathy. *Dis Model Mech* (2011) 4(6):721–6. doi: 10.1242/dmm.008052
25. Narendra U, Pauer GJ, Hagstrom SA. Genetic Analysis of Complement Factor H Related 5, CFHR5, in Patients With Age-Related Macular Degeneration. *Mol Vis* (2009) 15:731–6.
26. Monteferrante G, Brioschi S, Caprioli J, Pianetti G, Bettinaglio P, Bresin E, et al. Genetic Analysis of the Complement Factor H Related 5 Gene in Haemolytic Uraemic Syndrome. *Mol Immunol* (2007) 44(7):1704–8. doi: 10.1016/j.molimm.2006.08.004
27. Tortajada A, Yébenes H, Abarrategui-Garrido C, Anter J, García-Fernández JM, Martínez-Barricarte R, et al. C3 Glomerulopathy-Associated CFHR1 Mutation Alters FHR Oligomerization and Complement Regulation. *J Clin Invest* (2013) 123(6):2434–46. doi: 10.1172/JCI68280
28. Medjeral-Thomas NR, Lomax-Browne HJ, Beckwith H, Willicombe M, McLean AG, Brookes P, et al. Circulating Complement Factor H-Related Proteins 1 and 5 Correlate With Disease Activity in IgA Nephropathy. *Kidney Int* (2017) 92(4):942–52. doi: 10.1016/j.kint.2017.03.043
29. Booij JC, Baas DC, Beisekeeva J, Gorgels TG, Bergen AA. The Dynamic Nature of Bruch's Membrane. *Prog Retin Eye Res* (2010) 29(1):1–18. doi: 10.1016/j.preteyeres.2009.08.003
30. Byron A, Randles MJ, Humphries JD, Mironov A, Hamidi H, Harris S. Glomerular Cell Cross-Talk Influences Composition and Assembly of Extracellular Matrix. *J Am Soc Nephrol* (2014) 25(5):953–66. doi: 10.1681/ASN.2013070795
31. Sjoberg A, Onnerfjord P, Mörgelin M, Heinegård D, Blom AM. The Extracellular Matrix and Inflammation: Fibromodulin Activates the Classical Pathway of Complement by Directly Binding C1q. *J Biol Chem* (2005) 280(37):32301–8. doi: 10.1074/jbc.M504828200
32. Sjoberg AP, Manderson GA, Mörgelin M, Day AJ, Heinegård D, Blom AM. Short Leucine-Rich Glycoproteins of the Extracellular Matrix Display Diverse Patterns of Complement Interaction and Activation. *Mol Immunol* (2009) 46 (5):830–9. doi: 10.1016/j.molimm.2008.09.018
33. Melin Furst C, Åhrman E, Bratteby K, Waldemarson S, Malmström J, Blom AM. Quantitative Mass Spectrometry To Study Inflammatory Cartilage Degradation and Resulting Interactions With the Complement System. *J Immunol* (2016) 197(8):3415–24. doi: 10.4049/jimmunol.1601006
34. Clark SJ, McHarg S, Tilakaratna V, Brace N, Bishop PN. Bruch's Membrane Compartmentalizes Complement Regulation in the Eye With Implications for Therapeutic Design in Age-Related Macular Degeneration. *Front Immunol* (2017) 8:1778. doi: 10.3389/fimmu.2017.01778
35. Whitmore SS, Sohn EH, Chirco KR, Drack AV, Stone EM, Tucker BA, et al. Complement Activation and Choriocapillaris Loss in Early AMD: Implications for Pathophysiology and Therapy. *Prog Retin Eye Res* (2015) 45:1–29. doi: 10.1016/j.preteyeres.2014.11.005

36. Schmidt CQ, Herbert AP, Kavanagh D, Gandy C, Fenton CJ, Blaum BS, et al. A New Map of Glycosaminoglycan and C3b Binding Sites on Factor H. *J Immunol* (2008) 181(4):2610–9. doi: 10.4049/jimmunol.181.4.2610
37. Pangburn MK. Cutting Edge: Localization of the Host Recognition Functions of Complement Factor H at the Carboxyl-Terminal: Implications for Hemolytic Uremic Syndrome. *J Immunol* (2002) 169(9):4702–6. doi: 10.4049/jimmunol.169.9.4702
38. Clark SJ, Bishop PN, Day AJ. The Proteoglycan Glycomatrix: A Sugar Microenvironment Essential for Complement Regulation. *Front Immunol* (2013) 4:412. doi: 10.3389/fimmu.2013.00412
39. Happonen KE, Fürst CM, Saxne T, Heinegård D, Blom AM. PRELP Protein Inhibits the Formation of the Complement Membrane Attack Complex. *J Biol Chem* (2012) 287(11):8092–100. doi: 10.1074/jbc.M111.291476
40. Johnson JM, Young TL, Rada JA. Small Leucine Rich Repeat Proteoglycans (SLRPs) in the Human Sclera: Identification of Abundant Levels of PRELP. *Mol Vis* (2006) 12:1057–66.
41. Laabei M, Liu G, Ermert D, Lambris JD, Riesbeck K, Blom AM. Short Leucine-Rich Proteoglycans Modulate Complement Activity and Increase Killing of the Respiratory Pathogen Moraxella Catarrhalis. *J Immunol* (2018) 201 (9):2721–30. doi: 10.4049/jimmunol.1800734
42. Ferreira VP, Cortes C, Pangburn MK. Native Polymeric Forms of Properdin Selectively Bind to Targets and Promote Activation of the Alternative Pathway of Complement. *Immunobiology* (2010) 215(11):932–40. doi: 10.1016/j.imbio.2010.02.002
43. Pangburn MK. Analysis of the Natural Polymeric Forms of Human Properdin and Their Functions in Complement Activation. *J Immunol* (1989) 142 (1):202–7.
44. Kuhn S, Zipfel PF. The Baculovirus Expression Vector pBSV-8His Directs Secretion of Histidine-Tagged Proteins. *Gene* (1995) 162(2):225–9. doi: 10.1016/0378-1119(95)00360-I
45. Clark SJ, Schmidt CQ, White AM, Hakobyan S, Morgan BP, Bishop PN. Identification of Factor H-Like Protein 1 as the Predominant Complement Regulator in Bruch's Membrane: Implications for Age-Related Macular Degeneration. *J Immunol* (2014) 193(10):4962–70. doi: 10.4049/jimmunol.1401613
46. Poppelaars F, Goicoechea de Jorge E, Jongerius I, Baeumner AJ, Steiner MS, Józsi M, et al. A Family Affair: Addressing the Challenges of Factor H and the Related Proteins. *Front Immunol* (2021) 12:660194. doi: 10.3389/fimmu.2021.660194
47. Lores-Motta L, van Beek AE, Willems E, Zandstra J, van Mierlo G, Einhaus A, et al. Common Haplotypes at the CFH Locus and Low-Frequency Variants in CFHR2 and CFHR5 Associate With Systemic FHR Concentrations and Age-Related Macular Degeneration. *Am J Hum Genet* (2021) 108(8):1367–84. doi: 10.1016/j.ajhg.2021.06.002
48. Hebecker M, Józsi M. Factor H-Related Protein 4 Activates Complement by Serving as a Platform for the Assembly of Alternative Pathway C3 Convertase *via* its Interaction With C3b Protein. *J Biol Chem* (2012) 287(23):19528–36. doi: 10.1074/jbc.M112.364471
49. Seguin-Devaux C, Plesseria JM, Verschueren C, Masquelier C, Iserentant G, Fullana M, et al. FHR4-Based Immunoconjugates Direct Complement-Dependent Cytotoxicity and Phagocytosis Towards HER2-Positive Cancer Cells. *Mol Oncol* (2019) 13(12):2531–53. doi: 10.1002/1878-0261.12554
50. Martin Merinero H, Subías M, Pereda A, Gómez-Rubio E, Juana Lopez L, Fernandez C, et al. Molecular Bases for the Association of FHR-1 With Atypical Hemolytic Uremic Syndrome and Other Diseases. *Blood* (2021) 137 (25):3484–94. doi: 10.1182/blood.2020010069
51. Tortajada A, Gutiérrez E, Goicoechea de Jorge E, Anter J, Segarra A, Espinosa M, et al. Elevated Factor H-Related Protein 1 and Factor H Pathogenic Variants Decrease Complement Regulation in IgA Nephropathy. *Kidney Int* (2017) 92:953–63. doi: 10.1016/j.kint.2017.03.041
52. Cipriani V, Lorés-Motta L, He F, Fathalla D, Tilakaratna V, McHarg S, et al. Increased Circulating Levels of Factor H-Related Protein 4 are Strongly Associated With Age-Related Macular Degeneration. *Nat Commun* (2020) 11:778. doi: 10.1038/s41467-020-14499-3
53. Pouw RB, Gómez Delgado I, López Lera A, Rodríguez de Córdoba S, Wouters D, Kuijpers TW, et al. High Complement Factor H-Related (FHR)-3 Levels Are Associated With the Atypical Hemolytic-Uremic Syndrome-Risk Allele CFHR3*B. *Front Immunol* (2018) 9:848. doi: 10.3389/fimmu.2018.00848
54. Schafer N, Grosche A, Reinders J, Hauck SM, Pouw RB, Kuijpers TW, et al. Complement Regulator FHR-3 Is Elevated Either Locally or Systemically in a Selection of Autoimmune Diseases. *Front Immunol* (2016) 7:542. doi: 10.3389/fimmu.2016.00542

Author Disclaimer: Parts of this work were presented at the 16th European Meeting on Complement in Human Disease, September 8-12, 2017, Copenhagen, Denmark (*Mol. Immunol.* 2017, 89:145), and at the 27th International Complement Workshop, September 16-20, 2018, Santa Fe, New Mexico, USA (*Mol. Immunol.* 2018, 102:196).

Conflict of Interest: The authors declare that the research was conducted in the absence of any commercial or financial relationships that could be construed as a potential conflict of interest.

Publisher's Note: All claims expressed in this article are solely those of the authors and do not necessarily represent those of their affiliated organizations, or those of the publisher, the editors and the reviewers. Any product that may be evaluated in this article, or claim that may be made by its manufacturer, is not guaranteed or endorsed by the publisher.

frontiers | Frontiers in Immunology

CASE REPORT
published: 26 May 2022
doi: 10.3389/fimmu.2022.909503

Post-Transplant Thrombotic Microangiopathy due to a Pathogenic Mutation in Complement Factor I in a Patient With Membranous Nephropathy: Case Report and Review of Literature

Maryam Saleem[1†], *Sana Shaikh*[2†], *Zheng Hu*[3], *Nicola Pozzi*[4] *and Anuja Java*[1*]

[1] Division of Nephrology, Department of Medicine, Washington University School of Medicine, St. Louis, MO, United States, [2] Division of Nephrology, Department of Medicine, University of California, San Francisco, San Francisco, CA, United States, [3] Division of Rheumatology, Department of Medicine, Washington University School of Medicine, St. Louis, MO, United States, [4] Department of Biochemistry and Molecular Biology, Edward A. Doisy Research Center, Saint Louis University School of Medicine, St. Louis, MO, United States

OPEN ACCESS

Edited by:
Mihály Józsi,
Eötvös Loránd University, Hungary

Reviewed by:
Kevin James Marchbank,
Newcastle University, United Kingdom
Pilar Sánchez-Corral,
University Hospital La Paz Research Institute (IdiPAZ), Spain

***Correspondence:**
Anuja Java
ajava@wustl.edu

†These authors share first authorship

Specialty section:
This article was submitted to Molecular Innate Immunity, a section of the journal Frontiers in Immunology

Received: 31 March 2022
Accepted: 02 May 2022
Published: 26 May 2022

Citation:
Saleem M, Shaikh S, Hu Z, Pozzi N and Java A (2022) Post-Transplant Thrombotic Microangiopathy due to a Pathogenic Mutation in Complement Factor I in a Patient With Membranous Nephropathy: Case Report and Review of Literature Case Report: aHUS and Recurrent Membranous Nephropathy After Kidney Transplantation. Front. Immunol. 13:909503. doi: 10.3389/fimmu.2022.909503

Thrombotic microangiopathy (TMA) is characterized by microangiopathic hemolytic anemia, thrombocytopenia and organ injury occurring due to endothelial cell damage and microthrombi formation in small vessels. TMA is primary when a genetic or acquired defect is identified, as in atypical hemolytic uremic syndrome (aHUS) or secondary when occurring in the context of another disease process such as infection, autoimmune disease, malignancy or drugs. Differentiating between a primary complement-mediated process and one triggered by secondary factors is critical to initiate timely treatment but can be challenging for clinicians, especially after a kidney transplant due to presence of multiple confounding factors. Similarly, primary membranous nephropathy is an immune-mediated glomerular disease associated with circulating autoantibodies (directed against the M-type phospholipase A2 receptor (PLA2R) in 70% cases) while secondary membranous nephropathy is associated with infections, drugs, cancer, or other autoimmune diseases. Complement activation has also been proposed as a possible mechanism in the etiopathogenesis of primary membranous nephropathy; however, despite complement being a potentially common link, aHUS and primary membranous nephropathy have not been reported together. Herein we describe a case of aHUS due to a pathogenic mutation in complement factor I that developed after a kidney transplant in a patient with an underlying diagnosis of PLA2R antibody associated-membranous nephropathy. We highlight how a systematic and comprehensive analysis helped to define the etiology of aHUS, establish mechanism of disease, and facilitated timely treatment with eculizumab that led to recovery of his kidney function. Nonetheless,

ongoing anti-complement therapy did not prevent recurrence of membranous nephropathy in the allograft. To our knowledge, this is the first report of a patient with primary membranous nephropathy and aHUS after a kidney transplant.

Keywords: thrombotic microangiopathy, kidney transplantation, complement factor I, membranous nephropathy, atypical hemolytic uremic syndrome, complement functional analysis

INTRODUCTION

Atypical hemolytic uremic syndrome (aHUS) is a classic complement-mediated thrombotic microangiopathy (TMA) resulting from inadequately controlled activation of the alternative pathway (AP) of the complement system (1, 2). The etiology of aHUS is commonly a heterozygous, loss-of-function mutation in a regulator (Factor H, Factor I or Membrane Cofactor Protein). Less commonly a gain-of-function mutation in a complement activator (C3 or Factor B) may be identified (3). A TMA after a kidney transplantation can be *de novo* or recurrent (4, 5). Patients with recurrent TMA almost always have a complement-mediated disease. However, *de novo* TMA may be complement-mediated or secondary to transplantation-associated triggers such as immunosuppressive medications, ischemia reperfusion injury, viral infections, malignancy or antibody-mediated rejection. *De novo* TMA is reported in 1-15% patients, although the true frequency is unknown, and the implication of a dysregulated complement system may be underestimated.

Primary membranous nephropathy (MN) is an autoimmune-mediated glomerular disease and is one of the most common causes of nephrotic syndrome in adults (6). The disease may recur after kidney transplantation in 35-40% cases or occur as a *de novo* form. Over the last few years, several different podocyte antigens have been identified in association with MN, such as M-type phospholipase A2 receptor (PLA2R), thrombospondin type-1 domain-containing 7A, exostosin 1 and exostosin 2, NELL-1 and, most recently, protocadherin FAT1 (7, 8). Evidence from human and animal data has suggested that the complement system may play a role in the pathogenesis of MN, however, there has been substantial heterogeneity in the complement activation profiles reported in patients. One reason for the variation in the extent of complement activation may be due to differences in the subclass of IgG antibodies associated with the various antigens. We report a unique case of complement mediated *de novo* TMA (aHUS) in a patient after kidney transplantation who had an underlying diagnosis of PLA2R+ MN as the etiology of his native kidney disease. The patient responded successfully to anti-complement therapy without relapse of the TMA but developed early and aggressive recurrence of the membranous nephropathy in the allograft.

CASE DESCRIPTION

Patient Information

A 28-year-old African American male with end stage renal disease (ESRD) secondary to biopsy-proven membranous nephropathy (PLA2R antibody positive) underwent a 2A, 2B, 1DR mismatch, ABO incompatible living-unrelated kidney transplant. There was no history of kidney disease in the family. Due to the ABO incompatibility (donor A+, recipient O+ with an anti-A antibody titer of 64), he was treated with 10 sessions of plasmapheresis, rituximab and mycophenolic acid prior to transplant (per our center's protocol) with a decrease in the anti-A antibody titer to 4. Induction immunosuppression included methylprednisolone (7 mg/kg) and thymoglobulin (6 mg/kg).

Clinical Findings and Diagnostic Assessment

On postoperative day (POD) 1, the patient developed increased bleeding from the surgical incision site and was taken back to the operating room (OR) for exploration and washout. Diffuse oozing was noted with a hematoma in the retroperitoneum. Laboratory data were notable for anemia (hemoglobin 6.9-7.7 g/dL; reference range 13-17 g/dL), severe thrombocytopenia (platelet count 24-36 k/μL; reference range 150-400 k/μL), low haptoglobin (<10 mg/dL; reference range 30-200 mg/dL) and high lactate dehydrogenase (580-736 units/L; reference range 150-250 units/L) **(Figure 1).** Additional work-up revealed low C3 (58 mg/dL; reference range 90-180 mg/dL) and a low normal C4 (12.9 mg/dL; reference range, 10-40 mg/dL). ADAMTS13 (a disintegrin and metalloproteinase with a thrombospondin type 1 motif, member 13) activity and coagulation profile were normal. This raised concern for a TMA. Genetic testing for complement variants was sent.

Therapeutic Intervention

Tacrolimus was not initiated. Eculizumab was administered on POD 3. Patient returned to the OR on POD 4 for revision and closure and at that time an intraoperative biopsy was performed which confirmed a TMA with no evidence of acute cellular or antibody-mediated rejection (**Figure 2**).

Follow-Up and Outcomes

The patient remained oliguric and required hemodialysis on POD 5. Over the next 24 hours, signs of clinical recovery were evident with normalization of haptoglobin (86 mg/dL), improvement in lactate dehydrogenase (364 units/L) and C3 (112 mg/dL). Renal function improved and he did not require further dialysis. Serum creatinine on the day of discharge (POD 10) was 4.5 mg/dL. Eculizumab was continued as an outpatient. Creatinine stabilized at 1.8 mg/dL by POD 14, with no recurrence of TMA; however, the patient developed recurrent biopsy-proven membranous nephropathy a month later.

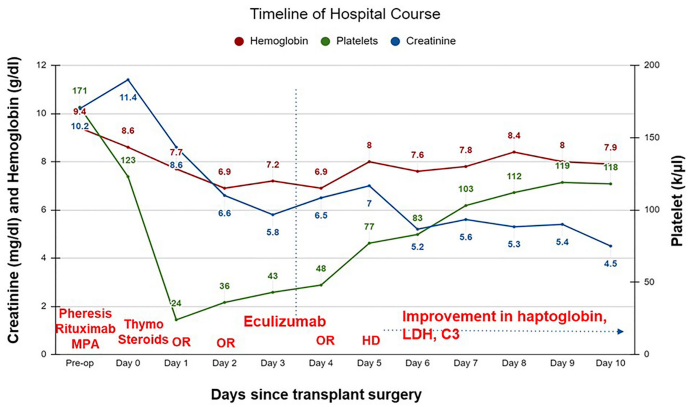

FIGURE 1 | Timeline of hospital course of patient after a living unrelated kidney transplantation. C3, complement 3; HD, hemodialysis; LDH, lactate dehydrogenase; OR, operative room; thymo, thymoglobulin; MPA, mycophenolic acid.

Genetic Variant Analysis

Genetic testing was conducted by the Genomic and Pathology services at Washington University in St. Louis and revealed a 'variant of uncertain significance' in Complement Factor I (*CFI*) (Ile357Met). This variant is located in the serine protease domain of FI which contains the catalytic site and has been reported at a frequency of 0.004% in population databases (gnomAd). We produced the variant protein recombinantly and conducted functional and structural analysis to define the significance of this variant using the methods described previously (9). As assessed by ELISA, the secretion of the recombinant protein by 293T cells compared to wild type (WT) was reduced [WT, 11.44 µg/ml ± 1.4 (standard error of mean); 357Met, 4.79 µg/ml ± 0.401(standard error of mean)]. However, patient's serum antigenic level of Factor I (FI) was normal (3.6 mg/dL, reference range for Blood Center of Wisconsin laboratory is 2.4-4.9 mg/dL). Although these results raised the question whether decreased secretion of FI *in vitro* in 293T cells accurately translates to low antigenic levels in the patient, the variant Ile357Met has been reported previously in patients with low levels (10). Therefore, we speculated that the normal serum level in our patient was likely reflective of an increase in the secretion of the WT allele (indicative of the acute phase nature of FI). Additionally, functional analysis demonstrated that the variant had defective complement regulatory activity with Factor H (**Figures 3A– C**) but no defect was seen with membrane cofactor protein or complement receptor 1 (**Figure 3D**).

Structural analysis showed that Ile357 was located 8 Å away from the catalytic serine (S525) and 3.5 Å away from the conserved disulfide bond (365–381). The disulfide bond plays a vital role of keeping the catalytic histidine (H380) in place for optimal enzymatic activity (**Figure 3E**). Given that Met is bulkier and less hydrophobic than Ile, the substitution of Ile to Met likely alters the position of the disulfide bond 365-381, thus lowering the FI activity. We also mapped the variant on the triple complex with FH and C3b (**Figure 3F**) (11) and it does not seem to lay close to FH, therefore, we speculate that the variant likely causes a conformational change that results in reduced functional activity. These analyses established that the *CFI* Ile357Met variant was deleterious (due to both decreased secretion and functional activity) and thereby consistent with the diagnosis of aHUS in our patient.

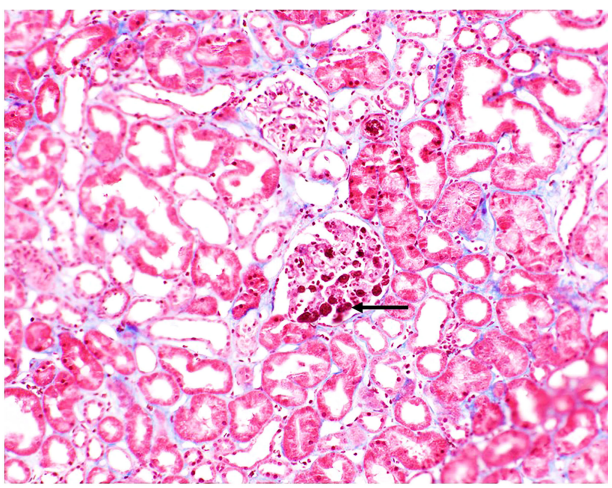

FIGURE 2 | Biopsy image from patient. Fibrin thrombi seen in glomeruli (black arrow). Small arteries and arterioles demonstrated focal fibrinoid necrosis of the arterial wall (not shown).

DISCUSSION

Thrombotic microangiopathy (TMA) characterized by over-activation and dysregulation of the alternative pathway (AP) of complement cascade is called a primary TMA or aHUS. The clinical outcome of aHUS is unfavorable, typified by progression to ESRD and relapse after kidney transplantation, if not diagnosed and treated timely. aHUS may be mimicked by other disease processes, currently classified under secondary TMA, including infections, pregnancy, autoimmune conditions,

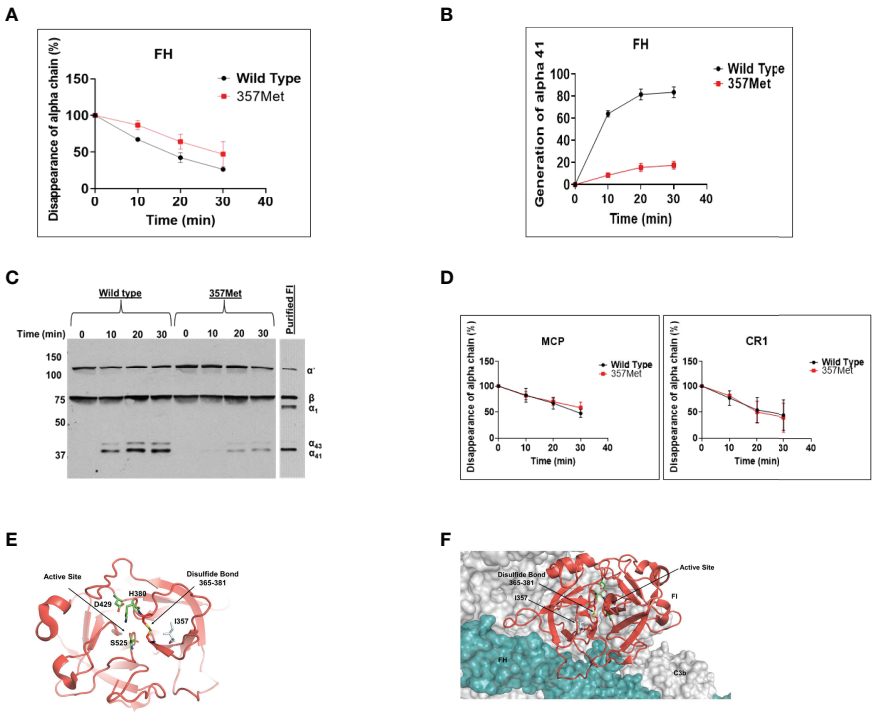

FIGURE 3 | Functional evaluation of Factor I (FI) variant Ile357Met: proteolytic activity. The fluid-phase C3b proteolytic activity of the variant factor I (357Met) with its cofactor proteins (Factor H [FH], membrane cofactor protein [MCP], or complement receptor 1 [CR1]) was assessed by cleavage of purified C3b to iC3b and compared to wild type (WT). For these assays, purified WT and FI variant proteins were diluted in physiologic salt (150 mM NaCl) buffer with C3b (10 ng; Complement Technologies, Inc, Tyler, TX USA) at 37°C. Concentrations of WT or variant FI used with the individual cofactors were 10 ng with MCP, 20 ng with FH and 15 ng with CR1. Concentration of cofactor used in the reactions were 100 ng MCP, 200 ng FH or 150 ng CR1. Reactions were carried out in a total volume of 15 µl/reaction at 37°C. Kinetic analysis of the WT and variants was achieved through collection of sample at 0, 10, 20 and 30 min. At each time point 7 µl of 3x Laemmli reducing sample buffer was added to individual reactions to stop the reaction and then heated at 95°C for 5 min. The samples were electrophoresed on 10% Tris-glycine gel and then transferred to nitrocellulose for WB analysis. Membranes were rinsed with TBS-T (0.05%Tween-20) for 5 min and blocked overnight with 5% nonfat dry milk in PBS. Blots were probed with a 1:5,000 dilution of goat anti-human C3 (Complement Technologies, Inc, Tyler, TX, USA) followed by HRP-conjugated rabbit anti-goat IgG and developed with SuperSignal substrate (Thermo Fisher Scientific, Waltham, MA, USA). The signal detected on radiographic films was scanned using a laser densitometer (Pharmacia LKB Biotechnology, Piscataway, NJ, USA). Multiple exposures were used to establish linearity. **(A, B)**. The percentage of α' chain remaining and generation of α41 fragment indicates cleavage of C3b to iC3b. Cleavage rate was measured by densitometric analysis of the α' chain remaining as well as generation of α41 relative to the β chain. Data represent 2 separate experiments with bars corresponding to the standard error of mean (SEM). Upon comparison to WT FI, the proteolytic activity of variant 357Met was defective with FH. The P value for the difference in the percentage of α'chain remaining between WT and variant was 0.05 and for the difference in the percentage of α41 generation was <0.05. **(C).** Representative WB demonstrating cofactor activity of Factor H with the variant (357Met) compared with wild type FI as well as purified FI **(D)** No defect was observed with MCP or CR1 as the cofactor protein. I, isoleucine; M, methionine. Structural evaluation of Ile357Met **(E)** Mapping of Ile357 on the structure of FI shows that it is located in the serine protease domain of FI which harbors the catalytic activity. Although the variant is away from the catalytic serine (S525)), the substitution of I to a bulkier amino acid M likely alters the position of the disulfide bond 365-381, thus affecting the FI activity. **(F)** Mapping of the Ile357 on the triple complex of Factor H and C3b shows that the variant is away from the binding surface of FH, therefore we speculate that it likely leads to a conformational change resulting in low functional activity.

and graft rejection. Kidney transplantation poses a problematic setting since there are multiple potential triggers (transplant surgery, drugs, rejection, and infections) for TMA development (12, 13). Consequently, it can be 'tricky" for transplant clinicians to distinguish aHUS from these secondary TMAs.

Our case is a prime example of such a challenging scenario. The patient had a history of ESRD secondary to biopsy-proven primary MN and manifested a *de novo* TMA after kidney transplantation. After a systematic work-up, the etiology of the TMA was determined to be a pathogenic mutation in *CFI*. We speculate that the genetic mutation in *CFI* conferred a low risk of TMA in the native kidneys, and that he developed an early and aggressive disease after kidney transplantation due to the multiple additional risk factors (transplant surgery, ischemia-reperfusion injury, etc) that predisposed him to endothelial injury. Our strategy of recombinant protein production followed by detailed functional assessment defined the functional repertoire of the *CFI* variant protein (demonstrating that it was defective due to both low secretion and low function of the protein) and ascertained the diagnosis of complement-mediated TMA or aHUS in this patient and helped to differentiate it from a secondary TMA after kidney transplantation. Further it provided critical guidance relative to the underlying pathophysiology and appropriate therapeutic regimen.

We also considered the possibility that complement dysregulation due to the *CFI* genetic variant could have played a role in the etiology of membranous nephropathy. This

speculation stems from the Heymann nephritis rat model that showed that subepithelial immune deposits initiate complement activation leading to C5b-9-mediated damage of the podocytes (14, 15). This has been further validated in human MN with evidence of C3 breakdown product deposition (C3c and C3d) on immuno-histologic staining and presence of C5b-9 in the urine (16). Although, the exact role of complement in MN and the predominant pathway involved remains unclear, several levels of evidence implicate the AP or lectin pathway. The absence of classical pathway components (C1q and C4) in glomeruli, IgG4 being the major subclass associated with PLA2R and the decrease in complement receptor 1 (CR1) expression on the podocyte observed in patients with primary MN have all led to the speculation that the AP activation may be dominant (17–20). There is also one case in the literature of MN in association with Factor H-autoantibodies in the absence of a TMA (21). These data indicate that a subset of patients with primary MN may have dysregulation of the AP and benefit from anti-complement therapy. Our patient developed recurrent MN within a month after transplantation despite being on eculizumab but did not develop recurrent TMA. Therefore, we believe that the MN in our patient was likely not complement-mediated, and he had two different primary immune processes (MN and aHUS) in the allograft. These two diseases have not been reported together before either in the native kidney or after a transplantation. Despite the discovery of multiple new antigens in MN, their precise role in complement activation remains unclear and more research is needed to better define the underlying pathogenic mechanisms of these antigens and to determine if and who would benefit from anti-complement therapy.

DATA AVAILABILITY STATEMENT

The original contributions presented in the study are included in the article/supplementary material. Further inquiries can be directed to the corresponding author.

ETHICS STATEMENT

The studies involving human participants were reviewed and approved by Institutional review board, Washington University School of Medicine, St. Louis, MO. The patients/participants provided their written informed consent to participate in this study. Written informed consent was obtained from the individual(s) for the publication of any potentially identifiable images or data included in this article.

AUTHOR CONTRIBUTIONS

MS, SS, and AJ drafted the manuscript. ZH performed the experiments. NP conducted the structural analysis. SS and AJ prepared the figures. AJ edited the manuscript. All authors contributed to the article and approved the submitted version.

FUNDING

Supported in part by Barnes Jewish Hospital Foundation Fund, Division of Nephrology, Washington University School of Medicine in St. Louis (AJ).

ACKNOWLEDGMENTS

The authors thank Dr. Joe Gaut (Washington University School of Medicine) for providing the biopsy image, Dr. Yun Ju Sung (Division of Biostatistics, Washington University School of Medicine) for performing the statistical analyses and Drs. John Atkinson and M. Kathryn Liszewski (Washington University School of Medicine) for their helpful comments during the preparation and revision of this manuscript.

REFERENCES

1. Moake JL. Thrombotic Microangiopathies. *N Engl J Med* (2002) 347(8):589–600. doi: 10.1056/NEJMra020528
2. George JN, Nester CM. Syndromes of Thrombotic Microangiopathy. *N Engl J Med* (2014) 371(7):654–66. doi: 10.1056/NEJMra1312353
3. Java A, Atkinson J, Salmon J. Defective Complement Inhibitory Function Predisposes to Renal Disease. *Annu Rev Med* (2013) 64:307–24. doi: 10.1146/annurev-med-072211-110606
4. Reynolds JC, Agodoa LY, Yuan CM, Abbott KC. Thrombotic Microangiopathy After Renal Transplantation in the United States. *Am J Kidney Dis* (2003) 42(5):1058–68. doi: 10.1016/j.ajkd.2003.07.008
5. Garg N, Rennke HG, Pavlakis M, Zandi-Nejad K. *De Novo* Thrombotic Microangiopathy After Kidney Transplantation. *Transplant Rev* (2018) 32 (1):58–68. doi: 10.1016/j.trre.2017.10.001
6. Passerini P, Malvica S, Tripodi F, Cerutti R, Messa P. Membranous Nephropathy (MN) Recurrence After Renal Transplantation. *Front Immunol* (2019) 10:1326. doi: 10.3389/fimmu.2019.01326
7. Brglez V, Boyer-Suavet S, Seitz-Polski B. Complement Pathways in Membranous Nephropathy: Complex and Multifactorial. *Kidney Int Rep* (2020) 5(5):572–74. doi: 10.1016/j.ekir.2020.02.1033
8. Sethi S, Madden B, Casal Moura M, Nasr SH, Klomjit N, Gross LA, et al. Hematopoietic Stem Cell Transplant-Membranous Nephropathy is Associated With Protocadherin Fat1. *J Am Soc Nephrol* (2022) 33(5):1033–44;. doi: 10.1681/ASN.2021111488
9. Java A, Pozzi N, Love-Gregory LD, Heusel JH, Sung YJ, Hu Z , et al. A Multimodality Approach to Assessing Factor I Genetic Variants in Atypical Hemolytic Uremic Syndrome. *Kidney Int Rep* (2019) 4(7):1007–17. doi: 10.1016/j.ekir.2019.04.003
10. Nilsson SC, Trouw LA, Renault N, Miteva M, Genal F, Zelazko M, et al. Genetic, Molecular and Functional Analyses of Complement Factor I Deficiency. *Eur J Immunol* (2009) 39(1):310–23. doi: 10.1002/eji.200838702
11. Forneris F, Wu J, Xue X, Ricklin D, Lin Z, Sfyroera G, et al. Regulators of Complement Activity Mediate Inhibitory Mechanisms Through a Common C3b-Binding Mode. *EMBO J* (2016) 35:1133–49. doi: 10.15252/embj.201593673
12. Scully M, Cataland S, Coppo P, de la Rubia J, Friedman KD, Hovinga JK, et al. Consensus on the Standardization of Terminology in Thrombotic Thrombocytopenic Purpura and Related Thrombotic Microangiopathies. *J Thromb Haemost* (2017) 15(2):312–22. doi: 10.1111/jth.13571
13. Palma LMP, Sridharan M, Sethi S. Complement in Secondary Thrombotic Microangiopathy. *Kidney Int Rep* (2021) 6(1):11–23. doi: 10.1016/j.ekir.2020.10.009

14. Salant DJ, Quigg RJ, Cybulsky AV. Heymann Nephritis: Mechanisms of Renal Injury. *Kidney Int* (1989) 35(4):976–84. doi: 10.1038/ki.1989.81
15. Luo W, Olaru F, Miner JH, Beck LH, Van derVlag J, Thurman JM , et al. Alternative Pathway Is Essential for Glomerular Complement Activation and Proteinuria in a Mouse Model of Membranous Nephropathy. *Front Immunol* (2018) 9:1433. doi: 10.3389/fimmu.2018.01433
16. Zhang MF, Huang J, Zhang YM, Ou Z, Wang X, Wang F, et al. Complement Activation Products in the Circulation and Urine of Primary Membranous Nephropathy. *BMC Nephrol* (2019) 20(1):313. doi: 10.1186/s12882-019-1509-5
17. Brglez V, Boyer-Suavet S, Seitz-Polski B. Complement Pathways in Membranous Nephropathy: Complex and Multifactorial. *Kidney Int Rep* (2020) 5(5):572–74. doi: 10.1016/j.ekir.2020.02.1033
18. Ma H, Sandor DG, Beck LHJr. The Role of Complement in Membranous Nephropathy. *Semin Nephrol* (2013) 33(6):531–42. doi: 10.1016/j.semnephrol.2013.08.004
19. Cunningham PN, Quigg RJ. Contrasting Roles of Complement Activation and its Regulation in Membranous Nephropathy. *J Am Soc Nephrol* (2005) 16 (5):1214–22. doi: 10.1681/ASN.2005010096
20. Ayoub I, Shapiro JP, Song H, Zhang XL, Parikh S, Almaani S, et al. Establishing a Case for Anti-Complement Therapy in Membranous Nephropathy. *Kidney Int Rep* (2020) 6(2):484–92. doi: 10.1016/j.ekir.2020.11.032
21. Seikrit C, Ronco P, Debiec H. Factor H Autoantibodies and Membranous Nephropathy. *N Engl J Med* (2018) 379(25):2479–81. doi: 10.1056/NEJMc1805857

Conflict of Interest: The authors declare that the research was conducted in the absence of any commercial or financial relationships that could be construed as a potential conflict of interest.

Publisher's Note: All claims expressed in this article are solely those of the authors and do not necessarily represent those of their affiliated organizations, or those of the publisher, the editors and the reviewers. Any product that may be evaluated in this article, or claim that may be made by its manufacturer, is not guaranteed or endorsed by the publisher.

frontiers | Frontiers in Immunology

ORIGINAL RESEARCH
published: 26 May 2022
doi: 10.3389/fimmu.2022.876776

OPEN ACCESS

Edited by:
Roberta Bulla,
University of Trieste, Italy

Reviewed by:
Marina Noris,
Mario Negri Pharmacological Research Institute (IRCCS), Italy
Andrea Balduit,
University of Trieste, Italy

***Correspondence:**
Taco W. Kuijpers
t.w.kuijpers@amsterdamumc.nl
Anna E. van Beek
a.vanbeek@sanquin.nl

†Present address:
Diana Wouters,
Sanquin Diagnostic Services,
Amsterdam, Netherlands

‡These authors have contributed equally to this work

Specialty section:
This article was submitted to Molecular Innate Immunity, a section of the journal Frontiers in Immunology

Received: 15 February 2022
Accepted: 29 April 2022
Published: 26 May 2022

Citation:
van Beek AE, Pouw RB, Wright VJ, Sallah N, Inwald D, Hoggart C, Brouwer MC, Galassini R, Thomas J, Calvo-Bado L, Fink CG, Jongerius I, Hibberd M, Wouters D, Levin M and Kuijpers TW (2022) Low Levels of Factor H Family Proteins During Meningococcal Disease Indicate Systemic Processes Rather Than Specific Depletion by Neisseria meningitidis. Front. Immunol. 13:876776. doi: 10.3389/fimmu.2022.876776

Low Levels of Factor H Family Proteins During Meningococcal Disease Indicate Systemic Processes Rather Than Specific Depletion by *Neisseria meningitidis*

Anna E. van Beek[1,2‡], Richard B. Pouw[1,2‡], Victoria J. Wright[3], Neneh Sallah[4], David Inwald[3], Clive Hoggart[3], Mieke C. Brouwer[1], Rachel Galassini[3], John Thomas[5], Leo Calvo-Bado[5], Colin G. Fink[5], Ilse Jongerius[1,2], Martin Hibberd[4], Diana Wouters[1†], Michael Levin[3] and Taco W. Kuijpers[2,6*] on behalf of the EUCLIDS Consortium*

[1] Sanquin Research, Department of Immunopathology, and Landsteiner Laboratory, Amsterdam University Medical Centre, Amsterdam Infection and Immunity Institute, Amsterdam, Netherlands, [2] Department of Pediatric Immunology, Rheumatology, and Infectious Diseases, Emma Children's Hospital, Amsterdam University Medical Centre, Amsterdam, Netherlands, [3] Section for Paediatric Infectious Disease, Department of Infectious Disease, Faculty of Medicine, Imperial College London, London, United Kingdom, [4] Department of Infection Biology, Faculty of Infectious and Tropical Diseases, London School of Hygiene and Tropical Medicine, London, United Kingdom, [5] Micropathology Ltd., University of Warwick, Warwick, United Kingdom, [6] Sanquin Research, Department of Blood Cell Research, and Landsteiner Laboratory, Amsterdam University Medical Centre, Amsterdam, Netherlands

Neisseria meningitidis, the causative agent of meningococcal disease (MD), evades complement-mediated clearance upon infection by 'hijacking' the human complement regulator factor H (FH). The FH protein family also comprises the homologous FH-related (FHR) proteins, hypothesized to act as antagonists of FH, and FHR-3 has recently been implicated to play a major role in MD susceptibility. Here, we show that the circulating levels of all FH family proteins, not only FH and FHR-3, are equally decreased during the acute illness. We did neither observe specific consumption of FH or FHR-3 by *N. meningitidis*, nor of any of the other FH family proteins, suggesting that the globally reduced levels are due to systemic processes including dilution by fluid administration upon admission and vascular leakage. MD severity associated predominantly with a loss of FH rather than FHRs. Additionally, low FH levels associated with renal failure, suggesting insufficient protection of host tissue by the active protection by the FH protein family, which is reminiscent of reduced FH activity in hemolytic uremic syndrome. Retaining higher levels of FH may thus limit tissue injury during MD.

Keywords: complement, factor H, FHR, *Neisseria meningitidis*, meningococcal disease

INTRODUCTION

Neisseria meningitidis is a Gram-negative commensal bacterium carried in the nasopharynx by up to 24% of the population (1). Upon infection, it can cause meningococcal meningitis and/or septicemia, collectively called meningococcal disease (MD). MD is a severe, debilitating and life-threatening disease with an occurrence of 2 – 20 per 100,000 in developed countries (2, 3). The complement system plays a major role in preventing MD, exemplified by deficiencies in components of its terminal pathway that are associated with recurrent *N. meningitidis* infection (4, 5).

N. meningitidis is known to exploit human complement regulator factor H (FH) to avoid complement-mediated clearance (6, 7). FH is a glycoprotein circulating in plasma at around 300 μg/mL (8, 9). It is the major regulator of the alternative pathway and is composed of 20 complement control protein (CCP) domains. FH is crucial in protecting human cells from complement-mediated damage and contains two regions involved in the binding to human cells, located in CCP6 to CCP8 and in CCP19 and CCP20 (10). *N. meningitidis* expresses various proteins to recruit FH to its surface (6, 7, 11–13). FH-binding protein (fHbp) plays a dominant role in evading complement-mediated clearance upon infection (14). This lipoprotein binds FH at CCP6 and CCP7, while leaving the complement regulatory capabilities of FH intact (15). The 'hijacking' of FH aids *N. meningitidis* in avoiding complement-mediated clearance, prolonging its survival in human circulation (6, 7, 16).

The FH protein family is encoded in tandem in the *CFH-CFHR* locus. *CFH* encodes FH and its short splice variant, FH like-1 (FHL-1), while the five *CFHR* genes encode the homologs FH-related (FHR)-1, FHR-2, FHR-3, FHR-4A and FHR-5 (17). FHR-1, FHR-2 and FHR-5 circulate in blood as dimers, with FHR-1 and FHR-2 also forming heterodimers (18, 19). The FHRs have high sequence identity to the ligand binding regions of FH (CCP6-8 and CCP19-20), but lack CCP domains homologous to FH CCP1-4, which are involved in complement regulation (20, 21). Therefore, FHRs are hypothesized to compete with FH binding to cellular surfaces, enhancing complement activation (17).

A previous genome-wide association study identified that, apart from SNPs in *CFH*, gene variations in *CFHR3* were also found to associate with MD susceptibility (22). This was the first indication that the FHRs might play a role in MD, with FHR-3 as the most promising candidate to compete with FH. FHR-3 has the highest sequence identity with FH CCP6 and CCP7 (91% and 85%, respectively), and was found to bind to fHbp *in vitro*, competing with FH for binding (23).

Since we recently developed FHR-specific ELISAs, we were now able to make the translation from genetics and *in vitro* data towards the study of FH family proteins and their levels during the acute stage of MD. We previously reported that the levels of FHRs are 10 – 100 fold lower in comparison to FH during steady-state (8, 19, 24). However, based on previous reports regarding the levels of FH (8, 25, 26) and FHR-3 (8) during sepsis, we hypothesized that the levels of FH and the FHRs may very well be altered during an episode of acute MD, possibly affecting their ratio and changing the balance of alternative pathway activation and regulation.

In this study, we analyzed the serum levels of FH and all FHRs from a cohort of pediatric MD patients during the acute stage of disease in relation to *N. meningitidis* serogroup, diagnosis and severity parameters and compared these with levels during convalescence in surviving patients. We report here that not only FH and FHR-3, but plasma concentrations of all FH family proteins are greatly decreased during the acute phase of MD. However, predominantly low FH plasma concentrations are associated with the severity of MD and renal failure.

MATERIALS AND METHODS

Study Cohort

Patients in this study ($n = 106$) were a subset of the cohort recruited at St. Mary's Hospital, London (UK) between 1992 and 2003, the details of which have been reported previously (16, 22, 27–29). All samples were obtained with informed consent of the parents or guardians of each patient according to the local ethics committee and the Declaration of Helsinki and were stored at -80°C until use. Cases included in this study had microbiologically confirmed MD and had acute serum samples taken during hospitalization, and a serum sample taken after convalescence (in survivors, $n = 91$).

Blood Markers of Disease Severity

White cell count (WCC), platelet count, activated partial thromboplastin time (aPTT), international normalized ratio (INR), base excess, and levels of fibrinogen, C-reactive protein (CRP), potassium, and lactate were all determined as part of routine diagnostics at St. Mary's Hospital, London (UK). Glasgow Meningococcal Septicemia Prognostic Score (GMSPS) and Pediatric Index of Mortality (PIM) score were determined as previously described (30, 31).

Measurement FH and FHR Proteins in Serum

FH family proteins and total human IgG levels in serum were determined by in-house developed ELISAs as previously described (8, 19, 24, 32). In short, FH was measured by ELISA using an in-house generated, specific mouse monoclonal antibody (mAb) directed against CCP domains 16/17 of FH (clone anti-FH.16, Sanquin Research, Amsterdam, the Netherlands) as the capture mAb and polyclonal goat anti-human FH (Quidel, San Diego, CA, USA), which was HRP-conjugated in-house, as the detecting Ab. FHR-1/1 homodimers and FHR-1/2 heterodimers were captured using clone anti-FH.02 (Sanquin Research), and detected with biotinylated anti-FH.02 (Sanquin Research) or anti-FHR-2 (clone MAB5484, R&D Systems, Minneapolis, MN, USA), respectively. For the specific detection of FHR-3, an in-house developed mAb directed against FHR-3 and FHR-4A (clone anti-FHR-3.1, Sanquin Research) was used as the capture mAb. A biotinylated mAb directed against FHR-3 and FH (clone anti-FHR-3.4, Sanquin Research) was used as detecting mAb. To measure

FHR-4A, a rat anti-mouse kappa mAb (RM-19, Sanquin Research) was coated on the plate before addition of the capture mAb (clone anti-FHR-4A.04, Sanquin Research), capturing specifically FHR-4A. The detecting mAb was a biotinylated polyclonal rabbit anti-human FHR-3 (Sanquin Research). FHR-5 was measured by using two specific mAbs: anti-FHR-5.1 as a capturing mAb and biotinylated anti-FHR-5.4 as detection mAb (both from Sanquin Research).

To determine whether fHbp affects the measurement of FH and FHRs by ELISA, *e.g.* by sterically hindering or otherwise affecting specific antibody binding to FH or any of the FHRs, the ELISAs were performed as described above, using pooled normal human serum (> 400 healthy donors, Sanquin diagnostics) with purified fHbp (a kind gift of Prof. Christoph Tang, University of Oxford, UK) added during the sample step. A concentration of 100 µg/mL fHbp was used relative to 100% serum, representing an approximate 1-to-1 molar ratio with FH, using fHbp wildtype variants 1 and 3, as well as the fHbp variant 1 mutant that is unable to bind FH.

N. meningitidis Quantification

Three sets of primers/probes widely used in molecular diagnostics laboratories targeting three different conserved genes (*metA*, *sodC* and *tauE*) in *N. meningitidis* were used for bacterial load quantification by qPCR (**Supplementary Table 1**). Master mixes (LightCycler® 480 II Master mix, 2X conc., Cat. nr. 04887301001, Roche, Basel, Switzerland) contained 2.5 µL primers (200 nM), 2.5 µL probe (100 nM) and 20 µL template DNA in a total reaction volume of 50 µL, following manufacturer's recommendations. Initial denaturation of 95°C for 7 minutes was followed by 50 cycles of 95°C for 10 s, 60°C for 40 s, and 72°C for 1 s and a final cooling step at 40°C for 10 s. Quantification was estimated using *N. meningitidis* DNA Standards copies/µL (dilution series of $1.15x10^{-6}$ to $1.15x10^{-3}$) AMPLIRUN® DNA Control ($1.15x10^{-7}$ copies/µL. Amplification data were analyzed by instrument software (Roche).

Statistical Analysis

Data were analyzed using GraphPad Prism, version 8 (GraphPad software, La Jolla, CA, USA) and R version 3.5.0 (33). Statistical significance between two groups was tested with a Mann-Whitney test. Statistical significance between multiple groups was tested by a Kruskal-Wallis test (unpaired data) or Friedman test (paired data), both followed by a Dunn's multiple comparison's test. Correlations (*r*) were assessed using Pearson's measure of association, followed by the Benjamini-Hochberg procedure to control for the false discovery rate (FDR, set to 0.05).

RESULTS

Study Cohort

Serum samples were available from 106 children with MD (**Table 1**). The patient age ranged from 0.1 – 16 years at admission with a median age of 2.9 years with equal gender distribution. Convalescent samples were drawn 10 – 2011 days after infection, with a median of 65 days. Acute stage samples were obtained at the first or second day of hospitalization. In seventeen patients, samples were also obtained during subsequent days. Fourteen patients (13%) were diagnosed with localized meningococcal meningitis, 75 (71%) with meningococcal septicemia, and seventeen (16%) with both (*i.e.* proven septicemia and meningitis). Fifteen out of the 106 patients did not survive. Death occurred at a median of one day (range 0 – 11). *N. meningitidis* serogroup was successfully typed in 69 cases, with serogroup B being the most prevalent (43 cases, 61%), followed by serogroup C (24 cases, 34%) and single cases of serogroup A and W135.

FH and FHR Protein Levels Decrease Equally During MD

We assessed the levels of FH and all FHRs in the first sample drawn at the acute stage and at convalescence from MD patients, using in-house developed ELISAs (**Figures 1A, B**) (8, 19, 24). FH, FHR-1/1, FHR-1/2, FHR-2/2 and FHR-5 levels at convalescence were comparable to those of healthy children (**Table 2**) (9). Levels of FHR-3 and FHR-4A were found to be higher at convalescence than FHR-3 and FHR-4A levels in healthy children. Two children appeared to carry a homozygous *CFHR3/CFHR1* deletion, as evidenced by the lack of either protein in their convalescent sample. No apparent *CFHR3/CFHR1* deletion was found among the non-survivors, based on their acute stage FHR-3 and FHR-1/1 levels.

At the acute stage, both FH and all FHRs were markedly decreased, with median levels 50-64% lower than found at convalescence (**Figure 1B**, **Table 2**). In contrast to all other FH family proteins, the acute stage FHR-4A levels, while being significantly decreased compared to those found at convalescence, were not significantly lower compared to the normal range found in healthy children. The relative decreases of all FH family proteins strongly correlated with each other, indicating a similar underlying mechanism (**Figures 1C, D**). Of note, the FH and FHR ELISAs were unaffected by the possible presence of circulating fHbp in human serum (**Supplementary Figure 1**).

FH Family Proteins Show Different Kinetics Following the Acute Stage of Infection

After having established that all FH family proteins were decreased proportionally during the acute phase of infection, we investigated the changes in concentration on subsequent days in a subset of seventeen patients. In contrast to the equal decrease upon infection, recovery of the FH family proteins in the subsequent days differed from each other (**Figures 2A, B**).

TABLE 1 | Patient characteristics.

Number of female cases (%)	**52 (49%)**
Median age (y) at admission (IQR)	2.9 (1.3 – 7.9)
Median time interval (days) of convalescence sample drawn after admission (IQR)	65 (49 – 78)
Cases of meningococcal meningitis (%)	14 (13%)
Cases of meningococcal septicemia (%)	75 (71%)
Cases of meningococcal septicemia and meningitis (%)	17 (16%)

Characteristics of pediatric MD cohort of 106 patients. IQR, interquartile range.

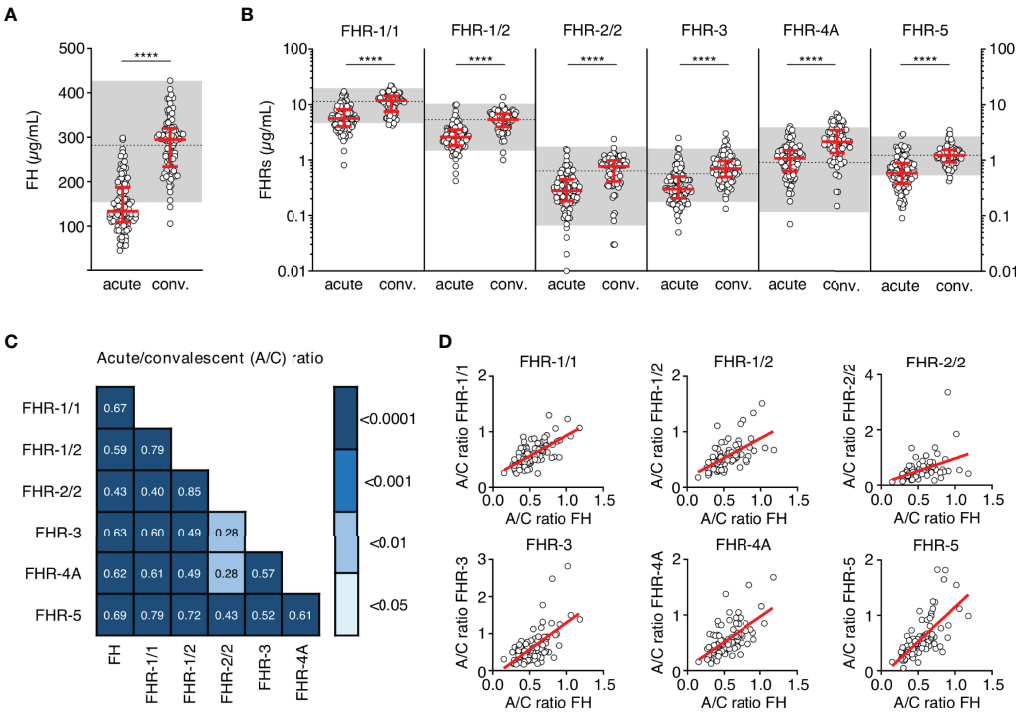

FIGURE 1 | FH family protein levels are low at the acute stage of MD. **(A, B)** Differences in FH, FHR-1/1 homodimers, FHR-1/2 heterodimers, FHR-2/2 homodimers, FHR-3, FHR-4A and FHR-5 homodimers as assessed at the acute stage (samples obtained during the first or second day of hospitalization, *n* = 106) compared to levels at convalescence (*n* = 91). Two children appeared to carry a homozygous *CFHR3/CFHR1* deletion, as evidenced by the lack of either protein in their convalescent sample. They were excluded from the analysis for FHR-1/1, FHR-1/2, FHR-2/2 and FHR-3 (*n* = 104 and *n* = 89 for acute stage and convalescence). Acute serum samples comprised 88 samples drawn at day 1 and 18 samples drawn at day 2 of hospitalization, for patients of whom no day 1 sample was available. Levels of FHR-2/2 were calculated based on FHR-1/1 and FHR-1/2 levels. Shaded area indicates 95% range in healthy patients, with dashed line indicating the median ****p < 0.0001. Scatter dot plots depict median and interquartile range (IQR) as red lines. Statistical significance was tested using a Mann-Whitney test. **(C)** Correlations (*r*) between the relative decreases of FH family proteins (ratios between acute and convalescent levels, by dividing acute levels over convalescent levels) were assessed using Pearson's measure of association, followed by the Benjamini-Hochberg procedure to control for the false discovery rate (FDR, set to 0.05). Blue shades indicate, from light to dark: $p < 0.05$; $p < 0.01$; $p < 0.001$; and $p < 0.0001$. **(D)** Examples of correlations in **(C)**, showing relative decrease in FH levels versus relative decrease in FHR levels. A/C ratio, acute/convalescent ratio; Conv., convalescent.

TABLE 2 | FH protein family ranges during MD.

Protein (µg/mL)	Reference interval (RI)	Convalescent level MD patients	Mann-Whitney test (*p* value) (RI *vs* conv.)	Acute level MD patients	Decrease (median)	Mann-Whitney test (*p* value) (conv. *vs* acute)
FH	282 (238 – 326)	295 (234 – 320)	0.8056	131 (109-181)	56%	< 0.0001
FHR-1/1	11.36 (7.39 – 14.26)	11.85 (7.50 – 14.48)	0.7445	5.59 (3.96 – 8.07)	53%	< 0.0001
FHR-1/2	5.40 (3.92 – 7.01)	5.39 (3.99 – 6.90)	0.9624	2.59 (1.81 – 3.53)	52%	< 0.0001
FHR-2/2	0.64 (0.40 – 1.11)	0.78 (0.41 – 0.98)	0.9316	0.28 (0.19 – 0.47)	64%	< 0.0001
FHR-3	0.57 (0.38 – 0.80)	0.69 (0.48 – 0.98)	0.0074	0.30 (0.20 – 0.50)	57%	< 0.0001
FHR-4A	0.91 (0.48 – 1.50)	2.16 (1.35 – 3.46)	<0.0001	1.07 (0.63 – 1.49)	50%	< 0.0001
FHR-5	1.23 (0.92 – 1.47)	1.23 (0.92 – 1.55)	0.9956	0.58 (0.37 – 0.88)	53%	< 0.0001

Reference intervals (RIs) as previously described for 110 healthy Dutch children (9). RIs and convalescent levels of MD patients of FHR-1/1, FHR-1/2, FHR-2/2 and FHR-3 exclude the non-detectable levels of those who presumably carry the homozygous CFHR3/CFHR1 deletion. All protein levels depict median and interquartile range (IQR) in µg/mL. Mann-Whitney tests describe comparisons between the RIs vs convalescent levels and between convalescent levels vs. during the acute stage.

The median FH levels remained low during the first days of hospitalization but showed a sign of recovery to normal levels at day four. In contrast, levels of FHR-1/1, FHR-1/2, FHR-2/2 and FHR-3 showed a quicker recovery. FHR-4A levels did not change during the first four days of hospitalization, remaining at approximately 50% of convalescent levels. Blood levels of FHR-5 recovered more steadily, similar to FH. The decrease in serum levels at the acute stage of MD was not unique to the FH family proteins, since total IgG levels, which were measured as a reference protein of similar molecular weight as FH, showed a similar decrease and dynamics (**Figure 2C**) (32).

FH and FHR Levels Associate With Clinical and Laboratory Parameters

Next, we analyzed whether the low FH and FHR levels at the acute stage were related to the classification or severity of MD. Levels of FH, FHR-1/1, FHR-1/2, FHR-3 and FHR-4A were lower in patients diagnosed with septicemia in comparison to those with meningitis alone (**Figure 3**). Levels of FHR-2/2 were comparable between the patient groups, while FHR-5 levels were lower in patients who were diagnosed with septicemia alone when compared to meningococcal meningitis with accompanying septicemia (**Figure 3**).

We also assessed whether the FH and FHR levels at acute stage correlated with the clinical parameters WCC, platelet count, aPTT, INR, fibrinogen, CRP, potassium, base excess, lactate, the severity scores PIM and GMSPS, and the bacterial load (**Table 3** and **Figure 4**). Overall, all correlations indicated a negative effect of low acute stage FH and/or FHR levels, *i.e.* low protein levels correlating with more adverse clinical values. Acute stage FH levels correlated with most clinical parameters, with only potassium, lactate and the PIM score showing no significant correlation with FH. Of the FHRs, FHR-1 and FHR-5 correlated most with various clinical parameters. There was a striking correlation between low levels of all FH family proteins and base excess. Although reduced base excess correlated with increased lactate levels in the patients (r = -0.56, $p < 0.0001$), the FH family protein levels were not correlated with lactate. Although both base excess and lactate are markers of impaired perfusion and shock, the correlation with base excess and not with lactate may have been influenced by the increase in base excess associated with resuscitation with high chloride-containing fluids (normal saline or 5% albumin), which cause a worsening of base excess due to hyperchloremic acidosis (34). FH family protein levels were lowest in those patients receiving renal support (**Figure 5** and **Supplementary Figure 2**). All patients receiving renal support were diagnosed with sepsis, precluding any further analysis of the relationship between FH levels and kidney function.

Acute stage levels FH, FHR-1/1, FHR-1/2, FHR-4A and FHR-5 correlated with bacterial load, which is a well-established marker of MD severity (**Figure 4**). We determined the *N. meningitidis* bacterial load in 62 patients of whom sufficient acute stage serum was available. The bacterial load ranged from $8.52*10^0$ to $1.04*10^9$ copies per mL serum (median = $5.68*10^4$). We did not observe a difference between serogroups B and C in bacterial load (p = 0.33, Mann-Whitney test), nor did we observe a difference in severity (by PIM score, p = 0.26, Mann-Whitney test). Except for FHR-5, we did not observe a significant association between *N. meningitidis* serogroups B or C and acute stage FH family protein levels (**Supplementary Figure 3**). Bacterial load correlated negatively with base excess (r = -0.42, $p < 0.001$) and positively with lactate (r = 0.68, $p < 0.0001$).

DISCUSSION

The role of complement in MD is complex and can be regarded as a "double-edged sword". While its activation is essential for the clearance of invading microbes, too much complement

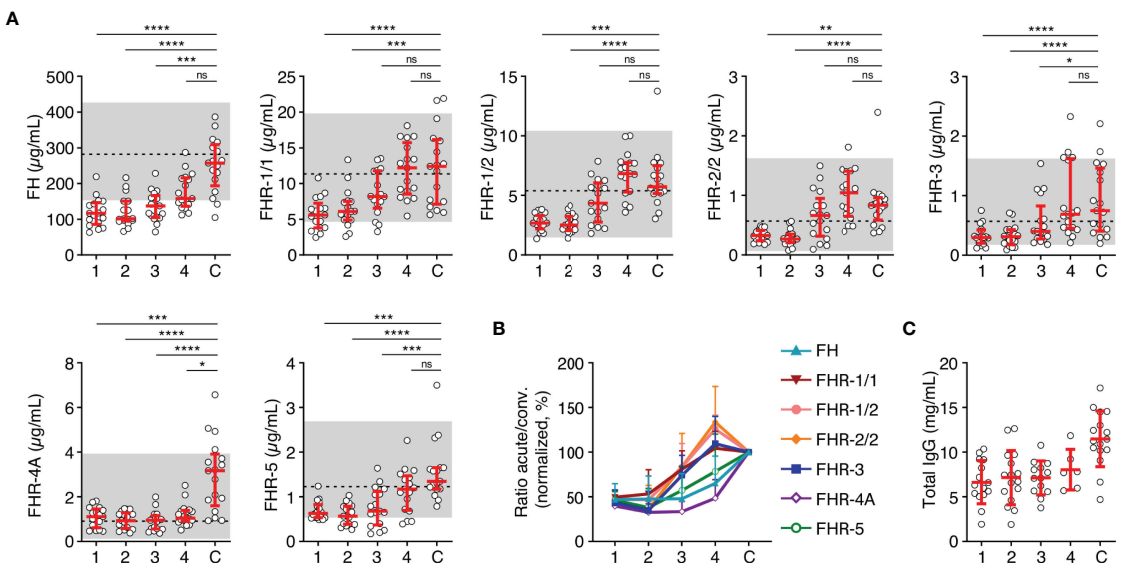

FIGURE 2 | FH family protein level dynamics during the acute stage of MD. **(A)** FH family protein levels in paired samples (n = 17) as assessed during the first four days of infection (day 1 until day 4), compared with the concentration at convalescence **(C)**. Shaded area indicates 95% range in healthy patients, with dashed line indicating the median. Friedman test followed by Dunn's multiple comparisons test, with every acute stage dataset compared to the levels found at convalescence. ****$p < 0.0001$; ***$p < 0.001$; **$p < 0.01$; *$p < 0.05$; ns, not significant. **(B)** FH family protein levels as in **(A)**, normalized to the levels found at convalescence. **(C)** Total IgG levels in unpaired samples (maximum n = 16) as assessed during the first four days of infection and at convalescence. The 95% range in healthy patients is not depicted, due to variability of total IgG levels during childhood. Lines depict median and IQR.

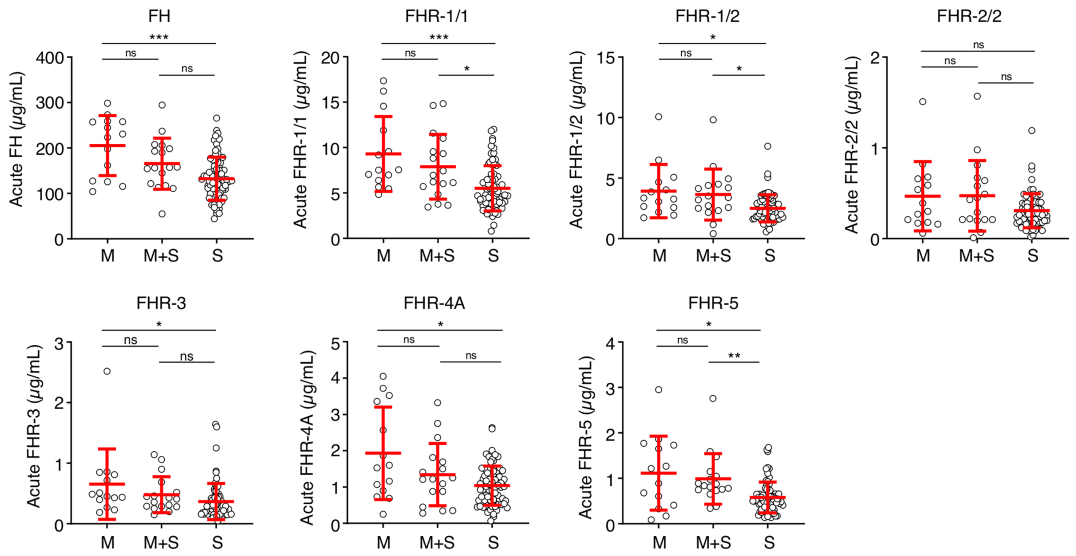

FIGURE 3 | FH family proteins per clinical syndrome. Protein levels of FH, FHR-1/1, FHR-1/2, FHR-3, FHR-4A and FHR-5 at the acute stage (first sample obtained during hospitalization, *n* = 106), according to the diagnosed clinical syndrome: meningococcal meningitis (M, *n* = 14), meningococcal septicemia (S, *n* = 75), or both (M+S, *n* = 17). Statistical significance was tested using a Kruskal-Wallis test, followed by a Dunn's multiple comparisons test. Lines depict median and IQR. $^{**}p < 0.01$; $^{*}p < 0.05$; $^{***}p < 0.001$; ns, not significant.

activation may contribute to immunopathology. Plasma levels of FH are subjected to a similarly delicate balance: high FH levels protect host tissues from complement-mediated damage, but this also increases survival of FH-binding pathogens such as *N. meningitidis* (16, 35). In contrast, low FH levels decrease complement evasion of FH-binding pathogens but renders host tissue more vulnerable to complement-mediated damage. This delicate balance in FH levels is further complicated by the presence of the proposed FH antagonists, the FHRs. It is hypothesized that the competition between FH and the FHRs determines to what extent and at what rate alternative pathway activation takes place on surfaces (17). With the recent insight that fHbp also binds FHR-3, it was suggested that the levels of FHR-3 determine if *N. meningitidis* successfully recruits FH and evades complement, and thereby would play a crucial role in developing MD (23). Our previous research demonstrated that a systemic competition between FH and FHR-3 is unlikely to occur during steady-state, where the molar excess of FH is ~130-fold compared with FHR-3 (8). However, it was unknown up until now whether this would also hold true during MD.

Although FH and possibly FHR-3 play an important role in MD susceptibility, the dynamics of their plasma levels during the acute stage of MD were unknown. By measuring all FH family protein levels during MD in the first days after admission, we observed that the protein levels of both FH and the FHRs were markedly decreased during the acute stage of MD, whereas their recovery towards normal levels showed different kinetics. FH and FHR-5 levels slowly progressed to normal levels, suggesting a low synthesis rate of these proteins by the liver, or alternatively, that their consumption or loss

TABLE 3 | Clinical and laboratory parameters.

Parameter	Normal range	*n*	MD patients Median (IQR)
WCC (*10^9/L)	4.0 – 11.0	105	9.3 (3.7 – 23.5)
Platelet count (*10^9/L)	150 – 400	105	196 (132 – 256)
aPTT (s)	30 – 40	99	45.9 (36 – 61.9)
INR	0.8 – 1.2	94	1.6 (1.3 – 1.8)
Fibrinogen (g/L)	1.5 – 4.0	84	3.1 (1.9 – 4.5)
CRP (mg/L)	5 – 10	93	92 (54 – 157)
Potassium (mM/L)	3.5 – 5.0	103	3.5 (3.2 – 3.9)
Base Excess (mEq/L)	-2 – 2	104	-7 (-10 – -5)
Lactate (mmol/L)	0.5 – 1	56	1.6 (0.9 – 3.7)
PIM	0	100	4.9 (2.4 – 14.0)
GMSPS	0	106	10 (7 – 12)

n, number of informative cases; IQR, interquartile range; WCC, white cell count; aPTT, activated partial thromboplastin time; INR, international normalized ratio; CRP, C-reactive protein; PIM, Pediatric Index of Mortality; GMSPS, Glasgow Meningococcal Septicemia Prognostic Score.

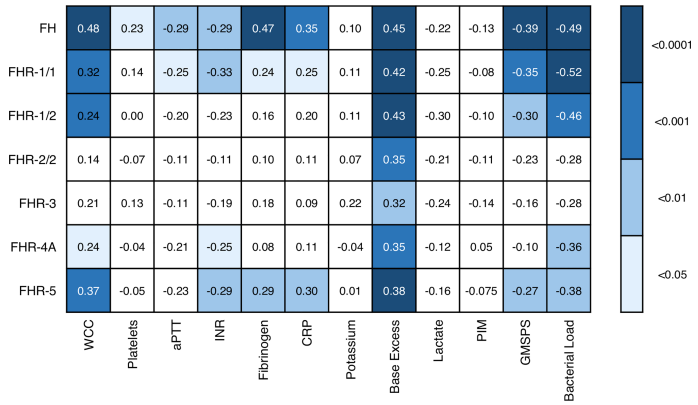

FIGURE 4 | Associations of acute stage FH family protein levels with clinical and laboratory parameters. Pearson correlation coefficients (*r*), considering twelve severity markers and seven FH family proteins (including the different dimers). Correlations were assessed using Pearson's measure of association, followed by the Benjamini-Hochberg procedure to control for the false discovery rate (FDR, set to 0.05). Blue shades indicate, from light to dark: $p < 0.05$; $p < 0.01$; $p < 0.001$; and $p < 0.0001$. WCC, white cell count; aPTT, activated partial thromboplastin time; INR, international normalized ratio; CRP, C-reactive protein; PIM, pediatric index of mortality; GMSPS, Glasgow Meningococcal Septicemia Prognostic Score.

from the circulation may be prolonged. FHR-1, FHR-2 and FHR-3 showed quicker recoveries within a few days after admission, while FHR-4A did not recover during the first four days. As the main production site of the FH protein family is the liver, the various observed recovery rates indicate that liver synthesis is not generally low during MD.

During the acute stage of MD, necrotic or damaged tissue, including the vasculature, will activate complement (36, 37). The reduction of FH and the FHRs in the circulation may therefore be due to the subsequent recruitment of these proteins to sites of complement activation. Alternatively, it can be hypothesized that the protein levels are low because of dilution due to

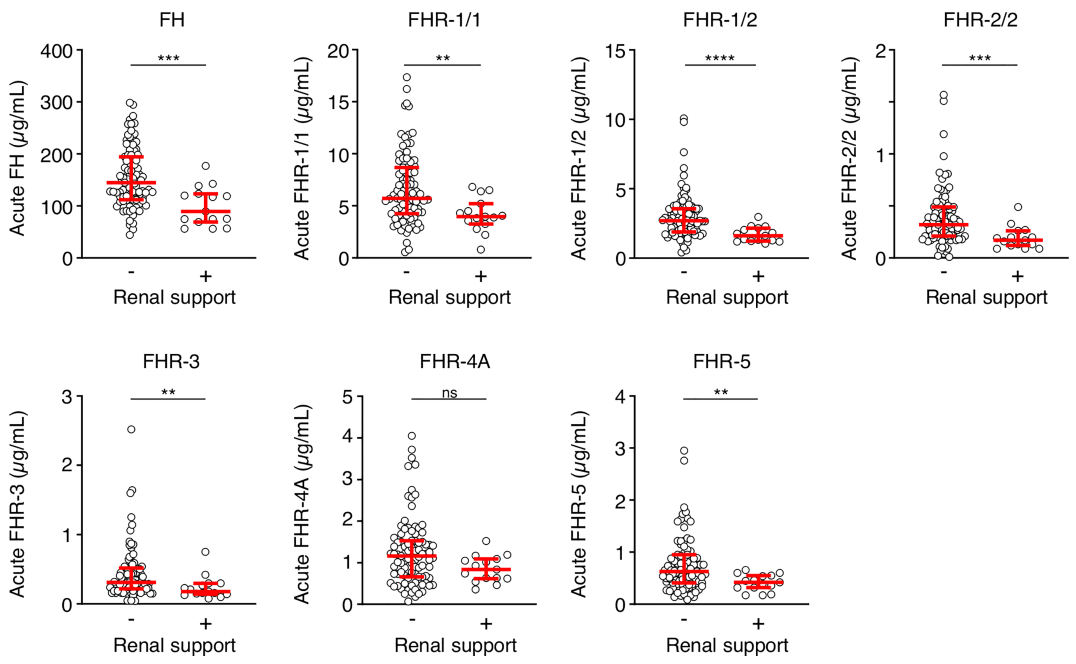

FIGURE 5 | FH family proteins are low in patients who receive renal support. Serum levels of FH, FHR-1/1, FHR-1/2, FHR-2/2, FHR-3, FHR-4A and FHR-5 at the acute stage of patients who did ($n = 15$) or did not ($n = 90$) receive renal support. Both surviving and non-surviving patients are included here. Statistical significance was tested using a Mann-Whitney test. Lines depict median and IQR. ****$p < 0.0001$; ***$p < 0.001$; **$p < 0.01$; ns, not significant.

administration of resuscitation fluids and additional passive leakage into the tissues due to increased vascular permeability (38). Both processes could account for the lower protein levels during the acute stage of meningococcal septicemia, which is a more systemic disease in comparison to meningococcal meningitis. In support of combined dilution and increased vascular permeability as underlying mechanisms, the serum levels of IgG (of similar molecular weight as FH) were also decreased, suggesting a non-selective lowering of proteins in the blood compartment. This is in line with clinical vascular leakage and edema formation known to occur during treatment at the early stage of the disease. If vascular leakage and dilution would be accounting completely for the initial loss of proteins, similar recovery rates are expected. However, the FH protein family showed different dynamics in subsequent days, suggesting that other processes are at play. We could not determine whether their different dynamics are reflecting different roles for each of the proteins during inflammatory responses or are due to different rates of synthesis.

Finally, FH levels could be low due to recruitment *via* fHbp on the meningococci. However, this was also observed for FHRs that are not bound by *N. meningitidis* (23). Moreover, the observed decreases of all FH family proteins correlated strongly with each other and were reduced to a similar extent as IgG. This suggests that the reduced plasma concentrations are due to general leakage from the circulation rather than consumption due to binding on meningococci.

FHR-3 is the only FHR bound by fHbp that can compete with FH *in vitro* and might affect *N. meningitidis* survival (23). However, its acute stage protein levels did not correlate with bacterial load. The vastly different molar concentrations of FH and FHR-3, with FH circulating at a >100-fold excess compared to FHR-3, make it unlikely that substantial amounts of FHR-3 would be bound by meningococci, and that this would be reflected in plasma levels. The proposed role of FHR-3 as competitor of FH in meningococcal disease therefore is unlikely to play a role in the circulation.

Of the FH protein family, FH was found to correlate most with MD severity parameters. Lower FH levels during the acute stage correlated with the prediction score GMSPS as well as the blood variables which are known to be associated with MD severity, including WCC, platelets, base excess, INR and aPTT. The correlation of FH with coagulation markers such as fibrinogen, INR and aPTT is in line with previous studies on sepsis and FH (25, 26), and corroborates an *in vitro* study that suggests a potential role for FH in coagulation (39). The association of FH with severity also explains the observed association of FH and FHRs with bacterial load. While, as discussed above, this is unlikely to reflect consumption, bacterial load is a strong predictor of severity, and thus the associations with FH and FHRs are suggestive of FH and FHR clearance due to severe inflammation and the accompanying complement activation (40, 41).

The lowest levels of most FH family proteins were associated with clinical manifestations of renal failure during hospitalization. While this may be part of the association of reduced FH and FHRs with disease severity, regulation of complement activation by FH is known to be involved in renal disease during hemolytic uremic syndrome and glomerulonephritis (17). We speculate that the association of FH (and FHRs) with impaired kidney function may not only be linked to disease severity, but rather could indicate a specific protective role of the FH family proteins in preventing renal failure when levels drop because of disease.

The double activity of FH, protecting both host tissue and meningococci against complement-mediated damage, makes analysis of its role in MD challenging. Following what has previously been found *in vitro* for *N. meningitidis* (16), where small changes in FH levels greatly affect survival, we propose that a balanced concentration of FH in blood is key in MD. Low steady-state FH levels may reduce susceptibility towards MD, but if MD does occur, the low FH levels may be insufficient to protect the vasculature and kidneys from complement-mediated damage (35). Indeed, it has previously been shown that inhibition of complement improves survival of mice suffering from bacterial meningitis (42). Therapeutic interventions that substantially increase the levels of FH activity on host surfaces (and not on microbial surfaces) may reduce tissue injury, when administered as soon as patients have been treated with antibiotics to eliminate meningococci from the circulation. A potentiating antibody that increases the function of FH on host surfaces without enhancing binding to meningococci might therefore be worth investigating in acute stages of systemic inflammation (35).

DATA AVAILABILITY STATEMENT

The raw data supporting the conclusions of this article will be made available by the authors, without undue reservation.

ETHICS STATEMENT

The studies involving human participants were reviewed and approved by Imperial College Research Ethics Committee. Written informed consent to participate in this study was provided by the participants' legal guardian/next of kin.

AUTHOR CONTRIBUTIONS

AB, RP, DW, ML, and TK designed research. AB, RP, VW, NS, MB, JT, and LC-B performed research. VW, DI, CH, and RG collected data and materials used in this study. CF, IJ, MH, DW, ML, and TK supervised aspects of the project. AB, RP, and NS analyzed data. AB, RP, IJ, DW, and TK drafted the manuscript. All authors critically reviewed the manuscript, gave final approval of the version to be published, and agreed to be accountable for all aspects of the work in ensuring that

questions related to the accuracy or integrity of any part of the work are appropriately investigated and resolved.

FUNDING

Research leading to these results has received funding from Meningitis Research Foundation and Imperial College BRC, and the European Union's seventh Framework program under EC-GA no. 279185 (EUCLIDS; www.euclids-project.eu). The funders had no role in study design, data collection and analysis, decision to publish, or preparation of the manuscript.

ACKNOWLEDGMENTS

The authors would like to thank the patients participating in the study.

SUPPLEMENTARY MATERIAL

The Supplementary Material for this article can be found online at: https://www.frontiersin.org/articles/10.3389/fimmu.2022.876776/full#supplementary-material

REFERENCES

1. Christensen H, May M, Bowen L, Hickman M, Trotter CL. Meningococcal Carriage by Age: A Systematic Review and Meta-Analysis. *Lancet Infect Dis* (2010) 10:853–61. doi: 10.1016/S1473-3099(10)70251-6
2. Borrow R, Alarcón P, Carlos J, Caugant DA, Christensen H, Debbag R, et al. The Global Meningococcal Initiative: Global Epidemiology, the Impact of Vaccines on Meningococcal Disease and the Importance of Herd Protection. *Expert Rev Vaccines* (2016) 16:313–28. doi: 10.1080/14760584.2017.1258308
3. Sridhar S, Greenwood B, Head C, Plotkin SA, Sáfadi MA, Saha S, et al. Global Incidence of Serogroup B Invasive Meningococcal Disease: A Systematic Review. *Lancet* (2015) 15:1334–46. doi: 10.1016/S1473-3099(15)00217-0
4. Kuijpers TW, Nguyen M, Th C, Hopman P, Nieuwenhuys E, Dewald G, et al. Complement Factor 7 Gene Mutations in Relation to Meningococcal Infection and Clinical Recurrence of Meningococcal Disease. *Mol Immunol* (2010) 47:671–7. doi: 10.1016/j.molimm.2009.10.017
5. Schejbel L, Fadnes D, Permin H, Tore K, Garred P, Eirik T. Primary Complement C5 Deficiencies – Molecular Characterization and Clinical Review of Two Families. *Immunobiology* (2013) 218:1304–10. doi: 10.1016/j.imbio.2013.04.021
6. Madico G, Welsch JA, Lewis LA, McNaughton A, Perlman DH, Costello CE, et al. The Meningococcal Vaccine Candidate GNA1870 Binds the Complement Regulatory Protein Factor H and Enhances Serum Resistance. *J Immunol* (2006) 177:501–10. doi: 10.4049/jimmunol.177.1.501
7. Schneider MC, Exley RM, Chan H, Feavers I, Kang Y, Sim RB, et al. Functional Significance of Factor H Binding to Neisseria Meningitidis. *J Immunol* (2006) 176:7566–75. doi: 10.4049/jimmunol.176.12.7566
8. Pouw RB, Brouwer MC, Geissler J, van Herpen LV, Zeerleder SS, Wuillemin WA, et al. Complement Factor H-Related Protein 3 Serum Levels Are Low Compared to Factor H and Mainly Determined by Gene Copy Number Variation in CFHR3. *PloS One* (2016) 11:e0152164. doi: 10.1371/journal.pone.0152164
9. van Beek AE, Kamp A, Kruithof S, Nieuwenhuys EJ, Wouters D, Jongerius I, et al. Reference Intervals of Factor H and Factor H-Related Proteins in Healthy Children. *Front Immunol* (2018) 9:1727. doi: 10.3389/fimmu.2018.01727
10. Dopler A, Stibitzky S, Hevey R, Mannes M, Guariento M, Höchsmann B, et al. Deregulation of Factor H by Factor H-Related Protein 1 Depends on Sialylation of Host Surfaces. *Front Immunol* (2021) 12:615748. doi: 10.3389/fimmu.2021.615748
11. Lewis LA, Ngampasutadol J, Wallace R, Reid JEA, Vogel U, Ram S. The Meningococcal Vaccine Candidate Neisserial Surface Protein a (NspA) Binds to Factor H and Enhances Meningococcal Resistance to Complement. *PloS Pathog* (2010) 6:1–20. doi: 10.1371/journal.ppat.1001027
12. Lewis LA, Vu DM, Vasudhev S, Shaughnessy J, Granoff DM, Ram S. Factor H-Dependent Alternative Pathway Inhibition Mediated by Porin B Contributes to Virulence of Neisseria Meningitidis. *MBio* (2013) 4:1–9. doi: 10.1128/mBio.00339-13
13. Giuntini S, Pajon R, Ram S, Granoff DM. Binding of Complement Factor H to PorB3 and NspA Enhances Resistance of Neisseria Meningitidis to Anti-Factor H Binding Protein Bactericidal Activity. *Infect Immun* (2015) 83:1536–45. doi: 10.1128/IAI.02984-14
14. Loh E, Kugelberg E, Tracy A, Zhang Q, Gollan B, Ewles H, et al. Temperature Triggers Immune Evasion by Neisseria Meningitidis. *Nature* (2013) 502:237–40. doi: 10.1038/nature12616
15. Schneider MC, Prosser BE, Caesar JJE, Kugelberg E, Li S, Zhang Q, et al. Neisseria Meningitidis Recruits Factor H Using Protein Mimicry of Host Carbohydrates. *Nature* (2009) 458:890–3. doi: 10.1038/nature07769
16. Haralambous E, Dolly SO, Hibberd ML, Litt DJ, Udalova IA, O'dwyer C, et al. Factor H, a Regulator of Complement Activity, is A Major Determinant of Meningococcal Disease Susceptibility in UK Caucasian Patients. *Scand J Infect Dis* (2006) 38:764–71. doi: 10.1080/00365540600643203
17. Sánchez-Corral P, Pouw RB, López-Trascasa M, Józsi M. Self-Damage Caused by Dysregulation of the Complement Alternative Pathway: Relevance of the Factor H Protein Family. *Front Immunol* (2018) 9:1607. doi: 10.3389/fimmu.2018.01607
18. Goicoechea de Jorge E, Caesar JJE, Malik TH, Patel M, Colledge M, Johnson S, et al. Dimerization of Complement Factor H-Related Proteins Modulates Complement Activation *In Vivo*. *Proc Natl Acad Sci U.S.A.* (2013) 110:4685–90. doi: 10.1073/pnas.1219260110
19. van Beek AE, Pouw RB, Brouwer MC, van Mierlo G, Geissler J, Ooijevaar-De Heer P, et al. Factor H-Related (FHR)-1 and FHR-2 Form Homo- and Heterodimers, While FHR-5 Circulates Only As Homodimer in Human Plasma. *Front Immunol* (2017) 8:1328. doi: 10.3389/fimmu.2017.01328
20. Kühn S, Skerka C, Zipfel PF. Mapping the Complement Regulatory Domains in the Human Factor H-Like Protein 1 and in Factor H. *J Immunol* (1995) 155:5663–70.
21. Gordon DL, Kaufman RM, Blackmore TK, Kwong J, Lublin DM. Identification of Complement Regulatory Domains in Human Factor H'. *J Immunol* (1995) 155:8–11.
22. Davila S, Wright VJ, Khor CC, Sim KS, Binder A, Breunis WB, et al. Genome-Wide Association Study Identifies Variants in the CFH Region Associated With Host Susceptibility to Meningococcal Disease. *Nat Genet* (2010) 42:772–6. doi: 10.1038/ng.640
23. Caesar JJ, Lavender H, Ward PN, Exley RM, Eaton J, Chittock E, et al. Competition Between Antagonistic Complement Factors for a Single Protein on N. Meningitidis Rules Disease Susceptibility. *Elife* (2014) 3:1–14. doi: 10.7554/eLife.04008
24. Pouw RB, Brouwer MC, van Beek AE, Józsi M, Wouters D, Kuijpers TW. Complement Factor H-Related Protein 4A is the Dominant Circulating Splice Variant of CFHR4. *Front Immunol* (2018) 9:729. doi: 10.3389/fimmu.2018.00729
25. Higgins SJ, De Ceunynck K, Kellum JA, Chen X, Gu X, Chaudhry SA, et al. Tie2 Protects the Vasculature Against Thrombus Formation in Systemic Inflammation. *J Clin Invest* (2018) 128:1471–84. doi: 10.1172/JCI97488
26. Shimizu J, Fujino K, Sawai T, Tsujita Y, Tabata T, Eguchi Y. Association Between Plasma Complement Factor H Concentration and Clinical Outcomes in Patients With Sepsis. *Acute Med Surg* (2021) 8:1–7. doi: 10.1002/ams2.625
27. Hibberd ML, Sumiya M, Summerfield JA, Booy R, Levin M. Association of Variants of the Gene for Mannose-Binding Lectin With Susceptibility to Meningococcal Disease. *Lancet* (1999) 353:1049–53. doi: 10.1016/S0140-6736(98)08350-0
28. Haralambous E, Weiss H, Radalowicz A, Hibberd M, Booy R, Levin M. Sibling Familial Risk Ratio of Meningococcal Disease in UK Caucasians. *Epidemiol Infect* (2003) 130:413–8. doi: 10.1017/S0950268803008513

29. Wright V, Hibberd M, Levin M. Genetic Polymorphisms in Host Response to Meningococcal Infection: The Role of Susceptibility and Severity Genes. *Vaccine* (2009) 27S:B90–B102. doi: 10.1016/j.vaccine.2009.05.002
30. Sinclair JF, Skeoch CH, Hallworth D. Prognosis of Meningococcal Septicaemia. *Lancet* (1987) 2:38. doi: 10.1016/S0140-6736(87)93067-4
31. Pollack MM, Patel KM, Ruttimann UE. PRISM III: An Updated Pediatric Risk of Mortality Score. *Crit Care Med* (1996) 24:743–52. doi: 10.1097/00003246-199605000-00004
32. Van De Bovenkamp FS, Derksen NIL, Ooijevaar-de Heer P, Van Schie KA, Kruithof S, Berkowska MA, et al. Adaptive Antibody Diversification Through N-Linked Glycosylation of the Immunoglobulin Variable Region. *Proc Natl Acad Sci U.S.A.* (2018) 115:1901–6. doi: 10.1073/pnas.1711720115
33. R Core Team. *R: A Language and Environment for Statistical Computing*. Austria: R Found Stat Comput Vienna (2015).
34. Levin M, Cunnington AJ, Wilson C, Nadel S, Lang HJ, Ninis N, et al. Effects of Saline or Albumin Fluid Bolus in Resuscitation: Evidence From Re-Analysis of the FEAST Trial. *Lancet Respir Med* (2019) 7:581–93. doi: 10.1016/S2213-2600(19)30114-6
35. Pouw RB, Brouwer MC, de Gast M, van Beek AE, van den Heuvel LP, Schmidt CQ, et al. Potentiation of Complement Regulator Factor H Protects Human Endothelial Cells From Complement Attack in aHUS Sera. *Blood Adv* (2019) 3:621–32. doi: 10.1182/bloodadvances.2018025692
36. Brandtzaeg P, Mollnes TE, Kierulf P. Complement Activation and Endotoxin Levels in Systemic Meningococcal Disease. *J Infect Dis* (1989) 160:58–65. doi: 10.1093/infdis/160.1.58
37. Huson MAM, Wouters D, Van Mierlo G, Grobusch MP, Zeerleder SS, van der Poll T. HIV Coinfection Enhances Complement Activation During Sepsis. *sJ Infect Dis* (2015) 212:474–83. doi: 10.1093/infdis/jiv074
38. Oragui EE, Nadel S, Kyd P, Levin M. Increased Excretion of Urinary Glycosaminoglycans in Meningococcal Septicemia and Their Relationship to Proteinuria. *Crit Care Med* (2000) 28:3002–8. doi: 10.1097/00003246-200008000-00054
39. Ferluga J, Kishore U, Sim RB. A Potential Anti-Coagulant Role of Complement Factor H. *Mol Immunol* (2014) 59:188–93. doi: 10.1016/j.molimm.2014.02.012
40. Darton T, Guiver M, Naylor S, Jack DL, Kaczmarski EB, Borrow R, et al. Severity of Meningococcal Disease Associated With Genomic Bacterial Load. *Clin Infect Dis* (2009) 48:587–94. doi: 10.1086/596707
41. Hackett S, Guiver M, Marsch J, Sills J, Thomson A, Kaczmarski E, et al. Meningococcal Bacterial DNA Load at Presentation Correlates With Disease Severity. *Arch Dis Child* (2002) 86:44–6. doi: 10.1136/adc.86.1.44
42. Kasanmoentalib ES, Valls Seron M, Morgan BP, Brouwer MC, van de Beek D. Adjuvant Treatment With Dexamethasone Plus Anti-C5 Antibodies Improves Outcome of Experimental Pneumococcal Meningitis: A Randomized Controlled Trial. *J Neuroinflamm* (2015) 12:1–7. doi: 10.1186/s12974-015-0372-y

Conflict of Interest: RP, MB, DW and TK are co-inventors of patents describing the potentiation of FH with monoclonal antibodies and therapeutic uses thereof. JT, LCB and CF are employed by Micropathology Ltd.

All other authors declare that the research was conducted in the absence of any commercial or financial relationships that could be construed as a potential conflict of interest.

Publisher's Note: All claims expressed in this article are solely those of the authors and do not necessarily represent those of their affiliated organizations, or those of the publisher, the editors and the reviewers. Any product that may be evaluated in this article, or claim that may be made by its manufacturer, is not guaranteed or endorsed by the publisher.

frontiers | Frontiers in Immunology

TYPE Mini Review
PUBLISHED 14 September 2022
DOI 10.3389/fimmu.2022.981375

OPEN ACCESS

EDITED BY
Mihály Józsi,
Eötvös Loránd University, Hungary

REVIEWED BY
Bradley Patton Dixon,
University of Colorado Anschutz Medical Campus, United States
Pilar Sánchez-Corral,
University Hospital La Paz Research Institute (IdiPAZ), Spain

*CORRESPONDENCE
Yoko Yoshida
yokoy122@gmail.com

SPECIALTY SECTION
This article was submitted to Molecular Innate Immunity, a section of the journal Frontiers in Immunology

RECEIVED 29 June 2022
ACCEPTED 25 August 2022
PUBLISHED 14 September 2022

CITATION
Yoshida Y and Nishi H (2022) The role of the complement system in kidney glomerular capillary thrombosis. *Front. Immunol.* 13:981375. doi: 10.3389/fimmu.2022.981375

The role of the complement system in kidney glomerular capillary thrombosis

Yoko Yoshida* and Hiroshi Nishi

Division of Nephrology and Endocrinology, The University of Tokyo Graduate School of Medicine, Tokyo, Japan

The complement system is part of the innate immune system. The crucial step in activating the complement system is the generation and regulation of C3 convertase complexes, which are needed to generate opsonins that promote phagocytosis, to generate C3a that regulates inflammation, and to initiate the lytic terminal pathway through the generation and activity of C5 convertases. A growing body of evidence has highlighted the interplay between the complement system, coagulation system, platelets, neutrophils, and endothelial cells. The kidneys are highly susceptible to complement-mediated injury in several genetic, infectious, and autoimmune diseases. Atypical hemolytic uremic syndrome (aHUS) and lupus nephritis (LN) are both characterized by thrombosis in the glomerular capillaries of the kidneys. In aHUS, congenital or acquired defects in complement regulators may trigger platelet aggregation and activation, resulting in the formation of platelet-rich thrombi in the kidneys. Because glomerular vasculopathy is usually noted with immunoglobulin and complement accumulation in LN, complement-mediated activation of tissue factors could partly explain the autoimmune mechanism of thrombosis. Thus, kidney glomerular capillary thrombosis is mediated by complement dysregulation and may also be associated with complement overactivation. Further investigation is required to clarify the interaction between these vascular components and develop specific therapeutic approaches.

KEYWORDS

complement, kidney, platelet, neutrophil, atypical hemolytic uremic syndrome, thrombosis, lupus nephritis, coagulation

Introduction

Complement system

The complement system is essential for the innate immune system to eliminate invading pathogens. The crucial step in activating the complement system is the generation and regulation of C3 convertase. All complement mechanisms in immune defense, namely opsonization, phagocytosis, inflammation, and target cell lysis, rely on the enzymatic step that generates C3 convertase. The complement system is activated by three different pathways: the classical (CP), lectin (LP), and alternative (AP) pathways (Figure 1). Although each of these routes has a different activation mechanism, they all produce C3 convertase, which cleaves C3 into C3a and C3b to activate the terminal complement pathway and generate C5b-9 (1).

The CP is activated by C1q recognition of antigen-bound antibodies, which eventually induces C1s to produce the CP C3 convertase (C4bC2b) through the cleavage of C2 and C4. In the LP, the binding of mannose-binding lectin (MBL) to microbial carbohydrates triggers the generation of C3 convertase (C4bC2b) *via* the MBL-associated serine proteases 1 and 2 (MASP-1 and MASP-2). In contrast, the AP is constitutively activated at low levels by the hydrolysis of C3 (C3(H_2O)). C3 (H_2O) rapidly reacts with complement factors B (FB) and D, resulting in the formation of an initial fluid-phase C3 convertase (C3(H_2O)Bb). This initial convertase can cleave C3 and generate C3b, which is generally inactivated by various complement regulatory proteins. However, in the presence of pathogens, C3b binds to the target surface and induces the formation of C3 convertase (C3bBb). All C3 convertases (CP/LP C4bC2b and AP C3bBb) can attach to the C3b fragment and form C5 convertases (CP/LP C4bC2bC3b and AP C3bBbC3b), which cleave C5 into C5a and C5b. The C5b molecule sequentially binds to C6, C7, and C8 to form C5b-8. Finally, C5b-8 binds to C9, which polymerizes and forms a transmembrane ring, leading

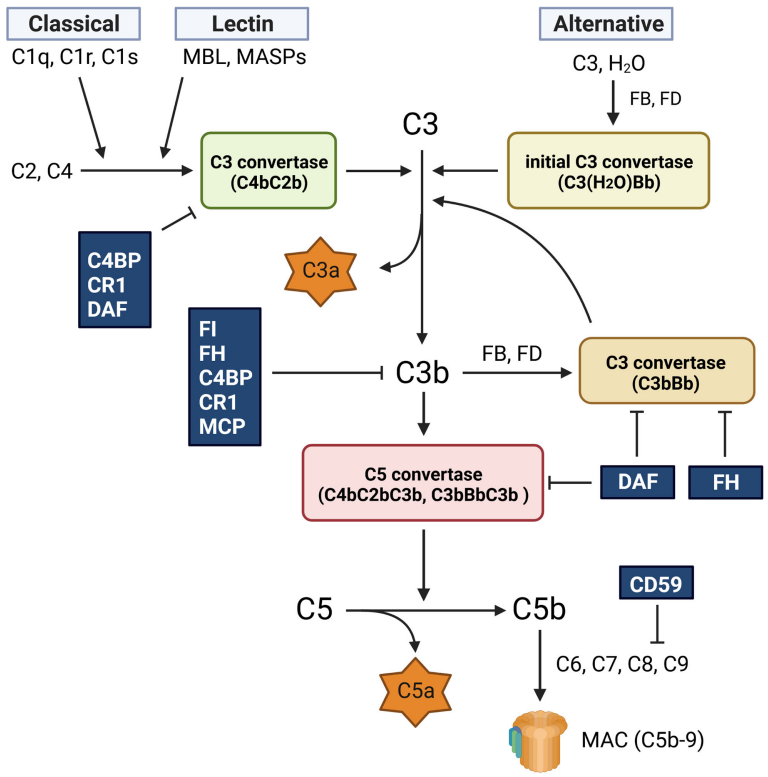

FIGURE 1
Complement activation pathway. The complement system is activated *via* three different pathways: classical (CP), lectin (LP), and alternative (AP). The CP is activated by the binding of C1q to antigen-bound antibodies. This reaction activates C1s and C1r, leading to the formation of the CP C3 convertase (C4bC2b). The LP generates the same C3 convertase as the CP, but its activation is caused by mannose-binding lectin (MBL) and MBL-associated serine proteases (MASPs). The AP is spontaneously activated *via* hydrolysis of C3 (C3 (H_2O)), which generates the initial C3 convertase (C3(H_2O)Bb). All three activation routes merge at the cleavage of C3 and lead to the formation of the C5 convertases (C4bC2bC3b and C3bBbC3b), which cleave C5 into C5a and C5b. The C5b fragment forms the membrane attack complex (C5b-9, MAC) by binding to C6, C7, C8, and C9. C9 polymerization is required for C5b-9 generation. C5b-9 creates pores in the membrane and lyses the target cells. The fragment of C3b is opsonin, and C3a and C5a are also known as anaphylatoxins and chemotactic factors, respectively.

to the formation of C5b-9, which is also known as the membrane attack complex (MAC).

Although cell lysis by C5b-9 is effective against gram-negative bacteria, the complement system also acts against gram-positive bacteria by promoting opsonization and neutrophil phagocytosis. The C3b and C4b fragments are opsonins, and opsonized pathogens are recognized by complement receptor type 1 (CR1) on neutrophils, which then phagocytose them. In addition to opsonization, complement C3b enhances antibody generation by B cells, and another important role of complement is the generation of two anaphylatoxins, C3a and C5a. These peptides support inflammation and activate cells expressing anaphylatoxin receptors (1).

Negative regulators of the complement system and their expression in the kidneys

Various complement-regulatory proteins tightly control complement activation to protect autologous tissues from complement attack (2–4). The plasma protein C1 inhibitor (C1-INH) prevents the initiation of the CP and LP by binding to and inactivating C1r, C1s, and MASPs (5). During C3 convertase formation, various complement regulators function as cofactors for factor I (FI), a serine protease that inactivates C3b and C4b. Some regulators also exhibit decay acceleration activity, which decreases the stability of C3 convertases by accelerating the dissociation of Bb from C3bBb and/or C2b from C4bC2b (1, 2, 4).

Factor H (FH) and C4b-binding protein (C4BP) are fluid-phase proteins associated with FI-mediated C3b or C4b cleavage, as well as the decay acceleration activity of the AP or CP C3 convertase (1, 2, 4). Cell membrane inhibitors, such as CR1 and membrane cofactor protein (MCP), also function as cofactors for the inactivation of C3b and C4b *via* FI. CR1 also shows decay acceleration activity with respect to the CP C3 convertase, but MCP does not. Decay accelerating factor (DAF or CD55) and CD59 are glycosylphosphatidylinositol (GPI)-anchored membrane inhibitors of the complement system. As its name implies, DAF accelerates the decay of C3/C5 convertases, and CD59 inhibits C5b-9 formation by binding to C8 and C9. CR1-related gene/-protein y (Crry) is a rodent-specific membrane regulator with both cofactor and decay-accelerating activities, and is similar to human MCP and DAF (6). Animal experiments using Crry-neutralizing antibodies have revealed that Crry is a critical complement regulator in rodent kidneys (2).

In the context of renal physiology, MCP, CR1, DAF, and CD59 are expressed in the glomeruli and protect them from complement attacks. The expression levels of these regulatory proteins can be altered by complement attack and in various glomerular disorders (2). MCP, DAF, and CD59 are ubiquitously expressed in all resident glomerular cells, although DAF is barely detectable in the glomerular cells of normal kidneys (2). The expression of MCP and DAF, but not that of CD59, is concentrated in the juxtaglomerular apparatus (3). In contrast, the expression of CR1 is mainly restricted to podocytes (2).

Although FH is a fluid phase complement regulatory protein, it is also present on the cell surface. The C-terminal region of FH can bind to glycosaminoglycans and sialic acid on the cell surface. After binding to the cell surface, it can trap deposited C3b to induce FI-mediated C3b inactivation (4). Clinically, FH dysfunction is highly associated with renal impairment caused by atypical hemolytic uremic syndrome (aHUS) and C3 glomerulopathy, suggesting that FH-mediated complement regulation plays an essential role in kidney health.

Roles of the complement system and inflammation in thrombosis

The complement system, coagulation-fibrinolytic system, platelets, and leukocytes all form a close network and interact with each other (7). Therefore, dysregulation of any component can lead to multiple diseases with different pathological conditions and clinical manifestations (8) (Figure 2).

Complement and coagulation systems

Both the complement and coagulation systems share common cascade pathways that involve proteolysis and enable an inflammatory response as a way of defending the host (9–11).

The complement system modulates the coagulation cascade in several ways. Both C5- and C3-deficient mice have longer tail bleeding time and reduced susceptibility to thrombosis, indicating that the complement system plays an essential role in the coagulation process (12). MASP-1 and MASP-2 cleave coagulation factors such as prothrombin, fibrinogen, factor XIII, and thrombin-activatable fibrinolysis inhibitors *in vitro* (13, 14). C5a and C5b-9 induce tissue factor (TF) expression, which initiates the extrinsic coagulation pathway in both endothelial cells and neutrophils (9, 15). C5a also induces the secretion of ultra large von Willebrand factor multimers and P-selectin and increases neutrophil adhesion to cultured endothelial cells (16). These suggest that C5a is an important inflammatory mediator between neutrophils and endothelial cells during the acute inflammatory response.

Coagulation factors can also activate the complement cascade at different levels. Thrombin cleaves C3 and C5 into C3a and C5a *in vitro*, which amplifies the activation of the complement system and the induction of chemotaxis and neutrophil activation (17, 18). Plasmin also cleaves C3 and C5 (17). Plasminogen, on the other hand, enhances FI-mediated cleavage of C3b in the presence of FH, and plasmin degrades C3b (19). Factor XIa (FXIa) and FH modulate each other. FXIa

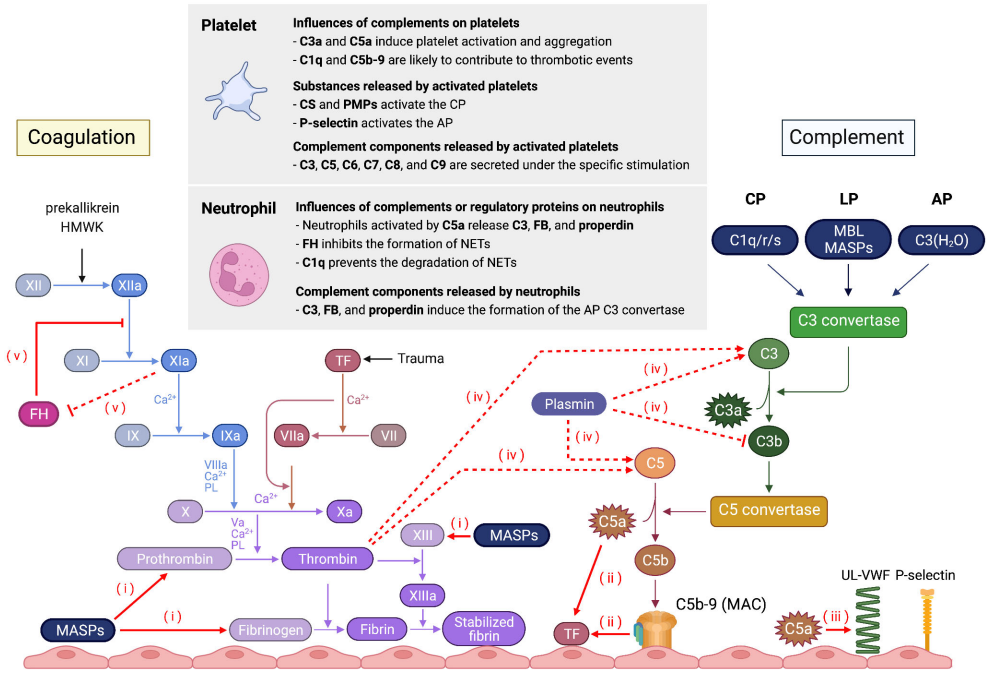

FIGURE 2
Schematic overview of the interaction between the complement system and the coagulation system, platelets, and neutrophils. (i) MASPs can cleave coagulation factors, such as prothrombin, fibrinogen, and factor XIII. (ii) C5a and C5b-9 enhance blood thrombogenicity through upregulation of TF in endothelial cells and neutrophils. (iii) C5a induces UL-VWF secretion and P-selectin expression. Conversely, coagulation factors activate the complement cascade. (iv) Thrombin and plasmin can generate C3a and C5a, whereas plasminogen enhances FI-mediated C3b cleavage in the presence of FH and plasmin degrades C3b. (v) Factor XIa decreases the cofactor and decay acceleration activity of FH and the ability binding of FH to bind to human endothelial cells. Conversely, FH inhibits FXIa activation.

cleaves FH, which decreases the cofactor and decay acceleration activity of FH and the ability of FH to bind to human endothelial cells. Conversely, FH inhibits FXIa activation *via* either thrombin or factor XIIa (20).

Complement system and platelets

Various complement components specifically activate platelets (10, 11). Thrombin-mediated platelet aggregation and release are enhanced by several complement components, such as C3, C5, C6, C7, C8, and C9 (21). Most of these proteins are stored in platelets and are secreted following activation (22–24). The binding of C1q to the C1q receptor (gC1qR/p33) expressed on platelets activates glycoprotein (GP) IIb-IIIa fibrinogen binding sites and P-selectin expression, which contributes to the thrombotic events associated with complement activation (25). The binding of C5b-9 induces a change in the membrane potential of platelets, thereby exposing the binding sites to factor Va and serving as a basis for the proteolytic generation of thrombin (26). In addition, anaphylatoxins C3a and C5a induce platelet activation and aggregation (27).

Platelets also release various molecules that activate or modulate the complement system (10, 11). Chondroitin sulfate released by thrombin-activated platelets induces fluid-phase activation of the CP in a C1q-dependent manner (28). Platelet microparticles also support the activation of the CP, whereas they induce the expression of C1-INH from the α-granules of platelets (29). Intriguingly, P-selectin expressed in activated platelets acts as a receptor for C3b, thereby initiating the activation of the AP (30). Experimental animal data have shown that C3, but not C5, is not redundant in platelet activation (12).

Furthermore, platelets have a complement regulatory system that limits complement activation on their surfaces. Platelets express MCP, CD55, and CD59 and carry C1-INH and FH (31, 32) in their α granules. In addition, activated platelets and neutrophils can remove C5b-9 in the form of microparticles (33). The absence or impairment of such regulatory proteins is associated with platelet dysfunction, alterations in platelet activation, or thrombocytopenia (8).

Complement system, leukocytes, and the endothelium

Neutrophils accumulate at inflamed sites with the help of the chemoattractant C5a and phagocytose bacteria with surface deposits of C3b or iC3b *via* CR1 and CR3 (34, 35). Neutrophil extracellular traps (NETs) are also considered part of the human innate immune system. These form when neutrophils respond to bacteria or immune complexes by ejecting nuclear chromatin and digestive enzymes to kill pathogens (36) and can sometimes evoke autoimmune tissue injury (37, 38).

Properdin is a positive complement regulator that stabilizes C3 convertase in the AP (39). Intriguingly, activated neutrophils (including those activated by C5a) release C3, FB, and properdin (40), and induce the formation of AP C3 convertase, leading to C5a generation. C5a activates additional neutrophils, which secrete key components of the AP. C3- and C3a receptor (C3aR)-deficient knockout mice fail to form NETs (41, 42), suggesting that the complement system also affects the formation of NETs. Furthermore, C3b opsonization promoted the release of NETs (43). In addition, neutrophils stimulated with phorbol myristate acetate (PMA) secrete properdin and deposit it on NETs and certain bacteria to induce the formation of C5b–9 (40).

FH, a negative regulator of the AP, binds to neutrophils, inhibits the formation of PMA-stimulated NETs (44), and reduces the inflammatory response (45). Conversely, binding of C1q prevents the degradation of NETs by directly inhibiting DNAse-I by C1q (46). NETs also exert thrombogenic activity through their expression of functionally active TF (47), which is disrupted by complement C3 inhibition (48).

Role of the complement system in glomerular capillary thrombosis in kidney disorders

Thrombotic microangiopathy

Thrombotic microangiopathy (TMA) is a pathological condition caused by the formation of microvascular thrombi that leads to thrombocytopenia, microangiopathic hemolytic anemia, and end-organ damage (49). TMA is caused by various hereditary or acquired factors, and is classified into four main categories: thrombotic thrombocytopenic purpura (TTP), hemolytic uremic syndrome (HUS) caused by Shiga toxin-producing *Escherichia coli* (STEC), atypical HUS (aHUS), and secondary TMA.

TTP is caused by a severe deficiency of ADAMTS13 (a disintegrin-like metalloprotease with thrombospondin type 1 motif, member 13) resulting from genetic or acquired defects (50). STEC-induced HUS is predominantly found in children and is diagnosed based on the direct detection of Shiga toxins in feces and the presence of anti-lipopolysaccharide immunoglobulin M antibodies (51).

aHUS is a complement-mediated TMA caused by the overactivation of the AP as a result of inherited and/or acquired complement abnormalities (52, 53). aHUS mainly targets the kidneys, and 50-70% of patients develop end-stage kidney disease (ESKD) unless they receive early and appropriate treatment (52). The efficacy and safety of the complement-inhibiting drug, eculizumab (54, 55) and ravulizumab (56, 57), have been described in many reports. Genetic variants of several complement regulators (FH, FI, and MCP) and activators (C3 and FB) have been identified in up to 50% of patients with aHUS (58). Thus, complementary diagnostic approaches have been developed to address the limitations of comprehensive gene analysis (59, 60). In addition, the acquisition of inhibitory autoantibodies against FH can cause aHUS (52, 61). In both genetic and acquired defects, impaired complement control on self-cell surfaces *via* the formation of C5b-9 leads to endothelial tissue damage and the generation of thrombi in the microvasculature (62).

Thrombocytopenia is a typical feature of TMA in which platelet thrombi are found in the capillaries and arterioles (62, 63). As mentioned above, various complement regulators normally protect platelets from complement attack; thus, defects in these regulators in aHUS may cause platelet activation and the formation of platelet-rich microvascular thrombi. Although there are few reports regarding the coagulation profile of aHUS (64), genetic variants of some coagulation-related proteins are associated with the pathogenesis of aHUS (65–67). Because the activations of complement and coagulation systems synergistically amplify each other as discussed earlier, this vicious cycle may be associated with the formation of microvascular thrombi in aHUS.

Patients with *FH* variants have a significantly increased risk of ESKD than those with variants in *CD46* (*MCP*) (68). *FH* variants associated with aHUS are primarily located at the C-terminus, and inhibitory autoantibodies also target the C-terminal region of FH (68–70). These genetic and acquired defects inhibit FH binding to the cell surface, resulting in C5b-9 formation in endothelial cells and platelets (62, 71). Although it is still unclear why complement damage seems to be restricted to the kidneys, heparan sulfate expressed in the kidneys appears critical for FH binding on cell surfaces (72).

In addition to TTP, STEC-induced HUS, and aHUS, a variety of pathological conditions such as autoimmune disease (73, 74), drug use (75), infection (76, 77), malignancy (78), malignant hypertension (79–81), pregnancy (82, 83), and transplantation (84, 85) can trigger secondary TMA. Although TTP and STEC-HUS have well-established diagnostic tests, the differentiation between aHUS and secondary TMA remains controversial because pathogenic variants in complement-related genes are only identified in about half of the patients

with aHUS. In addition, complement abnormalities have been found in some secondary TMA (86).

Complement abnormalities may play a role in secondary TMA caused by malignant hypertension (79–81) and pregnancy (82). Rare genetic variants in complement-related genes have been identified in approximately 30-70% of patients with malignant hypertension-associated TMA (79–81). In these cases, *ex vivo* analysis showed that patient sera induced massive C5b-9 formation in microvasculature endothelial cells, suggesting that these variants induced excessive complement activation. In addition, patients with over-deposition of C5b-9 in vascular endothelial cells had a higher incidence of ESKD, and the administration of anti-C5 antibodies improved renal function in these cases.

Lupus nephritis

Systemic lupus erythematosus (SLE) is a autoimmune disease that primarily affects young women. SLE affects the kidneys in approximately 50% of such patients as lupus nephritis (LN) (87). A variety of abnormal immune responses, such as defects in the clearance of immune complexes and apoptotic cells, nucleic acid-sensing abilities, lymphocyte signaling, and interferon-production have a central role in the pathogenesis of this disease (88, 89). Because immune complexes are deposited in tissues, and the deposition of C1q in tissues is relatively characteristic of SLE, it is plausible that these immune complexes activate the complement system and decrease complement levels (C3, C4, and CH50) in the peripheral blood. Activation of the complement system may cause inflammatory injury to tissues, as C3 or C4 fragments bind to complement receptors on B lymphocytes to enhance antibody generation (90, 91). However, this cannot explain why the deficiency of complement components such as C1q, C1s, C1r, C2, and C4 causes lupus-like symptoms (92). Deficiencies in this component activity may disturb the efficient disposal of dying and dead cells (93) or the normal tolerance mechanisms of lymphocytes (94), with both leading to the generation of autoantibodies.

The International Society of Nephrology/Renal Pathology Society meeting report mentioned the importance to have a standardized approach and terminology to distinguish ordinary arterial or arteriolar sclerosis from lupus-related lesions such as vasculopathy associated with immune complex deposition, vasculitis, and TMA (95). Indeed, within the glomerular capillaries and small arterioles in LN kidney specimens, microvascular thrombosis is conventionally recognized as one of the most common histopathological findings (96, 97). This characteristic finding has been variously described as “lupus vasculopathy (LV)” (97, 98), “immunoglobulin microvascular cast” (96), and “glomerular thrombosis” (99). LV is documented predominantly in diffuse proliferative LN, but the underlying etiology and its prognostic value remain undetermined (96, 97, 100). LV is characterized by the accumulation of immunoglobulins and complements in the vascular wall (98). This results in luminal narrowing and suggests the presence of immune-mediated vascular injury (98). Notably, unlike lupus vasculitis, LV does not involve the deposition of inflammatory cells in the vascular wall (98).

In lupus-prone MRL/lpr mice, treatment with aspirin and dexamethasone partially attenuates glomerular thrombosis (101). In rodents with nephrotoxic nephritis that mimics the downstream effector phase of LN (102), Fcγ receptors (103, 104) and components of the complement system (105, 106) have been implicated in the pathogenesis of tissue injury, including glomerular thrombosis. These experimental findings in animals suggest that inflammation may promote kidney glomerular thrombosis in LN.

Antiphospholipid syndrome (APS) frequently occurs in SLE and is characterized by vascular thrombosis, repeated miscarriages, and the presence of antiphospholipid antibodies (APLA) (107). Although patients with APS show a prolonged activated partial thromboplastin time, APLA exert prothrombotic effects because they inhibit β2-glycosylphosphatidylinisotol, which is an inhibitory regulator of phospholipid-dependent coagulation, protein C activation, thrombomodulin, and heparan sulfate on vascular endothelial cells (108, 109). Intriguingly, C4 deficiency attenuates fetal loss in mice with APS (110). Moreover, APLA stimulate TF activation in myelomonocytic cells, and mice deficient in C3, unlike mice deficient in C5, are protected from *in vivo* thrombus formation induced by cofactor-independent APLA, suggesting that C3 is required for TF activation and APLA-induced thrombosis (111). Because complement mediates TF enrichment in NETs (47, 48), neutrophils may be another player in thrombin formation in this context.

Primary glomerulonephritis

Glomerulonephritis refers to a group of kidney diseases affecting the glomeruli due to the damage mediated by immunological dysregulation. Hypocomplementemia is a significant feature of kidney glomerular diseases such as post-infectious glomerulonephritis, immune complex-mediated membranoproliferative glomerulonephritis, C3 glomerulopathy, dense deposit diseases, and IgG4-related kidney disease (112, 113). In addition, the majority of patients with IgA nephropathy (114) or membranous nephropathy (115) have local C3 deposits in the glomeruli. Other complement elements, such as the FH-related proteins 1 and 5 and lectin pathway products, also accumulate (114–116). These findings suggest that systemic or local activation of the complement system may cause kidney tissue damage.

However, thrombosis is rarely observed in these patients unless they develop heavy proteinuria (117), which evokes a hypercoagulable state due to the urinary loss of coagulation regulatory proteins, including antithrombin and protein S, which counterbalances the increase in the synthesis rate of hemostatic proteins in the liver (118). Further studies are needed to determine the association of the development of thrombosis with complement-mediated kidney injury.

Conclusion

The complement system has long been recognized as a central mediator of innate immune defenses that eliminate invading pathogens. Accumulating evidence has revealed how the complement system can modulate the function of the coagulation system, platelets, and neutrophils, and contribute to thrombosis. Further research on the link between the complement system and kidney disorders may deepen our understanding of complement-dependent mechanisms that promote glomerular capillary thrombosis and severely impair glomerular filtration. Such insights may provide novel therapeutic options for patients and clinicians.

Author contributions

YY drafted the original manuscript and HN revised it. Both authors approved the submitted version of the manuscript.

Funding

This work was supported by the Japan Society for the Promotion of Science Grant-in-Aid for Scientific Research 21K08272 (to YY) and the SENSHIN Medical Research Foundation (to HN).

Acknowledgments

The figures were created with BioRender.com.

Conflict of interest

The authors declare that the research was conducted in the absence of any commercial or financial relationships that could be construed as a potential conflict of interest.

Publisher's note

References

1. Merle NS, Church SE, Fremeaux-Bacchi V. Roumenina, LT: Complement system part I - molecular mechanisms of activation and regulation. *Front Immunol* (2015) 6:262. doi: 10.3389/fimmu.2015.00262

2. Nangaku M. Complement regulatory proteins in glomerular diseases. *Kidney Int* (1998) 54:1419–28. doi: 10.1046/j.1523-1755.1998.00130.x

3. Thurman JM, Renner B. Dynamic control of the complement system by modulated expression of regulatory proteins. *Lab Invest* (2011) 91:4–11. doi: 10.1038/labinvest.2010.173

4. Lesher AM, Song WC. Review: Complement and its regulatory proteins in kidney diseases. *Nephrol (Carlton)* (2010) 15:663–75. doi: 10.1111/j.1440-1797.2010.01373.x

5. Mollnes TE, Kirschfink M. Strategies of therapeutic complement inhibition. *Mol Immunol* (2006) 43:107–21. doi: 10.1016/j.molimm.2005.06.014

6. Naik A, Sharma S, Quigg RJ. Complement regulation in renal disease models. *Semin Nephrol* (2013) 33:575–85. doi: 10.1016/j.semnephrol.2013.08.008

7. Borkowska S, Suszynska M, Mierzejewska K, Ismail A, Budkowska M, Salata D, et al. : Novel evidence that crosstalk between the complement, coagulation and fibrinolysis proteolytic cascades is involved in mobilization of hematopoietic stem/progenitor cells (HSPCs). *Leukemia* (2014) 28:2148–54. doi: 10.1038/leu.2014.115

8. Verschoor A, Langer HF. Crosstalk between platelets and the complement system in immune protection and disease. *Thromb Haemost* (2013) 110:910–9. doi: 10.1160/TH13-02-0102

9. Markiewski MM, Nilsson B, Ekdahl KN, Mollnes TE, Lambris JD. Complement and coagulation: Strangers or partners in crime? *Trends Immunol* (2007) 28:184–92. doi: 10.1016/j.it.2007.02.006

10. Nording H, Langer HF. Complement links platelets to innate immunity. *Semin Immunol* (2018) 37:43–52. doi: 10.1016/j.smim.2018.01.003

11. Rawish E, Sauter M, Sauter R, Nording H, Langer HF. Complement, inflammation and thrombosis. *Br J Pharmacol* (2021) 178:2892–904. doi: 10.1111/bph.15476

12. Subramaniam S, Jurk K, Hobohm L, Jackel S, Saffarzadeh M, Schwierczek K, et al. Distinct contributions of complement factors to platelet activation and fibrin formation in venous thrombus development. *Blood* (2017) 129:2291–302. doi: 10.1182/blood-2016-11-749879

13. Hess K, Ajjan R, Phoenix F, Dobo J, Gal P, Schroeder V. Effects of MASP-1 of the complement system on activation of coagulation factors and plasma clot formation. *PloS One* (2012) 7:e35690. doi: 10.1371/journal.pone.0035690

14. Krarup A, Wallis R, Presanis JS, Gal P, Sim RB. Simultaneous activation of complement and coagulation by MBL-associated serine protease 2. *PloS One* (2007) 2:e623. doi: 10.1371/journal.pone.0000623

15. Ikeda K, Nagasawa K, Horiuchi T, Tsuru T, Nishizaka H, Niho Y. C5a induces tissue factor activity on endothelial cells. *Thromb Haemost* (1997) 77:394–8. doi: 10.1055/s-0038-1655974

16. Foreman KE, Vaporciyan AA, Bonish BK, Jones ML, Johnson KJ, Glovsky MM, et al. C5a-induced expression of p-selectin in endothelial cells. *J Clin Invest* (1994) 94:1147–55. doi: 10.1172/JCI117430

17. Amara U, Flierl MA, Rittirsch D, Klos A, Chen H, Acker B, et al. Molecular intercommunication between the complement and coagulation systems. *J Immunol* (2010) 185:5628–36. doi: 10.4049/jimmunol.0903678

18. Huber-Lang M, Sarma JV, Zetoune FS, Rittirsch D, Neff TA, McGuire SR, et al. Generation of C5a in the absence of C3: A new complement activation pathway. *Nat Med* (2006) 12:682–7. doi: 10.1038/nm1419

19. Barthel D, Schindler S, Zipfel PF. Plasminogen is a complement inhibitor. *J Biol Chem* (2012) 287:18831–42. doi: 10.1074/jbc.M111.323287

20. Puy C, Pang J, Reitsma SE, Lorentz CU, Tucker EI, Gailani D, et al. Cross-talk between the complement pathway and the contact activation system of coagulation: Activated factor XI neutralizes complement factor h. *J Immunol* (2021) 206:1784–92. doi: 10.4049/jimmunol.2000398

21. Polley MJ, Nachman RL. Human complement in thrombin-mediated platelet function: uptake of the C5b-9 complex. *J Exp Med* (1979) 150:633–45. doi: 10.1084/jem.150.3.633

22. Tedesco F, Densen P, Villa MA, Presani G, Roncelli L, Rosso di san Secondo VE. Functional C8 associated with human platelets. *Clin Exp Immunol* (1986) 66:472–80.

23. Jenkinson ML, Bliss MR, Brain AT, Scott DL. Rheumatoid arthritis and senile dementia of the alzheimer's type. *Br J Rheumatol* (1989) 28:86–8. doi: 10.1093/rheumatology/28.1.86-b

24. Martel C, Cointe S, Maurice P, Matar S, Ghitescu M, Theroux P, et al. Requirements for membrane attack complex formation and anaphylatoxins binding to collagen-activated platelets. *PloS One* (2011) 6:e18812. doi: 10.1371/journal.pone.0018812

25. Peerschke EI, Reid KB, Ghebrehiwet B. Platelet activation by C1q results in the induction of alpha IIb/beta 3 integrins (GPIIb-IIIa) and the expression of p-selectin and procoagulant activity. *J Exp Med* (1993) 178:579–87. doi: 10.1084/jem.178.2.579

26. Wiedmer T, Sims PJ. Effect of complement proteins C5b-9 on blood platelets. evidence for reversible depolarization of membrane potential. *J Biol Chem* (1985) 260:8014–9.

27. Polley MJ, Nachman RL. Human platelet activation by C3a and C3a des-arg. *J Exp Med* (1983) 158:603–15. doi: 10.1084/jem.158.2.603

28. Hamad OA, Ekdahl KN, Nilsson PH, Andersson J, Magotti P, Lambris JD, et al. Complement activation triggered by chondroitin sulfate released by thrombin receptor-activated platelets. *J Thromb Haemost* (2008) 6:1413–21. doi: 10.1111/j.1538-7836.2008.03034.x

29. Yin W, Ghebrehiwet B, Peerschke EI. Expression of complement components and inhibitors on platelet microparticles. *Platelets* (2008) 19:225–33. doi: 10.1080/09537100701777311

30. Del Conde I, Cruz MA, Zhang H, Lopez JA, Afshar-Kharghan V. Platelet activation leads to activation and propagation of the complement system. *J Exp Med* (2005) 201:871–9. doi: 10.1084/jem.20041497

31. Schmaier AH, Smith PM, Colman RW. Platelet C1- inhibitor. A secreted alpha-granule protein. *J Clin Invest* (1985) 75:242–50. doi: 10.1172/JCI111680

32. Devine DV, Rosse WF. Regulation of the activity of platelet-bound C3 convertase of the alternative pathway of complement by platelet factor h. *Proc Natl Acad Sci USA* (1987) 84:5873–7. doi: 10.1073/pnas.84.16.5873

33. Morgan BP. The membrane attack complex as an inflammatory trigger. *Immunobiology* (2016) 221:747–51. doi: 10.1016/j.imbio.2015.04.006

34. Ehrengruber MU, Geiser T, Deranleau DA. Activation of human neutrophils by C3a and C5A. comparison of the effects on shape changes, chemotaxis, secretion, and respiratory burst. *FEBS Lett* (1994) 346:181–4. doi: 10.1016/0014-5793(94)00463-3

35. van Kessel KP, Bestebroer J, van Strijp JA. Neutrophil-mediated phagocytosis of staphylococcus aureus. *Front Immunol* (2014) 5:467. doi: 10.3389/fimmu.2014.00467

36. Brinkmann V, Reichard U, Goosmann C, Fauler B, Uhlemann Y, Weiss DS, et al. Neutrophil extracellular traps kill bacteria. *Science* (2004) 303:1532–5. doi: 10.1126/science.1092385

37. Villanueva E, Yalavarthi S, Berthier CC, Hodgin JB, Khandpur R, Lin AM, et al. Netting neutrophils induce endothelial damage, infiltrate tissues, and expose immunostimulatory molecules in systemic lupus erythematosus. *J Immunol* (2011) 187:538–52. doi: 10.4049/jimmunol.1100450

38. Chen K, Nishi H, Travers R, Tsuboi N, Martinod K, Wagner DD, et al. Endocytosis of soluble immune complexes leads to their clearance by FcgammaRIIIB but induces neutrophil extracellular traps *via* FcgammaRIIA *in vivo*. *Blood* (2012) 120:4421–31. doi: 10.1182/blood-2011-12-401133

39. Kimura Y, Miwa T, Zhou L, Song WC. Activator-specific requirement of properdin in the initiation and amplification of the alternative pathway complement. *Blood* (2008) 111:732–40. doi: 10.1182/blood-2007-05-089821

40. Yuen J, Pluthero FG, Douda DN, Riedl M, Cherry A, Ulanova M, et al. NETosing neutrophils activate complement both on their own NETs and bacteria *via* alternative and non-alternative pathways. *Front Immunol* (2016) 7:137. doi: 10.3389/fimmu.2016.00137

41. Yipp BG, Petri B, Salina D, Jenne CN, Scott BN, Zbytnuik LD, et al. Infection-induced NETosis is a dynamic process involving neutrophil multitasking *in vivo*. *Nat Med* (2012) 18:1386–93. doi: 10.1038/nm.2847

42. Guglietta S, Chiavelli A, Zagato E, Krieg C, Gandini S, Ravenda PS, et al. Coagulation induced by C3aR-dependent NETosis drives protumorigenic neutrophils during small intestinal tumorigenesis. *Nat Commun* (2016) 7:11037. doi: 10.1038/ncomms11037

43. Palmer LJ, Damgaard C, Holmstrup P, Nielsen CH. Influence of complement on neutrophil extracellular trap release induced by bacteria. *J Periodontal Res* (2016) 51:70–6. doi: 10.1111/jre.12284

44. Schneider AE, Sandor N, Karpati E, Jozsi M. Complement factor h modulates the activation of human neutrophil granulocytes and the generation of neutrophil extracellular traps. *Mol Immunol* (2016) 72:37–48. doi: 10.1016/j.molimm.2016.02.011

45. Halder LD, Abdelfatah MA, Jo EA, Jacobsen ID, Westermann M, Beyersdorf N, et al. Factor h binds to extracellular DNA traps released from human blood monocytes in response to candida albicans. *Front Immunol* (2016) 7:671. doi: 10.3389/fimmu.2016.00671

46. Leffler J, Martin M, Gullstrand B, Tyden H, Lood C, Truedsson L, et al. Neutrophil extracellular traps that are not degraded in systemic lupus erythematosus activate complement exacerbating the disease. *J Immunol* (2012) 188:3522–31. doi: 10.4049/jimmunol.1102404

47. Stakos D, Skendros P, Konstantinides S, Ritis K. Traps n' clots: NET-mediated thrombosis and related diseases. *Thromb Haemost* (2020) 120:373–83. doi: 10.1055/s-0039-3402731

48. Skendros P, Mitsios A, Chrysanthopoulou A, Mastellos DC, Metallidis S, Rafailidis P, et al. Complement and tissue factor-enriched neutrophil extracellular traps are key drivers in COVID-19 immunothrombosis. *J Clin Invest* (2020) 130:6151–7. doi: 10.1172/JCI141374

49. George JN, Nester CM. Syndromes of thrombotic microangiopathy. *N Engl J Med* (2014) 371:654–66. doi: 10.1056/NEJMra1312353

50. Joly BS, Coppo P, Veyradier A. Thrombotic thrombocytopenic purpura. *Blood* (2017) 129:2836–46. doi: 10.1182/blood-2016-10-709857

51. Trachtman H, Austin C, Lewinski M, Stahl RA. Renal and neurological involvement in typical shiga toxin-associated HUS. *Nat Rev Nephrol* (2012) 8:658–69. doi: 10.1038/nrneph.2012.196

52. Kavanagh D, Goodship TH, Richards A. Atypical hemolytic uremic syndrome. *Semin Nephrol* (2013) 33:508–30. doi: 10.1016/j.semnephrol.2013.08.003

53. Yoshida Y, Kato H, Ikeda Y, Nangaku M. Pathogenesis of atypical hemolytic uremic syndrome. *J Atheroscler Thromb* (2019) 26:99–110. doi: 10.5551/jat.RV17026

54. Legendre CM, Licht C, Muus P, Greenbaum LA, Babu S, Bedrosian C, et al. Terminal complement inhibitor eculizumab in atypical hemolytic-uremic syndrome. *N Engl J Med* (2013) 368:2169–81. doi: 10.1056/NEJMoa1208981

55. Licht C, Greenbaum LA, Muus P, Babu S, Bedrosian CL, Cohen DJ, et al. Efficacy and safety of eculizumab in atypical hemolytic uremic syndrome from 2-year extensions of phase 2 studies. *Kidney Int* (2015) 87:1061–73. doi: 10.1038/ki.2014.423

56. Rondeau E, Scully M, Ariceta G, Barbour T, Cataland S, Heyne N, et al. The long-acting C5 inhibitor, ravulizumab, is effective and safe in adult patients with atypical hemolytic uremic syndrome naive to complement inhibitor treatment. *Kidney Int* (2020) 97:1287–96. doi: 10.1016/j.kint.2020.01.035

57. Ariceta G, Dixon BP, Kim SH, Kapur G, Mauch T, Ortiz S, et al. The long-acting C5 inhibitor, ravulizumab, is effective and safe in pediatric patients with atypical hemolytic uremic syndrome naive to complement inhibitor treatment. *Kidney Int* (2021) 100:225–37. doi: 10.1016/j.kint.2020.10.046

58. Noris M, Bresin E, Mele C, Remuzzi G. Genetic atypical hemolytic-uremic syndrome. In: MP Adam, GM Mirzaa, RA Pagon, SE Wallace, LJH Bean, KW Gripp and A Amemiya, editors. *GeneReviews*. Seattle (WA): University of Washington, Seattle (2021).

59. Sanchez-Corral P, Gonzalez-Rubio C, Rodriguez de Cordoba S, Lopez-Trascasa M. Functional analysis in serum from atypical hemolytic uremic syndrome patients reveals impaired protection of host cells associated with mutations in factor h. *Mol Immunol* (2004) 41:81–4. doi: 10.1016/j.molimm.2004.01.003

60. Yoshida Y, Miyata T, Matsumoto M, Shirotani-Ikejima H, Uchida Y, Ohyama Y, et al. A novel quantitative hemolytic assay coupled with restriction fragment length polymorphisms analysis enabled early diagnosis of atypical hemolytic uremic syndrome and identified unique predisposing mutations in Japan. *PloS One* (2015) 10:e0124655. doi: 10.1371/journal.pone.0124655

61. Jozsi M, Licht C, Strobel S, Zipfel SL, Richter H, Heinen S, et al. Factor h autoantibodies in atypical hemolytic uremic syndrome correlate with CFHR1/CFHR3 deficiency. *Blood* (2008) 111:1512–4. doi: 10.1182/blood-2007-09-109876

62. Jokiranta TS. HUS and atypical HUS. *Blood* (2017) 129:2847–56. doi: 10.1182/blood-2016-11-709865

63. Noris M, Remuzzi G. Atypical hemolytic-uremic syndrome. *N Engl J Med* (2009) 361:1676–87. doi: 10.1056/NEJMra0902814

64. Sakurai S, Kato H, Yoshida Y, Sugawara Y, Fujisawa M, Yasumoto A, et al. Profiles of coagulation and fibrinolysis activation-associated molecular markers of atypical hemolytic uremic syndrome in the acute phase. *J Atheroscler Thromb* (2020) 27:353–62. doi: 10.5551/jat.49494

65. Delvaeye M, Noris M, De Vriese A, Esmon CT, Esmon NL, Ferrell G, et al. Conway, EM: Thrombomodulin mutations in atypical hemolytic-uremic syndrome. *N Engl J Med* (2009) 361:345–57. doi: 10.1056/NEJMoa0810739

66. Lemaire M, Fremeaux-Bacchi V, Schaefer F, Choi M, Tang WH, Le Quintrec M, et al. Recessive mutations in DGKE cause atypical hemolytic-uremic syndrome. *Nat Genet* (2013) 45:531–6. doi: 10.1038/ng.2590

67. Bu F, Maga T, Meyer NC, Wang K, Thomas CP, Nester CM, et al. Comprehensive genetic analysis of complement and coagulation genes in atypical hemolytic uremic syndrome. *J Am Soc Nephrol* (2014) 25:55–64. doi: 10.1681/ASN.2013050453

68. Fremeaux-Bacchi V, Fakhouri F, Garnier A, Bienaime F, Dragon-Durey MA, Ngo S, et al. Genetics and outcome of atypical hemolytic uremic syndrome: a nationwide French series comparing children and adults. *Clin J Am Soc Nephrol* (2013) 8:554–62. doi: 10.2215/CJN.04760512

69. Jozsi M, Strobel S, Dahse HM, Liu WS, Hoyer PF, Oppermann M, et al. Anti factor h autoantibodies block c-terminal recognition function of factor h in hemolytic uremic syndrome. *Blood* (2007) 110:1516–8. doi: 10.1182/blood-2007-02-071472

70. Noris M, Caprioli J, Bresin E, Mossali C, Pianetti G, Gamba S, et al. Relative role of genetic complement abnormalities in sporadic and familial aHUS and their impact on clinical phenotype. *Clin J Am Soc Nephrol* (2010) 5:1844–59. doi: 10.2215/CJN.02210310

71. Lehtinen MJ, Rops AL, Isenman DE, van der Vlag J, Jokiranta TS. Mutations of factor h impair regulation of surface-bound C3b by three mechanisms in atypical hemolytic uremic syndrome. *J Biol Chem* (2009) 284:15650–8. doi: 10.1074/jbc.M900814200

72. Loeven MA, Rops AL, Berden JH, Daha MR, Rabelink TJ, van der Vlag J. The role of heparan sulfate as determining pathogenic factor in complement factor h-associated diseases. *Mol Immunol* (2015) 63:203–8. doi: 10.1016/j.molimm.2014.08.005

73. Kwok SK, Ju JH, Cho CS, Kim HY, Park SH. Thrombotic thrombocytopenic purpura in systemic lupus erythematosus: Risk factors and clinical outcome: a single centre study. *Lupus* (2009) 18:16–21. doi: 10.1177/0961203308094360

74. Yamashita H, Kamei R, Kaneko H. Classifications of scleroderma renal crisis and reconsideration of its pathophysiology. *Rheumatol (Oxford)* (2019) 58:2099–106. doi: 10.1093/rheumatology/kez435

75. Al-Nouri ZL, Reese JA, Terrell DR, Vesely SK, George JN. Drug-induced thrombotic microangiopathy: A systematic review of published reports. *Blood* (2015) 125:616–8. doi: 10.1182/blood-2014-11-611335

76. Bitzan M, Zieg J. Influenza-associated thrombotic microangiopathies. *Pediatr Nephrol* (2018) 33:2009–25. doi: 10.1007/s00467-017-3783-4

77. Tiwari NR, Phatak S, Sharma VR, Agarwal SK. COVID-19 and thrombotic microangiopathies. *Thromb Res* (2021) 202:191–8. doi: 10.1016/j.thromres.2021.04.012

78. Thomas MR, Scully M. How I treat microangiopathic hemolytic anemia in patients with cancer. *Blood* (2021) 137:1310–7. doi: 10.1182/blood.2019003810

79. Timmermans S, Abdul-Hamid MA, Vanderlocht J, Damoiseaux J, Reutelingsperger CP, van Paassen P, et al. Patients with hypertension-associated thrombotic microangiopathy may present with complement abnormalities. *Kidney Int* (2017) 91:1420–5. doi: 10.1016/j.kint.2016.12.009

80. Timmermans S, Abdul-Hamid MA, Potjewijd J, Theunissen R, Damoiseaux J, Reutelingsperger CP, et al. C5b9 formation on endothelial cells reflects complement defects among patients with renal thrombotic microangiopathy and severe hypertension. *J Am Soc Nephrol* (2018) 29:2234–43. doi: 10.1681/ASN.2018020184

81. Timmermans S, Werion A, Damoiseaux J, Morelle J, Reutelingsperger CP, van Paassen P. Diagnostic and risk factors for complement defects in hypertensive emergency and thrombotic microangiopathy. *Hypertension* (2020) 75:422–30. doi: 10.1161/HYPERTENSIONAHA.119.13714

82. Fakhouri F, Roumenina L, Provot F, Sallee M, Caillard S, Couzi L, et al. Pregnancy-associated hemolytic uremic syndrome revisited in the era of complement gene mutations. *J Am Soc Nephrol* (2010) 21:859–67. doi: 10.1681/ASN.2009070706

83. Yoshida Y, Matsumoto M, Yagi H, Isonishi A, Sakai K, Hayakawa M, et al. Severe reduction of free-form ADAMTS13, unbound to von willebrand factor, in plasma of patients with HELLP syndrome. *Blood Adv* (2017) 1:1628–31. doi: 10.1182/bloodadvances.2017006767

84. Nishi H, Hanafusa N, Kondo Y, Nangaku M, Sugawara Y, Makuuchi M, et al. Clinical outcome of thrombotic microangiopathy after living-donor liver transplantation treated with plasma exchange therapy. *Clin J Am Soc Nephrol* (2006) 1:811–9. doi: 10.2215/CJN.01781105

85. Schoettler M, Chonat S, Williams K, Lehmann L. Emerging therapeutic and preventive approaches to transplant-associated thrombotic microangiopathy. *Curr Opin Hematol* (2021) 28:408–16. doi: 10.1097/MOH.0000000000000687

86. Palma LMP, Sridharan M, Sethi S. : Complement in secondary thrombotic microangiopathy. *Kidney Int Rep* (2021) 6:11–23. doi: 10.1016/j.ekir.2020.10.009

87. Almaani S, Meara A. Rovin, BH: Update on lupus nephritis. *Clin J Am Soc Nephrol* (2017) 12:825–35. doi: 10.2215/CJN.05780616

88. Tsokos GC, Lo MS, Costa Reis P. Sullivan, KE: New insights into the immunopathogenesis of systemic lupus erythematosus. *Nat Rev Rheumatol* (2016) 12:716–30. doi: 10.1038/nrrheum.2016.186

89. Nishi H, Mayadas TN. Neutrophils in lupus nephritis. *Curr Opin Rheumatol* (2019) 31:193–200. doi: 10.1097/BOR.0000000000000577

90. Villiers MB, Villiers CL, Laharie AM, Marche PN. Amplification of the antibody response by C3b complexed to antigen through an ester link. *J Immunol* (1999) 162:3647–52.

91. Rossbacher J, Shlomchik MJ. The b cell receptor itself can activate complement to provide the complement receptor 1/2 ligand required to enhance b cell immune responses *in vivo*. *J Exp Med* (2003) 198:591–602. doi: 10.1084/jem.20022042

92. Macedo AC, Isaac L. Systemic lupus erythematosus and deficiencies of early components of the complement classical pathway. *Front Immunol* (2016) 7:55. doi: 10.3389/fimmu.2016.00055

93. Korb LC, Ahearn JM. C1q binds directly and specifically to surface blebs of apoptotic human keratinocytes: Complement deficiency and systemic lupus erythematosus revisited. *J Immunol* (1997) 158:4525–8.

94. Mitchell DA, Pickering MC, Warren J, Fossati-Jimack L, Cortes-Hernandez J, Cook HT, et al. C1q deficiency and autoimmunity: The effects of genetic background on disease expression. *J Immunol* (2002) 168:2538–43. doi: 10.4049/jimmunol.168.5.2538

95. Bajema IM, Wilhelmus S, Alpers CE, Bruijn JA, Colvin RB, Cook HT, et al. Revision of the international society of Nephrology/Renal pathology society classification for lupus nephritis: Clarification of definitions, and modified national institutes of health activity and chronicity indices. *Kidney Int* (2018) 93:789–96. doi: 10.1016/j.kint.2017.11.023

96. Descombes E, Droz D, Drouet L, Grunfeld JP, Lesavre P. Renal vascular lesions in lupus nephritis. *Med (Baltimore)* (1997) 76:355–68. doi: 10.1097/00005792-199709000-00003

97. Barber C, Herzenberg A, Aghdassi E, Su J, Lou W, Qian G, et al. Evaluation of clinical outcomes and renal vascular pathology among patients with lupus. *Clin J Am Soc Nephrol* (2012) 7:757–64. doi: 10.2215/CJN.02870311

98. Gonzalez-Suarez ML, Waheed AA, Andrews DM, Ascherman DP, Zeng X, Nayer A. Lupus vasculopathy: Diagnostic, pathogenetic and therapeutic considerations. *Lupus* (2014) 23:421–7. doi: 10.1177/0961203313520340

99. Miranda JM, Garcia-Torres R, Jara LJ, Medina F, Cervera H, Fraga A. Renal biopsy in systemic lupus erythematosus: significance of glomerular thrombosis. analysis of 108 cases. *Lupus* (1994) 3:25–9. doi: 10.1177/096120339400300106

100. Wu LH, Yu F, Tan Y, Qu Z, Chen MH, Wang SX, et al. : Inclusion of renal vascular lesions in the 2003 ISN/RPS system for classifying lupus nephritis improves renal outcome predictions. *Kidney Int* (2013) 83:715–23. doi: 10.1038/ki.2012.409

101. Gonzalo-Gil E, Garcia-Herrero C, Toldos O, Usategui A, Criado G, Perez-Yague S, et al. Microthrombotic renal vascular lesions are associated to increased renal inflammatory infiltration in murine lupus nephritis. *Front Immunol* (2018) 9:1948. doi: 10.3389/fimmu.2018.01948

102. Du Y, Fu Y, Mohan C. Experimental anti-GBM nephritis as an analytical tool for studying spontaneous lupus nephritis. *Arch Immunol Ther Exp (Warsz)* (2008) 56:31–40. doi: 10.1007/s00005-008-0007-4

103. Park SY, Ueda S, Ohno H, Hamano Y, Tanaka M, Shiratori T, et al. Resistance of fc receptor- deficient mice to fatal glomerulonephritis. *J Clin Invest* (1998) 102:1229–38. doi: 10.1172/JCI3256

104. Nishi H, Furuhashi K, Cullere X, Saggu G, Miller MJ, Chen Y, et al. Neutrophil FcgammaRIIA promotes IgG-mediated glomerular neutrophil capture *via* Abl/Src kinases. *J Clin Invest* (2017) 127:3810–26. doi: 10.1172/JCI94039

105. Sogabe H, Nangaku M, Ishibashi Y, Wada T, Fujita T, Sun X, et al. Increased susceptibility of decay-accelerating factor deficient mice to anti-glomerular basement membrane glomerulonephritis. *J Immunol* (2001) 167:2791–7. doi: 10.4049/jimmunol.167.5.2791

106. Robson MG, Cook HT, Botto M, Taylor PR, Busso N, Salvi R, et al. Accelerated nephrotoxic nephritis is exacerbated in C1q-deficient mice. *J Immunol* (2001) 166:6820–8. doi: 10.4049/jimmunol.166.11.6820

107. Afeltra A, Vadacca M, Conti L, Galluzzo S, Mitterhofer AP, Ferri GM, et al. Thrombosis in systemic lupus erythematosus: Congenital and acquired risk factors. *Arthritis Rheum* (2005) 53:452–9. doi: 10.1002/art.21172

108. Atsumi T, Khamashta MA, Amengual O, Donohoe S, Mackie I, Ichikawa K, et al. Binding of anticardiolipin antibodies to protein c *via* beta2-glycoprotein I (beta2-GPI): A possible mechanism in the inhibitory effect of antiphospholipid antibodies on the protein c system. *Clin Exp Immunol* (1998) 112:325–33. doi: 10.1046/j.1365-2249.1998.00582.x

109. Sang Y, Roest M, de Laat B, de Groot PG, Huskens D. Interplay between platelets and coagulation. *Blood Rev* (2021) 46:100733. doi: 10.1016/j.blre.2020.100733

110. Girardi G, Berman J, Redecha P, Spruce L, Thurman JM, Kraus D, et al. Complement C5a receptors and neutrophils mediate fetal injury in the antiphospholipid syndrome. *J Clin Invest* (2003) 112:1644–54. doi: 10.1172/JCI200318817

111. Muller-Calleja N, Ritter S, Hollerbach A, Falter T, Lackner KJ, Ruf W. Complement C5 but not C3 is expendable for tissue factor activation by cofactor-independent antiphospholipid antibodies. *Blood Adv* (2018) 2:979–86. doi: 10.1182/bloodadvances.2018017095

112. Hebert LA, Cosio FG, Neff JC. Diagnostic significance of hypocomplementemia. *Kidney Int* (1991) 39:811–21. doi: 10.1038/ki.1991.102

113. Couser WG, Johnson RJ. The etiology of glomerulonephritis: Roles of infection and autoimmunity. *Kidney Int* (2014) 86:905–14. doi: 10.1038/ki.2014.49

114. Tortajada A, Gutierrez E, Pickering MC, Praga Terente M, Medjeral-Thomas N. The role of complement in IgA nephropathy. *Mol Immunol* (2019) 114:123–32. doi: 10.1016/j.molimm.2019.07.017

115. Ma H, Sandor DG, Beck LHJr. The role of complement in membranous nephropathy. *Semin Nephrol* (2013) 33:531–42. doi: 10.1016/j.semnephrol.2013.08.004

116. Medjeral-Thomas NR, Cook HT, Pickering MC. Complement activation in IgA nephropathy. *Semin Immunopathol* (2021) 43:679–90. doi: 10.1007/s00281-021-00882-9

117. Kerlin BA, Ayoob R, Smoyer WE. Epidemiology and pathophysiology of nephrotic syndrome-associated thromboembolic disease. *Clin J Am Soc Nephrol* (2012) 7:513–20. doi: 10.2215/CJN.10131011

118. Schlegel N. Thromboembolic risks and complications in nephrotic children. *Semin Thromb Hemost* (1997) 23:271–80. doi: 10.1055/s-2007-996100

frontiers | Frontiers in Immunology

TYPE Original Research
PUBLISHED 01 December 2022
DOI 10.3389/fimmu.2022.1056153

OPEN ACCESS

EDITED BY
Mihály Józsi,
Eötvös Loránd University, Hungary

REVIEWED BY
Eleni Gavriilaki,
G. Papanikolaou General Hospital, Greece
Johannes Hofer,
Hospitaller Brothers of Saint John of God Linz, Austria

*CORRESPONDENCE
Romy N. Bouwmeester
Romy.Bouwmeester@radboudumc.nl

SPECIALTY SECTION
This article was submitted to Molecular Innate Immunity, a section of the journal Frontiers in Immunology

RECEIVED 28 September 2022
ACCEPTED 14 November 2022
PUBLISHED 01 December 2022

CITATION
Bouwmeester RN, Bormans EMG, Duineveld C, van Zuilen AD, van de Logt A-E, Wetzels JFM and van de Kar NCAJ (2022) COVID-19 vaccination and Atypical hemolytic uremic syndrome.
Front. Immunol. 13:1056153.
doi: 10.3389/fimmu.2022.1056153

COVID-19 vaccination and Atypical hemolytic uremic syndrome

Romy N. Bouwmeester[1*], Esther M.G. Bormans[1], Caroline Duineveld[2], Arjan D. van Zuilen[3], Anne-Els van de Logt[2], Jack F.M. Wetzels[2] and Nicole C.A.J. van de Kar[1]

[1]Radboud University Medical Center, Amalia Children's Hospital, Radboud Institute for Molecular Life Sciences, Department of Pediatric Nephrology, Nijmegen, Netherlands, [2]Radboud University Medical Center, Radboud Institute for Health Sciences, Department of Nephrology, Nijmegen, Netherlands, [3]University Medical Center Utrecht, Department of Nephrology and Hypertension, Utrecht, Netherlands

Introduction: COVID-19 vaccination has been associated with rare but severe complications characterized by thrombosis and thrombocytopenia.

Methods and Results: Here we present three patients who developed *de novo* or relapse atypical hemolytic uremic syndrome (aHUS) in native kidneys, a median of 3 days (range 2-15) after mRNA-based (Pfizer/BioNTech's, BNT162b2) or adenoviral (AstraZeneca, ChAdOx1 nCoV-19) COVID-19 vaccination. All three patients presented with evident hematological signs of TMA and AKI, and other aHUS triggering or explanatory events were absent. After eculizumab treatment, kidney function fully recovered in 2/3 patients. In addition, we describe two patients with dubious aHUS relapse after COVID-19 vaccination. To assess the risks of vaccination, we retrospectively evaluated 29 aHUS patients (n=8 with native kidneys) without complement-inhibitory treatment, who received a total of 73 COVID-19 vaccinations. None developed aHUS relapse after vaccination.

Conclusion: In conclusion, aHUS should be included in the differential diagnosis of patients with vaccine-induced thrombocytopenia, especially if co-occuring with mechanical hemolytic anemia (MAHA) and acute kidney injury (AKI). Still, the overall risk is limited and we clearly advise continuation of COVID-19 vaccination in patients with a previous episode of aHUS, yet conditional upon clear patient instruction on how to recognize symptoms of recurrence. At last, we suggest monitoring serum creatinine (sCr), proteinuria, MAHA parameters, and blood pressure days after vaccination.

KEYWORDS

COVID-19, vaccination, atypical hemolitic uremic syndrome, trigger, complement, SARS-CoV-2, thrombotic microagiopathy, aHUS

10.3389/fimmu.2022.1056153

Introduction

Atypical hemolytic uremic syndrome (aHUS) is a severe form of thrombotic microangiopathy (TMA) that is characterized by thrombocytopenia, microangiopathic hemolytic anemia (MAHA), and acute kidney injury (AKI) (1–3). Hematologically, TMA can be defined by at least two of the following parameters: platelet count <150 x10^9/L, lactate dehydrogenase (LDH) serum level above the upper limit of normal, and low or undetectable haptoglobin. Overactivation of the alternative pathway (AP) of the complement system is found to play the main role in the pathophysiology of aHUS and a genetic predisposition of a (likely) pathogenic variant in one or more of the complement (regulatory) proteins, or the presence of anti-complement factor H (CFH) antibodies can be found in up to 70% of aHUS patients (4–6). In aHUS, actual dysregulation of the AP requires a substantial triggering, complement activating event, such as (bacterial and viral) infections, surgery, kidney transplantation, and pregnancy (6, 7). Moreover, in pediatric patients, hepatitis B and diphtheria-pertussis-tetanus-polio (DPTP)) vaccination has been identified as a potential trigger for aHUS (7, 8). To confirm aHUS, a *diagnosis per exclusionem*, it is recommended to perform diagnostics to identify a triggering event, document genetic complement variant(s), and exclude secondary causes of TMA (4, 6, 9). Atypical HUS can be effectively treated with the complement C5-inhibitor eculizumab (which is the only complement-inhibiting therapy available in the Netherlands) (10).

Recently, vaccination campaigns against the coronavirus disease 2019 (COVID-19), also known as severe acute respiratory syndrome coronavirus-2 (SARS-CoV-2), have been implemented worldwide (11). Although rare, COVID-19 vaccination has been associated with severe thrombosis and thrombocytopenia-associated complications (12–14). In addition, a second or third COVID-19 vaccination has been statistically significant associated with (non-aHUS) glomerular disease relapse (15). Sporadically, patients developed complement-mediated HUS after COVID-19 infection and, even more rare, COVID-19 vaccination (14, 16–21). Yet to date it is unknown to what degree vaccination against COVID-19 could trigger aHUS in pediatric and adult patients with a pathogenic complement variant.

Here we describe the association between both Pfizer/BioNTech's (BNT162b2) mRNA-based and AstraZeneca (ChAdOx1 nCoV-19) adenoviral-based COVID-19 vaccination and aHUS in the Dutch population.

Method

Prospective case descriptions

From January 2021 to May 2022 we prospectively identified Dutch pediatric and adult patients who developed onset or relapse aHUS after COVID-19 vaccination with the mRNA-based Pfizer-BioNTech (BNT162b2) or Moderna (mRNA-1273) vaccine, and adenoviral-based AstraZeneca (ChAdOx1 nCoV-19) or Janssen (Ad26.COV2.S) vaccine. Diagnosis of aHUS was made by the treating physician, yet consultation with the aHUS working group was a prerequisite for inclusion in this study. The aHUS working group consists of one pediatric nephrologist and one nephrologist from each University Medical Center in The Netherlands and forms a platform for medical discussions and evaluation of individual cases with (suspected) aHUS. Patients with a confirmed secondary form of TMA and thrombotic thrombocytopenic purpura (TTP, ADAMTS13 activity level <10%) were excluded. In all patients, genomic analysis was performed to screen for variants in complement proteins, including factor H (CFH), factor B (CFB), factor I (CFI), C3, membrane cofactor protein (MCP/CD46), CFH-related proteins 1-5 (CFHR1-5), diacylglycerol kinase-ϵ (DGKE), and thrombomodulin (THBD). Genomic rearrangements in the CFH/CFHR region were assessed using Multiplex Ligation-dependent Probe Amplification (MLPA). In addition, the homozygous presence of at-risk *CFH-H3* and *MCPggaac* haplotypes were evaluated (22, 23). In all patients, detection of autoantibodies against CFH was performed using an in-house enzyme-linked immunosorbent assay (ELISA) (24).

Medical relevant data was obtained from the prospective observational CUREiHUS study (NTR5988), in which all patients were included after giving informed consent. For this study, ethical approval was obtained in the Netherlands from the Medical Research Ethics Committee of Oost-Nederland (NL52817.091.15).

Retrospective cohort analysis

To estimate the risk of developing aHUS after COVID-19 vaccination, we retrospectively evaluated the clinical course of patients known with aHUS and who received COVID-19 vaccination in the Radboud University Medical Center, the aHUS expertise center of the Netherlands. This cohort was subdivided into patients either treated with or without complement-inhibiting therapy. A potential aHUS relapse was defined as a ≥20% increase in serum creatinine (sCr) after COVID-19 vaccination, and/or ≥2 of the following TMA criteria: thrombocytopenia (platelet count <150 x 10^9/L), lactate dehydrogenase (LDH) above the upper limit of normal (>250 U/l) and low/undetectable haptoglobin (<0.3 mg/L). This retrospective evaluation required no formal ethical approval nor informed consent, in accordance with Dutch law. Of note, in the majority of patients, laboratory evaluation shortly after vaccination was protocolized due to participation in the RECOVAC study (NL76215.042.2).

Statistical analysis

Clinical characteristics, including among others medical history and genomic analysis, were descriptively expressed. Laboratory parameters were presented as absolute numbers (for individual values) or median and (min-max) range. Statistical analyses were performed using IBM SPSS Statistics (V.25.0) and figures were drawn using Microsoft Office Excel and Powerpoint (V.2016).

Results

Prospective case descriptions

From January 2021 to May 2022, two Caucasian adult patients and one Caucasian pediatric patient, all with the pathogenic C3 variant C.481 C>T (p.(Arg161Trp)) in heterozygosity, developed *de novo* (n=1) or relapse aHUS (n=2) in native kidneys. All three patients presented with evident hematological signs (≥2 parameters) of TMA and AKI (77-560% increase in sCr) (Figure 1). In addition, C3 levels were decreased (540 and 650 mg/L, reference range (ref) 700-1500 mg/L) in 2/3 patients (*cases 1* and *2*), but normal (1169 mg/L) in one patient (*case 3*). However, in this patient (*case 3*), levels of C3bBbP (38.0 CAU/ml, ref 0-12), sC5b-9 (0.78 CAU/ml, ref 0-0.5), C3d (15.6 mg/L, ref <8.3) and C3d/C3 ratio (13.3, ref <8.1) were elevated, indicating complement activation. Overall, aHUS was diagnosed a median of 3 days (range 2-15) after mRNA-based (Pfizer/BioNTech's, BNT162b2) or adenoviral-based (AstraZeneca, ChAdOx1 nCoV-19) COVID-19 vaccination. However, clinical symptoms (other than the most common side-effects after COVID-19 vaccination <48 hours after vaccination) were already reported after a median of 2 (1-3) days. Clinical characteristics and symptoms of all patients are provided in Table 1. Of note, in two patients (without complement-inhibitory treatment) no complications occurred after the first COVID-19 vaccination. In addition, the pediatric patient (*case 3*) had been vaccinated according to the Dutch National Immunization Program, yet these vaccinations did not result in aHUS onset.

An underlying infection as a trigger for aHUS could be excluded in all patients, as infection parameters were low (CRP <1-7 mg/L, leukocyte count 3.6-10.3x10^9/L) and viral (among others Influenza A/B and COVID-19) and bacterial (including STEC) serological diagnostics were negative. After eculizumab initiation (within 24 hours after first detection of TMA in 2/3 patients), rapid and complete recovery of TMA parameters was observed in all, which even enabled early (≤5 weeks) eculizumab withdrawal in two patients (*cases 1* and *3*). Kidney function fully recovered to baseline values in two patients but recovery was incomplete in one adult (*case 2*), who required dialysis for a duration of sixteen days in the acute phase. Notably, this latter patient had a medical history of hypertension and was known with proteinuria (UPCR 0.67 g/10mmol). A median of 28 (8-33) weeks after eculizumab discontinuation, kidney function has remained stable in all patients.

In addition to abovementioned patients, two patients with the C.481 C>T C3 variant were treated with eculizumab therapy due to a clinical diagnosis of aHUS relapse after COVID-19 vaccination. Although evident other explanatory factors were absent, in

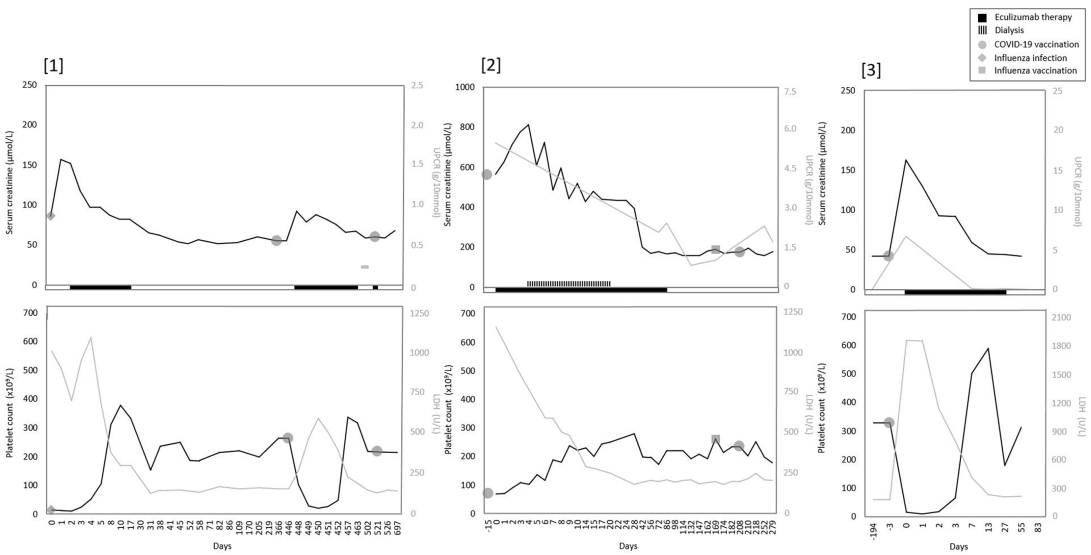

FIGURE 1
Overview of serum creatinine, proteinuria, and TMA parameters over time in all patients. Overview trend of serum creatinine, proteinuria and TMA parameters LDH and thrombocytes (platelet count). [1] Only one measurement of UPCR was available in patient one. Before the second COVID-19 vaccination, a prophylactic dose of eculizumab was given.

TABLE 1 Patient Characteristics.

ID	Sex, age[1] (at onset)	Relevant comorbidities	Native kidneys vs kidney transplant	Genetic complement analysis[2]	Family history	Type of vaccination	Days from vaccination to start of symptoms	Days from vaccination to start of TMA[3]	Clinical signs and symptoms at presentation	Treatment
Case 1	Female, 26 (21)	–	Native kidneys	Heterozygous C3 variant C.481 C>T (p.(Arg161Trp)) Homozygous haplotype MCP*ggaac*	Yes, aHUS in father and aunt (case 3)	AstraZeneca (ChAdOx1 nCoV-19) Adenoviral vector based vaccine [1st]	2	2	Fever, dark urine, ongoing epistaxis, nausea.	Eculizumab (start at TMA day 3) for 2.5 weeks
Case 2	Female, 58 (58)	Hypertension, proteinuria	Native kidneys	Heterozygous C3 variant C.481 C>T (p.(Arg161Trp))	Yes, aHUS in sibling and niece (case 1)	AstraZeneca (ChAdOx1 nCoV-19) Adenoviral vector based vaccine [2nd]	3	15	Headache, vomiting, dyspnoea on exertion, hypertension, petechiae	Dialysis for 16 days. Eculizumab (start at 1st day of TMA) for 12 weeks
Case 3	Male, 12 (10)	–	Native kidneys	Heterozygous C3 variant C.481 C>T (p.(Arg161Trp))	None	Pfizer/ BioNTech'sBNT162b2mRNA vaccine [2nd]	1	3	Nausea, abdominal pain, jaundice, dark urine, oliguria, petechiae, hypertension	Eculizumab (start at 1st day of TMA) for 4 weeks
Case 4	Female, 57 (57)	Crohn's disease	Native kidneys	Heterozygous C3 variant C.481 C>T (p.(Arg161Trp)) Homozygous haplotype MCP*ggaac*	None	Pfizer/BioNTech's (BNT162b2)mRNA vaccine [1st + 3rd]	2 2nd relapse: 10	7 2nd relapse: 26	Hypertension and diarrhea	Eculizumab for 12 weeks and (2nd relapse) 15 weeks. Eculizumab was started after respectively 10 and 8 days of TMA.[3]
Case 5	Male, 53 (50)	Antiphospholipid syndrome	Native kidneys	Heterozygous C3 variant C.481 C>T (p.(Arg161Trp)) Homozygous haplotype MCP*ggaac*	None	Pfizer/ BioNTech'sBNT162b2mRNA vaccine [2nd]	+/- 40	69 [delay]	Fatigue	Eculizumab (start at TMA day 13) for 12 weeks

1 Age at (first) episode of aHUS after COVID-19 vaccination.

2 Align GVGD, Sorting Intolerant From Tolerant (SIFT) and Polymorphism Phenotyping v2 (PolyPhen) databases/tools were used for prediction of clinical significance. The Genome Aggregation Database (gnomAD) was used to determine the minor allele frequency (MAF). Only variants of unknown significance, (likely) pathogenic variants, and MCPggaac or CFH-H3 risk haplotypes (if present in homozygosity) were reported.

3 Start of TMA was defined as first day of detected laboratory TMA parameters. In case 3, TMA parameters were absent. First day of TMA was defined as start of sCr increase (>15%) after COVID-19 vaccination.

10.3389/fimmu.2022.1056153

10.3389/fimmu.2022.1056153

retrospect, in both patients (*cases 4* and *5*) aHUS relapse but also the timely relation with COVID-19 vaccination could be debated (Table 1; Supplementary Figure 1). One patient (*case 5*) presented with relatively minor changes in TMA parameters and a sCr increase of only 8% (Supplementary Table 1; Supplementary Figure 1). In addition, TMA parameters were assessed with a delay of 69 days after vaccination and complement activity parameters were not determined. The other patient (*case 4*) was diagnosed with aHUS relapse, but did not present with TMA. This patient was known with chronic mild thrombocytosis due to a relatively small spleen (3.6 centimeters) and/or as a symptom of Crohn's disease. Although an increase in sCr (18-23%) and UPCR after Pfizer/BioNTech vaccination, TMA parameters all remained within ranges of normal. Complement C3 levels were normal (789 mg/L), but levels of C3bBbP (22.6 CAU/ml), sC5b-9 (0.96 CAU/ml), C3d (8.5 mg/L) and C3d/C3 ratio (10.8) were all mildly elevated, indicating some level of complement activation. In addition, aHUS recurrence could not be excluded due to the presence of unexplained diarrhea (which resembled the clinical picture of her first episode of aHUS), increased blood pressure, and the absence of other explanatory factors for this kidney function decline. In contrast to the abovementioned episodes and despite adequate complement inhibition (eculizumab through level 91µg/mL), in this patient, more evident but self-limiting changes in thrombocytes and LDH levels were observed after the second Pfizer/BioNTech vaccination (Supplementary Figure 1, *case 4*).

Retrospective cohort analysis

Laboratory results after COVID-19 vaccination were available from 29 (including 1 child) and 12 aHUS patients respectively without and with complement-inhibiting therapy, receiving a total of 73 and 31 vaccinations (Supplementary Table 1). The majority of patients (21/29 and 8/12) in this retrospective cohort were kidney transplant recipients. In addition, the presence of a complement genetic variant was confirmed in 88% (36/41) of the patients. In all but one patient, TMA was not reported after vaccination. In this one patient, a kidney transplant recipient, ≥2 TMA parameters were found after vaccination(s), however without an increase in sCr and despite adequate complement inhibition (CH50 <10%) with eculizumab. A kidney biopsy was performed, which showed signs compatible with CNI toxicity and no thrombosis. Tacrolimus was discontinued and TMA parameters normalized. Subclinical aHUS recurrence triggered by vaccination was thus deemed unlikely. A ≥20% increase in serum creatinine (sCr) values was found in 6 and 1 patient(s) without and with complement-inhibiting therapy. In all 7 episodes, sCr increase could either be assigned to other explanatory factors (e.g. intercurrent disease) or was temporary, and (re)start of eculizumab was not required. Therefore, clinically relevant aHUS recurrence due to COVID-19 vaccination in these patients was excluded.

Discussion

We presented two adult patients and one pediatric patient with a pathogenic complement variant, who developed evident new onset or relapse aHUS shortly after either the first, second, or even third COVID-19 vaccination with the mRNA-based Pfizer/BioNTech's (BNT162b2) or adenoviral-based AstraZeneca (ChAdOx1 nCoV-19) vaccine. To our knowledge, this is the first study to report (COVID) vaccination as a triggering event for aHUS in patients with a documented complement mutation. In all episodes, other aHUS triggering or explanatory events were absent. Atypical HUS onset or recurrence was diagnosed a median of 3 days (range 2-15) after COVID-19 vaccination, but clinical symptoms were reported after a median duration of 2 (1-3) days. In one patient with dubious aHUS relapse, we cannot exclude that aHUS episode could have been diagnosed more profoundly and earlier if TMA parameters were assessed at the time of the start of symptoms. Our data confirms the findings of three adult cases with a pathogenic complement variant, who developed aHUS 1-6 days after BNT162b2, ChAdOx1 nCoV, or mRNA-1273 vaccination (19–21). In addition, two cases of, respectively, a Caucasian and African adult patient who developed TMA onset 5 and 10 days after ChAdOx1 nCoV vaccination have been reported (25, 26). However, aHUS diagnosis in both cases could be debated, as genomic analysis revealed only a benign complement variant in one patient and was not even performed in the other. In addition, in this last patient, clinical symptoms improved by oral prednisolone treatment alone (26).

Last year, the number of reports on thrombocytopenia-associated disorders as a complication of COVID-19 vaccination increased significantly. A vaccine-induced immune thrombotic thrombocytopenia (VITT) was found approximately 5-20 days after AstraZeneca (ChAdOx1 nCoV-19) vaccination (13). VITT is characterized by (cerebral venous sinus) thrombosis, thrombocytopenia, and elevated D-dimer levels. It is caused by the formation of complexes of adenovirus hexon proteins with platelet factor 4 (PF4) on platelet surfaces (27, 28). Subsequently, anti-PF4 autoantibodies are produced and can directly activate platelets (12, 13). Besides VITT, cases of immune thrombocytopenia (ITP) after AstraZeneca (ChAdOx1 nCoV-19) vaccination have been reported, yet antibodies associated with this condition (including anti-PF4 antibodies) have not been identified to date (29, 30). Thrombotic thrombocytopenic purpura (TTP), another form of TMA, has also been associated with both mRNA and adenoviral-based COVID-19 vaccination (31, 32). In 95% of patients, TTP is caused by the presence of anti-ADAMTS13 autoantibodies, and a decreased (<10%) ADAMTS13 activity is found responsible for the low platelet count. Theoretically, TTP after COVID-19 vaccination could be caused by newly-formed autoantibodies. Yet, it is hypothesized that COVID-19 vaccination, especially in

early-onset TTP, can be a trigger of occult, undiagnosed TTP rather than inducing TTP. Particularly since ADAMTS-13 antigens and vaccine components (including SARS-CoV-2-spike (S) proteins) bear no resemblance, and the autoimmune process (the formation of autoreactive B-cells, plasma cells, and autoantibodies) and development of the clinical phenotype of TTP requires at least 7-10 days (33).

In aHUS, TMA is the result of overactivation of the alternative complement pathway (AP). COVID-19 infection can potentially trigger aHUS, as COVID-19 initiates an innate immune response (16–18, 34–36). The soluble SARS-CoV-2 spike protein binds to the ACE-2 receptor, expressed on (among others) endothelial cells (37). Subsequently, expression of pro-inflammatory factors (especially TNF-α and IL-1) will induce coagulation and activation of the complement system. In addition, *in vitro*, the SARS-CoV-2 spike protein (subunits 1 and 2) can directly and predominantly initiate the alternative complement pathway (APC) on cell surfaces (33). In their subsequent study, Yu et al. (38) found that dysregulation of the APC plays an important role in disease severity in COVID-19 patients. In example, spike protein 2 directly competes with CFH, and serum from COVID-19 patients could increase membrane attack complex (C5b-9) deposition on cell surface or induce complement-mediated cell death (39). At first, it was not expected that only localized and minor presence of the SARS-CoV-2 spike protein, as expressed after both mRNA and adenoviral-based vaccination, could induce massive acceleration of these mechanisms and thereby cause systemic (pro-thrombotic) conditions in healthy individiduals (13, 33, 39, 40). However, in aHUS patients, the synergistic effect of a local complement-amplifying condition and a pre-existing (pathogenic) complement genetic variant might cause conversion of a 'normal' pro-inflammatory state into an unrestrained overactivation of the AP.

Although three cases of aHUS after COVID-19 vaccination appears to be substantial (especially considering a yearly incidence rate in the Netherlands of approximately 10 aHUS episodes), signs of recurrent disease after vaccination were absent in our retrospective cohort of 29 aHUS patients without complement-inhibitory treatment. Of note, this retrospective cohort consisted of patients from (the largest but) a single-center academic hospital in the Netherlands. Unfortunately, the total number of vaccinated aHUS patients in the Netherlands is unknown and data on outpatient clinic visits after vaccination was predominantly available in kidney transplant recipients. All prospective patients (n=5) participated in the CUREiHUS study (in which a total of 49 patients have been included since January 2016), a national Dutch prospective observational study including aHUS patients with a first-time eculizumab treatment since January 2016. Although discussion of all possible aHUS patients in the national aHUS working group for indication to start eculizumab and inclusion in the CUREiHUS study is protocolized in the Netherlands, this is not an absolute prerequisite. Therefore, we cannot exclude missing a patient with aHUS relapse after COVID-19 vaccination in our prospective cohort. It should also be noted that aHUS was only diagnosed after Pfizer/BioNTech's and AstraZeneca vaccination, yet the majority of patients in our retrospective cohort were vaccinated with Moderna. Due to the small number of patients in both cohorts, an increased risk of aHUS after certain vaccines could not be confirmed nor the definite risk of recurrence be calculated. At last, we could only determine a temporal relationship between COVID-19 vaccination and aHUS, and data on the actual pathophysiological mechanism is not yet available.

In conclusion, we identified COVID-19 vaccination as a potential trigger for aHUS onset or relapse in pediatric and adult patients who are not treated with C5 inhibition. Therefore, aHUS should be included in the differential diagnosis of patients with vaccine-induced thrombocytopenia, especially if co-occurring with MAHA and severe AKI, but in absence of major neurological complications. This underlines the importance of clear patient instruction and routine (laboratory) monitoring after COVID-19 vaccination for kidney function, proteinuria, TMA parameters, and blood pressure days after COVID-19 vaccination. Of note, since the complement system is capricious, uncomplicated previous (COVID-19) vaccinations are no guarantee for future (non-)development of aHUS after vaccination. As the risk of aHUS recurrence after COVID-19 vaccination appears to be acceptable, we advise continuation of COVID-19 vaccination in aHUS patients, as this evidently reduces the risk of severe COVID-19 infection.

Data availability statement

The original contributions presented in the study are included in the article/Supplementary Material. Further inquiries can be directed to the corresponding author.

Ethics statement

This study involved human participants and was reviewed and approved by the Medical Research Ethics Committee of Oost-Nederland (registration number of the CUREiHUS study: NL52817.091.15) (only applicable for prospective patients). This trial is registered at the Dutch Trial Registry NTR5988. Written informed consent to participate in this study was provided by the participant or participants' legal guardian/next of kin.

Author contributions

RB recruited the patients. RB, EB, and CD collected the data. RB and EB wrote the manuscript, under critical supervision and review of AL, AZ, JW, and NK. All authors contributed to the article and approved the submitted version.

Funding

All prospective patients were included in the CUREiHUS study, which is supported by grants from Zorgverzekeraars Nederland and ZonMw, 'Goed Gebruik Geneesmiddelen' (project number 836031008). They did not have any role in data collection, analysis or submission of this manuscript.

Acknowledgments

We are very grateful to the patients for their willingness to participate in this study. In addition, we thank the research nurses and database managers for their local management and data collection: Yvet Kroeze, Nienke Sonneveld, and Helma Dolmans.

Conflict of interest

JW is a member of the international advisory board of Alexion and also received a grant from Alexion. NvdK has received a consultancy fee from Roche Pharmaceuticals and Novartis and is a sub-investigator in the APL2-C3G trial, Apellis. AB received a consultancy fee from Novartis, is a member of the DSMB Zoster-047 trial, GSK, and a sub-investigator in the Belatacept study, BMS. VG is sub-investigator in the APL2-C3G trial, Apellis.

The remaining authors declare that the research was conducted in the absence of any commercial or financial relationships that could be constructed as a potential conflict of interest.

Publisher's note

Supplementary material

The Supplementary Material for this article can be found online at: https://www.frontiersin.org/articles/10.3389/fimmu.2022.1056153/full#supplementary-material

References

1. Westra D, Wetzels JF, Volokhina EB, van den Heuvel LP, van de Kar NC. A new era in the diagnosis and treatment of atypical haemolytic uraemic syndrome. *Neth J Med* (2012) 70(3):121–9.

2. Fakhouri F, Zuber J, Frémeaux-Bacchi V, Loirat C. Haemolytic uraemic syndrome. *Lancet* (2017) 390(10095):681–96. doi: 10.1016/S0140-6736(17)30062-4

3. Fakhouri F, Fila M, Hummel A, Ribes D, Sellier-Leclerc AL, Ville S, et al. Eculizumab discontinuation in children and adults with atypical hemolytic-uremic syndrome: A prospective multicenter study. *Blood* (2021) 137(18):2438–49. doi: 10.1182/blood.2020009280

4. George JN, Nester CM. Syndromes of thrombotic microangiopathy. *N Engl J Med* (2014) 371(7):654–66. doi: 10.1056/NEJMra1312353

5. Loirat C, Frémeaux-Bacchi V. Atypical hemolytic uremic syndrome. *Orphanet J Rare Dis* (2011) 6:60. doi: 10.1186/1750-1172-6-60

6. Loirat C, Fakhouri F, Ariceta G, Besbas N, Bitzan M, Bjerre A, et al. An international consensus approach to the management of atypical hemolytic uremic syndrome in children. *Pediatr Nephrol* (2016) 31(1):15–39. doi: 10.1007/s00467-015-3076-8

7. Geerdink LM, Westra D, van Wijk JA, Dorresteijn EM, Lilien MR, Davin JC, et al. Atypical hemolytic uremic syndrome in children: Complement mutations and clinical characteristics. *Pediatr Nephrol* (2012) 27(8):1283–91. doi: 10.1007/s00467-012-2131-y

8. Avcı Z, Bayram C, Malbora B. Hepatitis b vaccine-associated atypical hemolytic uremic syndrome. *Turk J Haematol* (2013) 30(4):418–9. doi: 10.4274%2FTjh-2013.0226

9. Legendre CM, Licht C, Muus P, Greenbaum LA, Babu S, Bedrosian C, et al. Terminal complement inhibitor eculizumab in atypical hemolytic-uremic syndrome. *N Engl J Med* (2013) 368(23):2169–81. doi: 10.1056/NEJMoa1208981

10. Wijnsma KL, Duineveld C, Wetzels JFM, van de Kar N. Eculizumab in atypical hemolytic uremic syndrome: Strategies toward restrictive use. *Pediatr Nephrol* (2019) 34(11):2261–77. doi: 10.1007/s00467-018-4091-3

11. Kircheis R. Coagulopathies after vaccination against SARS-CoV-2 may be derived from a combined effect of SARS-CoV-2 spike protein and adenovirus vector-triggered signaling pathways. *Int J Mol Sci* (2021) 22(19). doi: 10.3390/ijms221910791

12. Sharifian-Dorche M, Bahmanyar M, Sharifian-Dorche A, Mohammadi P, Nomovi M, Mowla A. Vaccine-induced immune thrombotic thrombocytopenia and cerebral venous sinus thrombosis post COVID-19 vaccination; a systematic review. *J Neurol Sci* (2021) 428:117607. doi: 10.1016/j.jns.2021.117607

13. Greinacher A, Thiele T, Warkentin TE, Weisser K, Kyrle PA, Eichinger S. Thrombotic thrombocytopenia after ChAdOx1 nCov-19 vaccination. *N Engl J Med* (2021) 384(22):2092–101. doi: 10.1056/NEJMoa2104840

14. Fattizzo B, Pasquale R, Bellani V, Barcellini W, Kulasekararaj AG. Complement mediated hemolytic anemias in the COVID-19 era: Case series and review of the literature. *Front Immunol* (2021) 12:791429. doi: 10.3389/fimmu.2021.791429

15. Canney M, Atiquzzaman M, Cunningham AM, Zheng Y, Er L, Hawken S, et al. A population-based analysis of the risk of glomerular disease relapse after COVID-19 vaccination. *JASN* (2022) 33:2247–57. doi: 10.1681/ASN.2022030258

16. Kaufeld J, Reinhardt M, Schröder C, Bräsen JH, Wiech T, Brylka P, et al. Atypical hemolytic and uremic syndrome triggered by infection with SARS-CoV2. *Kidney Int Rep* (2021) 6(10):2709–12. doi: 10.1016/j.ekir.2021.07.004

17. Ville S, Le Bot S, Chapelet-Debout A, Blancho G, Fremeaux-Bacchi V, Deltombe C, et al. Atypical HUS relapse triggered by COVID-19. *Kidney Int* (2021) 99(1):267–8. doi: 10.1016/j.kint.2020.10.030

18. El Sissy C, Saldman A, Zanetta G, Martins PV, Poulain C, Cauchois R, et al. COVID-19 as a potential trigger of complement-mediated atypical HUS. *Blood* (2021) 138(18):1777–82. doi: 10.1182/blood.2021012752

19. Rysava R, Peiskerova M, Tesar V, Benes J, Kment M, Szilágyi Á, et al. Atypical hemolytic uremic syndrome triggered by mRNA vaccination against SARS-CoV-2: Case report. *Front Immunol* (2022) 13:1001366. doi: 10.3389/fimmu.2022.1001366

20. Dos Santos C, Chavarri A, Alberto MF, Fondevilla CG, Sánched-Luceros A. Recurrence of atypical hemolytic uremic syndrome after COVID-19 vaccination. *Can J Kidney Health Dis* (2022) 9:6.

21. Claes KJ, Geerts I, Lemahieu W, Wilmer A, Kuypers DRJ, Koshy P, et al. Atypical hemolytic uremic syndrome occurring after receipt of mRNA-1273 COVID-19 vaccine booster: A case report. *Am J Kidney Dis* (2022) 0272-6386. doi: 10.1053/j.ajkd.2022.07.012

22. Caprioli J, Castelletti F, Bucchioni S, Bettinaglio P, Bresin E, Pianetti G, et al. Complement factor h mutations and gene polymorphisms in haemolytic uraemic syndrome: the c-257T, the A2089G and the G2881T polymorphisms are strongly associated with the disease. *Hum Mol Genet* (2003) 12(24):3385–95. doi: 10.1093/hmg/ddg363

23. Esparza-Gordillo J, Goicoechea de Jorge E, Buil A, Carreras Berges L, López-Trascasa M, Sánchez-Corral P, et al. Predisposition to atypical hemolytic uremic syndrome involves the concurrence of different susceptibility alleles in the regulators of complement activation gene cluster in 1q32. *Hum Mol Genet* (2005) 14(5):703–12. doi: 10.1093/hmg/ddi066

24. Dragon-Durey MA, Sethi SK, Bagga A, Blanc C, Blouin J, Ranchin B, et al. Clinical features of anti-factor h autoantibody-associated hemolytic uremic syndrome. *J Am Soc Nephrol* (2010) 21(12):2180–7. doi: 10.1681/ASN.2010030315

25. Ferrer F, Roldão M, Figueiredo C, Lopes K. Atypical hemolytic uremic syndrome after ChAdOx1 nCoV-19 vaccination in a patient with homozygous CFHR3/CFHR1 gene deletion. *Nephron* (2022) 146(2):185–9. doi: 10.1159/000519461

26. Aku TA, Dordoye EK, Yamoah P, Apraku T, Gyamera A. Hemolytic uremic syndrome: A covid-19 vaccine reaction case report. *Research Square* (2022). doi: 10.21203/rs.3.rs-1254743/v1

27. Greinacher A, Selleng K, Palankar R, Wesche J, Handtke S, Wolff M, et al. Insights in ChAdOx1 nCoV-19 vaccine-induced immune thrombotic thrombocytopenia. *Blood* (2021) 138(22):2256–68. doi: 10.1182/blood.2021013231

28. Scully M, Singh D, Lown R, Poles A, Solomon T, Levi M, et al. Pathologic antibodies to platelet factor 4 after ChAdOx1 nCoV-19 vaccination. *N Engl J Med* (2021) 384(23):2202–11. doi: 10.1056/NEJMoa2105385

29. Pasin F, Calabrese A, Pelagatti L. Immune thrombocytopenia following COVID-19 mRNA vaccine: Casuality or causality? *Intern Emerg Med* (2022) 17 (1):295–7. doi: 110.1007%2Fs11739-021-02778-w

30. Uaprasert N, Panrong K, Tungjitviboonkun S, Dussadee K, Decharatanachart P, Kaveevorayan P, et al. ChAdOx1 nCoV-19 vaccine-associated thrombocytopenia: Three cases of immune thrombocytopenia after 107 720 doses of ChAdOx1 vaccination in Thailand. *Blood Coagul Fibrinol* (2022) 33(1):67–70. doi: 10.1097/mbc.0000000000001082

31. Osmanodja B, Schreiber A, Schrezenmeier E, Seelow E. First diagnosis of thrombotic thrombocytopenic purpura after SARS-CoV-2 vaccine - case report. *BMC Nephrol* (2021) 22(1):411. doi: 10.1186%2Fs12882-021-02616-3

32. Shah H, Kim AS, Sukumar S, Mazepa MA, Kohli R, Braunstein EM, et al. SARS-CoV-2 vaccination and immune thrombotic thrombocytopenic purpura. *Blood* (2022) 139(16):2570–73. doi: 10.1182/blood.2022015545

33. Yu J, Yuan X, Chen H, Chaturvedi S, Braunstein EM, Brodsky RA. Direct activation of the alternative complement pathway by SARS-CoV-2 spike proteins is blocked by factor d inhibition. *Blood* (2020) 136(18):2080–9. doi: 10.1182/blood.2020008248

34. Cugno M, Meroni PL, Gualtierotti R, Griffini S, Grovetti E, Torri A, et al. Complement activation in patients with COVID-19: A novel therapeutic target. *J Allergy Clin Immunol* (2020) 146(1):215–7.

35. Regis Peffault De L, Anne B, Etienne L, Thibault D, Armance M, Lionel G, et al. Complement C5 inhibition in patients with COVID-19 - a promising target? *Haematologica* (2020) 105(12):2847–50. doi: 10.3324/haematol.2020.260117

36. Magro C, Mulvey JJ, Berlin D, Nuovo G, Salvatore S, Harp J, et al. Complement associated microvascular injury and thrombosis in the pathogenesis of severe COVID-19 infection: A report of five cases. *Transl Res* (2020) 220:1–13. doi: 10.1016/j.trsl.2020.04.007

37. Defendi F, Leroy C, Epaulard O, Clavarino G, Vilotitch A, Le Marechal M, et al. Complement alternative and mannose-binding lectin pathway activation is associated with COVID-19 mortality. *Front Immunol* (2021) 12:742446. doi: 10.3389/fimmu.2021.742446

38. Kowarz E, Krutzke L, Reis J, Bracharz S, Kochanek S, Marschalek R. Vaccine-induced COVID-19 mimicry syndrome. *eLife* (2022) 11:e74974. doi: 10.7554/eLife.74974

39. Yu J, Gerber GF, Chen H, Yuan X, Chaturvedi S, Braunstein EM, et al. Complement dysregulation is associated with severe COVID-19 illness. *Haematologica* (2021) 107(5):1095–105. doi: 10.3324/haematol.2021.279155

40. Almehdi AM, Khoder G, Alchakee AS, Alsayyid AT, Sarg NH, Soliman SSM. SARS-CoV-2 spike protein: pathogenesis, vaccines, and potential therapies. *Infection* (2021) 49(5):855–76. doi: 10.1007/s15010-021-01677-8

frontiers | Frontiers in Immunology

TYPE Original Research
PUBLISHED 12 January 2023
DOI 10.3389/fimmu.2022.1058763

OPEN ACCESS

EDITED BY
Mihály Józsi,
Eötvös Loránd University, Hungary

REVIEWED BY
Marina Noris,
Mario Negri Institute for Pharmacological Research (IRCCS), Italy
Lubka T. Roumenina,
INSERM U1138 Centre de Recherche des Cordeliers (CRC), France

*CORRESPONDENCE
Ton J. Rabelink
a.j.rabelink@lumc.nl

SPECIALTY SECTION
This article was submitted to Molecular Innate Immunity, a section of the journal Frontiers in Immunology

RECEIVED 30 September 2022
ACCEPTED 12 December 2022
PUBLISHED 12 January 2023

CITATION
Gaykema LH, van Nieuwland RY, Dekkers MC, van Essen MF, Heidt S, Zaldumbide A, van den Berg CW, Rabelink TJ and van Kooten C (2023) Inhibition of complement activation by CD55 overexpression in human induced pluripotent stem cell derived kidney organoids.
Front. Immunol. 13:1058763.
doi: 10.3389/fimmu.2022.1058763

Inhibition of complement activation by CD55 overexpression in human induced pluripotent stem cell derived kidney organoids

Lonneke H. Gaykema[1,2], Rianne Y. van Nieuwland[1], Mette C. Dekkers[1], Mieke F. van Essen[1], Sebastiaan Heidt[3,4], Arnaud Zaldumbide[2], Cathelijne W. van den Berg[1,5], Ton J. Rabelink[1,5]* and Cees van Kooten[1]

[1]Department of Internal Medicine-Nephrology, Leiden University Medical Center, Leiden, Netherlands, [2]Department of Cell and Chemical Biology, Leiden University Medical Center, Leiden, Netherlands, [3]Department of Immunology, Leiden University Medical Center, Leiden, Netherlands, [4]Eurotransplant Reference Laboratory, Leiden University Medical Center, Leiden, Netherlands, [5]The Novo Nordisk Foundation Center for Stem Cell Medicine (reNEW), Leiden University Medical Center, Leiden, Netherlands

End stage renal disease is an increasing problem worldwide driven by aging of the population and increased prevalence of metabolic disorders and cardiovascular disease. Currently, kidney transplantation is the only curative option, but donor organ shortages greatly limit its application. Regenerative medicine has the potential to solve the shortage by using stem cells to grow the desired tissues, like kidney tissue. Immune rejection poses a great threat towards the implementation of stem cell derived tissues and various strategies have been explored to limit the immune response towards these tissues. However, these studies are limited by targeting mainly T cell mediated immune rejection while the rejection process also involves innate and humoral immunity. In this study we investigate whether inhibition of the complement system in human induced pluripotent stem cells (iPSC) could provide protection from such immune injury. To this end we created knock-in iPSC lines of the membrane bound complement inhibitor CD55 to create a transplant-specific protection towards complement activation. CD55 inhibits the central driver of the complement cascade, C3 convertase, and we show that overexpression is able to decrease complement activation on both iPSCs as well as differentiated kidney organoids upon stimulation with anti-HLA antibodies to mimic the mechanism of humoral rejection.

KEYWORDS

complement, CD55 (DAF), iPSCs, kidney organoids, CRISPR-Cas9, transplantation, immune modulation

Introduction

End stage renal disease is increasing in prevalence worldwide. The inadequate availability of donor organs is the critical limiting factor in curative treatment. Human induced pluripotent stem cells (iPSCs) are a promising approach for regenerative medicine to circumvent the shortage of organ donors. Lineage specific differentiation protocols allow for the generation of many tissues, including kidney. Our group and others have shown that iPSC-derived kidney organoids contain nephrons and are vascularized upon transplantation (1–4), indicating the potential use of these organoids in transplantation to improve kidney function in patients. The use of autologous iPSC-derived tissues is not feasible in most cases, but transplantation of allogeneic tissue has an increased risk of rejection because of human leukocyte antigen (HLA) mismatches. Currently several strategies have been envisaged to generate hypoimmunogenic stem cells. While a lot of effort has been made to prevent T cell mediated rejection by disrupting HLA expression or by the overexpression of inhibitory molecules (5–8), no studies have been conducted to limit the deleterious effect of complement activation, while it has a significant role in graft rejection.

The complement system is part of the innate immune system and provides protection against micro-organisms. Activation of the cascade can be initiated *via* three separate routes: *via* binding of C1q to the Fc domains of surface bound antibodies (classical pathway), *via* mannose-containing polysaccharides recognition (lectin pathway) or *via* spontaneous hydrolysis of the internal C3 thioester bond (alternative pathway). All three pathways converge at the level of the C3 convertase, and induce a similar set of bioactive split products C3a, C3b, C5a, and the terminal product C5b-9, also called the membrane attack complex (MAC) (9). Regulation of the complement cascade is crucial because otherwise uncontrolled activation leads to organ damage and chronic inflammatory (autoimmune) renal diseases, including atypical haemolytic uraemic syndrome (aHUS), C3 glomerulopathy (C3G), systemic lupus erythematosus (SLE) and transplant rejection (10).

In transplantation the complement cascade can be activated by various triggers. In kidney transplantation, ischemia reperfusion injury (IRI) can cause release of damage-associated molecular patterns (DAMPS) that trigger activation (11). Later after transplantation, the presence of donor specific antibodies can result in classical pathway activation and thereby increase the risk for allograft rejection (12, 13). Also transplantation of tissues like kidney organoids are at risk of inducing deleterious complement activation, illustrated by the islet transplantation model of Xiao et al., who showed that deposition of complement product C3b in the transplanted tissue was associated with rejection (14). Complement activation is able to induce direct allograft injury *via* the formation of the MAC, and indirectly *via* the production of active split products that stimulate both the innate and adaptive immune response (15). Especially anaphylatoxins C3a and C5a contribute significantly to allograft rejection by promoting leukocyte infiltration (mainly macrophages) (16, 17) and stimulating effector T cell survival (18), proliferation and activation (17, 18) *via* signaling through complement receptors on leukocytes and tissue resident cells (16). The broad influence of complement activation on the whole immune response underscores the potential as a target for immune modulation. Although systemic complement inhibition may expose patients to higher risk of infection, genetic modification of the transplanted tissue by expression of complement inhibitors would offer site-specific protection. Multiple natural regulators of the complement system have been identified, of which many interfere at the level of the C3 convertase (9). C3 convertase is a strategic target since it is the converging point of the different activation routes and the central driver of the cascade. Inhibition of C3 convertase shuts down the complete cascade, including the production of anaphylatoxins C3a and C5a, and formation of the MAC. The effectiveness of C3 inhibition is illustrated by a recent study where compstatin was used in a kidney transplantation model in non-human primates. Improved graft survival and kidney function were achieved together with decreased macrophage infiltration, a lower amount of circulating cytokines and decreased T and B cell proliferation and activation (19).

In the current study we evaluated the potential of complement regulator CD55, also known as decay accelerating factor (DAF), which acts as a complement regulatory protein by accelerating the decay of C3 convertase and preventing its reassembly (20). Expression of CD55 in renal allografts was shown to have a protective effect on graft survival and function (21). We genetically modified iPSCs to overexpress CD55 and evaluated the complement inhibitory potential in iPSCs and iPSC-derived kidney organoids. We show that CD55 is able to inhibit complement activation and is therefore a promising candidate in the development of hypoimmunogenic iPSCs for transplantation purposes.

Materials and methods

iPSC maintenance and kidney organoid differentiation

Human iPSCs used in this study were generated by the LUMC iPSC Hotel using RNA Simplicon reprogramming kit (Millipore) (LUMC0072iCTRL01, detailed information at Human Pluripotent Stem Cell Registry, https://hpscreg.eu/). iPSCs were cultured on recombinant human vitronectin in Essential 8 (E8) medium (Thermo Fisher Scientific) and passaged every 3-4 days using 0.5 mM UltraPure EDTA

(Thermo Fisher Scientific). iPSCs were differentiated to kidney organoids following a previously described protocol (1, 3). In short, iPSCs were incubated for 4 days in STEMdiff APEL2 medium (APEL2) containing 1% PFHMII (Life Technologies), 1% Antibiotic–Antimycotic (Life Technologies) and 8 µM CHIR99021 (Tocris). On day 4, the medium was changed to APEL2 with 200 ng mL^{-1} rhFGF9 (R&D Systems) and 1 µg mL^{-1} heparin (Sigma-Aldrich). On day 7, cells were pulsed with 5 µM CHIR for 1 hour, dissociated and transferred as small 3-dimensional clumps containing 5×10^5 cells on Transwell 0.4 mm pore polyester membranes (Corning) in APEL2 containing FGF-9 and heparin. Medium was refreshed on day 7 + 3. On day 7 + 5 growth factors were removed and the APEL2 medium was refreshed every 2 days for the remaining culture time until day 7 + 14.

Genetic modification by CRISPR-Cas9

Genetic modification of iPSCs was performed by transfection of DNA plasmids using Lipofectamine Stem Transfection Reagent (Invitrogen). iPSCs were passaged the day before transfection. For transfection 7.5 µL of Lipofectamine Stem (Thermo Fisher Scientific) was mixed with 3 µg DNA plasmids in 125 µl optiMEM and after 15 min incubation at room temperature added to iPSCs. After transfection, iPSCs were kept in culture with daily change of media for 4 days. On day 4 iPSCs were dissociated into a single-cell suspension using TrypLE select (Thermo Fisher Scientific) and 20×10^3 cells per cm^2 were transferred to new culture plates in E8 containing RevitaCell Supplement (Thermo Fisher Scientific) and 0.2 µg mL^{-1} puromycin (InvivoGen). Selection by puromycin was continued for 6 – 7 days after which plain E8 medium was added. Remaining colonies were kept in culture until they had reached a size of 2-3 mm in diameter which took roughly 10 – 13 days after the single cell passage. Single colonies were scraped off, submerged in 0.5 mM EDTA for 5 min at 37°C, washed and transferred to a new plate containing E8 medium. iPSC clones were propagated, cryopreserved and cellular material was collected to validate the genetic modification.

Plasmid production

In each transfection for genetic modification by CRISPR-Cas9, 3 plasmids were used for homology directed repair in the Adeno-Associated Virus Integration Site 1 (AAVS1) region. 1. plasmid containing the sequence for Cas9 driven by a CAG promoter (Cas9 plasmid), 2. plasmid containing the gRNA (gRNA plasmid), and 3. plasmid containing the donor DNA for homologous recombination (donor DNA plasmid). The generation of the Cas9 plasmid (AV62_pCAG.Cas9.rBGpA) (22) and the gRNA plasmid targeting the safe harbor human locus AAVS1 (23), have been detailed elsewhere. The 2 donor DNA plasmids were assembled by inserting either an ORF for GFP or CD55 in an Age1+Not1 enzymatically digested AAVS1-CAG-puroR-T2A acceptor plasmid. The final donor DNA plasmids (pdonor.AAVS1-CAG-puroR-T2A-GFP and pdonor.AAVS1-CAG-puroR-T2A-CD55) contain AAVS1 homology arms flanking a CAG promoter, followed by the ORF of puromycin resistance gene and GFP or CD55 separated by a T2A sequence. Transformation of plasmids was performed in chemo-competent E.Coli bacteria and plasmids were isolated using maxiprep (Genomed). Correct plasmid sequences were validated by sanger sequencing by the Leiden Genome Technology Center (LGTC).

DNA isolation and genomic PCR

DNA isolation was done on cell pellets of roughly 500 x 10^3 iPSCs using the DNeasy kit (Qiagen) and DNA concentrations measured with nanodrop. PCR reactions were performed using GoTaq® G2 Flexi DNA Polymerase (Promega) under the following conditions: 100-200 ng DNA, 1× Green GoTaq Flexi buffer, 1.25 units GoTaq G2 Flexi polymerase, 0.3 µM each primer, 0.3 mM each dNTP and 1.5 mM $MgCl_2$ in a 30 µl volume for 30-40 cycles in a C1000 Touch Thermal Cycler (Bio-Rad, Hercules, USA). Primers used for screening are described in Supplemental Table 1. PCR products were loaded on a 1% agarose gel for size separation and DNA bands were visualized by ethidium bromide detection in a Molecular Imager Gel Doc XR+ (Bio-Rad). Size was estimated by comparing with GeneRuler DNA Ladder mix (Thermo Scientific).

mRNA isolation and qPCR

Total RNA was isolated using a nucleospin RNA/protein kit (Bioké) and RNA concentrations were measured with nanodrop. SuperScript III Reverse Transcriptase (Invitrogen) was used for the production of cDNA that was used as a template in real-time polymerase chain reaction (RT-qPCR). RT-qPCR was performed using SYBR Green Supermix (Bio-Rad) in a CFX Connect Real-Time System (Bio-Rad). Primers used in RT-qPCR are described in Supplemental Table 1. The expression of each gene was normalized to the level of glyceraldehyde-3-phosphate dehydrogenase (GAPDH) expression and relative mRNA levels were determined based on the comparative Ct method ($2^{-\Delta\Delta Ct}$) to the respective controls.

Immunohistochemistry

Organoids were fixed in 2% PFA for 20 min at 4°C, washed with PBS and incubated with the following primary antibodies:

sheep anti-human NPHS1 (1:100, AF4269, R&D Systems), mouse anti-E-Cadherin (1:250, 610181, BD), biotinylated Lotus Tetragonolobus Lectin (LTL) (1:300, B-1325, Vector Laboratories) and mouse anti-human CD55 (1:500, ab1422, Abcam). Secondary antibodies were donkey anti-sheep Alexa-647 (A21448, Invitrogen), donkey anti-mouse Alexa-568 (A10037, Invitrogen), donkey anti-mouse Alexa-488 (A21202, Invitrogen), and Streptavidin conjugated with Alexa-532 (S11224, Invitrogen), all at 1:500 dilution. Nuclei were stained with Hoechst33342 (1:10000, H3576, Invitrogen) and organoids were mounted using ProLong Gold Antifade Mountant (Invitrogen) in glass bottom dishes (MatTek). Images were acquired using a White Light Laser Confocal Microscope TCS SP8 and LAS-X Image software.

In vitro complement activation assay

iPSCs or kidney organoids were stimulated with 500 IU mL^{-1} recombinant human IFN-γ (Invitrogen) 48 hours prior to the complement activation assay to increase HLA surface expression. iPSCs were dissociated into single cells using TrypLE select for 5 min at 37°C. Kidney organoids were dissociated to single cells by incubation in collagenase I buffer consisting of 600 U mL^{-1} collagenase Type I (Worthington) and 0.75 U mL^{-1} DNAse (Sigma Aldrich) in HBSS with calcium and magnesium (Thermo Fisher Scientific) for 40 minutes at 37°C with repeated pipetting, followed by TrypLE buffer consisting of 5 U mL^{-1} DNAse I (Sigma Aldrich) and 4 µg mL^{-1} heparin (Sigma Aldrich) in 80% TrypLE select 10x (Thermo Fisher Scientific) in DPBS (Thermo Fisher Scientific) for 5 min at 37°C. Dissociation was stopped by adding HBSS with 10% FBS. Cell clusters were removed by passing the cells over a 30 µm filter and the single cells were resuspended in PBS + 0,1% BSA. In the *in vitro* complement activation assay, iPSCs and kidney organoid cells were first incubated with a human anti- HLA-A2 (SN607D8) or human anti-HLA-A1 (GV2D5) antibody, generated as described previously (24) at 3 µg mL^{-1} for 30 min on ice. Normal human serum (NHS) was used as complement source and heat-inactivated normal human serum (dNHS), 45 min incubated at 56°C, was used as complement inactivated control. Cells were washed and incubated in 10% NHS or dNHS diluted in RPMI for 1 hour at 37°C, after which cells were processed for analysis by flow cytometry.

Flow cytometry

For flow cytometry the following antibodies were used: PE-conjugated mouse anti- HLA-ABC (1:100, 555553, BD Biosciences), human anti- HLA-A2 antibody (3 µg mL^{-1}, SN607D8), mouse anti-human CD55 (1:500, ab1422, Abcam), mouse anti-C3 (1:1000, RFK22, in-house generated), mouse anti-C5b-9 (1:100, AE11, Hycult Biotech), PE-conjugated mouse anti-human CD46 (1:100, 12-0469-42, Invitrogen), and APC-conjugated mouse anti-human CD59 (1:100, 17-0596-42, Invitrogen) were used as primary antibodies. Secondary antibodies used for detection were PE-conjugated goat anti-human IgG (1:1000, 109-116-098, Jackson) and PE-conjugated goat anti-mouse (1:100, R0480, DAKO). All antibody incubations were done for 30 min on ice with subsequent washing in PBS + 0,1% BSA. Flow cytometry was performed on a LSR-II (BD) and acquired results analyzed using FlowJo (BD).

Statistical analysis

Results were visualized and statistically analyzed using Graphpad Prism. Each sample was compared to the respective control by using T-test or one-way ANOVA with Dunnett correction for multiple comparisons as indicated. Values are shown as mean + SD and p-value < 0.05 was considered statistically significant.

Results

iPSCs are sensitive to antibody-induced complement activation

To evaluate the immunogenicity of iPSCs and the possible involvement of humoral immunity, we developed a system to study allo-antibody induced complement activation. iPSCs were shown to express HLA class I, which could be further increased by 48 hours incubation with IFN-γ (Figure 1A). iPSCs were further evaluated for expression of transmembrane complement regulators. iPSCs showed mRNA expression of the C3-convertase inhibitors CD46/MCP, CD55/DAF and the C5b-9 inhibitor CD59 (Figure 1B), as well as surface protein expression (Figure 1C).

To investigate complement activation at the surface, the HLA-A2-positive iPSCs were stimulated by IFN-γ and incubated with a human anti-HLA-A2 antibody. This was followed by exposure to complement active NHS, thereby mimicking classical pathway activation. Following 1 hour incubation at 37°C, iPSCs were analyzed for the deposition of complement activation fragments using flow cytometry (Figure 1D). 1 hour incubation with NHS did not affect the phenotype of the iPSCs (Supplemental Figure 1A), but did result in the deposition of C3 as the central complement component (Figure 1E) and C5b-9 as the end product of the terminal pathway (Figure 1F). Both the proportion positive cells as well as the MFI showed a significant increase compared to the negative control, using dNHS. Complement deposition was most prominent for C3 (mean 20 fold increase in MFI), implying an insufficient regulation of the

10.3389/fimmu.2022.1058763

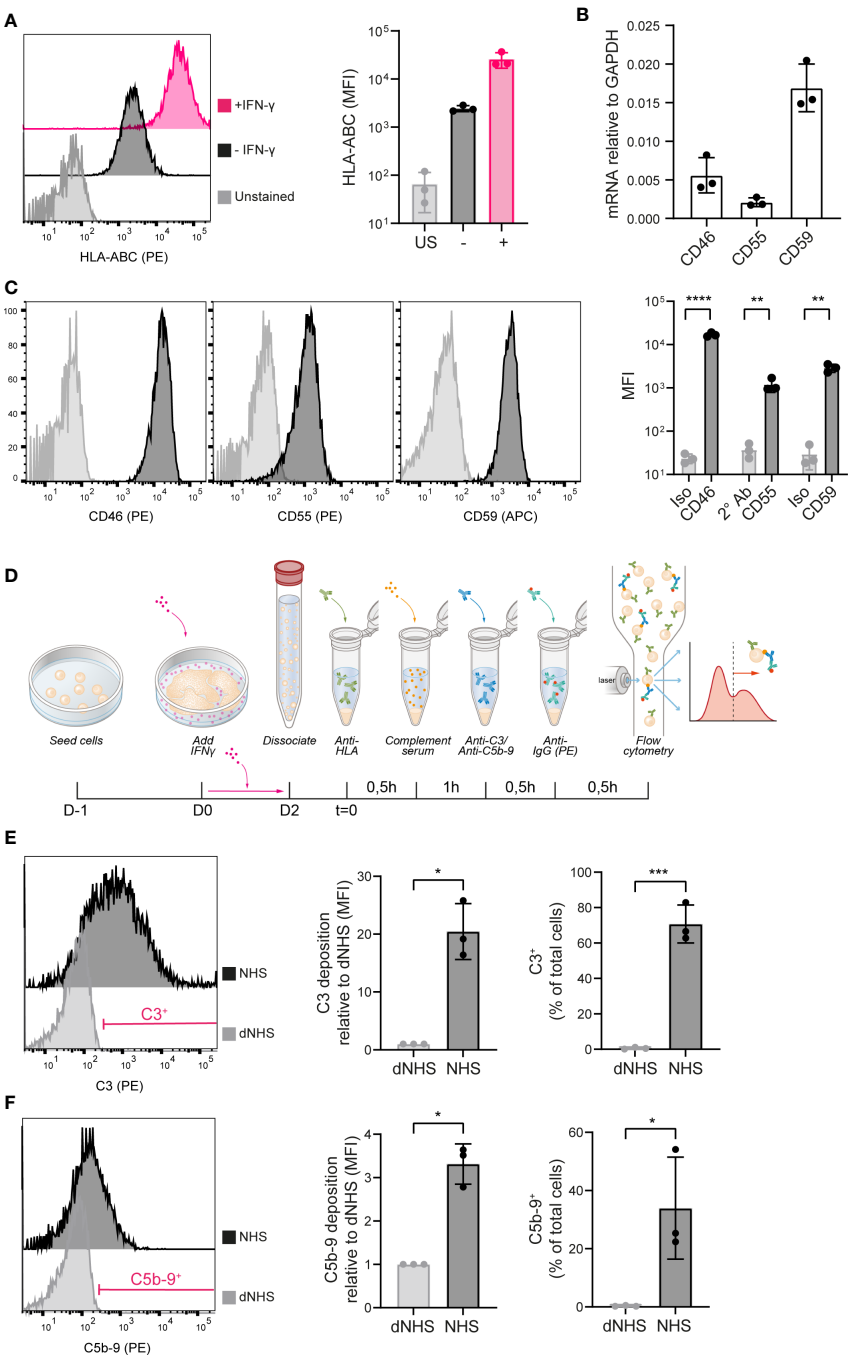

FIGURE 1
iPSCs are vulnerable to complement activation. **(A)** HLA-ABC surface protein expression measured by flow cytometry in unstained (US), unstimulated (–) and IFN-γ stimulated (+) iPSCs. A representative histogram is shown of three independent experiments (n=3). **(B)** mRNA expression of CD46, CD55 and CD59 in iPSCs measured by RT-qPCR (n=3). **(C)** Complement inhibitor CD46, CD55 and CD59 protein surface expression in iPSCs measured by flow cytometry. Representative histograms are shown of three independent experiments (n=3). **(D)** Schematic of the experimental procedure to measure complement deposition on iPSCs *in vitro*. **(E)** C3 deposition on iPSCs incubated with heat-inactivated (dNHS) or active normal human serum (NHS) measured by flow cytometry. Results are presented as relative mean fluorescence intensity (MFI) and $C3^+$ proportion. A representative histogram of three independent experiments (n=3) is shown and indicates the gate for the $C3^+$ proportion. **(F)** C5b-9 deposition on iPSCs incubated with heat-inactivated (dNHS) or active normal human serum (NHS) measured by flow cytometry. Results are presented as relative mean fluorescence intensity (MFI) and $C5b\text{-}9^+$ proportion. A representative histogram of three independent experiments (n=3) is shown and indicates the gate for the $C5b\text{-}9^+$ proportion. Error bars show standard deviation and significance (*$p < 0.05$; **$p < 0.01$; ***$p < 0.001$; ****$p < 0.0001$) was evaluated using T-test.

C3-convertase on the iPSCs. In addition, we showed that incubation of iPSCs with an anti-HLA-A1 antibody, an alloantigen not expressed on these iPSCs, did not result in complement activation, indicating an alloantigen-specific response (Supplemental Figure 1B).

Generation of iPSCs with stable overexpression of CD55

iPSCs were genetically modified to (over-)express either complement inhibitor CD55 or GFP. Following transfection and selection, CRISPR/Cas9 modified iPSC clones were selected and further characterized (Figure 2A). To ensure stable transgene expression, we selected a synthetic CAG promoter to drive CD55 or GFP expression and the adeno-associated virus integration site 1 (AAVS1) locus as target location. The insert sequence further contained a puromycin resistance (puroR) gene to allow for selection (Figure 2B).

In total 12 clones were selected for both CD55 and GFP modification. AAVS1 specific locus integration was assessed by PCR using primer sets spanning the homology arm and confirmed that 9 out of 12 CD55 clones (iPSC-CD55) and 10 out of 12 GFP clones (iPSC-GFP) were modified correctly (Figure 2B). iPSC-CD55 clone 2, 4 and 6, and iPSC-GFP clone 6 were selected for follow-up experiments, in which iPSC-GFP served as control to test the effectivity of CD55 overexpression.

CD55 gene and protein expression were validated by qPCR and flow cytometry analysis respectively and compared to iPSC-GFP and the parental (unmodified) iPSCs, indicated as control. CRISPR-Cas9 gene editing led to consistent 30-fold increase in CD55 mRNA expression in the iPSC-CD55 clones, compared to controls (Figure 2C). In line with this, also CD55 protein surface expression was on average 10 – 15 times higher in all three CD55-clones compared to iPSC-GFP (Figure 2D). As expected, GFP expression was exclusively detected in iPSC-GFP (Supplemental Figure 2).

CD55 overexpressing iPSCs are protected against complement activation

To evaluate whether CD55 surface overexpression affected complement activation, we used the same *in vitro* complement activation assay (Figure 1). iPSCs were maintained for 2 days in presence of IFN-γ to increase HLA surface expression. We confirmed that the CD55 and GFP-overexpressing clones showed a similarly increased expression of HLA-A2 (Figure 3A). In addition, also mRNA and surface expression of the complement regulators CD46 and CD59 were not affected by the gene modifications (Figure 3B; Supplemental Figure 3).

Complement C3 deposition at the surface of iPSC-GFP was comparable to the unmodified iPSCs. In contrast, all three CD55 overexpressing clones showed a significant inhibition of C3 deposition at the surface of these cells (Figure 3C), reducing it to the levels observed with dNHS. Similar results were observed for the deposition of C5b-9 (Figure 3D), albeit the level of C5b-9 deposition under control conditions was much lower. These data confirmed that CD55 overexpression is able to control complement activation at the surface of these iPSCs.

CD55 overexpressing iPSCs successfully differentiate to kidney organoids

Next, we differentiated the iPSC clones to kidney organoids and evaluated their ability to differentiate following genetic modification and compared their phenotype to the parental (unmodified) iPSC line (control). Macroscopic pictures showed a conserved phenotype in all the modified iPSC-CD55 and iPSC-GFP clones compared to unmodified iPSCs (Figure 4A). Immunohistochemical staining confirmed the presence of glomerular (NPHS1), proximal tubular (LTL) and distal tubular structures (ECAD) in all organoids (Figures 4B, C), demonstrating that kidney organoid differentiation was successful following genetic modification and overexpression of CD55.

Overexpression of CD55 on differentiated kidney organoid cells protects against anti-HLA-induced complement activation

Control kidney organoids showed low expression of CD55, as investigated by immunofluorescence staining (Figure 5A). On the other hand, CD55 overexpressing clones showed prominent CD55 staining throughout the organoid (Figure 5A; Supplemental Figure 4A). In line with the immunofluorescence analysis, the CD55 mRNA expression was low in control organoids, but strongly increased in the CD55 overexpressing clones (Figure 5B). This was confirmed by the difference in CD55 surface expression as shown by flow cytometry (Figure 5C). It should be noted that the CD55 expression was more heterogenous compared to the expression on iPSCs. Similar to CD55, GFP expression was maintained after differentiation of GFP-iPSCs towards kidney organoids (Supplemental Figures 4B, C).

To assess functionality of CD55 overexpression, we adapted the protocol used for iPSCs to measure complement deposition on single organoid cells. Kidney organoid cells showed an increased expression of HLA-A2 by IFN-γ stimulation (Figure 5D) and CD55 overexpressing clones showed a similar expression of CD46 and CD59 as control and iPSC-GFP-derived kidney organoids (Figure 5E; Supplemental Figure 5). When exposed to anti-HLA-A2 antibodies, followed by NHS, organoid cells showed a significant increase in complement activation, as

10.3389/fimmu.2022.1058763

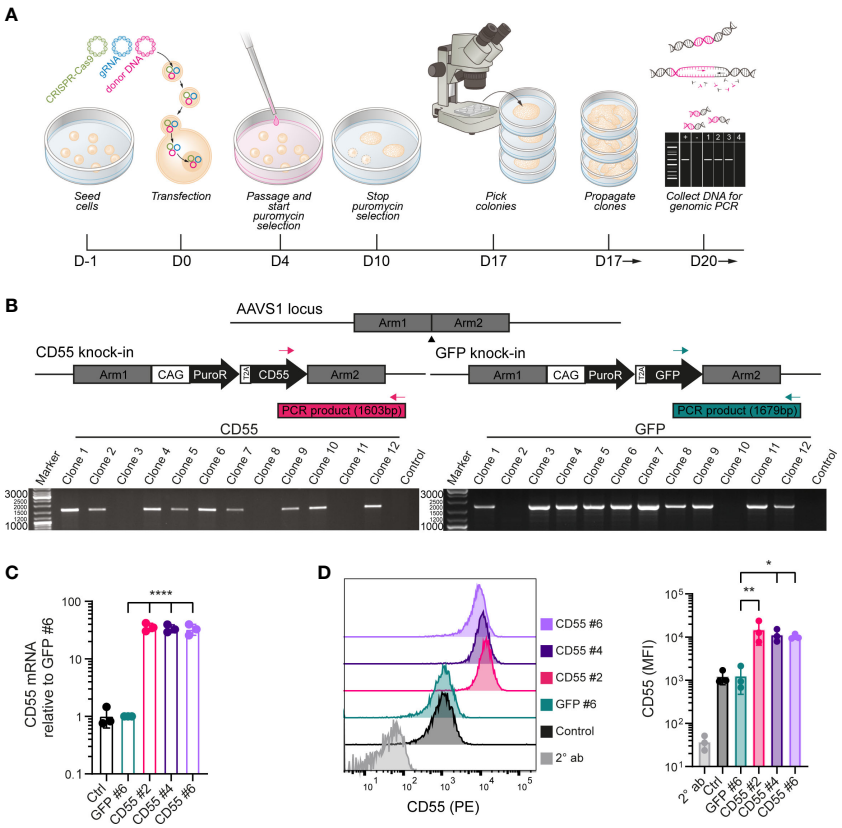

FIGURE 2
Genetic modification of iPSCs to induce over-expression of CD55. **(A)** Schematic of the genetic modification strategy by transfection of plasmids in iPSCs using lipofectamine and puromycin selection. **(B)** PCR strategy with inserted sequences for CD55 or GFP and a puromycin resistance (puroR) gene in the AAVS1 locus and analysis of puromycin selected iPSC clones with 2 distinct primer sets. DNA of the parental unmodified cell line was used as a negative control and clones were screened for the amplification of a PCR product with the indicated size (1603bp for CD55 insert or 1679bp for GFP insert). **(C)** mRNA expression of CD55 in control iPSCs and modified iPSC clones (GFP #6, CD55 #2, 4 and 6) measured by RT-qPCR (n=3). **(D)** CD55 protein expression in control iPSCs and modified iPSC clones measured by flow cytometry (n=3) showing a representative histogram. Staining with only PE-conjugated secondary antibody (2° ab) is shown in light grey. Error bars show standard deviation and significance (*p < 0.05; **p < 0.01; ****p < 0.0001) was evaluated using one-way ANOVA comparing each sample to iPSC-GFP with Dunnett correction for multiple comparisons.

shown by the deposition of C3 and C5b-9, compared to the negative control using dNHS (Figures 5F, G). Complement deposition was significantly inhibited in the CD55-overexpressing clones. All together these data show that CD55 overexpression can be an efficient tool to diminish antibody-mediated complement activation, both in undifferentiated iPSCs as well as differentiated kidney organoids.

Discussion

Since the generation of iPSCs (25, 26), the application of their derived tissues in regenerative medicine holds great expectations for solving the shortage of donor organs. Yet, immune surveillance of the host remains a barrier for further clinical applications. In this study we demonstrate the potential of CD55 overexpression in iPSCs and differentiated kidney organoids to improve resistance towards complement activation. Importantly, we show that knock-in of CD55 in the AAVS1, 'safe harbour' (27), locus did not influence the quality of the kidney organoids and allowed a stable and strong CD55 expression throughout the differentiation.

Our data illustrate a different sensitivity of iPSCs compared to kidney organoids to complement activation, shown by a higher intensity of complement deposition on differentiated cells. This observation underscores the importance of better control on complement activation when iPSC-derived cells and tissues are considered to be used in transplantation. Interestingly we found reduced CD55 expression during kidney organoid differentiation (Figures 1D, 5C), which is in line with our previous work on embryonic stem cell-derived beta cells that was accompanied with reduced CD55 expression (28). In

10.3389/fimmu.2022.1058763

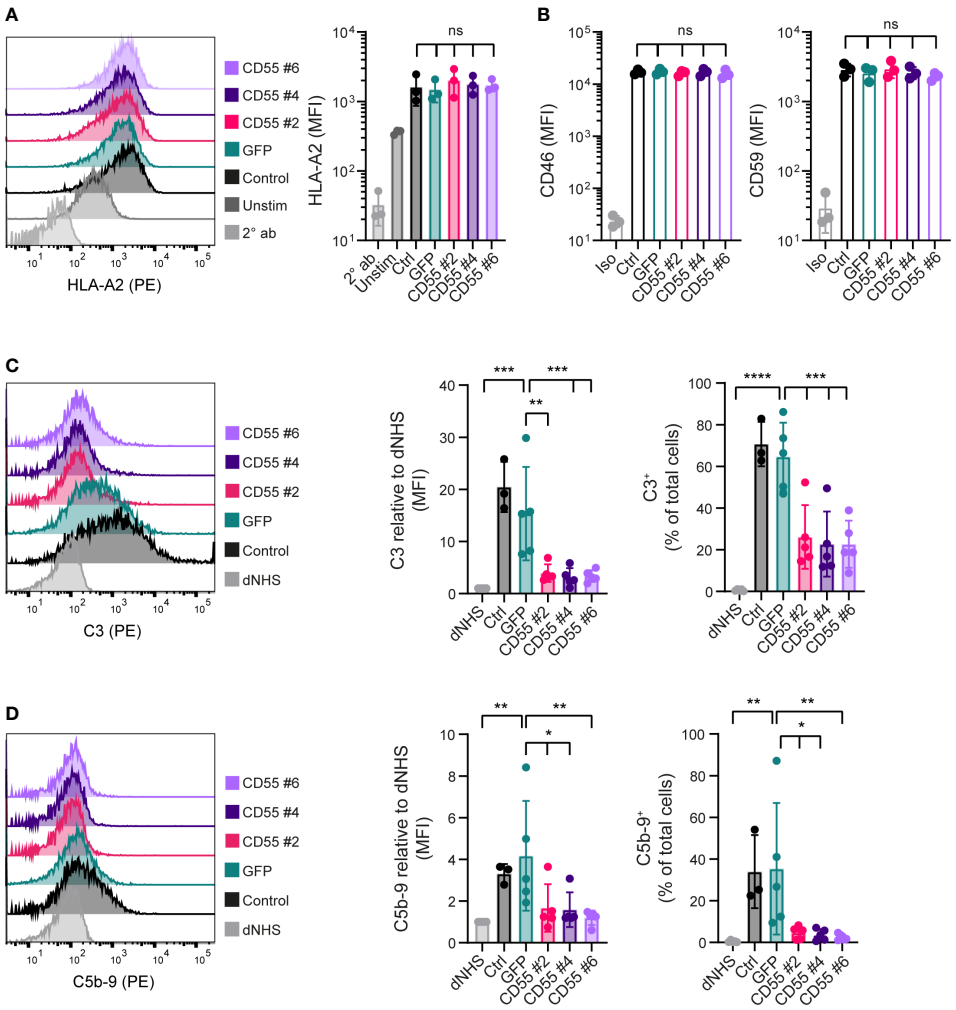

FIGURE 3
CD55 overexpression in iPSCs decreases complement deposition. **(A)** Cell surface opsonization by anti-HLA-A2 in unstimulated (Unstim) and IFN- γ stimulated (Ctrl, GFP, CD55 #2, 4 and 6) iPSCs measured by flow cytometry. A representative histogram is shown and results are presented as mean fluorescence intensity (MFI) in three independent experiments (n=3). Staining with only PE-conjugated secondary antibody (2° ab) is shown in light grey. **(B)** CD46 and CD59 protein surface expression on iPSCs measured by flow cytometry (n=3). Staining with isotype (Iso) is shown in light grey. (**C, D**) C3 and C5b-9 deposition on iPSCs incubated with normal human serum (NHS) measured by flow cytometry. Incubation with heat-inactivated NHS (dNHS) was used as negative control and is shown in light grey. Results are presented as relative mean fluorescence intensity (MFI) and $C3^+$ or $C5b\text{-}9^+$ proportion. A representative histogram is shown (n=3 for control, n=5 for others). Error bars show standard deviation and significance (*p < 0.05; **p < 0.01; ***p < 0.001; ****p < 0.0001) was evaluated using one-way ANOVA comparing each sample to iPSC-GFP with Dunnett correction for multiple comparisons. ns, non significant.

contrast, complement regulatory proteins, CD46 and CD59, remained present following kidney organoids differentiation (Supplemental Figure 5). Therefore the low surface CD55 expression detected in the kidney organoids may play a more prominent role in the increased vulnerability to complement activation and overexpression of CD55 provides the opportunity to increase resistance. CD55 knock-in iPSCs can be used for differentiation of any desirable tissue or cell type. Although we found that the complement inhibition by CD55 overexpression was evident for both undifferentiated iPSCs and iPSC-derived kidney organoids, this can not directly be translated to all differentiated cell types. Further research is necessary to validate the use of CD55 overexpression in other iPSC-derived cells.

In our studies on complement reactivity to iPSC-derived kidney organoids we focused on analysis of dissociated cells. The use of flow cytometry to evaluate complement activation provides higher sensitivity and offers the possibility for quantification. For future research however, it would be valuable to extend the complement reactivity and apply the experimental setup to whole organoids. Additionally it would be of critical importance to validate the findings in an *in vivo*

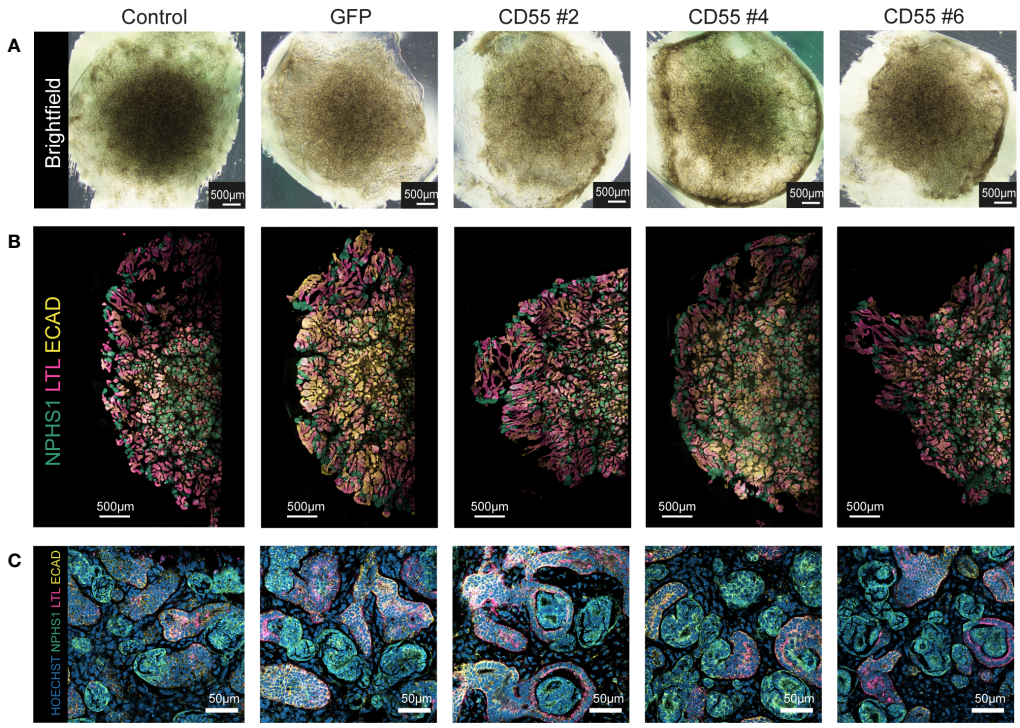

FIGURE 4
Modified iPSC-derived kidney organoids contain nephron structures upon differentiation. **(A)** Representative brightfield images of kidney organoids from unmodified iPSCs (control) and genetically modified iPSCs at day 7 + 14 of differentiation. **(B)** Representative fluorescent images of half an organoid, with detection of NPHS1 (podocytes, green), LTL (proximal tubule, pink), and ECAD (distal tubule, yellow). **(C)** Representative images of a higher magnification of the staining shown in **(B)** with additional detection of nuclei (Hoechst, blue).

situation, which could also allow for the evaluation of the interaction with other immune components.

The use of CD55, which intervenes in the complement cascade at C3 convertase, is strategically chosen, since it targets the converging point of all three complement activation routes. Our results showed that CD55 overexpression inhibited deposition of both C3 and C5b-9, confirming that the complement cascade was inhibited from C3 to the end of the cascade where the C5b-9 complex, or MAC, is formed. Moreover, overexpression of CD55 may have additional beneficial effects that we did not investigate here (20), since other immune regulation effects have been found including the regulation of T cell proliferation and activation *via* CD97 binding (29), and reduction of NK cell reactivity (30).

In our study, CD55 overexpression did not fully prevent complement deposition, raising the question if additional inhibitory molecules are required. The necessary degree of complement protection is greatly dependent on the application of the transplantable tissue. Intraportal transplantation, commonly used for islet transplantation in patients with type I diabetes, involves a great impact of complement activation as part of the immediate blood mediated immune reaction (IBMIR), and might need a higher grade of protection (31, 32). Furthermore, combination of multiple complement regulatory proteins has shown additive effect in other conditions. In mice it was shown that CD55 is protective against IRI and co-expression with CD59 provided additional protection (33). The need for combining complement regulators is further illustrated by the recent developments in the field of xenotransplantation. For instance higher CD55 and CD59 expression in pig fibroblasts increased their resistance towards human serum mediated cytolysis (34). Similarly in cytotoxicity assays using porcine peripheral blood mononuclear cells of genetically modified pigs, the combination of CD55 and CD59 offered higher protection than either of them alone (35). Also in experimental xenotransplant models, genetic modifications were applied to pigs to overcome these immunological barriers and the addition of complement regulatory proteins CD46, CD55 and/or CD59 was advantageous for transplant outcome (35–37). This has resulted in the first pig to human xenotransplants using 10-gene modified pigs, which include the overexpression of CD55 and CD46 (38, 39).

Complement activation can cause cytotoxicity directly but also functions as an important inducer of innate immune cell infiltration and bridges the innate with the adaptive immune response. In accordance with this, it was shown that C3 inhibition

10.3389/fimmu.2022.1058763

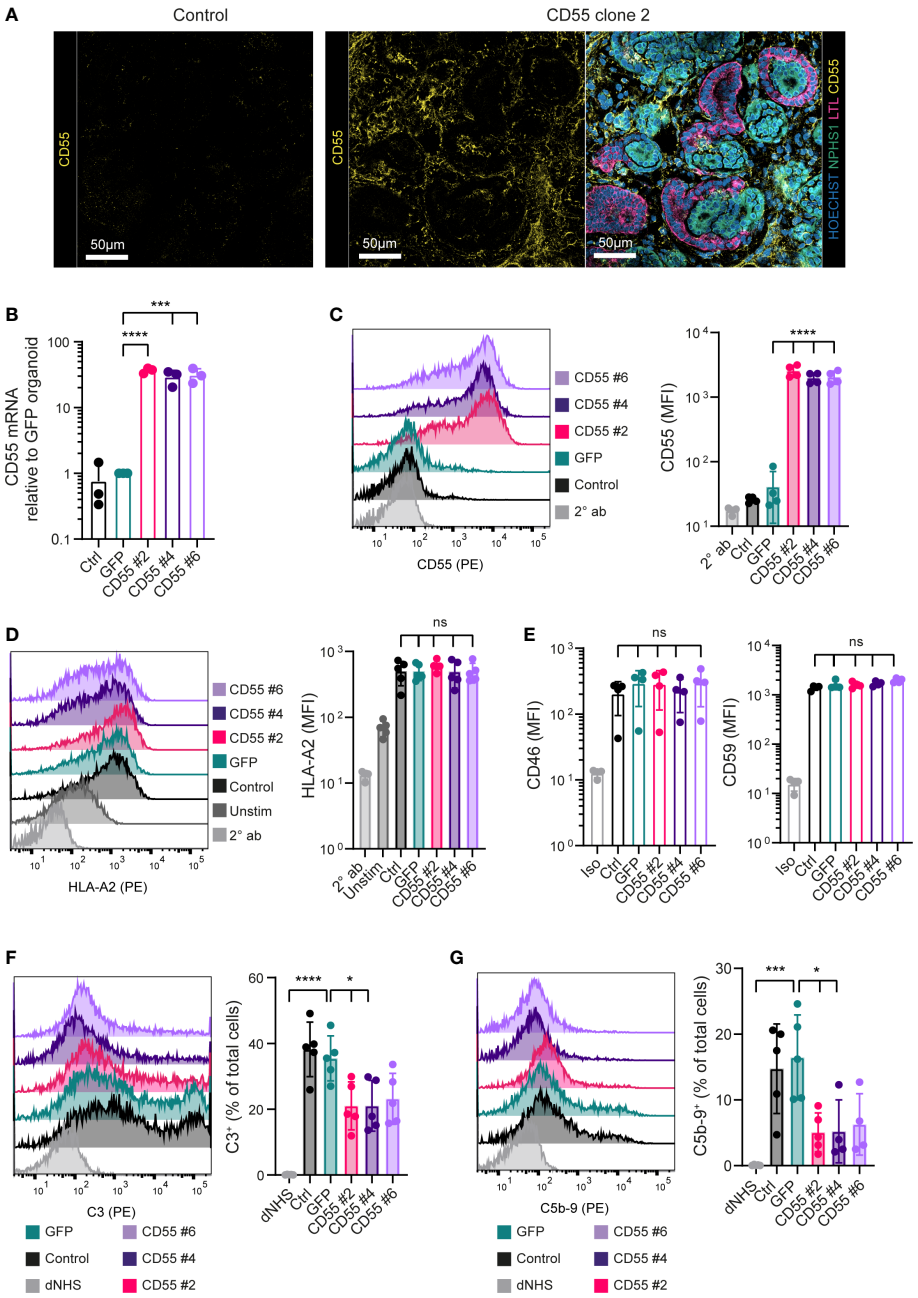

FIGURE 5
CD55 overexpression in kidney organoids decreases complement deposition. **(A)** Representative fluorescent images of organoids with detection of CD55 (yellow) in high magnification. For the CD55 #2 organoid an image with detection of Hoechst (blue), NPHS1 (green), LTL (pink) and CD55 (yellow) of the same area as the separate CD55 image is included. Other clones are included in Supplemental Figure 4. **(B)** CD55 mRNA expression in organoids at day 7 + 14 measured by RT-qPCR (n=3). **(C)** CD55 protein expression in dissociated kidney organoids at day 7 + 14 measured by flow cytometry showing a representative histogram of 5 independent experiments (n=5). Staining with only PE-conjugated secondary antibody (2° ab) is shown in light grey. **(D)** Cell surface opsonization by anti-HLA-A2 in unstimulated (Unstim) and IFN-γ stimulated (Ctrl, GFP, CD55 #2, 4 and 6) kidney organoid cells measured by flow cytometry. A representative histogram is shown of 5 independent experiments (n=5) and staining with only PE-conjugated secondary antibody (2° ab) is shown in light grey. **(E)** CD46 and CD59 protein surface expression on kidney organoid cells measured by flow cytometry (n=5). Staining with isotype (Iso) is shown in light grey. (**F**, **G**) C3 and C5b-9 deposition on kidney organoid cells incubated with normal human serum (NHS) measured by flow cytometry. Incubation with heat-inactivated NHS (dNHS) was used as negative control and is shown in light grey. Results are presented as $C3^+$ or $C5b\text{-}9^+$ proportion. A representative histogram is shown of 5 independent experiments (n=5). Error bars show standard deviation and significance (*p < 0.05; ***p < 0.001; ****p < 0.0001) was evaluated using one-way ANOVA comparing each sample to iPSC-GFP-derived kidney organoids with Dunnett correction for multiple comparisons. ns, non significant.

by the compstatin analog Cp40 in kidney transplantation in primates reduced macrophage infiltration, cytokine production and T and B cell activation (19). However, it is unlikely that complement inhibition alone will prevent alloimmune rejection since this study also showed progressive adaptive immune responses despite complement inhibition.

In conclusion, our results demonstrate that CD55 over-expressing iPSCs and their derived kidney organoids are less susceptible to complement activation *in vitro*, providing evidence for the use of CD55 genetic manipulation to improve transplant outcomes of iPSC-derived tissues.

Data availability statement

The datasets presented in this study can be found in online repositories. The names of the repository/repositories and accession number(s) can be found in the article/Supplementary Material.

Author contributions

LG performed the experiments, analyzed results and wrote the manuscript, RN and MD performed experiments, SH provided the anti-HLA-A1 and anti-HLA-A2 antibody, ME advised the project and reviewed the manuscript, AZ and CB supervised the project and wrote the manuscript, TJR arranged funding and supervised the project, CK supervised the project and wrote the manuscript. All authors contributed to the article and approved the submitted version.

Funding

This study was funded by LUF/Stichting Prof. Jaap de Graeff-Lingling Wiyadharma Fonds 2020-01 and an unrestricted grant from Novo Nordisk. The Novo Nordisk Foundation Center for Stem Cell Medicine (reNEW) is supported by Novo Nordisk Foundation grants (NNF21CC0073729). The funders had no involvement in the study design, collection, analysis, interpretation of data, the writing of this article, or the decision to submit it for publication.

Acknowledgments

We thank Christian Freund (LUMC human iPSC Hotel, Leiden, the Netherlands) for providing hiPSC line LUMC0072iCTRL01. We gratefully acknowledge Steve Cramer and Manuel Goncalves (LUMC, Leiden, the Netherlands) for their expert assistance and Manon Zuurmond for her illustrations. We also thank Ellen Lievers and Anneloes Verwey (LUMC, Leiden, the Netherlands) for their support and the Light & Electron Microscopy Facility (LUMC, Leiden, the Netherlands).

Conflict of interest

The authors declare that the research was conducted in the absence of any commercial or financial relationships that could be construed as a potential conflict of interest.

Publisher's note

Supplementary material

The Supplementary Material for this article can be found online at: https://www.frontiersin.org/articles/10.3389/fimmu.2022.1058763/full#supplementary-material

SUPPLEMENTARY FIGURE 1
Single cell gating and alloantigen-specific complement activation. **(A)** The gating strategy for iPSCs in flow cytometry experiments is indicated for iPSCs incubated with normal human serum (NHS) and heat-inactivated NHS (dNHS). **(B)** C3 and C5b-9 deposition on IFN-γ stimulated and unstimulated (Unstim) iPSCs incubated with allo-antibodies followed by normal human serum (NHS) measured by flow cytometry (n=2). Complement deposition is compared between cells incubated with binding HLA-A2 allo-antibody (Allo ab +) and incubation with HLA-A1 (Allo ab -) that is unable to bind to the cells. Incubation with heat-inactivated NHS (dNHS) was used as negative control and error bars show standard deviation.

SUPPLEMENTARY FIGURE 2
GFP expression in modified iPSCs. **(A)** mRNA expression of GFP in control iPSCs and modified iPSC clones measured by RT-qPCR (n=3). **(B)** GFP protein expression in iPSCs measured by flow cytometry (n=3) showing a representative histogram. Error bars show standard deviation and significance (****p<0.0001) was evaluated using one-way ANOVA comparing each sample to Control iPSCs with Dunnett correction for multiple comparisons.

SUPPLEMENTARY FIGURE 3
mRNA and protein expression of complement regulatory proteins CD46 and CD59 in iPSCs. **(A)** CD46 mRNA expression in iPSCs measured by RT-qPCR (n=3). **(B)** CD46 protein surface expression measured by flow cytometry showing a representative histogram of 3 independent experiments (n=3) of which combined results are presented in Figure 3B. **(C)** CD59 mRNA expression in iPSCs measured by RT-qPCR (n=3). **(D)** CD59 protein surface expression measured by flow cytometry showing a representative histogram of 3 independent experiments (n=3) of which combined results are presented in Figure 3B. Staining with isotype (Iso) is shown in light grey. Error bars show standard deviation and significance was evaluated using one-way ANOVA comparing each sample to iPSC-GFP with Dunnett correction for multiple comparisons.

SUPPLEMENTARY FIGURE 4
CD55 and GFP expression in kidney organoids derived from modified iPSCs. **(A)** Representative fluorescent images in high magnification of organoids with detection of CD55 (yellow) in the upper panel, and an

image with detection of Hoechst (blue), NPHS1 (green), LTL (pink) and CD55 (yellow) of the same area in the lower panel. **(B)** mRNA expression of GFP in kidney organoids at day 7 + 14 measured by RT-qPCR (n=3). **(C)** GFP protein expression in dissociated kidney organoids at day 7 + 14 measured by flow cytometry (n=5) showing a representative histogram. Error bars show standard deviation and significance (****p<0.0001) was evaluated using one-way ANOVA comparing each sample to Control kidney organoids with Dunnett correction for multiple comparisons.

SUPPLEMENTARY FIGURE 5

mRNA and protein expression of complement regulatory proteins CD46 and CD59 in iPSC-derived kidney organoids. **(A)** CD46 mRNA expression in kidney organoids at d7+14 measured by RT-qPCR (n=3). **(B)** CD46 protein expression in kidney organoids at d7+14 measured by flow cytometry including a representative histogram of 5 independent experiments (n=5) of which combined results are presented in Figure 5E. **(C)** CD59 mRNA expression in kidney organoids at d7+14 measured by RT-qPCR (n=3). **(D)** CD59 protein expression in kidney organoids at d7+14 measured by flow cytometry including a representative histogram of 5 independent experiments (n=5) of which combined results are presented in Figure 5E. Staining with isotype (Iso) is shown in light grey. Error bars show standard deviation and significance was evaluated using one-way ANOVA comparing each sample to iPSC-GFP-derived kidney organoids with Dunnett correction for multiple comparisons.

References

1. Takasato M, Er PX, Chiu HS, Maier B, Baillie GJ, Ferguson C, et al. Kidney organoids from human iPS cells contain multiple lineages and model human nephrogenesis. *Nature* (2015) 526(7574):564–8. doi: 10.1038/nature15695

2. Bantounas I, Ranjzad P, Tengku F, Silajdzic E, Forster D, Asselin MC, et al. Generation of functioning nephrons by implanting human pluripotent stem cell-derived kidney progenitors. *Stem Cell Rep* (2018) 10(3):766–79. doi: 10.1016/j.stemcr.2018.01.008

3. van den Berg CW, Ritsma L, Avramut MC, Wiersma LE, van den Berg BM, Leuning DG, et al. Renal subcapsular transplantation of PSC-derived kidney organoids induces neo-vasculogenesis and significant glomerular and tubular maturation in vivo. *Stem Cell Rep* (2018) 10(3):751–65. doi: 10.1016/j.stemcr.2018.01.041

4. Sharmin S, Taguchi A, Kaku Y, Yoshimura Y, Ohmori T, Sakuma T, et al. Human induced pluripotent stem cell-derived podocytes mature into vascularized glomeruli upon experimental transplantation. *J Am Soc Nephrol.* (2016) 27(6):1778–91. doi: 10.1681/ASN.2015010096

5. Gornalusse GG, Hirata RK, Funk SE, Riolobos L, Lopes VS, Manske G, et al. HLA-e-expressing pluripotent stem cells escape allogeneic responses and lysis by NK cells. *Nat Biotechnol* (2017) 35(8):765–72. doi: 10.1038/nbt.3860

6. Deuse T, Hu X, Gravina A, Wang D, Tediashvili G, De C, et al. Hypoimmunogenic derivatives of induced pluripotent stem cells evade immune rejection in fully immunocompetent allogeneic recipients. *Nat Biotechnol* (2019) 37(3):252–8. doi: 10.1038/s41587-019-0016-3

7. Han X, Wang M, Duan S, Franco PJ, Kenty JH, Hedrick P, et al. Generation of hypoimmunogenic human pluripotent stem cells. *Proc Natl Acad Sci U.S.A.* (2019). doi: 10.1073/pnas.1902566116

8. Xu H, Wang B, Ono M, Kagita A, Fujii K, Sasakawa N, et al. Targeted disruption of HLA genes *via* CRISPR-Cas9 generates iPSCs with enhanced immune compatibility. *Cell Stem Cell* (2019) 24(4):566–78 e7. doi: 10.1016/j.stem.2019.02.005

9. Mathern DR, Heeger PS. Molecules great and small: The complement system. *Clin J Am Soc Nephrology.* (2015) 10(9):1636–50. doi: 10.2215/CJN.06230614

10. Ricklin D, Mastellos DC, Reis ES, Lambris JD. The renaissance of complement therapeutics. *Nat Rev Nephrology.* (2018) 14(1):26–47. doi: 10.1038/nrneph.2017.156

11. Nieuwenhuijs-Moeke GJ, Pischke SE, Berger SP, Sanders JSF, Pol RA, Struys M, et al. Ischemia and reperfusion injury in kidney transplantation: Relevant mechanisms in injury and repair. *J Clin Med* (2020) 9(1). doi: 10.3390/jcm9010253

12. Bouquegneau A, Loheac C, Aubert O, Bouatou Y, Viglietti D, Empana JP, et al. Complement-activating donor-specific anti-HLA antibodies and solid organ transplant survival: A systematic review and meta-analysis. *PloS Med* (2018) 15(5):e1002572. doi: 10.1371/journal.pmed.1002572

13. Loupy A, Lefaucheur C, Vernerey D, Prugger C, Duong van Huyen JP, Mooney N, et al. Complement-binding anti-HLA antibodies and kidney-allograft survival. *N Engl J Med* (2013) 369(13):1215–26. doi: 10.1056/NEJMoa1302506

14. Xiao F, Ma L, Zhao M, Huang GC, Mirenda V, Dorling A, et al. Ex vivo expanded human regulatory T cells delay islet allograft rejection *via* inhibiting islet-derived monocyte chemoattractant protein-1 production in CD34(+) stem cells-reconstituted NOD-scid IL2r gamma(null) mice. *PloS One* (2014) 9(3). doi: 10.1371/journal.pone.0090387

15. Zhou W, Farrar CA, Abe K, Pratt JR, Marsh JE, Wang Y, et al. Predominant role for C5b-9 in renal ischemia/reperfusion injury. *J Clin Invest.* (2000) 105(10):1363–71. doi: 10.1172/JCI8621

16. Peng Q, Li K, Smyth LA, Xing G, Wang N, Meader L, et al. C3a and C5a promote renal ischemia-reperfusion injury. *J Am Soc Nephrol.* (2012) 23(9):1474–85. doi: 10.1681/ASN.2011111072

17. Gueler F, Rong S, Gwinner W, Mengel M, Brocker V, Schon S, et al. Complement 5a receptor inhibition improves renal allograft survival. *J Am Soc Nephrol.* (2008) 19(12):2302–12. doi: 10.1681/ASN.2007111267

18. Lalli PN, Strainic MG, Yang M, Lin F, Medof ME, Heeger PS. Locally produced C5a binds to T cell-expressed C5aR to enhance effector T-cell expansion by limiting antigen-induced apoptosis. *Blood* (2008) 112(5):1759–66. doi: 10.1182/blood-2008-04-151068

19. Schmitz R, Fitch ZW, Schroder PM, Choi AY, Manook M, Yoon J, et al. C3 complement inhibition prevents antibody-mediated rejection and prolongs renal allograft survival in sensitized non-human primates. *Nat Commun* (2021) 12(1). doi: 10.1038/s41467-021-25745-7

20. Dho SH, Lim JC, Kim LK. Beyond the role of CD55 as a complement component. *Immune Netw* (2018) 18(1). doi: 10.4110/in.2018.18.e11

21. Brodsky SV, Nadasdy GM, Pelletier R, Satoskar A, Birmingham DJ, Hadley GA, et al. Expression of the decay-accelerating factor (CD55) in renal transplants-a possible prediction marker of allograft survival. *Transplantation* (2009) 88(4):457–64. doi: 10.1097/TP.0b013e3181b0517d

22. Chen XY, Rinsma M, Janssen JM, Liu J, Maggio I, Goncalves MAFV. Probing the impact of chromatin conformation on genome editing tools. *Nucleic Acids Res* (2016) 44(13):6482–92. doi: 10.1093/nar/gkw524

23. Maggio I, Zittersteijn HA, Wang Q, Liu J, Janssen JM, Ojeda IT, et al. Integrating gene delivery and gene-editing technologies by adenoviral vector transfer of optimized CRISPR-Cas9 components. *Gene Ther* (2020) 27(5):209–25. doi: 10.1038/s41434-019-0119-y

24. Mulder A, Kardol M, Regan J, Buelow R, Claas F. Reactivity of twenty-two cytotoxic human monoclonal HLA antibodies towards soluble HLA class I in an enzyme-linked immunosorbent assay (PRA-STAT (R)). *Hum Immunol* (1997) 56(1-2):106–13. doi: 10.1016/S0198-8859(97)00146-8

25. Takahashi K, Tanabe K, Ohnuki M, Narita M, Ichisaka T, Tomoda K, et al. Induction of pluripotent stem cells from adult human fibroblasts by defined factors. *Cell* (2007) 131(5):861–72. doi: 10.1016/j.cell.2007.11.019

26. Takahashi K, Yamanaka S. Induction of pluripotent stem cells from mouse embryonic and adult fibroblast cultures by defined factors. *Cell* (2006) 126(4):663–76. doi: 10.1016/j.cell.2006.07.024

27. Smith JR, Maguire S, Davis LA, Alexander M, Yang FT, Chandran S, et al. Robust, persistent transgene expression in human embryonic stem cells is achieved with AAVS1-targeted integration. *Stem Cells* (2008) 26(2):496–504. doi: 10.1634/stemcells.2007-0039

28. van der Torren CR, Zaldumbide A, Duinkerken G, Brand-Schaaf SH, Peakman M, Stange G, et al. Immunogenicity of human embryonic stem cell-derived beta cells. *Diabetologia* (2017) 60(1):126–33. doi: 10.1007/s00125-016-4125-y

29. Spendlove I, Ramage JM, Bradley R, Harris C, Durrant LG. Complement decay accelerating factor (DAF)/CD55 in cancer. *Cancer Immunol Immun* (2006) 55(8):987–95. doi: 10.1007/s00262-006-0136-8

30. Miyagawa S, Kubo T, Matsunami K, Kusama T, Beppu K, Nozaki H, et al. Delta-short consensus repeat 4-decay accelerating factor (DAF : CD55) inhibits complement-mediated cytolysis but not NK cell-mediated cytolysis. *J Immunol* (2004) 173(6):3945–52. doi: 10.4049/jimmunol.173.6.3945

31. Moberg L, Johansson H, Lukinius A, Berne C, Foss A, Kallen R, et al. Production of tissue factor by pancreatic islet cells as a trigger of detrimental

thrombotic reactions in clinical islet transplantation. *Lancet* (2002) 360 (9350):2039–45. doi: 10.1016/S0140-6736(02)12020-4

32. Tjernberg J, Ekdahl KN, Lambris JD, Korsgren O, Nilsson B. Acute antibody-mediated complement activation mediates lysis of pancreatic islets cells and may cause tissue loss in clinical islet transplantation. *Transplantation* (2008) 85 (8):1193–9. doi: 10.1097/TP.0b013e31816b22f3

33. Bongoni AK, Lu B, Salvaris EJ, Roberts V, Fang D, Mcrae JL, et al. Overexpression of human CD55 and CD59 or treatment with human CD55 protects against renal ischemia-reperfusion injury in mice. *J Immunol* (2017) 198 (12):4837–45. doi: 10.4049/jimmunol.1601943

34. Zhao H, Li YY, Wiriyahdamrong T, Yuan ZM, Qing YB, Li HH, et al. Improved production of GTKO/hCD55/hCD59 triple-gene-modified diannan miniature pigs for xenotransplantation by recloning. *Transgenic Res* (2020) 29 (3):369–79. doi: 10.1007/s11248-020-00201-2

35. Zhou CY, McInnes E, Copeman L, Langford G, Parsons N, Lancaster R, et al. Transgenic pigs expressing human CD59, in combination with human membrane cofactor protein and human decay-accelerating factor. *Xenotransplantation* (2005) 12 (2):142–8. doi: 10.1111/j.1399-3089.2005.00209.x

36. Pan D, Liu T, Lei T, Zhu H, Wang Y, Deng S. Progress in multiple genetically modified minipigs for xenotransplantation in China. *Xenotransplantation* (2019) 26(1):e12492. doi: 10.1111/xen.12492

37. Liu F, Liu J, Yuan Z, Qing Y, Li H, Xu K, et al. Generation of GTKO diannan miniature pig expressing human complementary regulator proteins hCD55 and hCD59 *via* T2A peptide-based bicistronic vectors and SCNT. *Mol Biotechnol* (2018) 60(8):550–62. doi: 10.1007/s12033-018-0091-6

38. Porrett PM, Orandi BJ, Kumar V, Houp J, Anderson D, Killian AC, et al. First clinical-grade porcine kidney xenotransplant using a human decedent model. *Am J Transplantation.* (2022) 22(4):1037–53. doi: 10.1111/ajt.16930

39. Montgomery RA, Stern JM, Lonze BE, Tatapudi VS, Mangiola M, Wu M, et al. Results of two cases of pig-to-Human kidney xenotransplantation. *New Engl J Med* (2022) 386(20):1889–98. doi: 10.1056/NEJMoa2120238

frontiers | Frontiers in Immunology

TYPE Original Research
PUBLISHED 18 January 2023
DOI 10.3389/fimmu.2022.1073802

OPEN ACCESS

EDITED BY
Mihály Józsi,
Eötvös Loránd University, Hungary

REVIEWED BY
Christoph Licht,
University of Toronto, Canada
Pilar Sánchez-Corral,
University Hospital La Paz Research Institute (IdiPAZ), Spain

*CORRESPONDENCE
Richard J. H. Smith
richard-smith@uiowa.edu

SPECIALTY SECTION
This article was submitted to Molecular Innate Immunity, a section of the journal Frontiers in Immunology

RECEIVED 18 October 2022
ACCEPTED 28 December 2022
PUBLISHED 18 January 2023

CITATION
Pisarenka S, Meyer NC, Xiao X, Goodfellow R, Nester CM, Zhang Y and Smith RJH (2023) Modeling C3 glomerulopathies: C3 convertase regulation on an extracellular matrix surface. *Front. Immunol.* 13:1073802. doi: 10.3389/fimmu.2022.1073802

Modeling C3 glomerulopathies: C3 convertase regulation on an extracellular matrix surface

Sofiya Pisarenka[1,2], Nicole C. Meyer[1], Xue Xiao[1], Renee Goodfellow[1], Carla M. Nester[1], Yuzhou Zhang[1] and Richard J. H. Smith[1,2]*

[1]Molecular Otolaryngology and Renal Research Laboratories, Caver College of Medicine, University of Iowa, Iowa City, IA, United States, [2]Molecular Medicine Graduate Program, Caver College of Medicine, University of Iowa, Iowa City, IA, United States

Introduction: C3 glomerulopathies (C3G) are ultra-rare complement-mediated diseases that lead to end-stage renal disease (ESRD) within 10 years of diagnosis in ~50% of patients. Overactivation of the alternative pathway (AP) of complement in the fluid phase and on the surface of the glomerular endothelial glycomatrix is the underlying cause of C3G. Although there are animal models for C3G that focus on genetic drivers of disease, in vivo studies of the impact of acquired drivers are not yet possible.

Methods: Here we present an in vitro model of AP activation and regulation on a glycomatrix surface. We use an extracellular matrix substitute (MaxGel) as a base upon which we reconstitute AP C3 convertase. We validated this method using properdin and Factor H (FH) and then assessed the effects of genetic and acquired drivers of C3G on C3 convertase.

Results: We show that C3 convertase readily forms on MaxGel and that this formation was positively regulated by properdin and negatively regulated by FH. Additionally, Factor B (FB) and FH mutants impaired complement regulation when compared to wild type counterparts. We also show the effects of C3 nephritic factors (C3Nefs) on convertase stability over time and provide evidence for a novel mechanism of C3Nef-mediated C3G pathogenesis.

Discussion: We conclude that this ECM-based model of C3G offers a replicable method by which to evaluate the variable activity of the complement system in C3G, thereby offering an improved understanding of the different factors driving this disease process.

KEYWORDS

C3 glomerulopathies, extracellar matrix, complement regulation, C3 nephritic factor (C3Nef), factor H (FH), factor B (FB), C3 convertase

10.3389/fimmu.2022.1073802

Introduction

C3 Glomerulopathies (C3G) are a group of ultra-rare complement-mediated renal diseases defined by specific histopathological findings on renal biopsy. The C3G definition includes presence of glomerulonephritis with C3-dominant immunofluorescence staining: C3 intensity must be at least two orders of magnitude more than any other immunoreactant. Electron microscopy (EM) is used to distinguish between the two major subtypes of C3G: Dense Deposit Disease (DDD) and C3 Glomerulonephritis (C3GN). DDD presents with extremely electron-dense, "sausage-shaped" deposits in the lamina densa of the glomerular basement membrane (GBM), a kidney-specific type of an extracellular matrix (ECM). In comparison, C3GN presents with subendothelial, subepithelial and/or mesangial deposits that are less electron-dense and have a less compact, "cloudy" appearance (1–3). The most important outcome associated with C3G diagnosis is the progression to end-stage renal disease (ESRD): ~50% of patients reach ESRD within 10 years of diagnosis (2, 4, 5). If kidney transplantation is offered, C3G recurrence in allografts is common (~60-80%), contributing to graft loss in ~50% of the cases (4, 6–10).

C3G pathogenesis is primarily driven by dysregulation of complement in the circulation and/or glomerular microenvironment (Figure 1). Complement is an integral part of the innate immune system, responsible for pathogen clearance and recruitment of immune cells to the site of complement activation. Of the three complement-initiating pathways (classical, lectin, alternative), the alternative pathway (AP) is the main contributor to C3G pathogenesis. The AP is continuously activated at a low rate in a process known as tick-over, resulting in cleavage of complement component 3 (C3) into an anaphylatoxin C3a and an opsonin C3b, which deposits on pathogen and self surfaces to drive formation of C3 convertase of the AP, C3bBb (17, 18). This process is tightly controlled by regulators of complement activation (RCA) which control complement activity to prevent injury to the host. In C3G, C3 convertase regulation is impaired, resulting in complement deposits in the renal glomeruli. While the source of disease is unknown in a subset of C3G cases (~35-40%), C3 convertase dysregulation and the subsequent development of disease is driven by acquired (~40-50%) or genetic drivers (~15-25%) in most (4, 19). Known drivers act on different parts of the complement cascade. For example, acquired drivers such as C3 nephritic factors (C3Nefs) stabilize C3 convertase (18, 20, 21), while genetic drivers like mutations in the *CFH* gene decrease inhibition of complement activity (22–24). Understanding the molecular processes underlying complement dysregulation is imperative for patient-specific management of C3G (2, 25, 26).

End organ renal damage begins in the glomeruli, which are high-flow, high-pressure capillary beds. The glomerular endothelial cells (GEnC) are highly fenestrated, with fenestrae comprising ~20-50% of total GEnC surface area (11–16). Complement control over the fenestrae depends on fluid-phase RCA proteins, which bind to heparin sulfate proteoglycans and sialic acids in the overlaying glycocalyx (27–30). Factor H (FH) and its related proteins (FHRs) are examples of the

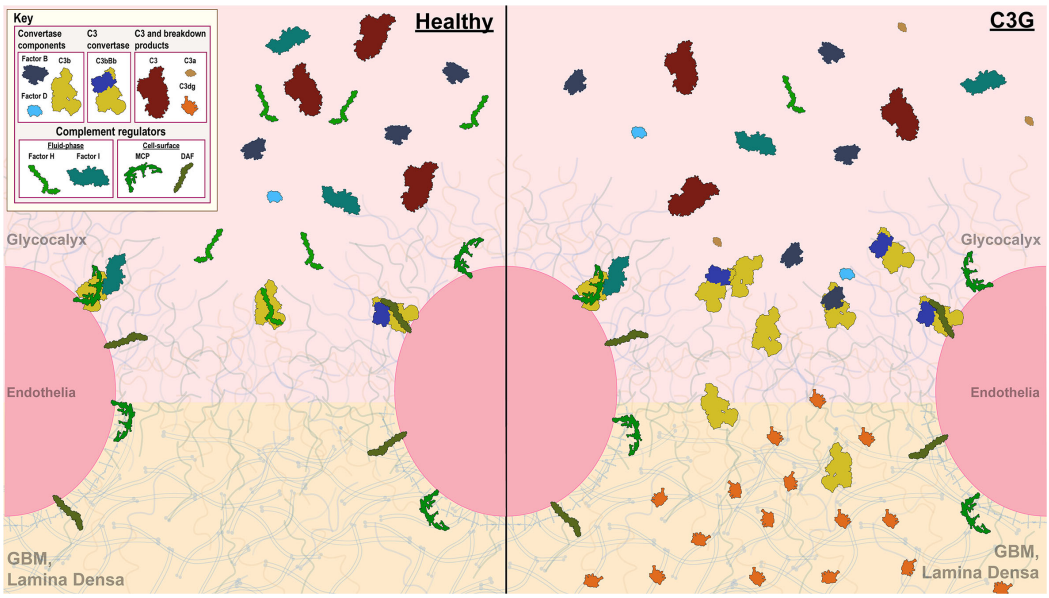

FIGURE 1
Complement control in the glomerular microenvironment. The glomerulus is the filtration unit of the kidney. Its filtration barrier is composed of the glycocalyx, glomerular endothelial cells (GEnC), glomerular basement membrane (GBM) and podocytes. The glycocalyx, a network of proteoglycans and glycoproteins, overlays highly fenestrated GEnCs. GEnC pores comprise ~20-50% of total cell surface area (11–16), allowing filtration of waste products through the glycomatrix (glycocalyx and the GBM), underlying podocytes and further into the Bowman's capsule to be excreted as urine. Complement activity on GEnCs is controlled by both cell-bound (MCP and DAF depicted) and fluid-phase complement regulators (Factor H (FH) and Factor I (FI) depicted), while complement control over the GEnC pores relies on fluid-phase regulators alone. A healthy glomerular microenvironment exhibits adequate cell-surface and fluid-phase complement control thereby preventing injury to the GEnCs and complement deposition in the glycomatrix. In contrast, in the C3G glomerular microenvironment, fluid-phase complement dysregulation occurs (an example of C3G driven by FH deficiency depicted) in presence of adequate cell-surface complement control. Here, GEnCs are still protected by the cell-bound regulators, but the lack of fluid-phase complement control over the GEnC pores allows complement amplification and complement deposition to occur as reflected by changes in the lamina densa of the GBM.

most important fluid-phase RCAs responsible for complement control in the glomeruli (22, 31, 32). Ultimately, it is the dysregulation of complement control in the fluid phase and at the glycomatrix (glycocalyx and the GBM) surface that gives rise to C3G.

We therefore developed an *in vitro* extra-cellular matrix (ECM) based model to test fluid phase complement regulation. Our goal was to model normal regulation of the C3 convertase on ECM surface and then determine how acquired and genetic drivers of C3G impact convertase activity. These studies advance our understanding of C3G pathogenesis, provide a diagnostic tool to monitor patient-specific complement dysregulation, and, potentially, may become a screening tool to test complement therapeutics based on a patient's complement profile.

Materials and methods

Patient cohort selection

Six patients were selected from our C3G research cohort. All patients had biopsy-proven C3G and sufficient purified Immunoglobulin G (IgG) samples to complete all assays multiple times. Selection was based on complement biomarker data (Table 1). Three C3G patients had elevated C3Nef activity (>20% activity as determined by C3CSA, C3Nef+), and three C3G patients had normal C3Nef activity (≤20%, C3Nef-). Control normal human serum (NHS) IgG was purified from pooled sera of persons with no history of renal disease. All patients gave informed consent before donating samples and were enrolled in this study under the guidelines approved by the institutional review board of the University of Iowa.

IgG purification

Patient IgG was purified using the Melon Gel IgG Purification Kit (Thermo Scientific, Rockford, IL) according to the manufacturer's instructions (33) and adjusted to 0.75 mg/ml.

C3Nef activity assay

C3 Convertase Stabilizing Assay (C3CSA) was performed as described previously (18). Briefly, AP C3 convertase was formed on the surface of sheep erythrocytes (SE), followed by adding patient-purified

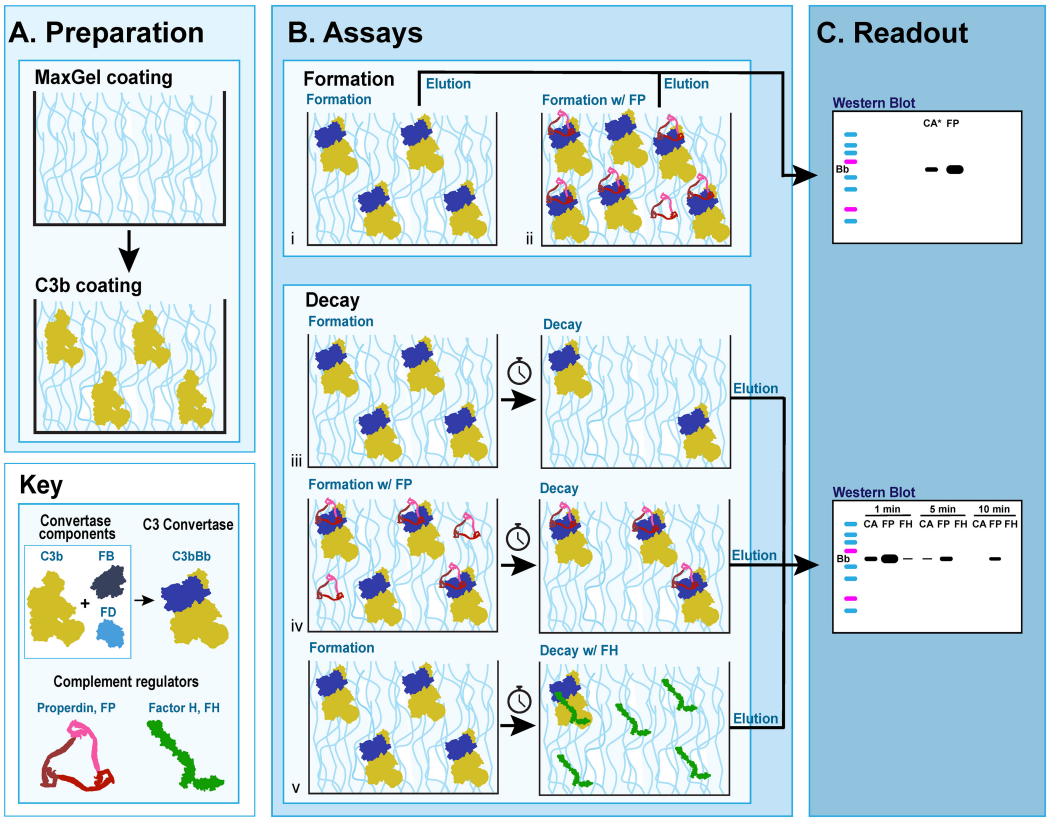

FIGURE 2
C3 convertase assays on MaxGel surface. **(A)** Preparation for all assays involves coating microtiter plates with MaxGel (ECM) followed by coating with C3b. **(B)** Formation assay: Factor B (FB) and Factor D (FD) are added to C3b-coated MaxGel, subsequently generating C3bBb over the course of 10 min in the absence (i) or presence (ii) of Properdin. Decay assay: C3bBb is generated as described above in absence (iii, v) or presence of Properdin (iv), and then allowed to decay over time naturally (iii, iv) or in presence of Factor H (v). **(C)** The amount of C3 convertase present on MaxGel surface at the time of elution is quantitated by western blot and observing the Bb complement fragment.

10.3389/fimmu.2022.1073802

TABLE 1 Patient biomarkers.

	Patient #	C3Nef (C3CSA) (<20%)	Factor H Autoantibodies FHAA (<200 AU)	Factor B Autoantibodies FBAA (<200 AU)
C3Nef + patients	P1	3+ (67%)	<50	<50
	P2	1+ (40%)	<50	<50
	P3	1+ (25%)	<50	77
C3Nef + patients	P4	Negative (17%)	<50	<50
	P5	Negative (15%)	<50	<50
	P6	Negative (12%)	<50	55

IgG to C3 convertase coated SE. Next, C3 convertase was allowed to decay for 20 and 60 minutes. At each time point, 50 ul was removed and mixed with rat EDTA serum, which served as a source of terminal complement components. C3CSA activity was reported as a function of the degree of hemolysis at 20 minutes as measured by OD at λ415.

Generation of recombinant FB and FH mutants

Recombinant FB and FH proteins were obtained through GeneArt, a division of ThermoFisher Scientific (Regensburg, Germany), as described previously (24). Briefly, the DNA coding region of select FB and FH variants with His-tag at the C- terminus was synthesized and cloned into a mammalian expression vector. Plasmids were then transfected into Expi 293 cells, followed by purification of the resulting Fb and FH protein directly from the culture supernatants using Ni2+ columns. After purification, all proteins were adjusted to 1 mg/mL in PBS and stored at -80°C until use (24).

C3 convertase formation assay

The C3 convertase formation assay (C3CFA) is a novel assay that measures the amount of C3 convertase formed on MaxGel™ (Sigma-Aldrich, St. Louis, MO) in the presence or absence of RCAs (Figure 2B i-ii). All complement proteins were obtained from Complement Technology Inc., Tyler, TX.

Preparation

96-well ELISA microtiter plates were coated with MaxGel (100 ul of 1:4 MaxGel:1xELISA coating buffer (Bio-Rad Laboratories, Inc., Hercules, CA)). Conditions were prepared in duplicate. Plates were incubated overnight (o/n) at 4°C. The following day, plates were washed with 1xPBS x3, then blocked with 4%BSA in 1xPBS for two hours at room temperature. Plates were then washed with 1xPBS x3 and wells were incubated with purified C3b (50 ul at 130 ug/ml) in 1xELISA coating buffer for at 4°C 2 o/n. C3b concentration was approximated using the normal physiological concentration of C3 (normal range, 900-1800 ug/ml) and was set at 1/10 of this value (concentration used, 1300 ug/ml); all other complement proteins and human IgG were used at 1/20 of their respective physiological concentrations (Table 2).

Assays

Fresh assay buffer (AB) was used for each experiment (8.1mM Na2HPO4, 1.8mM NaH2PO4, 0.05%Tween20, 75mM NaCl, 10mM $MgCl_2$, 2% BSA in PBS, distilled H_2O, pH = 7.0). Factor B (FB, 10.5 ug/ml) and Factor D (FD, 0.1 ug/ml) were added. 50 ul was added to each well (p/w). The same composition of reagents was used for all experiments.

C3b-coated wells were washed three times with AB to remove unbound C3b. C3 convertase was then formed by incubating the wells with control (FB+FD) or experimental (FB+FD+Reactant) assay mixtures (50 ul p/w) for 10 min at 37°C. Wells were washed with AB x3 to ensure that only MaxGel-bound C3 convertase remained.

TABLE 2 Concentration of complement proteins in circulation.

Protein	Normal Range, ug/ml	Concentration used, ug/ml	Physiological concentration scaling factor	Assay concentration, ug/ml
C3	900-1800	1,300	1/10	130
Factor B	188-219	210	1/20	10.5
Factor D	1-26	2	1/20	0.1
Factor H	116-562	450	1/20	22.5
Properdin	17.5-25.2	20	1/20	1
Purified IgG	7,000-16,000	15,000	1/20	750

Readout

Elution buffer (10mM EDTA and 1%SDS) was added to the plates at 25 ul p/w, followed by 1h incubation at room temperature on an orbital shaker. Eluants from duplicate wells were pooled, 35 ul of the pooled eluant was then added to 35 ul of 2x Laemmli Sample Buffer (Bio-Rad Laboratories, Inc., Hercules, CA) and heated at 95°C for 15 min in preparation for SDS-PAGE.

C3 convertase decay assay

The C3 convertase decay assay (C3CDA) is a novel assay that measures the rate of decay of C3 convertase formed on MaxGel™ in presence or absence of RCAs or decay of C3 convertase alone (Figure 2B iii-v). Preparation and assay steps of the C3CFA protocol were followed for each timepoint assessed. Washed plates were incubated with AB alone or AB+Reactant (50 ul p/w) for a determined period at 37°C, then washed with AB x3. The readout for C3CDA was identical to the readout for C3CFA. The impact of properdin, FH and C3Nefs on C3 convertase decay was assessed.

Visualization *via* SDS-PAGE and western blotting

Samples were separated by 10% SDS-PAGE gel (Bio-Rad Laboratories, Inc., Hercules, CA), and transferred to nitrocellulose membrane. Membranes were blocked with 5% skim milk in 1x PBST (1xPBS, 0.075% Tween20) at 4°C o/n, then incubated with a mouse monoclonal Factor B antibody specific for the Bb subunit (1:200 in 5% BSA, 1xPBST; Santa Cruz Biotechnology, Inc., Dallas, TX; F-7: sc-271636) at 4°C o/n. Membranes were washed x3 with 1xPBST, followed by a 2-hour incubation at room temperature with polyclonal HRP-conjugated goat anti-mouse secondary antibody (1:4000, Jackson ImmunoResearch Inc, West Grove, PA, 115-035-062, RRID: AB_2338504, in 5% BSA, 1xPBST). Membranes were washed x5 in 1xPBST, then incubated with SuperSignal West Pico PLUS Chemiluminescent Substrate (Thermo Scientific, Rockford, IL) for 1 min. Protein bands were visualized using Classic X-ray Film (Research Products International, Mt. Prospect, IL).

Quantification and normalization of western blot data

Western blots were quantified using ImageJ (http://imagej.nih.gov/ij/; National Institutes of Health, Bethesda, MD). C3 convertase alone (CA) at the first assayed timepoint (as indicated in the legend) was set as 1; all other values in a replicate were normalized to this value.

Statistical analyses

Statistical analyses were performed using GraphPad Prism 8 (GraphPad Software, San Diego, CA). All experiments were repeated a minimum of three times. Student's t-test and one-way ANOVA with Dunnett's multiple comparisons test were used to assess the difference between conditions. Half-life in decay assays was determined by fitting a curve with non-linear regression using second order polynomial equation. Difference was considered statistically significant at $P \leq 0.05$.

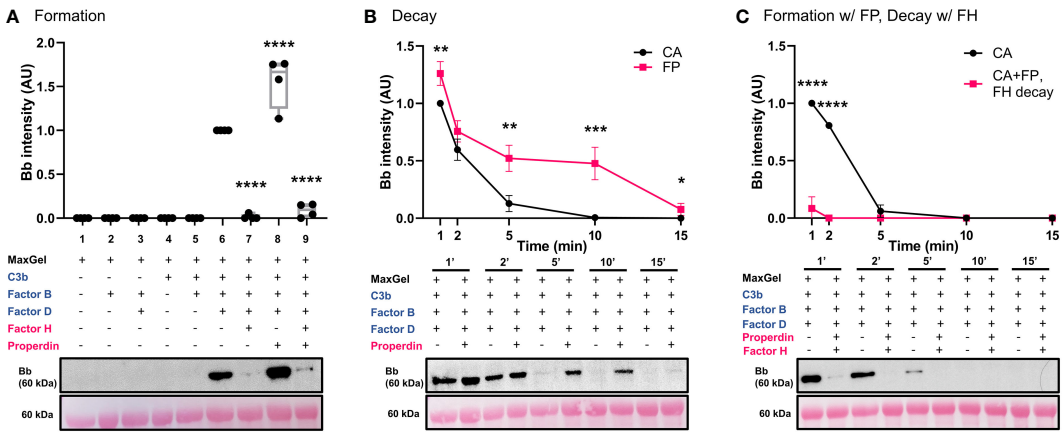

FIGURE 3
C3 convertase assembles, decays on ECM surface and is regulated by RCA proteins. **(A)** Western blot analysis of C3 convertase formation on ECM surface. MaxGel does not contain complement proteins necessary to form C3 convertase (lanes 1-5). C3 convertase alone (CA) forms in presence of C3b, FB and FD (lane 6), and is regulated by inhibitory FH (lane 7), stabilizing FP (lane 8) or a mix of FH+FP (lane 9). Results were normalized to CA and presented as relative protein expression. Box plots show median, 1st and 3rd quartile ranges, and the individual data points of four independent experiments. Significance calculated for CA. **(B)** Western blot analysis of timed decay (1-15 min) of CA formed alone or in presence of Properdin. FP increases C3bBb half-life more than 2-fold (CA $t_{1/2}$ =3.1min; FP $t_{1/2}$ =7.4min). **(C)** Western blot analysis of timed decay (1-15 min) of CA formed alone or in presence of properdin (C3bBb(P)), followed by FH-mediated decay of C3bBb(P). FH increases decay of C3bBb(P) (CA $t_{1/2}$ =3.2min; C3bBb(P)+FH $t_{1/2}$<1min). Results were normalized to CA at 1 min and presented as relative protein expression. Ponceau S Staining was used as a measure of total protein load. Mean ± SD of four independent experiments. Significance calculated for CA at respective timepoints. * P ≤ 0.05, ** P ≤ 0.01, *** P ≤ 0.001, **** P ≤ 0.0001.

Results

Validation of the method

C3 convertase assembles, decays on ECM surface and is regulated by RCA proteins

A novel *in vitro* model of complement activity and regulation was designed to assess C3 convertase activity on ECM surface (Figure 2). We first ensured that MaxGel, the ECM used as a base for all the assays, does not contain complement proteins capable of forming C3 convertase. To do so, we separately added necessary components of C3 convertase (C3b, FB, FD) or their combinations to MaxGel-coated wells (Figure 3A, lanes 1-5). Further, we demonstrated that C3bBb was only able to form on MaxGel surface in presence of all necessary components (Figure 3A, lane 6) and its formation was inhibited by Factor H (FH) and stabilized by Properdin (FP) (Figure 3A, lanes 7-8). Together, these experiments show that C3 convertase forms on MaxGel surface and that complement regulators act in the physiologically expected manner.

Properdin, the only known positive regulatory protein of the AP of complement, is capable of increasing the half-life of the C3 convertase up to 10 times (34). We hypothesized that physiological amounts of FP would stabilize C3bBb on MaxGel surface. To test this hypothesis, we assessed the differences in C3bBb decay rates when formed alone (CA) or in presence of FP (C3bBb(P)) (Figure 3B), following natural decay rates. Addition of FP led to 2.4-fold increase in convertase half-life (FP $t_{1/2}$ =7.4min) when compared to untreated control (CA $t_{1/2}$ =3.1min). Notably, though not statistically significant, some C3bBb(P) complexes were still present after 15 min of decay. C3bBb(P) decayed rapidly in the presence of FH (CA $t_{1/2}$ =3.2min), with complexes disappearing within 2 minutes (Figure 3C).

FH inhibits C3 convertase formation on ECM surface in dose-dependent manner

Factor H can disrupt formation of C3 convertase, perform decay acceleration activity (DAA) on already existing C3bBb complexes and act as a cofactor for another complement inhibitor, Factor I (FI) (32, 35, 36). Here we used the convertase formation assay to assess the impact of FH on C3 convertase formation. Decreasing concentrations of FH increased C3 convertase formation in dose-dependent manner (Figure 4A). Similarly, increasing concentrations of stabilizing properdin promoted dose-dependent increase in C3bBb formation (Figure 4B).

We modeled a range of Factor H:Properdin ratios by decreasing FH concentration while maintaining FP concentration to determine how changes in the relative ratio affect C3 convertase regulation on ECM surface (Figure 4C, lanes 4-9). A significant difference was observed at a ratio of FH : FP 0.25:1 (lane 7) which corresponds to 112.5 ug/ml FH and 20 ug/ml FP. We also modeled FH : FP ratios from two C3G patients with very high FP values (Table 1) (lanes 10-11). Neither reached significance when compared to the normal physiological ratio (lane 4, Figure 4C).

Assessment of genetic drivers of C3G

Genetic variation in *CFB* may lead to variation in C3 convertase activity and regulation

Three variants in *CFB* were assessed using our ECM-based model: one in the region encoding for the CCP2 subunit of Ba and two in the VWA subunit of Bb (Figure 5A). Convertase formation was significantly less with recombinant WT FB (FB his) (Figure 5B, lane

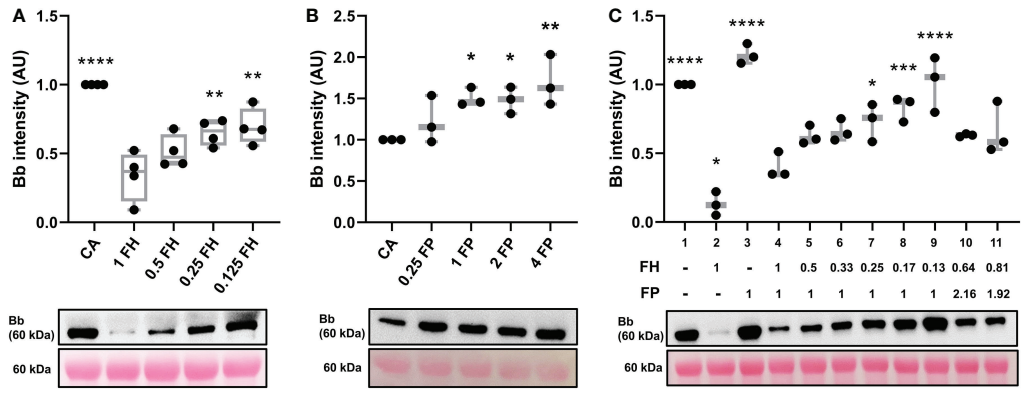

FIGURE 4
FH inhibits C3 convertase formation in dose dependent manner. **(A)** Western blot analysis of C3 convertase formed in presence of varying amounts of FH. Decreasing the concentration of FH (lanes 3-5) leads to decreased inhibition of C3 convertase formation in dose-depended manner, as compared to the normal physiological concentration of FH (lane 2). Box plots show median, 1st and 3rd quartile ranges, and the individual data points of four independent experiments. **(B)** Western blot analysis of C3 convertase formed in presence of varying amounts of properdin. Increasing the concentration of FP (lanes 3-5) leads to increased formation of C3 convertase in dose-depended manner, as compared to convertase alone (CA, lane 1). **(C)** Western blot analysis of C3 convertase formed in presence of decreasing FH : FP ratio. Decreasing the ratio of FH : FP (lanes 5-9) leads to decreased FH inhibition of complement formation in dose-dependent manner. Low FH : FP ratios allow for a significant increase (lanes 7-9) in convertase formation as compared to the physiological FH : FP ratio (lane 4). FH and FP biomarkers of two C3G patients with elevated FP levels from MORL C3G cohort are shown in lanes 10 (FH: 287ug/mL, FP: 43.2 ug/mL) and 11 (FH: 363 ug/mL, FP: 38.4 ug/mL). Results were normalized to CA and presented as relative protein expression. Ponceau S Staining was used as a measure of total protein load. Box plots show median, 1st and 3rd quartile ranges, and the individual data points of three independent experiments. Significance calculated for CA. * P ≤ 0.05, ** P ≤ 0.01, *** P ≤ 0.001, **** P ≤ 0.0001.

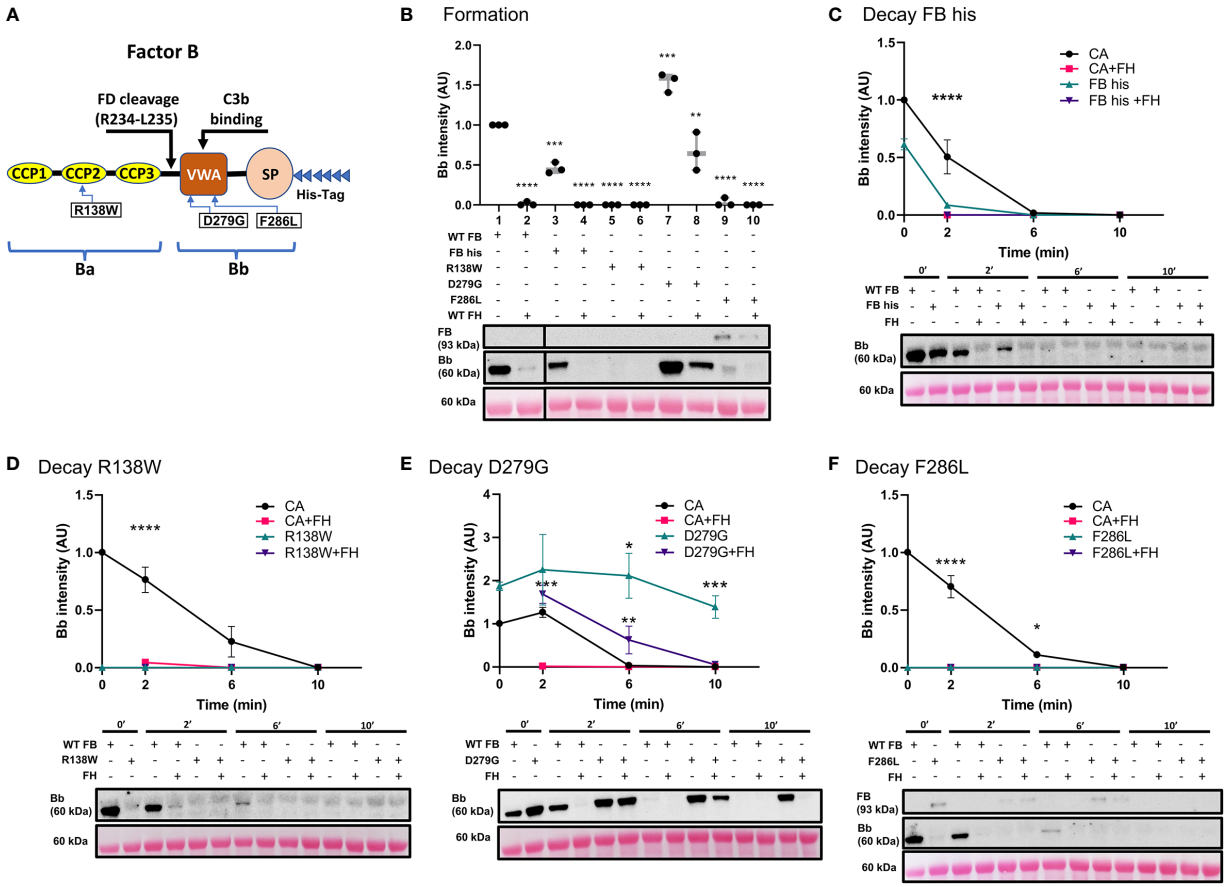

FIGURE 5
Variants in *CFB* can affect its affinity for C3b binding and rate of C3 convertase decay in presence/absence of FH. **(A)** Schematic of recombinant FB proteins, blue arrows denoting the positions of specific mutants. **(B)** Western blot analysis of C3 convertase formation. Recombinant WT FB (FB his) shows decreased ability to form C3 convertase (lanes 3) as compared to WT FB (CA, lanes 1). There is no formation in presence of FH (lanes 2 and 4). Both p.Arg138Trp (lanes 5-6) and p.Phe286Leu (lanes 9-10) fail to form C3bBb in absence/presence of FH. p.Asp279Gly increases C3 convertase formation ~1.5-fold (lane 7) as compared to CA (lane 1) and is able to form C3bBb even in presence of FH (lane 8). Results were normalized to CA and presented as relative protein expression. Box plots show median, 1st and 3rd quartile ranges, and the individual data points of three independent experiments. Significance calculated for WT FB. **(C)** Western blot analysis of CA formed using WT FB or FB his, then decayed in presence/absence of FH. Decrease in C3 convertase at 0 and 2 min is observed as compared to WT FB. **(D)** Western blot analysis of CA formed using WT or p.Arg138Trp, then decayed in absence/presence of FH. No mutant convertase activity is observed at 0 min as compared to WT FB. **(E)** Western blot analysis of CA formed using WT or p.Asp279Gly, then decayed in absence/presence of FH. Decrease in natural and FH-mediated decay of p.Asp279Gly C3bBb is observed as compared to WT FB at all timepoints. **(F)** Western blot analysis of CA formed using WT or p.Phe286Leu, then decayed in absence/presence of FH. No mutant convertase activity is observed at 0 min as compared to WT FB. For all decay experiments, results were normalized to CA at 0 min and presented as relative protein expression. Ponceau S Staining was used as a measure of total protein load. Statistical significance shown for comparisons between CA/recombinant protein and CA+FH/recombinant protein+FH respectively at the same timepoint. Mean ± SD of three independent experiments. * P ≤ 0.05, ** P ≤ 0.01, *** P ≤ 0.001, **** P ≤ 0.0001.

3) as compared to WT FB (lane 1); addition of FH prevented convertase formation entirely (lanes 2 and 4). The p.Arg138Trp failed to form active C3 convertase alone (lane 5) as well as in presence of FH (lane 6). The p.Asp279Gly, a gain-of-function mutation characterized by a high affinity for C3b and resistance to natural and FH-assisted decay (37–39), resulted in increased amounts of C3 convertase formation (lane 7). FH was not able to prevent C3 convertase formation by p.Asp279Gly (lane 8). No active C3bBb was observed for the p.Phe286Leu (lanes 9-10), but C3bB formed in absence and presence of FH, lanes 9-10).

The C3 convertase decay assay was used to assess the mutants' natural and FH-mediated decay. As predicted from the results of the formation assay, FB his showed significantly less C3bBb after 2 min as compared to WT FB (FB his $t_{1/2}$~0.24 min, CA $t_{1/2\ =}$2.2 $_{min}$). Addition of FH resulted in complete decay of C3 convertase at 2 min (Figure 5C). Both p.Arg138Trp (Figure 5D) and p.Phe286Leu (Figure 5F) failed to form C3bBb, thus the observed absence of C3 convertase at 0 and 2 min of decay with or without FH was expected. C3bB resulting from the p.Phe286Leu was present after 10 min of natural and FH-mediated decay. Natural decay of C3bBb formed with p.Asp279Gly was significantly slower as compared to WT FB (D279G $t_{1/2}$>10 min, CA $t_{1/2\ =}$ 4.2min). Decaying p.Asp279Gly C3 convertase with FH resulted in decreased DAA (D279G+FH $t_{1/2\ =}$ 6.6 $_{min}$), with convertase complexes still seen at 6 min (Figure 5E).

Pathogenic variation in SCR 1-3 of *CFH* leads to decreased inhibitory function of FH on ECM surface

We performed functional studies on three reported pathogenic variants in *CFH* (Figure 6A). The C3 convertase formation assay was performed to assess the ability of recombinant WT FH (FH his) and FH

10.3389/fimmu.2022.1073802

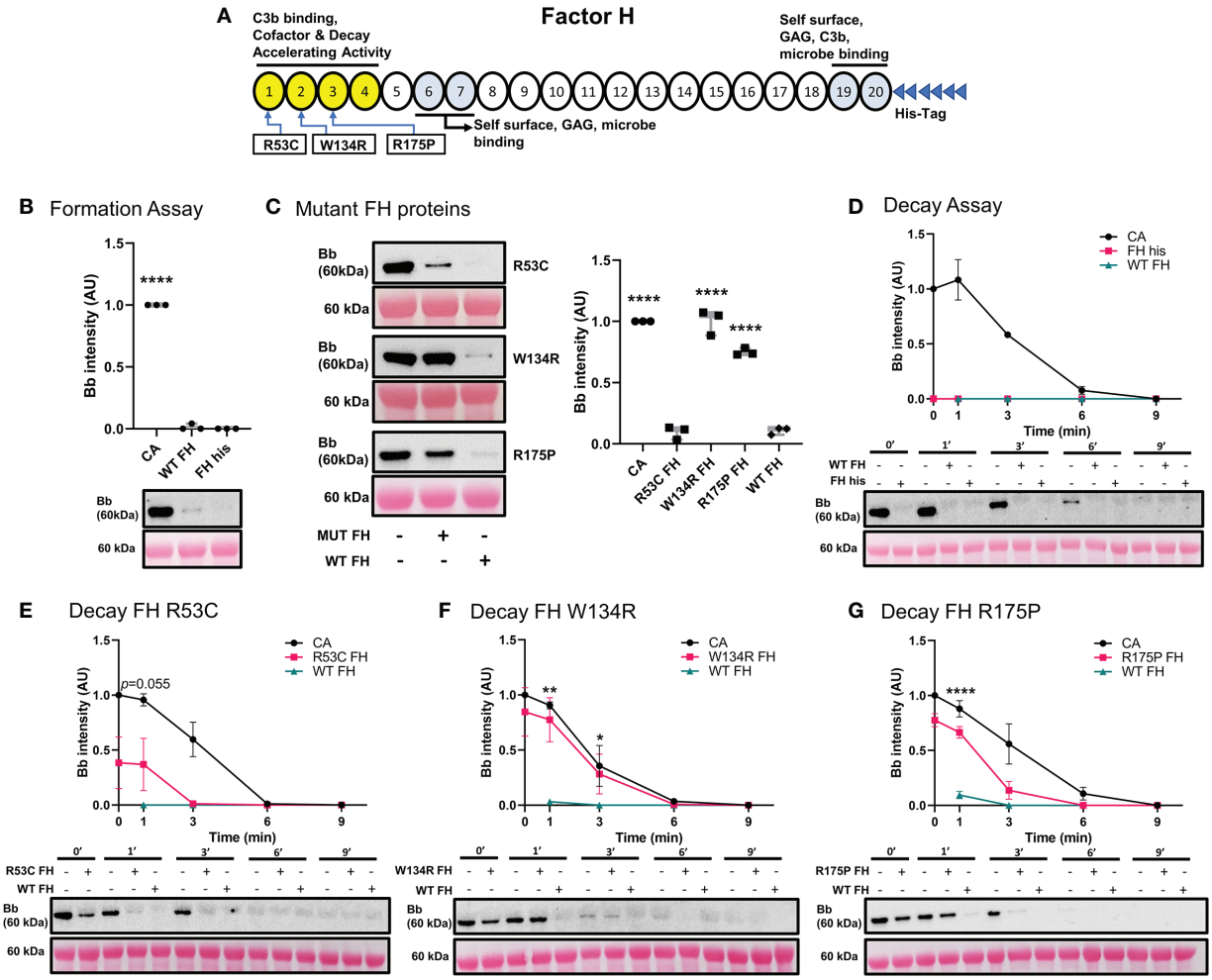

FIGURE 6
Variants in *CFH* can affect its ability to inhibit C3 convertase formation and promote Decay Acceleration Activity. **(A)** Schematic of recombinant FH proteins, blue arrows denoting the positions of specific mutants. **(B)** Western blot analysis of C3 convertase formed alone (CA), or in presence of WT FH or recombinant WT FH (FH his). Recombinant WT FH inhibits C3bBb formation to the same degree as WT FH. **(C)** Western blot analysis of CA formed alone, or in presence of recombinant FH variants or WT FH. p.Arg53Cys inhibits C3bBb formation to the same degree as WT FH, while p.Trp134Arg and p.Arg175Pro shows significant impairment in their ability to prevent C3 convertase formation. Results were normalized to CA and presented as relative protein expression. Box plots show median, 1st and 3rd quartile ranges, and the individual data points of three independent experiments. Significance calculated for WT FH. **(D)** Western blot analysis of CA formed alone, then decayed in buffer, or with WT FH or recombinant WT FH. There is no difference between the two FH conditions. **(E)** Western blot analysis of CA formed alone, then decayed in buffer, or with p.Arg53Cys or WT FH. p.Arg53Cys almost reached significance at 1 min as compared to WT FH (p=0.055). **(F)** Western blot analysis of CA formed alone, then decayed in buffer, or with p.Trp134Arg or WT FH. p.Trp134Arg ($t_{1/2}$ =2 min, $t_{1/2}$ =2.5 min) shows very poor DAA, providing only 20% decrease in C3bBb half-life as compared to CA. **(G)** Western blot analysis of CA formed alone, then decayed in buffer, or with p.Arg175Pro or WT FH. p.Arg175Pro ($t_{1/2}$~1.5 min, CA $t_{1/2}$ =3.1 min) decreases DAA as compared to WT FH. For all decay experiments, results were normalized to CA at 0 min and presented as relative protein expression. Ponceau S Staining was used as a measure of total protein load. Mean ± SD of three independent experiments. Statistical significance shown for comparisons between WT FH/recombinant FH at the same timepoint. * P ≤ 0.05, ** P ≤ 0.01, *** P ≤ 0.001, **** P ≤ 0.0001.

mutants to prevent C3 convertase formation. Non-recombinant WT FH and FH his prevented C3 convertase formation equally well (Figure 6B). p.Arg53Cys also prevented C3bBb formation. In contrast, p.Trp134Arg and p.Arg175Pro showed diminished ability to inhibit C3 convertase formation as compared to WT FH (Figure 6C).

Next, we tested the decay accelerating activity of FH his and FH mutants. FH his was as effective as WT FH in accelerating C3 convertase decay (Figure 6D). C3 convertase decay rate in presence of p.Arg53Cys (CA $t_{1/2}$ =3.1 min) was not significantly different from WT FH (P=0.055) at 1 min (Figure 6E). The presence of either p.Trp134Arg (Figure 6F) or p.Arg175Pro ($t_{1/2}$~1.5 min, CA $t_{1/2}$ =3.1 min) (Figure 6G) exhibited a significantly slower DAA at 1 min as compared to WT FH. Notably, p.Trp134Arg mutant showed particularly poor DAA; its $t_{1/2}$ =2 min compared to untreated CA $t_{1/2}$ =2.5 min.

Assessment of acquired drivers of C3G

IgG derived from C3Nef-positive C3G patients stabilized C3 convertase, some promoted formation

Antibodies against AP C3 convertase called C3 Nephritic Factors (C3Nefs) are a common driver of disease (2, 40). Here, we used C3 convertase decay and formation assays to assess the stabilization

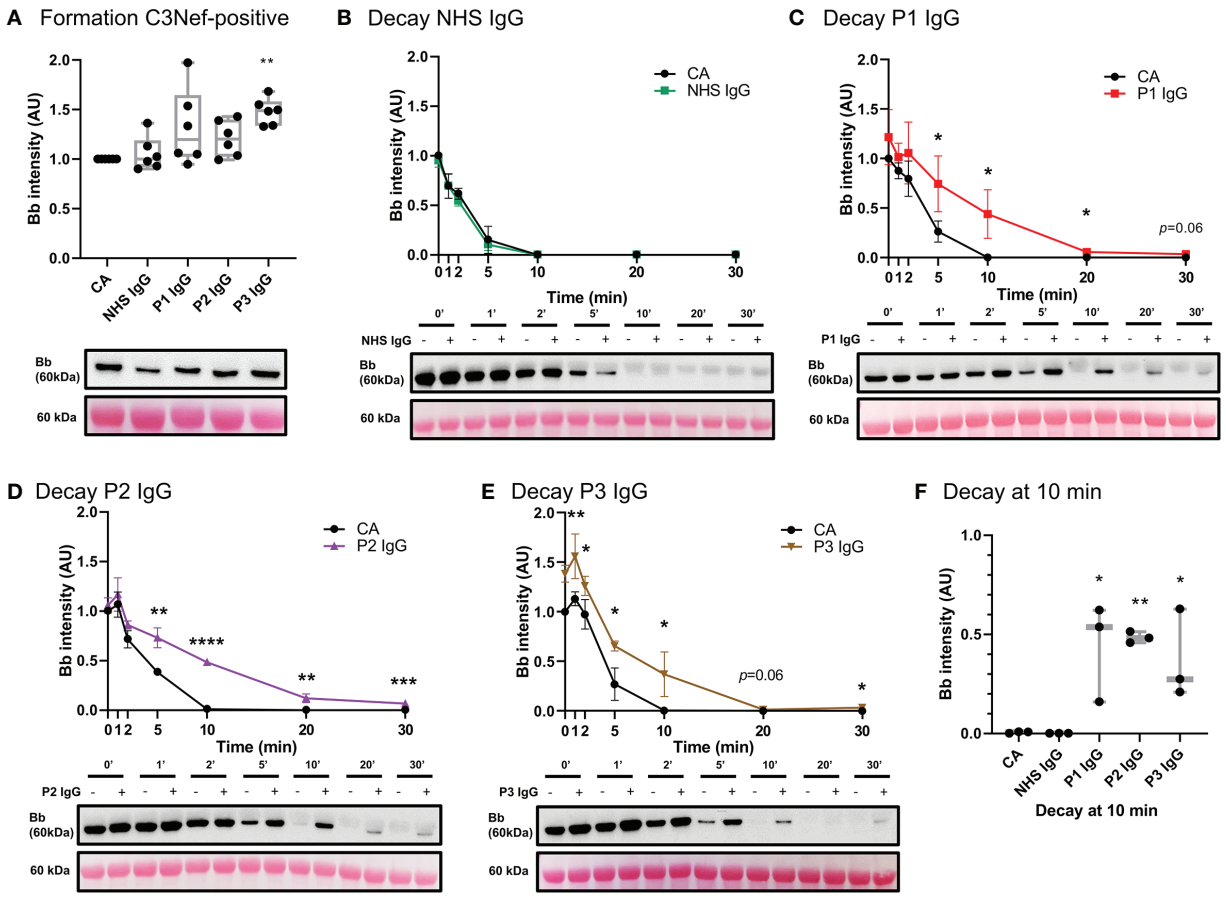

FIGURE 7
IgG from C3Nef+ C3G patients stabilize C3 convertase and decrease its decay rate. **(A)** Western blot analysis of CA formed alone, or in presence of NHS, P1, P2 or P3 IgG. P3 IgG significantly increases C3bBb formation. Results were normalized to CA and presented as relative protein expression. Box plots show median, 1st and 3rd quartile ranges, and the individual data points of six independent experiments. Significance calculated for NHS IgG. **(B)** Western blot analysis showing C3 convertase formed alone (CA) or in presence of NHS IgG, then decayed for up to 30 min. NHS IgG do not stabilize C3 convertase (NHS IgG $t_{1/2}$ = 3 min, CA $t_{1/2}$ = 3.36 min). **(C–E)** Western blot analyses showing C3 convertase formed alone (CA) or in presence of IgG derived from C3Nef+ patients, then decayed for up to 30 min. **(C)** P1 IgG stabilizes C3bBb 2-fold (P1 $t_{1/2}$ = 8.9 min, CA $t_{1/2}$ = 4.3min). **(D)** P2 IgG stabilizes C3bBb 1.9-fold (P2 $t_{1/2}$ = 9.4 min, CA $t_{1/2}$ = 4.9 min). **(E)** P3 IgG stabilizes C3bBb 1.7-fold (P3 $t_{1/2}$ = 8.7 min CA $t_{1/2}$ = 5 min). Mean ± SD of three independent experiments. Statistical significance shown for comparisons between CA/Patient IgG at the same timepoint. **(F)** Composite box plots showing C3 convertase stabilization by IgG from C3Nef+ C3G patients after 10 min of decay in buffer. For all decay experiments, results were normalized to CA at 0 min and presented as relative protein expression. Ponceau S Staining was used as a measure of total protein load. Box plots show median, and the individual data points of three independent experiments. Significance calculated for NHS IgG at 10 min. * P ≤ 0.05, ** P ≤ 0.01, *** P ≤ 0.001, **** P ≤ 0.0001.

capacity of IgG derived from C3Nef-positive C3G patients (Figure 7) (Table 1). Addition of normal human serum IgG (NHS IgG) in C3CDA did not affect the decay rate of convertase (Figure 7B). Stabilization of C3 convertase was observed most prominently with P1 IgG (P1 $t_{1/2}$ = 8.9 min, CA $t_{1/2}$ = 4.3min) (Figure 7C) and P2 IgG (P2 $t_{1/2}$ = 9.4 min, CA $t_{1/2}$ = 4.9 min) (Figure 7D), which showed 2- and 1.9-fold increases in half-life, respectively. Addition of P3 IgG (P3 $t_{1/2}$ = 8.7 min CA $t_{1/2}$ = 5 min) allowed for 1.7-fold increase in convertase half-life (Figure 7E). All C3Nef-positive patient IgG promoted C3 convertase stabilization past 10 min, as compared to NHS IgG (Figure 7F). Interestingly, P3 IgG consistently formed more C3 convertase in the C3CFA than did P1 or P2 IgG (Figure 7A).

Three C3Nef-negative patient IgG (Table 1) showed increased stabilization of C3bBb in decay assays: 1.3-fold increase in C3bBb half-life in the presence of P4 IgG (P4 $t_{1/2}$ = 7 min, CA $t_{1/2}$ = 5.5 min), 1.7-fold with P5 IgG (P5 $t_{1/2}$ = 5.5 min, CA $t_{1/2}$ = 3.3 min) and 1.2-fold with P6 IgG (P6 $t_{1/2}$ = 5.6 min CA $t_{1/2}$ = 4.6 min) (Figure 8C–E). While P6 IgG and P7 IgG allowed for some convertase stabilization at 10 min post formation (Figure 8F), it is evident that little to no C3bBb complexes were present on the ECM surface past that timepoint. The convertase formation assay showed no significant change in any C3Nef-negative patient IgG (Figure 8A).

Discussion

In this body of work, we present an *in vitro* model of C3G that utilizes human ECM (MaxGel), purified human complement proteins, and patient-derived antibodies to improve our understanding of C3G pathogenesis and promote patient-specific diagnostics. The first step in the development and validation of this

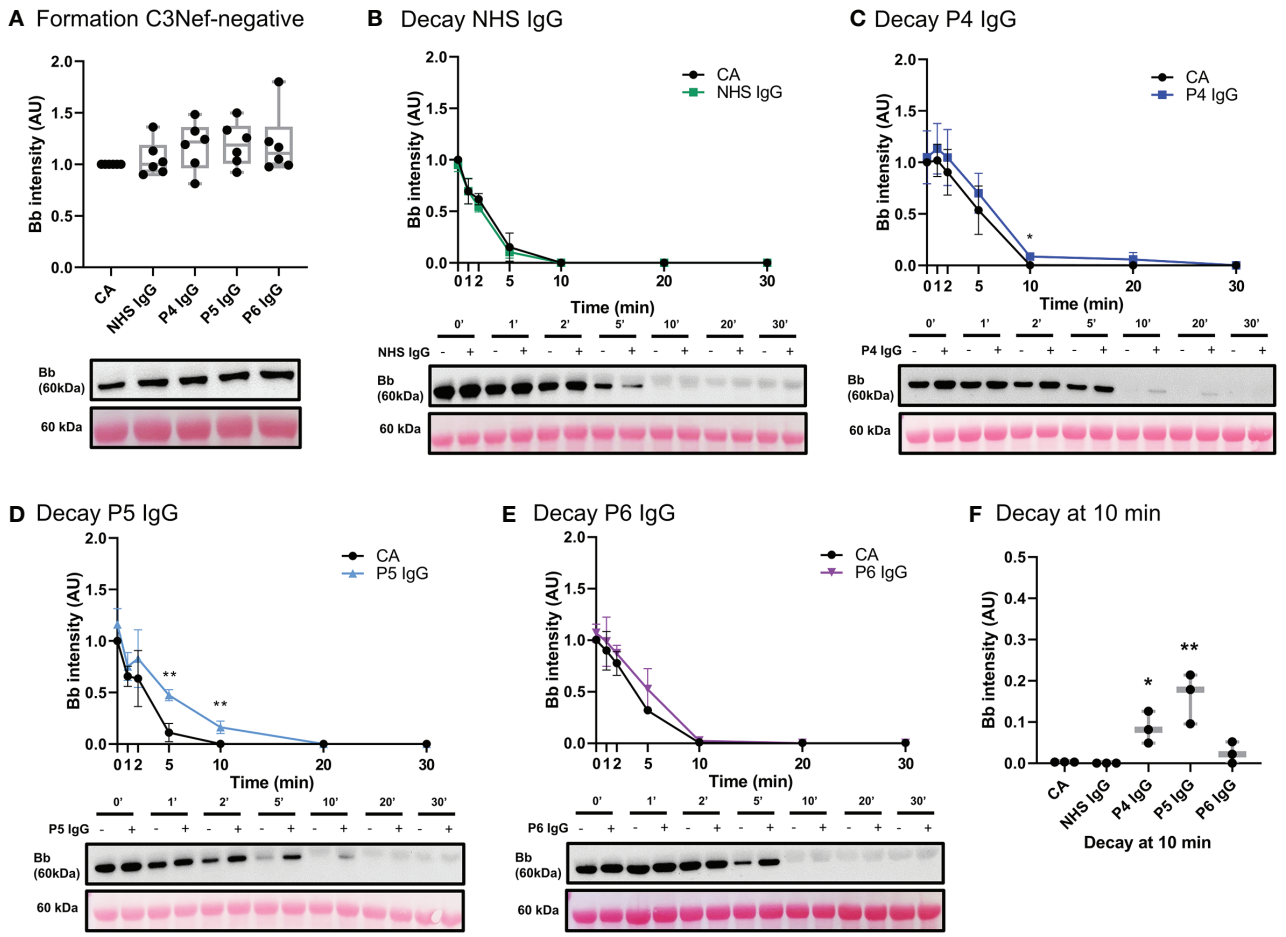

FIGURE 8
IgG from C3Nef- C3G patients do not promote C3 convertase formation but can increase its stability. **(A)** Western blot analysis of CA formed alone, or in presence of NHS, P4, P5 or P6 IgG. IgG from C3Nef-negative C3G patients does not affect C3bBb formation. Results were normalized to CA and presented as relative protein expression. Box plots show median, 1st and 3rd quartile ranges, and the individual data points of six independent experiments. Significance calculated for NHS IgG. **(B)** Western blot analysis showing C3 convertase formed alone (CA) or in presence of NHS IgG, then decayed for up to 30 min. NHS IgG do not stabilize C3 convertase (NHS IgG $t_{1/2}$ = 3 min, CA $t_{1/2}$ = 3.36 min). **(C–E)** Western blot analyses shows C3 convertase formed alone (CA) or in presence of IgG derived from C3Nef- patients, then decayed for up to 30 min. **(C)** P4 IgG increases C3bBb half-life 1.3-fold (P4 $t_{1/2}$ = 7 min, CA $t_{1/2}$ = 5.5 min). **(D)** P5 IgG increases C3bBb half-life 1.7-fold (P5 $t_{1/2}$ = 5.5 min, CA $t_{1/2}$ = 3.3 min). **(E)** P6 IgG increases C3bBb half-life 1.2-fold (P6 $t_{1/2}$ = 5.6 min CA $t_{1/2}$ = 4.6 min). Mean ± SD of three independent experiments. Statistical significance shown for comparisons between CA/Patient IgG at the same timepoint. **(F)** Composite box plots showing C3 convertase stabilization by IgG from C3Nef-negative patients (P4, P5) after 10 min of decay in buffer. For all decay experiments, results were normalized to CA at 0 min and presented as relative protein expression. Ponceau S Staining was used as a measure of total protein load. Box plots show median, and the individual data points of three independent experiments. Significance calculated for NHS IgG at 10 min. * P ≤ 0.05, ** P ≤ 0.01, *** P ≤ 0.001, **** P ≤ 0.0001.

model was to ensure that any change in C3bBb observed was due to the proteins added and not potential contamination of the ECM. We show that MaxGel does not permit C3 convertase formation unless all three essential components of the convertase are added, and that fluid-phase complement regulators successfully inhibit (FH) or promote (FP) convertase formation (Figure 3A). These outcomes are consistent with previous studies (41–47) and confirm the expected negative and positive regulation of C3bBb on ECM surface by FH and properdin, respectively. We also show that when formed in presence of properdin, the decay of C3bBb is >2 times slower (Supplemental Table 1) as compared to untreated C3 convertase (Figure 3B). These results align with the findings of a classical 1975 study where C3 convertase assembled with FP on sheep erythrocyte surface was stabilized 1.5- to 10-fold (34). It is important to note that different surfaces used as a base for C3 convertase reconstitution have been shown to result in different C3bBb half-lives (plastic = ~90 sec (48), sheep erythrocytes ~4 min (34), MaxGel ~ 3.8 min), highlighting the importance of studying complement activation on a surface that is relevant to disease pathogenesis. Next, we also showed the expected dose-response of the addition of FH and/or FP on C3bBb regulation, as confirmed by their concentration gradients and a combined assessment of FH : FP ratios (Figure 4). The results of patient-specific FH : FP assessments aligned with the gradient curve established in lanes 4-9 (Figure 4C), suggesting that the FH : FP ratio alone is not necessarily a predictor of pathogenicity.

To assess the genetic drivers of C3G, the impact of three variants each in *CFB* and *CFH* on C3 convertase formation and decay was characterized. With respect to *CFB*, we largely recapitulated the described phenotypes (Figure 5). p.Arg138Trp and p.Asp279Gly caused loss-of-function and gain-of-function effects, respectively

(38, 49). With p.Phe286Leu, we observed very few active C3bBb complexes; uncleaved C3bB (50, 51) complexes were present instead, even when formed and decayed with FH. These data suggest that under physiological concentrations of FB and FD, p.Phe286Leu FB may have a high affinity for C3b while not being successfully cleaved by FD. A similar phenotype of p.Phe286Leu was shown in a 2007 study, where this mutant's high affinity for C3b and decreased cleavage by FD was hypothesized to result in generation of abundant, rapidly cycling C3 convertase if supplied with unlimited FB (39). Considering both sets of data, we instead hypothesize that under normal physiological concentrations, the impaired cleavage of FB p.Phe286Leu by FD compensates for its increased affinity towards C3b. In light of a recent finding describing FD-independent AP activation (52), we also hypothesize that the incorporation of highly decay-resistant FB p.Phe286Leu into C3(H_2O)B may lead to increased C3 cleavage over time, thus propagating the complement amplification process.

C3 convertase formation and decay assays were used to assess three well-characterized pathogenic variants (p.Arg53Cys, p.Trp134Arg, p.Arg175Pro) in short consensus repeats 1-3 of *CFH*. Their respective inhibitory functions recapitulated the results from the previous studies (Figure 6) (23, 24).

We next assessed the acquired drivers of C3G. IgG from six C3G patients was assessed for C3bBb stabilization capacity (Table 1), and a spectrum of outcomes was found. While showing no effect on convertase formation rate, some IgG derived from C3Nef-negative patients had a mild stabilizing effect on C3bBb up to 10 min post formation. This finding suggests that some IgG derived from C3Nef-negative patients may stabilize C3bBb for a short period of time, likely contributing to the overall disease pathogenesis when other disease factors are present. Assessments of C3Nef-positive patient-derived IgG resulted in expected increases in C3 convertase half-life, consistent with described C3Nef functions (3, 18, 20). Importantly, unlike any other IgG tested, P3 IgG increased C3bBb formation while providing weak stabilization (Table 1), suggesting a novel method of C3G pathogenesis whereby C3Nefs promote increased formation of C3bBb.

There are two main limitations to the proposed model. First, while MaxGel is a human basement membrane extract, we cannot ensure that it recapitulates the exact composition of the ECM found in human kidneys. Differences in glycosaminoglycan composition may need to be considered when evaluating convertase regulation by FH and FP on the surface of these ECM. Second, His-tags on the recombinant proteins may change complement dynamics and pathway activity, as demonstrated by the His-tagged WT FB (Figure 5B, lanes 3-4; 5C). Decreased C3bBb formation and faster convertase decay with recombinant WT FB indicate the need to control for the effects of His-tags on these processes and adjust the data interpretation accordingly.

In summary, we have developed a new model to test complement activity and regulation on an ECM surface. This model recapitulates normal complement activity and when used to test both genetic and acquired drivers of C3G, provides valuable insights into how complement activity can be altered in this microenvironment. Its further applications to complement-mediated glomerular diseases may facilitate patient-specific insights into disease pathogenesis.

Data availability statement

The original contributions presented in the study are included in the article/Supplementary Material. Further inquiries can be directed to the corresponding author.

Ethics statement

The studies involving human participants were reviewed and approved by Institutional Review Board of the University of Iowa. The patients/participants provided their written informed consent to participate in this study.

Author contributions

RS and YZ conceived the study. SP and XX designed the protocol. SP troubleshot the protocol, designed and carried out the experiments, analyzed the data, made the figures and drafted the manuscript. NM and RG quantified C3Nefs. RS, YZ, CN, NM and SP revised the manuscript. All authors contributed to the article and approved the submitted version.

Funding

National Institutes of Health, Grant/Award. Number: R01 DK110023.

Acknowledgments

The authors would like to sincerely thank the patients enrolled in the study. We would also like to thank Dr. Mikhail Kulak for sharing his expertise with western blots.

Conflict of interest

The authors declare that the research was conducted in the absence of any commercial or financial relationships that could be construed as a potential conflict of interest.

Publisher's note

Supplementary material

The Supplementary Material for this article can be found online at: https://www.frontiersin.org/articles/10.3389/fimmu.2022.1073802/full#supplementary-material

References

1. Pickering MC, D'agati VD, Nester CM, Smith RJ, Haas M, Appel GB, et al. C3 glomerulopathy: Consensus report. *Kidney Int* (2013) 84(6):1079–89. doi: 10.1038/ki.2013.377

2. Smith RJH, Appel GB, Blom AM, Cook HT, D'Agati VD, Fakhouri F, et al. C3 glomerulopathy — understanding a rare complement-driven renal disease. *Nat Rev Nephrol.* (2019) 1 5:129–43. doi: 10.1038/s41581-018-0107-2

3. Heiderscheit AK, Hauer JJ, Smith RJH. C3 glomerulopathy : Understanding an ultra-rare complement- mediated renal disease. *Am J Med Genet* (2022) 190(3):344–57. doi: 10.1002/ajmg.c.31986

4. Servais A, Noël LH, Roumenina LT, Le Quintrec M, Ngo S, Dragon-Durey MA, et al. Acquired and genetic complement abnormalities play a critical role in dense deposit disease and other C3 glomerulopathies. *Kidney Int* (2012) 82(4):454–64. doi: 10.1038/ki.2012.63

5. Rabasco C, Cavero T, Román E, Rojas-Rivera J, Olea T, Espinosa M, et al. Effectiveness of mycophenolate mofetil in C3 glomerulonephritis. *Kidney Int* (2015) 88 (5):1153–60. doi: 10.1038/ki.2015.227

6. Iatropoulos P, Noris M, Mele C, Piras R, Valoti E, Bresin E, et al. Complement gene variants determine the risk of immunoglobulin-associated MPGN and C3 glomerulopathy and predict long-term renal outcome. *Mol Immunol* (2016) 71:131–42. doi: 10.1016/j.molimm.2016.01.010

7. Angelo JR, Bell CS, Braun MC. Allograft failure in kidney transplant recipients with membranoproliferative glomerulonephritis. *Am J Kidney Dis* (2011) 57(2):291–9. doi: 10.1053/j.ajkd.2010.09.021

8. Zand L, Lorenz EC, Cosio FG, Fervenza FC, Nasr SH, Gandhi MJ, et al. Clinical findings, pathology, and outcomes of C3GN after kidney transplantation. *J Am Soc Nephrol.* (2014) 25(5):1110–7. doi: 10.1681/ASN.2013070715

9. Li P, Ponnala L, Gandotra N, Wang L, Si Y, Tausta SL, et al. The developmental dynamics of the maize leaf transcriptome. *Nat Genet* (2010) 42(12):1060–7. doi: 10.1038/ng.703

10. Regunathan-Shenk R, Avasare RS, Ahn W, Canetta PA, Cohen DJ, Appel GB, et al. Kidney transplantation in C3 glomerulopathy: A case series. *Am J Kidney Dis* (2019) 73 (3):316–23. doi: 10.1053/j.ajkd.2018.09.002

11. Satchell SC, Braet F. Glomerular endothelial cell fenestrations: An integral component of the glomerular filtration barrier. *Am J Physiol - Ren Physiol* (2009) 296 (5):F947–56. doi: 10.1152/ajprenal.90601.2008

12. Butler MJ, Down CJ, Foster RR, Satchell SC. The pathological relevance of increased endothelial glycocalyx permeability. *Am J Pathol* (2020) 190(4):742–51. doi: 10.1016/j.ajpath.2019.11.015

13. Pollak MR, Quaggin SE, Hoenig MP, Dworkin LD. The glomerulus: The sphere of influence. *Clin J Am Soc Nephrol.* (2014) 9(8):1461–9. doi: 10.2215/CJN.09400913

14. Arkill KP, Qvortrup K, Starborg T, Mantell JM, Knupp C, Michel CC, et al. Resolution of the three dimensional structure of components of the glomerular filtration barrier. *BMC Nephrol.* (2014) 15(1):1–13. doi: 10.1186/1471-2369-15-24

15. Brenner BM, Hostetter TH, Humes HD. Molecular basis of protenuria of glomerular origin. *N Engl J Med* (1978) 298(15):826–33. doi: 10.1056/NEJM197804132981507

16. Myers BD, Guasch A. Selectivity of the glomerular filtration barrier in healthy and nephrotic humans. *Am J Nephrol.* (1993) 13(5):311–7. doi: 10.1159/000168645

17. Ricklin D, Reis ES, Mastellos DC, Gros P, Lambris JD. Complement component C3 - the "Swiss army knife" of innate immunity and host defense. *Immunol Rev* (2016) 274 (1):33–58. doi: 10.1111/imr.12500

18. Zhang Y, Meyer NC, Wang K, Nishimura C, Frees K, Jones M, et al. Causes of alternative pathway dysregulation in dense deposit disease. *Clin J Am Soc Nephrol.* (2012) 7(2):265–74. doi: 10.2215/CJN.07900811

19. Iatropoulos P, Daina E, Curreri M, Piras R, Valoti E, Mele C, et al. Cluster analysis identifies distinct pathogenetic patterns in c3 glomerulopathies/immune complex–mediated membranoproliferative GN. *J Am Soc Nephrol.* (2018) 29(1):283–94. doi: 10.1681/ASN.2017030258

20. Daha MR, Fearon DT, Austen KF. C3 nephritic factor (C3NeF): Stabilization of fluid phase and cell-bound alternative pathway convertase. *J Immunol* (1976) 116(1):1–7. doi: 10.4049/jimmunol.116.1.1

21. Michels MAHM, van de Kar NCAJ, Okrój M, Blom AM, van Kraaij SAW, Volokhina EB, et al. Overactivity of alternative pathway convertases in patients with complement-mediated renal diseases. *Front Immunol* (2018) 9(APR):1–13. doi: 10.3389/fimmu.2018.00612

22. Rodríguez De Córdoba S, Esparza-Gordillo J, Goicoechea De Jorge E, Lopez-Trascasa M, Sánchez-Corral P. The human complement factor h: Functional roles, genetic variations and disease associations. *Mol Immunol* (2004) 41(4):355–67. doi: 10.1016/j.molimm.2004.02.005

23. Merinero HM, García SP, García-Fernández J, Arjona E, Tortajada A, Rodríguez de Córdoba S. Complete functional characterization of disease-associated genetic variants in the complement factor h gene. *Kidney Int* (2018) 93(2):470–81. doi: 10.1016/j.kint.2017.07.015

24. Martín Merinero H, Zhang Y, Arjona E, del Angel G, Goodfellow R, Gomez-Rubio E, et al. Functional characterization of 105 factor h variants associated with aHUS: lessons for variant classification. *Blood* (2021) 138(22):2185–201. doi: 10.1182/blood.2021012037

25. Nester CM, Smith RJ. Diagnosis and treatment of C3 glomerulopathy. *Clin Nephrol.* (2013) 80(6):395–404. doi: 10.5414/CN108057

26. Nester CM, Smith RJH. Complement inhibition in C3 glomerulopathy. *Semin Immunol* (2016) 28(3):241–9. doi: 10.1016/j.smim.2016.06.002

27. Nangaku M. Complement regulatory proteins in glomerular diseases. *Kidney Int* (1998) 54(5):1419–28. doi: 10.1046/j.1523-1755.1998.00130.x

28. Li X, Ding F, Zhang X, Li B, Ding J. The expression profile of complement components in podocytes. *Int J Mol Sci* (2016) 17(4):471. doi: 10.3390/ijms17040471

29. Dane MJC, Van Den Berg BM, Lee DH, Boels MGS, Tiemeier GL, Avramut MC, et al. A microscopic view on the renal endothelial glycocalyx. *Am J Physiol - Ren Physiol* (2015) 308(9):F956–66. doi: 10.1152/ajprenal.00532.2014

30. Yilmaz O, Afsar B, Ortiz A, Kanbay M. The role of endothelial glycocalyx in health and disease. *Clin Kidney J* (2019) 12(5):611–9. doi: 10.1093/ckj/sfz042

31. Kouser L, Abdul-Aziz M, Nayak A, Stover CM, Sim RB, Kishore U. Properdin and factor h: opposing players on the alternative complement pathway "see-saw". *Front Immunol* (2013) 4:93. doi: 10.3389/fimmu.2013.00093

32. Parente R, Clark SJ, Inforzato A, Day AJ. Complement factor h in host defense and immune evasion. *Cell Mol Life Sci* (2016)74:1605–24. doi: 10.1007/s00018-016-2418-4

33. Scientific T. Melon^{TM} gel IgG spin purification kit (45206). (2012) 0747(815):.

34. Fearon DT, Austen KF. PROPERDIN : BINDING TO C3b AND STABILIZATION OF THE C3b-DEPENDENT C3 CONVERTASE. *J Exp Med* (1975) 142:856–63. doi: 10.1084/jem.142.4.856.

35. Nilsson SC, Sim RB, Lea SM, Fremeaux-Bacchi V, Blom AM. Complement factor I in health and disease. *Mol Immunol* (2011) 48(14):1611–20. doi: 10.1016/j.molimm.2011.04.004

36. Kopp A, Hebecker M, Svobodová E, Józsi M. Factor h: A complement regulator in health and disease, and a mediator of cellular interactions. *Biomolecules* (2012) 2(1):46–75. doi: 10.3390/biom2010046

37. Hourcade DE, Mitchell LM, Teresa J, Hourcade DE, Mitchell LM, Oglesby TJ. Mutations of the type a domain of complement factor b that promote high-affinity high-affinity C3b-binding. *J Immunol* (1999)162:2906–11. doi: 10.4049/jimmunol.162.5.2906

38. Roumenina LT, Jablonski M, Hue C, Blouin J, Dimitrov JD, Dragon-Durey MA, et al. Hyperfunctional C3 convertase leads to complement deposition on endothelial cells and contributes to atypical hemolytic uremic syndrome. *Blood* (2009) 114(13):2837–45. doi: 10.1182/blood-2009-01-197640

39. Goicoechea De Jorge E, Harris CL, Esparza-Gordillo J, Carreras L, Aller Arranz E, Abarrategui Garrido C, et al. Gain-of-function mutations in complement factor b are associated with atypical hemolytic uremic syndrome. *Proc Natl Acad Sci U S A.* (2007) 104 (1):240–5. doi: 10.1073/pnas.0603420103

40. Zhang Y, Nester CM, Martin B, Skjoedt MO, Meyer NC, Shao D, et al. Defining the complement biomarker profile of C3 glomerulopathy. *Clin J Am Soc Nephrol.* (2014) 9 (11):1876–82. doi: 10.2215/CJN.01820214

41. Dopler A, Guntau L, Harder MJ, Palmer A, Höchsmann B, Schrezenmeier H, et al. Self versus nonself discrimination by the soluble complement regulators factor h and FHL-1. *J Immunol* (2019) 202(7):2082–94. doi: 10.4049/jimmunol.1801545

42. Schmidt CQ, Hipgrave Ederveen AL, Harder MJ, Wuhrer M, Stehle T, Blaum BS. Biophysical analysis of sialic acid recognition by the complement regulator factor h. *Glycobiology* (2018) 28(10):765–73. doi: 10.1093/glycob/cwy061

43. Clark SJ, Ridge LA, Herbert AP, Hakobyan S, Mulloy B, Lennon R, et al. Tissue-specific host recognition by complement factor h is mediated by differential activities of its glycosaminoglycan-binding regions. *J Immunol* (2013) 190(5):2049–57. doi: 10.4049/jimmunol.1201751

44. van Essen MF, Schlagwein N, van den Hoven EMP, van Gijlswijk-Janssen DJ, Lubbers R, van den Bos RM, et al. Initial properdin binding contributes to alternative pathway activation at the surface of viable and necrotic cells. *Eur J Immunol* (2022) 52 (4):597–608. doi: 10.1002/eji.202149259

45. Harboe M, Johnson C, Nymo S, Ekholt K, Schjalm C, Lindstad JK, et al. Properdin binding to complement activating surfaces depends on initial C3b deposition. *Proc Natl Acad Sci U S A.* (2017) 114(4):E534–9. doi: 10.1073/pnas.1612385114

46. Zaferani A, Vivès RR, van der Pol P, Navis GJ, Daha MR, Van Kooten C, et al. Factor h and properdin recognize different epitopes on renal tubular epithelial heparan sulfate. *J Biol Chem* (2012) 287(37):31471–81. doi: 10.1074/jbc.M112.380386

47. Zaferani A, Vivès RR, van der Pol P, Hakvoort JJ, Navis GJ, Van Goor H, et al. Identification of tubular heparan sulfate as a docking platform for the alternative complement component properdin in proteinuric renal disease. *J Biol Chem* (2011) 286 (7):5359–67. doi: 10.1074/jbc.M110.167825

48. Pangburn MK, Muller-Eberhardt HJ. The C3 convertase of the alternative pathway of human complement enzymic properties of the bimolecular proteinase the association of factor b with C3b (the major fragment of complement component C3) in the presence of Mg2+ results in the formation of. *Biochem J* (1986) 235:723–30. doi: 10.1042/bj2350723

49. Marinozzi MC, Vergoz L, Rybkine T, Ngo S, Bettoni S, Pashov A, et al. Complement factor b mutations in atypical hemolytic uremic syndrome-disease-

relevant or benign? *J Am Soc Nephrol* (2014) 25(9):2053–65. doi: 10.1681/ASN.2013070796

50. Torreira E, Tortajada A, Montes T, De Córdoba SR, Llorca O. 3D structure of the C3bB complex provides insights into the activation and regulation of the complement alternative pathway convertase. *Proc Natl Acad Sci U S A.* (2009) 106(3):882–7. doi: 10.1073/pnas.0810860106

51. Torreira E, Tortajada A, Montes T, Rodríguez de Córdoba S, Llorca O. Coexistence of closed and open conformations of complement factor b in the alternative pathway C3bB(Mg 2+) proconvertase. *J Immunol* (2009) 183(11):7347–51. doi: 10.4049/jimmunol.0902310

52. Zhang Y, Keenan A, Dai DF, May KS, Anderson EE, Lindorfer MA, et al. C3(H2O) prevents rescue of complementmediated C3 glomerulopathy in cfh-/- cfd-/- mice. *JCI Insight* (2020) 5(9):e135758. doi: 10.1172/jci.insight.135758

frontiers | Frontiers in Immunology

TYPE Original Research
PUBLISHED 30 January 2023
DOI 10.3389/fimmu.2022.1011580

OPEN ACCESS

EDITED BY
Mihály Józsi,
Eötvös Loránd University, Hungary

REVIEWED BY
Dorottya Csuka,
Semmelweis University, Hungary
Kevin James Marchbank,
Newcastle University, United Kingdom

*CORRESPONDENCE
Rossella Piras
rossella.piras@marionegri.it

SPECIALTY SECTION
This article was submitted to Molecular Innate Immunity, a section of the journal Frontiers in Immunology

RECEIVED 04 August 2022
ACCEPTED 28 December 2022
PUBLISHED 30 January 2023

CITATION
Piras R, Valoti E, Alberti M, Bresin E, Mele C, Breno M, Liguori L, Donadelli R, Rigoldi M, Benigni A, Remuzzi G and Noris M (2023) *CFH* and *CFHR* structural variants in atypical Hemolytic Uremic Syndrome: Prevalence, genomic characterization and impact on outcome. *Front. Immunol.* 13:1011580. doi: 10.3389/fimmu.2022.1011580

CFH and *CFHR* structural variants in atypical Hemolytic Uremic Syndrome: Prevalence, genomic characterization and impact on outcome

Rossella Piras*, Elisabetta Valoti, Marta Alberti, Elena Bresin, Caterina Mele, Matteo Breno, Lucia Liguori, Roberta Donadelli, Miriam Rigoldi, Ariela Benigni, Giuseppe Remuzzi and Marina Noris

Istituto di Ricerche Farmacologiche Mario Negri IRCCS, Clinical Research Center for Rare Diseases Aldo e Cele Daccò and Centro Anna Maria Astori, Science and Technology Park Kilometro Rosso, Bergamo, Italy

Introduction: Atypical hemolytic uremic syndrome (aHUS) is a rare disease that manifests with microangiopathic hemolytic anemia, thrombocytopenia, and acute renal failure, and is associated with dysregulation of the alternative complement pathway. The chromosomal region including *CFH* and *CFHR1-5* is rich in repeated sequences, favoring genomic rearrangements that have been reported in several patients with aHUS. However, there are limited data on the prevalence of uncommon *CFH-CFHR* genomic rearrangements in aHUS and their impact on disease onset and outcomes.

Methods: In this study, we report the results of *CFH-CFHR* Copy Number Variation (CNV) analysis and the characterization of resulting structural variants (SVs) in a large cohort of patients, including 258 patients with primary aHUS and 92 with secondary forms.

Results: We found uncommon SVs in 8% of patients with primary aHUS: 70% carried rearrangements involving *CFH* alone or *CFH* and *CFHR* (group A; n=14), while 30% exhibited rearrangements including only *CFHRs* (group B; n=6). In group A, 6 patients presented *CFH::CFHR1* hybrid genes, 7 patients carried duplications in the *CFH-CFHR* region that resulted either in the substitution of the last *CFHR1* exon(s) with those of *CFH* (*CFHR1::CFH* reverse hybrid gene) or in an internal *CFH* duplication. In group A, the large majority of aHUS acute episodes not treated with eculizumab (12/13) resulted in chronic ESRD; in contrast, anti-complement therapy induced remission in 4/4 acute episodes. aHUS relapse occurred in 6/7 grafts without eculizumab prophylaxis and in 0/3 grafts with eculizumab prophylaxis. In group B, 5 subjects had the $CFHR3_{1-5}$::$CFHR4_{10}$ hybrid gene and one had 4 copies of *CFHR1* and *CFHR4*. Compared with group A, patients in group B exhibited a higher prevalence of additional complement abnormalities and

10.3389/fimmu.2022.1011580

earlier disease onset. However, 4/6 patients in this group underwent complete remission without eculizumab treatment. In secondary forms we identified uncommon SVs in 2 out of 92 patients: the *CFHR3*$_{1-5}$*::CFHR4*$_{10}$ hybrid and a new internal duplication of *CFH*.

Discussion: In conclusion, these data highlight that uncommon *CFH-CFHR* SVs are frequent in primary aHUS and quite rare in secondary forms. Notably, genomic rearrangements involving the *CFH* are associated with a poor prognosis but carriers respond to anti-complement therapy.

KEYWORDS

atypical hemolytic uremic syndrome (aHUS), eculizumab, factor H (FH), factor H-related proteins (FHRs), complement, copy number variations (CNVs), structural variants (SVs), single molecule real-time (SMRT)

Introduction

Atypical hemolytic uremic syndrome (aHUS) is an ultra-rare kidney disease characterized by microangiopathic hemolytic anemia, thrombocytopenia, and renal impairment (1). Primary aHUS is associated with genetic and acquired defects that led to dysregulation of the alternative pathway (AP) of complement system, resulting in endothelial damage in the microcirculation of the kidney and other organs (2). About 50% of patients carry genetic abnormalities that affect genes coding for complement regulators (*CFH*, *CD46*, *CFI* and *THBD*) and components (*C3* and *CFB*), while in 10% of patients anti-FH autoantibodies have been reported (3).

Atypical HUS can be secondary to autoimmune or systemic disease, pregnancy/postpartum, malignant hypertension, drug treatments, cancer and transplantation (4, 5). In the secondary forms, the prevalence of genetic defects is variable, ranging from almost 60% in cases associated with malignant hypertension or pregnancy to less than 10% in drug-induced TMA.

The gene most commonly involved in aHUS is *CFH*, encoding complement factor H (FH). *CFH* is mapped on chromosome 1q31 within the RCA (Regulation of Complement Activation) gene cluster, which also includes the *CFHR3*, *CFHR1, CFHR4, CFHR2* and *CFHR5* genes, derived from genomic duplication events (6). The resulting FH and FHR proteins are organized in short consensus repeats (SCRs), each consisting of about 60 amino acids (Figure 1), and are mainly produced by the liver and circulate in the blood.

Factor H is the main plasma regulator of the AP of complement and consists of 20 SCRs. FH regulatory activity is mediated by its N-terminal domains (SCR1-4) acting as a cofactor for complement protease Factor I (FI) and accelerating the decay of C3 convertase. In addition, through the SCR6-7 and C-terminal domains (SCR19-20), FH binds C3b and polyanions, such as glycosaminoglycans, heparan sulfate, and sialic acids, and mediates cell surface protection from complement activation. The large majority of *CFH* genetic abnormalities in aHUS cluster in the C-terminal part of the protein, leading to reduced complement regulation on endothelial cells. However, not all the carriers of heterozygous *CFH* genetic defects manifest aHUS, due to incomplete penetrance.

FHRs were originally thought to be negative complement inhibitors, but later studies indicated that these molecules may instead enhance complement activation (8). The C-terminal domains of FHRs have a high level of amino acidic sequence identity with SCR18-19-20 of FH leading them to be able to bind the same FH ligands (Figure 1) (8–11). The N-terminal SCRs (SCR1-2) of FHR-1, FHR-2 and FHR-5, are very similar (85-100%) and include a dimerization domain (Figure 1), which explains their presence in the circulation as homo- and hetero- dimers or tetramers (12–14). This oligomerization increases FHR avidity for C3b and C3-opsonized surfaces and for polyanionic surface ligands, which results in the activation of the alternative pathway (12, 13). The N-terminal domains of FHR-3 and FHR-4 (SCR1-3 of both) share high residue sequence similarity with FH SCR6 to SCR8 and FH SCR6-8-9, respectively, which are involved in binding to heparin, C-reactive protein, and microbial surface ligands. However, none of the FHR protein domains have any similarity to the N-terminal regulatory domains of FH, indicating that FHRs lack direct complement regulatory activity, although this point remains controversial (15).

The FH gene cluster is characterized by large repeated regions, which favors genomic rearrangements and copy number variations (CNVs) like the duplications, deletions and inversions that have been reported in association with aHUS and other complement-mediated diseases (16, 17). Genomic alterations involving DNA segments larger than 1kb are defined as structural variants (SVs) and the most frequent SV in the *CFH* gene cluster is the ~84 kb deletion of *CFHR3* and *CFHR1* (*CFHR3-CFHR1* del), which is associated with a high risk of developing anti-FH autoantibody (anti-FHs)-mediated aHUS (18). Rare SVs involving *CFH* and *CFHRs* that lead to hybrid genes such as *CFH::CFHR1, CFH::CFHR3*, and the reverse *CFHR1::CFH* hybrids have been reported in patients with primary aHUS, and a few functional analyses have confirmed their involvement in disease pathogenesis (7, 16, 17).

However, data on the prevalence of *CFH-CFHR* genomic rearrangements in primary and secondary aHUS, their impact on disease penetrance, disease onset, response to therapy and outcome are limited to case reports or case-series.

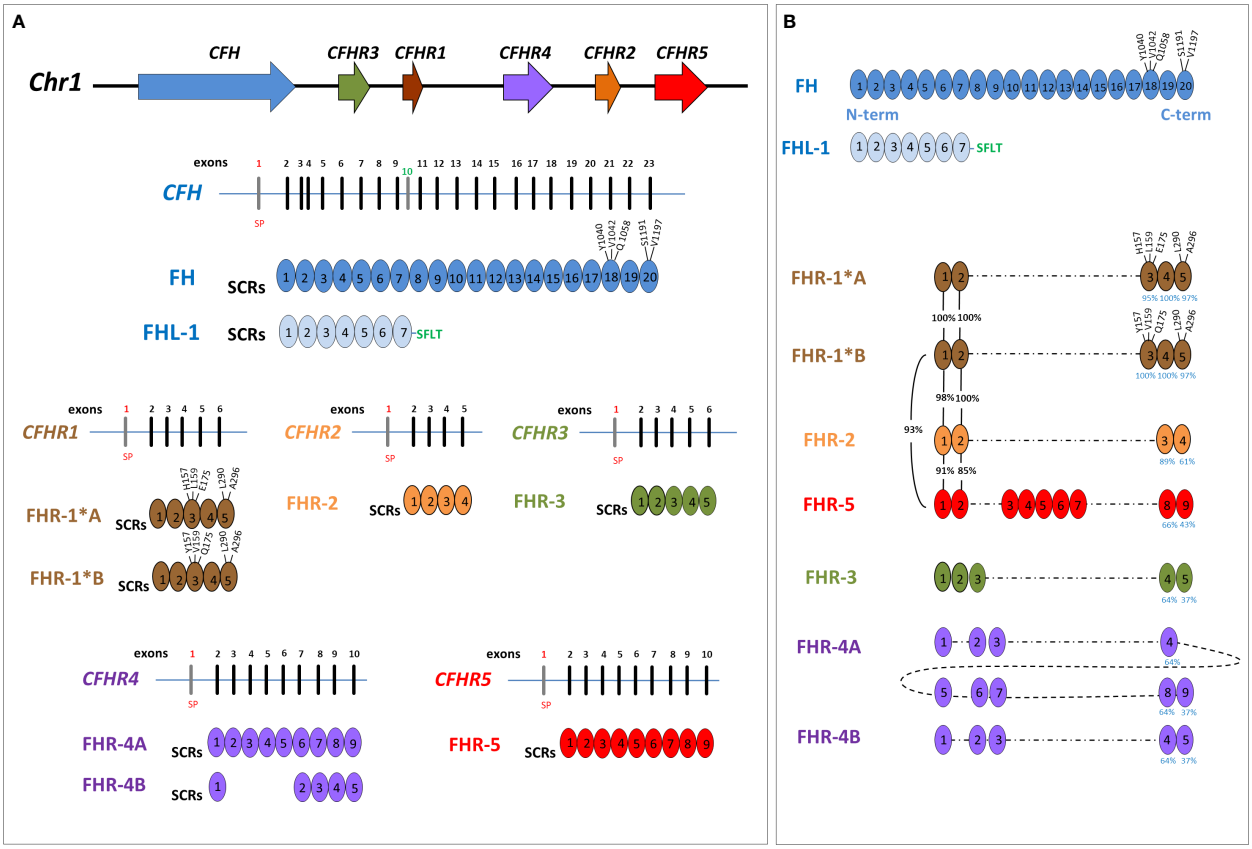

FIGURE 1
Structure of Factor H family: genes and proteins. **(A)** The human complement factor H (*CFH*) gene family is located on chromosome 1q31.3 and includes six genes: *CFH, CFHR3, CFHR1, CFHR4, CFHR2* and *CFHR5*. For each gene, the corresponding protein was represented. Each short consensus repeat (SCR) is composed of about 60 amino acids and is encoded by a single exon, with the exception of SCR2 of Factor H (FH), encoded by exon 3 and 4. Exon 1 of each gene encodes 18 amino acids of the signal peptide (SP). *CFH* gene is composed of 23 exons and, through two alternative splicing, produces FH, deriving from 22 exons, and Factor H-like protein 1 (FHL-1), deriving from 10 exons. Exon 10 is not included in the FH transcript and encodes the C-terminal four amino acids (Ser-Phe-Leu-Thr; indicated in the Figure with the green SFLT) and the 3'UTR of FHL-1. FHR-1 exists in two isoforms that differ in three amino acids in the SCR3: FHR-1*A is known as acidic isoform and has His at position 157 (H157), Leu at 159 (L159) and Glu at 175 (E175); FHR-1*B is the basic isoform with Tyr at position 157 (Y157), Val at 159 (V159) and Gln at 175 (Q175). **(B)** Factor H-related proteins (FHRs) share a high degree of conservation within the C-terminal domains of FH (SCR18-SCR19-SCR20), and FHR-1 is the most similar (the percentage of amino acids identity between each SCR of FHR and those of FH is indicated by blue numbers under the SCRs). As represented in the Figure, SCR3 of FHR-1*A differs from SCR18 of FH for 3 amino acids (H157, L159 and E175) while SCR5 differs from FH-SCR20 for 2 amino acids (L290 and A296). At variance, SCR3 of FHR-1*B has the same amino acids of SCR18 of FH. Of note, the N-terminal domains of FHR-1, FHR-2 and FHR-5 (SCR1 and SCR2) have a high sequence identity (indicated by black percentage numbers) and include a dimerization motif which explains their presence in plasma as either homo-or heterodimers. This image was inspired by Jozsi et al. (7) Trends immunology, 2015.

Here, we report a retrospective study of *CFH-CFHR* copy number variations (CNVs) in a large cohort of unrelated patients affected by primary (n=258) or secondary aHUS (n=92). We evaluated the prognosis of patients carrying *CFH-CFHR* SVs and the contribution of the concomitant presence of rare complement gene variants or anti-FHs abnormalities to disease development. To overcome the limits of next generation sequencing (NGS) to detect SVs in the *CFH-CFHR* region, we applied Multiplex Ligation-dependent Probe Amplification (MLPA), long-read sequencing (Single -Molecule Real-Time, SMRT) and direct sequencing to identify and characterize rare genomic rearrangements. We found them in the 6% of patients, including 2 patients with secondary forms. Furthermore, we identified a group of patients carrying rearrangements that included only *CFHR* genes, which have so far been reported in association with C3G or Immune complex-mediated membranoproliferative glomerulonephritis (IC-MPGN) (17). This group presented a milder disease phenotype than patients with rearrangements involving *CFH*.

Our results confirm the important role of *CFH* genomic rearrangements in the pathogenesis of aHUS and highlight the potential impact of SVs involving *CFHR* genes in disease predisposition and phenotype.

Material and methods

Study participants

Patients included in this study were recruited through the International Registry of HUS/TTP, under the coordination of the Aldo and Cele Daccò Clinical Research Center for Rare Diseases (Ranica, Bergamo, Italy).

Clinical information and demographic/laboratory data for patients and their available relatives were collected using a case report form. Biochemical and genetic tests were performed using blood, plasma or serum samples, and DNA was collected for each patient and available relatives.

Healthy controls were recruited among blood donors and were analyzed for copy number variations (CNVs). The samples used for the research were stored at the Centro Risorse Biologiche (CRB) Mario Negri, Malattie Rare e Malattie Renali biobank.

Atypical HUS was diagnosed in all cases with microangiopathic hemolytic anemia and thrombocytopenia (hematocrit less than 30%, hemoglobin level less than 10 g/dL, serum lactate dehydrogenase level higher than 500 U/L, undetectable haptoglobin, fragmented erythrocytes in peripheral blood smear, and platelet count less than $150x10^3$/μl) associated with acute renal failure (serum creatinine>1.3 mg/dl for adults, >0.5 mg/dl for children under 5 years of age and >0.8 mg/dl for children aged 5-10 years old; and/or urinary protein/creatinine ratio >200 mg/g; or an increase of serum creatinine or urinary protein/creatinine ratio>15% compared to baseline levels). Thrombotic thrombocytopenic purpura was ruled out in the presence of ADAMTS13 activity >10% and no anti-ADAMTS13 antibodies. Patients were classified as having primary aHUS when both secondary underlying conditions and Stx-*E.Coli* infections were ruled out; a secondary form was considered when aHUS was associated with hypertension, autoimmune diseases, infections, pre-existing nephropathy, transplantation, drug exposure or other coexisting conditions (pneumococcal infections and malignancy).

Familial aHUS was diagnosed when two or more members of the same family were affected by the disease at least 6 months apart and exposure to a common trigger infectious agent was excluded. Sporadic aHUS was diagnosed when one or more episodes of the disease manifested in a subject with no familial history of the disease.

The study was approved by the Ethics Committee of the Azienda Sanitaria Locale, Bergamo (Italy) and informed consent was obtained in accordance with the Declaration of Helsinki.

Complement profile assessment

FH and anti-FH autoantibody serum levels were measured using Enzyme-Linked Immunosorbent Assay (ELISA) as previously reported (3).

Genetic screening and biochemical testing

Genomic DNA was extracted from peripheral blood leukocytes (Nucleon™ BACC2 kit, GE Healthcare; NucleoSpin Blood columns, Macherey-Nagel). All coding exons and the intronic flanking regions of membrane cofactor protein (*CD46)*, complement factor H (*CFH*), complement factor I (*CFI)*, complement factor B (*CFB)*, complement C3 (*C3)* and thrombomodulin (*THBD)* genes were amplified by polymerase chain reaction (PCR) and were directly sequenced (48-capillary 3730 DNA Analyzer), as previously reported (19). Patients recruited more recently were analyzed using a next generation sequencing (NGS) panel for the simultaneous sequencing of *CFH*, *CD46*, *CFI*, *CFB, C3*, and *THDB* through Ion Torrent platform (Life technologies). Since recessive LPVs in the gene encoding diacylglycerol kinase DGKε (*DGKE)* have been identified in patients with aHUS with an onset in infancy, we also sequenced *DGKE*, by NGS, in patients carrying uncommon SVs and with a disease onset below 4 years (20, 21).

Patients with uncommon SVs and their available relatives, were genotyped by NGS or direct sequencing for the *CFH* and *CD46* single-nucleotide polymorphisms (SNPs) that define the aHUS-risk haplotypes *CFH-H3* and $CD46_{GGAAC}$, respectively (19, 22–25).

Genetic variants with a reported minor allelic frequency (MAF) below 0.001 in the Genome Aggregation Database (gnomAD) and with a Combined Annotation Dependent Depletion (CADD) phred score ≥10 were considered likely pathogenic variants (LPVs).

CFH-CFHR copy number variations

Multiplex ligation dependent probe amplification (SALSA MLPA P236, MRC Holland, Netherlands) and in-house probes for *CFHR4* and *CFHR5* were used to evaluate the presence of copy number variations (CNVs) in *CFH*, *CFHR1*, *CFHR2*, *CFHR3*, *CFHR4*, and *CFHR5* genes in all the patients, as previously reported (17).

Two hundred and fourteen healthy subjects were also analyzed for *CFHR4* CNVs using multiplex polymerase chain reaction (mPCR) amplifying intron 1 and exon 2 of *CFHR4* and intron 3 of *CFHR1* (18).

Single molecule real-time (SMRT) sequencing

Probes targeting *CFH-CFHRs* on the human genome, reference hg19 (from chr: 196619000 to chr: 196979303) were designed by Nimble Design Software (Roche Sequencing, Pleasanton, CA, US). Selected DNA samples previously identified with CNVs through MLPA analysis, were sequenced at the Norwegian Sequencing Centre using the PacBio Sequel system. Methodology details have previously been published in Piras R et al. (17)

Direct sequencing

PCR was carried out in 25 μl of reaction volume using 125 ng of genomic DNA from patients with abnormal MLPA pattern and the Accuprime Taq DNA Polymerase (Thermo Fisher Scientific; 35 cycles of amplification: 94°C for 30 seconds, 59°C for 30 seconds, 68°C for 10 minutes). The breakpoint regions were identified by bidirectional sequencing of the long-range PCR product, using BigDye® Terminator v3.1 Cycle Sequencing Kit (Thermo Fisher Scientific) following the manufacturer's instructions. The BigDye XTerminator® Purification Kit (Thermo Fisher Scientific) was used to purify DNA sequencing reactions removing non-incorporated BigDye® terminators and salts. Sequencing analyses were carried out on the 48-capillary 3730 DNA Analyzer (Life Technologies). Sequences of primers used for long-range PCR are reported in Supplementary Table 1.

Western blot

The molecular pattern of FH-FHRs was studied by Western Blot (WB) using serum/plasma (diluted 1:40 for FHRs and 1:80 for FH). Proteins were separated by 10–12% SDS-PAGE, under non-reducing conditions and transferred by electroblotting to polyvinylidene Difluoride (PVDF) membrane (Bio-Rad). Membranes were developed using specific FH/FHR antibodies (the FHR-3 polyclonal antiserum was a kind gift from Prof. Zipfel (15); the anti-FHR1-2-5 monoclonal antibody was kindly provided by Prof. de Cordoba (12); the commercial monoclonal anti-human Factor H - OX-23, LSBio-), followed by HRP- conjugated secondary antibodies and ECL chemiluminescence detection system (Amersham).

Statistical analysis

All statistical tests were executed using MedCalc software. The Chi-square test or the Fisher's exact test were used to make comparisons, as appropriate.

Results

CFH-CFHR structural variants in aHUS

We report a retrospective MLPA analysis in a cohort of 350 unrelated patients with a diagnosis of aHUS, including 258 with primary aHUS and 92 with secondary aHUS.

Common structural variants (SVs), namely the *CFHR3-CFHR1* deletion (*CFHR3-CFHR1*del) and/or the *CFHR1-CFHR4* deletion (*CFHR1-CFHR4*del), were observed in 165 patients (47%; Table 1). The homozygous *CFHR3-CFHR1*del was significantly more frequent in aHUS cases than in healthy controls (11% vs 3%, respectively, p-value = 0.01).

The prevalence of common SVs was comparable in primary and secondary aHUS patients (47% vs 48%, respectively, ns), although the homozygous *CFHR3-CFHR1*del was more frequent in primary than in secondary aHUS (14% vs 4%, respectively, p-value = 0.01).

Specifically, in the primary aHUS group, common SVs were detected in 121 patients (47%) (Table 1): the heterozygous *CFHR3-CFHR1*del was found in 77 patients (30% vs 32% in healthy controls, ns); 36 patients exhibited the homozygous *CFHR3-CFHR1*del (14% vs 3% controls, p-value = 0.002); in addition, 7 patients were carriers of both *CFHR3-CFHR1*del and *CFHR1-CFHR4*del (3% vs 0% controls, ns) and a single case had the heterozygous *CFHR1-CFHR4*del (0.4% vs 2% controls, ns).

Among patients with secondary aHUS, common SVs were detected in 44 patients (48%). As shown in Table 1, 37 patients were heterozygous for the *CFHR3-CFHR1*del (40% vs 32% controls, ns) and 4 patients exhibited the same deletion on both alleles (4% vs 3% controls, ns). In addition, 2 patients were carriers of both the *CFHR3-CFHR1*del and the *CFHR1-CFHR4*del (2% vs 0% controls, p-value = *0.09*) and one patient had the heterozygous *CFHR1-CFHR4*del (1% vs 2% controls, ns).

Twenty-two patients (6%) carried uncommon SVs, including new or rare duplications and hybrid genes. These uncommon SVs were mainly found in patients with primary aHUS (n=20 out of 22 carriers; 91%), with a prevalence in this group of 8%.

Seventy % are rearrangements involving *CFH* gene alone or *CFH* and *CFHR* genes (n=14) and 30% are rearrangements including only *CFHR* genes (n=6; Table 2) that were mainly reported in C3G (17).

From here on we divided patients with rearrangements in *CFH* alone or *CFH* and *CFHR* genes (group A) from those involving only *CFHRs* (group B) to investigate differences in prevalence, age of onset, outcome and response to therapy.

Primary aHUS group A

***CFH::CFHR1* hybrid genes**: Six unrelated patients (#1; #2; #3; #4; #5; #6) shared a similar MLPA pattern in which probes showed one copy of exon 23 (n=1) or exons 22 and 23 (n=4) or exon 21-23 (n=1) of *CFH* and a gain of exon 6 or exons 5-6 or exons 4-6 of *CFHR1*, respectively (Table 2 and Figure 2A). In patients #1, #2, #3 and #4 the abnormal MLPA pattern is consistent with a deletion giving rise to $CFH_{1\text{-}21}$::$CFHR1_{5\text{-}6}$ hybrid gene, described for the first time in a family in UK (29). Notably, patient #1 also exhibited an extra copy of both *CFHR3* and

TABLE 1 Frequency of common and uncommon Structural Variants (SVs) in controls and patients.

	Controls	Total aHUS cases (n=350)		Primary aHUS (n=258)		Secondary aHUS (n=92)	
	n/tot (%)	n (%)	*P*-value[a]	n (%)	*P*-value[a]	n (%)	*P*-value[a]
Common SVs							
Het *CFHR3-CFHR1* del	32/100 (32%)	114 (32.6%)	ns	77 (29.8%)	ns	37 (40.2%)	ns
Hom *CFHR3-CFHR1*del	3/100 (3%)	40 (11.4%)	**0.01**	36 (14%)	**0.002**	4 (4.3%)	ns
Het *CFHR1-CFHR4*del	4/214 (1.9%)	2 (0.6%)	ns	1 (0.4%)	ns	1 (1.1%)	ns
*CFHR3-CFHR1*del + *CFHR1-CFHR4*del	0/214 (0%)	9 (2.6%)	ns	7 (2.7%)	*0.02*	2 (2.2%)	*0.09*
Uncommon SVs							
	1 (1%)*	22 (6%)	ns	20 (7.8%)	ns	2 (2.2%)	ns

[a]P-value have been calculated considering patients versus controls; Significant values are reported in bold; ns, not statistically significant.
*$CFHR3_{1\text{-}5}$::$CFHR4_{10}$ hybrid gene.

10.3389/fimmu.2022.1011580

TABLE 2 List of patients with new/rare *CFH-CFHR* structural variants (SVs) and/or other complement abnormalities.

Rare abnormalities							
Pat.	Uncommon SVs	LPVs	gnomAD MAF_all	CADD	FH levels (mg/L)	Anti-FH abs	g.A>G rs7542235 snp (*CFHR3-CFHR1*Δ tag)
Primary aHUS							
Group A							
#1	CFH_{1-21}::$CFHR1_{5-6}$ hybrid gene + *de novo CFHR3-CFHR1* dupl				408	Neg	AA
#2	CFH_{1-21}::$CFHR1_{5-6}$ hybrid gene				NA	NA	AA
#3	CFH_{1-21}::$CFHR1_{5-6}$ hybrid gene	*CFH*: p.R1210C	2.00E-04	11.77	377	Neg	AA
#4 [1]	CFH_{1-21}::$CFHR1_{5-6}$ hybrid gene	*CFI*: c.1429+1G>C	2.80E-05	24.7	NA	NA	AA
#5	CFH_{1-22}::$CFHR1_{6}$ hybrid gene				NA	Neg	AA
#6	CFH_{1-20}::$CFHR1_{4-5-6}$ hybrid gene + *CFHR1*dupl				327	Neg	AA
#7	Reverse $CFHR1_{1-5}$::CFH_{23} hybrid gene				332	Neg	AG
#8 [2]	Reverse $CFHR1_{1-5}$::CFH_{23} hybrid gene+ *CFHR3* dupl				218	Neg	AA
#9	Reverse $CFHR1_{1-5}$::CFH_{23} hybrid gene				363	NA	AG
#10	Reverse $CFHR1_{1-4}$::CFH_{22-23} hybrid gene + *CFHR3* dupl				182	Neg	AA
#11	Reverse $CFHR1_{1-4}$::CFH_{22-23} hybrid gene				221	Neg	AG
#12	Reverse $CFHR1_{1-4}$::CFH_{22-23} hybrid gene				283	Neg	AA
#13	CFH_{1-18} duplication				210	Neg	AA
#14	Reverse hybrid $CFHR1_{1-3}$::CFH_{21-23} gene + $CFHR3_{1-3}$ dupl				327	Neg	AA
Group B							
#15	$CFHR3_{1-5}$::$CFHR4_{10}$ hybrid gene	*C3*: p.D1115H	0	27.4	304	Neg	AA
#16	$CFHR3_{1-5}$::$CFHR4_{10}$ hybrid gene				308	Pos	GG
#17	$CFHR3_{1-5}$::$CFHR4_{10}$ hybrid gene				376	Neg	AA
#18	$CFHR3_{1-5}$::$CFHR4_{10}$ hybrid gene	*CD46*: c.286+2T>G	5.21E-05	14.54	NA	NA	GG
#19	$CFHR3_{1-5}$::$CFHR4_{10}$ hybrid gene				233	Neg	AA
#20 [3]	*CFHR1-CFHR4* duplication (4 copies)	*GRHPR:* p.R96H (hom)	3.98E-06	16.1	316	Neg	AA
Secondary aHUS							
#21	$CFHR3_{1-5}$::$CFHR4_{10}$ hybrid gene				388	Neg	AA
#22	CFH_{2-9} duplication				NA	NA	AA

Abbreviations and limits of normal range:
SVs, structural variants defined as genomic rearrangements resulting in duplications, deletions and inversions larger than 1 kb;
NA, not available;
Normal serum/plasma FH levels: ≥193 mg/L;
LPV, likely pathogenic variants, defined as genetic variants in coding and splicing regions of complement genes (*CFH, CFI, CD46, CFB, C3,* and *THBD*) with MAF< 0.001 in the gnomAD Database and with a CADD phred score ≥10;
[1]Bresin et al. (26);[2] Valoti et al. (27);[3]Valoti et al. (28).

10.3389/fimmu.2022.1011580

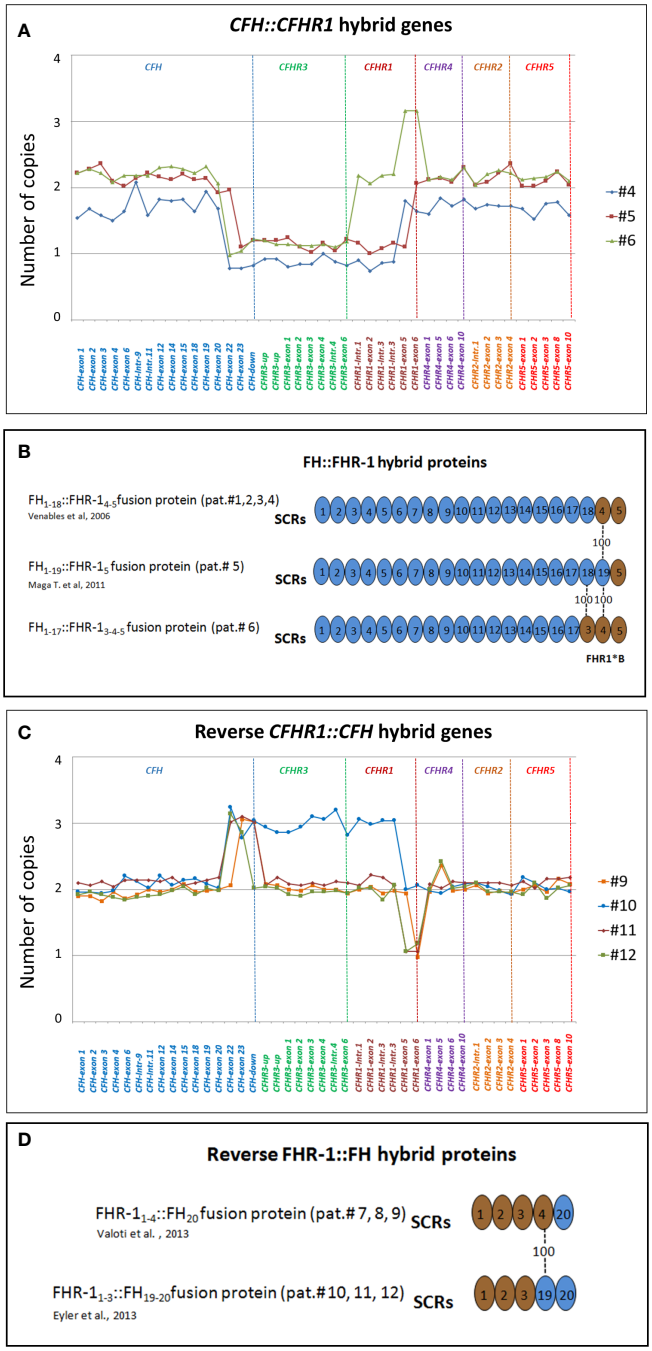

FIGURE 2
Graphic representation of MLPA results from aHUS patients carrying structural variants (SVs) in the *CFH* and *CFHR* genes. **(A)** MLPA patterns consistent with *CFH::CFHR1* hybrid genes. In patient #4, MLPA pattern shows one copy of exons 22 and 23 of *CFH*, one copy of *CFHR3*, one copy of *CFHR1* until intron 3, 2 copies of exons 5 and 6 of *CFHR1* and two normal copies of *CFHR4, CFHR2* and *CFHR5*, consistent with CFH_{1-21}::$CFHR1_{5-6}$ hybrid gene (29). In patient #5 MLPA results evidence 1 copy of exon 23 of *CFH*, one copy of *CFHR3*, one copy of *CFHR1* until exon 5, 2 copies of exons 6 of *CFHR1* and two normal copies of *CFHR4, CFHR2* and *CFHR5*, consistent with CFH_{1-22}::$CFHR1_6$ hybrid gene (30). In patient #6 MLPA analysis shows one copy of exons 22 and 23 of *CFH*, one copy of *CFHR3*, normal copy number from the *CFHR1*-intron 1 to *CFHR1*-intron 3, 3 copies of exons 5 and 6 of *CFHR1*, and two normal copies of *CFHR4, CFHR2* and *CFHR5*. This abnormal MLPA pattern was further characterized through long PCR, Sanger sequencing and SMRT which, as reported in Figure 3, led to the identification of the CFH_{1-20}::$CFHR1_{4-6}$ hybrid gene. **(B)** Representation of FH::FHR-1 hybrid proteins resulting from SVs identified in patients #1, #2, #3, #4, #5 and #6. SCRs translated from *CFH* are indicated in blue while SCRs deriving from *CFHR1* are indicated in brown. The number "100" indicates that SCR4 of FHR-1 is identical to SCR19 of FH; similarly, SCR3 of FHR-1*B is identical to SCR18 of FH. The total identity between FH and FHR-1 indicates that the translated FH::FHR-1 protein is the same in all the above described cases. **(C)** MLPA pattern consistent with reverse *CFHR1::CFH* hybrid genes. MLPA results in patient #9 show 3 copies of *CFH*-exon 23, normal *CFHR3* copies, two *CFHR1* copies until exon 5, one copy of *CFHR1*-exon 6, two normal copies of *CFHR4, CFHR2* and *CFHR5*, consistent with the reverse $CFHR1_{1-5}$::CFH_{23} hybrid gene. In patient #10, #11 and #12 MLPA analysis shows a gain starting from *CFH*-exon 22 until *CFHR1*-intron 3 and a loss of *CFHR1*-exon 5-6 consistent with a reverse $CFHR1_{1-4}$::CFH_{22-23} hybrid gene. In addition, patient #10 carries 3 copies of *CFHR3* and 2 copies of normal *CFHR1*. In patient #11 MLPA provides a copy of normal *CFHR1* and 2 copies of *CFHR3*, consistent with the presence of $CFHR1_{1-4}$-CFH_{22-23} on one allele and *CFHR3-CFHR1 del* on the other allele (see Supplementary Figure 1). Unlike patient #11, the abnormal MLPA pattern of patient #12 does not involve the probe located downstream of *CFH*. **(D)** Representation of reverse FHR-1::FH hybrid proteins resulting from SVs identified in patients #7, #8, #9, #10, #11 and #12. The translated fusion protein is the same in all cases due to the 100% of identity between SCR19-FH and SCR4-FHR-1.

CFHR1. CNV analysis of his relatives found the $CFH_{1\text{-}21}$::$CFHR1_{5\text{-}6}$ hybrid gene in the patient and in his healthy brother – with the latter lacking the extra copy of *CFHR3* and *CFHR1*– and a normal copy number in his healthy mother. Biological samples from the father were not available. Nonetheless, these results suggest that the patient inherited the hybrid $CFH_{1\text{-}21}$::$CFHR1_{5\text{-}6}$ gene from his father and evidenced the presence of a *de novo CFHR3-CFHR1* duplication (Figure 3). In patients #2, #3 and #4, the breakpoints of the $CFH_{1\text{-}21}$::$CFHR1_{5\text{-}6}$ hybrid gene were located to different genomic positions within intron 21 (#2, #3 chr1: 196712875-196797547; #4 chr1: 196712997-196797845).

Patient #4 is a familial aHUS case with an affected first cousin (III-4; Supplementary Figure 1). MLPA studies revealed the $CFH_{1\text{-}21}$::$CFHR1_{5\text{-}6}$ hybrid gene in both patients and in three unaffected family members (26).

In patient #5 we identified the same $CFH_{1\text{-}22}$::$CFHR1_{6}$ genomic rearrangement described by Maga et al., which encodes the same fusion protein as the $CFH_{1\text{-}21}$::$CFHR1_{5\text{-}6}$ hybrid gene ($FH_{1\text{-}19}$::FHR-1_5 and $FH_{1\text{-}18}$::FHR-$1_{4\text{-}5}$ respectively, Figure 2B) (30).

As shown in Figure 4, in patient #6, a large deletion extending from intron 20 of *CFH* to intron 3 of *CFHR1* was identified by MLPA and long PCR followed by Sanger sequencing (Figures 4A, B), indicating a novel $CFH_{1\text{-}20}$::$CFHR1_{4\text{-}6}$ hybrid gene, which resulted in a $FH_{1\text{-}17}$::FHR-$1_{3\text{-}5}$ protein (Figure 4C). Since SCR3 and SCR4 of FHR-1 are identical to SCR18 and SCR19 of FH, the $FH_{1\text{-}17}$::FHR-$1_{3\text{-}5}$ protein is indistinguishable from $FH_{1\text{-}19}$::FHR-1_5 and $FH_{1\text{-}18}$::FHR-$1_{4\text{-}5}$ (Figure 2B). The genomic breakpoints were mapped between chr1: 196712504 (intron 20 of *CFH*) and chr1: 196797138 (intron 3 of *CFHR1*). The identification of the $CFH_{1\text{-}20}$::$CFHR1_{4\text{-}6}$ hybrid gene, confirmed also by SMRT sequencing (Figure 4D), did not fully clarify the abnormal *CFHR1* MLPA pattern, characterized by the presence of 2 copies of intron 1, exon 2 and intron 3 and 3 copies of exons 5-6 of *CFHR1*. Together, these data indicated the presence of an extra copy of *CFHR1*.

Results of WB analysis of patients' plasma/serum are shown in Supplementary Figure 2A.

Reverse *CFHR1::CFH* genes: In patients #7, #8 and #9, the exon 6 of *CFHR1* was replaced by the exon 23 of *CFH*, generating a reverse $CFHR1_{1\text{-}5}$::CFH_{23} hybrid gene, in addition to the normal *CFHR1* (Figure 2C). As we showed in a previously published study, we also observed an extra copy of *CFHR3* in patient #8 (27). Both the $CFHR1_{1\text{-}5}$::CFH_{23} hybrid and the extra *CFHR3* genes were transmitted to his progeny: his daughter developed aHUS, while his son was an unaffected carrier (Supplementary Figure 1). We previously showed that both these abnormalities were the result of a genomic duplication (27).

Patients #7 and #9 showed 3 copies of *CFH*-exon 23 and *CFH*-downstream probes and one copy of the *CFHR1*-exon 6 probe, consistent with the reverse $CFHR1_{1\text{-}5}$::CFH_{23} hybrid gene, but they had a normal *CFHR3* and *CFHR1* copy number. The presence in both patients of the heterozygous rs7542235 snp that tags the *CFHR1–CFHR3* deletion suggests the presence of the reverse $CFHR1_{1\text{-}5}$::CFH_{23} hybrid gene, with a normal *CFHR1* copy and the extra *CFHR3* copy on one allele and the common *CFHR3-CFHR1*del on the other allele (31).

In patients #10, #11 and #12, exons 5 and 6 of *CFHR1* were replaced by exons 22 and 23 of *CFH* (Reverse $CFHR1_{1\text{-}4}$::$CFH_{22\text{-}23}$ hybrid gene; Figure 2C). Similar to patient #8, in patient #10 we also identified a third copy of *CFHR3* and 2 copies of *CFHR1*, as a result of a large genomic duplication.

The MLPA pattern of patient #11 was consistent with the extra reverse $CFHR1_{1\text{-}4}$::$CFH_{22\text{-}23}$ hybrid gene, two copies of *CFHR3* and one copy of *CFHR1* (Figure 2C). The pedigree study showed that the proband inherited the reverse $CFHR1_{1\text{-}4}$::$CFH_{22\text{-}23}$ hybrid gene from his mother and the common *CFHR3-CFHR1*del from his father (Supplementary Figure 1), indicating that the allele with the reverse hybrid carries a large genomic duplication, involving *CFHR3*, as reported in patient #10.

A similar but not identical MLPA pattern (not involving the probe located downstream of *CFH*; Figure 2C) was observed in patient #12. In both patients #11 and #12, Sanger sequencing

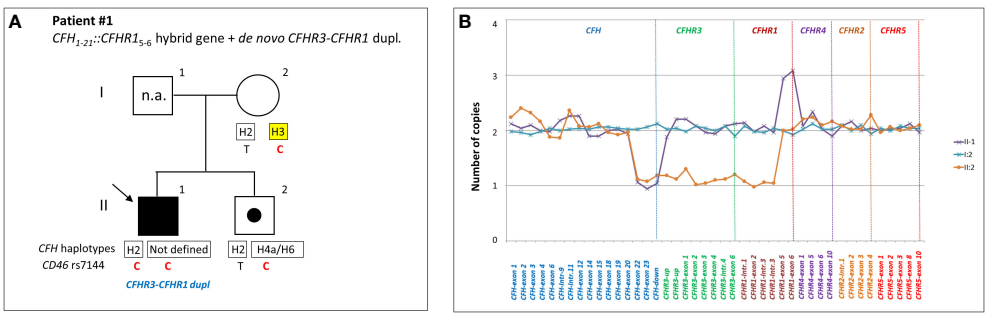

FIGURE 3
Patient #1 with a hybrid $CFH_{1\text{-}21}$::$CFHR1_{5\text{-}6}$ gene and a *de novo CFHR3-CFHR1* duplication. **(A)** The proband (black arrow) is patient II:1, his father is I:1 (samples are not available, n.a.), his mother is I:2 and his brother (unaffected carrier of hybrid $CFH_{1\text{-}21}$::$CFHR1_{5\text{-}6}$ gene) is II:2. Genotype of *CFH* single nucleotide polymorphisms (snps) targeting the *CFH-H3* risk (TGTGT) haplotype (c.1−331C>T, rs3753394; c.184G>A, p.V62I, rs800292; c.1204T>C, p.Y402H, rs1061170; c.2016A>G, p.Q672Q, rs3753396; c.2808G>T, p.E936D, rs1065489) and the *CD46* snp (rs7144, c.*897 T>C) targeting the $CD46_{GGAAC}$ risk haplotype are reported with a yellow square and in red, respectively. **(B)** MLPA analysis over the *CFH-CFHR* region in proband's relatives shows three different patterns. Patient (II:1) exhibits one copy of *CFH* exons 22 and 23 and 3 copies of *CFHR1* exons 5 and 6. His brother (II:2) exhibits a large heterozygous deletion from *CFH* exon 22 to *CFHR1* intron 3, consistent with the presence of hybrid $CFH_{1\text{-}21}$-$CFHR1_{5\text{-}6}$ gene. The mother (I:2) has a normal copy number. These results suggest that the patient and his brother inherited the hybrid $CFH_{1\text{-}21}$::$CFHR1_{5\text{-}6}$ gene from their father and evidenced the presence of a *de novo CFHR3-CFHR1* duplication only in the patient.

FIGURE 4
Identification of *CFH*$_{1-20}$::*CFHR1*$_{4-6}$ hybrid gene in patient #6. **(A)** The abnormal MLPA pattern found in patient #6 involves *CFH*, *CFHR3* and *CFHR1* genes. It results in: 1) loss of one copy of exons 22-23 of *CFH; 2)* loss of 1 copy of the entire *CFHR3* gene; 3) 2 copies of intron 1-2 and 3 of *CFHR1;* 4) 3 copies of exon 5 and 6 of *CFHR1.* **(B)** Electropherogram including the sequence of the genomic breakpoint. Arrows indicate the nucleotide differences between *CFH* and *CFHR1.* The first part of the sequence corresponded to *CFH;* the red asterisk indicates the genomic position where the intron 4 *CFHR1* sequence started. Four nucleotide differences were found in exon 4 *CFHR1:* c.469, c.475, c.523 (indicated in brown) and c.588 (not reported). Three of them led to three FHR-1 amino acid changes (p.Tyr157-Val159-Gln175, respectively) and are characteristic of the basic isoform of *CFHR1 (CFHR1*B).* The green bar highlights the target sequence of the "*CFHR1*-intron 3" probe, located in intron 3 of *CFHR1* (194 nucleotides before exon 4), upstream of the breakpoint region, explaining the 2 copies identified by this probe. **(C)** Representation of ~84 kb deletion involving *CFH*, *CFHR3* and *CFHR1*, resulting in the generation of *CFH*$_{1-20}$::*CFHR1*$_{4-6}$ hybrid gene that encodes the FH$_{1-17}$::FHR1$_{3-5}$ fusion protein. **(D)** Screenshot from IGV (Integrative Genomics Viewer) showing reads from SMRT sequencing. SMRT sequencing identified both *CFH*$_{1-20}$::*CFHR1*$_{4-6}$ hybrid gene and the *CFHR1* duplication. Misaligned reads in the *CFHR1-CFHR4* intragenic region and the *CFHR2* are also shown.

placed the genomic breakpoints between intron 4 of *CFHR1* and intron 21 of *CFH*, confirming a reverse *CFHR1-CFH* gene, but the genomic locations were different (#11: chr1: 196799104-196714588; #12: chr1: 196797930-196713442). Patient #12 did not carry the rs7542235 snp linked to the *CFHR3-CFHR1* deletion, which does not indicate the presence of a deletion on the other allele, unlike patient #11. Altogether these data show that the reverse hybrid in patients #11 and #12 could derive from different genomic rearrangements. A schematic representation of the reverse FHR-1:: FH proteins is shown in Figure 2D. Results of WB analysis of patients' plasma/serum are shown in Supplementary Figure 2B.

New genomic rearrangements: We identified a 98 kb tandem duplication in *CFH* extending from exon 1 to exon 18 (chr1: 196611131-196708834) in a single case affected by a primary form of aHUS (#13; Figures 5A, B). The duplication was inherited from the unaffected father (II-2) and was also found in his healthy brother (III-5) and in an unaffected paternal uncle (II-1; Figure 5C). Their family history shows that a paternal cousin (III-2; son of II-1) had recurrent aHUS and died at 10 years of age. FH levels in the proband and in the available relatives were normal (≥193 mg/L) although the proband had lower FH levels (210 mg/L) than his relatives (Figure 5C). WB using a monoclonal anti-human FH antibody and samples from all carriers of the *CFH*$_{1-18}$ duplication showed: 1) the band of normal FH protein, around 155 kDa; 2) a shorter than normal band with a MW around 100 kDa (Figure 5D). These results indicate that the *CFH*$_{1-18}$ duplication produces a short FH, likely composed by the first fifteen SCRs of FH (FH$_{1-15}$) (Figure 5E).

An additional new SV was observed in patient #14, characterized by 3 copies of *CFH* intron 21-exons 22-23 and *CFHR3* exons 1-2-3, with the concomitant presence of 2 copies of *CFHR1*, one of them lacking exons 4-5-6 (Figure 6A). PCR, using a forward primer located in intron 2 of *CFHR1* and a reverse primer located in intron 21 of *CFH*, and Sanger sequencing revealed the presence of a *CFHR1*$_{1-3}$::*CFH*$_{21-23}$ hybrid gene, likely resulting in a reverse FHR-1$_{1-2}$::FH$_{18-20}$ (Figures 6B, C). Western Blot analysis using an anti-FHR-1-2-5

10.3389/fimmu.2022.1011580

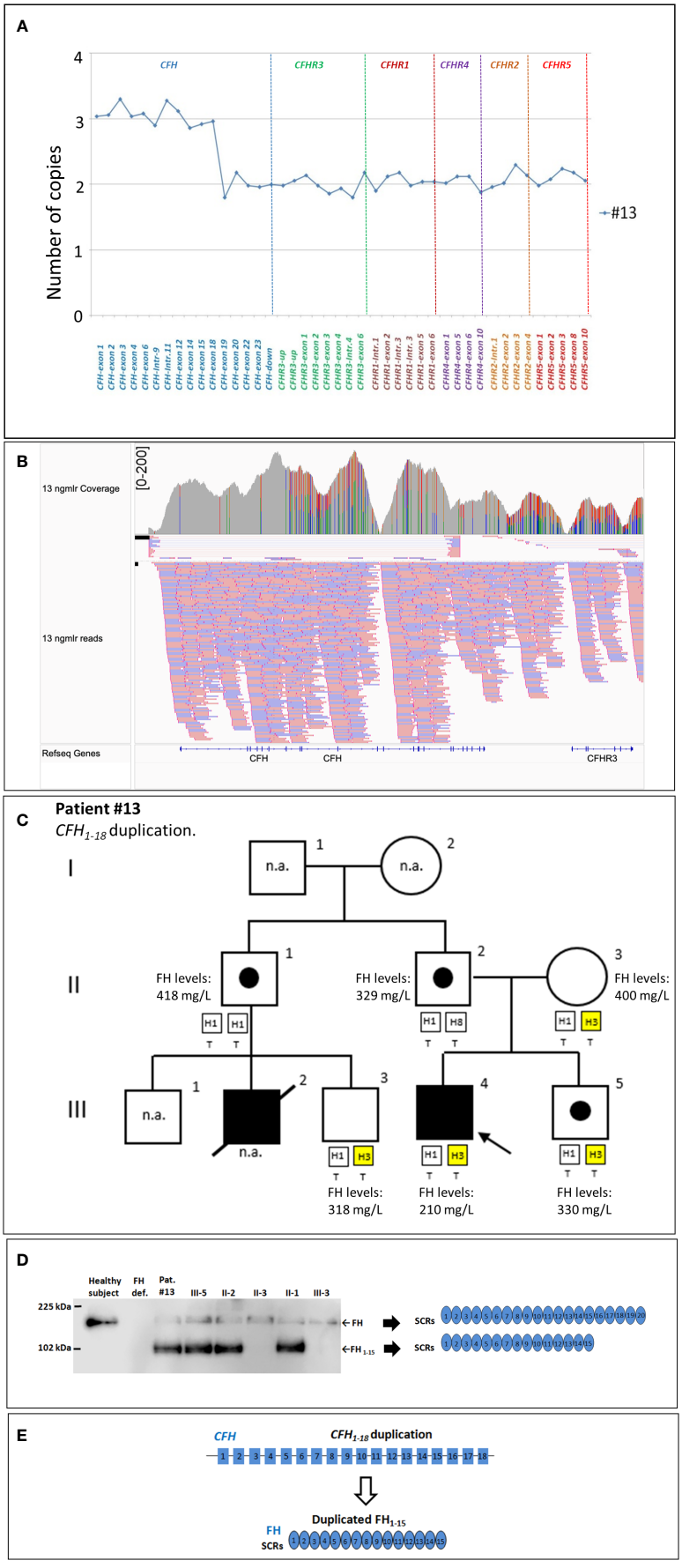

FIGURE 5 (Continued)

FIGURE 5 (Continued)
The $CFH_{1\text{-}18}$ duplication identified in patient #13. **(A)** MLPA pattern showing 3 copies of *CFH* until exon 18 and 2 normal copies in the remaining *CFH*, *CFHR* exons. **(B)** Screenshot from IGV (Integrative Genomics Viewer) showing reads from SMRT sequencing of patient #13, carrying a tandem $CFH_{1\text{-}18}$ duplication. Reads originating from across the breakpoint were mapped as chimeric alignments (split-reads) with the second part of the read mapped upstream of the first part (and vice versa for the reverse reads). **(C)** Pedigree of patient #13 and FH levels: the $CFH_{1\text{-}18}$ was inherited from the unaffected father and was also found in both his healthy brother (III-5) and in unaffected paternal uncle (II-1). FH levels resulted in the normal range in all tested samples (n.r.: ≥193 mg/L) although in the proband's sample were lower (210 mg/L) than in the other relatives. **(D)** Western Blot (WB) to detect FH was performed using a monoclonal anti-human FH antibody (OX-23, LSBio), under non-reducing conditions, using sample from the proband (III-4), his available relatives, a patient with FH deficiency (negative control) and a healthy control with normal FH (positive control). The presence of a band with a MW (around 100 kDa) lower than normal FH in all carriers of the $CFH_{1\text{-}18}$ duplication indicates that a short FH, likely missing the C-terminal domains [$FH_{1\text{-}15}$; **(E)**], is secreted. n.a., not available.

antibody did not discriminate between the wt FHR1 and the reverse hybrid FHR-$1_{1\text{-}2}$::$FH_{18\text{-}20}$ (same molecular weight, Figure 6D). Analysis using an anti-FHR-3 antiserum revealed in the serum from patient #14: 1) three bands corresponding to normal glycosylated isoforms of FHR-3 (Figure 6E and Supplementary Figure 2C); 2) a single band at lower MW (around 15 kDa; Figure 6E) compatible with a shorter FHR-$3_{1\text{-}2}$ protein.

Primary aHUS group B

***$CFHR3_{1\text{-}5}$::$CFHR4_{10}$* hybrid gene and *CFHR1- CFHR4* duplication:** This group was characterized by uncommon genomic rearrangements involving only *CFHR* genes (Table 2).

In five patients (#15, #16, #17, #18, and #19) we identified the $CFHR3_{1\text{-}5}$::$CFHR4_{10}$ hybrid gene that we previously described in C3G (17). Among these, case #16 also carried the polymorphic *CFHR3-CFHR1*del, leading to the lack of *CFHR1*.

In this group the only available pedigree was that of patient #15. MLPA studies revealed the presence of the $CFHR3_{1\text{-}5}$::$CFHR4_{10}$ hybrid gene in his healthy mother, too (Supplementary Figure 1). Results of WB analysis of patients' plasma/serum are shown in Supplementary Figure 2D.

Finally, four copies of both the *CFHR1* and *CFHR4* genes were observed in patient #20, a previously described case of aHUS concomitant to primary hyperoxaluria due to *GRPHR* gene abnormalities (Supplementary Figure 1) (28).

Genetic and serum abnormalities in primary aHUS

To better characterize patients with uncommon SVs, we also evaluated the presence of LPVs in complement genes and or/anti-FH antibodies (anti-FHs).

We observed that group B had a higher prevalence of concomitant complement abnormalities (4/6) compared to group A (2/14) even though the difference was not statistically significant (p-value= 0.04).

In detail, only two patients out of 14 (14%; patients #3 and #4) of group A, both carrying the $CFH_{1\text{-}21}$::$CFHR1_{5\text{-}6}$ hybrid gene, had additional complement abnormalities (*CFH* p. R1210C and *CFI* c.1429+1G>C LPVs, respectively).

In group B, three of six patients (50%; patients #15, #16 and #18), all carrying the $CFHR3_{1\text{-}5}$::$CFHR4_{10}$ hybrid gene, also had concomitant LPVs (#15: *C3* p.D1115H and #18: *CD46* c.286+2T>G, respectively) or anti-FHs (patient #16, with the $CFHR3_{1\text{-}5}$::$CFHR4_{10}$ hybrid gene on one allele and the *CFHR3-CFHR1*del on the other allele) (Table 2).

To evaluate whether the presence of SVs impaired circulating factor H (FH) levels we tested serum/plasma FH concentrations in all patients carrying uncommon SVs, for whom samples were available. Only patient #10, with the reverse $CFHR1_{1\text{-}4}$::$CFH_{22\text{-}23}$ hybrid gene (group A), had FH levels that were slightly lower than normal (182 mg/L; n.v.≥ 193 mg/L), indicating that *CFH-CFHR* SVs did not substantially impact FH levels (Table 2).

Finally, to evaluate whether in our cohort of primary aHUS patients, the complete *CFHR1* deficiency was associated with the presence of anti-FHs, patients carrying the homozygous *CFHR3-CFHR1*del or the combined *CFHR3-CFHR1*del and *CFHR1-CFHR4*del were tested for anti-FHs, when samples were available. We found that 26 out of 39 tested patients had anti-FHs (67%), consistently with the already known correlation between *CFHR1* deficiency and development of anti-FHs in patients with aHUS (3, 18).

Incomplete penetrance of rare structural variants

Among the nine studied pedigrees, we found 17 asymptomatic relatives carrying rearrangements in *CFH* or *CFHR* genes, indicating that SVs are associated with an incomplete penetrance of the phenotype aHUS (11 affected/28 carriers; 39%).

As reported above, in patients #3, #4, #15, #16 and #18 we identified additional complement abnormalities. Samples from relatives were available for patients #4 and #15 only. In the pedigree of patient #4, the *CFI* LPV (c.1429+1G>C) was found in the proband (IV-3), but also in her healthy mother (III-1) and in the younger sister (IV-4), who do not carry the $CFH_{1\text{-}21}$::$CFHR1_{5\text{-}6}$ hybrid gene (Supplementary Figure 1). These results suggested that the concomitant presence of SVs and LPVs synergized in determining disease development in the proband. Accordingly, her father (III-2) and the older sister (IV-2) carried only the $CFH_{1\text{-}21}$::$CFHR1_{5\text{-}6}$ hybrid gene and did not have aHUS. However, the $CFH_{1\text{-}21}$::$CFHR1_{5\text{-}6}$ hybrid gene but not the *CFI* LPV (c.1429+1G>C), were also found in a healthy grand-uncle of the proband (II-3) and his daughter (III-4), who developed ESRD after an episode of aHUS. These findings indicate that in this arm of the pedigree, other risk factors synergized with the $CFH_{1\text{-}21}$::$CFHR1_{5\text{-}6}$ hybrid to the final phenotype. As shown in Supplementary Figure 1, the affected subject in this arm (III-4) is homozygous for the $CD46_{GGAAC}$ risk haplotypes, whereas her unaffected father is heterozygous.

10.3389/fimmu.2022.1011580

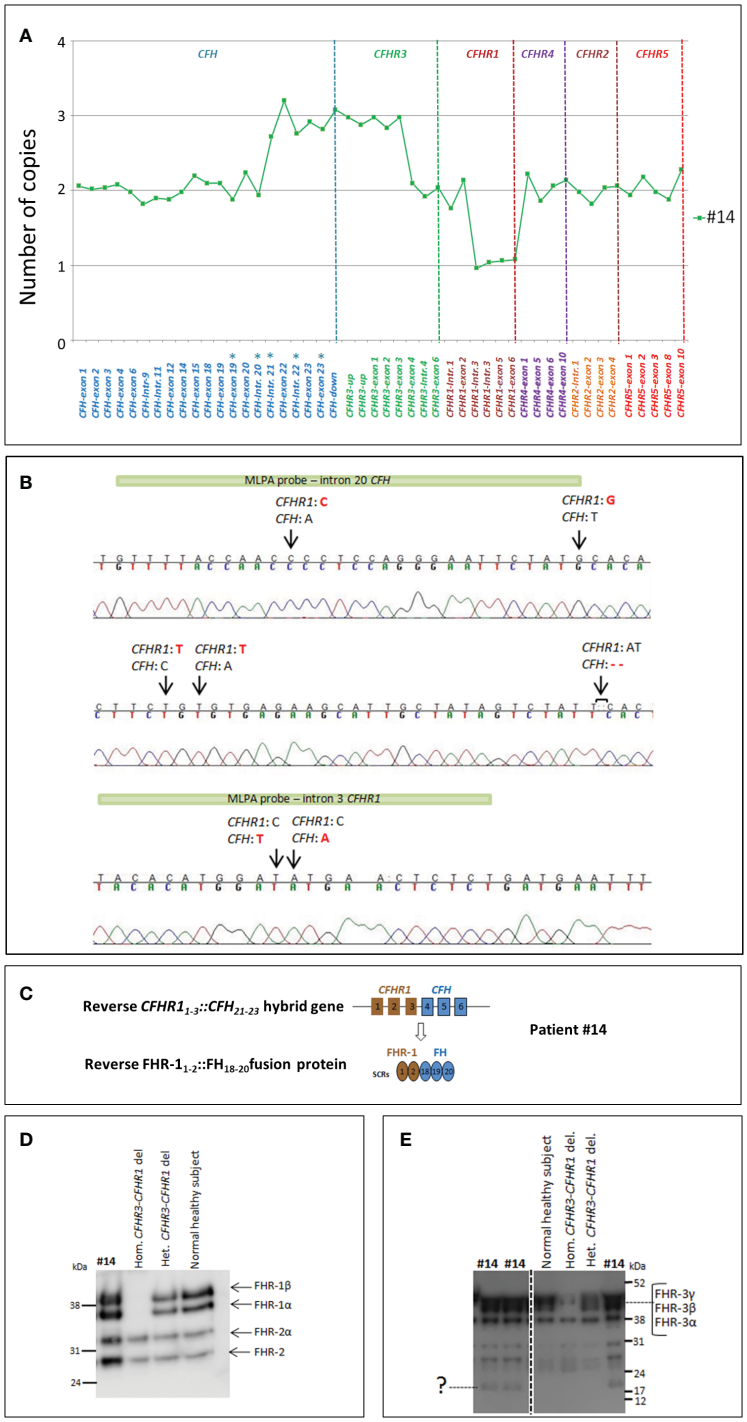

FIGURE 6
Identification of the reverse *CFHR1*$_{1-3}$::*CFH*$_{21-23}$ hybrid gene in patient #14. **(A)** The results of MLPA show in patient #14 three copies of both *CFH* exons 21-22-23 and *CFHR3* exons 1-2-3, 2 copies of *CFHR1*, one of them lacking exons 4-5-6. These data suggest the presence of a reverse *CFHR1*$_{1-3}$::*CFH*$_{21-23}$ hybrid with a partial duplication of *CFHR3*$_{1-3}$. The analysis has been performed with the SALSA MLPA P236-*CFH*-region Kit (MRC Holland) implemented with homemade probes (indicated by asterisks) analyzed in a separate assay and covering the last exons and introns of the *CFH* gene (27). **(B)** Sequence of the genomic breakpoint of the *CFHR1*$_{1-3}$::*CFH*$_{21-23}$ hybrid gene, mapped between chr1:196796490 (intron 3 of *CFHR1*) and chr1:196711901 (intron 20 of *CFH*). Arrows indicate the nucleotide differences between *CFH* and *CFHR1*. The green bars highlight the target sequence of "*CFH*-intron 20" probe (located 747 nucleotides before exon 21) and the "*CFHR1*-intron 3" probe (located 396 nucleotides after exon 3). **(C)** Representation of reverse *CFHR1*$_{1-3}$::*CFH*$_{21-23}$ and the corresponding FHR-1$_{1-2}$::FH$_{18-19-20}$ fusion protein. **(D, E)** To investigate the effect of *CFHR3*$_{1-3}$ duplication at protein level, we performed a WB analysis, under non-reducing conditions, using both an anti-FHR-1-2-5 monoclonal antibody and a FHR-3 polyclonal antiserum. FHR-1 staining showed FHR-1 bands at the same MW of the normal healthy control **(D)**. Staining of FHR-3 showed both the bands corresponding to the three normal glycosylated isoforms of FHR-3 and a faint band at low MW consistent with a short FHR-3$_{1-2}$ **(E)**.

10.3389/fimmu.2022.1011580

Incomplete penetrance was also observed in the pedigree of patient #15 carrying the *CFHR3*$_{1-5}$*::CFHR4*$_{10}$ hybrid gene, the *C3* LPV (p.D1115H), and the *CFH-H3* risk haplotype, all inherited from the unaffected mother (Supplemantary Figure 1).

Clinical data of patients with primary aHUS carrying rare SVs

In group A, infectious triggers were reported in all patients with available data (7/7) and the median age at disease onset was 6.5 years (IQR, 1-25.75). Two out of 14 patients were treated with eculizumab: one of them (patient #9) underwent full remission with complete recovery of renal function, the other (patient #7) had an aHUS relapse in the kidney graft. Eculizumab treatment enabled stable normalization of hematological parameters and partial recovery of graft function, but thereafter the patient lost the graft due to chronic rejection. In contrast, 11 out of 12 patients in this group who did not receive eculizumab (either because disease onset antedated anti-complement therapy or the drug was not available) did not recover from the acute episode and developed end-stage renal disease (ESRD; Table 3).

Atypical HUS relapses occurred in 6/7 grafts without eculizumab prophylaxis and in 0/3 grafts with eculizumab prophylaxis.

In group B, infectious triggers were associated with aHUS onset in 5/5 cases with available data, and the median age of disease onset was 2 years (IQR, 1.5-7.5).

Disease was less severe in group B than in group A. Indeed, 4 out of 5 patients in this group achieved complete remission without eculizumab treatment (p=0.0099, vs group A no eculizumab). No clinical data are available for patient #19.

One group B patient (patient #15) lost two kidney grafts for aHUS recurrence; he did not receive eculizumab (Table 3).

Rare structural variants and clinical data of patients with secondary aHUS

Two cases of secondary aHUS, associated with malignant and severe hypertension, respectively, had uncommon **SV** (#21; #22; Table 2). One of them carried the hybrid *CFHR3*$_{1-5}$*::CFHR4*$_{10}$ gene, previously described in a patient with DDD (17) while the other patient had an internal duplication in *CFH*, extending from part of exon 2 to exon 9 (Figure 7A). Direct sequencing of a long-PCR product and SMRT sequencing allowed us to map the duplication within *CFH* (chr1:196642182-196661791; Figures 7B, C) with partial intron 9 sequence followed by part of exon 2 sequence. *In silico* analysis (Genscan) predicted that the *CFH*$_{2-9}$ duplication may generate a longer *CFH* gene, characterized by the first nine exons of *CFH*, followed by exon 3 of *CFH* (Figure 7D).

In both patients no LPVs in complement genes were identified (Table 2).

The outcome of the patient with the hybrid *CFHR3*$_{1-5}$*::CFHR4*$_{10}$ gene (#21) was unfavorable as she developed ESRD (no eculizumab treatment; Table 3). The patient carrying the internal duplication of *CFH* was treated with eculizumab, which partially improved renal function and hematological parameters at one month after disease onset (Table 3).

Discussion

In the present study, through a retrospective analysis of a large cohort of patients affected by either primary or secondary forms of aHUS, we documented that: I) the prevalence of the homozygous *CFHR3-CFHR1*del is higher in primary aHUS than in secondary aHUS; II) uncommon SVs in *CFH* and *CFHR* genes are more frequent in primary aHUS than in secondary forms; III) the disease penetrance of aHUS in carriers of rare *CFH-CFHR* SVs is incomplete; IV) these genomic abnormalities occur often in combination with other complement abnormalities; V) the prognosis for rare SV carriers is strongly related to the specific abnormality.

Among common SVs, we observed an enrichment of the homozygous *CFHR3-CFHR1*del in primary aHUS and confirmed previous data in the literature about the association between this common SV and the development of anti-FH autoantibodies, an acquired driver reported in 10% of aHUS patients (3, 18). In contrast, the finding that in secondary aHUS patients the prevalence of the homozygous *CFHR3-CFHR1*del was comparable to controls does not support the hypothesis that this deletion plays a role in secondary aHUS. Similarly, we identified rare SVs, including duplications or hybrid genes, in a substantial fraction (8%) of patients with aHUS, but we rarely did so in secondary forms (2%).

Consistent with earlier data in literature, in our cohort uncommon SVs most frequently involved *CFH* and *CFHR1* leading to the formation of *CFH::CFHR1* hybrid genes or reverse *CFHR1::CFH* hybrid genes (16, 27, 29, 30, 32).

Specifically, we identified the *CFH*$_{1-21}$*::CFHR1*$_{5-6}$ and the *CFH*$_{1-22}$*::CFHR1*$_{6}$ SVs in 2% of patients with primary aHUS. Even though they formed through different rearrangements, as documented by the identification of different DNA breakpoints, hybrid *CFH::CFHR1* genes caused the loss of one copy of *CFHR3* and encoded for the same FH::FHR-1 fusion protein characterized by a FH protein in which SCR19 and 20 were substituted by the FHR-1 specific SCR4-SCR5 C-terminal residues (29, 30). Notably, the FH SCR19 is identical to FHR-1 SCR4, while FH SCR20 differs from FHR-1 SCR5 only at 2 amino acids: FH Ser1191 (which corresponds to Leu290 in FHR-1) and FH Val1197 (corresponding to Ala296 in FHR-1). Thus, the FH-FHR-1 fusion proteins encoded by the *CFH*$_{1-21}$*::CFHR1*$_{5-6}$ and the *CFH*$_{1-22}$*::CFHR1*$_{6}$ hybrids share the FHR-1-specific C-terminus with the Leu1191 and Ala1197 changes. As reported in published studies, the FH with 1191Leu and 1197Ala residues can also derive from a gene conversion event that is the result of the unidirectional transfer of *CFHR1* exon 6 into the *CFH* gene (33, 34). Functional studies have shown that these FH mutants have a normal regulatory activity in the fluid phase but have a limited capacity to protect cells from complement activation (33). This is also consistent with recent findings showing that the two amino acid differences that differentiate the C-terminus of FH from that of FHR-1 are responsible for distinctive interactions with C3 and sialic acid glycans (35, 36). Indeed, while the C-terminus of FH binds to proteoglycans and C3b, thus driving the recruitment of FH to cell

TABLE 3 Demographic and clinical findings of aHUS patients carrying uncommon *CFH-CFHR* SVs.

Pat.	Sex	Age	Trigger	Outcome	Therapy	Eculizumab (Yes/no)	Relapses (Yes/No)	N° of Tx	Eculizumab prophylaxis Tx1	Relapses Tx1	Eculizumab treatment Tx1	Outcome of Tx1	Eculizumab prophylaxis Tx2	Relapses Tx2	Eculizumab treatment Tx2	Outcome of Tx2
Pat.	**Sex**	**Age**	**Trigger**	**Outcome**	**Therapy**	**Eculizumab (Yes/no)**	**Relapses (Yes/ No)**	**N° of Tx**	**Eculizumab prophylaxis Tx1**	**Relapses Tx1**	**Eculizumab treatment Tx1**	**Outcome of Tx1**	**Eculizumab prophylaxis Tx2**	**Relapses Tx2**	**Eculizumab treatment Tx2**	**Outcome of Tx2**
Primary aHUS - Group A																
#1	M	1	Upper resp tract infection	ESRD	Antihypertensive, steroids, BT, PI	No	Yes	0	-	-	-	-	-	-	-	-
#2	F	1	na	ESRD	Antihypertensive	No	na	1	No	Yes	No	ESRD	-	-	-	-
#3	M	1	Viral infection	ESRD	BT, Igs, PI, PEX	No	Yes	0	-	-	-	-	-	-	-	-
#4	F	0.5	Upper resp tract infection	Recovery renal fx	PI, BT, PEX	No	No	0	-	-	-	-	-	-	-	-
#5	F	0.4	gastroenteritis	ESRD	BT	No	na	2	No	Yes	No	ESRD	Yes	No	No	Normal renal fx
#6	F	21	Na	ESRD	na	No	na	1	No	Yes	No	ESRD	-	-	-	-
#7	M	3	gastroenteritis	ESRD	na	No	na	1	No	Yes	Yes	ESRD [a]	-	-	-	-
#8	M	49	Upper resp tract infection	ESRD	BT, PI, PEX	No	na	1	Yes	No	na	Normal renal fx	-	-	-	-
#9	M	25	na	Recovery renal fx	BT, PEX	Yes	No	0	-	-	-	-	-	-	-	-
#10	F	1	na	ESRD	Antihypertensive, PEX	No	na	1	No	No	na	ESRD	-	-	-	-
#11	M	48	na	ESRD	PEX, hemodialysis	Yes [b]	No	0	-	-	-	-	-	-	-	-
#12	F	26	na	ESRD	BT, PI, PEX	No	No	2	No	na	No	ESRD	No	Yes	No	ESRD
#13	M	10	flu-like	ESRD	PI	No	na	1	Yes	No	na	Normal renal fx	-	-	-	-
#14	M	2	na	ESRD	na	No	na	na	-	-	-	-	-	-	-	-
Primary aHUS - Group B																
#15	M	1	Upper resp tract infection	ESRD	PEX	No	Yes	2	No	Yes	No	ESRD	No	Yes	No	ESRD
#16	F	11	gastroenteritis	Recovery renal fx	BT, PI, PEX	No	na	0	-	-	-	-	-	-	-	-
#17	M	2	Upper resp tract infection	Recovery renal fx	BT, PI, PEX	No	No	0	-	-	-	-	-	-	-	-
#18	F	2	Upper resp tract infection	Recovery renal fx	BT, PI, PEX	No	Yes	0	-	-	-	-	-	-	-	-
#19	F	4	na	Na	na	No	na	0	-	-	-	-	-	-	-	-
#20	M	0.5	gastroenteritis	Recovery renal fx	BT, PI	No	No	0	-	-	-	-	-	-	-	-
Secondary aHUS																
#21	F	48	Malignant hypertension	ESRD	Antihypertensive	No	na	0	-	-	-	-	-	-	-	-
#22	F	22	Severe hypertension	Partial recovery renal fx	BT, PI	Yes	No	0	-	-	-	-	-	-	-	-

PI, plasma infusion; BT, blood transfusion; PEX, plasma exchange; Igs, immunoglobulins; ESRD, end-stage renal disease; fx, function; tx, transplant;. [a] ESRD 8 days after transplant for chronic rejection; [b]After 21 PEX; na, not available.

10.3389/fimmu.2022.1011580

10.3389/fimmu.2022.1011580

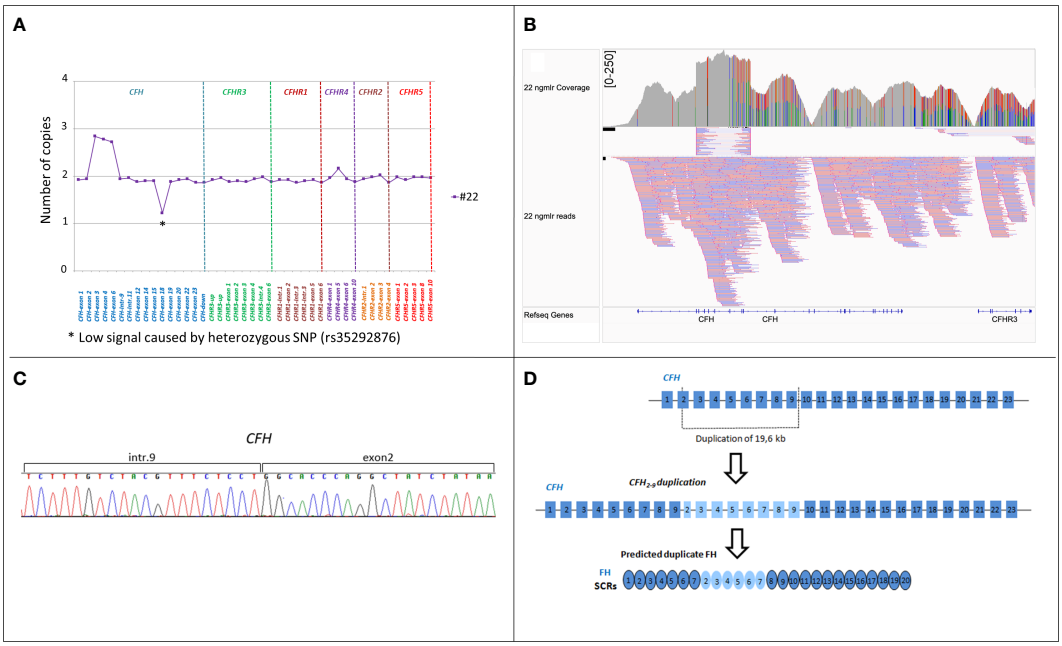

FIGURE 7
Identification of $CFH_{2\text{-}9}$ duplication in patient #22. **(A)** MLPA pattern in patient #22 shows a high signal on the exon 3, exon 4 and exon 6-*CFH* probes consistent with a heterozygous duplication. **(B)** Screenshot from IGV (Integrative Genomics Viewer) showing reads from SMRT sequencing. SMRT sequencing identified $CFH_{2\text{-}9}$ duplication. **(C)** Electropherogram of the genomic breakpoint. The first part of the sequence corresponds to intron 9 of the *CFH* and the second part is the sequence of *CFH* exon 2. **(D)** Representation of 19,6 kb internal duplication of the *CFH* and the predicted resulting FH protein consisting of 26 SCRs.

surfaces and to the cell matrix, the C-terminus of FHR-1 strongly interacts with native C3 (nC3), C3b, iC3b and C3dg, attracting nC3 to the proximity of the cell surface. The latter acquired property of FH::FHR-1 fusion proteins, along with the loss of the capacity to bind sialic acids, causes a shift from complement regulation to complement activation on cell surfaces (35).

Another *CFH* and *CFHR1* genomic rearrangement reported in association with aHUS leads to reverse *CFHR1::CFH* genes. A *de novo* $CFHR1_{1\text{-}4}$::$CFH_{22\text{-}23}$ gene was described in 2013 in a patient with sporadic aHUS, and in 2015 we reported a reverse $CFHR1_{1\text{-}5}$::CFH_{23} gene in a family with 2 affected subjects over 2 generations (27, 32). Here, we identified 5 additional patients carrying the above reverse *CFHR1::CFH* genes, which derived from different DNA breakpoints. Notably, all these genes encode the same FHR-1::FH fusion protein characterized by the FH specific C-terminus with amino acid 290Ser (which corresponds to Ser1191 in FH) and 296Val (that corresponds to Val1197 in FH) (37). The reverse FHR-1::FH hybrid, through its FHR-1 N-terminal domain forms multimers that interact with other FHR-1 and/or FHR-2 molecules, while with its FH C-terminal domain competes with FH for the binding to cell ligands, thus promoting surface restricted complement activation (16, 35). Consistently, FHR-1 isolated from heterozygous carriers of the $CFHR1_{1\text{-}5}$::CFH_{23} hybrid induced complement-dependent sheep erythrocytes hemolysis when added to normal human serum (27).

In this study, we have also identified a new reverse $CFHR1_{1\text{-}3}$::$CFH_{21\text{-}23}$ gene including a partial duplication of the first three exons of *CFHR3* likely resulting in a FHR-$1_{1\text{-}2}$-$FH_{18\text{-}20}$ protein and in a short $FHR3_{1\text{-}2}$ protein that requires further investigation. We speculate that the greater sequence similarity to FH, makes the FHR-$1_{1\text{-}2}$-$FH_{18\text{-}20}$ protein a stronger competitor of FH for its surface ligands, than the reverse FHR-$1_{1\text{-}4}$::FH_{20} and FHR-$1_{1\text{-}3}$::$FH_{19\text{-}20}$ hybrids.

Another novel finding of this study is the association of large *CFH* gene duplications with aHUS. In a 10-year boy with primary aHUS, we identified a *CFH* tandem duplication involving a large portion of the gene, including exons 1 to 18, and encoding a shorter than normal FH (likely $FH_{1\text{-}15}$) that lacks the five C-terminal SCRs. We speculate that the abnormal FH cannot properly bind and inhibit AP on cell surfaces while maintaining its inhibitory functions in fluid phase. In addition, in a 22-year-old woman with secondary aHUS associated with severe hypertension, we found an internal *CFH* duplication extending from part of exon 2 to exon 9 and located after *CFH* intron 9. We hypothesize that similarly to partial duplications described in other genes, this *CFH* duplication may either cause a reading frame shift in the mRNA, producing a truncated FH, or result in a longer than normal protein with conformational changes and dysfunctional activity (38–40). Consistently, *in silico* analysis of the $CFH_{2\text{-}9}$ duplication predicts a longer translated FH product (Figure 7D).

Notably, we observed incomplete penetrance of aHUS in carriers of *CFH-CFHRs* SVs, which is consistent with earlier studies on patients with LPVs in *CFH* and other complement genes (23, 41, 42). The identification of additional rare complement gene abnormalities in 3 probands with *CFH-CFHRs* SVs is in line with the above observation. Specifically, in a pedigree with the $CFH_{1\text{-}21}$::$CFHR1_{5\text{-}6}$ hybrid gene we found a *CFI* variant, predicted to alter splicing in the region encoding serine protease domain of Factor I, in the proband who developed aHUS in the first year of life, whereas this variant was absent in all unaffected carriers of the hybrid gene. However, the finding that in this family a carrier of the $CFH_{1\text{-}21}$::

CFHR1$_{5\text{-}6}$ alone developed aHUS, whereas there were none among the subjects with the *CFI* LPV alone, documents that the *CFH*$_{1\text{-}21}$::*CFHR1*$_{5\text{-}6}$ hybrid gene is the main driver of the disease. In a patient with the *CFH*$_{1\text{-}21}$::*CFHR1*$_{5\text{-}6}$ hybrid gene we also identified the FH R1210C LPV, which was previously reported as a predisposing factor to a range of pathologies, including aHUS, C3G and AMD. The FH-1210C mutant forms covalently linked complexes with human serum albumin that interfere with FH binding to surface-bound C3b (43, 44). Thus, due to the combination of the FH 1210C mutant from one allele and the hybrid FH with the 1191L and 1197A changes from the other allele, all FH molecules in this patient have a dysfunctional C-terminus, leading to defective regulation of complement on cellular surfaces. Finally, in a third patient carrying the *CFH*$_{1\text{-}21}$::*CFHR1*$_{5\text{-}6}$ hybrid gene, familial studies revealed that the proband also has a *de novo* duplication involving *CFHR3* and *CFHR1* genes that was not found in unaffected relatives carrying the hybrid gene.

We found additional genetic or acquired abnormalities even more frequently in the group of patients with SVs involving only *CFHR* genes, which mostly result in the formation of a *CFHR3*$_{1\text{-}5}$::*CFHR4*$_{10}$ hybrid. Indeed, 4 out of 6 patients in this group also carry either LPVs or anti-FH antibodies, which would indicate a lower pathogenic impact of *CFHR* SVs versus those involving *CFH*. The *CFHR3*$_{1\text{-}5}$::*CFHR4*$_{10}$ hybrid has already been reported in association with C3G, and it has been suggested that it binds cell surface ligands and favors C3 convertase activity, but functional studies are required to clarify its pathogenic impact (17). The finding that a proband shared the *CFHR3*$_{1\text{-}5}$::*CFHR4*$_{10}$ hybrid gene, a *C3* LPV and *CFH* H3 risk haplotype with their unaffected mother, underlines the complexity of aHUS, which may not manifest even in subjects with multiple genetic risk factors. It is likely that in such susceptible individuals, environmental factors or an underlying condition that activates complement or perturbs the endothelium are required to trigger the disease. This possibility is in line with the report here of two cases of aHUS secondary to chronic severe hypertension in patients who carried SVs affecting the *CFH* or *CFHRs* genes, respectively. It is known that microvascular endothelium can move to a pro-thrombotic phenotype during stress stimuli due to hypertension (45, 46). So in the above patients, the concomitance of hypertension-mediated endothelial stress injury and genetically-determined defective regulation of the complement system may irreversibly compromise the homeostatic equilibrium of the endothelium.

Our data also show relevant associations between the specific SV and disease phenotype, response to therapies and risk of recurrence after kidney transplant. Thus, *CFH::CFHR1* hybrid genes were commonly found in patients who manifested the disease in their first year of life, a finding consistent with previously published data (33). The FH::FHR-1 hybrids mimic the effect of LPV in the FH C-terminus that have been often associated with disease onset in infancy (2). Finding that in the majority of *CFH::CFHR1* carriers aHUS was triggered by infections, would suggest that in these patients dysfunctional FH could not adequately control the complement activation induced upon the first exposure to viruses or bacteria. As previously reported (37), the reverse *CFHR1::CFH* hybrid genes were associated with a later disease onset, mostly in adulthood. It is tempting to speculate that in these patients FH produced by the 2 normal copies of *CFH*, could partially counteract the competitive action of the reverse FHR-1::FH protein (27, 37).

Nonetheless, both patients with hybrid *CFH::CFHR1* genes and those with reverse *CFHR1::CFH* genes from our cohort who did not receive anti-complement therapy had an unfavorable prognosis, while those treated with eculizumab went into full remission.

At variance, the outcome in patients with *CFHR* hybrids was more favorable than in patients with *CFH* SVs, even when they did not receive eculizumab, confirming a lower pathogenic impact of *CFHR* SVs than *CFH* SVs.

Previous reports from the pre-eculizumab era documented a strong association between *CFH* genetic abnormalities and the risk of relapses after kidney transplant, almost invariably leading to graft loss (2). In recent studies the use of prophylactic eculizumab was independently associated with a reduced risk of recurrence and with longer graft survival (47, 48). Consistent with this, here we observed overall unfavorable outcomes in 8 out of 9 grafts without prophylactic eculizumab, while 3 grafts transplanted under eculizumab prophylaxis have maintained normal function.

In conclusion, this work highlights the association between aHUS and genomic rearrangements in the *CFH-CFHR* region and describes both known genomic alterations and new large aberrations, which are often hard to identify and solve. These structural variants have a different impact on risk of disease manifestation, age of onset, and severity. Not surprisingly, our findings further highlight the prevalent role of factor H genetic defects in the pathogenesis of aHUS but also propose that abnormalities in factor H-related proteins may play a role. Altogether, our data definitely support including a *CFH-CFHR* SV search in routine genetic analysis for patients with aHUS to improve prognosis and treatment approaches.

Data availability statement

The data presented in the study are deposited in the EBI European Nucleotide Archive, accession number: PRJEB44176.

Ethics statement

The studies involving human participants were reviewed and approved by Ethics Committee of the Azienda Sanitaria Locale, Bergamo (Italy). Written informed consent to participate in this study was provided by the participants' legal guardian/next of kin.

Author contributions

RP, EV, MA and MN designed research, interpreted data, and wrote the paper. EV, RP, MA, LL, CM, MB, and RD performed the research and analyzed the data. EB and MR provided detailed clinical information on patients. MN, AB and GR critically revised the manuscript. All authors contributed to the article and approved the submitted version.

Funding

This work was partially supported by Kidneeds Foundation (Kidneeds projects 735/8215 and 698/7603) and by UNEARTH project (project ID 1745126). We would also like to thank Associazione Nazionale Anziani Pensionati di Confartigianato Imprese Bergamo for its support. RP, EV, MB and MR are recipients of a research contract from Progetto DDD Onlus-Associazione per la lotta alla DDD (Milan, Italy). CM is recipient of a grant from Fondazione Regionale per la Ricerca Biomedica (FRRB; UNEARTH project 1745126). LL is recipient of a fellowship from Fondazione Aiuti per la Ricerca sulle Malattie Rare ARMR ONLUS (Bergamo, Italy). The funding sources had no role in study design, nor in the collection, analysis or interpretation of data, nor in the writing of the report or in the decision to submit the paper for publication.

Acknowledgments

We acknowledge Silvia Prandini, Veruska Lecchi, Diana Cadè, Sara Gamba, Elena Bresin and Erica Daina for sample and clinical data collection. Authors thank all clinicians from the other centers and patients for their membership in and support for the International Registry of HUS/TTP. The authors would like to thank Ave Tooming-Klunderud for SMRT sequencing service, which was provided by the Norwegian Sequencing Centre (www.sequencing.uio.no), a national technology platform hosted by the University of Oslo and supported by the Functional Genomics and Infrastructure programs of the Research Council of Norway and the Southeastern Regional Health Authorities, and David Stucki and Deborah Moine from PacBio for bioinformatic assistance. The authors also are grateful to Kerstin Mierke for editing the manuscript and Davide Martinetti for editing the figures.

Conflict of interest

MN has received honoraria from Alexion Pharmaceuticals for giving lectures, and for participating in advisory boards, and she has received research grants from Omeros, Gemini, Novartis and BioCryst Pharmaceuticals. AB has received honoraria from Alexion Phamaceuticals and BioCryst Pharmaceuticals. GR has consultancy agreements with AbbVie, Alexion Pharmaceuticals, Novartis Pharma and BioCryst Pharmaceuticals. Since 1st May 2022, the co-author EV has been employed by Frontiers Media SA. EV declared her affiliation with Frontiers, and the handling Editor states that the process nevertheless met the standards of a fair and objective review.

The remaining authors declare that the research was conducted in the absence of any commercial or financial relationships that could be constructed as a potential conflict of interest.

Publisher's note

Supplementary material

The Supplementary Material for this article can be found online at: https://www.frontiersin.org/articles/10.3389/fimmu.2022.1011580/full#supplementary-material

SUPPLEMENTARY FIGURE 1
Analyzed pedigrees. Each proband is indicated by a black arrow. Black squares and cicles indicate affected subject. The black dots show carriers of the SV. Genotype of *CFH* single nucleotide polymorphisms (snps) targeting the *CFH-H3* risk (TGTGT) haplotype (c.1−331C>T, rs3753394; c.184G>A, p.V62I, rs800292; c.1204T>C, p.Y402H, rs1061170; c.2016A>G, p.Q672Q, rs3753396; c.2808 G>T, p.E936D, rs1065489) and the *CD46*snp (rs7144 c.*897 T>C) targeting the $CD46_{GGAAC}$ risk haplotype are reported with a yellow square and in red, respectively.

SUPPLEMENTARY FIGURE 2
Western blot images. **(A)** Staining of FH detecting FH_{1-18}::FHR-1_{4-5} hybrid protein in patients #1 and #3 and FH_{1-17}::FHR-1_{3-5} in patient #6 that have the same MW of normal FH. Similarly, reverse FHR-1::FH hybrid proteins tested in serum from patients #7 (FHR-1_{1-4}::FH_{20}), #10, #11 (FHR-1_{1-3}::FH_{19-20}) and #14 (FHR-1_{1-2}::FH_{18-20}) share the same MW of normal FHR-1 **(B)**. **(C)** WB using a FHR-3 antiserum was performed to evaluate the protein pattern of patients also carrying *CFHR3* duplications (#1 and #10). The image shows in #1 and #10, bands of increased intensity compared to healthy subject and patient #11 (both carrying normal copies of *CFHR3*) and with the same MWs of the 3 normal glycosylated isoforms of FHR-3. WB analysis using the sample from patient #14, carrying the $CFHR3_{1-3}$ duplication was also analyzed and results show the presence of FHR-3 bands with expected MWs. A single band at lower MW (around 15kDa) compatible with a shorter FHR-3_{1-2} protein was observed in the WB reported in . **(D)** WB images showing the 3 bands of FHR-3 in patients #15, #16 and #17 (all carrying the $CFHR3_{1-5}$-$CFHR4_{10}$) indicating that the FHR3_{1-4}-FHR4_9 hybrid protein is secreted and has the same MW of normal FHR-3 since patient #16 carries the *CFHR3-CFHR1* deletion on the other allele.

References

1. Noris M, Remuzzi G. Hemolytic uremic syndrome. *J Am Soc Nephrol* (2005) 16 (4):1035–50. doi: 10.1681/ASN.2004100861

2. Noris M, Caprioli J, Bresin E, Mossali C, Pianetti G, Gamba S, et al. Relative role of genetic complement abnormalities in sporadic and familial aHUS and their impact on clinical phenotype. *Clin J Am Soc Nephrol* (2010) 5(10):1844–59. doi: 10.2215/CJN.02210310

3. Valoti E, Alberti M, Iatropoulos P, Piras R, Mele C, Breno M, et al. Rare functional variants in complement genes and anti-FH autoantibodies-associated aHUS. *Front Immunol* (2019) 10:853. doi: 10.3389/fimmu.2019.00853

4. Goodship TH, Cook HT, Fakhouri F, Fervenza FC, Fremeaux-Bacchi V, Kavanagh D, et al. Atypical hemolytic uremic syndrome and C3 glomerulopathy: conclusions from a "Kidney disease: Improving global outcomes" (KDIGO) controversies conference. *Kidney Int* (2017) 91(3):539–51. doi: 10.1016/j.kint.2016.10.005

5. Cavero T, Rabasco C, Lopez A, Roman E, Avila A, Sevillano A, et al. Eculizumab in secondary atypical haemolytic uraemic syndrome. *Nephrol Dial Transplant* (2017) 32 (3):466–74. doi: 10.1093/ndt/gfw453

6. Diaz-Guillen MA, Rodriguez de Cordoba S, Heine-Suner D. A radiation hybrid map of complement factor h and factor h-related genes. *Immunogenetics* (1999) 49(6):549–52. doi: 10.1007/s002510050534

7. Jozsi M, Tortajada A, Uzonyi B, Goicoechea de Jorge E, Rodriguez de Cordoba S. Factor h-related proteins determine complement-activating surfaces. *Trends Immunol* (2015) 36(6):374–84. doi: 10.1016/j.it.2015.04.008

8. Jozsi M, Zipfel PF. Factor h family proteins and human diseases. *Trends Immunol* (2008) 29(8):380–7. doi: 10.1016/j.it.2008.04.008

9. Skerka C, Zipfel PF. Complement factor h related proteins in immune diseases. *Vaccine* (2008) 26(Suppl 8):I9–14. doi: 10.1016/j.vaccine.2008.11.021

10. Zipfel PF, Jokiranta TS, Hellwage J, Koistinen V, Meri S. The factor h protein family. *Immunopharmacology* (1999) 42(1-3):53–60. doi: 10.1016/S0162-3109(99)00015-6

11. Lucientes-Continente L, Marquez-Tirado B, Goicoechea de Jorge E. The factor h protein family: The switchers of the complement alternative pathway. *Immunol Rev* (2022). doi: 10.1111/imr.13166

12. Goicoechea de Jorge E, Caesar JJ, Malik TH, Patel M, Colledge M, Johnson S, et al. Dimerization of complement factor h-related proteins modulates complement activation *in vivo*. *Proc Natl Acad Sci U.S.A.* (2013) 110(12):4685–90. doi: 10.1073/pnas.1219260110

13. Tortajada A, Yebenes H, Abarrategui-Garrido C, Anter J, Garcia-Fernandez JM, Martinez-Barricarte R, et al. C3 glomerulopathy-associated CFHR1 mutation alters FHR oligomerization and complement regulation. *J Clin Invest* (2013) 123(6):2434–46. doi: 10.1172/JCI68280

14. van Beek AE, Pouw RB, Brouwer MC, van Mierlo G, Geissler J, Ooijevaar-de Heer P, et al. Factor h-related (FHR)-1 and FHR-2 form homo- and heterodimers, while FHR-5 circulates only as homodimer in human plasma. *Front Immunol* (2017) 8:1328. doi: 10.3389/fimmu.2017.01328

15. Skerka C, Chen Q, Fremeaux-Bacchi V, Roumenina LT. Complement factor h related proteins (CFHRs). *Mol Immunol* (2013) 56(3):170–80. doi: 10.1016/j.molimm.2013.06.001

16. Zipfel PF, Wiech T, Stea ED, Skerka C. CFHR gene variations provide insights in the pathogenesis of the kidney diseases atypical hemolytic uremic syndrome and C3 glomerulopathy. *J Am Soc Nephrol* (2020) 31(2):241–56. doi: 10.1681/ASN.2019050515

17. Piras R, Breno M, Valoti E, Alberti M, Iatropoulos P, Mele C, et al. CFH and CFHR copy number variations in C3 glomerulopathy and immune complex-mediated membranoproliferative glomerulonephritis. *Front Genet* (2021) 12:670727. doi: 10.3389/fgene.2021.670727

18. Moore I, Strain L, Pappworth I, Kavanagh D, Barlow PN, Herbert AP, et al. Association of factor h autoantibodies with deletions of CFHR1, CFHR3, CFHR4, and with mutations in CFH, CFI, CD46, and C3 in patients with atypical hemolytic uremic syndrome. *Blood* (2010) 115(2):379–87. doi: 10.1182/blood-2009-05-221549

19. Piras R, Iatropoulos P, Bresin E, Todeschini M, Gastoldi S, Valoti E, et al. Molecular studies and an ex vivo complement assay on endothelium highlight the genetic complexity of atypical hemolytic uremic syndrome: The case of a pedigree with a null CD46 variant. *Front Med (Lausanne)* (2020) 7:579418. doi: 10.3389/fmed.2020.579418

20. Lemaire M, Fremeaux-Bacchi V, Schaefer F, Choi M, Tang WH, Le Quintrec M, et al. Recessive mutations in DGKE cause atypical hemolytic-uremic syndrome. *Nat Genet* (2013) 45(5):531–6. doi: 10.1038/ng.2590

21. Mele C, Lemaire M, Iatropoulos P, Piras R, Bresin E, Bettoni S, et al. Characterization of a new DGKE intronic mutation in genetically unsolved cases of familial atypical hemolytic uremic syndrome. *Clin J Am Soc Nephrol* (2015) 10(6):1011–9. doi: 10.2215/CJN.08520814

22. Caprioli J, Castelletti F, Bucchioni S, Bettinaglio P, Bresin E, Pianetti G, et al. Complement factor h mutations and gene polymorphisms in haemolytic uraemic syndrome: the c-257T, the A2089G and the G2881T polymorphisms are strongly associated with the disease. *Hum Mol Genet* (2003) 12(24):3385–95. doi: 10.1093/hmg/ddg363

23. Esparza-Gordillo J, Goicoechea de Jorge E, Buil A, Carreras Berges L, Lopez-Trascasa M, Sanchez-Corral P, et al. Predisposition to atypical hemolytic uremic syndrome involves the concurrence of different susceptibility alleles in the regulators of complement activation gene cluster in 1q32. *Hum Mol Genet* (2005) 14(5):703–12. doi: 10.1093/hmg/ddi066

24. Fremeaux-Bacchi V, Kemp EJ, Goodship JA, Dragon-Durey MA, Strain L, Loirat C, et al. The development of atypical haemolytic-uraemic syndrome is influenced by susceptibility factors in factor h and membrane cofactor protein: evidence from two independent cohorts. *J Med Genet* (2005) 42(11):852–6. doi: 10.1136/jmg.2005.030783

25. Bernabeu-Herrero ME, Jimenez-Alcazar M, Anter J, Pinto S, Sanchez Chinchilla D, Garrido S, et al. FHR-3 and FHR-1 variants associate in an extended haplotype conferring increased risk of atypical hemolytic uremic syndrome. *Mol Immunol* (2015) 67(2 Pt B)::276–86. doi: 10.1016/j.molimm.2015.06.021

26. Bresin E, Rurali E, Caprioli J, Sanchez-Corral P, Fremeaux-Bacchi V, Rodriguez de Cordoba S, et al. Combined complement gene mutations in atypical hemolytic uremic syndrome influence clinical phenotype. *J Am Soc Nephrol* (2013) 24(3):475–86. doi: 10.1681/ASN.2012090884

27. Valoti E, Alberti M, Tortajada A, Garcia-Fernandez J, Gastoldi S, Besso L, et al. A novel atypical hemolytic uremic syndrome-associated hybrid CFHR1/CFH gene encoding a fusion protein that antagonizes factor h-dependent complement regulation. *J Am Soc Nephrol* (2015) 26(1):209–19. doi: 10.1681/ASN.2013121339

28. Valoti E, Alberti M, Carrara C, Breno M, Yilmaz Keskin E, Bresin E, et al. Hemolytic uremic syndrome in an infant with primary hyperoxaluria type II: An unreported clinical association. *Nephron* (2019) 142(3):264–270. doi: 10.1159/000497823

29. Venables JP, Strain L, Routledge D, Bourn D, Powell HM, Warwicker P, et al. Atypical haemolytic uraemic syndrome associated with a hybrid complement gene. *PloS Med* (2006) 3(10):e431. doi: 10.1371/journal.pmed.0030431

30. Maga TK, Meyer NC, Belsha C, Nishimura CJ, Zhang Y, Smith RJ. A novel deletion in the RCA gene cluster causes atypical hemolytic uremic syndrome. *Nephrol Dial Transplant* (2011) 26(2):739–41. doi: 10.1093/ndt/gfq658

31. Raychaudhuri S, Ripke S, Li M, Neale BM, Fagerness J, Reynolds R, et al. Associations of CFHR1-CFHR3 deletion and a CFH SNP to age-related macular degeneration are not independent. *Nat Genet* (2010) 42(7):553–5. doi: 10.1038/ng0710-553

32. Eyler SJ, Meyer NC, Zhang Y, Xiao X, Nester CM, Smith RJ. A novel hybrid CFHR1/CFH gene causes atypical hemolytic uremic syndrome. *Pediatr Nephrol* (2013) 28(11):2221–5. doi: 10.1007/s00467-013-2560-2

33. Heinen S, Sanchez-Corral P, Jackson MS, Strain L, Goodship JA, Kemp EJ, et al. *De novo* gene conversion in the RCA gene cluster (1q32) causes mutations in complement factor h associated with atypical hemolytic uremic syndrome. *Hum Mutat* (2006) 27(3):292–3. doi: 10.1002/humu.9408

34. Chen JM, Cooper DN, Chuzhanova N, Ferec C, Patrinos GP. Gene conversion: mechanisms, evolution and human disease. *Nat Rev Genet* (2007) 8(10):762–75. doi: 10.1038/nrg2193

35. Martin Merinero H, Subias M, Pereda A, Gomez-Rubio E, Juana Lopez L, Fernandez C, et al. Molecular bases for the association of FHR-1 with atypical hemolytic uremic syndrome and other diseases. *Blood* (2021) 137(25):3484–94. doi: 10.1182/blood.2020010069

36. Dopler A, Stibitzky S, Hevey R, Mannes M, Guariento M, Hochsmann B, et al. Deregulation of factor h by factor h-related protein 1 depends on sialylation of host surfaces. *Front Immunol* (2021) 12:615748. doi: 10.3389/fimmu.2021.615748

37. Goicoechea de Jorge E, Tortajada A, Garcia SP, Gastoldi S, Merinero HM, Garcia-Fernandez J, et al. Factor h competitor generated by gene conversion events associates with atypical hemolytic uremic syndrome. *J Am Soc Nephrol* (2018) 29(1):240–9. doi: 10.1681/ASN.2017050518

38. White SJ, Aartsma-Rus A, Flanigan KM, Weiss RB, Kneppers AL, Lalic T, et al. Duplications in the DMD gene. *Hum Mutat* (2006) 27(9):938–45. doi: 10.1002/humu.20367

39. Hu X, Wonton RG. Partial gene duplication as a cause of human disease. *Hum Mutat* (1992) 1(1):3–12. doi: 10.1002/humu.1380010103

40. Lalic T, Vossen RH, Coffa J, Schouten JP, Guc-Scekic M, Radivojevic D, et al. Deletion and duplication screening in the DMD gene using MLPA. *Eur J Hum Genet* (2005) 13(11):1231–4. doi: 10.1038/sj.ejhg.5201465

41. Arjona E, Huerta A, Goicoechea de Jorge E, Rodriguez de Cordoba S. The familial risk of developing atypical hemolytic uremic syndrome. *Blood* (2020). doi: 10.1182/blood.2020006931

42. Caprioli J, Noris M, Brioschi S, Pianetti G, Castelletti F, Bettinaglio P, et al. Genetics of HUS: the impact of MCP, CFH, and IF mutations on clinical presentation, response to treatment, and outcome. *Blood* (2006) 108(4):1267–79. doi: 10.1182/blood-2005-10-007252

43. Sanchez-Corral P, Perez-Caballero D, Huarte O, Simckes AM, Goicoechea E, Lopez-Trascasa M, et al. Structural and functional characterization of factor h mutations associated with atypical hemolytic uremic syndrome. *Am J Hum Genet* (2002) 71(6):1285–95. doi: 10.1086/344515

44. Recalde S, Tortajada A, Subias M, Anter J, Blasco M, Maranta R, et al. Molecular basis of factor h R1210C association with ocular and renal diseases. *J Am Soc Nephrol* (2016) 27(5):1305–11. doi: 10.1681/ASN.2015050580

45. Wenzel UO, Kemper C, Bode M. The role of complement in arterial hypertension and hypertensive end organ damage. *Br J Pharmacol* (2021) 178(14):2849–62. doi: 10.1111/bph.15171

46. Lip GY. Hypertension and the prothrombotic state. *J Hum Hypertens* (2000) 14(10-11):687–90. doi: 10.1038/sj.jhh.1001051

47. Zuber J, Frimat M, Caillard S, Kamar N, Gatault P, Petitprez F, et al. Use of highly individualized complement blockade has revolutionized clinical outcomes after kidney transplantation and renal epidemiology of atypical hemolytic uremic syndrome. *J Am Soc Nephrol* (2019) 30(12):2449–63. doi: 10.1681/ASN.2019040331

48. Fayek SA, Allam SR, Martinez E, Pan G, Dao A, Rofaiel G. Atypical hemolytic uremic syndrome after kidney transplantation: Lessons learned from the good, the bad, and the ugly. *A Case Ser With Lit Review Transplant Proc* (2020) 52(1):146–52. doi: 10.1016/j.transproceed.2019.10.015

Frontiers in Immunology

Explores novel approaches and diagnoses to treat immune disorders.

The official journal of the International Union of Immunological Societies (IUIS) and the most cited in its field, leading the way for research across basic, translational and clinical immunology.

Discover the latest Research Topics

See more →

Frontiers

Avenue du Tribunal-Fédéral 34
1005 Lausanne, Switzerland
frontiersin.org

Contact us

+41 (0)21 510 17 00
frontiersin.org/about/contact